ASD-TDR-62-493
Part I

TEMPERATURE CONTROL SYSTEMS FOR SPACE VEHICLES

TECHNICAL DOCUMENTARY REPORT NO. ASD-TDR-62-493, Part I

May 1963

Directorate of Aeromechanics
Aeronautical Systems Division
Air Force Systems Command
Wright-Patterson Air Force Base, Ohio

Project No. 6146, Task No. 614609

(Prepared under Contract No. AF 33(616)-8323
by North American Aviation, Inc., Space and Information Systems Division, Downey, California; C. P. Bacha, F. I. Honea and D. Watanabe, authors)

NOTICES

When Government drawings, specifications, or other data are used for any purpose other than in connection with a definitely related Government procurement operation, the United States Government thereby incurs no responsibility nor any obligation whatsoever; and the fact that the Government may have formulated, furnished, or in any way supplied the said drawings, specifications, or other data, is not to be regarded by implication or otherwise as in any manner licensing the holder or any other person or corporation, or conveying any rights or permission to manufacture, use, or sell any patented invention that may in any way be related thereto.

ASTIA release to OTS not authorized.

Qualified requesters may obtain copies of this report from the Armed Services Technical Information Agency, (ASTIA), Arlington Hall Station, Arlington 12, Virginia.

Copies of this report should not be returned to the Aeronautical Systems Division unless return is required by security considerations, contractual obligations, or notice on a specific document.

35-853M, 300, 7-15-63

Aeronautical Systems Division, Dir/Aeromechanics, Flight Accessories Lab, Wright-Patterson AFB, Ohio.
Rpt. Nr. ASD TDR 62-493, Part I, TEMPERATURE CONTROL SYSTEMS FOR SPACE VEHICLES. May 63, 553 p., incl illus, tables and refs.

Unclassified Report

Passive, semi-passive, active, and heat storage methods for temperature control are described. Comparisons between the various methods are made indicating their advantages and disadvantages. Thermal design consideration of space vehicle equipment indicating various means for controlling equipment

(over)

1. Environmental Control Systems
2. Temperature Control Systems
3. Thermal Design
4. Space Vehicle Cooling Systems
5. Heat Transfer

I. Project 6146 Task 614609
II. Contract AF33(616) 8323
III. Contractor: North American Aviation, Inc., Downey, California
IV. C. P. Bacha, F. I. Honea and D. Watanabe

temperature is presented. Methods of thermal analysis and examples of analysis are presented which include steady-state and transient heat transfer. A brief discussion on dynamic response is also included.

V. SID 62-335
VI. Not aval fr OTS
VII. In ASTIA collection

Aeronautical Systems Division, Dir/Aeromechanics, Flight Accessories Lab, Wright-Patterson AFB, Ohio.
Rpt. Nr. ASD TDR 62-493, Part I, TEMPERATURE CONTROL SYSTEMS FOR SPACE VEHICLES. May 63, 553 p., incl illus, tables and refs.

Unclassified Report

Passive, semi-passive, active, and heat storage methods for temperature control are described. Comparisons between the various methods are made indicating their advantages and disadvantages. Thermal design consideration of space vehicle equipment indicating various means for controlling equipment

(over)

1. Environmental Control Systems
2. Temperature Control Systems
3. Thermal Design
4. Space Vehicle Cooling Systems
5. Heat Transfer

I. Project 6146 Task 614609
II. Contract AF33(616) 8323
III. Contractor: North American Aviation, Inc., Downey, California
IV. C. P. Bacha, F. I. Honea and D. Watanabe

temperature is presented. Methods of thermal analysis and examples of analysis are presented which include steady-state and transient heat transfer. A brief discussion on dynamic response is also included.

V. SID 62-335
VI. Not aval fr OTS
VII. In ASTIA collection

FOREWORD

This is the first part of Technical Documentary Report ASD 62-493 prepared by the Space and Information Systems Division (S&ID) of North American Aviation, Inc. This is one of a series of reports prepared during Phase II of a planned three year study of thermal and atmospheric control systems for manned and unmanned space vehicles. Other reports completed during this phase are:

ASD TR 61-164 (Part II)	Environmental Control Systems Selection for Unmanned Space Vehicles
ASD TR 61-240 (Part II)	Environmental Control Systems Selection for Manned Space Vehicles, Volume I (unclassified) and Volume II (secret)
ASD TR 61-161 (Part II)	Space Vehicle Environmental Control Requirements Based on Equipment and Physiological Criteria
ASD TR 61-119 (Part II)	Radiation Heat Transfer Analysis for Space Vehicles
ASD TR 61-176 (Part II)	Integration and Optimization of Space Vehicle Environmental Control Systems
ASD TR 61-162 (Part II)	Analytical Methods for Space Vehicle Atmospheric Control Processes
ASD TR 62-527 (Part I)	Atmospheric Control Systems for Space Vehicles

This study program was conducted by the Space and Information Systems Division (S&ID) of North American Aviation, Inc., under contract AF 33(616)-8323. It was sponsored by the Flight Accessories Laboratory of the Aeronautical Systems Division. The Los Angeles Division of North American Aviation, Inc. and AiResearch Manufacturing Company of Los Angeles, a division of the Garrett Corporation were sub-contractors in the study effort.

The thermal and atmospheric control study program was under the direction of A. L. Ingelfinger and Arnold Gross of the Environmental Control Section, Flight Accessories Laboratory of the Aeronautical Systems Division. C. Feldmanis of the Environmental Control Section acted as monitor of this project. R. E. Sexton of S&ID served as Project Manager of the study program.

The authors wish to acknowledge the contribution by Dr. N. Van Le of AiResearch Manufacturing Company, (A Division of Garrett Corporation) for providing a major portion of the material in Section IV and to R. K. Breeze and D. Goldenberg of Los Angeles Division of North American Aviation, Inc. for contributing Section VII.

ABSTRACT

Passive, semi-passive, active and heat storage methods for temperature control are described, which include mathematical equations, tables and graphs. Comparisons between the various methods are made indicating their advantages and disadvantages.

A section is presented on thermal design consideration of space vehicle equipment indicating various means for controlling equipment temperature. Methods of thermal analysis and examples of analyses are presented which include steady-state and transient heat transfer. A brief discussion on dynamic response is also included. Conclusions are reached concerning advances in analysis and design techniques. Recommendations cover areas needing investigation and further studies.

This report has been reviewed and is approved.

William C. Savage

WILLIAM C. SAVAGE
Chief, Environmental Branch
Flight Accessories Laboratory

CONTENTS

ILLUSTRATIONS

TABLE

SECTION I

INTRODUCTION

STUDY PROGRAM

The Thermal and Atmospheric Control Study made for the Aeronautical Systems Division is an analytical and experimental program concerned with the problems of the control of the environments of future military space vehicles. Three broadly defined tasks were designated for this study. They are:

1. Development of improved methods of analysis for predicting the requirements for and performance of space environmental control systems.

2. Development of methods, techniques, systems, and equipment required for this environmental control

3. Development of criteria and techniques for the optimization of environmental control systems and the integration of these systems with other vehicle systems.

One endeavor to accomplish these tasks is a survey of industrial organizations and military establishments to obtain data concerned with current and future state-of-the-art of thermal and atmospheric control. Other endeavors include evaluating existing and newly created methods of analysis, selection, integration, and optimization of control systems and components. The refurbishing and developing of existing and new analog or digital computer programs, applicable to this study, are included. In addition, laboratory verification of analyses and new design concepts form a part of the effort associated with these tasks.

To guide all these endeavors along lines which will find immediate and practical application, components and systems associated with specific vehicles have been studied. The vehicles selected are representative of a number of earth orbital and cislunar missions. These hypothetical vehicles are carried through preliminary design and used as thermal and atmospheric control models.

Manuscript released by the authors January 1963 for publication as an ASD Technical Documentary Report.

The principal purpose of the study program and its several tasks is to provide vehicle designers with a useful source of information and with the best analytical procedures to be used in the design of new vehicles. It is anticipated that vehicles going into service about 1966 will be the first to benefit from this program.

ROLE OF TEMPERATURE CONTROL

The control of equipment and compartment temperatures within safe and reliable limits is an important consideration in vehicle design. Temperature control is necessary in order to protect the equipment and compartments from the extremes of high surface temperatures of reentry and of low temperatures of absolute zero space radiation. This control is also necessary for maintaining the temperatures within close limits for precision equipment which is affected by temperature.

Temperature control is achieved basically by controlling the heat transfer rate to or from the equipment, compartment, or vehicle. In order to properly control this heat transfer rate, a knowledge of temperature control methods and analysis techniques for predicting heat transfer rates and dynamics response characteristics is necessary.

ORGANIZATION OF REPORT

The purpose of Part I of this report is to describe many temperature control methods, to compare these methods and to show some techniques of analysis and examples. Future parts of this report will deal more directly with design considerations and dynamic response characteristics of the control method.

Analyses of the temperature control system requirements for the hypothetical vehicles used in this program are presented in References 1 and 2. Reference 3 gives examples of system integration.

In order to properly choose a temperature control system for a space vehicle, the vehicle designer must know (1) methods of temperature control and heat storage, (2) trade-offs and comparisons between these methods, (3) thermal considerations of the vehicle equipment, and (4) heat transfer rates and thermal control dynamic response requirements of the vehicle. This report has been organized around these four major considerations.

The first three sections of the report describe methods of temperature control. These methods have been grouped as passive, semi-passive and active methods. Passive methods are those which have no moving parts; semi-passive methods are those which have

moving parts, flowing fluids or expendable coolants, and active methods are those which require heat pumps. Comparisons of some methods and coolants are also presented in these sections.

Aside from temperature control by heat transfer, another method of control is available by use of a heat storage material with a high heat of sublimation or vaporization within the desired temperature limits. These heat storage methods and materials are described in Section V.

All of the temperature control methods described in the preceding sections are summarized and compared for advantages, disadvantages, limitations, and trade-offs in Section VI. This section gives some weight, volume, and surface area equations and comparisons for various methods and maps the regions of application of these methods in terms of temperature and heat load. However, before the temperature control method can be chosen from the previous sections, a determination of the vehicle equipment temperature requirements and methods of heat removal and of heat transfer rates and control method dynamics response are necessary. Section VII presents the thermal considerations of space vehicle equipment in terms of temperature requirements, methods of heat removal, and future trends in equipment thermal limits. Since heat transfer rates and dynamic response of the control method are associated closely with the exact vehicle and its requirements, the determination of these quantities usually will require analyses. Some of these methods of analyses are presented in Section VIII.

Future parts of this report will add to the content of these subjects and describe design procedures for temperature control methods and a detailed method of analysis of control dynamic response.

SECTION II

PASSIVE TEMPERATURE CONTROL METHODS

Passive methods for the control of temperatures are characterized by containing no moving parts or fluids and requiring no input of power for their operation. The inherent simplicity of these methods is readily apparent. Many of the early space vehicles have depended solely on these methods for temperature control. Future spacecraft, because of their complexity, perhaps will require more complex methods for temperature control; but nonetheless, passive methods will continue to serve as an important part of an overall thermal control system.

Passive methods discussed in this section depend upon conduction, radiation or a combination of conduction and radiation as a means for heat transfer. Since natural convection does not occur in zero-gravity environment, heat transfer by this process will not be considered here.

Figure 1 illustrates a simple passive temperature control system which depends on conduction and radiation for heat transfer.

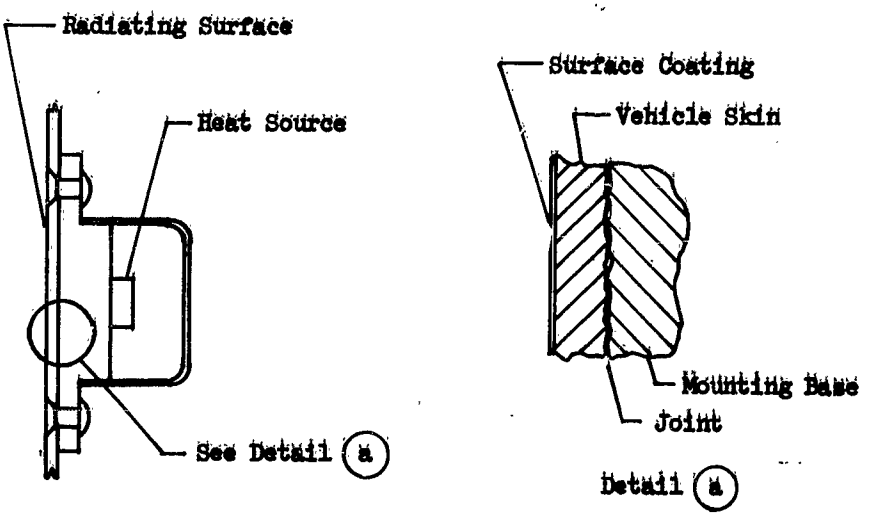

Figure 1 Temperature Control by Passive Method

Principal mode of heat transfer from heat source to the outer skin surface is by conduction. From the outer skin surface heat is dissipated to space, the ultimate heat sink, by radiation. The prime requirement of this simple system is to provide an efficient heat path from the source to sink. One very important consideration, which will be discussed, is the heat transfer across the interface of mating surfaces illustrated in detail (a) of Figure 1.

In addition to discussing means for providing efficient heat transfer by conduction and by radiation, methods for providing effective heat resistance or insulation will also be considered. This is very important in providing thermal protection for space vehicles while in orbit and particularly during reentry.

NOMENCLATURE

A	Area, (sq ft)
C_a, C_b, C_c	Constants (See Equation 14, 15 and 16)
c_p	Specific heat at constant pressure, Btu/(lb)(^oF)
E_E	Planetary emission, Btu/(hr)(sq ft)
F	Geometric form factor
f	Fractional volume of insulation occupied by fibers, dimensionless
h	Altitude, miles
h_c	Interface conductance, Btu/(hr)(sq ft)(^oF)
K_{ϵ,ϵ_s}	Heat transfer coefficient defined by Equation 23
k	Thermal conductivity, Btu/(hr)(sq ft)(^oF/ft)
k	Apparent thermal conductivity, Btu/(hr)(sq ft)(^oF/ft)
L	Length, ft
n	Number of shields
p	Pressure, psf
Q	Internal heat load rate, Btu/hr

q	Heat transfer rate, Btu/hr
q'	Heat transfer rate per unit area, Btu/(hr)(sq ft)
R	Earth radius, miles
R_E	Reflected solar energy from planet Btu/(hr)(sq ft)
r_e	Albedo
S	Solar constant, Btu/(hr)(sq ft)
T	Temperature, ^oF or ^oR
t	Time, hr
W	Mass of vehicle skin, lb
α	Absorptivity
ϵ	Emissivity
θ	Angle between the incident solar rays and the normal to the surface
θ_s	Angle between earth-sun line and vertical from planet to satellite
ρ	Density, lb/cu ft
σ	Stefan-Boltzmann constant 0.1713×10^{-8} Btu/(hr)(sq ft)($^oR^4$)

Subscripts

cd	Conductivity of gas
cv	Conductivity due to convection
E	Earth (or planet)
m	Designation number (n 1, 2, 3 .....m-1)
o	Internal body surface
ra	Conductivity due to radiation
R	Reflected solar
s	Solar

sc	Conductivity of solid conduction due to fiber contacts
T	Over all or total

CONDUCTION

The subject of heat conduction has been treated extensively in many books on heat transfer, such as References (26) and (89), therefore the discussion here is limited to selected material on this subject.

Study of heat flow through many materials has established the fact that materials differ in their ability to conduct heat. Those that are good conductors of heat are also good conductors of electricity. This includes well known metals such as silver, copper and aluminum. Many non-metallic materials such as wood, acid stones, liquids and gases are poor heat conductors, and are classified as insulators. Thus, depending upon the material utilized, either high thermal conductance or high thermal resistance can be achieved.

Thermal Conductance

To obtain efficient heat transfer by conduction requires more than just the consideration of the conducting material. As indicated by the fundamental law of conduction, Fourier's equation

$$q = \left(\frac{kA}{L}\right) \Delta T \qquad (1)$$

high heat flow rate can be achieved by obtaining large values for the term (kA/L) or the temperature difference ΔT.

To obtain a large temperature difference between the heat source and sink requires for a given heat source temperature, the determination of a heat sink at the desired lower temperature. For the temperature control system illustrated in Figure 1, the intermediate heat sink is the vehicle skin, so that ΔT is dependent upon the skin temperature, which in turn is governed by the net energy exchange by radiation.

The term (kA/L) is a combination of the conducting property of the conductor and its physical dimensions. Good heat conductors, such as copper and aluminum, have specific gravity values greater than one, therefore weight is an important consideration in addition to conductivity.

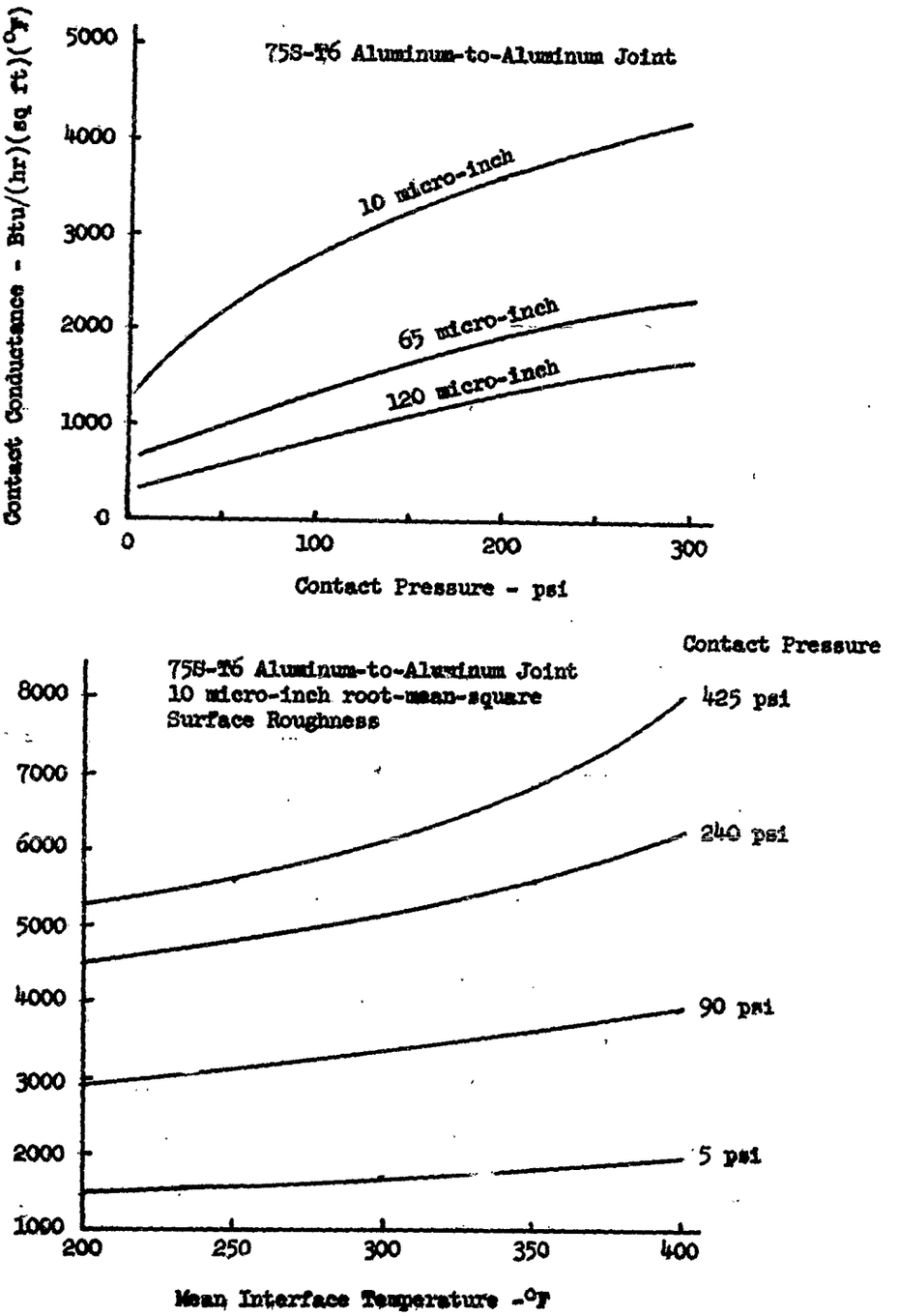

Figure 2 Thermal Conductance Across Interface of Conductor Joint

Increase in area A would increase heat flow rate, but it would also result in larger conductor, and hence increase in weight. The most significant quantity is the length L, since smaller the value would not only result in higher heat flow rate, but also lighter weight conductor. For the simple system illustrated in Figure 1, the heat source should be placed as close to the thermal radiating surface as possible.

The conduction path as shown in Figure 1 is composed of several solid conductors which introduces joints; thus, joint effects on heat flow becomes an important consideration.

Joint Resistance

For efficient design of conduction paths, knowledge of joint resistance is necessary. A survey of available literature indicates a lack of analysis and experimental data directly applicable to spacecraft, particularly for extremely low pressure environment. Many variables (which include contact pressure, temperature, heat flow rate, interstitual pressure, interstitual fluid, joint materials, surface finish, material hardness and surface flatness) must be taken into consideration to provide useful data on this subject. Some of the more important earlier work on joint resistance was published in 1949. Weills and Ryder, Reference 4, conducted tests using copper, steel and aluminum for varying temperature and pressure. Brunot and Buckland, Reference 5, used laminated and machined joints, using steel with cement, steel, and aluminum foils sandwiched between the surfaces. Only pressure was varied. In 1953, WADC, Reference 6, reported on an experimental method of measuring thermal resistance by using a Mach-Zehnder interferometer. The results of these measurements were tabulated. Fenech, Reference 7, developed an idealized model for thermal contact and compared the theoretical analysis with experimental data for Armco-Iron contact surfaces of 600 RMS roughness for varying pressure and temperature. Graff, Reference 8, introduced a dimensionless conductance ($h_c p/k\epsilon$) which was used to correlate test data presented by other investigations. Investigators for NACA, References 9, 10, 11 and 12, have presented considerable amount of experimental data on aircraft joints at atmospheric pressure for surface finish ranging from 10 to 120 microinch root-mean-square surface roughness. Contact pressure, temperature and heat load were the principal variables. Figure 2 presents a portion of the data given in Reference 10. The influence of surface finish and contact pressure on joint conductance is clearly indicated. Recently, Fried and Costello, Reference 13, have presented the results of experimental work for tests conducted at ambient pressures of 10^{-4} to 10^{-6} mm Hg absolute and relatively low range of contact pressures, from 2 to 35 psi. The experimental values indicate that joint conductance is lower at vacuum conditions.

Tests were also conducted utilizing various interface shim materials. The results of these tests are presented in Figure 3, indicating the marked influence of soft materials, such as lead foil, in increasing the joint conductance.

Based on the review of available reports, joint resistance can be decreased by: (1) increasing contact pressure, (2) reducing surface roughness, (3) maintaining surface flatness, and (4) utilizing shim materials with lower hardness than the joint material.

The problem of analyzing thermal resistance of joints consists of (1) determining the true contact area through which heat flows by solid conduction and (2) the modes of heat transfer other than solid conduction and their relative importance. True contact area is difficult to establish because it is made up of many small points of contact; which depend upon the surface roughness, contact pressure, contact material hardness, and surface flatness. The amount of deformation of the contact points establishes the true or effective contact area.

Reference 13 suggests gaseous, molecular, or other conduction through the interstitual fluid or filler, and radiation as possible modes of heat transfer in addition to solid conduction through the contact area. The contribution of each mode to the total heat transfer has not been established.

The problem of joint resistance associated with cooling electronic packages and components is discussed in Section VII.

Thermal Resistance

There are many materials available which can be used to achieve good thermal resistance. Solids, solid particles, liquids and gases are used in various combinations to provide the necessary insulation. The selection of the material is dependent upon, in addition to low thermal conductivity, whether structural rigidity is important. For example, insulation for cryogenic storage vessels must not only have high thermal resistance but must have structural rigidity.

Solid insulating material, such as wood, stone and plastics are not considered here because there are other insulations which not only have much lower thermal conductivity, but also have lower densities. Table 1 presents a list of representative insulations that are commonly used and are readily available.

These insulating materials are non homogeneous and porous so that thermal conductivity is a function composition, density, temperature and particularly pressure. For materials of this type,

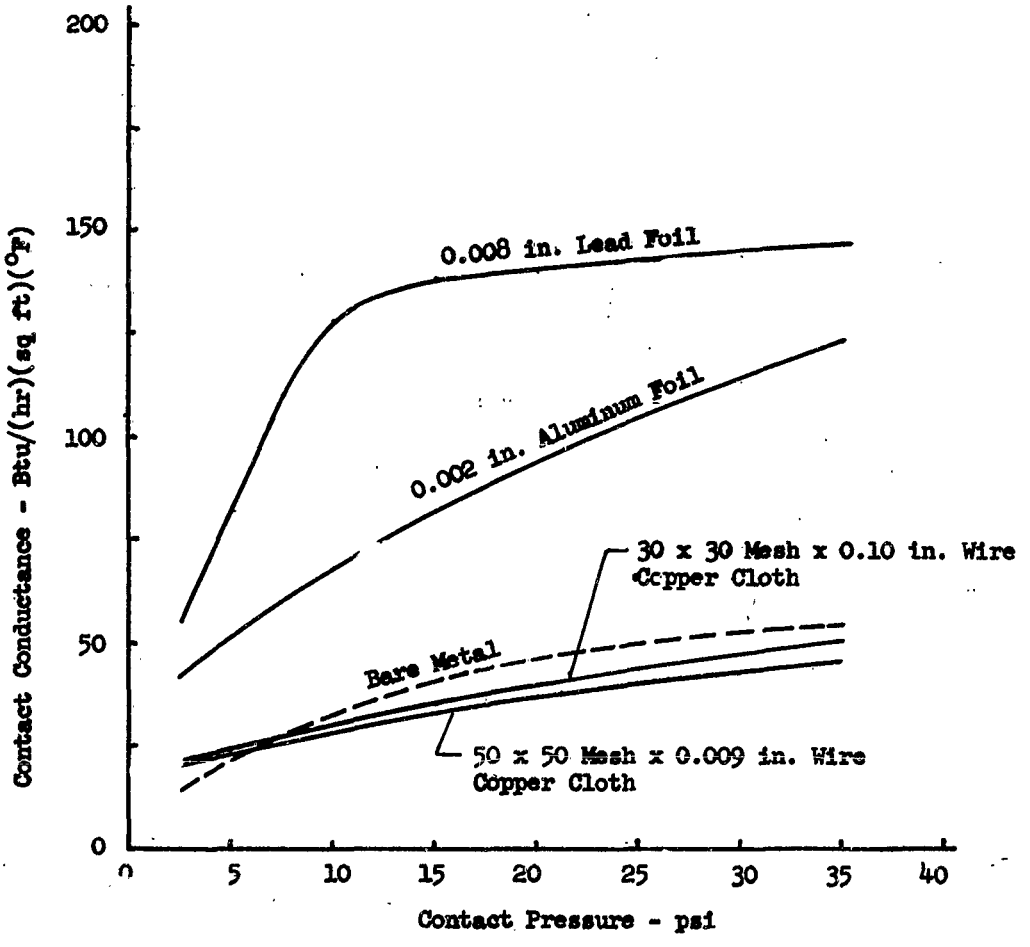

Figure 3 Thermal Conductance vs Contact Pressure for Joints with Shim Material

Table 1 - The Effect of Air Removal Upon the Thermal Conductivity of Various Materials at 100°F Mean Temperature

MATERIAL	Density, lb/cu ft	Thickness, inches	Thermal Conductivity, k			
			k at one atmosphere	at reduced pressure		Percent reduction
				microns Hg	k	
Air Space-Copper Surfaces		1	0.572	0.07	0.187	67.3
Corkboard	6.67	1	0.283	0.06	0.106	62.5
Corkboard	12.4	1	0.314	0.13	0.120	61.8
Cotton	0.78	1	0.288	0.07	0.072	75.0
Cotton	1.53	1	0.257	0.12	0.052	79.8
Cotton	2.62	1	0.248	0.14	0.033	86.7
Coarse glass wool	2.8	1	0.267	0.04	0.055	79.4
Fine glass wool "A"	0.58	1	0.2505	0.08	0.050	80.0
Fine glass wool "A"	1.94	1	0.2145	0.05	0.0195	90.0
Fine glass wool "A"	3.8	1	0.211	0.11	0.012	94.3
Fine glass wool "B"	0.78	1	0.302	0.04	0.0665	78.0
Hairfelt	11.1	3/4	0.260	0.10	0.031	88.1
Kapok	0.26	1	0.366	0.10	0.091	75.1
Kapok	0.99	1	0.245	0.10	0.0375	84.7
Kapok	3.96	1	0.244	0.12	0.0175	92.8
Mineral wool	7.7	1	0.258	0.05	0.037	85.7
Silica Aerogel	8.6	1	0.1715	0.07	0.0255	85.1
Special specimen	3.1	1	0.231	0.00	0.0145	93.7
Wood fiber board	15.5	3/4	0.353	0.05	0.075	78.8
Wood fiber	3.5	1	0.2715	0.08	0.052	80.8
Wood fiber	6.9	1	0.277	0.09	0.033	88.1

(19) General Dynamics-Astronautics Report AZJ-55-005, "Thermal Insulation of Space Vehicles", page 19
From: (16) Rowley, F. B., et al, "Gas is an Important Factor in the Thermal Conductivity of Most Insulating Materials", ASHVE Trans, Vol 58 p 155-170

heat transfer is not by conduction alone but also by convection and radiation. Reference 14 suggests for fibrous insulation, the term apparent thermal conductivity rather than thermal conductivity should be used and gives the following expression for the overall thermal conductivity

$$k'_T = \frac{(k_{cd} + k'_{cv} + k'_{ra})}{1 - f} + k_{sc} \qquad (2)$$

Table 2 of Reference 14 shows measured thermal conductivity values for various densities of fiber insulation with four gases, helium, air, carbon dioxide, and Freon 12 at atmospheric pressure except for one test at 76 mm of Hg pressure. The results indicate that at atmospheric pressure, gas conduction is by far the most important mode of heat transfer in fibrous insulation, contributing from 50 to 90 per cent to the overall thermal conductivity. Also at atmospheric pressure, helium gas gives the highest thermal conductivity and Freon-12 gives the lowest value.

Figure 4, which is reproduced from Figure 6 of Reference 14, shows the contribution by each of the different modes of heat transfer, at atmospheric pressure for changes in insulation density. It is readily apparent that air conduction is the major mode of heat transfer and does not change with change in insulation density. Radiation and convection decreases rather rapidly with increase in insulation density, up to about 3 lb/cu ft and further increase in density has less influence on these two modes of heat transfer. Solid conduction due to fiber contacts contribute very little to the heat transfer in the fibrous insulations.

Since gas conduction is the predominant mode of heat transfer, this can be minimized or eliminated by evacuating the gas from the insulation. The marked effect of low pressure on decreasing the thermal conductivity is clearly indicated in Table 1. The variation of thermal conductivity with pressure for powdered insulation is given in Figure 13.

By eliminating gas conduction by lowering the insulation pressure, radiation becomes the predominate mode of heat transfer. This mode of heat transfer can be minimized by the use of powdered or solid particle insulation or fibrous materials or by multiple layers of highly reflective surfaces. This latter method is discussed more fully in the part on radiation.

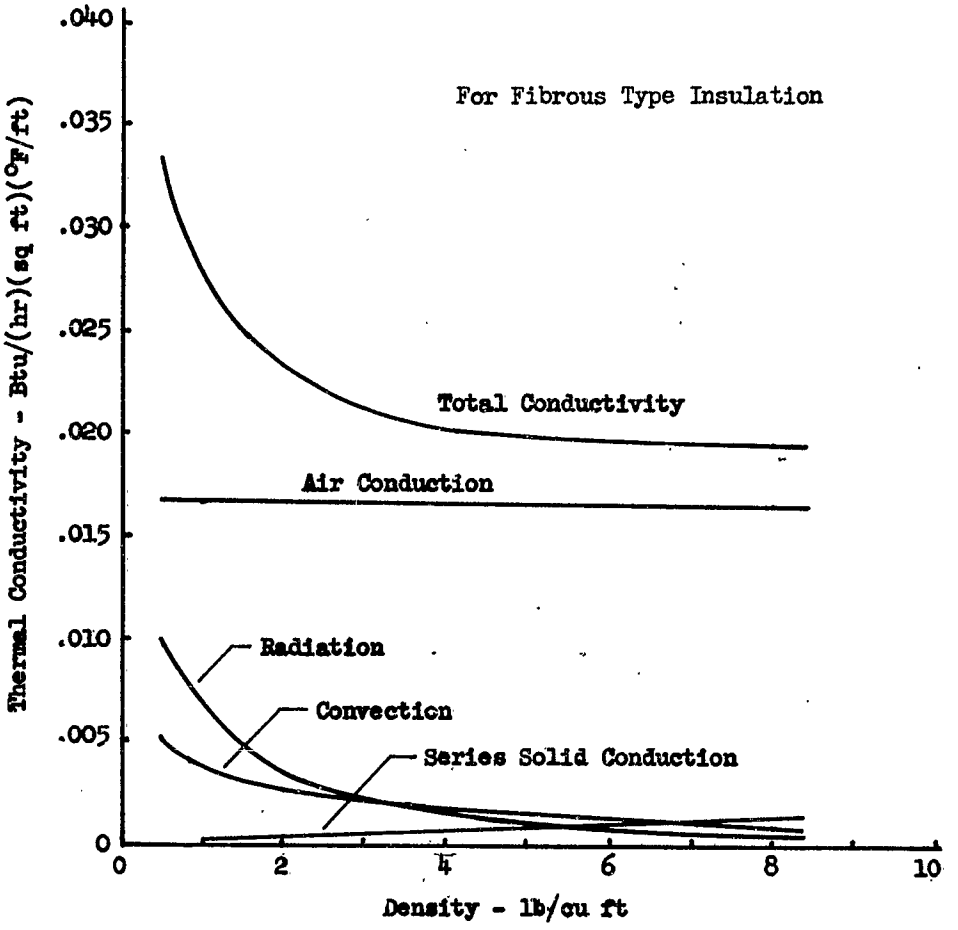

Figure 4 Contribution by Various Modes of Heat Transfer
Thermal Conductivity vs Density

Highly efficient insulating materials with lower thermal conductivities than those listed on Table 1 have been developed through improvements in cryogenic insulation. Table 6 of Reference 25 lists a number of such materials. As indicated in Reference 25, the best forms of insulation are the laminated types of insulation which have mean thermal conductivities in the order of .000025 Btu/(hr)(ft)(^{o}F). However, they are not load-bearing so that for applications such as insulating cryogenic storage vessel require additional structural members which introduces the additional problem of heat leaks. Evacuated powders and fibers have been used extensively, particularly in small vessels. The thermal conductivities of these materials are approximately ten times as high as those of laminated materials.

Christensen, Reference 15, draws the following conclusions with regards to some of the commonly used insulation materials.

(1) Cellular foams are not the best insulations for space environments because the totally enclosed interstices cannot be evacuated by the vacuum of space.

(2) Fiberglass mats may be the best conventional insulation for space application because they are vibration and pressure resistant and have conductivities as low as 0.001 (Btu-ft)/(hr)(sq ft)(^{o}F), at low temperatures.

(3) Fiberglass mats and powders must be used at the relatively high densities of 5 lb/cu ft and more in order to reduce radiation transfer through the insulation.

(4) Powders, while having the best thermal properties as insulators, have the disadvantages of being non load bearing or vibration resistant, and are susceptible to effects of moisture.

These insulating materials are applicable primarily for extremely low temperatures and are not suitable for specific application such as for reentry bodies. The insulation requirements during reentry are low thermal conductivity at high temperatures for short duration. This insulation problem is discussed in Part II of this report and Reference 1.

RADIATION

Radiation is a very important means of heat transfer for temperature control of space vehicles. Vehicle surface temperature, disposal of waste or excess heat, highly efficient insulation are all dependent upon radiation or the control of radiation. Knowledge

of thermal radiation and means for its control is vital for the design of temperature control systems. Reference 18 gives a comprehensive treatment on radiation heat transfer analysis. Reference 48 gives a detailed analysis for the design of efficient radiating surfaces. A more general discussion of thermal radiation is presented in many books on heat transfer, such as Reference 26, 29, and 89.

The selection of surface coatings for space vehicles is one of the important tasks to provide proper temperature control. Surface coatings must have appropriate values of solar absorptivity and emissivity to keep the vehicle surface temperature within required range. The importance of both α_s and ϵ is shown in Section VIII, Methods of Analysis.

Vehicle Surface Radiation

Many of the satellites placed in orbit have had surfaces made up of several different coatings arranged in strips or patches, the percentage of each area having been carefully calculated. Table 2 illustrates the variety of materials and finishes which were found on the internal or external surfaces of Explorer VII, Reference 17. In order to determine the required surface coating a vehicle heat balance equation must be used such as Equation 63 of Reference 18.

$$Wc_p \frac{dT}{dt} = \alpha_s A F_S S + \alpha_R A F_R R_E + \alpha_E A F_E E + Q - \epsilon \sigma T^4 \qquad (3)$$

In this equation the first three terms on the right represent direct solar, reflected solar and planetary emission incident on the vehicle surface. For each of these terms, a geometric form factor must be determined for every orbit position of the vehicle with respect to radiating bodies, such as the sun and the earth. A method for determining these quantities utilizing a computer program is described in Reference 18.

The term Q represents the internal heat load that is flowing into the surface. As illustrated in Figure 1, only that portion of the surface which heat is flowing into would this term apply. The last term represents the thermal energy that is radiated to space.

To illustrate how the required values for solar absorptivity and emissivity can be determined, the following example is presented. A sphere, which is in a circular orbit around the earth, is considered to be spinning about its own axis so that the temperature is uniform over all the surface. Furthermore, it is assumed that the temperature varies very slowly with time, thus $dT/dt \approx 0$. Equation 3 becomes

$$\epsilon \sigma T^4 = \alpha_s F_S S + \alpha_R F_R R_E + \alpha_E F_E E + Q \qquad (4)$$

By assuming $\alpha_s = \alpha_R$ and $\epsilon = \alpha_E$, and introducing the following constants into Equation 4,

$S = 443$ Btu/(hr)(sq ft)

$r_e = 0.35$ (Earth albedo)

$R = 3960$ Miles

$h = 300$ Miles

$F_S = 0.25$ (Eq. 45, Reference 18)

$F_E = \frac{1}{2}\left[1 - \frac{\sqrt{h(h+2R)}}{h+R}\right] = 0.316$ (Eq. 48, Reference 18)

$F_R = F_E \cos\theta_s = 0.316 \cos\theta_s$ (Eq. 49, Reference 18)

$R_E = Sr_e = 151$ (Eq. 64, Reference 18)

$E = \left[\frac{1-r_e}{4}\right]S = 72.1$ (Eq. 64, Reference 18)

$\sigma = 0.1713 \times 10^{-8}$ Btu/(hr)(sq ft)($^\circ R^4$)

The following equation is derived for T,

$$T = 100\sqrt[4]{648\left(\frac{\alpha_s}{\epsilon}\right) + 278\left(\frac{\alpha_s}{\epsilon}\right)\cos\theta_s + 133 + 5.48\left(\frac{\alpha_i}{\epsilon}\right)} \qquad (5)$$

For the specific case when the orbiting sphere is at the sun-earth line, surface temperature T is computed from Equation 5 for various values of emissivity and solar absorptivity. The results are plotted on Figure 5. For a desired surface temperature, there are many combinations of values for emissivity and solar absorptivity which can be used. Several coatings are indicated on the figure, illustrating the wide range of temperatures that can be obtained, high temperature by using polished aluminum and low temperature by using white lacquer. Also shown on the figure is that surface temperature of 120 F can be obtained by using either aluminum silicone paint or black silicone paint.

The curves plotted on Figure 5 are suitable only for preliminary calculations for low mass vehicles with low power output. The assumption that $dT/dt \approx 0$ would not be valid for most cases and Equation 3 should be used to determine the instantaneous temperature. Additional discussion on temperature determination of orbiting vehicles is given in Section VIII.

TABLE 2

Absorptance and Emittance of Materials Found in Explorer VII Satellite Vehicle (17)

Material	Short Wave Absorptance (Solar Radiation)	Long Wave Emittance
Sandblasted Aluminum	0.42	0.21
Polished Aluminum	0.31	0.07
Sandblasted Magnesium	0.63	0.54
Rokide A	0.15	0.77
Gray TiO_2 Paint	0.87	0.87
White TiO_2 Paint	0.19	0.94
Solar Cells	0.80	0.40
Sauereisen	0.34	0.88
Fused Silica	0.06	0.84
Gold Foil	0.21	0.07

(17) NASA TN D-608, "Juno II Summary Project Report, Vol I, Explorer VII Satellite" page 152

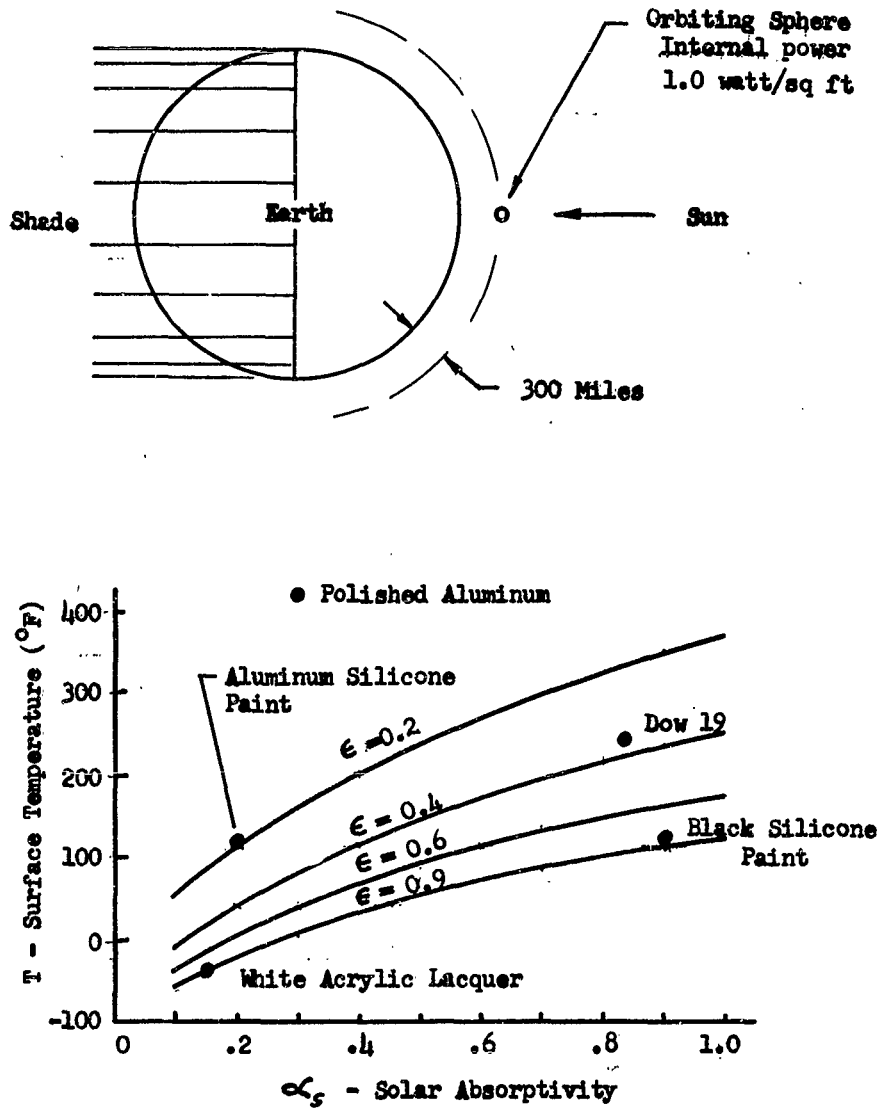

Figure 5 Orbital Vehicle Surface Temperature
(For Vehicle at Sun-Earth Line)

In some cases, no surface coating may be suitable to provide adequate protection from direct solar radiation. For such cases, radiation shields, composed of highly reflective surfaces can be used. The following pages present a derivation of equations from Dr. D. B. MacKay of S & ID for the relationship of multiple shields with respect to solar radiation to a vehicle. These equations are applicable to insulation problems, such as those mentioned in that part on cryogenic insulation.

Thermal Radiation Shield

Dr. D. B. MacKay showed a detailed analysis for a method of temperature control for lunar vehicles utilizing multilayer shields. The following derivation of equations is essentially as it was presented in an internal S & ID document.

The heat transfer equations derived here are for a vehicle whose surface is shielded by n layers of protecting material. It is assumed that a vacuum exists in the space between the body and the shield, as well as between the individual layers, and that no heat flows by conductivity between the elements under consideration. One further assumption is that the layers are flat, parallel and infinitely large, so that the configuration factor is equal to one.

Each of the several layers is assumed to have an emissivity ϵ except for the outside surface of the last layer (the most external one) which has an emissivity ϵ_m. The rate at which radiant energy leaves the body whose temperature is T_0 and emissivity is ϵ_0 can be analyzed with the use of the sketch given below.

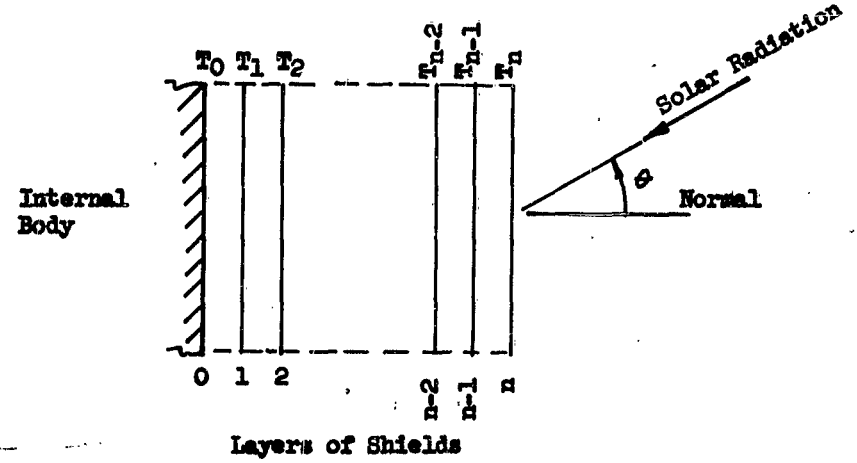

Figure 6. Schematic of Multilayer Shielding

Heat transfer between surface 0 and layer 1 is

$$q_{0,1} = \frac{1}{\frac{1}{\epsilon_0} + \frac{1}{\epsilon} - 1} \sigma \left(T_0^4 - T_1^4\right) = \frac{\epsilon_0 \epsilon}{\epsilon + \epsilon_0 - \epsilon_0 \epsilon} \sigma \left(T_0^4 - T_1^4\right) \tag{6}$$

and the heat transfer between layers 1 and 2 is

$$q_{1,2} = \frac{1}{\frac{1}{\epsilon} + \frac{1}{\epsilon} - 1} \sigma \left(T_1^4 - T_2^4\right) = \frac{\epsilon}{2 - \epsilon} \sigma \left(T_1^4 - T_2^4\right) \tag{7}$$

Similarly, it follows that heat transfer between layers (n-1) and n is

$$q_{n-1,n} = \frac{\epsilon}{2 - \epsilon} \sigma \left(T_{n-1}^4 - T_n^4\right) \tag{8}$$

Heat transfer equation between the n^{th} layer and the environment is

$$q_n = \epsilon_n \sigma T_n^4 - S \alpha_s \cos \phi \tag{9}$$

For steady state condition, heat flow rate is the same through all the layers, and thus equating Equation 7 and 8, the following relation is obtained.

$$T_1^4 - T_2^4 = T_{n-1}^4 - T_n^4 \tag{10}$$

Equation 10 is typical for any of the layers and shows the change in the value of the fourth power of the temperatures between succeeding layers. For n layers, there will be n-1 changes in value between the first and the n^{th} layer, or

$$T_1^4 - T_n^4 = \left(T_{n-1}^4 - T_n^4\right)(n-1) \tag{11}$$

Equating Equations 6 and 8

$$\frac{\epsilon_0 \epsilon}{\epsilon + \epsilon_0 - \epsilon_0 \epsilon} \sigma \left(T_0^4 - T_1^4\right) = \frac{\epsilon}{2 - \epsilon} \sigma \left(T_{n-1}^4 - T_n^4\right) \tag{12}$$

It follows that

$$T_o^4 = T_1^4 + \frac{\epsilon + \epsilon_o - \epsilon_o\epsilon}{\epsilon_o(2-\epsilon)} \left(T_{m-1}^4 - T_m^4 \right) \tag{12}$$

Also equating Equations 8 and 9, and simplifying,

$$T_{m-1}^4 - T_m^4 = \frac{\epsilon_m(2-\epsilon)}{\epsilon} T_m^4 - \frac{2-\epsilon}{\epsilon\sigma} S\alpha_s \cos\phi \tag{13}$$

By combining Equations 11, 12 and 13, and simplifying,

$$T_o^4 = T_m^4 + \left[\frac{\epsilon_m(2-\epsilon)}{\epsilon} T_m^4 - \frac{2-\epsilon}{\epsilon\sigma} S\alpha_s \cos\phi \right] \left[\frac{\epsilon + \epsilon_o - \epsilon_o\epsilon}{\epsilon_o(2-\epsilon)} + m - 1 \right] \tag{14}$$

which may be expressed simply as

$$T_o^4 = T_m^4 + \left(C_a T_m^4 - C_c \right) C_b \tag{15}$$

where

$$C_a = \frac{\epsilon_m(2-\epsilon)}{\epsilon} \tag{16}$$

$$C_b = \frac{\epsilon + \epsilon_o - \epsilon_o\epsilon}{\epsilon_o(2-\epsilon)} + n - 1 \tag{17}$$

$$C_c = \frac{2-\epsilon}{\epsilon\sigma} S\alpha_s \cos\phi \tag{18}$$

and finally,

$$T_m^4 = \frac{T_o^4 + C_b C_c}{C_a C_b + 1} \tag{19}$$

Substituting Equation 19 and Equation 9, the general equation for the amount of heat radiated through a cover consisting of n layers as a function to T_o and angle θ is obtained as

$$q_m = \epsilon_m \sigma \frac{T_o^4 + C_b C_c}{C_a C_b + 1} - S\alpha_s \cos\theta \tag{20}$$

When in free space, if a side of the vehicle is not exposed to the sun

$$q_m = \frac{\epsilon_m \sigma T_o^4}{C_a C_b + 1} \tag{21}$$

since $C_c = 0$

Further in the particular case where $\epsilon_m = \epsilon$, Equation 21 reduces to

$$q_m = K_{\epsilon,\epsilon_o} \sigma T_o^4$$

where

$$K_{\epsilon,\epsilon_o} = \frac{\epsilon\epsilon_o}{\epsilon + \epsilon_o(1-\epsilon) + \epsilon_o[2m-1-(m-1)\epsilon]} \tag{23}$$

If $\epsilon_o = \epsilon$ Equation 23 reduces to

$$K_{\epsilon,\epsilon_o} = \frac{\epsilon}{1 + m(2-\epsilon)} \tag{24}$$

Heat transfer coefficient K_{ϵ,ϵ_o} versus n, the number of shields, is plotted in Figure 7 for the case in which an enclosed body is in free space receiving no solar energy. Figure 7 indicates a rapid decrease in the value of heat transfer coefficient as the number of shields increases from zero to 2. As n increases beyond 3, the reduction in the value for K_{ϵ,ϵ_o} becomes negligible. Also indicated on the figure, coefficient K_{ϵ,ϵ_o} is reduced by decreasing the value for emissivity. By using three or four shields of low emissive material such as aluminum foil, $\epsilon = 0.05$, very low values for the heat transfer coefficient can be obtained.

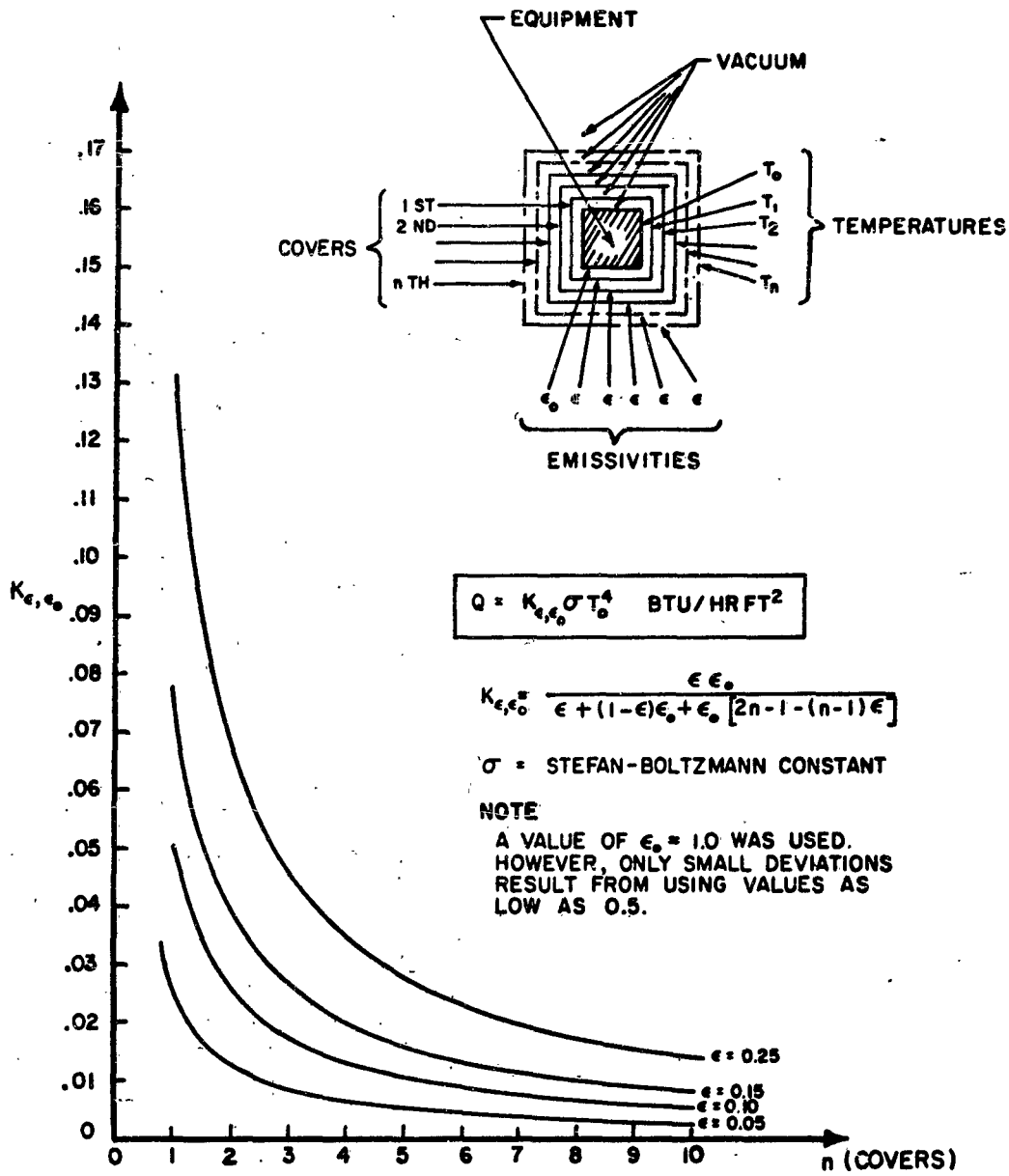

Figure 7. Multishield Heat Transfer Coefficient (Box in free space and no solar heat)

Figures 8 and 9 show a plot of Equation 20 for $n = 3$ and $n = 4$, for the case the body is exposed to solar radiation for which the incident angle and varies from 0° to 90°. Curves are plotted for several values of body temperature from 400° to $800^{\circ}R$. For a given sun angle θ, the heat transfer rate increases almost exponentially with increase in body temperature. Comparison of Figures 8 and 9 indicates the reduction of heat transfer rate by increasing the number of shield from 3 to 4, which is as expected.

The preceding analysis is limited for the case of infinite flat plates but it does illustrate the effectiveness of using multilayer shielding. For surfaces of finite size, the interchange factor between the layers must be computed since the geometric form factor is not equal to one. This can be readily accomplished by utilizing the radiosity analog method described in References 18 and 30.

Other types of radiation shields, such as the bumper type located in front of the vehicle, will be discussed in Part II of this report.

CONCLUSIONS

Passive methods, because of their relative simplicity, have been the sole means for temperature control of first generation space vehicles. Although more complex control methods will be required in the future vehicles, passive methods will be an integral part of the over-all temperature control system.

High conductance heat paths can be achieved by utilizing high heat conducting material and by placing the heat source close to the heat sink, such as the vehicle skin. The conduction path should be designed with a minimum number of joints.

An important consideration for the efficient design of conduction path is the joint effect on heat transfer. Currently, there is a need for more data, particularly at very low pressures, and a development of methods for analysis. Limited information currently available indicate thermal resistance of joints can be minimized by: (1) increasing contact pressure, (2) reducing surface roughness, (3) maintaining surface flatness, and (4) utilizing shim materials which have lower hardness then joint materials.

Through continued development effort, highly efficient insulations have been developed. Most efficient insulations required very low interstitial pressure to minimize or eliminate gas conduction, which is the major node of heat transfer accounting for 50 to 90 per cent at the total conductance. In addition, radiation heat transfer is minimized by use of powder and fibrous materials and by

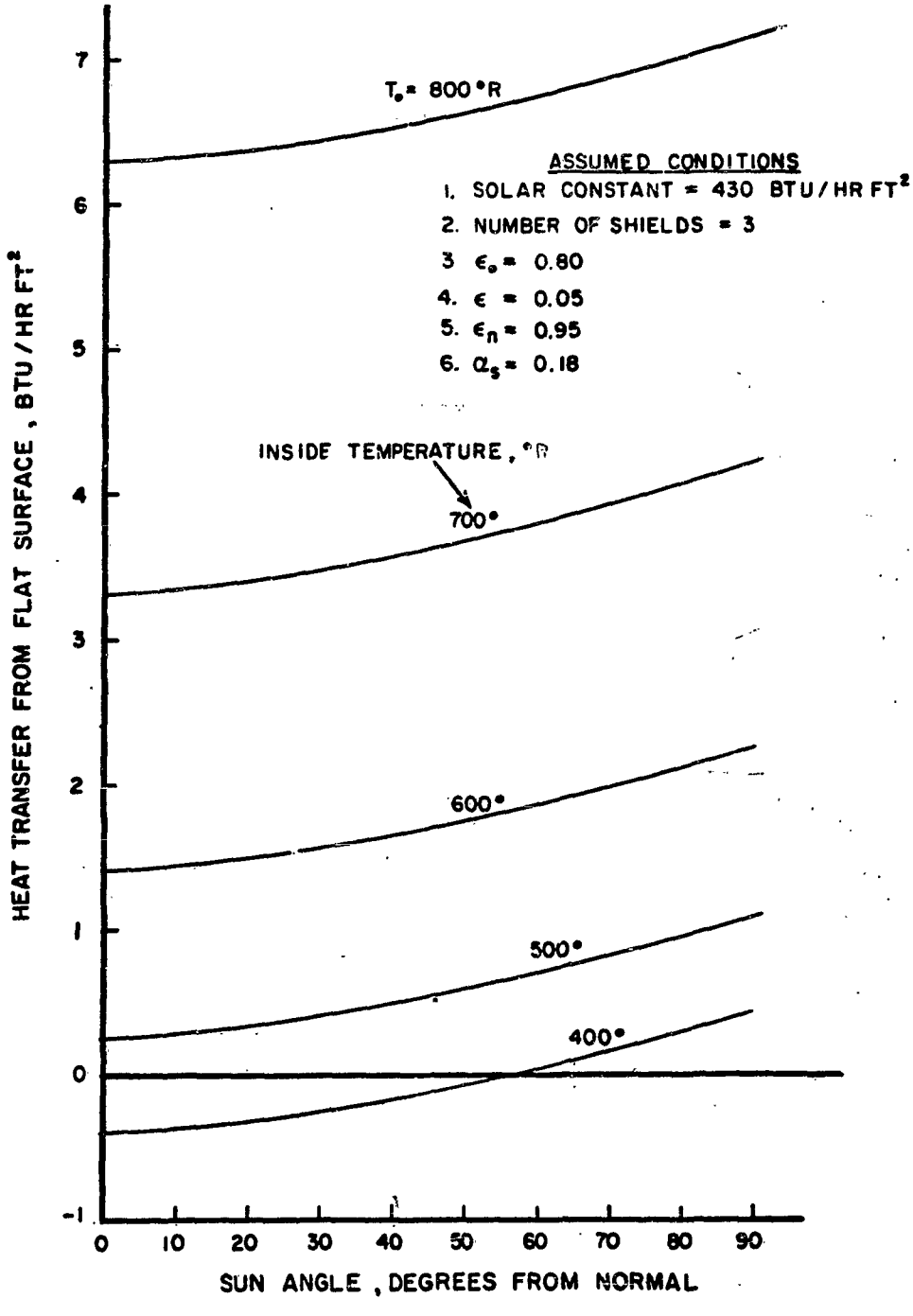

Figure 8. Heat Transfer in Space (Three Shields)

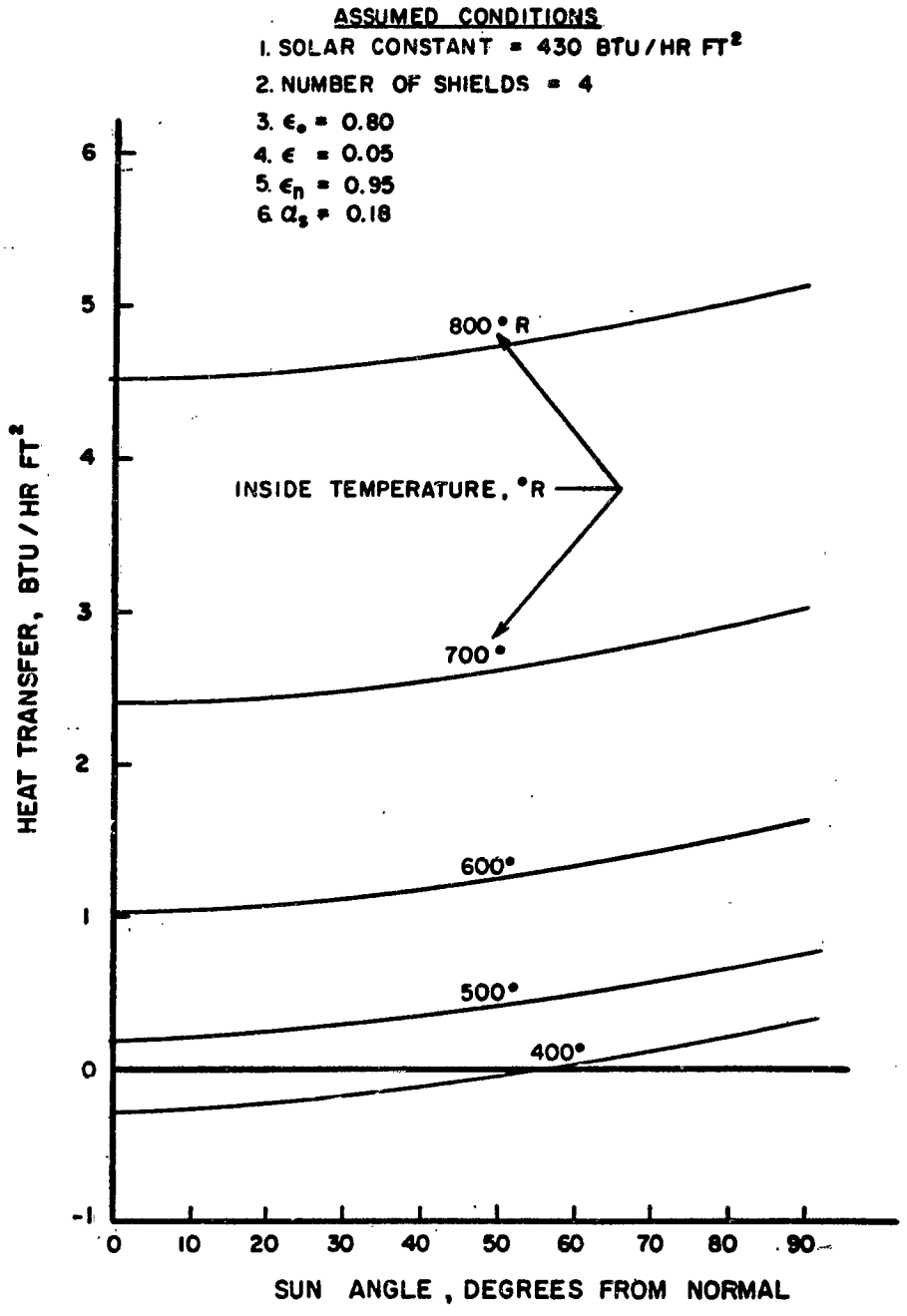

Figure 9. Heat Transfer in Space (Four Shields)

utilizing multilayer foils. Foil type insulations are available for vehicle thermal conductivity of 0.000025 Btu/(hr)(sq ft)(F/ft) can be obtained. Being none load bearing, this type of insulation usually requires additional structure for rigidity.

Proper selection of surface coating for space vehicles is a very important consideration for the efficient design of temperature control system. Vehicle skin temperature has direct influence on the interior temperature and thus effects temperature control requirements. Many surface coatings have been developed which provide wide range of values for α_s/ϵ.

An analysis for multilayer radiation shields has been presented and the plots of equations developed indicate the marked effect of shields to reduce radiation heat transfer. As shown on Figure 7, 3 or 4 shields should be used for maximum reduction in the value of heat transfer coefficient. Increasing the number beyond 4 has only a small effect in reducing the heat transfer coefficient. Shielding material should have low values for emissivity, such as aluminum foil for which $\epsilon = 0.05$.

Section III

SEMI-PASSIVE TEMPERATURE CONTROL METHODS

Semi-passive control methods differ from passive systems in having moving mechanical parts, components or fluids to assist in transporting heat. However, there is no heat pump in the system, so that the heat is dissipated at a lower temperature than that of the source (except for expendable methods). The dynamic parts and components of the system include shutters, moving masks, variable insulation, fluid pumps, and controlled valves.

Semi-passive methods can be classified in a number of different ways. The one used here is by the mode of heat transfer; that is, by systems involving variations in conduction, in convection or in radiation. It should be noted that the use of some methods to be discussed, namely differential metallic expansion or fluid expansion, can also be used to operate switches, relays or other means to reduce or halt the heat-producing activity of some component. This type of operation is not considered here. A simplified method of analyzing semi-passive control requirements with example problems is presented in Section VIII.

NOMENCLATURE

A	Area, sq ft
C_p	Specific heat (Constant Pressure), Btu/(lb)(^oF)
C	Specific heat (Constant Volume), Btu/(lb)(^oF)
D	Hydraulic Diameter, ft
E	Black body emissivity power, Btu/(hr)(sq ft)
F	Wind Force, lb
F	Configuration Factor
f	Friction Factor or Interchange Factor
G	Sum of all incident radiation, Btu/(hr)(sq ft)
H	Film Heat Transfer Parameter
h	Film Heat Transfer Coefficient, Btu/(hr)(sq ft)(^oF)

h_r	Radiation heat transfer coefficient, Btu/(hr)(sq ft)(^oF)
HP	Power, ft-lb/hr
J	Radiosity, Btu/(hr)(sq ft)
K	Thermal Conductivity, Btu/(hr)(sq ft)(^oF/ft)
L, L_u	Latent (or useful latent) heat of vaporization, Btu/lb
m	Fluid Mass, lb
$\dot{m}$	Mass Flow Rate, lb/hr
P	Power Parameter
P	Pressure, psi or psf
Q	Heat Input, Btu/hr
q	Heat Transfer Rate, Btu/hr
R	Thermal Resistance, (^oF)(hr)/Btu
T	Temperature, ^oR
t	Time, hr
u	Velocity, ft/hr
v	Volume, cu ft
W	Weight, lb
α	Absorptivity
ϵ	Dielectric Constant or Emissivity
θ_z	Irradiation Angle with Respect to the Normal to the Surface
μ	Viscosity, lb/(ft)(hr), (or poises)
ρ	Density, lb/cu ft
σ	Steffan-Boltzmann constant 0.1713×10^{-8} Btu/(hr)(sq ft)(^oR)^4

θ_1	Slat Angle Measured from Skin Surface

Subscripts:

b	Boiling
c	Critical
E	Equipment or Compartment
f	Fluid
g	Gas
H	Plumbing Hardware
Hx	Heat Exchanger or Fin
0	Reference Properties
P	Pump
T	Tank
m, n	Index number - 1, 2, 3

VARIABLE CONDUCTION METHODS

Differential Metallic Expansion

The simplest type of thermal switch is one made up of welded parallel strips of two metals having different coefficients of thermal expansion. Changes in temperature cause expansions or contractions of the strips, but the differences in coefficient cause a bending or warping that can be used to make or break a thermal conductive path. This is illustrated in Figure 10. A number of bimetallic elements and applications are illustrated in Truflex catalog TRU-1 (Reference 20).

While simple in operation, this switch can be made quite sensative to temperature changes, the make-or-break being controlled to within a degree or less of temperature. The rate of heat transfer may be less easy to regulate, being subject to the degree of finish and contamination on the surfaces, and the forces between surfaces.

Fluid Expansion

The use of fluid expansion or contraction to regulate heat flow can take many forms. For example, a variation of the differential-strip switch just described would be one in which contact was made or broken between the elements by temperature induced fluid pressure. A thermal switch actuated by fluid volumetric change is illustrated in Figure 11.

The thermal switch of Figure 11 is characterized by on-off operation. Figure 12 illustrates a method of temperature control employing a variable resistance heat path. This device also employs a bellows containing a temperature - sensitive fluid, but this material is not required to conduct heat. Heat transfer takes place across surfaces of soft materials, the contacting area being variable and related to the amount of heat to be conducted. These soft materials may be rubber, cork or any other that deflects easily. Thermal conductivity of such materials is usually low, but may be improved by impregnating with metal fibers, ribbons, springs, chips or other flexible paths, (21).

Variable Gas Conduction

The difference in conductivities of insulating materials before and after degassing has been discussed in Section II and Table 1 of this report. By regulating the amount of gas within the insulation, it is possible to produce conductivities to meet specific requirements.

Table 3 shows the variation of several insulating materials with pressure. The pattern of change is shown graphically in Figure 13. This illustrates the general behavior of reduced-pressured insulation: the very slow increase of conductivity with pressure increase, followed by a rapid rise, and then a region of little change of conductivity.

VARIABLE CONVECTION METHODS

The methods examined here are of two principal classes: those using expendable coolants and those having closed loops in which the coolant is recovered for reuse. The environment assumed for all systems is that of zero-gravity so that fans, blowers, pumps or some other device is necessary to force convection.

Expendable Coolant Convection Method

Expendable coolant methods are those in which a coolant absorbs heat, usually with one or two changes of phase, and is then vented overboard. Such systems are practicable only for missions of short duration because of the relatively large weight and volume requirements of the coolant for the amount of cooling done. Two classes

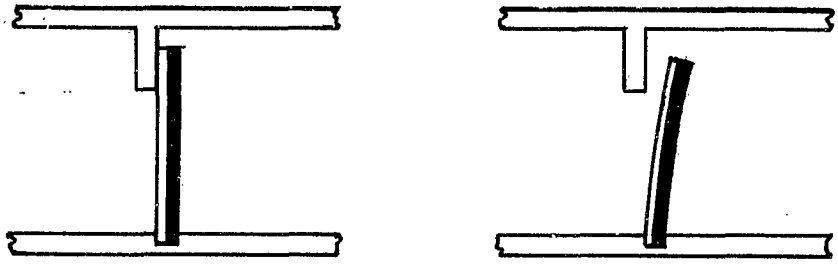

Figure 10. Differential Metallic Expansion Device for Controlling a Thermal Path

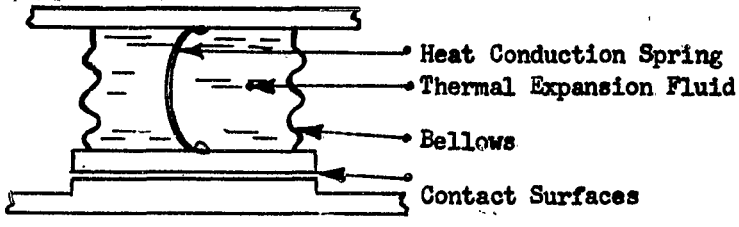

Figure 11. Thermal Switch For On-Off Conductivity Control

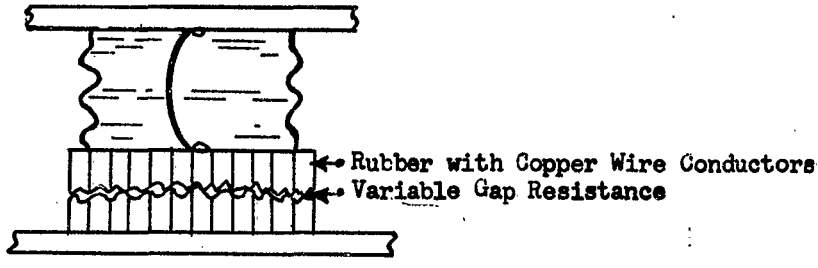

Figure 12. Thermal Switch For Variable Conductivity Control

Table 3 Variation Of Thermal Conductivity At 100°F
Of Various Insulating Materials With Interstitial Pressure (15)

Insulating Material	Thickness, Inches	Density, lb/cu ft	Pressure Microns of Hg	Thermal Conductivity, k (BTu)(m)(hr)(sq ft) (°F)
Air Space Between Copper Surfaces	1		Atmospheric	0.572
			0.10	0.245
			0.07	0.187
			0.0	0.145*
Corkboard	1	6.67	Atmospheric	0.283
			0.08	0.121
			0.06	0.106
Cotton	1	0.78	Atmospheric	0.288
			0.11	0.0805
			0.07	0.072
Fine Glass Wool	1	0.78	Atmospheric	0.302
			0.05	0.0695
			0.04	0.0665
Mineral Wool	1	7.7	Atmospheric	0.258
			9.0	0.059
			3.0	0.0425
			0.02	0.037

* Calculated

(15) General Dynamics - Astronautics Report AZJ 55-005, "Thermal Insulation of Space Vehicles", page 20

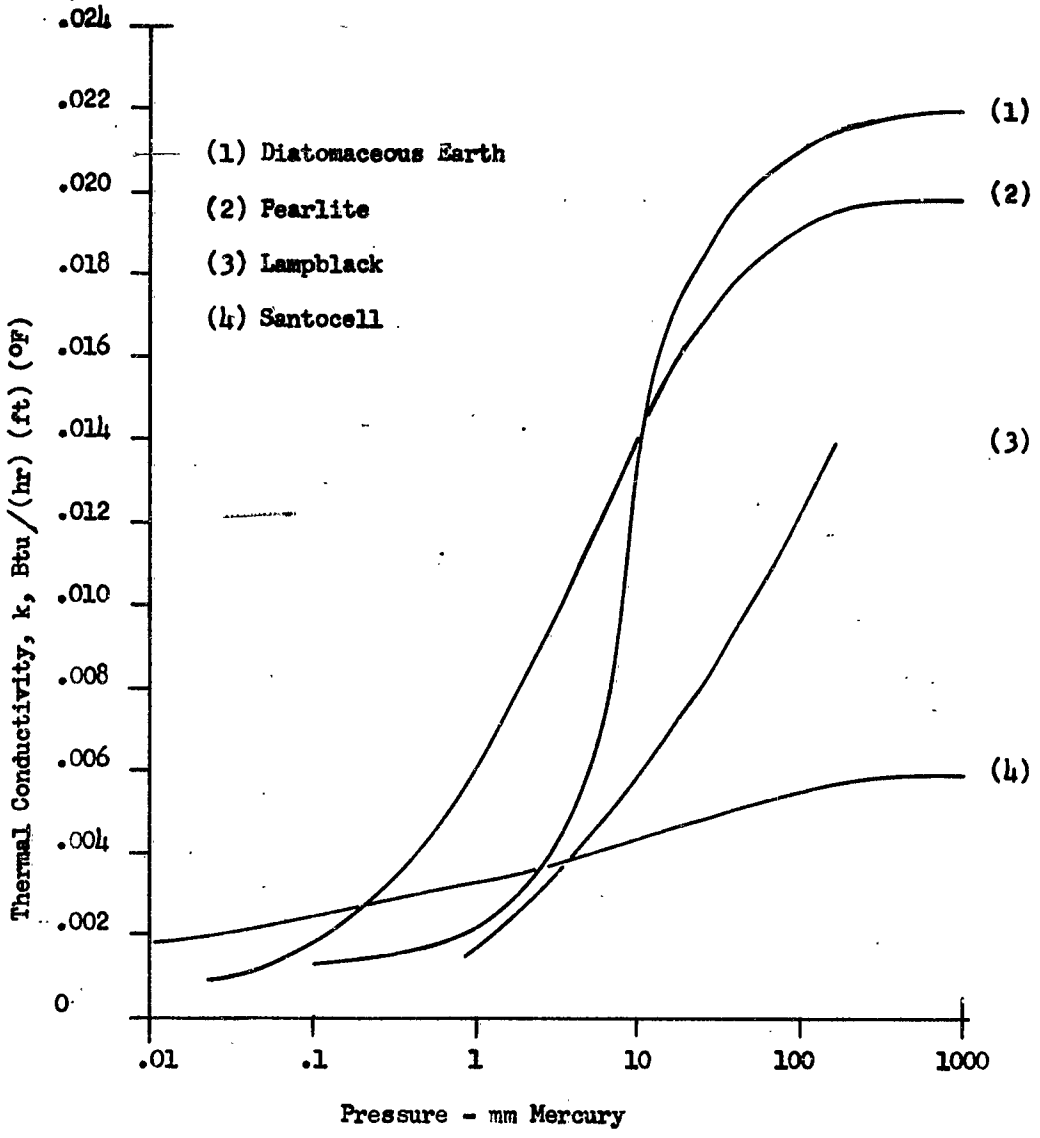

Figure 13. Variation of Thermal Conductivity, K, with Pressure of Powdered Insulations at Temperatures Between 138°R and 540° with Tave = 339°R (15)

are recognized: those having separate coolant storage and heat exchange components; and those in which storage and heat exchange are combined in one component. These are illustrated in Figures 14 and 15 respectively. It can be seen that in the integral system, no pressurant is required.

A comparative analysis of these two types of system (Reference 22) led to the conclusion that the separate storage arrangement had decided advantages of weight and volume, while the reliability of the integrated system was only very slightly higher. The greater weight and volume of the latter resulted from two necessities: (1) that of keeping an adequate portion of the heat transfer surfaces wet (a) with acceleration possible in any direction, and (b) at the end of a mission when the liquid level would be low because of coolant losses, and (2) that of preventing the carryover of liquid coolant through the vent. By providing heat transfer surfaces, storage volume, and quantity of coolant in excess of the minimum requirement, and by packing the coolant space of the exchanger with Fiberglass wicking to disperse the liquid, a sufficient area of the exchanger was kept wet to insure good heat transfer rates. The Fiberglass wicking and the location of the vent entrance at the geographical center of the exchanger will prevent the carryover of unvaporized coolant. Although simple and reliable, these provisions add considerably to the weight and space requirements of the integrated system.

One of the problems in expendable methods is the expulsion of the coolant from the tank. This becomes a major problem in space where gravity cannot be used as an aid to expulsion. Usually some form of bladder with a pressurized gas such as helium or nitrogen is used. The gas is kept in a high pressure tanks and bled into the coolant tanks to force the coolant out. The bladder is used to prevent mixing of the gas and coolant. Control of the coolant tank pressure is maintained by a pressure regulator between the gas pressurant tank and the coolant tank. Another method of expulsion is to spin the tank so that the liquid is forced out by centrifugal force.

Selection of Expendable Fluids

Analyses of expendable fluid cooling methods will almost always show the best fluids to be water and ammonia. While water will hold most of the advantages, ammonia has a lower freezing point and can therefore be used at lower temperature. In addition, ammonia vapor can be used for certain pressurization applications where steam would condense. Table 5 lists a number of materials that could be used as expendable coolants and the important properties that would have to be considered in making a selection. Note that the relative temperature level between the coolant boiling temperature and the equipment operating

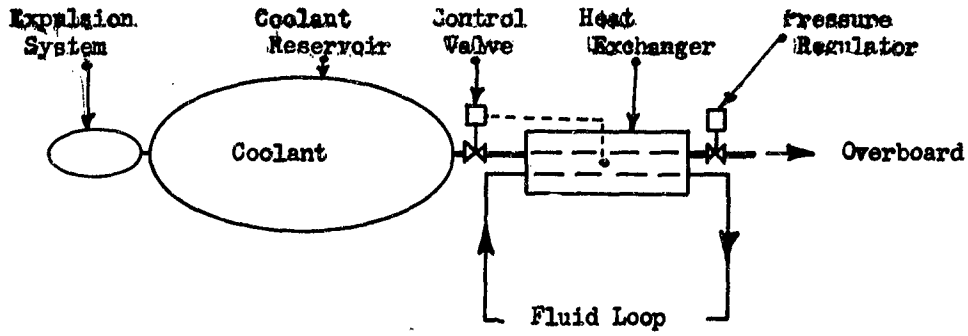

Figure 14. Separate Expendable Coolant Storage

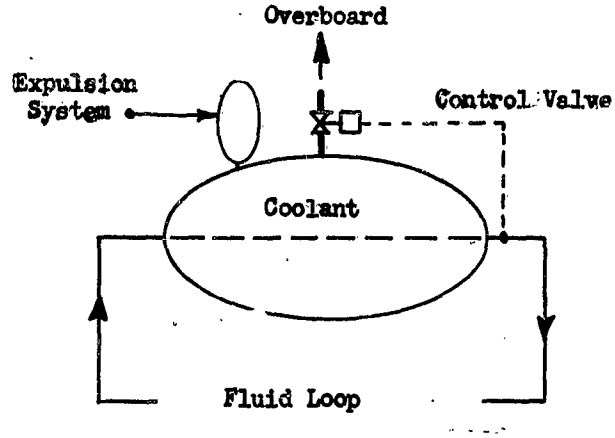

Figure 15. Integral Expendable Coolant Storage

temperature is also important in choice of coolant.

A relationship that may be of assistance in the selection of a suitable expendable liquid is known as Trouton's Rule. This rule states that the molal latent heat divided by the normal absolute temperature of evaporation is equal to constant. However, this ratio actually varies considerably, as seen in Table 4, but averages about 21. The polar or associated liquids, such as water and ethyl alcohol, have higher values than the nonassociated liquids. This results from the high heat of vaporization of these substances, and while it is true that their boiling points are also relatively high, the difference in temperatures is not as great as the difference in latent heat. Attention should therefore be directed toward liquids having high values of the latent heat of vaporization temperature ratio for expendable coolants.

Figures 16 and 17 show the value of latent heat at various boiling temperatures, for a number of possible liquids. It appears from this that water has more ability to absorb heat than any other liquid in the temperature range covered. The vapor pressures of these liquids are shown in Figures 18 and 19.

A more complex method of comparing expendable coolants, than Trouton's rule is the weight comparison technique developed in the following part of this section.

Evaluation of Expendable Coolant Liquids

A number of comparisons, including Trouton's rule of L/T_B have been used to choose a coolant fluid. However, most comparisons do not seem to carry through to an ultimate goal of showing which coolant requires the least total weight for a given heat load q, equipment temperature T_E, and time interval Δt.

Considering Figure 14, a useful coolant comparison can be made for given values of q, T_E, Δt.

The weight of the tank can be considered as a function of coolant pressure, density, the heat load, and latent heat of vaporization. The thickness of the tank varies directly with the pressure so that $W_T \propto P_T$. Since the volume of the tank varies directly with the inverse of density of the stored coolant, a spherical container with volume $\frac{4}{3}\pi R^3$ and surface area $4\pi R^2$ yields $V_T \propto 1/\rho_T$, $A_T \propto W_T$, $A_T \propto (V_T)^{2/3}$ or $W_T \propto 1/\rho_T^{2/3}$. Finally, consideration of the latent heat of vaporization of the fluid determines the amount required which also influences the tank weight as a volume change, $W_T \propto \sqrt{\dot{m}\,\Delta t} = \sqrt{\frac{q\,\Delta T}{L}}$. Combining these

Table 4 Liquid Properties And Trouton's Rule (96)

SUBSTANCE	BOILING TEMPERATURE	CRITICAL TEMPERATURE	$\frac{T_b}{T_c}$	LATENT HEAT OF VAPORIZATION, L_u	$\frac{L_u}{T_b}$
Helium	4.2°K	5.2°K	0.81	22 cal/mol	5.2
Hydrogen	20.3	33.2	0.61	216	10.6
Oxygen	90.2	154.3	0.58	1610	16.9
Ammonia	239.7	405.5	0.59	5560	23.2
Carbon Tetrachloride	350	556	0.63	7140	20.4
Ethanol	351	516	0.68	9450	26.9
Benzene	353	562	0.63	7500	21.2
Water	373	647	0.58	9700	26.0

(96) The Elements of Physical Chemistry, Samuel Glasstone, D. Van Nostrand Co., Inc., N. Y., N. Y. 1946, page 145

Table 5. Properties Of Some Substances Suitable As Expendable Coolants (23)

SUBSTANCE	CHEMICAL FORMULA	LIQUID DENSITY LB/CU FT	* BO PT °F	HEAT OF VAPORIZATION BTU/LB	SPECIFIC HEAT BTU/(LB)(°F) AT				TOTAL HEAT ABSORPTION BTU/LB			TOTAL HEAT ABSORPTION BTU/CU FT		RANK ON THE BASIS OF	
					Bo Pt	200°F	450°F	1500°F	Bo Pt to 200°F	Bo Pt to 450°F	Bo Pt to 1500°F	Bo Pt to 200°F	Bo Pt to 450°F	VOL.	WT.
Hydrogen	H_2	4.37	-423	194	3.42	3.45	3.47	3.62	2335	3200	6966	10,200	13,980	18	1
Water	H_2O	62.4	212	970	0.45	0.45	0.47	0.52	970**	1131	1671	60,500**	70,500	1	2
Helium	He	7.62	-452	11	1.24	1.24	1.24	1.24	821	1132	2437	6,250	8,620	20	3
Ammonia	NH_3	40.6	-28	589	0.48	0.53	0.59	0.81	703	844	1572	28,550	34,250	3	4
Hydrogen Fluoride	HF	62.0	67	650	0.34	0.34	0.35	0.38	695	782	1165	43,000	48,500	2	5
Methane	CH_4	25.9	-258	248	0.50	0.58	0.71	1.09	495	675	1638	12,800	17,500	11	6
Methanol	CH_3OH	48.1	148	472	0.39	0.39	0.46	-	492	600	-	23,650	28,850	4	7
Ethanol	CH_3CH_2OH	48.1	173	367	0.41	0.41	0.45	-	377	486	-	18,100	23,350	7	8
Methanol-Water	-	53.1	148	596	0.41	0.41	0.46	-	369**	733	-	19,600**	38,900	6	9
Ethane	C_2H_6	34.1	-127	210	0.33	0.50	0.63	1.0	345	486	1290	11,750	16,600	14	10
Ethylene	C_2H_4	35.3	-155	208	0.33	0.45	0.55	0.83	345	474	1168	12,200	16,700	12	11
Carbon Dioxide*	CO_2	62.0	-110	252	0.20	0.22	0.24	0.30	317	377	656	19,650	23,400	5	12
Carbon Monoxide	CO	49.3	-313	91	0.25	0.25	0.26	0.29	219	283	577	10,790	13,950	17	13
Nitrogen	N_2	50.2	-320	86	0.25	0.25	0.25	0.28	216	279	569	10,820	14,000	16	14
Air	-	57.4	-318	87	0.24	0.24	0.25	0.28	211	276	556	12,140	15,850	13	15
Oxygen	O_2	71.2	-297	92	0.22	0.22	0.23	0.26	201	260	525	14,330	18,540	9	16
Neon	Ne	75.2	-411	37	0.25	0.25	0.25	0.25	187	249	507	14,080	18,700	10	17
Nitrous Oxide	NO	62.4	-129	161	0.21	0.23	0.25	0.31	164	226	514	10,020	14,100	19	18
Agron	A	88.0	-302	68	0.13	0.13	0.13	0.13	130	161	292	11,450	14,190	15	19
Krypton	Kr	162.3	-241	47	0.13	0.13	0.13	0.13	103	135	268	16,750	21,910	8	20

Note: All values at 14.7 psia except as noted
Boiling Point
* Solid Carbon Dioxide assumed cubed and occupying 65% of total volume. Sublimes without evaporation.
** Boiling assumed at 11.5 psia and 200°F
(23) WADC TR 59-253 "Study of Equipment Cooling Systems", pages 17, 18

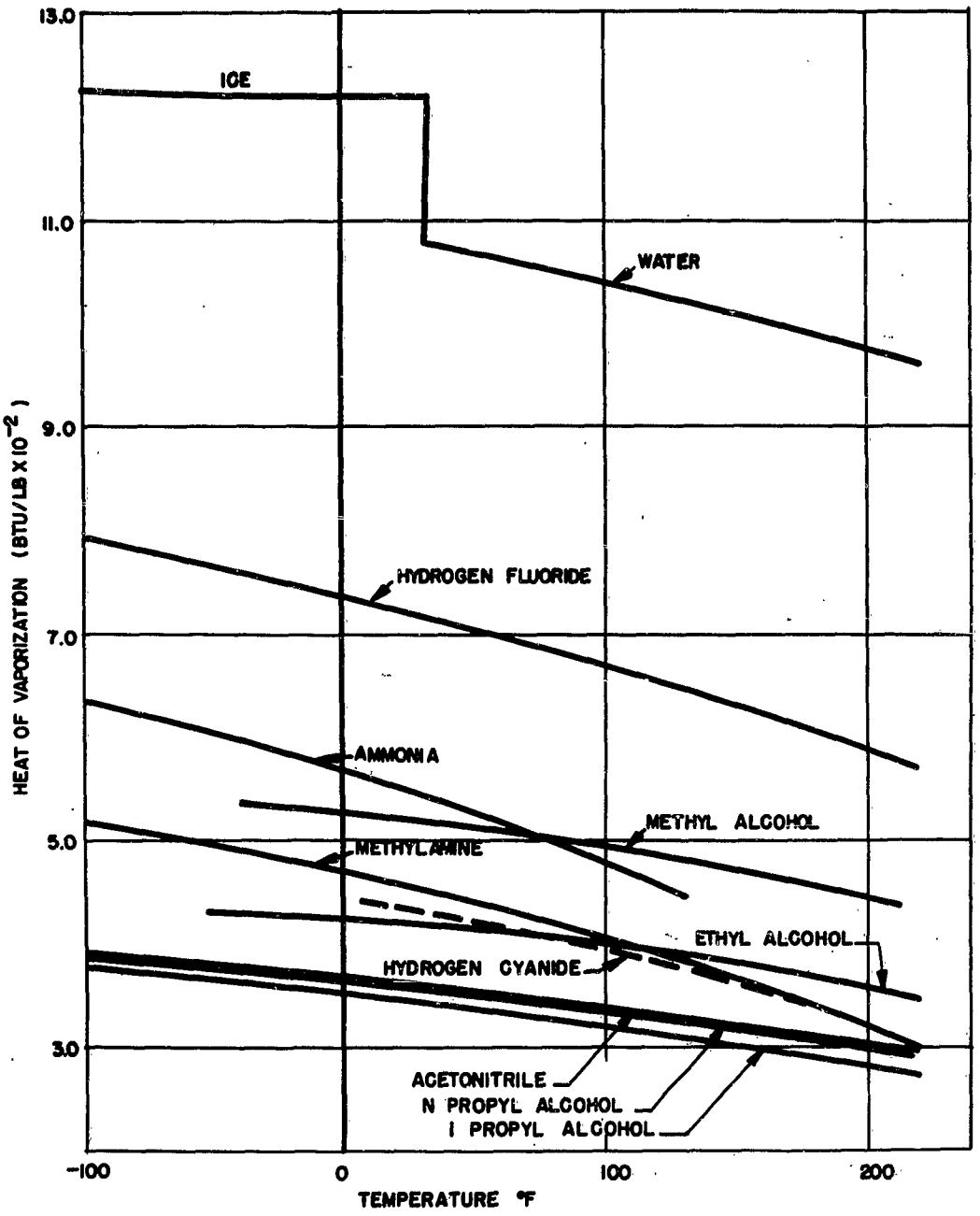

Figure 16 High Latent Heat Liquids

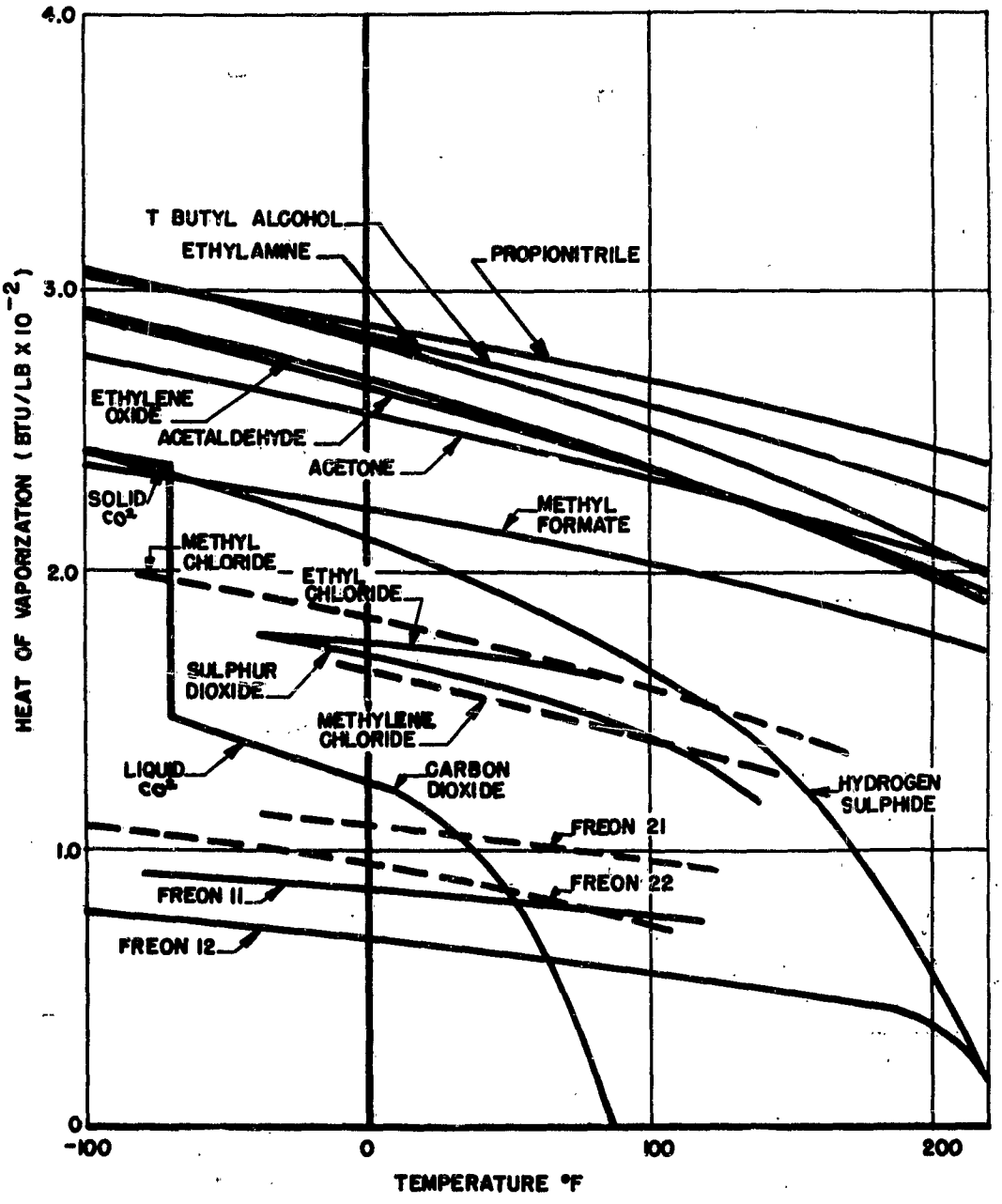

Figure 17 Moderatly High Latent Heat Liquids

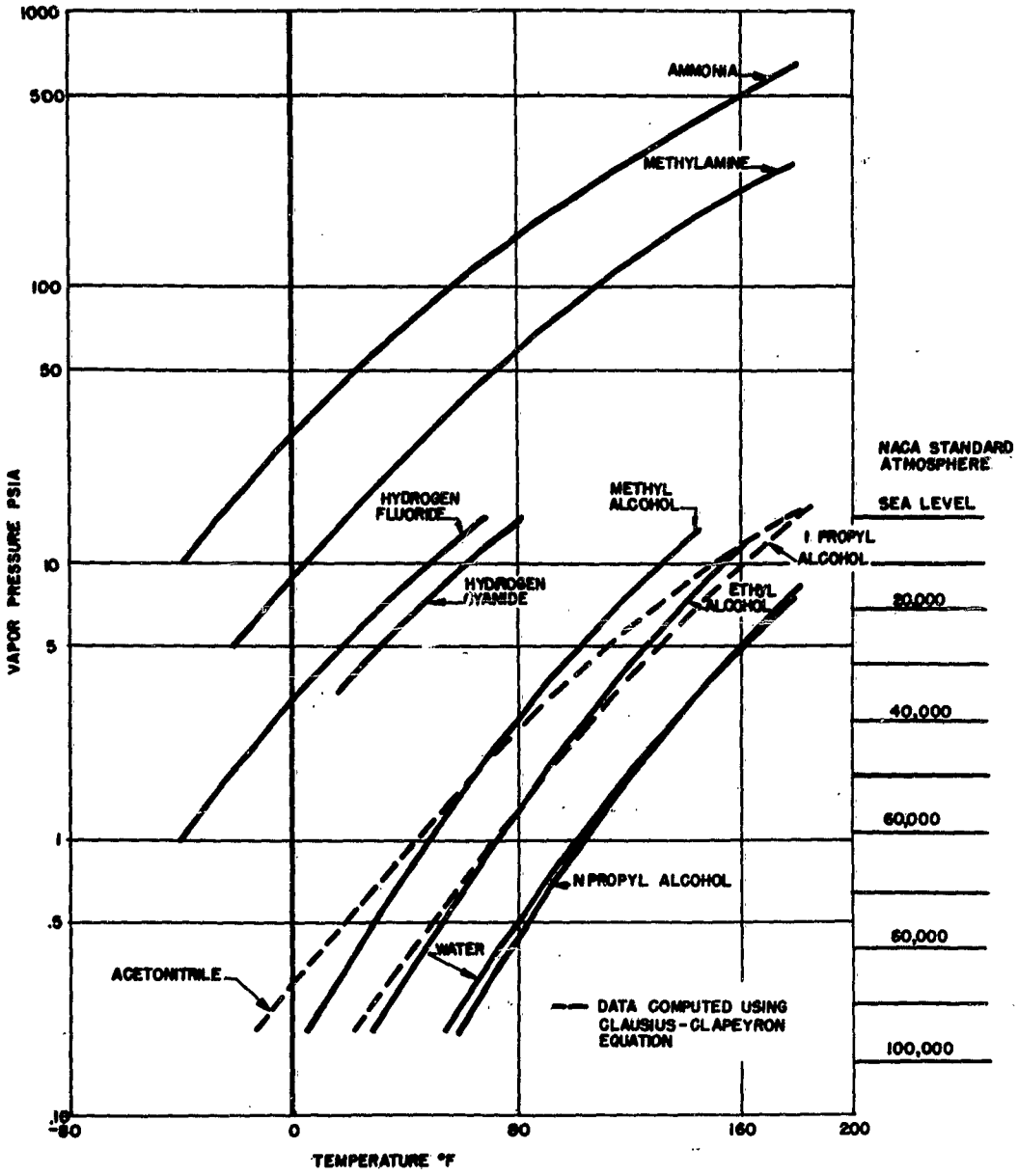

Figure 18 Vapor Pressure of Liquids With High Latent Heats

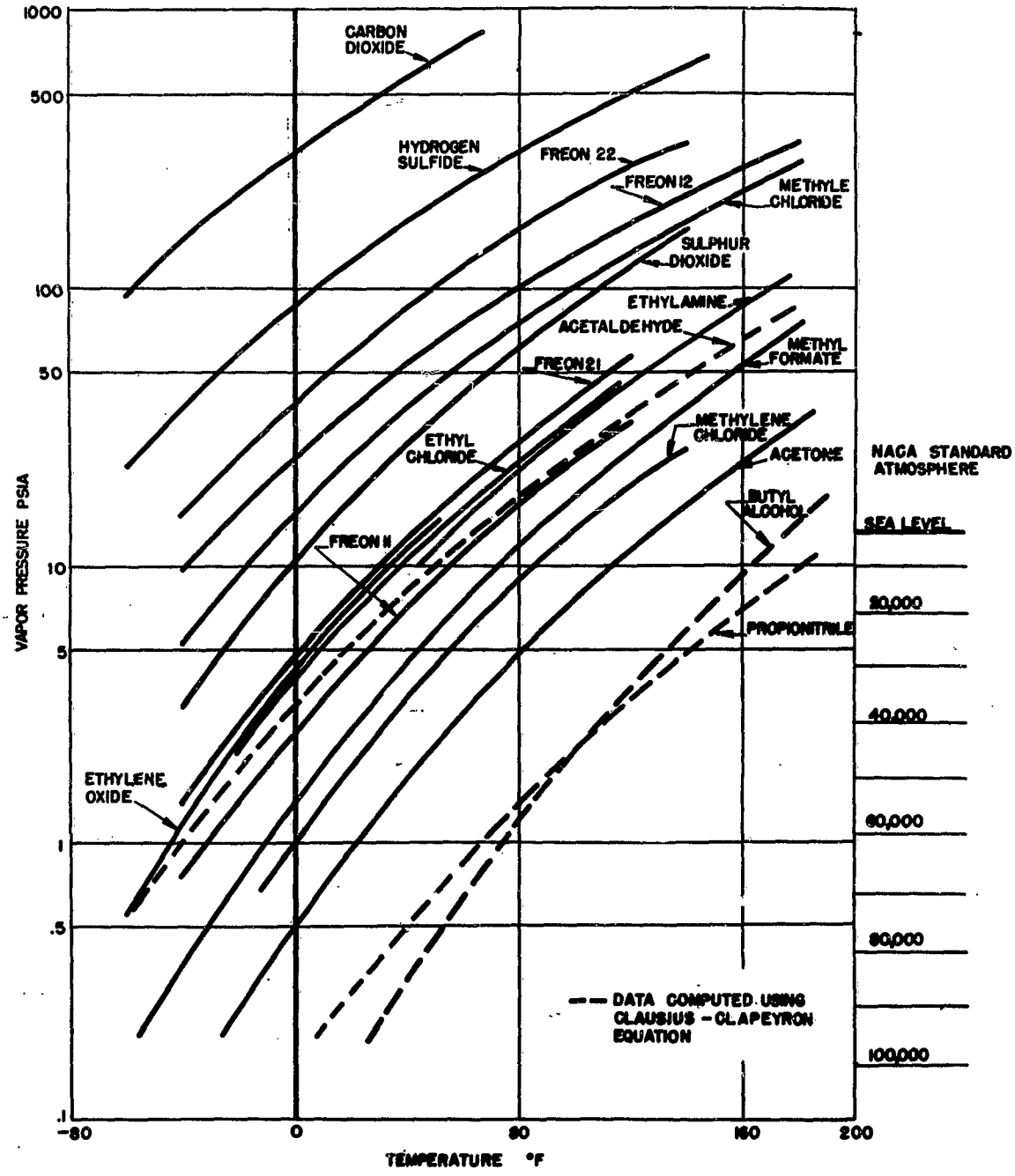

Figure 19 Vapor Pressures of Liquids with Moderatly High Latent Heats

terms, $W_T \propto P_T \sqrt{q\Delta t / L\rho_T}$ or the weight of tank can be expressed as $W_T = K P_T \sqrt{\frac{q\Delta t}{L\rho_T}}$ where K is a constant.

The weight of the heat exchanger can be considered as an inverse of the film coefficient of the coolant and the temperature difference between this compartment and the coolant, $W_{HX} \propto \frac{1}{h(T_E - T_b)}$ or $W_{HX} = \frac{K_2}{h(T_E - T_b)}$ where K_2 is a constant.

The weight of the coolant can be considered as $\dot{m} = \frac{q}{L} = \frac{\Delta m}{\Delta t}$ or $W_f = \Delta m = \frac{q\Delta t}{L}$. Of course, the coolant flow path may include other weight considerations such as tubing, fittings, pressure regulators and valves but the weight of these components is usually not a direct function of the coolant. Therefore this weight can be neglected or considered as a constant $W_H = K_3$.

Combining the weight, described in the previous paragraphs, the total weight becomes

$$W = W_T + W_f + W_{HX} + W_H = K P_T \sqrt{\frac{q\Delta t}{L\rho_T}} + \frac{K_2}{h(T_E - T_b)} + \frac{q\Delta t}{L} + K_3 \qquad (25)$$

Equation 25 can be simplified for comparison purposes by non-dimensionalizing the terms in the equation. Such nondimensionalizing could be based on a known coolant and flow system so that K, K_2, K_3 can be estimated. The nondimensionalized equation would appear as

$$\frac{W}{W_o} = K'\left(\frac{P_T}{P_{T_o}}\right)\left(\frac{L_o \rho_{T_o}}{L \rho_T}\right)^{1/2} + K'_2 \frac{h_o(T_E - T_{b_o})}{h(T_E - T_b)} + K'_4\left(\frac{L_o}{L}\right) + K'_3 . \qquad (26)$$

where O is a known coolant and K', K'2, K'3, and W'0 are known values,

$$K' = \frac{W_{T_o}}{W_o} , \quad K'_2 = \frac{W_{HX_o}}{W_o} , \quad K'_3 = \frac{W_{H_o}}{W_o} , \quad K'_4 = \frac{W_{f_o}}{W_o}$$

This equation can be reduced even farther if the boiling film coefficient of the liquids is held constant by varying the heat exchanger or cold plate flow area. Then $h/h_o = 1$ and Equation 26 becomes

$$\frac{W}{W_o} = K'\left(\frac{P_T}{P_{T_o}}\right)\left(\frac{L_o \rho_{T_o}}{L \rho_T}\right)^{1/2} + K'_2\left(\frac{T_E - T_{b_o}}{T_E - T_b}\right) + K'_3 + K'_4\left(\frac{L_o}{L}\right) \qquad (27)$$

Equation 27 can be used to compare coolants for use in an open-loop coolant method with known compartment heat load (q) and temperature (T_E). Tank weights and volumes can coolant method parameters, estimated by Schroeder, Towe, Lake, and Wunderman of Boeing (Ref. 23) are presented in Figures 21, 22, and 23 for use in comparisons.

Comparison Of Coolants For A Simple Open-Loop Expendable Coolant Method

Consider the sketch Figure 14, if the weight of the coolant lines, fittings and pressure regulators is neglected then $K'_3 = 0$, and the weight of the method is dependent on the heat exchanger, coolant, and tank. For a known ammonia method of this form with

Q = 1000 watts and $T_E = 130^{\circ}F$, the equation constants can be evaluated. Figure 20 shows a possible expendable water method and weight comparison to ammonia.

The properties of the ammonia method are

$c_{p_o} = 1.07$ Btu/lb ($^{\circ}F$

$k_o = 0.29$ Btu/(hr)(ft)($^{\circ}F$)

$\rho_o = 42.6$ lb/cu ft

$\mu_o = 0.0024$ poises

$L_o = 300$ Btu/lb (15% to 85% quality)14.7 psia

$T_{b_o} = -28^{\circ}F$

$P_{T_o} = 130$ psia ($70^{\circ}F$ saturated NH_3 liquid)

and the weights are

$W_{HX_o} = 1.5$ lb

$W_{f_o} = 10.4$ lb

$W_{T_o} = 14.6$ lb

$W_o = 26.5$ lb

Or evaluation K' constants:

$$K' = \frac{W_{To}}{W_o} = \frac{14.6}{26.5} = 0.551$$

$$K_2' = \frac{W_{HX_o}}{W_o} = \frac{1.5}{26.5} = 0.057$$

$$K_4' = \frac{W_{f_o}}{W_o} = \frac{10.4}{26.5} = 0.392$$

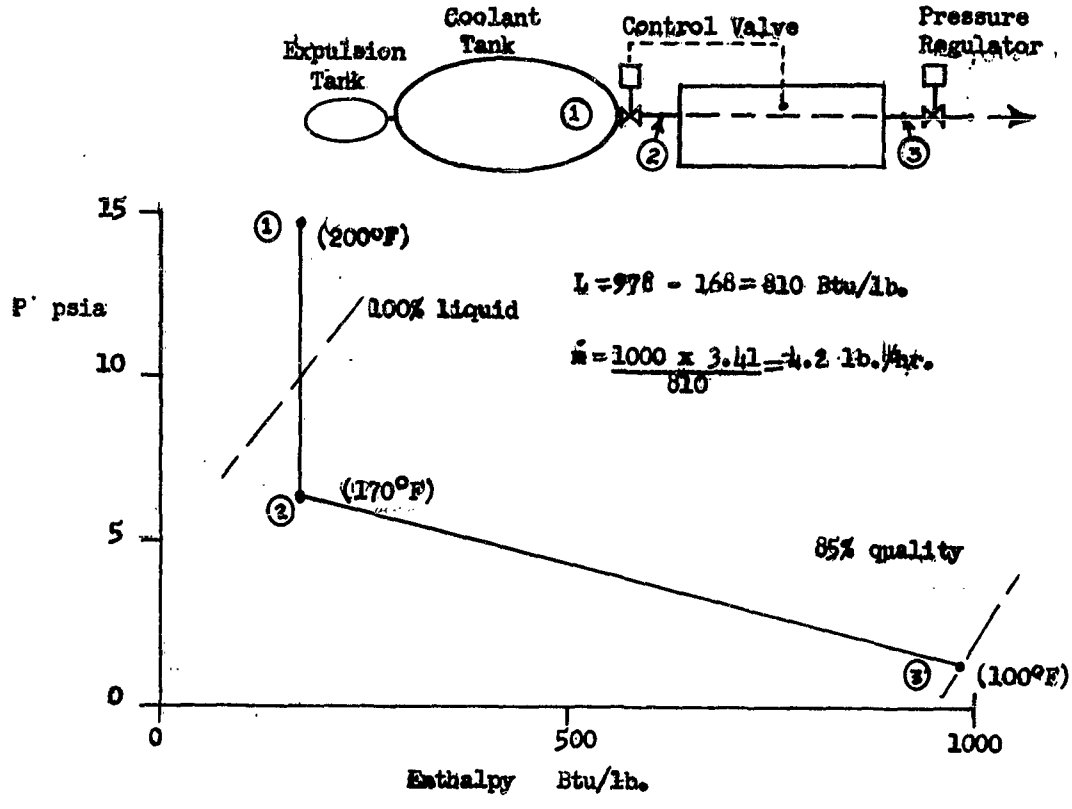

Comparison to Ammonia

	WEIGHT (Lb)		VOLUME (in^3)	
	H_2O	NH_3	H_2O	NH_3
Tank	2	14.6	55.5	278
Heat Exchanger	5.2	1.0		
Fluid	4.2	10.4		
Total*	11.4	26	55.5	278

*Does not include tubing, valves, cold plates

Figure 20. Expendable Water Method

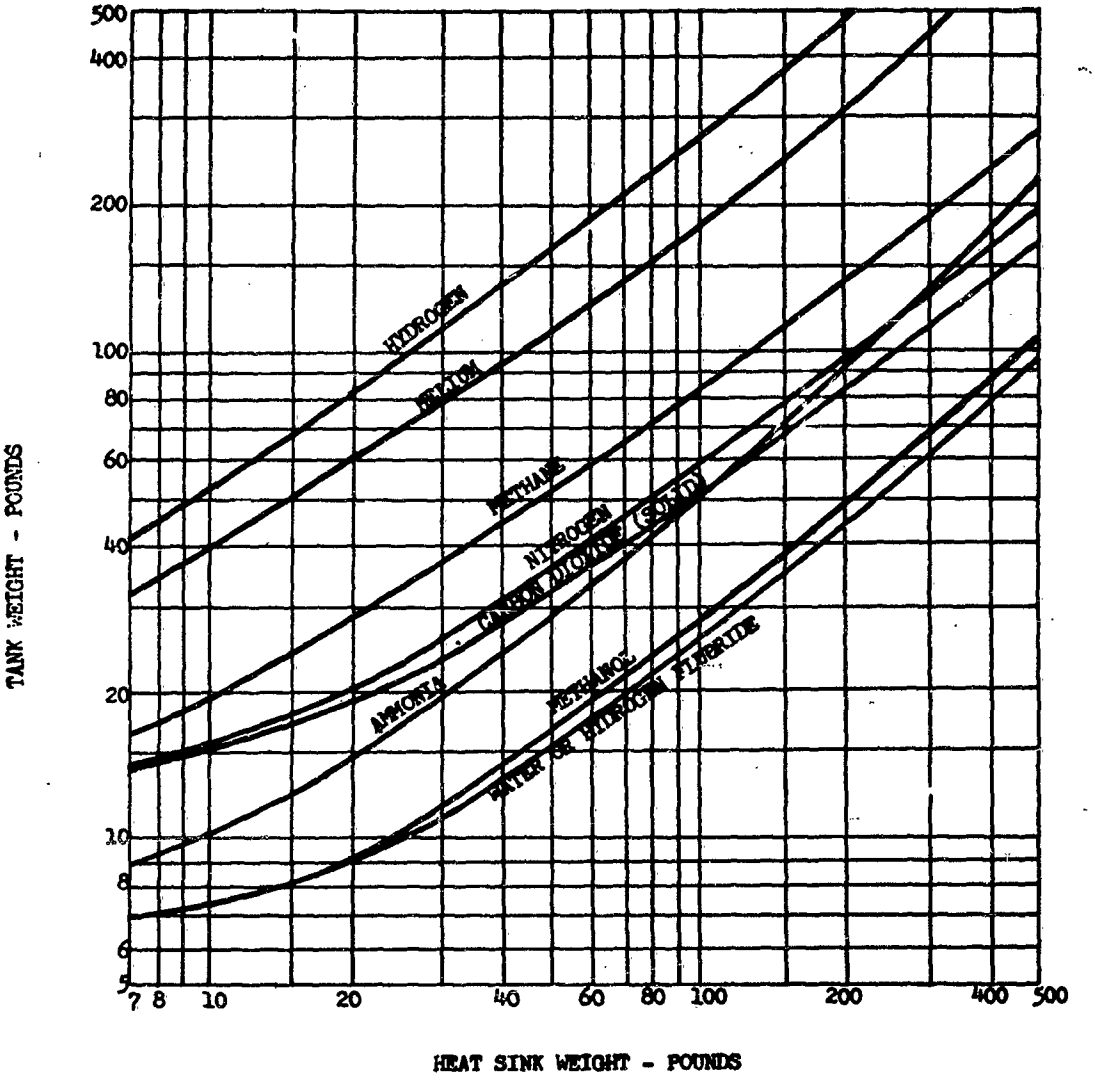

Includes tank, insulation where applicable, supports and fill, vent, and safety valving.

Figure 21. Liquid Heat Sink Storage Weight
(Reference 23)

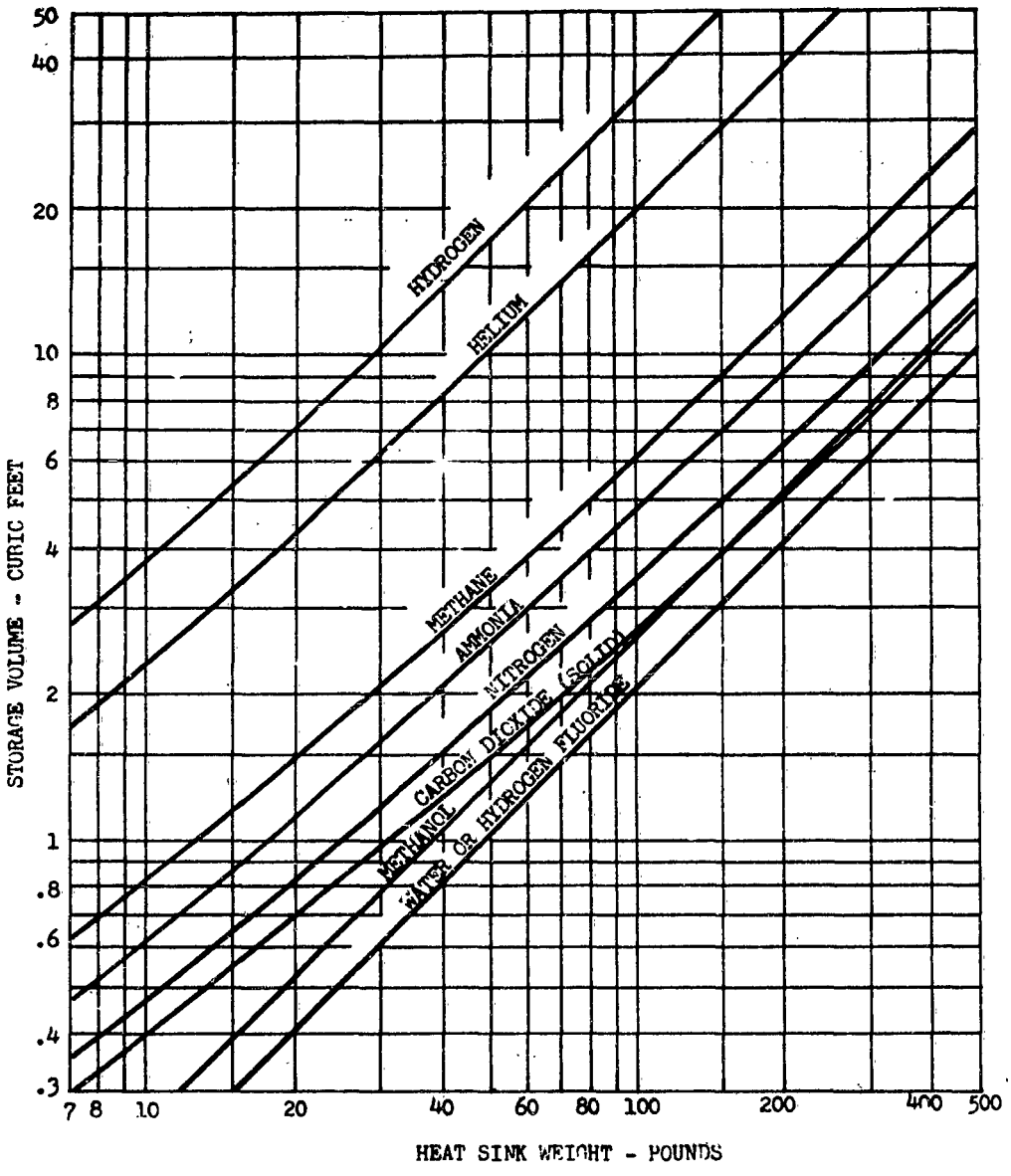

Assumes 80% volume utilization factor.

Figure 22. Liquid Heat Sink Storage Volume
(Reference 23)

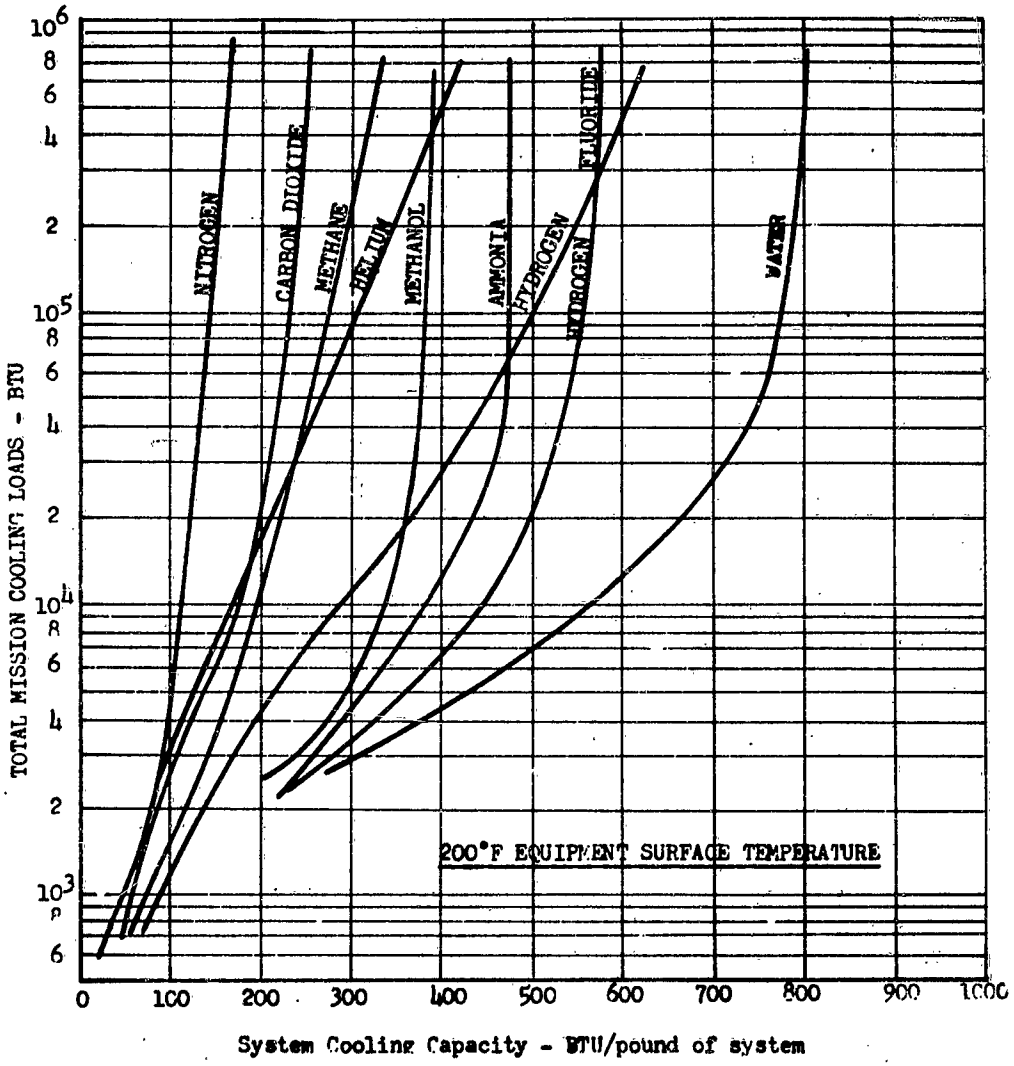

NOTES: 1. System weight includes coolant, tank, and a volume allowance of 1.5 pounds of structure per cubic foot of storage.
2. Coolant heated from stored liquid to 200°F vapor.
3. Tank weight and volume taken from curves 21 and 22 All assumptions from these curves apply.
4. No ground standby time assumed.

Figure 23. Capacity of Expendable Heat Sinks (200°F. Equipment Surface) (Reference 23)

Use of these values in Equation 27 gives the following ratios of W/W_O for coolant fluids.

Table 6. Weight Comparison Of Expendable Coolants
(Q = 1000 watts, T_E = 130°F, Δt = 1 hour)

Coolant	Tank Pressure P_T*	Vapor Pressure P_L	Boiling Temp. T_L	Useable Latent Heat L**	Weight Ratio $\frac{W}{W_O}$	Volume Ratio $\frac{V}{V_O}=\frac{L_2\rho_2}{L\rho}$	
	psia	psia	°F	Btu/lb			
Water	14.7	1.0	100	810	0.5	0.3	
Ammonia	130	14.7	-28	330	1.0	1.0	
Ethanol	14.7		100	200	1.0+	1.5	
Freon 21	80	14.7	48	80	2.2	2.1	
Nitrogen	14.7	14.7	-322	70	2.0	4.0	Stored at -322°F
CO_2 Solid	14.7	14.7	-110	246	0.9	0.6	Stored at -110°F

* Tank Pressure at 70°F except Nitrogen and CO_2 (Solid).

** Useful latent heat of vaporization to 85% quality for high film coefficients.

Except Nitrogen and CO_2 (Solid).

Closed Cycle Convection Methods

There are a number of different closed cycle methods, all having in common the conservation of the coolant for repeated use in heat transportation. In the open cycle or expendable coolant systems, the disposal of the coolant served the purpose of removing the unwanted heat from the vehicle. Since radiation is the only means by which heat may be rejected in space without this loss of the coolant, all closed systems have a radiator as a necessary component. Aside from these two common characteristics, closed cycle systems may differ from each other quite widely. A comparison of expendable and recycle methods is included in Section VI. A number of methods of the recycle type are described in the following paragraphs.

Forced Convection

The basic convection loop accomplishes transfer of heat from a heat sink to a heat-transport fluid, transporting the fluid to a radiator, and a return of the cooled fluid to a reservoir or to the heat exchanger. Such a method is illustrated in Figure 24. The degree of complexity can be changed by the addition or removal of controls for regulating the temperature of the heat sink. The transport fluid may be water, air, ammonia, or any one of other liquids and gases.

The weight, volume and power requirements of a forced convection loop depend upon the heat load, temperature range, fluid, and ducting. One analysis has been made for a system employing ethylene glycol, a pump-motor efficiency of 40 percent, a fluid pressure drop of 100 psi and a temperature change of 20°F of the fluid in passing through the radiator. The power requirement was found to be 0.025 kw/kw of heat rejected, and the weight to be from 3 to 10 pounds/kw. (Reference 3, Page 22).

Comparison Of Liquid Coolants For Closed Loop Semi-Passive Control Methods

The semi-passive closed loop liquid cooling method consists of a flow-control valve, a space radiator exchanger, a pump and a compartment exchanger (See Figure 24).

Ideally, the comparison of various liquids for this method would include detailed design of the complete loop for each coolant. However, such a comparison is time consuming and costly. Therefore, the use of parameters for comparison purposes is advisable. Several parameters which appear to affect the weight and effectiveness of the loop are the pump power and the forced convection film coefficient parameters.

The pump power parameter P has been derived in Reference 25.

This parameter is

$$P = \frac{\mu}{(\rho c_p)^2} \qquad \text{for laminar flow} \qquad (28)$$

and

$$P = \frac{\mu^{0.2}}{\rho^2 c_p^{2.8}} \qquad \text{for turbulent flow.} \qquad (29)$$

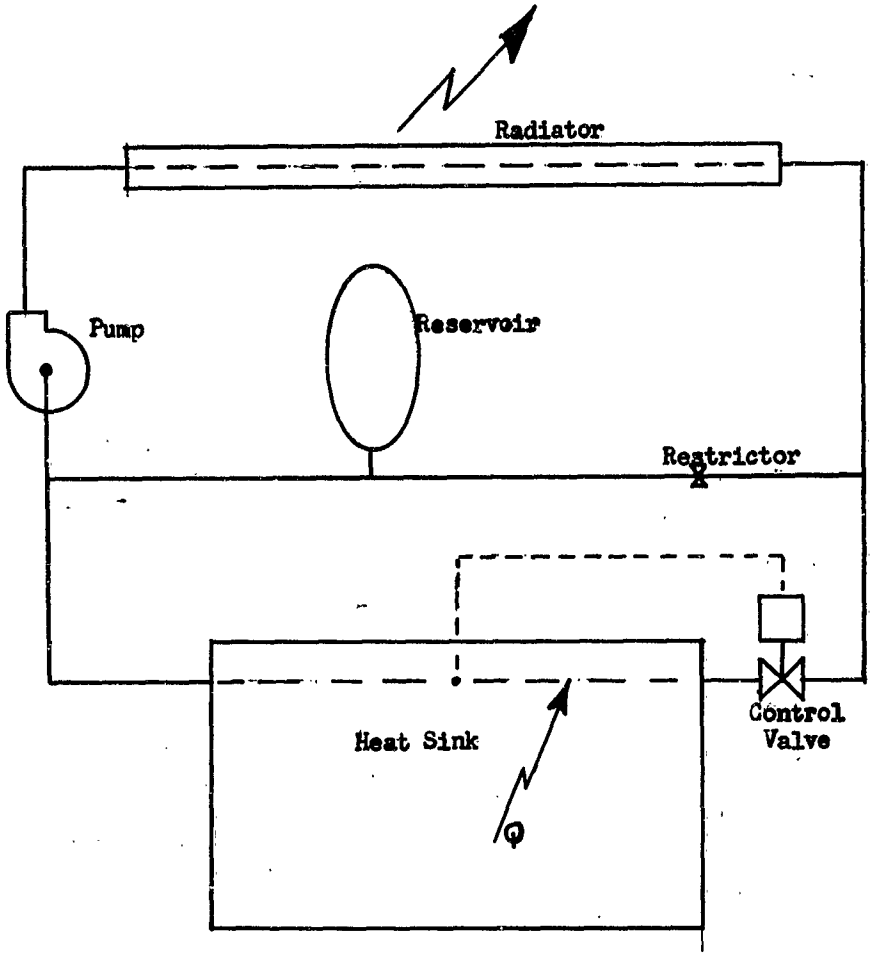

Figure 24. Schematic Diagram of Forced Convection Loop Temperature Control Method

Table 7. Comparison of Liquids for Semi-Passive Closed-Loop Cooling

Fluid and Temperatures	Properties				Pump Power Ratio to Turbulent Water		Film Coefficient Parameter	Temperatures °F			Dielectric Constant	Corrosivness	Toxicity
	Conduc - tivity $\frac{Btu}{(ft)^{o}F(hr)}$ k	Viscosity $\frac{lb}{(ft)hr}$ μ	Density $\frac{lb}{(ft)^3}$ ρ	Specific Heat $\frac{Btu}{(lb)(^{o}F)}$ c_p	Laminar $\frac{\mu}{(\rho c_p)^2} \Big/ \frac{\mu_o}{(\rho_o c_{p_o})^2}$	Turbulent $\frac{\mu^{0.2}}{\rho^{0.2} c_p^{0.8}} \Big/ \frac{\mu_o^{0.2}}{\rho_o^{0.2} c_{p_o}^{0.8}}$	$0.023 k \left(\frac{\rho}{\mu}\right)^{0.8} \left(\frac{c_p \mu}{k}\right)^{0.4}$	Freezing	Boiling	Flash			
Water[o]													
50°F	0.33	3.17	62.4	1.0	1.1	1.3	0.20	+32	212	Non		Inert	Non
80	0.367	2.0	62.4	1.0	0.7	1.0	0.275						
200	0.406	0.738	60.1	1.01	0.3	0.9	0.41						
Anhydrous Ammonia													
0°F	0.290	0.52	41.2	1.08	0.4	2.4	0.29	-108	-28	Ignition 1204		Corrosive to copper and aluminum alloys	Toxic
80		0.232	37.0	1.13	0.2	1.3							
28.3% Ammonia Water													
40°F	0.26	3.95	57.0	0.95	1.9	1.6	0.15	-85	80	Ignition 1204 (NH_3)		Corrosive to copper and aluminum alloys	Toxic
80		2.18	56.2	1.0	0.8	1.2							
57% Methanol-Water								-44	180	Closed Cup 54 (Methanol)			Toxic
40°F	0.234	5.82	58.7	0.83	4.8	4.5	0.12						
80	0.234	3.35	56.0	0.82	1.9	2.1	0.14						
200	0.234	0.80	52.2	0.87	0.5	1.8	0.17						
60% Ethylene Glycol - Water								-51	220	Closed cup 232 (ethylene glycol)			Non
0°F	0.226	82.2	68.8	0.643	82.3	6.0	0.04						
40		20.3	67.2	0.688	18.4	3.9	0.075						
80	0.224	14.8	67.2	0.75	5.0	2.5	0.082						
200	0.208	2.2	67.2	0.808	1.1	1.7	0.312						

Table 7. Comparison of Liquids for Semi-Passive Closed-Loop Cooling (Continued)

Fluid and Temperatures	Properties				Pump Power Ratio to Turbulent Water		Film Coefficient Parameter	Temperatures °F			Dielectric Constant	Corrosivness	Toxicity
	Conduc - tivity $\frac{Btu}{(ft)(^oF)(hr)}$ k	Viscosity $\frac{lb}{(ft)(hr)}$ μ	Density $\frac{lb}{(ft)^3}$ ρ	Specific Heat $\frac{Btu}{(lb)(^oF)}$ c_p	Laminar $\frac{\mu}{(\rho c_p)^{2/3}} \Big/ \frac{\mu_o}{(\rho_o c_{p_o})^{2/3}}$	Turbulent $\frac{\mu^{0.2}}{\rho^{0.8} c_p^{0.6}} \Big/ \frac{\mu_o^{0.2}}{\rho_o^{0.8} c_{p_o}^{0.6}}$	$0.023 k \left(\frac{\rho}{\mu}\right)^{0.8} \left(\frac{c_p \mu}{k}\right)^{0.4}$	Freezing	Boiling	Flash			
(CCl_3F) Freon 11								-168	+75	Non	2.28	Inert	Toxic above 750°F
0°F	0.072	1.64	98.3	0.207	5.4	32.6	0.082						
86	0.0609	0.94	91.4	0.209	2.3	32.2	0.087						
200	0.046	0.64	80.7	0.225	2.7	31.0	0.080						
FC-75 + (Minnesota Mining & Mfg)								-100	224	Non	1.86	Inert	Toxic above 750°F
0°F	0.092	9.05	116.5	0.221	26.5	25.7	0.06						
80	0.0813	3.99	109.0	0.245	7.6	19.2	0.071						
200	0.0705	1.1	95.5	0.278	2.1	13.4	0.104						
Coolanol 45 (Monsanto)								-100	630	Non	2.65 1kc (77°F)	Inert	Toxic above 759°F
0°F	0.087	260	57.1	0.40		40.8	0.0044						
80	0.082	38.5	55.8	0.45	78.5	21.0	0.0216						
200		8.0	52.2	0.512	15.2	12.2							
Dowtherm A (Dipheryl - Dipheyl oxide)										Non			
80° F		6.15	62.4	0.40	15.0	16.0							
200		2.92	62.4			6.1							
400		1.01	56.8										
Air* 70°F	0.0148	0.044	0.070	0.24	2.97×10^5	4.25×10^7	7.31×15^4			Non		Inert	Non

* Incompressible, for comparison purposes only.

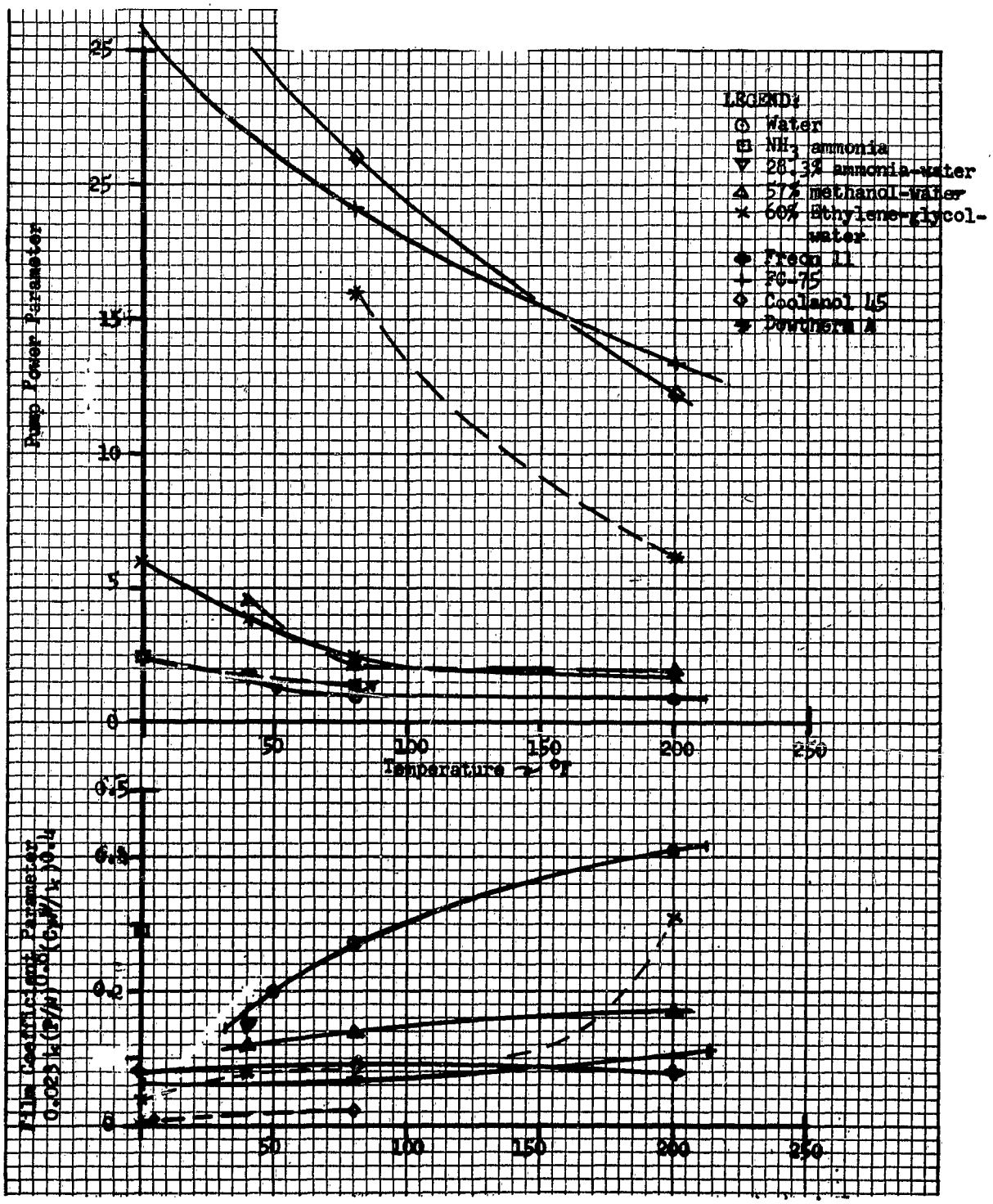

Figure 25. Turbulent Flow Liquid Coolant Parameters

For comparison purposes μ, ρ, and C_p are used as ratios relative to turbulent water at 80°F.

The film coefficient parameter H is based on McAdams' equation (Reference 29) with D = 1 ft and V = 1 ft/hr where fluid properties are evaluated at the average fluid bulk temperature. Note that $c_p\mu/k$ = Prandtl number is raised to the 0.4 power for use with the bulk fluid temperature properties. Whereas, the more accurate Colburn "j factor" has ($c_p\mu/k$) raised to the 1/3 power. However, the Colburn equation as shown in Giedt (Reference 26, p. 169) is based on fluid properties at the average film temperature. Since for evaluation purposes it is felt that the bulk temperature of a liquid is more likely to be known than the average film temperature, the bulk temperature equation has been used. In the gas comparison, the difference is less noticeable so that the more accurate Colburn equation is used.

$$H = 0.023\,k\left(\frac{\rho}{\mu}\right)^{0.8}\left(\frac{c_p\mu}{k}\right)^{0.4} \qquad (30)$$

These two parameters, as well as other comparison information such as freezing and boiling temperature, toxicity, flambility, corrosiveness, and dielectric strength are presented for some liquids in Table 7. A curve, Figure 25, shows the comparison of H and P for various coolants at different temperatures.

Comparison Of Gaseous Coolants For Closed Loop Semi-Passive Control Methods

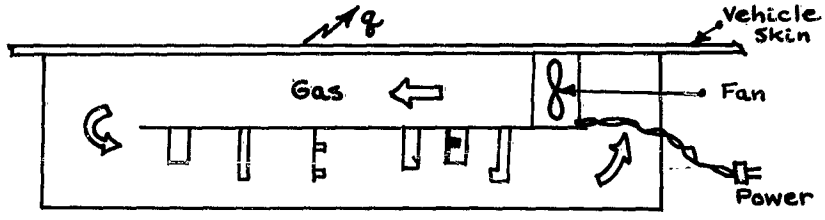

Figure 26. Typical Closed Cycle Gaseous Coolant Loop

From this sketch, the fan power, CFM, pressure drop, heat transfer film coefficient and dielectric constant can be seen to be parameters for comparison of gaseous coolants. In addition, if a sensitive component such as a stabilized inertial platform is part of the equipment, the wind force becomes a parameter.

For purposes of comparison of different gases the following assumptions were made.

1) The heat load to be removed by the gas is the same for all gases.

2) The maximum temperature rise in the gas is set. (ΔT_{gas} = constant)

3) The flow of the gases is turbulent.

4) All parameters will be computed as ratios relative to air at 70°F.

The following parameters were derived using these assumptions. (g = gas, a = air)

Weight Flow Rate

$$\frac{\dot{m}_g}{\dot{m}_a} = \frac{c_{p_a}}{c_{p_g}} \tag{31}$$

CFM

$$\frac{U_g}{U_a} = \frac{\dot{m}_a \rho_a}{\dot{m}_g \rho_g} \tag{32}$$

Film Coefficient

For turbulent flow in ducts or tubes:

$$h = 0.023 \frac{k}{D} \left(\frac{DU\rho}{\mu}\right)^{0.8} \left(\frac{c_p \mu}{k}\right)^{0.33}$$ (Giedt, Ref. 21, p.169)

(where properties are evaluated at the arithmetic mean boundary film temperature)

$$\frac{h_g}{h_a} = \left(\frac{k_g}{k_a}\right)\left(\frac{U_g \rho_g \mu_a}{U_a \rho_a \mu_g}\right)^{0.8}\left(\frac{c_{p_g} \mu_g k_a}{c_{p_a} \mu_a k_g}\right)^{0.33} = \left(\frac{k_g}{k_a}\right)^{0.67}\left(\frac{\mu_a}{\mu_g}\right)^{0.47}\left(\frac{c_{p_a}}{c_{p_g}}\right)^{0.47} \tag{33}$$

Pressure Drop $\Delta p = f\frac{L u^2 \rho}{2gD}$ where $f = 0.184\left(\frac{\mu}{uPD}\right)^{0.2}$ For $\frac{UPD}{\nu} > 2100$

$$\text{or} \quad \frac{\Delta P_g}{\Delta P_a} = \left(\frac{u_g}{u_a}\right)^{1.8}\left(\frac{\rho_g}{\rho_a}\right)^{0.8}\left(\frac{\mu_g}{\mu_a}\right)^{0.2} = \left(\frac{c_{p_a}}{c_{p_g}}\right)^{1.8}\left(\frac{\mu_g}{\mu_a}\right)^{0.2}\left(\frac{\rho_a}{\rho_g}\right) \tag{34}$$

Power Requirement $HP \propto \frac{\Delta P \cdot W}{\rho}$

$$\frac{HP_g}{HP_a} = \left(\frac{\Delta P_g}{\Delta P_a}\right)\left(\frac{W_g}{W_a}\right)\left(\frac{\rho_a}{\rho_g}\right) = \left(\frac{\mu_g}{\mu_a}\right)^{0.2}\left(\frac{\rho_a}{\rho_g}\right)^{2}\left(\frac{c_{p_a}}{c_{p_g}}\right)^{2.8} \tag{35}$$

Wind Force on Platform $F \propto \rho S' \frac{u^2}{2g}$

$$\frac{F_g}{F_a} = \left(\frac{\rho_g}{\rho_a}\right)\left(\frac{u_g}{u_a}\right)^2 = \left(\frac{\rho_g}{\rho_a}\right)\left(\frac{\rho_a}{\rho_g}\right)^2\left(\frac{c_{p_a}}{c_{p_g}}\right) = \frac{\rho_a c_{p_a}}{\rho_g c_{p_g}} \tag{36}$$

Dielectric Ratio

$$\frac{\epsilon_g}{\epsilon_a}$$

These ratios have been used for comparison of various gases and results are presented in Table 8.

Reference 27 shows a comparison of gases for use as artificial atmospheres in space vehicles. This report compares blower power requirements and heat transfer coefficients for these atmospheres. These ratios along with ratios for constant heat load are shown in Table 9.

The forced convection loop usually represents a relatively simple method with good reliability, easy control, good stability and relatively low power requirements. Size and weight may impose excessive penalties while leakage is probably the greatest danger of failure.

Most of the lightweight fans (and pumps) available for space or airborne use have small bearings and high RPM to keep weight and volume low. As a result, the life expectancy of these fans is seldom in excess of 500 hours. More reliable fans for long life such as one year continuous duty must be developed. Otherwise, the alternative is to add more fans for redundancy.

Table 8. Comparison Of Gases For Semi-Passive Closed-Loop Cooling

Gas and Molecular Weight	Thermal Properties (14.7 psia, $70°F$)				(Constant Heat Load and Gas Temperature) Parameters						Dielectric Constant	Flamability	Toxicity
	Density ρ $\frac{lb.}{ft.^3}$	Conductivity k $\frac{Btu}{(ft)(°F)(hr)}$	Specific Heat c_p $\frac{Btu}{(lb)(°F)}$	Viscosity μ $\frac{lb.}{(ft)(hr)}$	Weight Flow Rate	CFM	Heat Transfer Film Coefficient	Pressure Drop	Fan Power	Wind Force			
Air (28.96)	0.070	0.0148	0.24	0.044	1.0	.10	1.0	1.0	1.0	1.0	1.0	Non	Non
Helium (4.00)	0.0096	0.092	1.24	0.046	0.192	1.40	1.52	0.376	0.93	0.268	0.13	Non	Non
SF_6 (146.066)	0.372	0.00822	0.18	0.037	1.33	0.250	0.84	0.322	0.11	0.354	2.0	Non	Non
Nitrogen (28.02)	0.072	0.0138	0.248	0.0424	0.97	1.0	1.0	1.04	0.88	1.03	1.0	Non	Non
Hydrogen (2.016)	0.0050	0.101	3.44	0.022	0.07	0.98	1.44	0.104	0.097		0.07	Explosive	Non
Carbon Dioxide (44.00)	0.107	0.0096	0.21	0.0344	1.14	0.68	1.05	0.655	0.59	0.708		Non	Non
Argon (39.90)	0.097	0.010	0.124	0.0533	1.94	1.40	0.62	2.47	3.45	2.71		Non	Non
Sulfur Dioxide (64.07)	0.173	0.0057	0.154	0.0293	1.56	0.63	1.03	0.827	0.52	0.98		Non	Yes can form H_2SO_4

Table 9. Comparison Of Artificial Atmospheres

Gas	Pressure* PSIA	Thermal Properties*							Blower Power Ratio To Air			Heat Transfer Coefficient Ratio To Air		
		Gas Constant	Specific Heats		c_p/c_v	Density	Viscosity	Conductivity	Constant heat load	Constant* volume flow	Constant mass flow	Constant heat load	Constant volume flow	Constant mass flow
			Btu / lb·F			$\frac{lb}{ft^3}$	$\frac{lb}{ft \cdot hr.}$	$\frac{Btu}{ft. \cdot F\ hr.}$						
		R	c_p	c_v	γ	e	μ	k						
A IR	14.7	53.3	0.240	0.172	1.40	0.0735	0.0446	0.0152	1.00	1.00	1.00	1.00	1.00	1.00
$O_2 - N_2$	11.0	52.6	0.238	0.170	1.40	0.0559	0.0456	0.0153	1.78	0.95	1.74	1.00	0.77	0.98
$O_2 - He$	6.5	75.2	0.302	0.205	1.47	0.0234	0.0503	0.0177	5.30	0.82	1.10	0.94	0.40	1.14
$O_2 - He$	11.0	109.4	0.405	0.264	1.53	0.0274	0.0510	0.0208	1.70	0.90	8.00	0.91	0.57	1.34
O_2	5.0	48.2	0.220	0.157	1.39	0.0276	0.0500	0.0155	9.28	0.88	7.86	1.00	0.37	0.91
O_2	11.0	48.2	0.220	0.157	1.39	0.0608	1.0500	0.0155	1.92	0.89	1.62	1.00	0.80	0.91
$O_2 - Ne$	11.0	63.7	0.234	0.152	1.54	0.046	0.0605	0.0210	2.51	0.92	3.27	0.69	0.66	1.01

* From (27) Selection of The Closed System Atmosphere", By J. L. Heldenbrand; in Report WADD 60-574, "Closed Circuit Respiratory Systems Symposium"

Vacuum Cooling Method

The vacuum cooling system is similar to an expendable coolant method, but has the advantage that the coolant is recovered for subsequent reuse. In it, the coolant picks up heat from the heat sink, is vaporized, and then flows to a radiator-condenser where it is reliquified or solidified. The reduction in volume of the fluid brought about by the change of phase creates the vacuum that gives the method its name. The low temperature necessary for condensation is easily obtained in space.

The vacuum cooling method may operate with liquids which are aboard for other purposes, such as coolants or fuels to be used during reentry. The power required may be a very small amount or none at all. A schematic diagram is shown in Figure 27A.

If the coolant is liquified in the condenser, it can be returned to the reservoir simply by pumping. When the coolant is solidified, it must first be liquified. This can be done by having the radiator act as a collector of solar energy, as is illustrated in Figure 27B. The operation of this arrangement depends upon the orientation of radiator and absorber to deep space and sun, but by the manipulation of valves, the functions of the two loops become interchangeable.

Silica Gel Cooling Method

The silica gel cooling method is a type of vacuum method in which the vacuum is maintained by adsorbing the coolant in a silica gel bed. The refrigerant comes from another silica gel bed where it had been adsorbed previously.

The cycle commences with the driving off of the adsorbed refrigerant from a silica gel bed by the application of heat. A typical refrigerant would be sulfur dioxide, SO_2. The vapor is then condensed in a radiator and the liquid passed through a throttle valve where the pressure is reduced. It next goes through an evaporator where it is vaporized by heat picked up from the heat sink. The vapor is then adsorbed by the silica gel bed. After all refrigerant has been driven off from the first bed and adsorbed by the second, the roles of the two beds are reversed. By the use of appropriate interconnections, the same path through the radiator, throttle valve and evaporator can be followed with either bed as the source of refrigerant. A schematic diagram is shown in Figure 28.

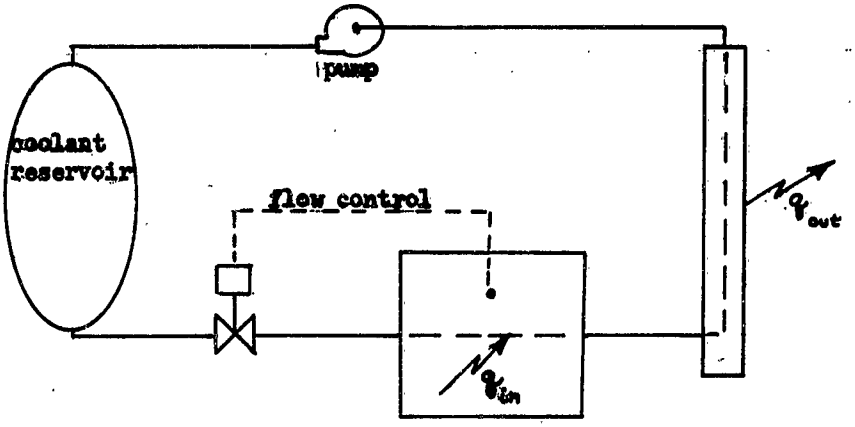

Figure 27a. Basic Method

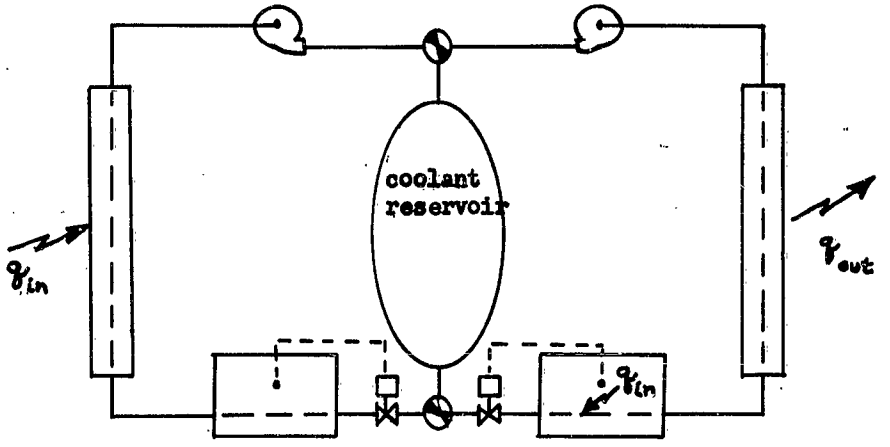

Figure 27b. Two-Loop Method

Figure 27. Vacuum Cooling Method

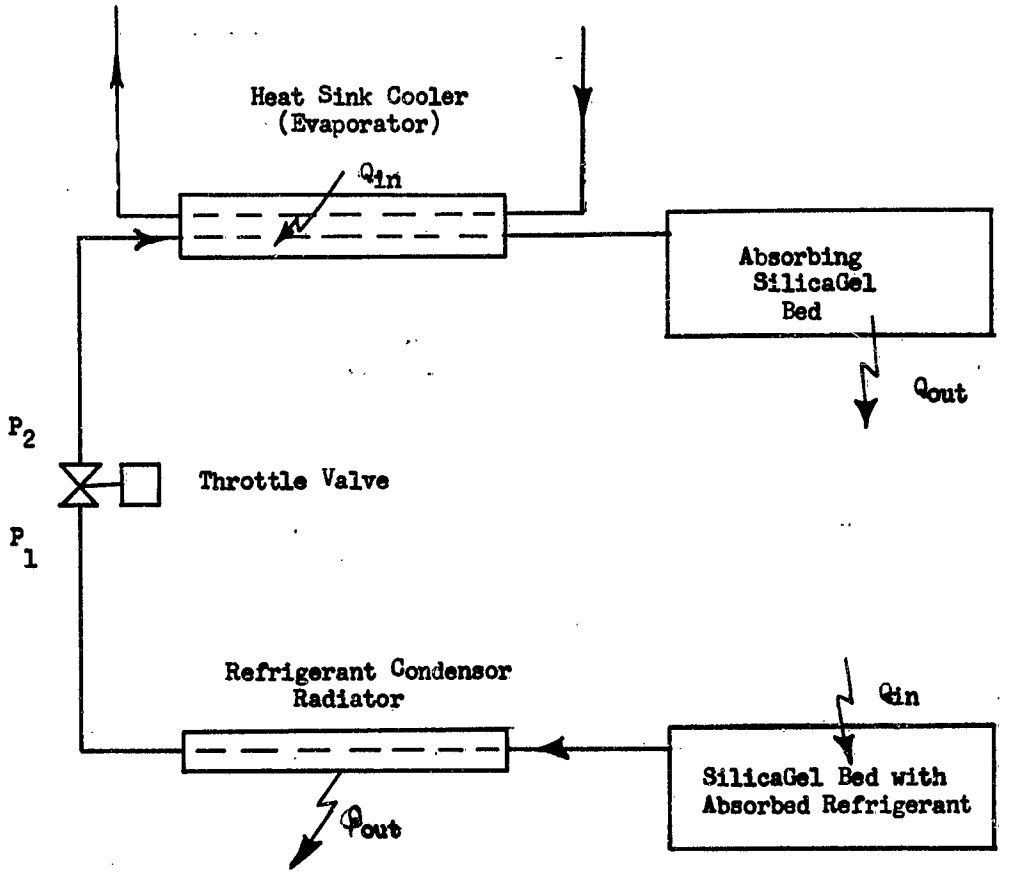

Figure 28. Schematic Diagram of Silica Gel Cooling Method

VARIABLE RADIATION METHODS

One means of controlling the surface temperature of a space vehicle for the condition of varying internal heat load and varying solar radiation incident on the surface is to change the emissivity or reflectivity of the surface. Several methods for varying the emissivity are discussed in the following paragraphs. These methods are characterized by a movable element whose position or attitude is varied in order to change the emissivity or reflectivity of the outer surface of the vehicle.

Venetian Blind - Shutter Type Method

This type of controller is shown in Figure 29. With the shutter open, the exposed area presents a surface of one emissivity, while the outside surfaces of the "slats" in the closed position can be made to have a different emissive and/or reflective character. By varying the degree of opening, any value between the open and closed emittance can be obtained.

One way of mounting the slats has been illustrated in Figure 29, in which the slats are mounted to the vehicle surface by hinges. This method permits some heat to be transmitted by conduction so that the slats serve as "radiating fins". Another way would be to pivot the slats along their longitudinal axis, and thus no contact would be made with the radiating surface. The slats can be positioned by a single mechanism actuated by volumetric or pressure changes in a temperature sensing bulb, by photo-electric cell and by bimettalic thermostatic elements.

The following discussion is a presentation of a way in which the required values for emissivity of the vehicle surface and both sides of the slats may be determined for a given heat load and vehicle surface temperature. It will not be a complete discussion on the design of the slats. This will be given in Part II of this report.

To make a rapid estimate for the required values for emissivity, the following equations may be used:

$$\sigma \epsilon_{effective} F A T_s^4 - \sum \alpha A G - Q = 0 \qquad (37)$$

$$\epsilon_{effective} = \epsilon_{slat} \cos\phi + \epsilon_{skin} (1 - \cos\phi) \qquad (38)$$

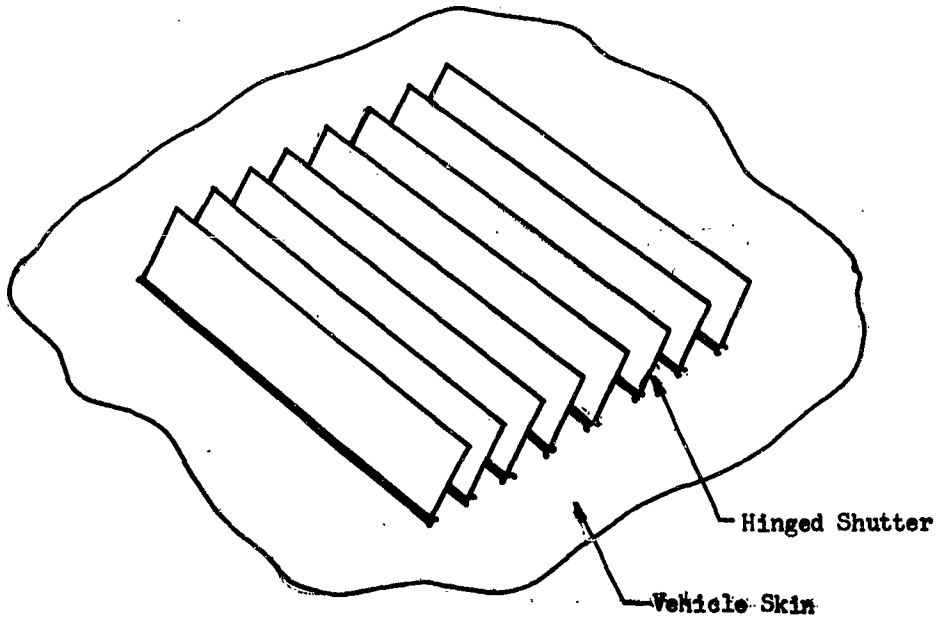

Figure 29 Venetian Blind Shutter, Hinged Type

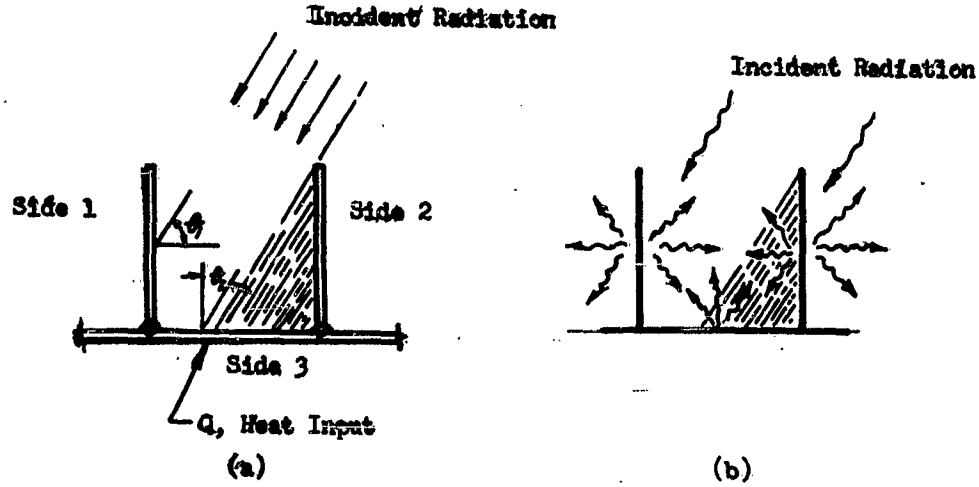

Figure 30. Cross-Section Through Shutter Arrangement

These two equations illustrate the complexity involved in determining required values for emissivity since there may be many combinations of values for ϵ and the slat angle ϕ. Further complexity is introduced for an orbiting vehicle because the solar radiation incident on the various surfaces varies with the vehicle orientation with respect to the various radiating bodies such as the sun and the earth.

The above equations are not sufficient to accurately determine the required values for emissivity since the radiation interchange between the various surfaces are not considered and the equations are limited to steady-state conditions only. A method which does not have the above restrictions is presented in the following paragraphs. This method utilizes the radiosity analog and thermal analog networks described in Reference 18. The use of networks greatly facilitates in visualizing and accounting for the various modes of heat transfer and to establish the necessary relationships for the analysis of the problem through the use of digital computers.

For illustrative purpose; the case in which the slats are perpindicular to the vehicle surface will be considered and this is shown in Figure 30. The incident angle of the solar radiation is shown to be less than 90° so that a shadow is cast on side 3 and a portion of side 2.

As shown in Figure 30, there are two sources which add thermal energy, the heat load added to side 2 and the solar radiation incident to the three sides. The heat load Q is assumed to be applied directly to side 2 for the purposes of this discussion and requires no further elaboration. Solar radiation requires careful consideration because of the interreflection of the three sides. Only part of the solar radiation impinging directly on a side is absorbed, the remaining energy is reflected to the other sides, which in turn reflects energy not absorbed back again. This is illustrated in Figure 30 b.

The most convenient way to determine the amount of solar radiation absorbed by the three sides is to use the radiosity method described in References 18 and 30, and the radiosity analog network illustrated in Figure 31a. A single mode for each side is used for illustrative purposes. For a more refined analysis, more nodes would be introduced. The radiosity method is limited to diffuse emission and reflection so that it is assumed that the surfaces considered here are of the diffuse form. One further assumption is that the surfaces are similar to "gray-bodies", $\epsilon = \alpha$, with the exception that the value for solar absorptivity α_s is different from

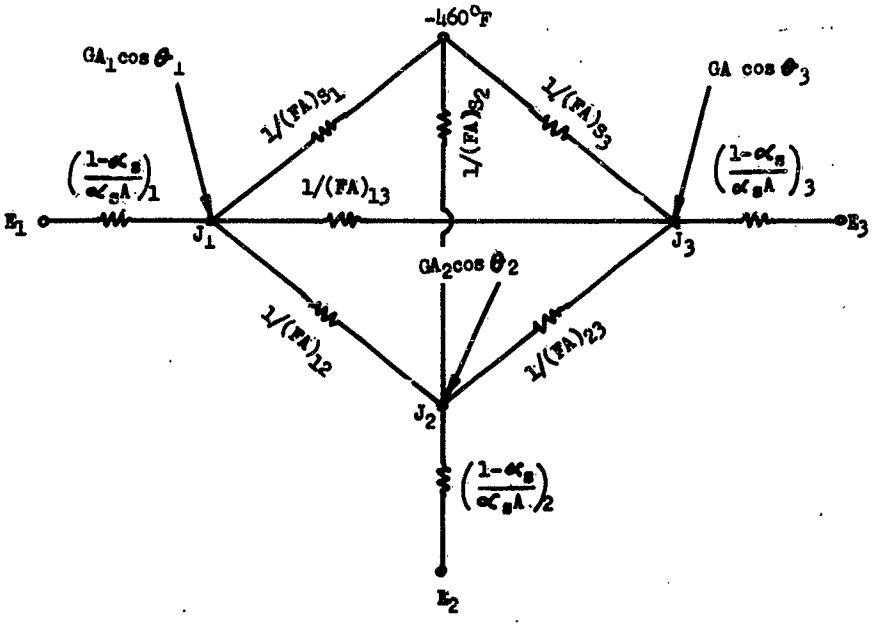

(a)

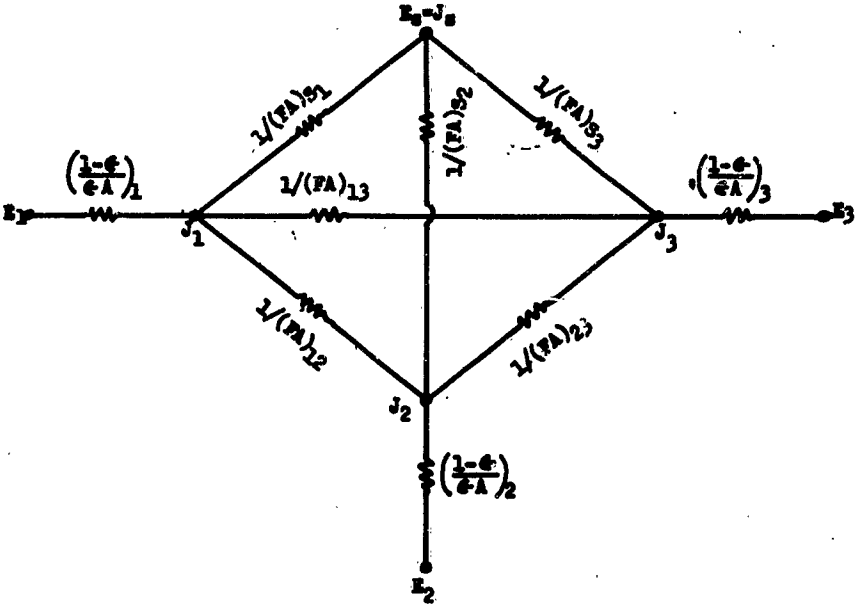

(b)

Figure 31 Radiosity Analog Network for Venetian Blind Shutter

infra-red absorptivity or emissivity.

The configuration factor F, for the three sides can be readily determined by using the string method discussed in Reference 18, if it is assumed that the "slats" are infinitely long.

By applying Kirchoff's laws for electric networks, three equations are written for heat flow into the radiosity nodes. The surface temperatures or potential, E_1, E_2 and E_3 are set to zero and the radiosities, J_1, J_2 and J_3 are determined from the three equations.

$$GA_1\cos\phi_1 + (FA)_{s_1}J_1 + (FA)_{13}(J_1-J_3) + (FA)_{12}(J_1-J_2) + \left(\frac{\alpha_s A}{1-\alpha_s}\right)_1 J_1 = 0 \qquad (39)$$

$$GA_2\cos\phi_2 + (FA)_{s_2}J_2 + (FA)_{12}(J_2-J_1) + (FA)_{23}(J_2-J_3) + \left(\frac{\alpha_s A}{1-\alpha_s}\right)_2 J_2 = 0 \qquad (40)$$

$$GA_3\cos\phi_3 + (FA)_{s_3}J_3 + (FA)_{13}(J_3-J_1) + (FA)_{23}(J_3-J_2) + \left(\frac{\alpha_s A}{1-\alpha_s}\right)_3 J_3 = 0 \qquad (41)$$

The values for J_1, J_2 and J_3 are then substituted into the following equation to determine the amount of solar radiation absorbed by each of the surfaces.

$$Q_{absorbed} = \left(\frac{\alpha_s A}{1-\alpha_s}\right)J \qquad (42)$$

Since the incident radiation G on each side varies with vehicle orbit position, which is time dependent, it is possible to obtain the variation of Q absorbed with respect to time such as illustrated in Figure 33.

Radiation heat transfer involves proper accounting of all inter-reflections between the slat surfaces and the skin. This can be readily accomplished by utilizing the radiosity analog network similar to the one illustrated in Figure 31b. Since no energy is reflected from space, the potential E_s is equal to the radiosity J_s. Also, the emissivity is different from the one used in determining the solar energy absorbed, Figure 31a, since the emitted radiation is assumed to be in the infrared band, which has a longer wave length.

Again, three network equations are written from which radiosities J_1, J_2 and J_3 are determined. These values are then used to determine the interchange factor f, between the various surfaces and space.

$$\left(\frac{\epsilon A}{1-\epsilon}\right)_1 (E_1 - J_1) + (FA)_{S_1}(E_S - J_1) + (FA)_{13}(J_3 - J_1) + (FA)_{12}(J_2 - J_1) = 0 \tag{43}$$

$$\left(\frac{\epsilon A}{1-\epsilon}\right)_2 (E_2 - J_2) + (FA)_{S_2}(E_S - J_2) + (FA)_{12}(J_1 - J_2) + (FA)_{23}(J_3 - J_2) = 0 \tag{44}$$

$$\left(\frac{\epsilon A}{1-\epsilon}\right)_3 (E_3 - J_3) + (FA)_{S_3}(E_S - J_3) + (FA)_{13}(J_1 - J_3) + (FA)_{23}(J_2 - J_3) = 0 \tag{45}$$

To determine the interchange factor between space and sides 1, 2 and 3, let $E_s = J_3 = 1$ and $E_1 = E_2 = E_3 = 0$ and solve for J_1, J_2 and J_3. Then since

$$(fA)_{S_1}(E_S - E_1) = \left(\frac{\epsilon A}{1-\epsilon}\right)_1 (J_1 - E_1),$$

$$(fA)_{S_1} = \left(\frac{\epsilon A}{1-\epsilon}\right)_1 J_1 . \tag{46}$$

Similarly

$$(fA)_{S_2} = \left(\frac{\epsilon A}{1-\epsilon}\right)_2 J_2 \tag{47}$$

$$(fA)_{S_3} = \left(\frac{\epsilon A}{1-\epsilon}\right)_3 J_3 \tag{48}$$

To determine the interchange factor between side 1 and sides 2 and 3, let $E_1 = 1$ and $E_s = E_2 = E_3 = 0$; and again solve for J_1, J_2 and J_3. Then since

$$(fA)_{12}(E_1 - E_2) = \left(\frac{\epsilon A}{1-\epsilon}\right)_2 (J_2 - E_2),$$

$$(fA)_{12} = \left(\frac{\epsilon A}{1-\epsilon}\right)_2 J_2 . \tag{49}$$

similarly,

$$(fA)_{13} = \left(\frac{\epsilon A}{1-\epsilon}\right)_3 J_3 \tag{50}$$

also

$$(fA)_{23} = (fA)_{12} \tag{51}$$

The above procedure is repeated to determine the remaining interchange factors. These factors are then used to determine the radiation thermal resistance between the three surfaces and space from the following equation.

$$R_R = \frac{1}{h_r A} = \frac{1}{\sigma (fA)_{mm} (T_m^2 + T_\infty^2)(T_m + T_\infty)} \tag{52}$$

The values for thermal resistance and solar radiation absorbed are then utilized in the thermal analog network to compute the temperature of the three surfaces. A typical network is shown in Figure 32. In this network, R_T represents the combined conduction resistance and radiation resistance between sides 1 and 2 and sides 2 and 3.

$$R_T = \frac{1}{\frac{1}{R_c} + \frac{1}{R_R}} = \frac{1}{\frac{KA}{L} + h_r A} \tag{53}$$

By utilizing a computer program similar to the one described in Section VIII, the surface temperatures can be readily determined.

The above procedure will require several iterations to establish the desired emissivities for the specified heat load and surfaces temperatures.

Rotating Mask Method

A temperature control method employing rotating masks was used on the Atlas Able-4 Lunar Satellite (28). This is illustrated in Figure 34. The spirally wound bimetallic strip sensed the internal payload temperature and these temperature changes cause the rotation of the mask through differential expansion or contraction. On the surface of the vehicle were alternating 45-degree segments of high and low absorbtivity-to-emissivity ratio materials. The rotation of the mask covered one and uncovered the other as required. Fifty of these units were used on the surface of the spherical satellite, placed as uniformly as possible to reduce the influence of varying sun angle. About 20 percent of the satellite surface is so controlled.

Advantages claimed for this method include the fact that there is, essentially, only one moving part. This adds to the simplicity and reliability and helps to keep the weight relatively low. Sensitivity to vibration is reduced because the unit is balanced about its pivot point. The large number of individual units contributes to the reliability of the whole system, since the failure of a single unit will affect the degree of temperature control for less than a similar failure would in some other systems.

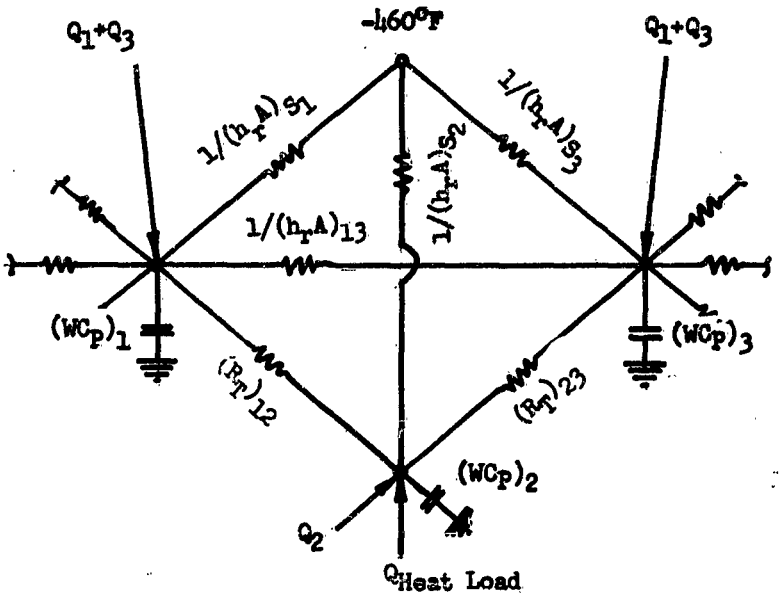

Figure 32. Thermal Analog Network For Venetian Blind Shutter

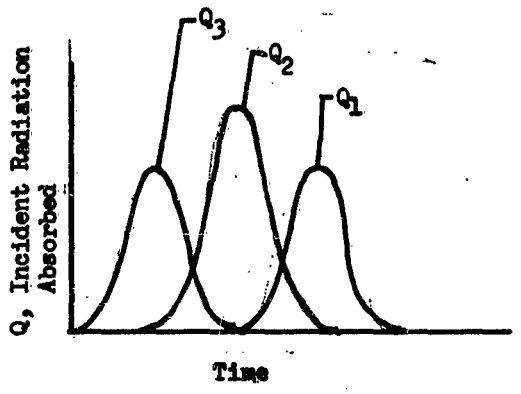

Figure 33, Incident Radiation Absorbed

Translating Mask Method

The translating type mask operates in very much the same fashion as the rotary mask. The essential difference is that the mask does not pivot about a central point but moves laterally to cover and uncover surfaces of differing thermal characteristics. Figure 34 shows the form of one translational mask method.

Four pairs of ribs are seen to radiate from the life cell to a narrow cylindrical band. This band has an outer surface of polished aluminum partially covered by alternating strips of aluminum oxide paint. An outer concentric band has openings in it of approximately the same size as the alternating polished aluminum and painted strips. A battery-powered motor moves the outer band to expose the required proportion of each surface in response to signals from a thermostat in the life cell. The heat generated in the life cell is conducted to the inner band through the radial ribs.

It is interesting to observe some of the reasons which favored the choice of this method. The proponents note that:

"Since the shields represent added weight, it is desirable to place them where they would have the maximum effect in raising the moment of inertia about the spin axis, i.e., at the periphery of the central plane."

"To prevent large axial temperature gradients in the life cell, heat generated in it is best removed from near its middle, rather than from its ends."

"Placement of the shields at the largest diameter of the satellite would assure the least possible variation of incident radiation, since the controllable surface can then not be shaded by other parts of the satellite, but can at worst only be turned at right angles to the incoming radiation."

The purpose in quoting these statements here is to emphasize that some methods have certain advantages not possessed by any other method. For example, the rotating mask method would be of no help in stabilizing spin, but could prevent large axial temperature gradients and would have far less variation of incident radiation than the method described here.

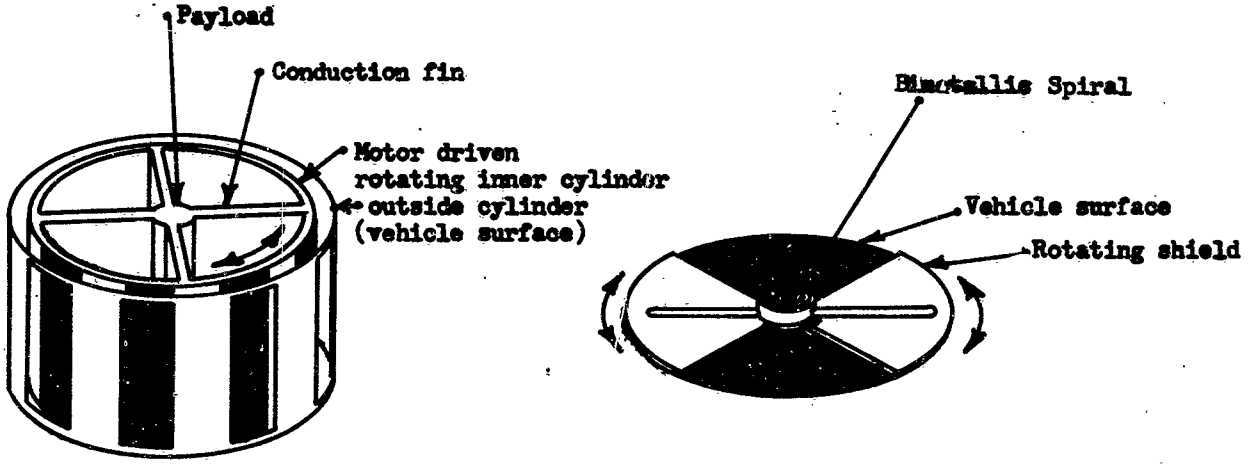

Figure 34. Translating and Rotating Mask
Temperature Control Units

Mercury Film Temperature Control Method

A temperature control method has been suggested that would utilize the fluid and reflective properties of liquid mercury in a manner illustrated by Figure 35. In operation, the temperature sensing bulb, containing mercury, would be located in the region where temperature is to be controlled. Increased or decreased temperature would cause a volumetric expansion or contraction of mercury with a consequent rise or fall of a continuous thin film, in the space between a glass or quartz "window" and a suitable backing. This backing could be of high absorptivity or high emissivity material, depending upon a requirement to bring solar heat into or reject internal heat from the vehicle.

At the present time, this system is undergoing an analysis which shows some promise for satisfactory operation. The arrangement has simplicity and reliability.

Other variants of this principle involve the use of pressure changes to actuate bellows or pistons to move the mercury. The use of a photoelectric cell to signal the start of a pump also suggests itself. In each case, the object is to cover more or less of a critical area with a reflective shield, capable of adjustment to any position within a range and free, in the shield itself, of moving mechanical parts.

Particle Cloud Shield

In this method, the evacuated space between the window and the backing plate would contain a cloud of particles sufficiently dense to be opaque to solar radiation. In an evacuated space in zero gravity, the distribution of particles could be expected to form a cloud of uniform density. The window would be cleared to permit the passage of thermal energy into or heat out of the vehicle by the formation of an electric field. This field would be formed by applying an electric current to electrodes at the outside edges of the system with the particles then collecting at these electrodes. To opacify the window, the current would be shut off and the brief actuation of a vibrating device would then send the particles out in a random distribution.

The particle cloud shield operates in a similar manner to that of electrostatic precipitators used to remove fly ash from flue gas. No development work has been done on this concept.

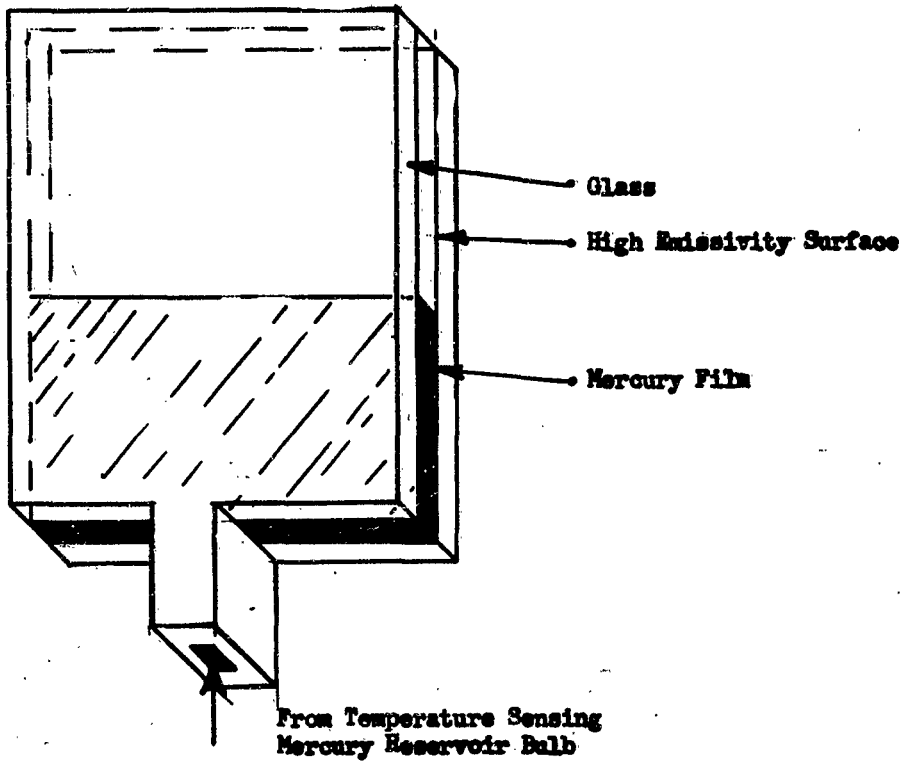

Figure 35. Mercury Film Temperature Control Method

CONCLUSION

The wide range of available semi-passive temperature control methods gives a choice of control through variation in surface coating or variation in the internal heat transfer rate. The variable coating and variable conduction type control will usually be restricted to equipment with small heat loads. Whereas, the forced convection fluid loops and expendable methods adapt better to equipment with high heat loads since cold plate or direct forced convection cooling is available for removing heat from high dissipating components.

The semi-passive methods are usually only limited by the requirement that the heat sink (heat exchanger, vehicle skin, or radiator) must be at a lower temperature than the equipment. However, the expendable, vacuum, and silica gel methods do not even have this restriction.

At the present time semi-passive methods of variable surfaces and fluid loops have been used on some space vehicles. These methods have proven to be reliable and fairly light. However, some coatings have deteriorated and fluid loops have an inherent danger of leakage. Much research is needed in improving coating and fluid loop reliabilities.

Since extensive research in surface coatings is already underway, recommendation is made that some research be directed toward fluid components and loops. If the probability of leakage is decreased, toxicity, corrosiveness and dielectric strength become negligible considerations in most fluid loops. As a result, basic coolant considerations of weight, volume, and surface area can be used as the only criteria needed for optimization. Increase in the efficiencies and operating life of fans and pumps is also desirable.

SECTION IV

ACTIVE TEMPERATURE CONTROL METHODS

Active temperature control methods have been defined in this report as methods which require a heat pump - - removing heat from a source or evaporator to a sink or radiator-condenser at a higher temperature. The cycles discussed in this section include vapor cycles, gas cycles, and thermoelectric cycles. Modified gas cycles which incorporate a vortex tube is also included.

The zero-gravity effects of the space environment can create major problems in the design and operation of the vapor cycles. Consequently, detailed discussion of methods of design for evaporators and radiator-condensers for operation in zero gravity is included. Note that although the term "heat pump" is used here most of these cycles are refrigeration cycles and cannot be reversed as in the usual "heat pump" sense because the evaporators and condensers are completely different in design due to the zero-gravity requirements. The usual "heat pump" is less efficient than a refrigeration cycle since dual purpose condensers and evaporators are required resulting in lower condensation and evaporation efficiencies.

The preceding zero-gravity effects are not a problem in the gas and thermoelectric cycles. However, all of the refrigeration cycles have one drawback in common - - a high power requirement. The power requirements are evident in the COP relationship of

$$\text{COP} = \frac{\text{COOLING LOAD}}{\text{METHOD POWER}}$$

Unfortunately, increasing the efficiency of the compressor or system does not drastically change the COP relationship, since the COP is more a function of the thermodynamics of the cycle. Thus, power penalties in weight, surface area, and volume must always be considered in comparisons of active methods with passive and semi-passive methods.

VAPOR CYCLE METHODS

For several reasons, vapor cycle methods should be considered for certain space applications. These methods have high performance characteristics, are able to provide refrigeration for large heat loads at the required location, and can operate over a wide range of altitudes from ground to outer space. The extensive development of vapor cycle systems for aircraft and missiles provides a wealth of data and experience for space applications. The use of the vapor cycle in space introduces, however, special problems involving the operation of components in a weightless environment. In addition, the continued exposure of refrigerants to space radiation may create new problems not considered in the past.

Nomenclature

COP	Coefficient of performance
c_p	Specific heat at constant pressure per unit mass
$\bar{c}_p$	Molal specific heat at constant pressure
L	Latent heat of vaporization
$\bar{L}$	Molal latent heat of vaporization
p	Pressure
Q_R/V_1	Cooling effect per unit volume of refrigerant at compressor inlet
R	Gas constant
r	Pressure ratio
T	Temperature
σ	Surface tension
η_c	Compressor efficiency

Compressor

H_{ad}	Adiabatic head
N	Rotational Speed
n_s	Specific speed
Q	Volumetric flow rate

Evaporator

A	Evaporator heat transfer surface
B_o	Bonde number
g_o	Gravity acceleration on earth
L	Hydraulic diameter
Q	Cooling load
W_e	Weber number
σ	Surface tension
ω	Rotational Speed

Condenser

a	Tapered ratio
D	Tube inside diameter, ft
d_h	Equivalent hydraulic diameter, ft
F	Fraction of vapor condensed in tube
$\bar{f}$	Mean friction factor
h	Heat transfer coefficient
h_{fg}	Heat of vaporization, Btu/lb
L	Fin length, ft
k	Conductivity of liquid
N	Number of parallel tubes
p	Pressure
Q	Heat rejection rate, Btu/sec
Q_c	Cooling load
Q_R	Condenser heat rejection rate
Re	Reynolds number
T	Tube temperature at which heat is radiated to outer space

Nomenclature

Condenser (Cont)

V	Velocity
t	Tube wall thickness, in.
W_e	Weber number
W_T	Combined tube and fin weight, lb
X_1	Tube length, ft
η_{ct}	Efficiency based on Carnot cycle
ϵ	Emissivity
σ	Stefan-Boltzmann constant
δ	Fin thickness, in.
ρ_t	Tube specific weight, lb/ft
ρ_f	Fin specific weight, lb/ft
μ	Vapor viscosity, lb/(ft)(sec)
ϵ	Surface emissivity
σ	Stefan-Boltzmann constant, 48×10^{-14} Btu/(sec)(sq ft)$(R)^4$
K	Fin thermal conductivity, Btu/(sec)(ft)(^oF)

Thermodynamics and Operation

Basic Vapor Refrigeration Cycle - The ideal vapor cycle consists of the following processes (see Figure 36):

1-2 Isentropic compression of saturated vapor to high-slide pressure P_2 (compressor)

2-3 Isobaric condensation to saturated liquid at high-side pressure P_2 (condenser). The refrigerant may reject heat directly to the outer environment or through an intermediate heat transfer loop.

3-4 Isenthalpic expansion of liquid to two-phase mixture at low-side pressure P_1 (expansion valve).

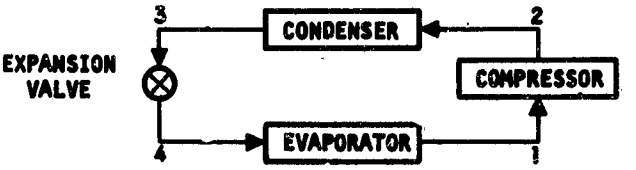

(a) Schematic Arrangement of Equipment

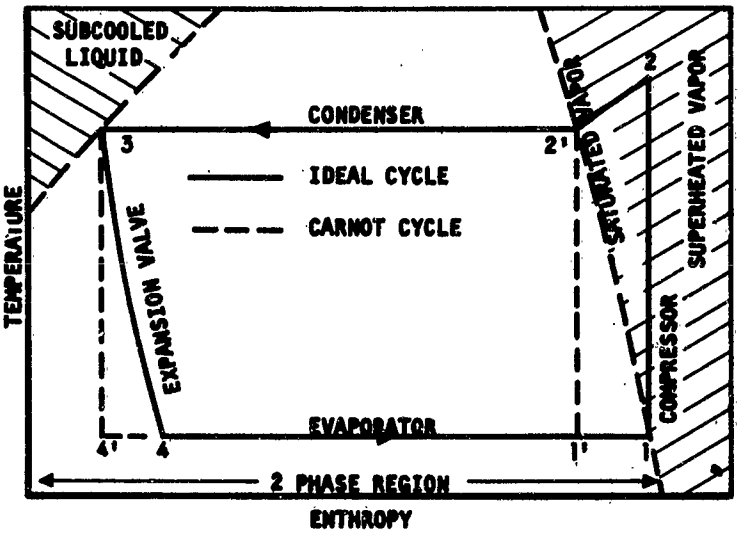

(b) The Vapor and the Carnot Refrigeration Cycles on the T-S Plane.

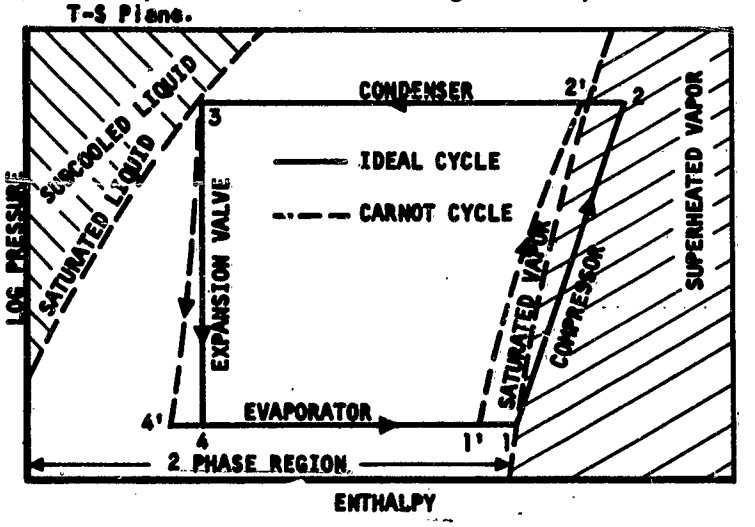

(c) The Vapor and the Carnot Refrigeration Cycles on the P-H Plane.

Figure 36. The Basic Vapor Refrigeration Cycle (Reference 32)

4-1 Isobaric isothermal evaporation to saturated vapor at low-side pressure P_1 (evaporator).

The cycle closely resembles a Carnot cycle operating at the same condenser and evaporator temperature, as indicated by 1'-2'-3-4'. This similarity contributes to the high performance characteristics of the vapor cycle. The coefficient of performance of the ideal vapor cycle given by Reference 31 expresses:

$$COP = \frac{A - B(r-1)}{\frac{1}{r(1-B)} \cdot (A + B - 1)\,(1 - 1/r)^{-1}} \qquad (54)$$

where $A = \dfrac{L_1}{c_{pg} T_1}$

$B = \dfrac{c_{pl}}{c_{pg}}$

$r = \dfrac{T_2}{T_1}$

This expression shows that the specific heats of the refrigerants and operating temperatures of condenser and evaporator are the principal influences on cycle performance.

Basic Vapor Refrigerating Cycle with Superheating

To avoid compressing a two-phase mixture, actual vapor cycles usually operate with superheat vapor at the inlet to the compressor. In addition, a small amount of subcooling is necessary at the inlet to the expansion valve to prevent premature vapor flashing. These considerations lead to the basic cycle with superheating shown on Figure 37. Assuming perfect thermodynamic behavior of the refrigerant vapor, Reference 31 expresses the COP of the cycle with superheating in terms of the COP of the previous basic cycle as:

$$\frac{COP_s}{COP} = \frac{1 + \dfrac{c_{pg}(T_s - T_1)}{L_1 - c_{pR}(T_2 - T_1)}}{1 + \dfrac{T_s - T_1}{T_1}} \qquad (55)$$

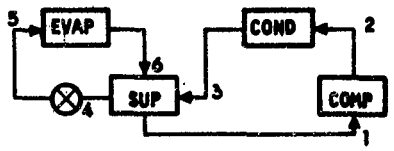

(a) Schematic Arrangement of Equipment

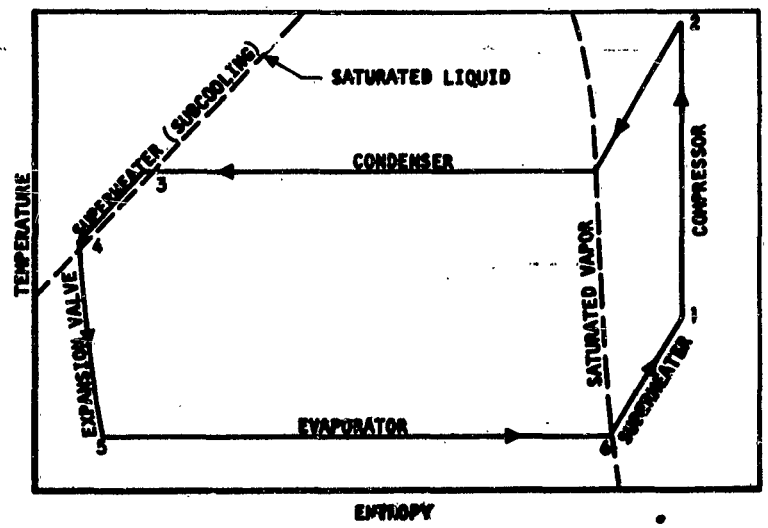

(b) Superheated Vapor Refrigerating Cycle on the T-S Plane.

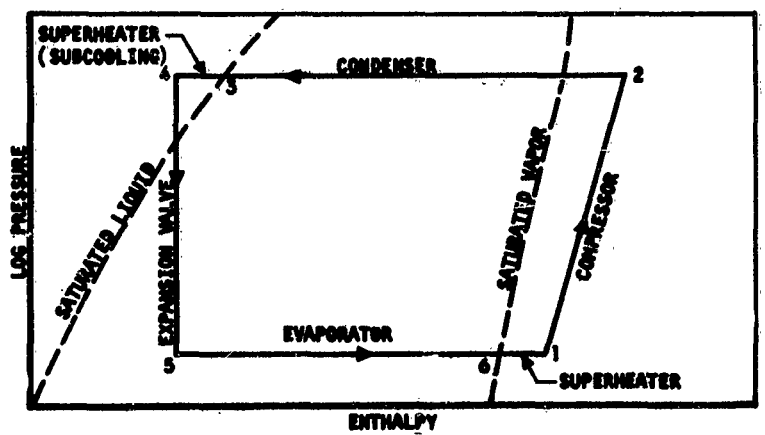

(c) Superheated Vapor Refrigerating Cycle on the P-H Plane.

Figure 37. The Basic Vapor Refrigerating Cycle with Superheating (Reference 31)

For typical operating conditions with Freon 11 and Freon 12 as refrigerants, Figures 38 and 39 show the beneficial effects of superheating in COP and flow requirements. To reduce total weight and volume of heat transfer equipment, a separate superheater, such as that shown in Figure 37, is preferable to superheating within the evaporator.

Basic Vapor Refrigerating Cycle with Subcooling

As liquid subcooling degrades the quality of the vapor-liquid mixture at the evaporator inlet, the heat transfer coefficient increases on the refrigerant side. This has only a small effect on the size of the condenser. If subcooling is accomplished in the condenser, the cycle COP is increased but at the expense of a considerable increase in condenser size (Reference 31). Subcooling by heat transfer with expanded liquid refrigerant, as shown in Figure 40, has negligible effect on the COP.

Cycle with Expander or Compressor Operating with a Two-Phase Fluid

A COP rise of approximately 30 per cent has been calculated for an expander operating with a two-phase fluid instead of the expansion valve of the previous cycles (Reference 32). However, realization of this cycle depends upon availability of efficient expanders which operate with a two-phase mixture. Similiarily, compressors operating with two-phase fluids as in Reference 33 have yet to be developed.

Compound Cycles

Figure 41 presents the compound cycle, a vapor cycle with two or more stages of compression. This approach is required to avoid pressure ratios that exceed compressor capacity. The compound cycle is identical in COP to the basic vapor cycle of Figure 36, but the individual stage pressure ratios and compressor displacement are different. Table 10 presents the performance, pressure ratios, and displacement data for an ideal two-stage compression cycle.

Cascade Systems

Cascade cycles may find wide application in space because of their ability to reach high sink temperatures, a requirement for light and compact radiators. As shown on Figure 42, a cascade cycle consists of two or more vapor cycles interconnected to utilize the heat sink of the low temperature cycle as the heat source for the high temperature cycle. This cycle might be used for a single heat source as presented in Figure 42, or for two heat sources at different temperatures. In the latter case, the high temperature cycle of the cascade would contain two evaporators, one to receive the heat from the high temperature source and the other to receive heat from the condensing refrigerant of the low temperature cycle of the cascade.

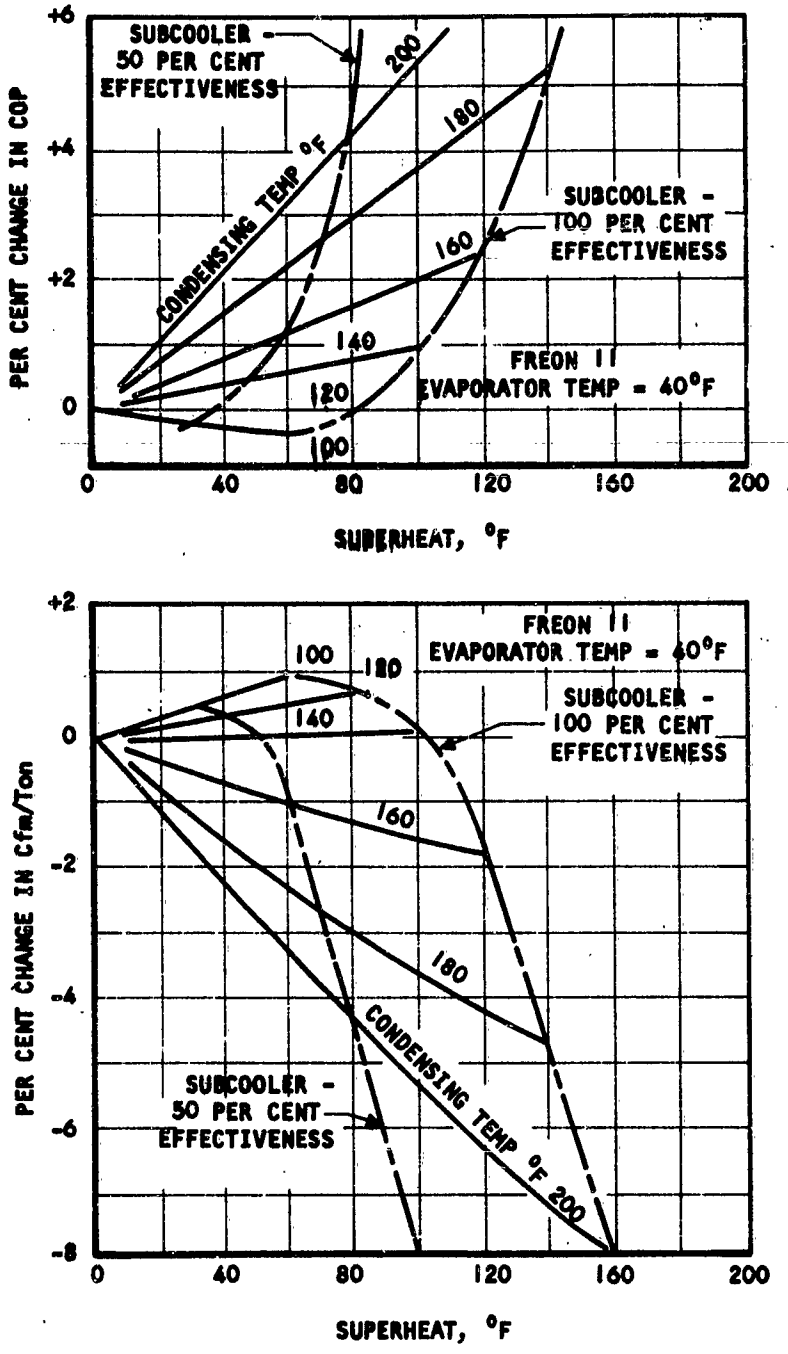

Figure 38. Effect Gained by Use of Superheating in Performing Useful Cooling with Freon 11.

(Reference 31)

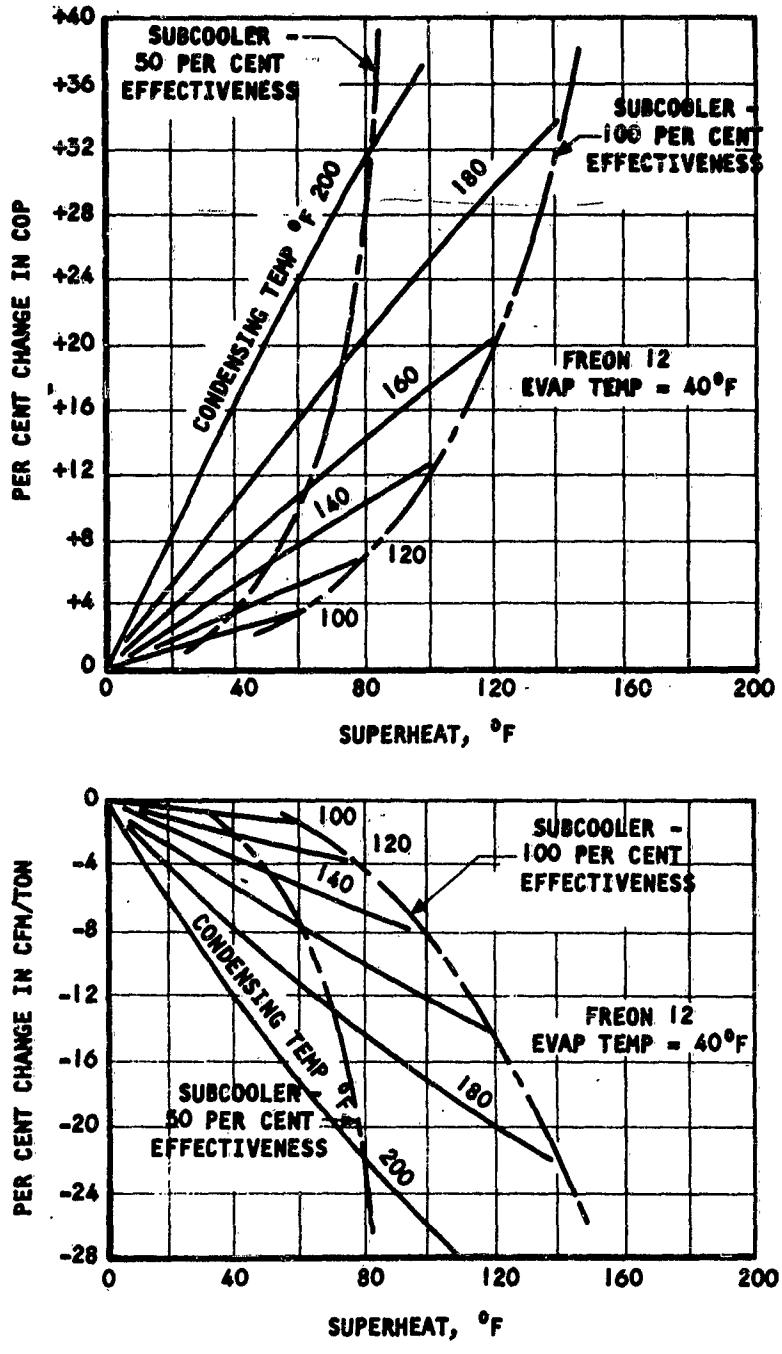

Figure 39. Effect Gained by Use of Superheating in Performing Useful Cooling with Freon 12.

(Reference 31.)

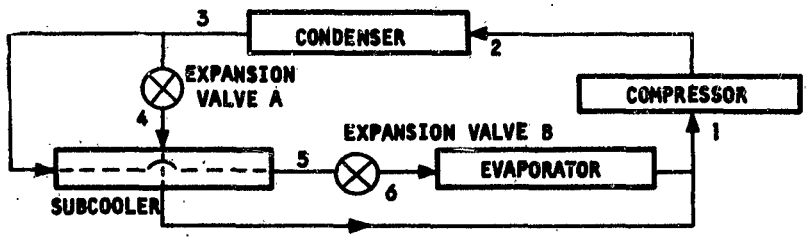

(a) Schematic Arrangement of Equipment

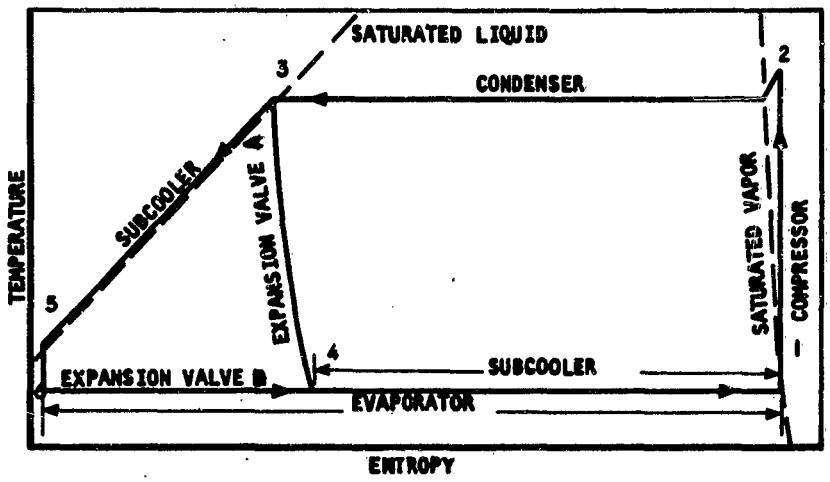

(b) Subcooled Liquid Refrigerating Cycle on T-S Plane

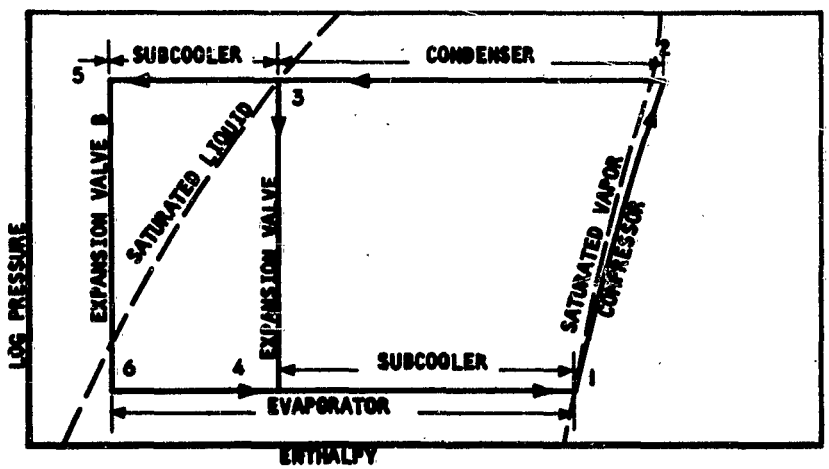

(c) Subcooled Liquid Refrigerating Cycle in P-H Plane.

Figure 40. The Basic Vapor Refrigerating Cycle With Subcooling (Reference 31)

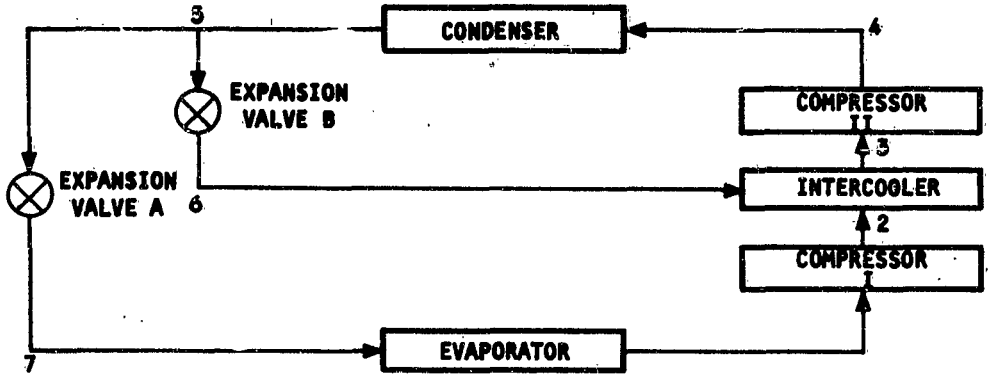

(a) Schematic Arrangement of Equipment

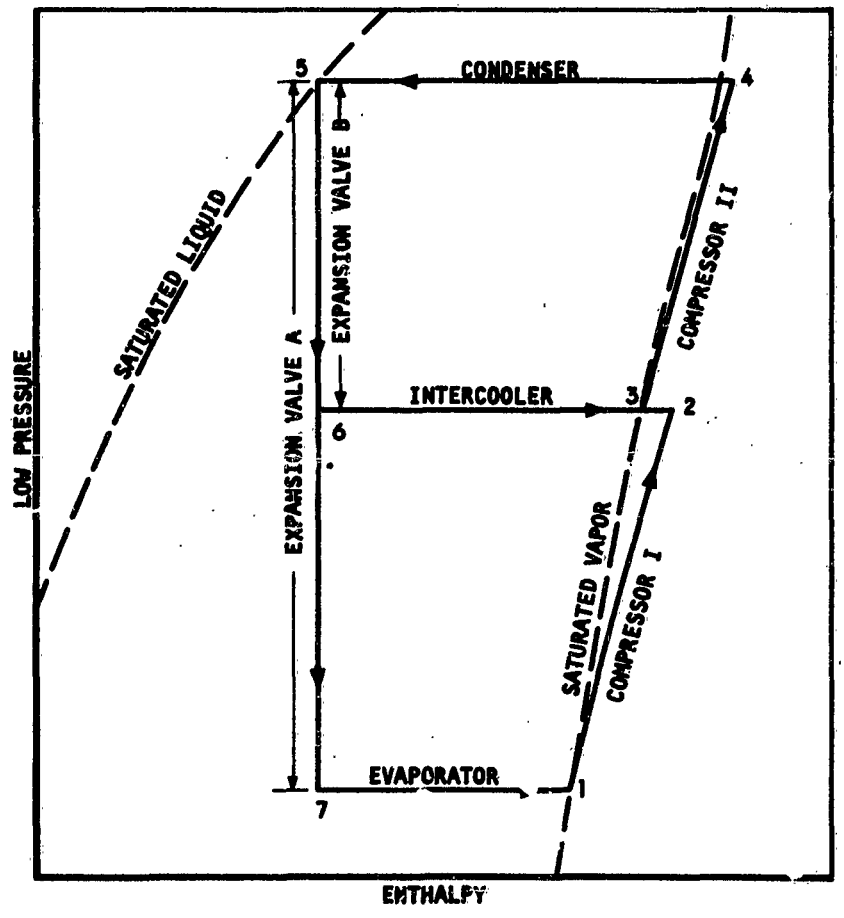

(b) Two-Stage Refrigerating Cycle on P-H Plane.

Figure 41. Vapor Refrigerating Cycle with Two-Stage Compression and Interstage Cooling.

(Reference 31)

Table 10

Ideal Performance Of
Compound Vapor Refrigeration Cycles

(Reference 31)

Over-all COP	LOW PRESSURE STAGE				HIGH PRESSURE STAGE			
	Refrigerant	COP	P_2/P_1	V_1/Q_r cfm/ton	Refrigerant	COP	P_2/P_1	V_1/Q_r cfm/ton
2.02	F-11		32.0	90.5				
1.64	F-12		14.4	14.3				
2.02	F-11		5.66	90.5	F-11		5.66	19.4
1.64	F-12		3.76	14.3	F-12		3.82	4.29
1.96	F-12	4.93	4.44	8.95	F-12	3.94	3.85	4.11
2.12	F-22	4.84	4.40	5.44	F-11	4.55	5.66	19.0
1.95	F-22	4.84	4.40	5.44	F-12	3.94	3.83	4.11
2.02	F-11		5.66	90.8	F-11		5.66	19.3
1.64	F-12		3.76	14.3	F-12		3.83	4.39
2.32	F-11		5.66	68.2	F-11		5.66	17.3
2.09	F-12		3.76	8.93	F-12		3.83	3.87
2.05	F-11		5.66	97.5	F-11		5.66	
1.82	F-12		3.76	12.9	F-12		3.83	
2.32	F-11		5.66	70.0	F-11		5.66	18.45
2.15	F-12		3.76	8.90	F-12		5.83	3.73

CONDITIONS: T_1 = -20°F; T_2 = 140°F

The intermediate pressure corresponds to saturation at 46°F; 10°F approach in heat transfer equipment (subcoolers, superheaters).

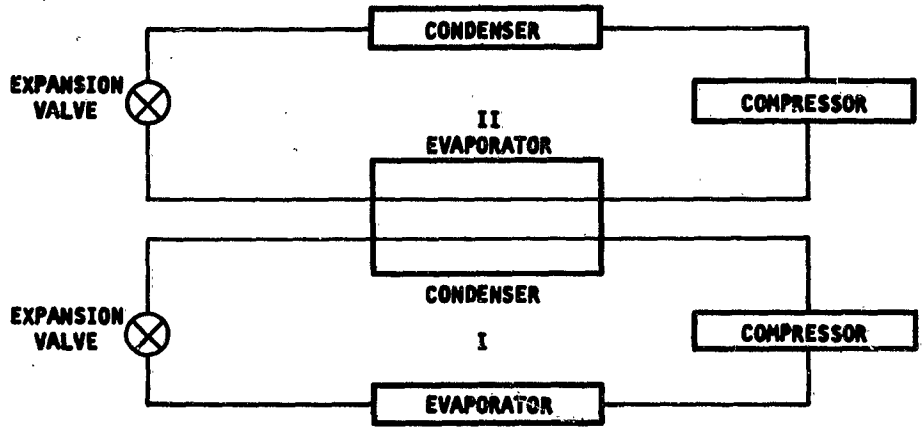

(a) Schematic Arrangement of Equipment

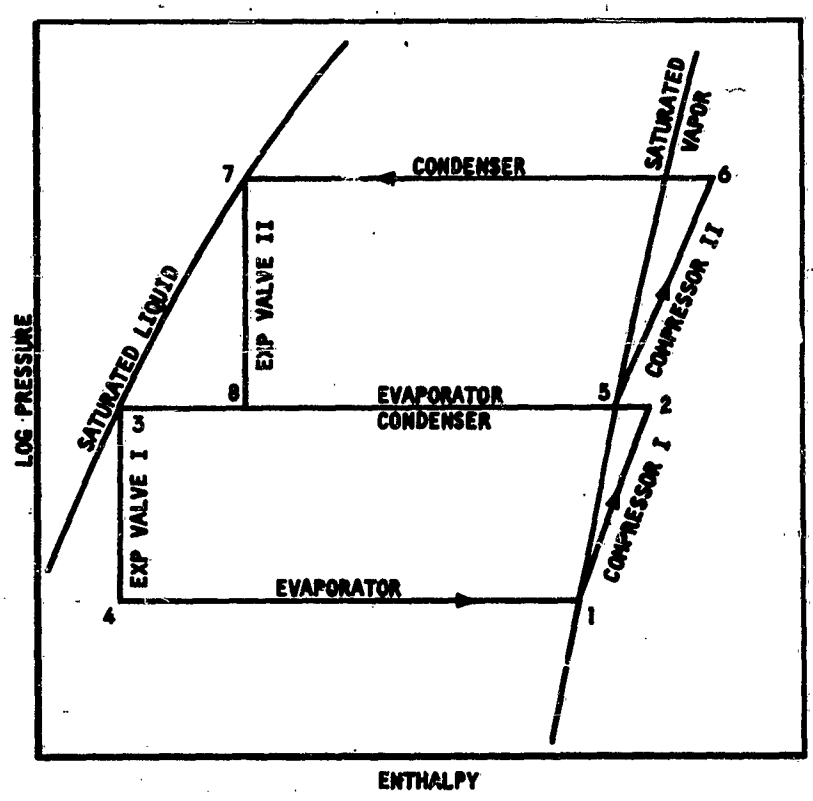

(b) The Cascade Refrigerating Cycle on the P-H Plane.

Figure 42. The Cascade Vapor Refrigerating Cycle (Reference 31)

The important feature of a cascade cycle is the improved COP over the simple cycle. For a typical cascade of two cycles, Reference 31 gives for the COP:

$$COP = \frac{1}{\eta_c} \left[\frac{1}{COP_1} + \frac{1}{COP_2} + \frac{1}{\eta_c} \times \frac{1}{COP_1} \times \frac{1}{COP_2} \right] \qquad (56)$$

where COP = coefficient of performance of the cascaded system

η_c = efficiency of the compressors of the cycle.

Figure 43 illustrates the COP of a cascade vapor refrigeration cycle as a function of the evaporator-condenser temperature.

Many authors (Reference 31 and others) recognize that this improvement in COP may not be an overwhelming superiority over other cycles, such as the compound. For space applications, however, the cascade cycle permits the use of different refrigerants to accommodate the heat sink temperatures. Ordinarily, this advantage is at the expense of increased mechanical complexity.

Cycle Variants

There are many variants of the cycles studied previously, and Reference 31 presents a detailed treatment of their characteristics. Compound cycles with intercooling and subcooling, with superheating, or with combinations of subcoolers and superheaters have been considered by many authors. Their complexity precludes their being recommended for space applications at this time.

Refrigerants

Previous study of the thermodynamics of vapor cycles shows that the practical realization of these systems depends primarily on the availability of the refrigerants. In selecting these refrigerants, two types of criteria are generally considered. These are the thermodynamic factors and the qualitative factors.

Thermodynamic Factors

Thermodynamic factors, which determine the desirability of a refrigerant from a performance standpoint, are considered below.

Refrigerating Effect Per Unit Volume. The refrigeration effect per unit volume of refrigerant measured at the inlet to the compressor, Q_r/v_1, establishes the rate of refrigerant flow through the system. The size of components, particularly compressors, can be compared by the following approximate expression, as obtained from Reference 31:

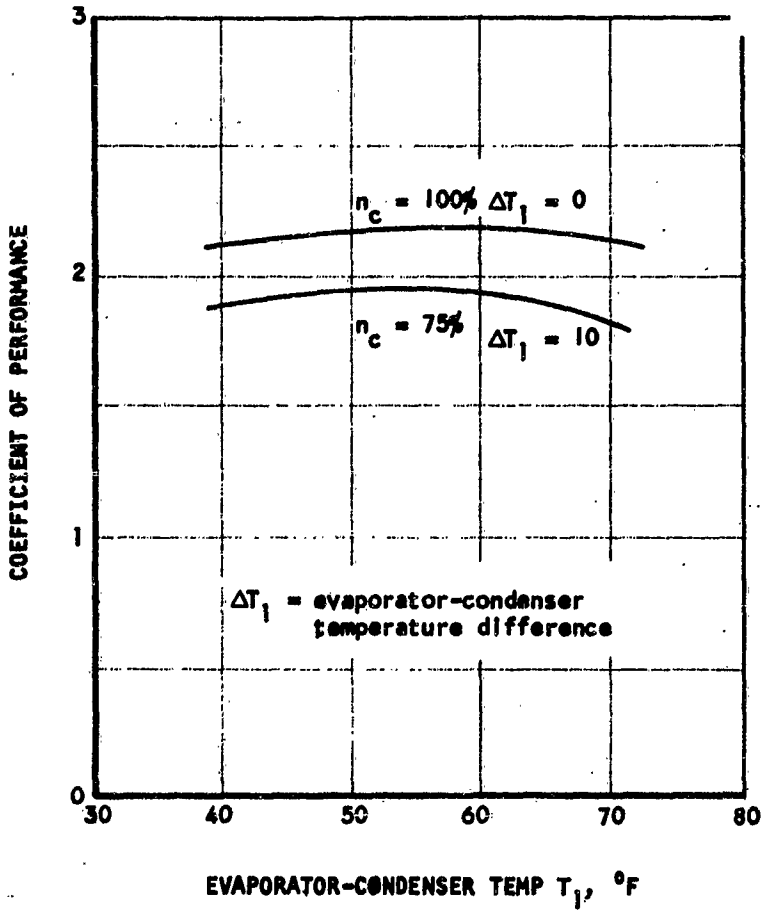

Figure 84. Relationship of the COP of a Cascade Vapor Refrigeration Cycle to the Evaporator - Condenser Temperature.

(Reference 1)

$$\frac{Q_r}{V_1} = \frac{L_1 - c_{p_1}(T_2 - T_1)}{V_1}$$

$$= \frac{P_1}{R}\left[\frac{L_1}{T_1} - c_{p_1}\left(\frac{T_2}{T_1} - 1\right)\right] \qquad (57)$$

It can be seen that the vapor pressure P_1 of the refrigerant at the evaporator temperature is an important factor. Volatile Freons like Freon 22 have a large value of Q_r/V_1, while the less volatile Freon 11 and 113 have lower values. Table 11 presents some typical values of this ratio.

Critical Temperature of Refrigerant, T_c. The condenser temperature is generally set far below the critical temperature to avoid any deterioration in performance and problems of thermal stability. Since space requirements may call for high condenser temperatures to satisfy optimization requirements, a high critical refrigerant temperature would be most desirable. At the same time, the corresponding pressure ratio must be within practical limits; otherwise, penalties would be imposed on the compressor. To illustrate, the critical properties of common refrigerants are presented in Table 12.

An extensive search for high temperature refrigerants has been made (Reference 34) for aircraft applications. The results indicate the availability of refrigerants permitting a condenser operation above 200°F. Table 13 presents the comparative performance of some high temperature refrigerants. No promising refrigerant has been found for operation at 500°F.

Coefficient of Performance. To compare the COP attained with different refrigerants, it is adequate to use the expression for the COP of the ideal cycle given by Equation 54. Figure 44 shows the variation of the COP as a function of the fluid variables A and B for a typical operating temperature ratio of r = 1.2. For comparison, the attained values of COP for some common refrigerants (Freons) have been placed on the same graph. The characteristic values associated with the variables A and B are tabulated in Table 11.

When a wide range of temperatures is considered in the selection of refrigerants, it is common practice to consider their relative merits by calculating and comparing their COP's. A typical comparison is shown in Figure 45, where it appears that within a conventional range of temperatures, Freon 11 has a good COP. For a higher temperature range, mercury, water, or some of the high temperature refrigerants of Table 13 are better.

Table 11. Refrigerant Properties (Reference 31)

Refrigerant	$\frac{P_2}{P_1}^{*}\ \frac{136}{40}$	P_2, psia	$\frac{Q_r}{V_1}^{*136}_{40}$ $\frac{Ton}{cfm}$	L^{**} $\frac{Btu}{lb}$	c_{PL}^{**} $\frac{Btu}{lb\,^{\circ}F}$	c_{PE}^{**} $\frac{Btu}{lb\,^{\circ}F}$	$A = \frac{L}{c_{pg} T_1}$	$B = \frac{c_{PL}}{c_{pg}}$	Cycle COP Calc from tabulated data
Freon 11	6.09	42.60	.0561	77.16	0.208	0.136	1.135	1.53	4.38
Freon 12	4.07	209.9	.268	59.35	0.244	0.157	0.758	1.55	3.84
Freon 21	5.80	71.49	.0973	98.84	0.258	0.169	1.170	1.53	4.36
Freon 22	4.02	356.6	.422	75.63	0.337	0.173	0.874	1.95	-
Freon 113	7.75	20.6	.0222	65.32	0.217	0.154	0.850	1.41	4.28
Freon 114	5.27	80.15	.0905	54.26	0.239	0.161	0.674	1.49	3.82
Water	21.4	2.60	.002	1044.1	0.998	0.450	4.65	2.22	3.92

Name	Chemical Formula	Critical Temp. T_c °F	Compressor Type	Usual Evap. Temp. Range, °F
Freon 11***	CCl_3F	388.4	Centrifugal-Rotary	30 to 50
Freon 12	CCl_2F_2	232.7	Reciprocal-Rotary	0 to 50
Freon 21	$CHCl_2F$	353.3	Rotary	0 to 50
Freon 22	$CHClF_2$	204.8	Reciprocal	-130 to 0
Freon 113	$C_2Cl_3F_3$	417.4	Centrifugal	30 to 50
Freon 114	$C_2Cl_2F_4$	294.3	Rotary	0 to 50
Carrene 1****	CH_2Cl_2	421.0	Centrifugal	30 to 50
Carrene 7	74.2% CCl_2F_2 25.8% $C_2H_4F_2$	-	Reciprocal	0 to 50
Dielene	$C_2H_2Cl_2$	470.0	Centrifugal	30 to 50

*Values evaluated between 40°F evaporator and 136°F condenser
**Evaluated at 88°F
***Same as Carrene 2
****"Carrene" and "Dielene" are registered trademarks of the Carrier Corporation

Table 12. Properties of Common Refrigerants

PHYSICAL PROPERTIES OF FREON* FAMILY OF FLUORINATED COMPOUNDS□

Manufactured by E. I. DU PONT DE NEMOURS & CO. (INC.), "FREON" PRODUCTS DIVISION
Wilmington 98, Delaware

		METHANES							ETHANES			
		"FREON-11"	"FREON-12"	"FREON-13"	"FREON-13B1"	"FREON-14"	"FREON-21"	"FREON-22"	"FREON-112"	"FREON-113"	"FREON-114"	"FREON-115"
Chemical Formula		CCl_3F	CCl_2F_2	$CClF_3$	$CBrF_3$	CF_4	$CHCl_2F$	$CHClF_2$	CCl_2F-CCl_2F	CCl_2F-$CClF_2$	$CClF_2$-$CClF_2$	$CClF_2$-CF_3
Molecular Weight		137.38	120.92	104.47	148.9	88.01	102.93	86.48	203.84	187.39	170.93	154.48
Boiling Point at 1 atm.	°C. °F.	23.77 74.78	−29.79 −21.62	−81.4 −114.6	−57.8 −72.0	−128.0 −198.4	8.92 48.06	−40.80 −41.44	92.8 199.0	47.57 117.63	3.55 38.39	−38.7 −37.7
Freezing Point	°C. °F.	−111 −168	−158 −252	−181 −294	−168 −270	−184 −299	−135 −211	−160 −256	26 79	−35 −31	−94 −137	−106 −159
Critical Temperature	°C. °F.	198.0 388.4	112.0 233.6	28.9 83.9	67.0 152.6	−45.5 −49.9	178.5 353.3	96.0 204.8	278 532	214.1 417.4	145.7 294.3	80.0 175.9
Critical Pressure	atm. lbs/sq in abs	43.2 635	40.6 596.9	38.2 561	39.1 575	36.9 542	51.0 750	48.7 716	34* 500*	33.7 495	32.2 474	30.8 453
Critical Volume	cc/mol cu ft/lb	247 0.0289	217 0.0287	181 0.0277	200 0.0215	140 0.0250	197 0.0307	164 0.0305	370* 0.029*	325 0.0278	293 0.0275	259 0.0269
Critical Density	g/cc lbs/cu ft	0.554 34.6	0.558 34.8	0.578 36.1	0.745 46.5	0.64 40	0.522 32.6	0.525 32.8	0.55* 34*	0.576 36.0	0.582 36.3	0.596 37.2
Density, Liquid at 30° C. at 86° F.	g/cc lbs/cu ft	1.464 91.38	1.292 80.67	1.298 @ −30°C. 81.05 @ −22°F.	1.499 93.59	1.32 @ −80°C. 82.2 @ −112°F.	1.366 85.22	1.175 73.36	1.634 102.1	1.565 96.96	1.440 89.91	1.265 78.99
Density, Sat'd Vapor at b.p.	g/l lbs/cu ft	5.86 0.366	6.33 0.395	7.01 0.438	8.71 0.544	3.94 0.246	4.57 0.285	4.82 0.301	7.02** 0.438**	7.38 0.461	7.83 0.489	8.37 0.522
Specific Heat, Liquid (Heat Capacity) at 30° C. at 86° F.	cal/(g) (°C) Btu/(lb) (°F)	0.208	0.232	0.247 @ −30°C. −22°F.	0.217	0.27 @ −80°C. −112°F.	0.256	0.335		0.218	0.238	0.285
Specific Heat, Vapor, at Const. Pressure (Heat Capacity)‡ (1 atm.) at 30° C. at 86° F.	cal/(g) (°C) Btu/(lb) (°F)	0.135	0.145	0.133 @ −30°C. −22°F.	0.11	0.132 @ −80°C. −112°F.	0.140	0.152		0.161 @ 60°C. 140°F.	0.160	0.164
Specific Heat Ratio, at 30° C. and 1 atm. (C_p/C_v)‡		1.135	1.137	1.172 @ −30°C. −22°F.	1.136	1.220 @ −80°C. −112°F.	1.175	1.184		1.080 @ 60°C. 140°F.	1.088	1.091
Heat of Vaporization at b.p.	cal/g Btu/lb	43.51 78.31	39.47 71.04	35.47 63.85	28.38 51.08	32.50 58.44	57.86 104.15	55.92 100.66	32.8 41.0	35.07 63.12	32.78 59.00	30.11 54.20
Thermal Conductivity at 30° C. or 86° F. Liquid / Vapor (1 atm.)	Btu per (hr)(sq ft) (°F per ft)	0.0609 0.00484	0.0492 0.00557	0.09 @ −70°C. −94°F.	0.0040	0.10 @ −112°C. −170°F.	0.0687 0.00569	0.0696 0.00670		0.0521 0.00400 (0.5 atm.)	0.0447 0.00646	
Viscosity at 30° C. or 86° F. Liquid / Vapor (1 atm.)	centipoise centipoise	0.405 0.0111	0.251 0.0127	0.27 @ −70°C. −94°F.	0.212 0.0148	0.34 @ −112°C. −170°F.	0.330 0.0116	0.229 0.0131	1.21	0.679 0.0104 (0.1 atm.)	0.386 0.0117	
Surface Tension at 25° C. or 77° F.	dynes/cm	19	9		4		19	9	23 (30° C.)	19	13	
Refractive Index of Liq.	n_D^{25}	1.384	1.286				1.361	1.252	1.413 (25° C.)	1.358	1.288	
Relative Dielectric Strength at 1 atm and 23° C. (nitrogen = 1)		3.1	2.4	1.4		1.0	1.3	1.3		2.6 (0.44 atm.)	2.8	2.8
Dielectric Constant Liquid / Vapor (0.5 atm.)	temp. in °C. temp. in °C.	2.28[29] 1.0019[24]	2.13[29] 1.0016[29]	1.0013[29]		1.0006[24.5]	5.34[28] 1.0035[28]	6.11[24] 1.0035[25.4]		2.44[25]	2.17[25] 1.0021[26.8]	1.0018[27.4]
Solubility of "Freon" in Water at 1 atm. and 25° C. (77° F.)	wt. %	0.11	0.028	0.009	0.03	0.0015	0.95	0.30	0.012 (Sat'n Press.)	0.017 (Sat'n Press.)	0.013	0.006
Solubility of Water in "Freon" at 30° C. (86° F.) / at 0° C. (32° F.)	wt. % wt. %	0.013 0.0036	0.012 0.0026		0.0095 (70°F.)		0.16 0.066	0.15 0.060		0.013 0.0036	0.011 0.0026	
Flammability		nonflammable	nonflammable	nonflammable	nonflammable	nonflammable	nonflammable	nonflammable	nonflammable	nonflammable	nonflammable	nonflammable
Toxicity		Group 5A†	Group 6†	probably Group 6Δ	Group 6†	probably Group 6Δ	much less than Group 4, somewhat more than Group 5†	Group 5A†	probably less than Group 4, more than Group 5Δ	much less than Group 4, somewhat more than Group 5†	Group 6†	probably Group 6o

*"FREON" and combinations of FREON- or F- with numerals are Du Pont's registered trademarks for its fluorinated hydrocarbon compounds.

NOTES

□ A bibliography giving the source of the data used in this chart is on the reverse side

*Critical constants calculated according to Meissner and Redding, Ind. Eng. Chem., Vol. 34, 1942, p. 521 et seq.

**Calculated value based on normal deviation from ideal gas law

‡With the "Freon" compounds the value of this property varies considerably with changes of pressure and temperature

†Result of Underwriters Laboratories test; rating devised by them: Group 1, very toxic; Group 6, no evident toxicity (See U.L. Reports MH-2375 for "Freon-11", "Freon-12", "Freon-114"; MH-2630 for "Freon-21"; MH-3134 for "Freon-22"; and MH-3072 for "Freon-113", which are available from Du Pont on request)

ΔResult based on preliminary toxicological data

oResult based only on assumptions from chemical structure and analogy to other "Freon" compounds

E. I. DU PONT DE NEMOURS & CO. (Inc.)
"FREON" PRODUCTS DIVISION
WILMINGTON 98, DELAWARE

TABLE 13

Power Requirements For
Various High Temperature Refrigerants

(Reference 34)

Compound	Evaporator Temp °F	Condenser Temp °F	Required Power hp/ton (isentropic)	Condenser Heat Rejection Btu/min-ton (Compressor, 65 per cent efficiency)
1, 2-Dichlorohexafluorocyclopentene-1	120	300	2.90	389
Dibromotetrafluoroethane	120	300	3.90	455
Water	250	450	1.79	317
Dichlorobenzene	250	450	2.36	354
Freon 113	80	200	1.57	303

NOTE: Drag values assume 50 per cent momentum loss in cooling air circuit

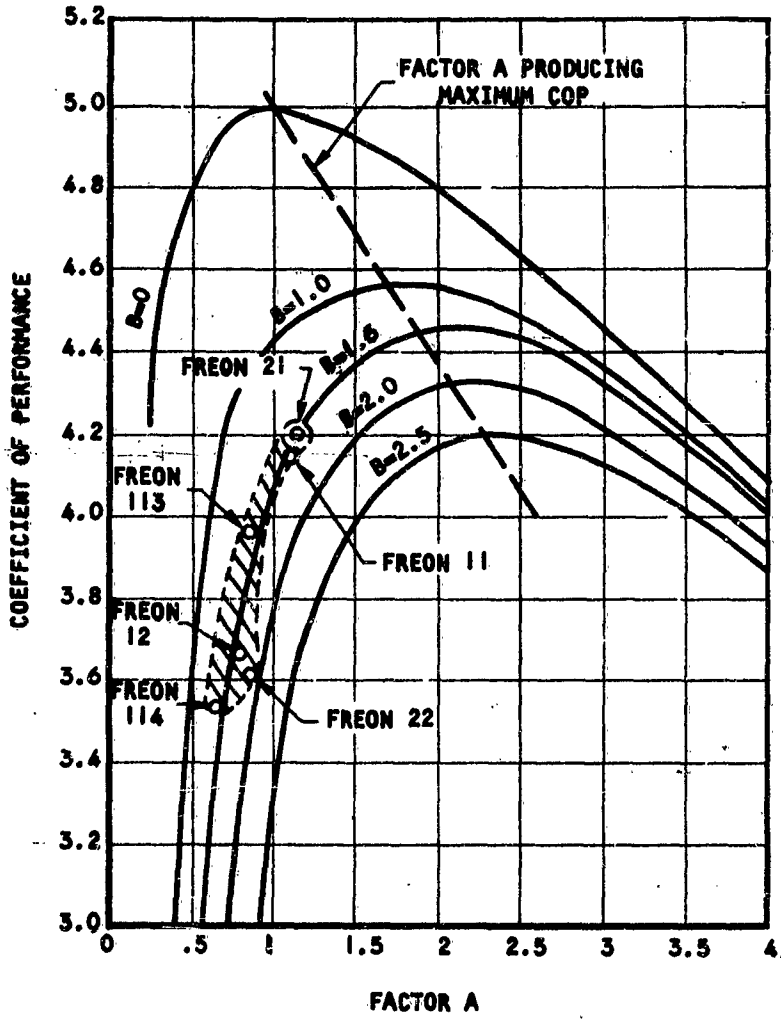

Figure 44. Relationship of Coefficient of Performance of Vapor Cycle with Factors A and B.

(Reference 31)

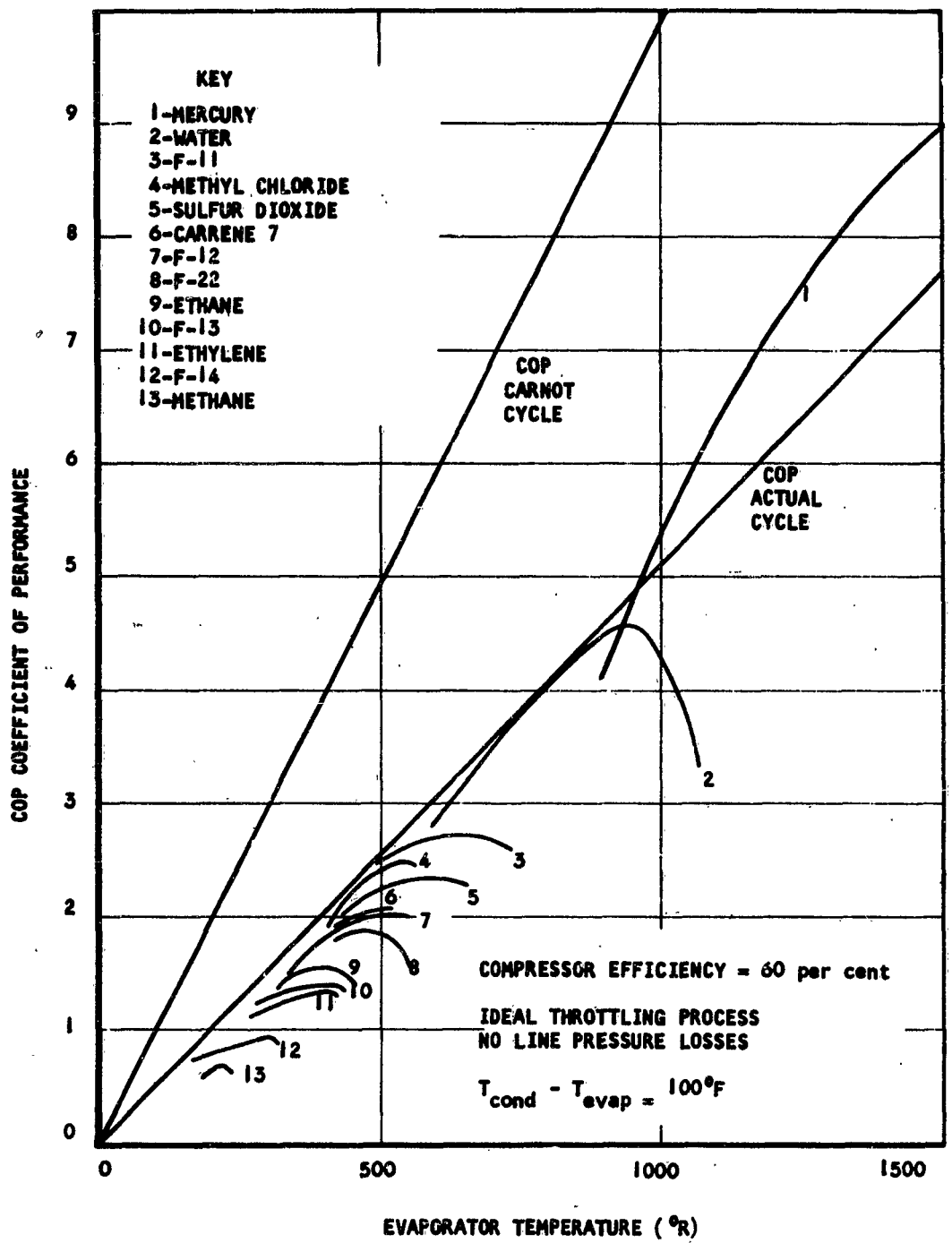

Figure 45. COP of Various Refrigerants as a Function of Evaporator Temperature (Reference 46)

Qualitative Factors

Qualitative factors, as well as thermodynamic properties, contribute to the selection of the most suitable refrigerant. The qualitative factors generally considered most important in earth-surface applications are:

corrosiveness
toxicity
flammability
handling problems
availability

In addition to these factors, space operation places emphasis on other characteristics such as behavior in weightless environments and properties associated with radiation resistance.

Among the physical properties of the refrigerants, surface tension is considered most influential in a weightless environment. For example, if mercury is used as a refrigerant, all design concepts must be modified to accommodate its non-wetting property. The commonly known refrigerants of the Freon family are wetting liquids with relatively small values of surface tension, as shown in Table 14. These low surface tensions would reduce the influence of capillary effects in components of refrigeration systems.

Refrigerants selected for space applications must have radiation resistant qualities. Fluorinated organic compounds of the Freon family are reported to break down in space environments. While refrigerant behavior under radiation has been reported principally in classified publications, Reference 35 does present data on the breakdown on Freon 11 and gamma radiation. A detailed investigation is needed on this subject since space radiation includes particles as well as electromagnetic waves.

Compressors for Vapor Cycles

Various types of compressors have been used successfully in vapor cycle refrigeration. In space application, the centrifugal type appears promising because of its light weight, small volume, and high reliability.

As in all types of compressors, the centrifugal compressor is defined by its specific speed,

$$n_s = \frac{N\sqrt{Q}}{6270\,(H_{ad})^{.75}} \qquad (58)$$

where n_s = specific speed

N = rotational speed, rpm

Q = volumetric flow at the inlet to the compressor, cu ft/min.

H_{ad} = abiabatic head, ft

Table 14

Surface Tension Of Liquids (Against Air)

(Reference 32)

Liquid	σ (dynes/cm)
Benzene	28.9
Carbon Tetrachloride	26.8
Ethyl Alcohol	22.3
Mercury	465
Water	72.8
Freon 11	19
Freon 12	9
Freon 13B1	4
Freon 21	19
Freon 22	9
Freon 112	23
Freon 113	19
Freon 114	13

For good performance, the design of these compressors should place them in the specific speed range of 0.060 to 0.20. On this basis, Figures 46 and 47 give the rotational speed required by these compressors for operation with Freon 11 and Freon 113. Assuming that good reliability can be achieved with a single-stage compressor operating at 80,000 rpm, these curves establish the lowest practical limits of application of centrifugal compressors to cooling capacity of 3.5 Ton and 1.0 Ton, for Freon 11 and Freon 113, respectively. The use of multistage compressors further lowers these limits.

Table 11 presents the possibility of the application of other types of compressors, such as the rotary or reciprocal types.

The rotary compressor of the type known under the trade name of "Hell Rotor" can be considered for application in the lower range of cooling capacity. While its performance is on a parity with other types, its mechanical design is more complex than that of the centrifugal compressor.

The reciprocating compressor can be used in very small cooling capacity (fractional tonnage) following development of high piston speeds.

Physical Characteristics of Compressors and Drive Mechanisms

Compressor physical characteristics are most important in system studies. Presently, most of the centrifugal compressors considered for active temperature control systems are driven by 400 a-c motors. They are directly driven or geared to the motor. In general, the weight of these compressors represents 15 to 30 per cent of the total weight of the compressor and motor unit. Table 15 presents the physical characteristics of these compressors. With availability of high frequency current, direct drive using a high speed electric motor would reduce considerably the weight of these units.

Table 15 provides a comparison of the physical characteristics of typical rotary and piston compressors.

Evaporators

The evaporator in a vapor cycle refrigeration system is the heat exchanger in which heat is transferred from the source to the refrigerant. In conventional evaporators operating on earth, the heat transfer regime is a mixture of two basic boiling mechanisms, one a transfer due to forced convection and the other a contribution due to pool boiling. Boiling takes place by the formation of bubbles around nuclei of unknown nature. These vapor bubbles grow and collapse with a rate controlled by the liquid temperature, pressure, and surface tension. For effective transfer, these bubbles must be continuously removed from the heat transfer area, which thus remains wet. Removal of a bubble takes place by its collapsing upon contact with a subcooled liquid, or under the influence of the inertia of the surrounding liquid. In a zero-gravity environment, there are no body forces. A still liquid without inertia does not contribute toward the removal of these bubbles. The coefficients of boiling heat transfer would therefore be

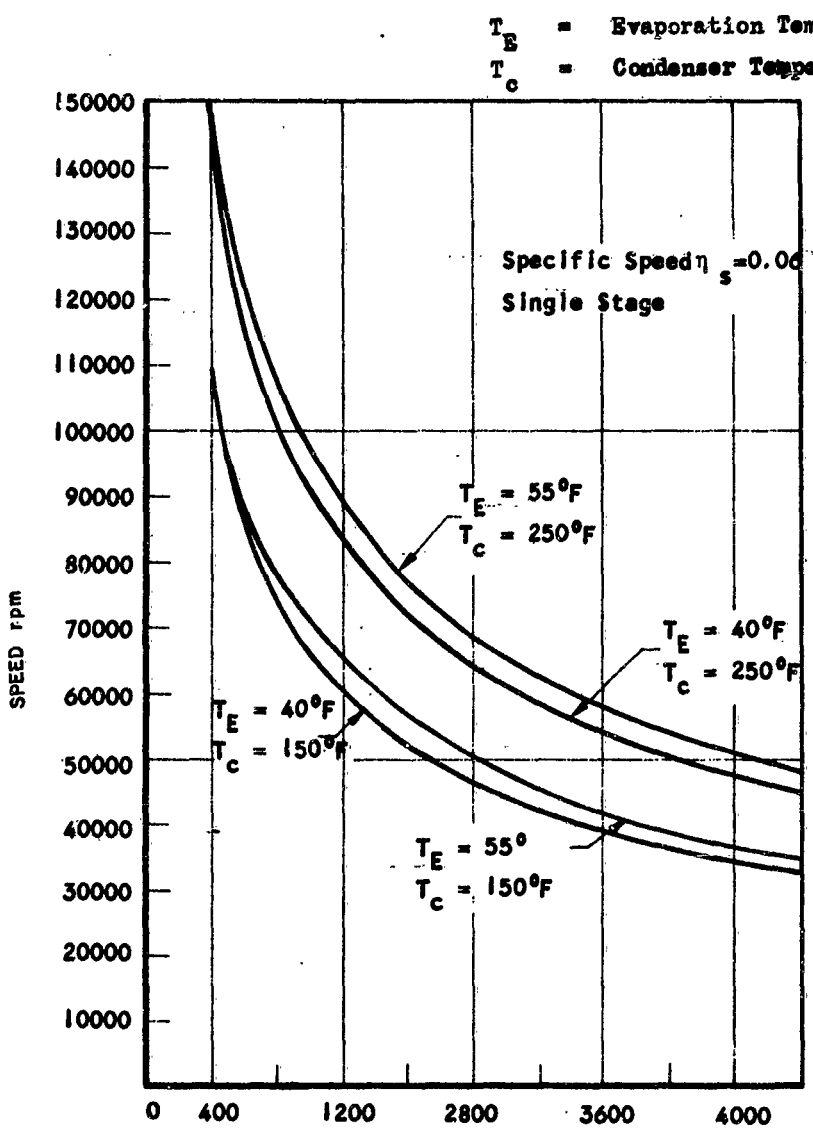

Figure 46.

Speed of Centrifugal Compressors for Various Cooling Capacity - Freon 11

(Reference 32)

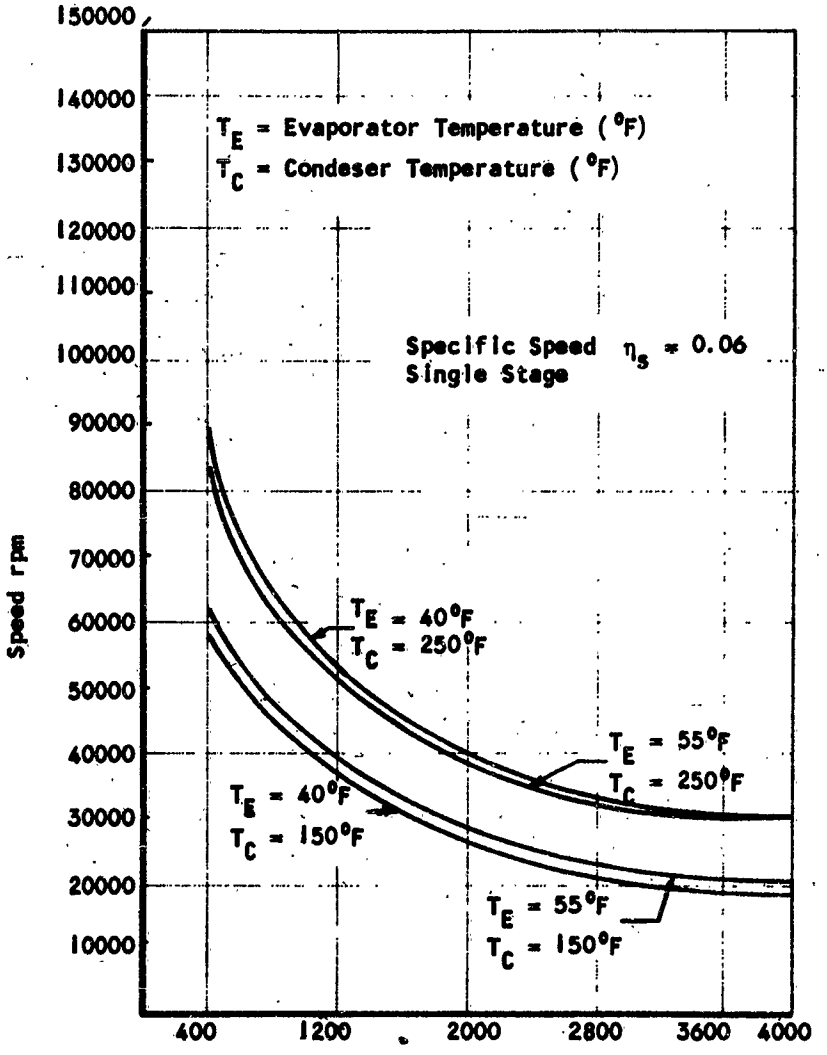

Figure 47.

Speed of Centrifugal Compressors For Various Cooling Capacities Freon 113

(Reference 32)

Table 15

Physical Characteristics Of
Typical Compressor Units

TYPE	NOMINAL HP RATING	LENGTH (in.)	DIAMETER (in.)	WEIGHT (lb)	SOURCE
Centrifugal and Electric Motors, 400 a-c	5	12.75	8.8	22.0	AiResearch Units
	10	12.75	8.8	27.5	
	25	12.75	8.8	33.5	
	50	16.00	9.0	53.0	
	100	20.00	9.25	90.0	
Heli Rotor and Electric Motor	13			35.0	Stratos
Reciprocating Electric Motor 400 a-c	1/6	7.25	4.0	7.5	Great Lakes Company
	1/3	7.50	4.0	10.0	
	1	9.10	5.0	15.5	
	5	14.00	8.0	50.4	

several orders of magnitude lower than those usually accepted. Forced convection would then remedy and help maintain the heat transfer coefficients at a higher level by contributing to the removal of the vapor bubbles.

Conventional Design

It appears that a conventional evaporator can be used for zero-g applications if the amount of forced convection is increased. This will occur at the expense of a higher pressure drop or a reduction in ΔT across the heat transfer surface.

If conventional designs are to be applied effectively to space equipment, the parameters characterizing these processes must be maintained close to the values known to yield satisfactory operation on earth, since the boiling heat transfer is a mixture of dynamic and thermal processes. For dynamic similarity, dimensionless Bonde and Weber numbers must be introducted, along with the usual Reynolds number.

The following example illustrates the evaluation of these numbers for a typical earth application design.

Given these conditions:

Freon 11 of density ρ = 91.4 lb/cu ft or 1.413 gr/ccm

Surface tension σ = 19 dynes/cm

Hydraulic diameter L = 0.1 in. or 0.254 cm

Acceleration of gravity on earth g_o = 986 cm/(sec)(sec)

Local gravity field $g = kg_o$

Flow of fluid in evaporator, V = 1 fps or 30.48 cm/sec

Bonde Number, $B_o = \frac{L^2 \rho K g_o}{\sigma} = 4.9K$

Weber Number, $W_e = \frac{\rho V^2 L}{\sigma} = 18.15$

For a Bonde number smaller than 1, the gravity field has a preponderant effect on capillary forces. In the above example, this takes place in an environment with $g = \frac{1}{4.9} g_o$. To maintain this similarity in low gravity operation, the evaporator requires a larger L and thus becomes heavier and more voluminous. As the gravity field is almost non-existent, there is increasing difficulty in keeping the Bonde number at the same magnitude as in conventional design. An investigation must be made into this deviation to determine a rational design approach.

Inertia force will be preponderant in comparison to capillary force if the Weber number is larger than 1. From the above example, a velocity of 1 fps still yields a good Weber number. Thus, it appears that this number can be easily maintained in designing for zero-gravity.

Since the thermal process is generally correlated in terms of the previous physical parameters, the heat transfer parameters possibly can be maintained within a range of practical values. Pending further investigation of the problem of zero-g boiling, these arguments are presented to support a design approach based on the conventional technique for evaporation design (Reference 31 and 32).

The size and volume of some light weight evaporators using the plate-fin, tube-fin construction are presented on Figures 48, 49 and 50. The success of the conventional approach is presently supported by the operation of the plate-fin evaporators used on the Project Mercury environmental system as shown in Figure 51. The heat transfer surface on this unit is made from offset finned packages. The offset fins act as turbulators, creating a flow field that aids vapor bubble entrainment.

Vortex Evaporators

Vortex evaporators have been considered for space applications to take advantage of the artificial gravity field induced by rotating the fluid in stationary passages. Physically, the evaporators consist of tubes with twisted tapes inserted internally. The boiling refrigerant flows inside these tubes in a helicoidal path. The rotational motion imparts an artificial gravity field in which

$$g' = \omega^2 r \tag{59}$$

where g' = "gravitational" force, in/(sec)(sec)

ω = rotational speed, radians/sec

r = radius of rotation, in.

The rotational speed ω can be calculated as shown from Reference 6 by assuming that the flow follows the twist Y of the blade with a mean axial velocity V_a,

$$\omega = \frac{30\ V_a}{Y D \left(1 - \left(\frac{\pi}{2Y}\right)^2\right)^{1/2}} \tag{60}$$

where ω = revolutions per minute

V_a = axial velocity, fps

D = diameter, ft

Y = number of diameters advanced per 180° twist

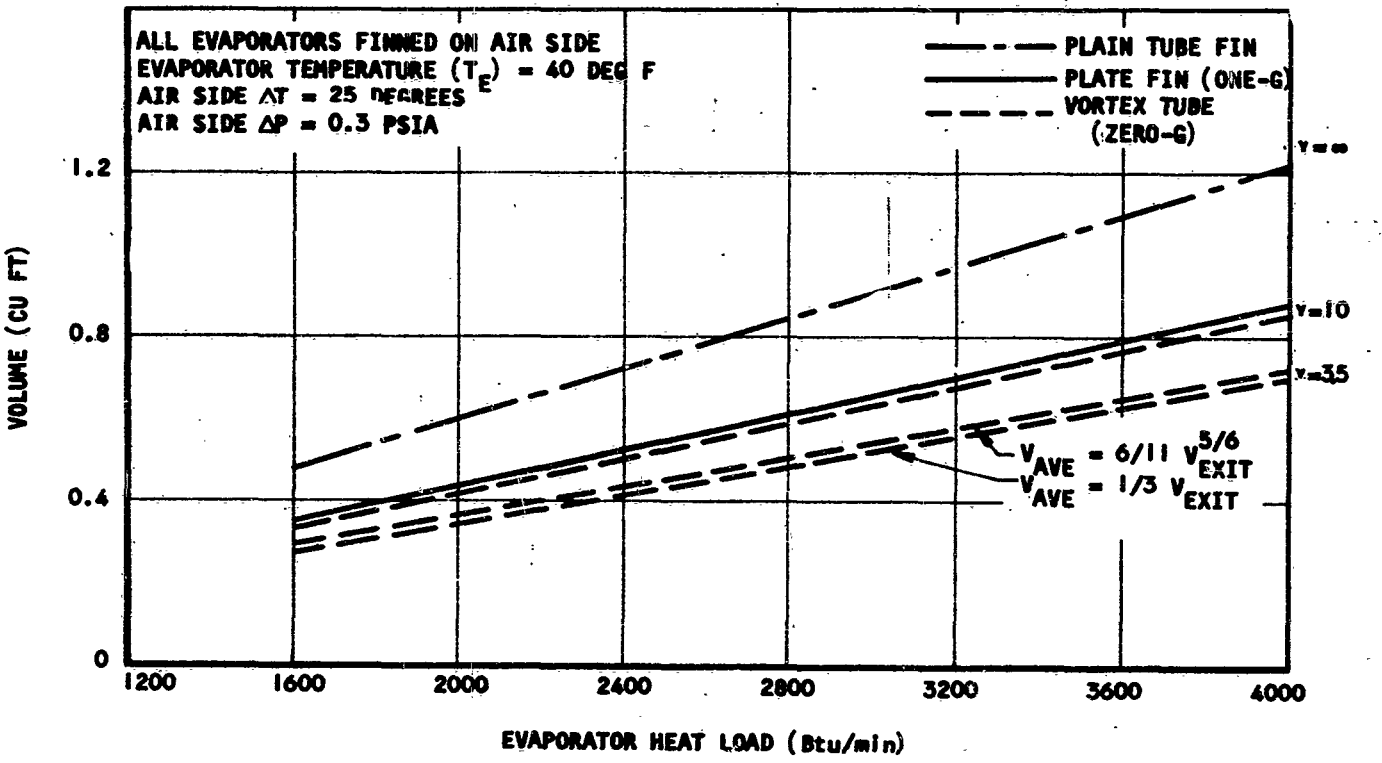

Figure 48. Comparison of Volumes of Freon 11 Plate Fin Vortex Tube and Plain Fin-Tube Evaporators.

(Reference 32)

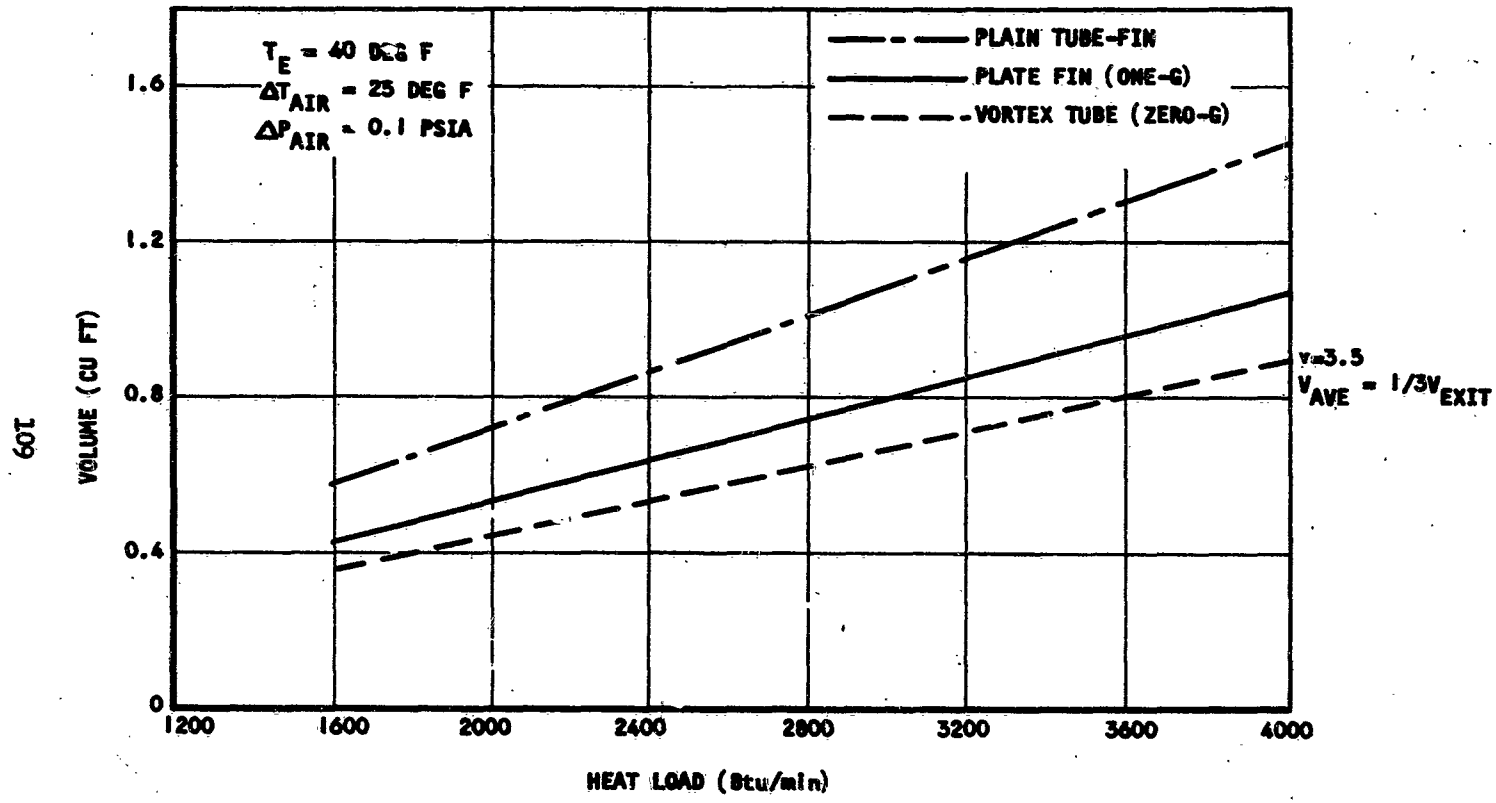

Figure 49. Comparison of Volumes of Freon 11 Plate Fin, Vortex Tube and Plain Fin-Tube Evaporators.

(Reference 32)

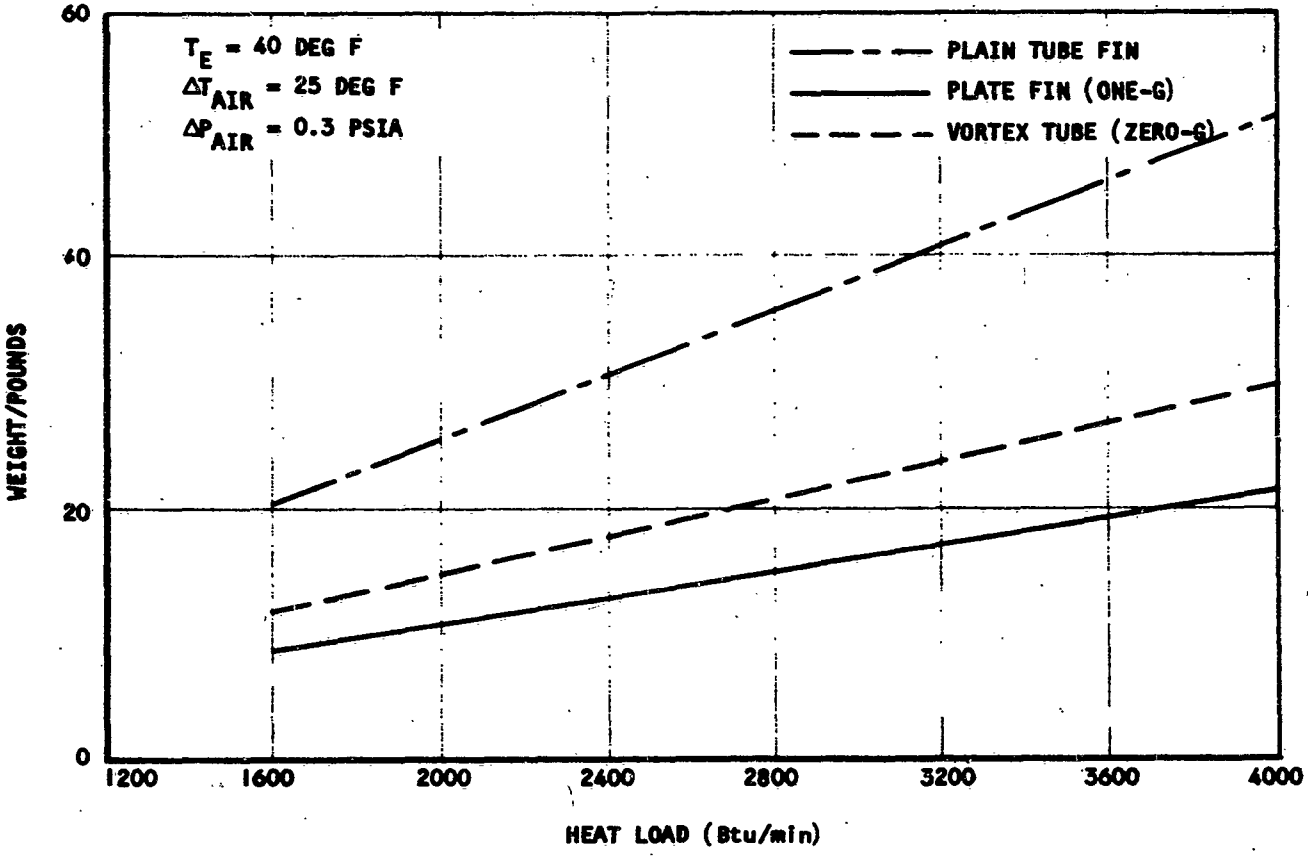

Figure 50. Comparison of Weights of Freon 11, Plate Fin, Vortex Tube and Plain Fin-Tube Evaporators.

(Reference 32)

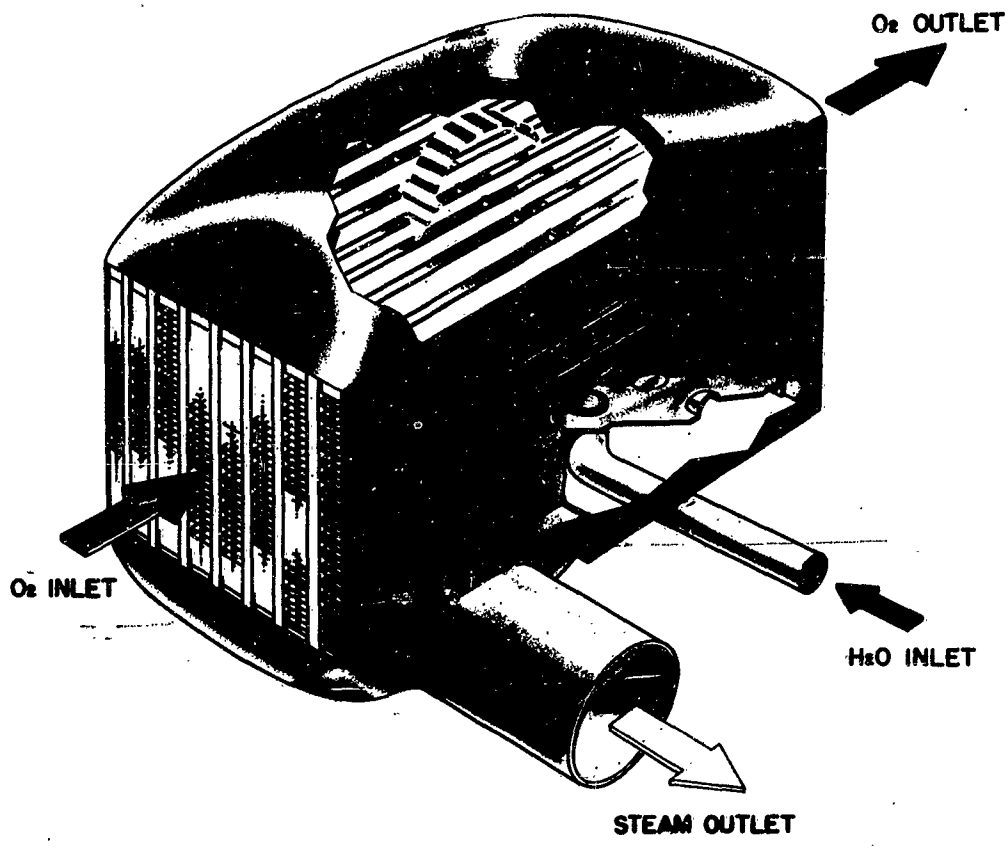

Figure 51. Environmental Control System Evaporator For Zero-gravity Operation

Preliminary evaluation of the merits of the vortex evaporators has been made with a simple modification of the Roshenow correlation for boiling heat transfer:

$$h = K \left[\frac{\omega^2 r}{g_o}\right]^{0.1} \left[\frac{Q}{A}\right]^{2/3} \qquad (61)$$

where

h = boiling heat transfer coefficient, Btu/hr-ft^2-^{o}F

g_o = acceleration on earth

K = a grouping of physical properties of this fluid (Reference 32)

Evaluation of the pressure drop due to the two-phase flow on the vortex side of the evaporator can be made from data in Reference 36 and Lockhart-Martinelli theory.

The results of the calculations of vortex evaporators carried out by Reference 32 are shown in Figures 48, 49 and 50. It appears that the vortex evaporator does offer an advantage in weight and volume accompanied by a reasonable pressure drop. These comparisons have been made with a one-g evaporator. If due consideration is given to the reasoning of the previous discussion calling for a relatively higher forced evaporation, the conventional evaporater would not take the more favorable position in the competitive picture. Although these preliminary calculations have been made with data of reasonable reliability, further investigation is still needed to insure the definite advantage of the vortex evaporator for zero-g application.

Evaporators Using Capillary Material

Capillary material has been proposed in space evaporator design to provide a liquid feed to all surfaces. Reference 32 describes a typical design using capillary material in an ice-water evaporator in which a wick, having the trade name of Liquid Lock, fills the boiling side of the heat exchanger.

A capillary evaporator for use in space applications must present some free passages for the boiling bubble to escape. Such an approach is shown in Figure 52. Here a cross-flow evaporator is presented. Air flows in one side through the plate face surfaces. Fibrous material originating from water storage lines up the other side of the heat transfer surface. The surface tension properties of the fibrous material move and distribute the water along the heat transfer surface. When evaporation takes place, the vapor escapes through the perforated spacer fin.

Besides the possibility of use in connection with a storage reservoir, the capillary material may require a forced convection lower than in other designs. Heat transfer data on these materials, particularly in zero-g

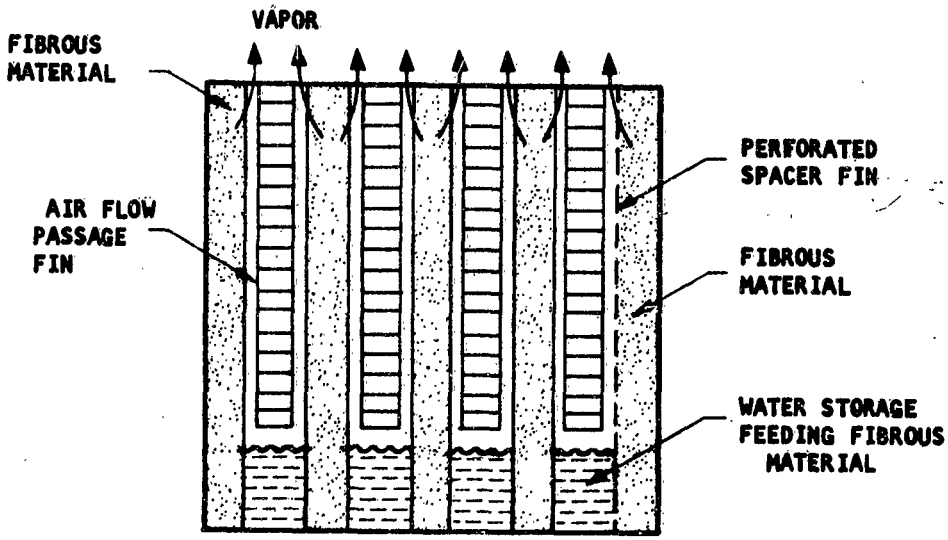

Figure 52. Proposed Design of an Evaporator Using Wick Material.

Table 16

Physical Properties And Absorption Characteristics Of Wick Materials

Sample Number and Material	Width in	Height in	Thickness in	Volume cu in	Weight lb	Density lb/cu ft	Maximum Rise in *	Time min*	Volume Ratio W_w/V_d	Weight Ratio W_w/W_d	Density Ratio P_w/P_d	Maximum Water Absorption lb/lb	Maximum Water Absorption lb/cu ft
1.Refrasil Batt							1.5	35	0.675	11.78	17.4	10.77	26.6
Dry Condition	4.0	5.0	1.0	20.0	0.0287	2.47							
Wet Condition	4.125	5.25	0.625	13.5	0.337	43.2							
2.Refrasil Bulk							6.25	31	1.00	3.87	3.87	2.87	40.9
Dry Condition	Dia.												
	Length	1.875		24.8	0.205	14.2							
Wet Condition	"	1.875		24.8	0.793	55.1							
3.DuPont Cellulose Sponge							3.5	60	1.35	10.10	7.51	9.09	31.9
Dry Condition	1.613	5.0	0.75	5.98	0.0121	3.54							
Wet Condition	1.75	5.25	0.875	8.04	0.122	26.3							
4.American Felt Co.No.7546							4.375	6600	1.03	3.68	3.58	2.68	53.4
Dry Condition	Dia.	0.28											
	Length	11.33		0.717	0.0084	20.2							
Wet Condition	Dia.	0.28											
	Length	11.94		0.737	0.038	72.3							
5.American Felt Co. 17/3 No.7545							5.25	1440	1.00	3.49	3.49	2.49	42.0
Dry Condition	2.813	6.125	0.813	14.01	0.137	16.9							
Wet Condition	2.813	6.125	0.813	14.01	0.477	58.8							

* Maximum height to which water rose in the dry specimen against gravity and the time to reach this height.

operation, are still scarce. Pending further experimentation, Reference 32 suggests using the correlation due to Gilmour

$$\left(\frac{h}{c_p G'}\right)\left(\frac{c_p \mu}{k}\right)^{0.6}\left(\frac{\rho_L \sigma}{p^2}\right)^{0.21} = 0.072\left(\frac{D_e G'}{\mu}\right)^{-0.77} \qquad (62)$$

where

$G' = \dfrac{q}{A \epsilon h_{fg}}$

q/A = heat flow Btu/(hr)(sq ft)

h = heat transfer coefficient, Btu/(hr)(sq ft)(^{o}F)

c_p = liquid specific heat Btu/(lb)(^{o}F)

k = liquid thermal conductivity Btu/(hr)(ft)(^{o}F)

p = absolute pressure lb/sq ft

D_e = dimension parameter

μ = liquid viscosity lb/(hr)(ft)

ρ = liquid density lb/cu ft

σ = surface tension, lb/ft

ϵ = porosity factor = $1 - \dfrac{\rho_{wick}}{\rho_{fiber}}$

A preliminary investigation of these materials by Reference 32 shows that material stability is the major problem. Unless the material is properly selected or the additional forced convection is kept within a limiting value, the behavior of the material alters after a period of operation. Table 16 presents the physical characteristics of some wick materials reported to be promising in Reference 32.

Condenser-Radiator

In some instances, the refrigerant of the vapor cycle rejects heat directly to the outer space without an intermediate heat transfer loop. This rejection takes place in a condenser-radiator. For simple analysis, the heat rejected per unit of cooling load is calculated as:

$$\frac{Q_R}{Q_c} = 1 + \frac{1}{\eta_{ct}\, COP_{ct}} \qquad \text{and } COP_{ct} = \frac{T_1}{T_1 - T_2} \qquad (63)$$

where Q_R = Heat rejected

η_{ct} = Carnot efficiency

Q_c = Coolant load

COP_{ct} = Carnot coefficient of performance of the vapor cycle

T_1 = Condenser temperature

T_2 = Evaporator temperature

If this heat rejection is to an absolute-zero outer space, the radiator area is then given by

$$Q_R = \left(1 + \frac{1}{\eta_{CT}} \frac{1}{COP_{CT}}\right) Q_c = A \sigma \epsilon T_1^4$$

$$\frac{A}{Q_c} = \frac{\sigma \epsilon T_1^4}{1 + \frac{1}{\eta_{CT} COP_{CT}}} \qquad (64)$$

Equation 64 is shown on Figure 53 to offer a rapid estimate of the required radiator area. It is calculated for an evaporator temperature of 40^0F (T_2) and an assumed emissivity of the radiator surface of 1.

Conventional Condensers: Design with Tapered Tubes

In applying conventional techniques to the design of condensers required to operate in weightless environments, the main problems are:

a. Maintaining a reasonably stable flow at the interface of the condensing film and the vapor.

b. Coalescing and collecting the condensed refrigerant.

Stability of the Flow

With wetting refrigerants, such as Freon, a thin layer of condensate tends to form on the condensation. Non-wetting fluid such as mercury appears in the form of condensate droplets. If the vapor velocity is sufficiently high, the interface between vapor and liquid becomes unstable. Any small perturbation will be amplified and thus tend to destroy the continuity of the interface. A "sluggy" flow takes place with an increase in pressure drop and with the resulting possibility of completely clogging the condensing side of the condenser. The decrease in condensing heat transfer coefficient may be a negligible adverse effect since the controlling coefficient is generally on the cooling side, that is, the radiating of intermediate heat transfer loop sides.

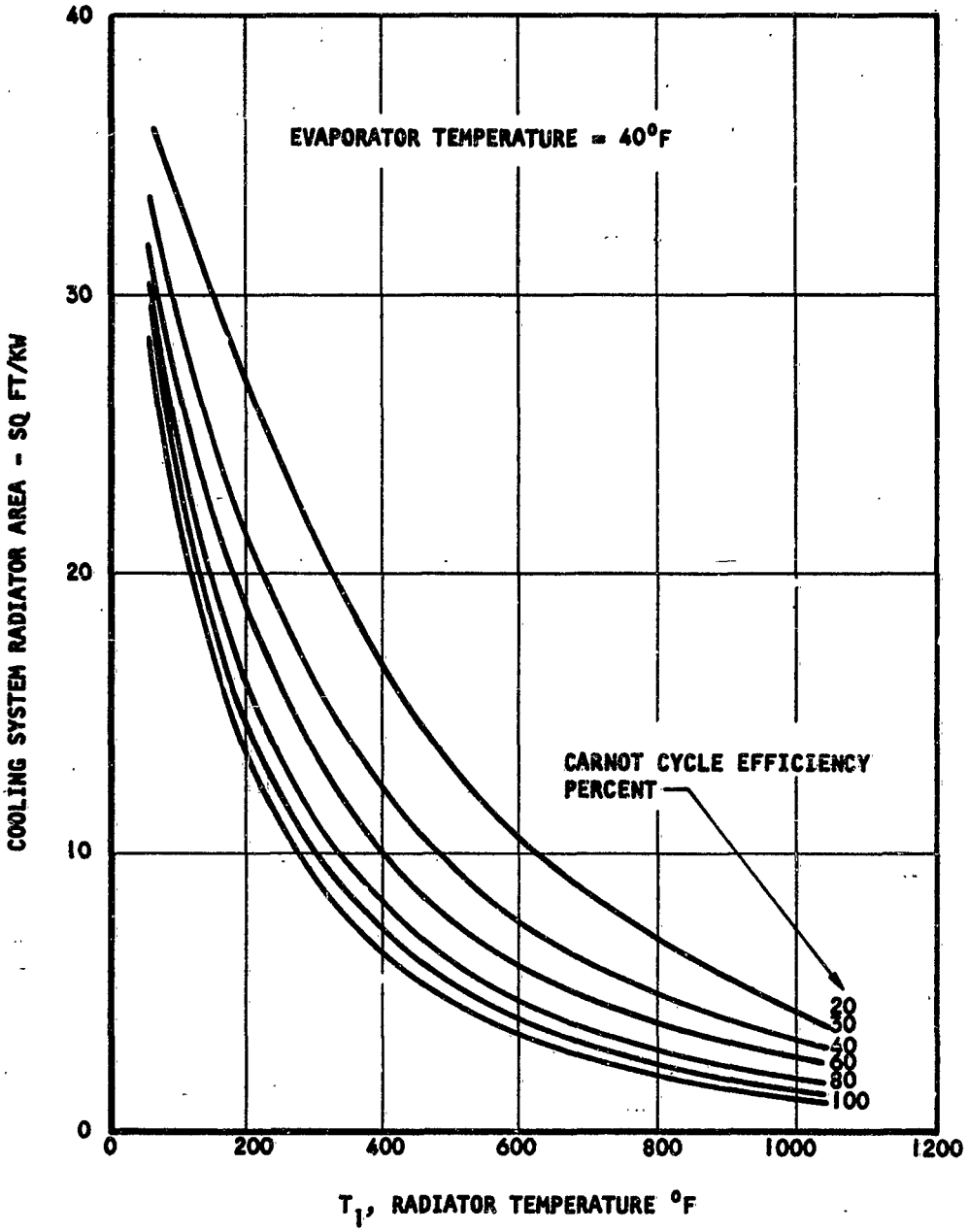

Figure 53. Radiator Area vs Radiator Temperature for Cooling System.

(Reference 44)

Factors contributing to the stability of the interface are discussed below:

Viscosity. Higher viscosity results in an increase in the damping of all the disturbances. For Freon type refrigerants the viscosity is relatively small; thus, in laminar flow stabilizing with viscosity effect is less feasible.

Turbulence. A condensate film with a turbulent flow regime will have good damping characteristics. As Freons have low kinematic viscosity, the condensate film will soon reach the transition Reynolds number and benefit from the subsequent turbulence.

Gravity Field and Surface Tension. The stabilizing effects due to gravity and surface tensions have been extensively examined. In a zero-g field, condenser operation is closely related to surface tension effect. Stability then consists of maintaining the velocity of the vapor phase below the critical value. Theoretical investigations of the hydrodynamic stability of thin films of condensate reported in Reference 39 show that if the Reynolds number and Weber number of the condensate are kept within the range shown in Figure 54, stability exists for a wide range of small disturbances. The following examples illustrate the use of this relationship.

Given:

Condensing Freon 11 = 250°F

Tube diameter = 0.2 in.

Condensate thickness = .001 in.

The corresponding Reynolds and Weber numbers are tabulated for typical vapor velocities, V, in the following:

Velocity, fps	Reynolds Number	Weber Number
1	1.37½	.15
10	13.74	15.0
50	68.7	395.0
100	137.4	------

Figure 54 shows that the velocity of 1 fps an absolute stability exists. For velocity of the order of 50 fps or higher there is a possibility of instability. The tolerable degree of instability for a satisfactory condensing process has not been determined. Therefore, the theoretical analyses can at best serve as a guide to the designer.

Coalescing and Collecting the Condensed Refrigerant

This will also be a problem in zero-g environment. Although sponge materials have been suggested, the most practical solution currently

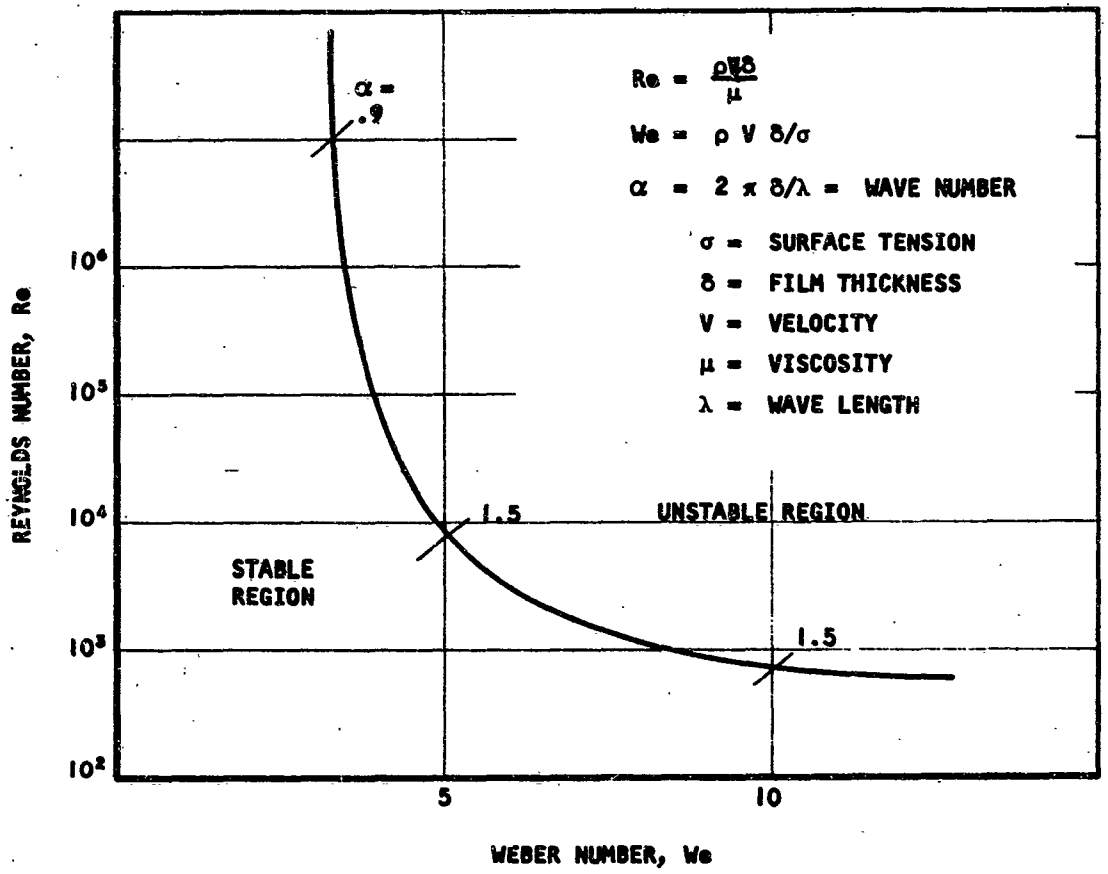

Figure 54. Domains for Two-Phase Flow Stability.
(Reference 39)

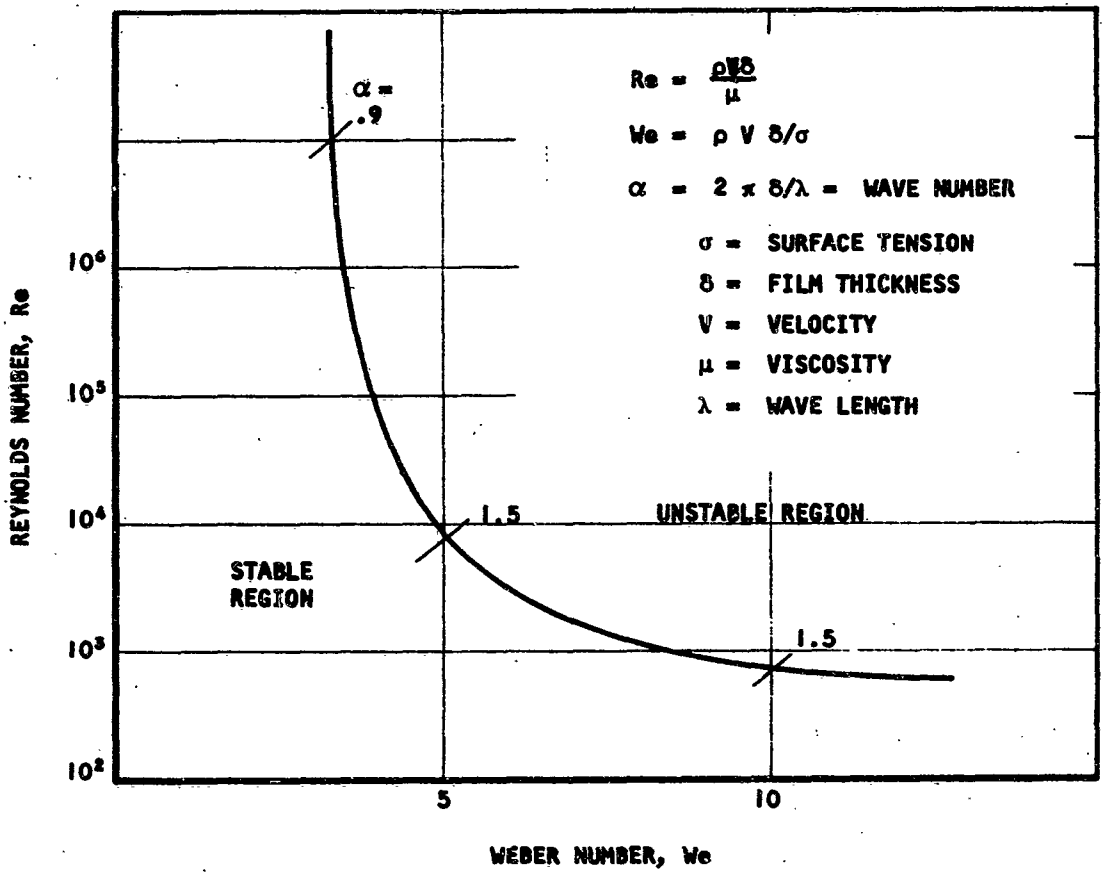

Figure 54. Domains for Two-Phase Flow Stability.
(Reference 39)

seems to be in a tapered tube configuration. In Figure 55, the surface forces acting on the fluid (pressure and surface tension) will cause a slug of a wetting liquid to migrate towards the larger end and a non-wetting liquid toward the smaller end. Under forced condensation in a tapered tube, a slug will be drawn into the header of the condenser in one direction or the other. Besides this, the taper helps to maintain the vapor velocity constant, thereby avoiding the usual deceleration of flow found in a constant diameter tube. Because of potential advantages of the condenser-radiator with tapered tubes, a detail treatment of the subject is warranted.

Heat Transfer Coefficient on the Condensate Side

For space design, it is generally assumed that the controlling thermal resistance is on the radiating side; the film condensation coefficient is much higher than the radiating coefficient. In the design of ground equipment, the film condensation coefficient is given by well-known heat transfer correlation data. The question now arises, however, as to the applicability of this relationship to space equipment. Pending further classification on this matter, a low limit to this coefficient can be evaluated by assuming that heat transfer takes place by conduction only. The relative values of the h_c and h_r are given as

$$h_c = \frac{4k}{d_h}$$

$$h_r = \sigma \epsilon T^3$$

$$\text{then} \quad \frac{h_c}{h_r} = \frac{4k}{\sigma \epsilon d_h T^3} \tag{65}$$

Reference 32 gives the numerical values of the ratio shown in Table 17. It appears that for Freon 11, the assumption of the radiating side as the controlling thermal resistance is still valid.

Size and Weight of Condenser-Radiators

To arrive at the size and weight of a radiator using tapered tubes, the following assumptions are made:

a. Condensation in the tube is uniform, and 90 percent or more of the entering saturated vapor is condensed in the tube. This condition must exist to produce the situation pictured in Figure 55 which permits easy coalescing and collecting of the liquid condensate in a zero-g environment.

b. The thickness of the condensate film in the tube is negligible compared to the tube diameter. The vapor velocity and the tube length are constant.

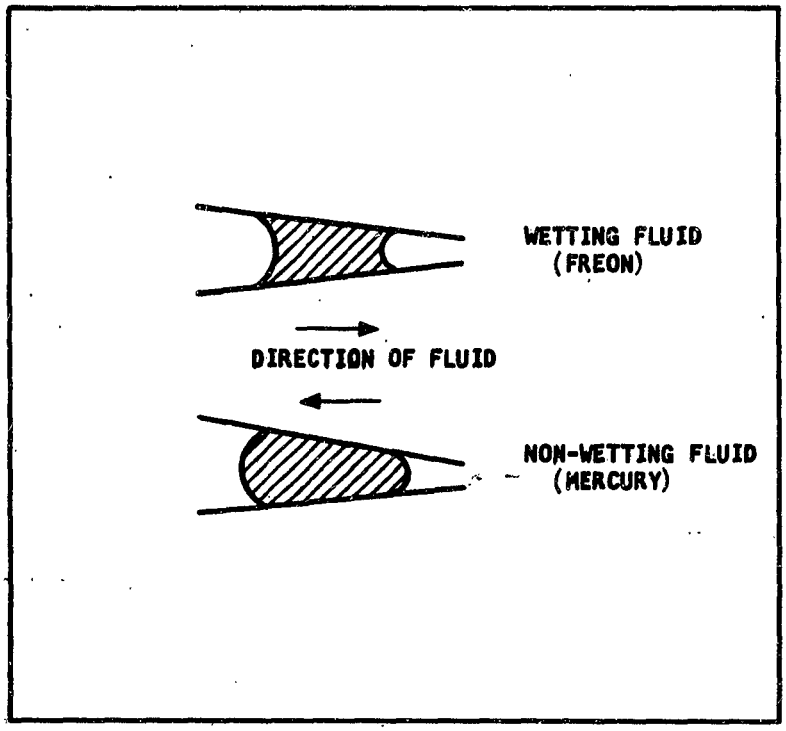

Figure 55. Influence of Surface Tension on Tapered Tubes

Table 17

Minimum Ratios For Condensing-Side To Radiating-Side
Heat Transfer Coefficients For Integral Condenser-Radiators

Fluid	Saturation Temperature °F	Condensation Tube Diameter in.	$(h_c/h_r)_{min}$
Freon 11	320	0.5	3.6
Freon 11	320	2.0	0.9
Freon 11	250	0.5	1.57
Freon 11	150	2.0	3.25
Mercury	400	0.5	640
Mercury	400	0.5	160
Sodium	800	0.5	1120
Sodium	1250	0.5	396
Sulphur	400	2.0	2.0
Sulphur	1100	2.0	0.5

c. The physical dimensions of a radiator element consisting of a tapered tube and the corresponding fin area are shown in Figure 56. Mean arithmetic values have been taken wherever integration of a variable dimension is required.

d. The elemental radiator is designed around a fin of aluminum weight, which according to Reference 40, occurs with

$$\eta_f \cong 0.575 \; ; \; \sqrt{\frac{48\sigma\epsilon T^3}{K\delta}}\,\bar{L} \cong 1.8 \; . \tag{66}$$

The equations for determining the required length of the tube to condense a fraction F of the entering mass of vapor is given by:

$$\frac{Q_R}{N} = \rho V\left(\frac{\pi}{4} D_o^2\right) F h_{fg}$$

$$= \epsilon\sigma T^4 X_1 \left[\bar{D} + 2.07\sqrt{\frac{K\delta}{48\sigma\epsilon T^2}}\right] \tag{67}$$

The weight of the radiator element is calculated from the expression

$$\frac{W_{NT}}{N} = \rho_f X_1 \frac{\delta}{12}\left(\bar{D} + 2\bar{L}\right) + \rho_t X_1 \pi\left(\bar{D} + \frac{t}{12}\right)\frac{t}{12} \tag{68}$$

The specific weight of the radiator is given by Equations 67 and 68

$$\frac{W_T}{Q_R} = \frac{\rho_f \frac{\delta}{12}\left(\bar{D} + 2\bar{L}\right) + \rho_t \pi\left(\bar{D} + \frac{t}{12}\right)\frac{t}{12}}{\epsilon\sigma T^4\left(\bar{D} + 2.07\sqrt{\frac{K\delta}{48\sigma\epsilon T^2}}\right)} \tag{69}$$

With this design approach, the specific weight is seen to be independent of the rate of heat transfer. It depends only on the physical dimensions of the passages and the radiator temperature.

From Reference 40 the pressure drop in the elemental radiator is,

$$\frac{\Delta P}{X_1} = \frac{1}{12}\left[\frac{4 - 11a + 10a^2 - 3a^3}{(1-a)^4}\right]\frac{dP}{dx_o}$$

$$\frac{dP}{dx_o} = 0.1007\,\frac{f}{\sigma g}\left(\frac{W}{N}\right)^2 \tag{70}$$

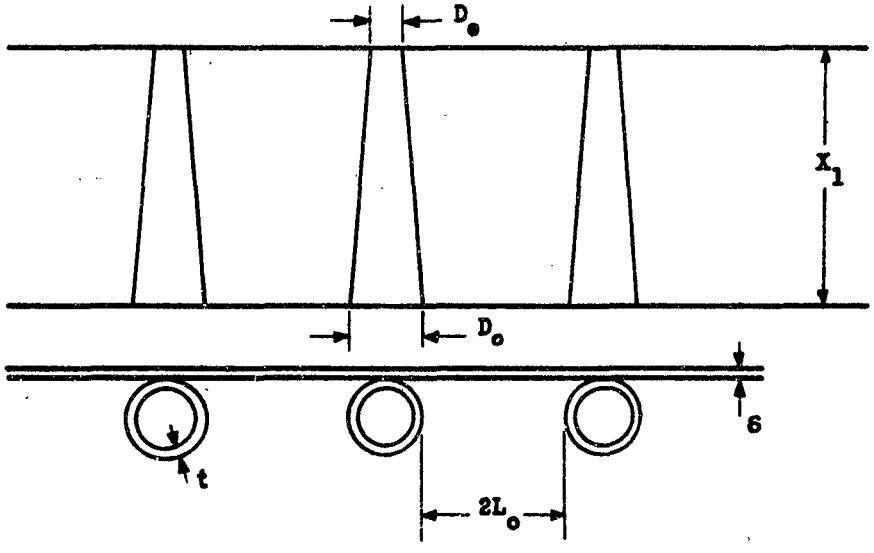

$$a = 1 - D_e/D_o$$

$$\bar{D} = \frac{D_o + D_e}{2}$$

$$\bar{L} = L_o + \frac{D_o - D_e}{2}$$

Figure 56. Geometry of Tapered Tube Condenser - Radiator.

TAPERED TUBE RADIATOR

EMISSIVITY	=	0.9
TUBE THICKNESS	t =	0.020 IN.
FIN THICKNESS	=	0.020
TUBE MATERIAL		
FIN MATERIAL	=	173 LB/FT^3
95% CONDENSATION IN TUBE		
VAPOR VELOCITY		1 FPS at 250°F Condenser
		10 FPS 150°F Condenser

FREON 11

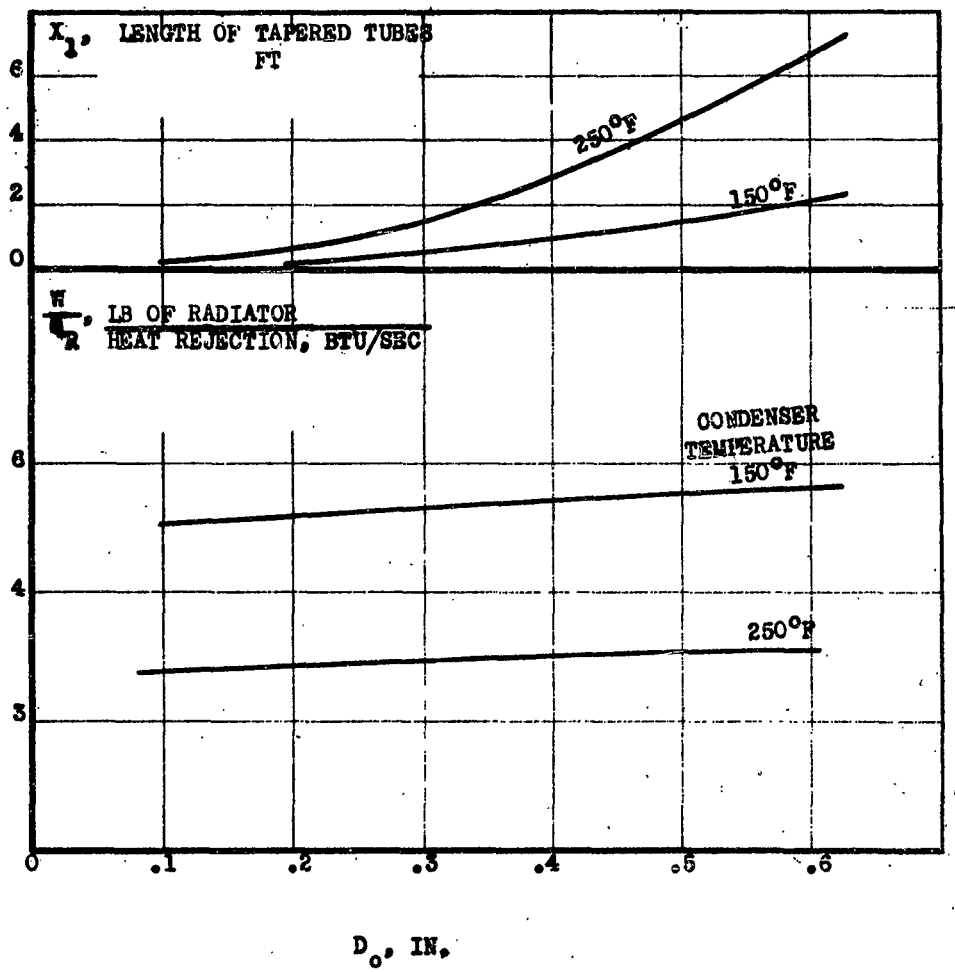

Figure 57. Condenser Radiator Characteristics with Freon 11

The friction factor is that of a two-phase flow given by the correlation of Martinelli, Bergland-Gazley or Koster in Reference 41.

As an illustration of this design procedure, Figure 57 presents the characteristics of a condenser-radiator for Freon 11 at 150°F and 250°F, where 95 per cent of the entering vapor is assumed to be condensed. The specific weight shown applies also to other refrigerants operating at the same temperatures, in accordance with the previous analytical expression. The pressure drop, calculated with extrapolated data of Bergland-Gazley, is of small magnitude, a condition that satisfies the assumptions used in the design approach presented here. From Figure 57 it is seen that the specific weight changes little with tube diameter. Proper diameter is determined by the space available for the radiator length and also the taper angle of the tube. For instance, very small tubes have considerable taper angle that precludes all the assumptions used in the calculation.

Condensers with Curved Passages

Curved passages have been proposed for space condensers to provide a force similar to that of gravity. Here, the entire mass of the condensing refrigerant flows over a helicoidal path. At any point along its trajectory, the fluid is subject to centrifugal force due to local acceleration defined by the tengential speed and the corresponding radius of curvature of the path.

Two contributions account for the heat transfer in curved passages of the condensing refrigerant shown in Figure 58. As the condensate layer on Wall B is relatively thin due to centrifugal action, there is good heat transfer. On the other wall, the condensate layer

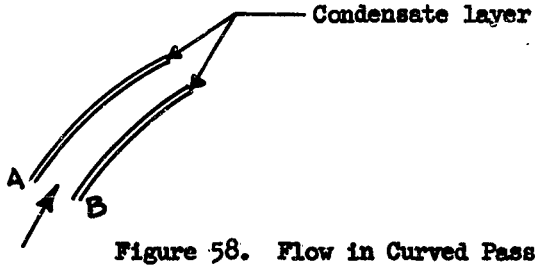

Figure 58. Flow in Curved Passages

is thicker. The heat transfer rate is compensated, however, on mixing due to the secondary flow inherent in curved passages, and the fluid temperature will be closer to that of the Wall A. As a result, heat transfer rates are practically the same on both walls. Usually, these rates are taken as those of the flat plates (Reference 42).

A conceptual design of a condenser with curved passages is given in Reference 32 and shown in Figure 59. This spiral condenser consists of curved layers in which the coolant and condensing refrigerant flow is

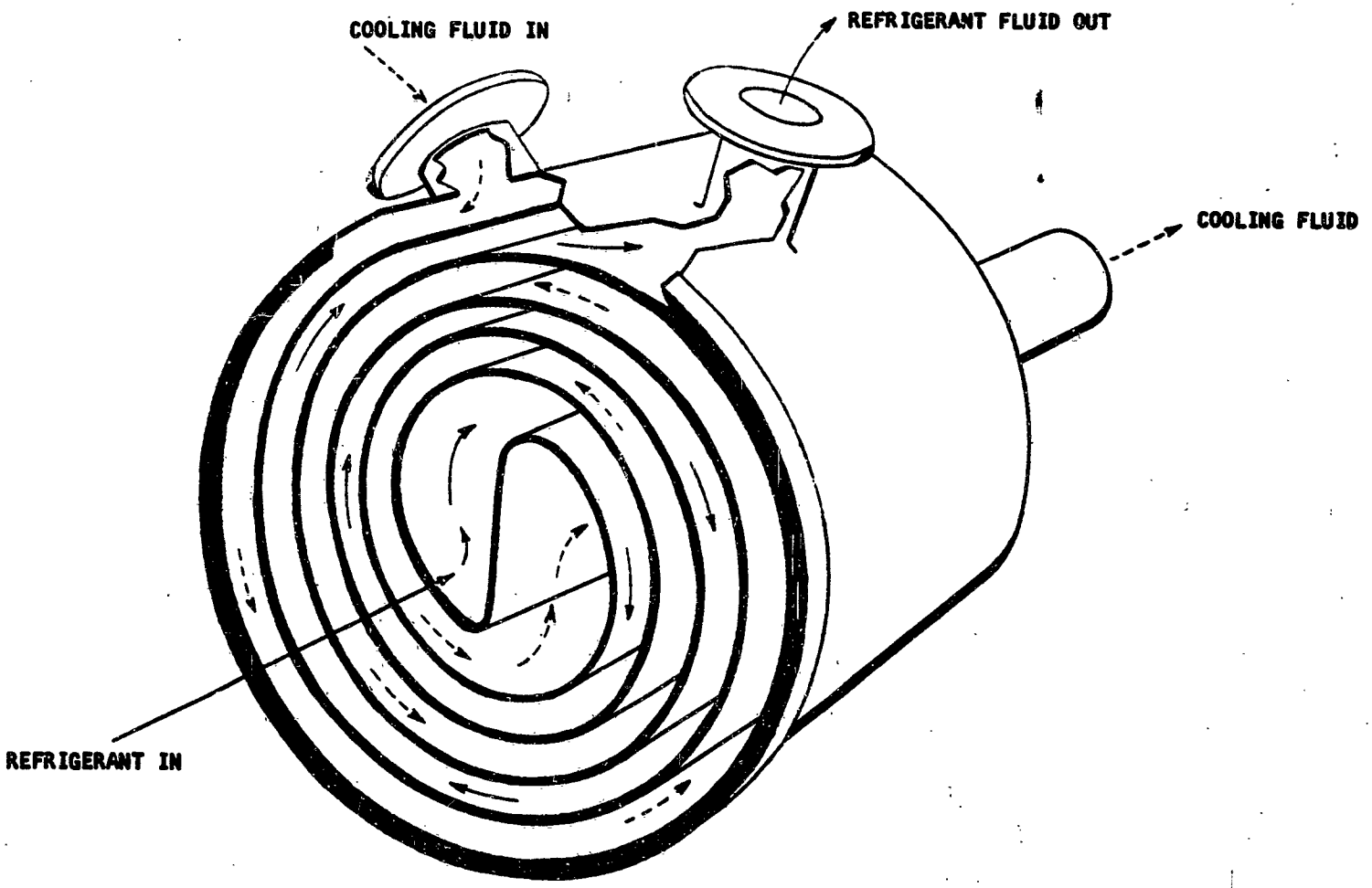

Figure 59. Diagram of a Spiral Condenser (Fluids in Counterflow)
Reference 32

counter-current. For some typical operation of vapor cycle systems, Reference 32 reports a preliminary design study yielding the characteristics of spiral condensers. The heat transport fluid was taken as an alloy of sodium and patassium (22% Na - 78% K) that melts at 12°F and has a high conductivity.

Pending further experimental work, the feasibility study has been made with the same design procedure as for a ground-use condenser. A relatively good vapor velocity (20 fps) and a resulting condensing heat transfer coefficient of 275 Btu/(hr)(sq ft)(°F) have been used. Flat plate data have been applied without consideration of the stability of flow or the slugging under zero-g operation. The computed characteristics of the spiral condenser derived from this study are shown in Figure 60 through 62.

Rotating Condensers

Another method for providing the body forces required for satisfactory condensation in zero-gravity environment is to use a centrifugal force supplied by rotating the equipment itself, the principle of operation in a rotating condenser.

Figure 63 illustrates a rotating condenser design. Vapor from the compressor is sprayed on a series of rotating hollow discs cooled by coolant flow. The vapor condenses in these discs and the liquid condensate, in the form of droplets or thin film, is centrifuged outward by the rotation of the discs. The liquid is collected in an annular channel from which it is returned to the liquid main due to a pressure difference.

Though a rotating condenser, with its extra power requirements and complex design, is thought to offer little promise compared to other approaches, a fully detailed design study has been carried out in Reference 32. The weight and power requirements of vapor cycle systems using Freon 11 are shown in Figure 64 and 65 for some typical operating conditions.

Actual Performances of Vapor Cycle Systems

Actual performances of vapor cycle systems are often needed for comparative studies such as system analysis. While system performance can be calculated from that of the components, it is desirable to get a rapid approximation of the actual value without detailed calculation. This is best handled by the introduction of a cycle efficiency defined as:

$$\eta_{cycle} = \frac{\text{Actual COP of cycle}}{\text{Ideal COP of cycle}}$$

The actual COP is calculated, accounting for the performance of all the components, while the ideal COP is evaluated from purely thermodynamic processes. For illustrative purposes, Figure 66 presents the cycle efficiency achieved on a high speed aircraft vapor cycle system as derived from preliminary calculations found in Reference 1.

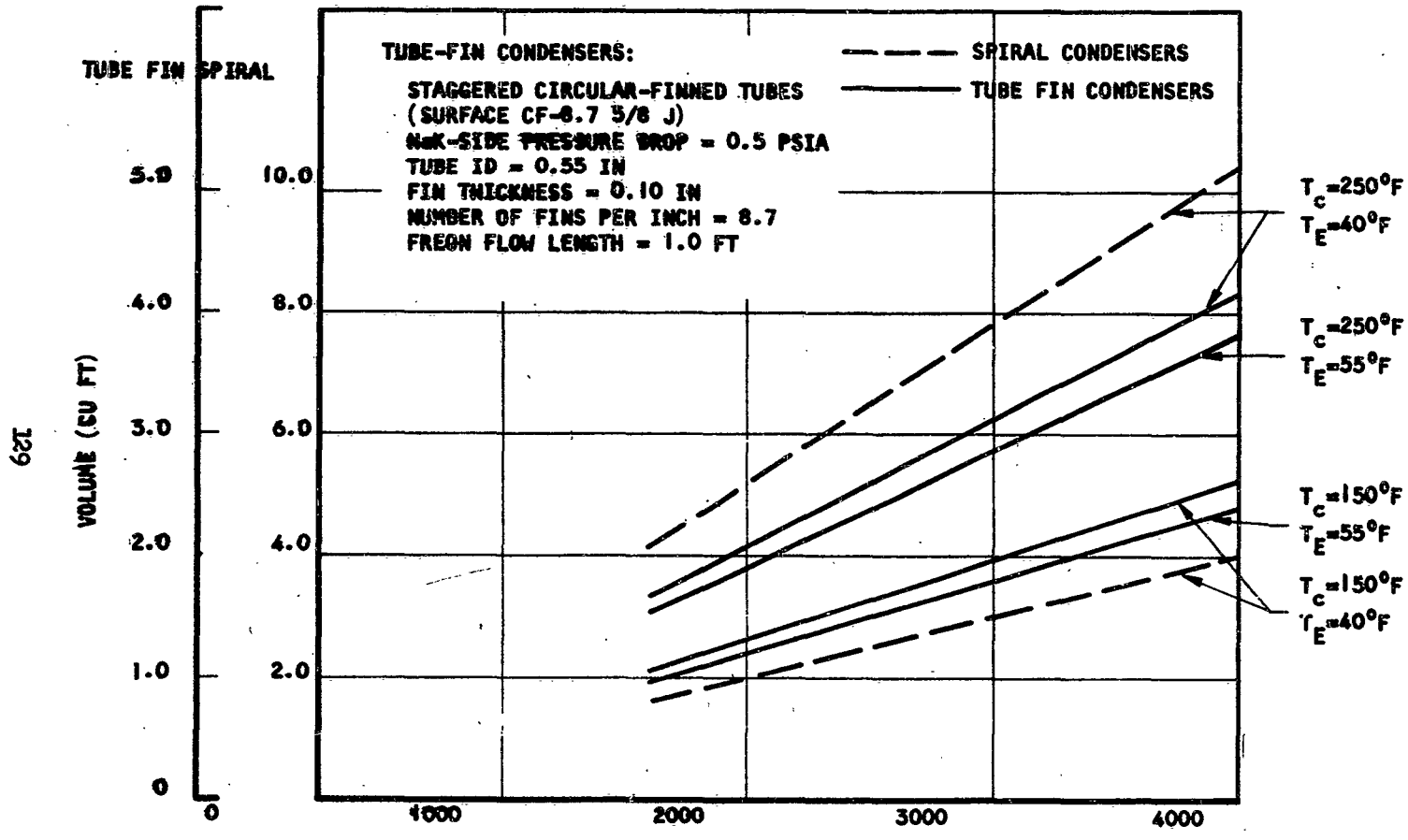

Figure 60. Comparison of Volumes of Freon 11 Spiral Condenser (Zero-G) With Large Tube-Fin Condensers (One-G)

Reference 32

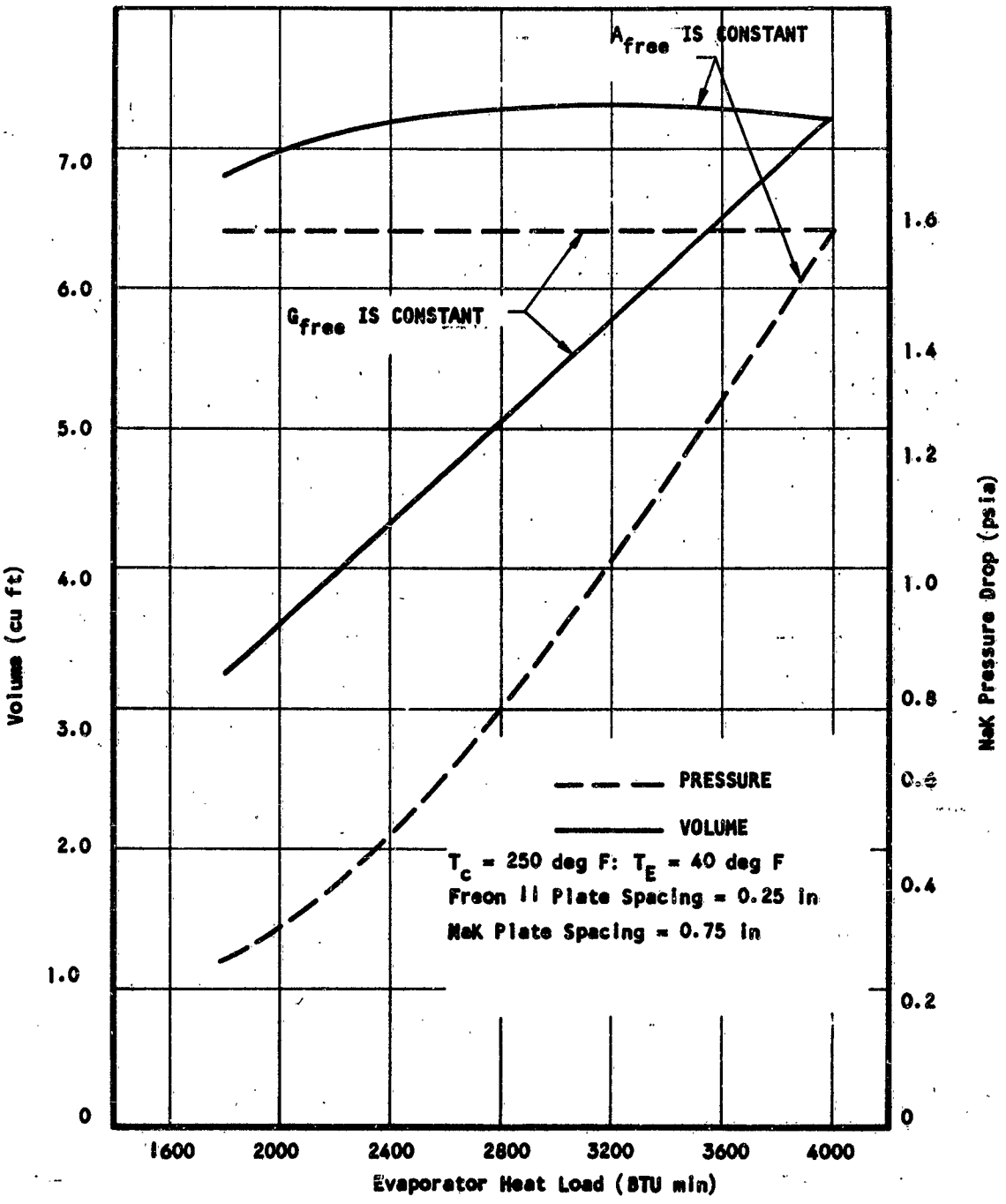

Figure 61. Volume and Pressure Drop for Freon 11 Spiral Condenser Reference 32

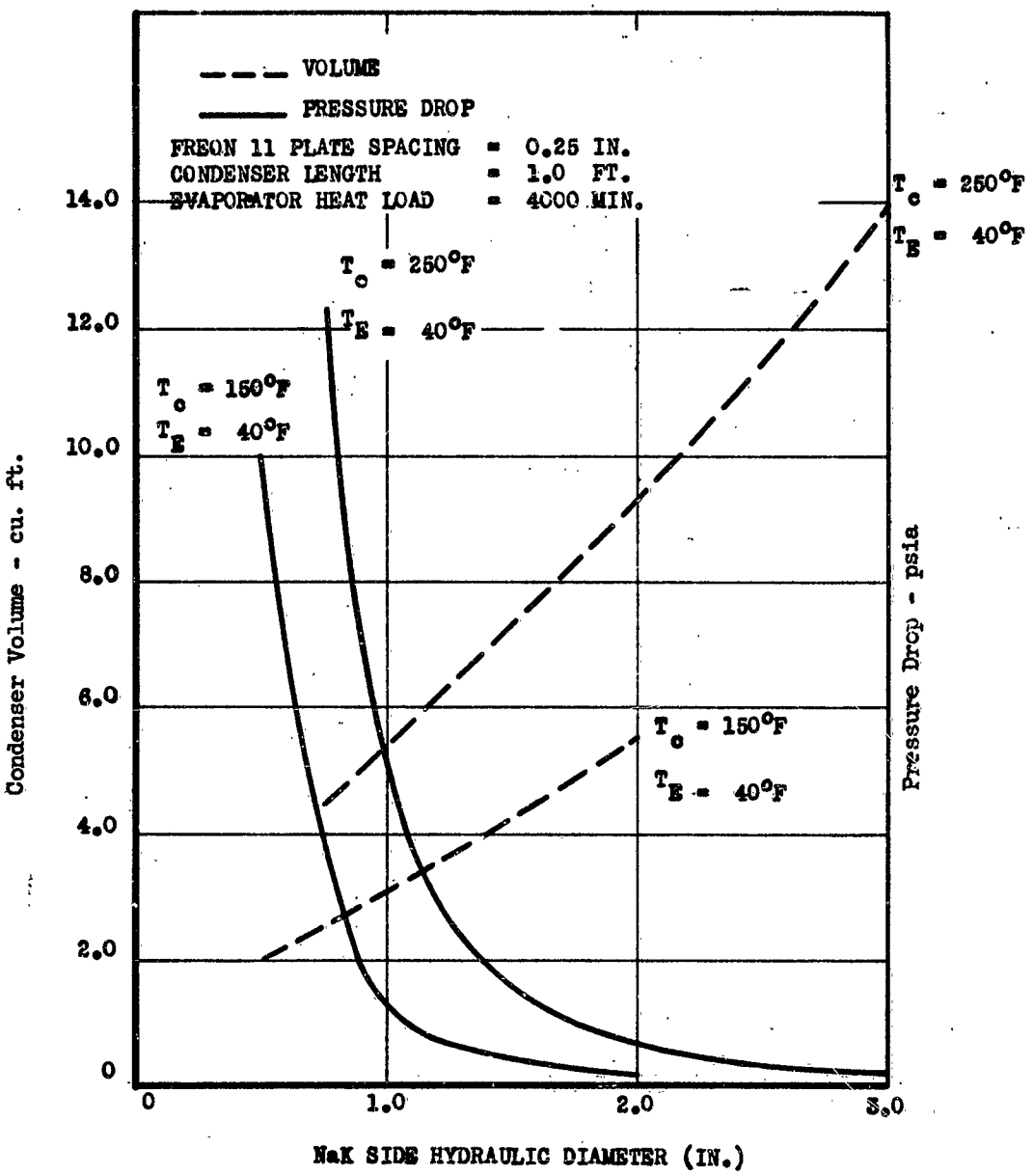

Figure 62. Variation of Freon 11 Spiral Condenser Volume and Pressure with NaK-Side Hydraulic Diameter (Reference 32)

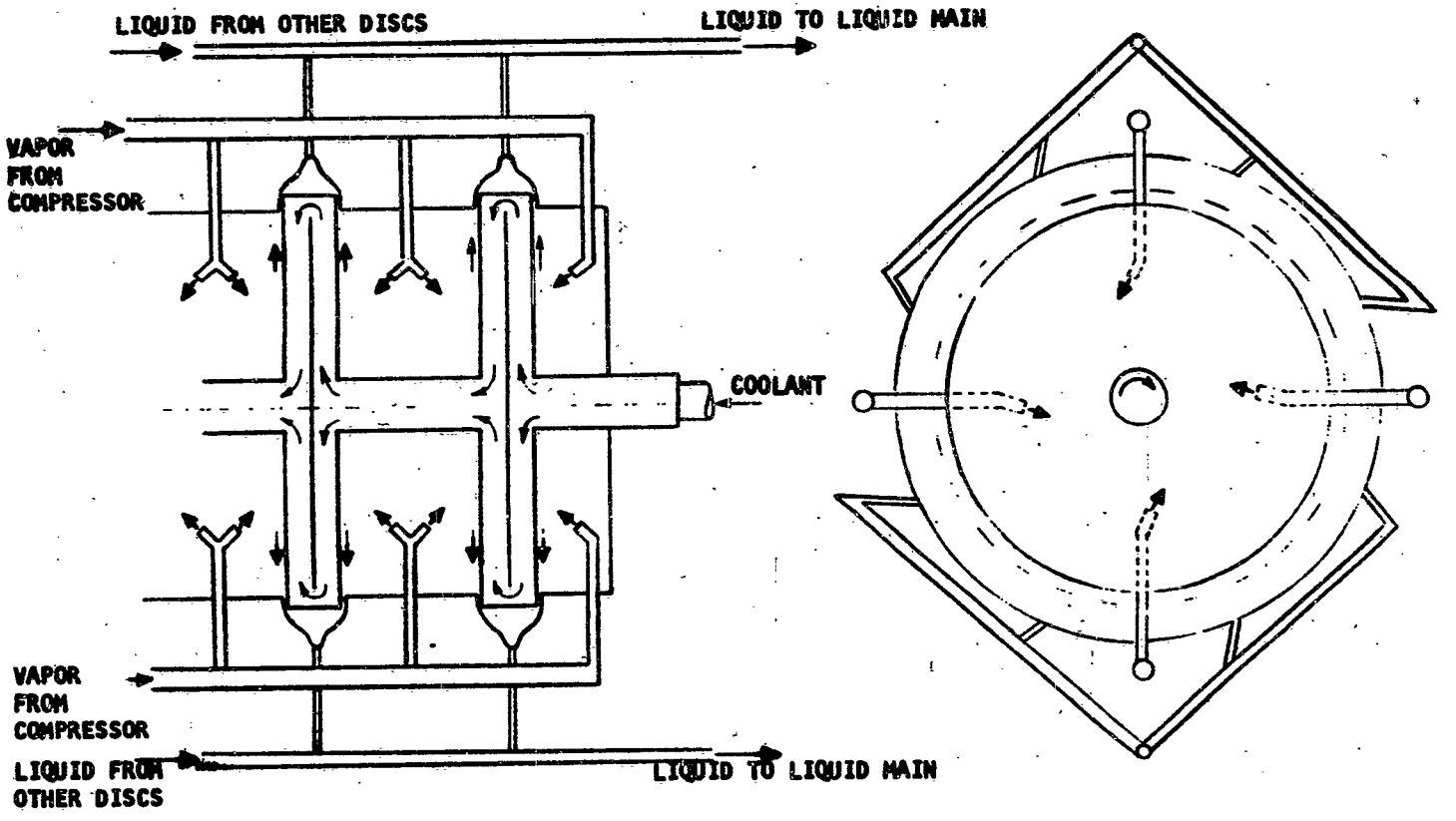

Figure 63. Rotating Condenser
(Reference 32)

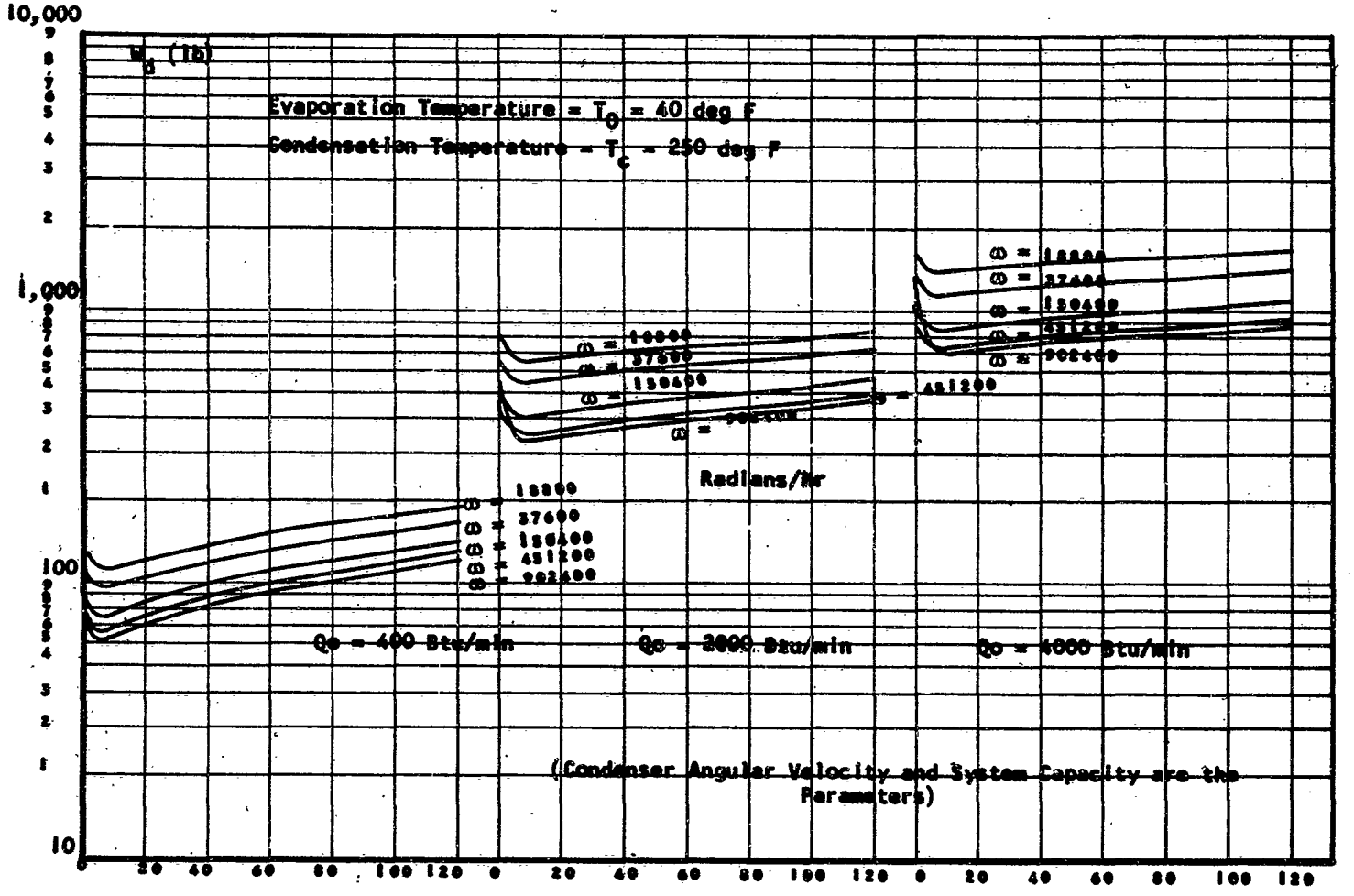

Figure 64. Condenser System Dead Weight vs. Number of Discs.
(Reference 32)

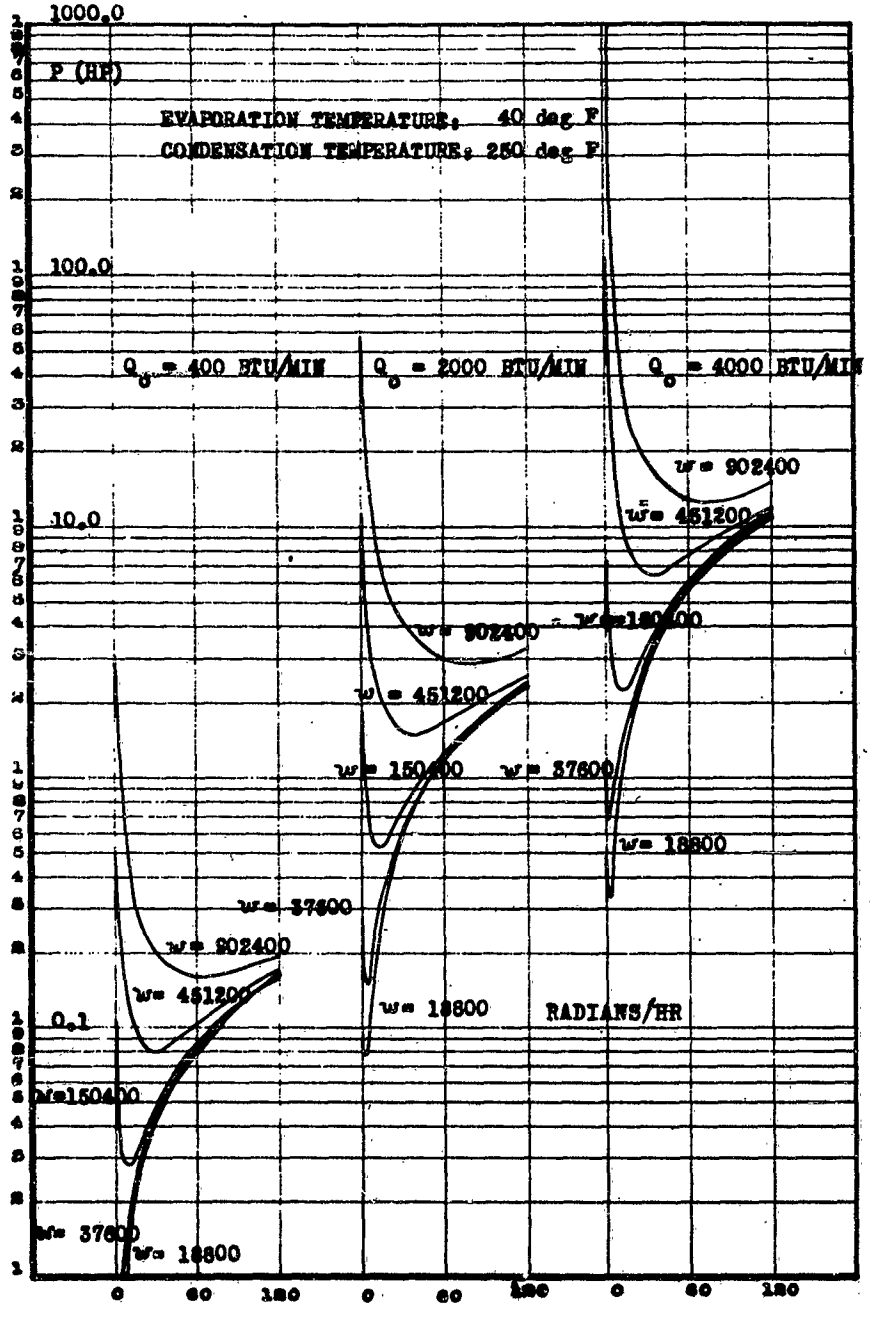

Figure 65

Total Power Requirement Vs. Number of Discs

(Condenser Angular Velocity and System Capacity are the Parameters)

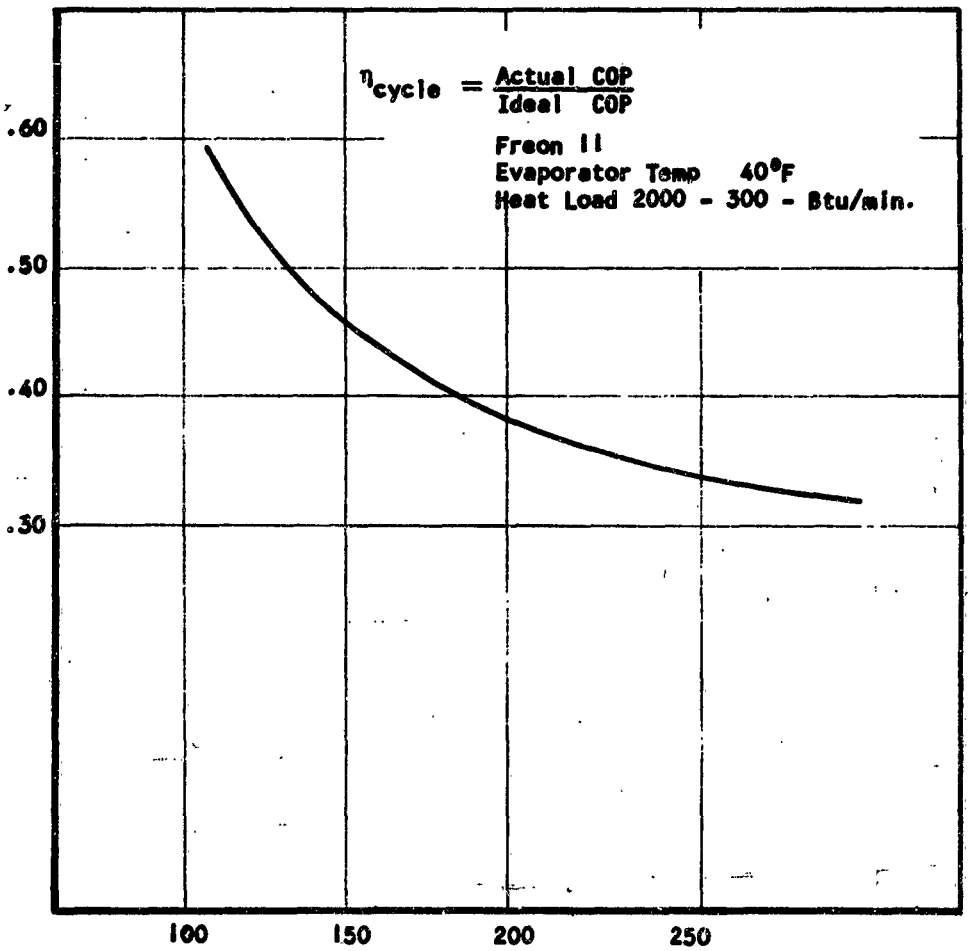

Figure 66. Performance of Vapor Cycle
(Reference 2)

Demonstration of Vapor Cycle System Analysis

Consider a vapor cycle system to be designed for space application. The requirements are as follows:

Evaporator temperature = 40°F

Condenser temperature = 150-250°F

Cooling capacity = 1000-2000 Btu/min

A simple cycle with a superheat of 20°F and a compressor efficiency of 60 per cent will be assumed.

Selection of the Refrigerants. Following the steps presented in this study, the factors governing the refrigerant selection are evaluated. The COP of the common refrigerants, the refrigeration effect Q/V_1, and the pressure ratios of the compressor cycle are shown in Figures 67, 68 and 69. Table 18 lists these refrigerants in order of COP for a condenser temperature of 250°F.

There appears to be little to choose from when the relative standings of each refrigerant are added on a basis of 1, 2, 3, 4. Other factors, such as state-of-the-art in component development, must be taken into consideration in a final selection. For illustrative purposes, Freon 11 has been chosen in this example.

Performance Characteristics and Estimate of System Weight. 250°F Condenser. Table 19 represents the characteristics of a Freon 11 system operating at a condenser temperature of 250°F. With a COP of 0.85, the compressor power required for a system with a cooling capacity of 2000 Btu/min (10 tons) is 55.4 hp. The radiator accounts for 69 per cent of the total. The estimated radiator weight would be considerably higher with protection from meteoritic damage.

Table 19 also shows the weight estimate for a system with 1000 Btu/min in cooling capacity. It can be seen that the system weight variation relates principally to radiator weight. Thus, for a reasonable range of cooling capacities, the system weight can be written as:

$$W_{T2} = W_{T1} + Q_c \left(1 + \frac{1}{COP}\right)\left(\frac{W_{T2} + W'}{Q_R}\right) \qquad (71)$$

where W_T = system total weight, lb

W_{T1} = weight of system components compressor, refrigerants, evaporators, etc., except condenser-radiator, lb.

W_{T2} = condenser radiator weight, such as given in Figure 57, lb.

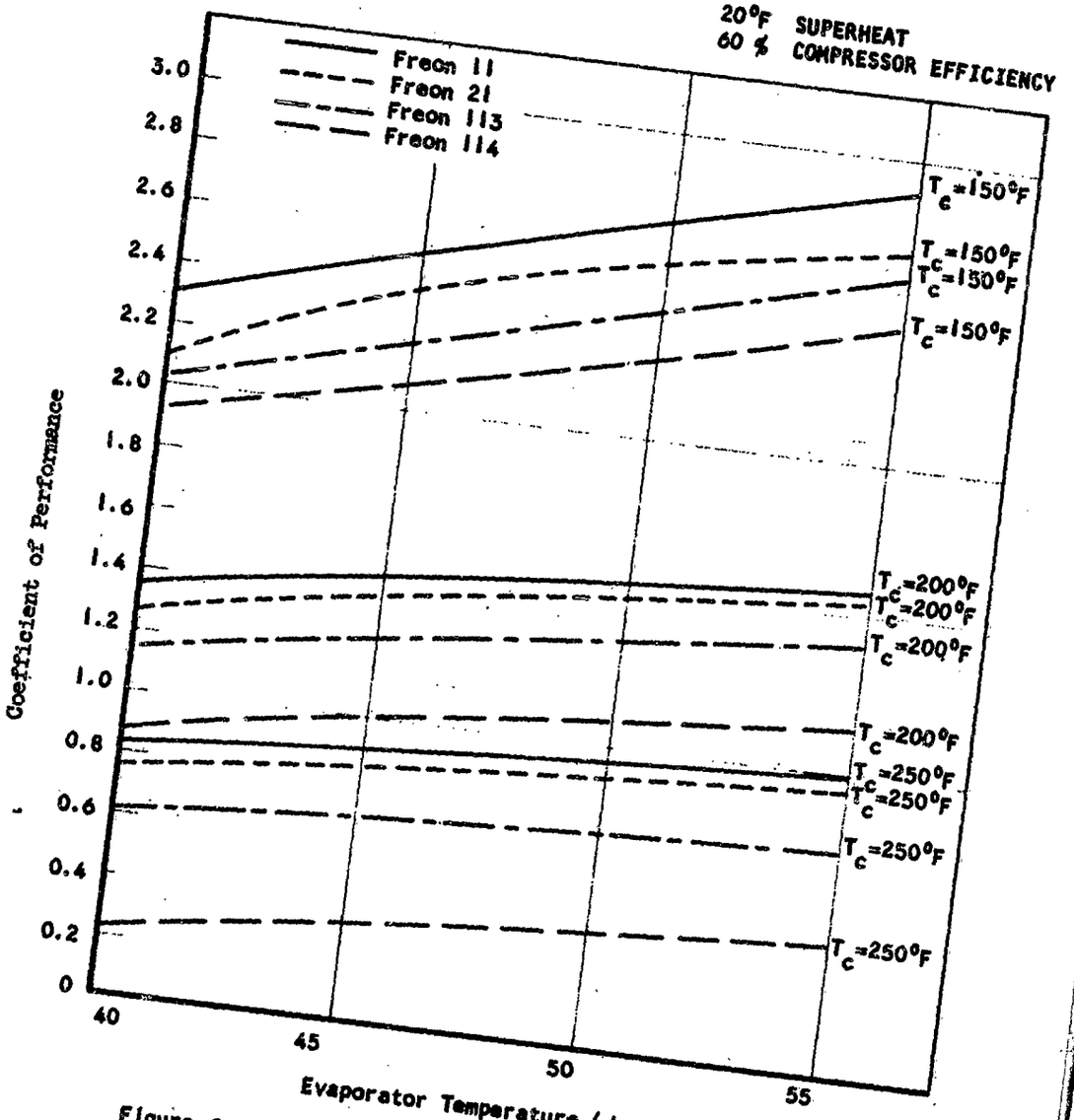

Figure 67. Coefficient of Performance of Freon Refrigerants (Reference 32)

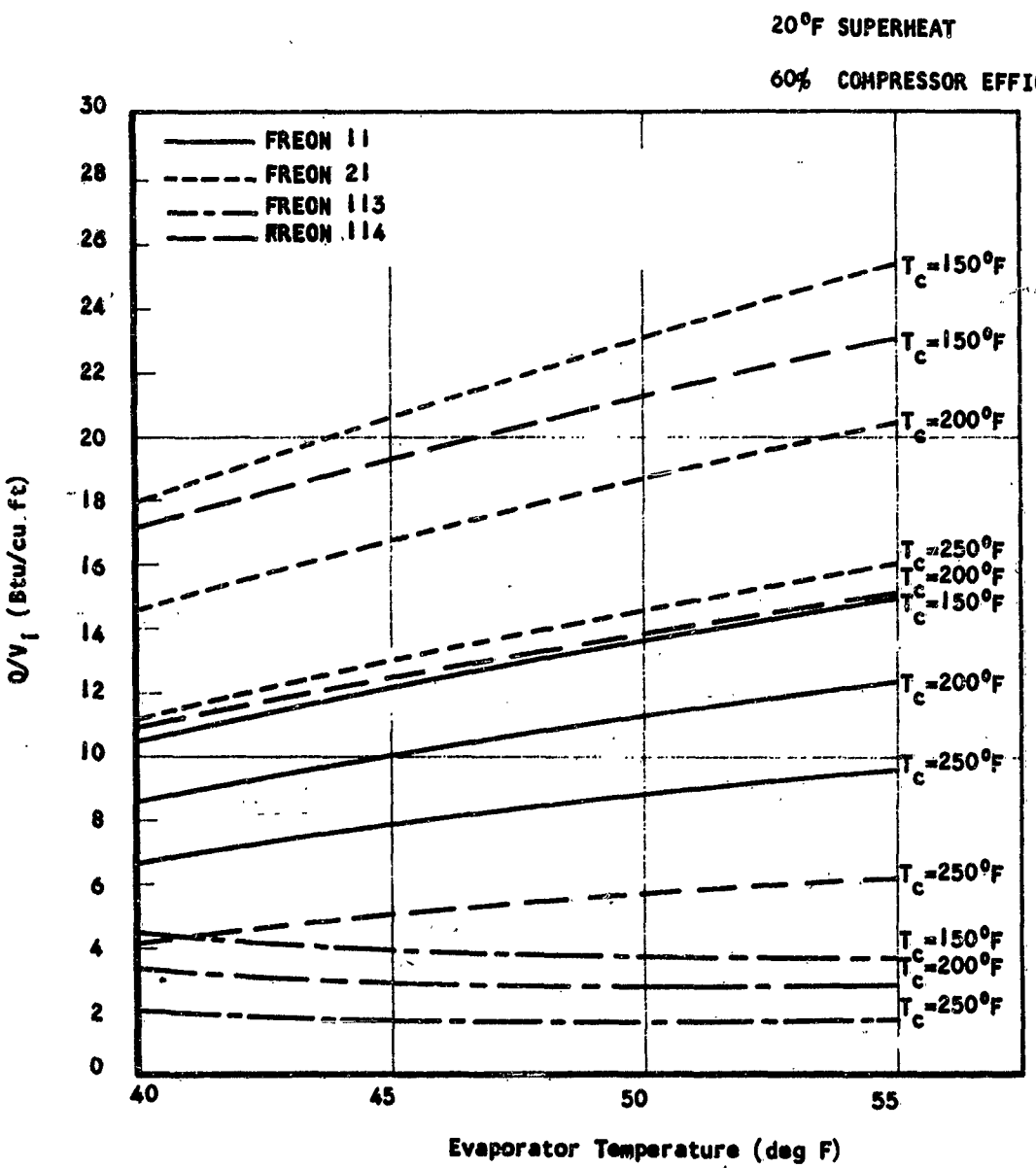

Figure 68. Refrigeration Effect Per Unit Volume For Freon Refrigerants (Reference 32)

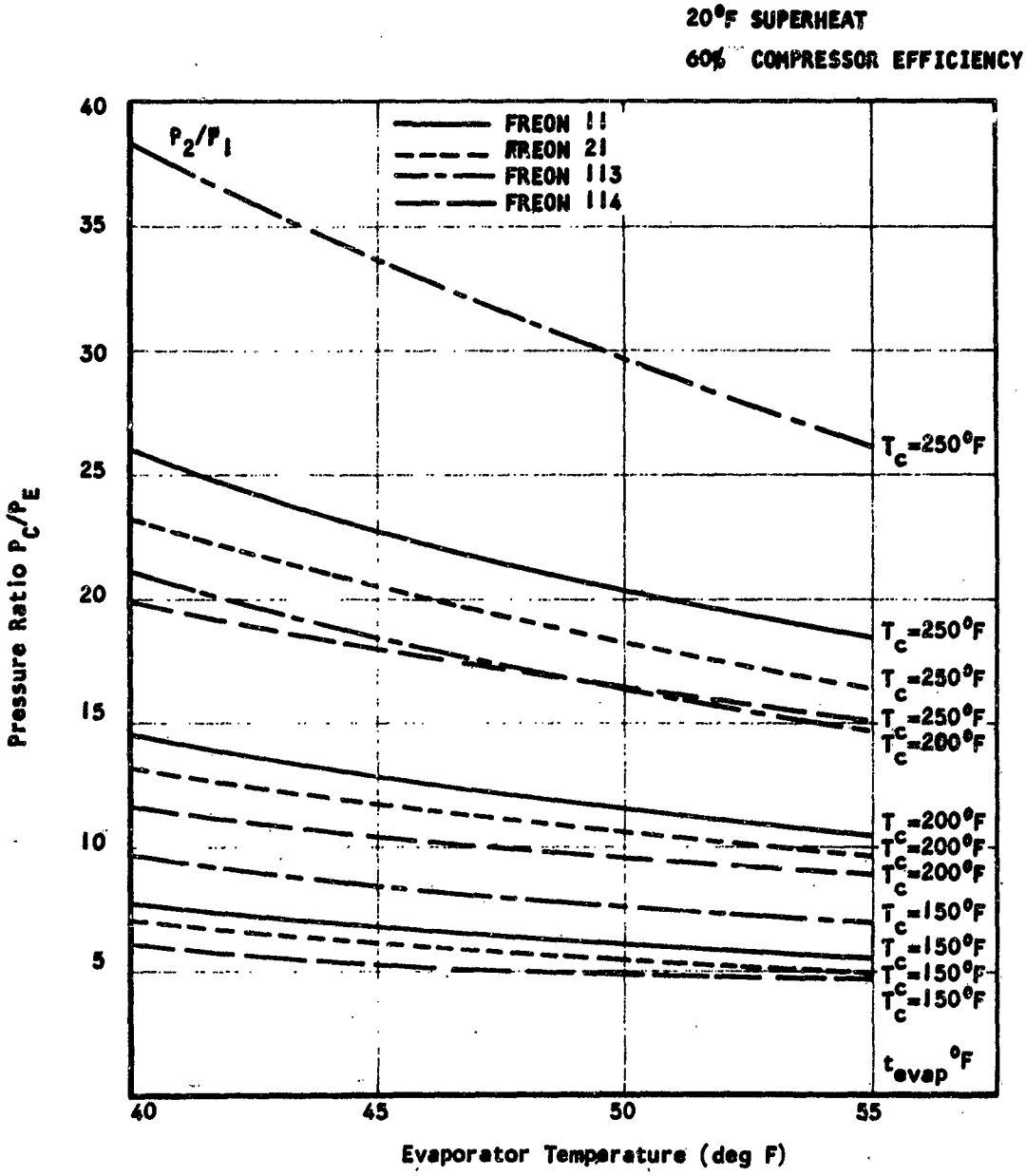

Figure 69. Ratio of Condenser Pressure to Evaporator Pressure For Freon Refrigerants

(Reference 32)

Table 18

Summary Of Properties Of Selected Refrigerants

Evaporator Temperature = 40°F
Condenser Temperature = 250°F

Coefficient of Performance (COP)		Q/V_1		Pressure Ratio P_C/P_E		Condenser Pressure P_C psia		Evaporator $\frac{\Delta T}{\Delta P}$		Σ of Relative Positions in Preceding Columns
F-11	0.85	F-113	2.06	F-114	20.4	F-113	102	F-114	3	12
F-21	0.77	F-114	4.15	F-21	23.2	F-11	182	F-21	3.5	13
F-113	0.63	F-11	6.7	F-11	26	F-21	295	F-11	6	13
F-114	0.28	F-21	11.1	F-113	28.5	F-114	310	F-113	13	12

Table 19

Vapor Cycle System
Weight and Performance Characteristics

CONDITIONS OF OPERATION: FREON 11 EVAPORATOR 40°F
RADIATOR CONDENSER 250°F
20° SUPERHEAT: 60% COMPRESSOR EFFICIENCY

CHARACTERISTIC	WEIGHT, LB, FOR COOLING CAPACITY, IN Btu/min, of		SOURCE OF INFORMATION
	1000	2000	
Evaporator Plate Fin Design P = 0.3 psia; T airside = 25°F	7.5	13.5	Data from Ref. 32 25% for header
Superheater	7	10	Reference 31
Expansion valve	3	5	Reference 31
Receiver	3	4	Reference 31
Refrigerant	7	10	Reference 31
Temperature Control	6	6	Reference 31
Centrifugal compressor and 400 cycle a-c electric motor	35	50	AiResearch Mfg. Co.
Condenser radiator with tapered tubes and conventional design	104	218	Figure 57, $\frac{W_T}{Q_R}$ = 3 lb/(sec)(Btu)
Total	172.5	316.5	
COP	.85	.85	
Compressor hp required	27.7	55.4	

W' = Increment in radiator weight for meteoritic protection, lb.

Q_C = Cooling capacity, Btu/sec

Q_R = Heat rejected to outer space, Btu/sec

This formula, valid within a given range of capacities, is predicated upon a radiator weight that is large compared to that of other components. For a wide range of capacities, variation with capactity of the evaporator weight, electric motor weight, and of other component weights must be taken into account.

150°F Condenser. Table 20 presents the characteristics of a Freon 11 system operating with a condenser temperature of 150°F. With the thermodynamic properties of Freon, a COP of 2.3 is achieved as compared to 0.85 for the 250°F condenser. Thus, a 10-ton cooling system requires a compressor power of only 20.5 hp.

Because of operation at a lower temperature level, the radiator specific weight (weight per unit of heat rejection rate, lb/(Btu)(sec) increases. Relatively, resulting radiator weight is even larger than in the previous case.

Condenser Temperature for Optimum Vapor Cycle System Weight

The demonstration estimate indicates reasons for high condenser temperature operation to decrease the system weight. The examples indicate a difference of only 6.5 per cent between 150°F and 250°F operation. With the 150°F condenser, this difference would be further reduced with a compressor of higher efficiency (compatible with present day technology). Retaining Freon 11 as a refrigerant, operation at a temperature higher than 250°F will not be advantageous, from the weight viewpoint, as the COP begins to deteriorate considerably, introducing a larger amount of heat to be rejected to the environment. This problem must be considered in addition to that of refrigerant stability. Thus, the feasibility of higher condenser temperature operation is to be sought in the high temperature refrigerants mentioned earlier in this study.

The Vapor Cycle Subsystem in the Thermal Environmental Control System

If integration of the vapor cycle subsystem in an environmental control system is considered, an optimum weight of both the vapor cycle and power systems may require a condenser operating temperature different from the optimum of the vapor cycle system alone. From the previous numerical examples, the ratio

$$COP_{150°F}/COP_{250°F} = 2.71$$

Table 20

Vapor Cycle System
Weight and Performance Characteristics

CONDITIONS OF OPERATION: FREON 11 EVAPORATOR 40°F
RADIATOR CONDENSOR 150°F
20° SUPERHEAT: 60% COMPRESSOR EFFICIENCY

CHARACTERISTIC	WEIGHT, LB, FOR COOLING CAPACITY, IN Btu/min, of		SOURCE OF INFORMATION
	1000	2000	
Evaporator Plate fin design P = 0.3 psia, T airside = 25°F	7.5	13.5	Data from Fig. 48, 49, 50 25% for header
Superheater	7	10	Reference 31
Expansion Valve	3	5	Reference 31
Receiver	3	4	Reference 31
Refrigerant	7	10	Reference 31
Temperature control	6	6	Reference 31
Centrifugal compressor and 400 a-c electrical motor	25	35	AiResearch Mfg. Co.
Condenser radiator with tapered tubes and conventional design	129	258	Fig. 57, $\frac{W_T}{Q_R}$ = 5.4 lb/Btu/sec
Total	187.5	341.5	
COP	2.3	2.3	
Compressor hp	10.25	20.5	

indicates that operation at 250°F requires 2.71 times more power. The energy rejected due to inefficiency in the generation of the necessary compressor power is then much more.

In Reference 44, the optimization of this system assumes that the energy associated with the inefficiency of power generation is rejected to the environment at the same temperature as that of the condenser of the vapor cycle system. For optimization, this study calls for a high condenser temperature, even beyond the limits of existing refrigerants.

While the weight consideration is of prime importance, the integrity of the vapor cycle system must still be considered. Previous numerical examples consider Freon 11 for operation at 250°F. Practically, such a system would require a change in refrigerant after short periods of operation. There also exists the possibility of using Freon 113 with a lower COP, a higher system weight, and a considerable improvement in reliability.

GAS CYCLE METHOD

Gas cycle cooling methods should be considered for space application for several reasons. For example, the problems usually associated with vapor cycles, such as toxicity, leakage, and availability of the refrigerant, can be avoided by proper selection of the working fluid. More important, however, is the absence of problems associated with weightlessness and with two-phase flow.

Gas cycle cooling can operate in an open or a closed loop. In the open circuit, the gas circulating through the cooling loop is supplied directly from the source. After being processed in the cooling system, it is then returned to the same source. In the closed cycle, the same amount of refrigerant, continuously circulated through the cooling system, absorbs heat from the environment through a heat exchanger.

Nomenclature

A	Radiator area
c_p	Specific heat at constant pressure
H_{ad}	Adiabatic head
J	Conversion factor
K	Gas adiabatic exponent
N	Rotational speed
n_s	Specific speed of compressor
P	Pressure

Nomenclature (Cont)

Q	Cooling load
r	Pressure ratio
T	Temperature
V	Volumetric flow rate
w	Flow rate
η	Efficiency
σ	Stefan-Boltzmann constant
ϵ	Emissivity

Subscript

c	Compressor
E	Source heat exchanger
m	Arithmetic mean value
t	Turbine
*	Reference area

Thermodynamics and Operation

Gas cycle cooling systems usually operate on the reversed Brayton cycle, though cooling systems using Stirling and other cycles have been successful. The Brayton cooling cycle is shown on the T-S diagram of Figure 70. The system diagram of this closed cycle is shown schematically in Figure 71. The cycle consists of four major components: compressor, turbine, radiator, and heat exchanger. In an open cycle, the heat exchanger is eliminated as the cooling fluid is allowed to flow directly to the environment.

The gas entering the compressor is at Condition 1 and relatively warm. In going through the compressor during Process 1-2, its temperature and pressure are raised. This gas then flows at constant pressure through the radiator, rejecting heat to the sink, which must be at a lower temperature, during Process 2-3. The cooled gas is then expanded in a turbine during Process 3-4, where work is abstracted from the fluid. At the turbine exit, the gas temperature is low enough to absorb heat from the environment, as it does during the constant pressure Process 4-1.

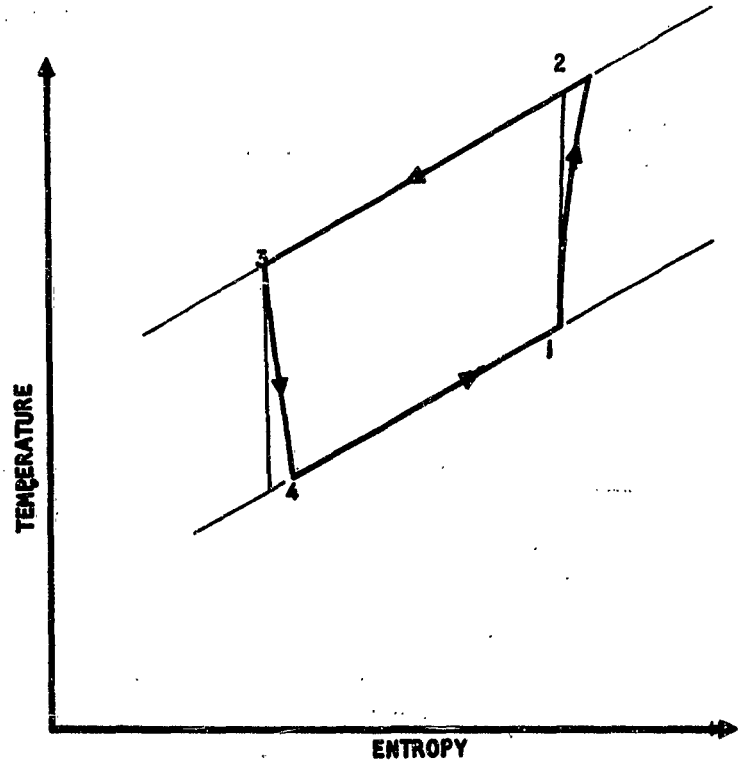

Figure 70. Temperature - Entropy Diagram of The Brayton Cycle

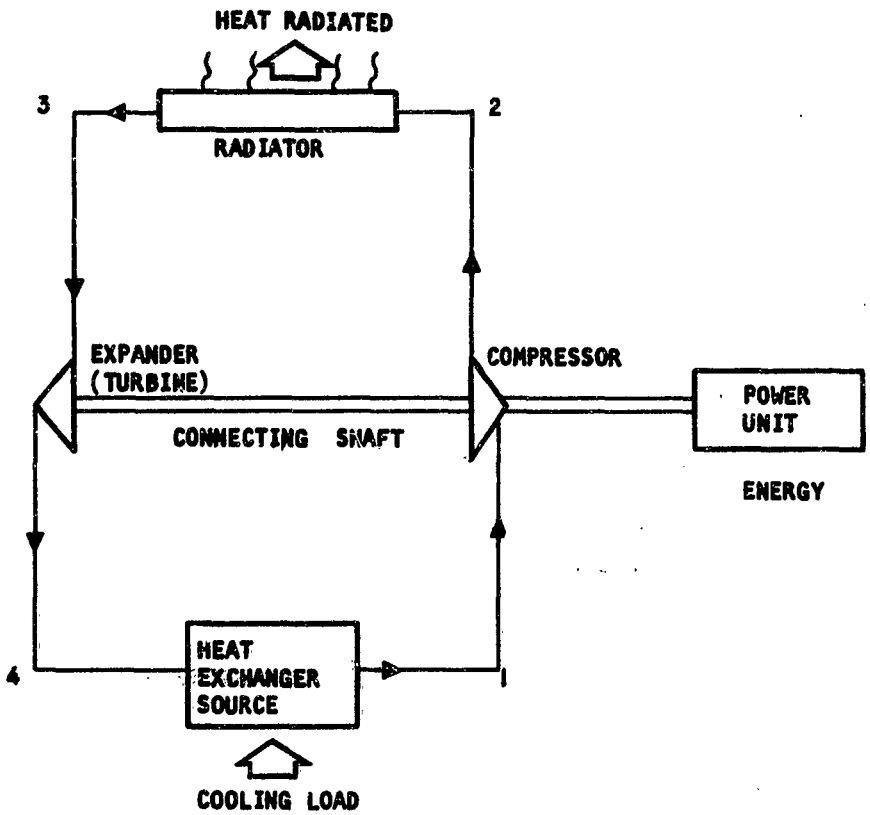

Figure 71. Schematic Diagram of a Gas Cycle Cooling System

Performance Characteristics

Gas cycle system performance is measured by its coefficient of performance, defined in the same way for gas as for vapor cycles:

$$\text{COP} = \frac{\text{Heat Extracted}}{\text{Cycle Work}}$$

In making a generalized study of the influence on the performance of the cycle, it is assumed that the circulating fluid is a perfect gas and that the evaporator and radiator operate with a 100 per cent efficiency. Pressure drops in these components are not taken into account.* The COP of the cycle of Figure 70 can then be written as

$$\text{COP} = \frac{\frac{\Delta T_E}{T_4}}{\frac{\Delta T_E}{T_4} - \frac{\Delta T_c}{T_t}} \tag{72}$$

where ΔT_E = Temperature rise in the source heat exchanger

ΔT_c = Temperature rise in the compressor

ΔT_t = Temperature drop in the turbine

T_4 = Temperature of the turbine exit

The ratio $\Delta T_E/T_4$ is of interest to the designer of cooling systems, for it establishes the heat transfer from the environment to the system.

Effect of the Adiabatic Exponent

The above temperature ratios can be calculated in terms of the cycle pressure ratio r, of the turbine and compressor efficiencies η_t and η_c, and of the adiabatic exponent of the gas k. That is:

$$r = \frac{P_2}{P_1};$$

$$\frac{\Delta T_t}{T_4} = \frac{\eta_t \gamma_t}{(1-\eta_t)\gamma_t + 1}; \tag{73}$$

$$\frac{\Delta T_c}{T_4} = \left(1 + \frac{\Delta T_c}{T_4}\right)\frac{\gamma}{\eta_c} \tag{74}$$

*Effects of the inefficiency of the components on cycle performance are discussed in Reference 31.

where

$$Y = r^{(k-1)/k} - 1$$

For a given value of the design ratio of temperatures, $\Delta T_E/T_4$, it can be seen that the nature of the fluid influences COP only through the exponent k. Figures 72 and 73 present the COP that can be achieved for two typical values of the ratio $\Delta T_c/T_4$ and assumed values of the compressor and turbine efficiency. In addition, these figures carry the lines of constant $\frac{Tm}{T_4}$, where Tm is the arithmetic mean of the inlet and exit radiator temperatures.

Air, a refrigerant that has many advantages in the gas cycle, shows a low COP compared to that of conventional vapor cycles. To achieve comparable COP values, air cycles would have to operate between pressure ratios of 1 and 2 with a resulting low value of Tm/T_4, a characteristic indicating the requirement for a larger radiator area. These figures also show that the coefficient of performance does improve with fluids of lower values of k, and that there is not an appreciable difference in COP for k values between 1.4 and 1.666.

Effect of Specific Heat, c_p

From the analytical expression for COP, it appears that the specific heat of the gas does not affect cycle performance. In a gas refrigeration system it does influence the flow rate through the system in accordance with the relationship:

$$w = \frac{Q}{c_p \Delta T_E} \tag{75}$$

where w = Refrigerant flow rate, lb/sec

Q = Cooling load, Btu/sec

ΔT_E = Temperature rise in source heat exchanger, ^oF

c_p = Specific heat at constant pressure, Btu/(lb)(^oF)

To introduce the concept of specific flow rate, i.e., the flow rate required per unit of cooling load, the above relation is written as:

$$\frac{w}{Q} = \frac{1}{c_p T_4 \left(\Delta T_E/T_4\right)} \tag{76}$$

It can be seen that the specific flow rate, w/Q, is inversely proportional to the specific heat, c_p. This flow rate is often used as an approximate measure of the size of the equipment required for the cooling system.

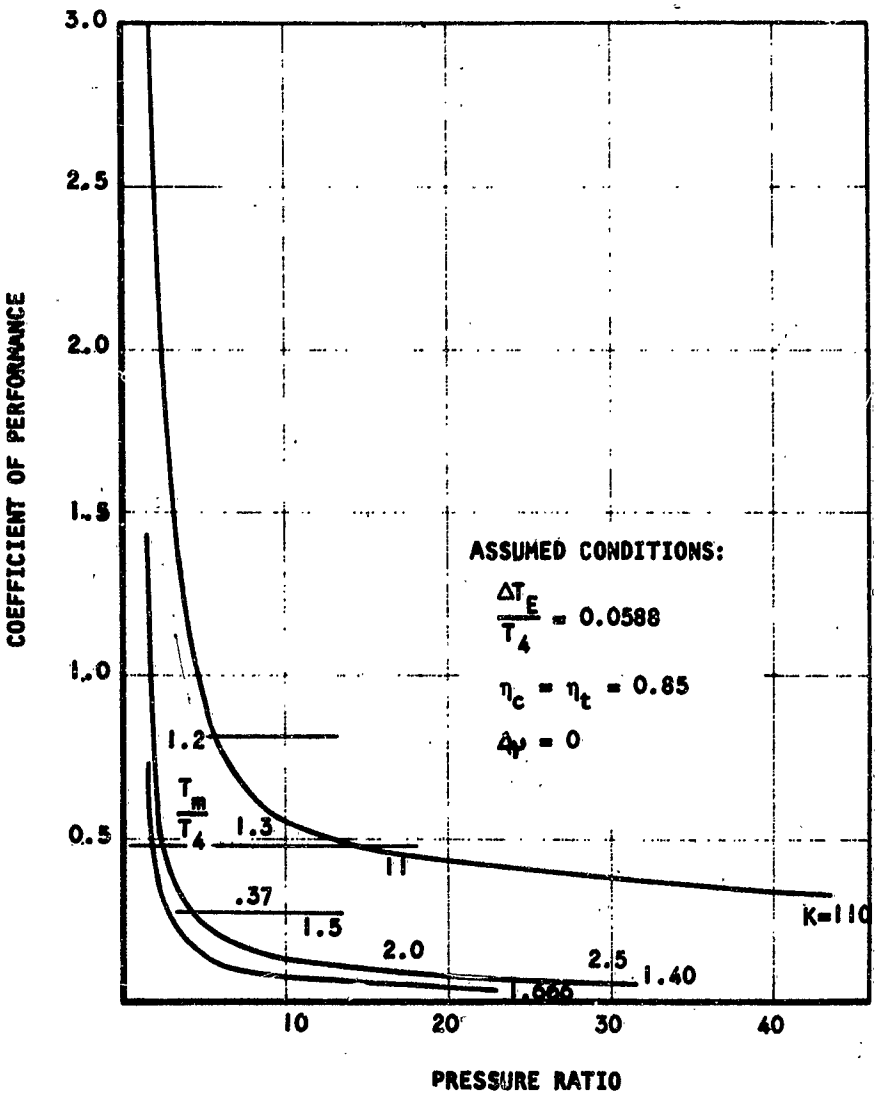

Figure 72. Relationship of Gas Cycle Coefficient of Performance to Pressure Ratio.

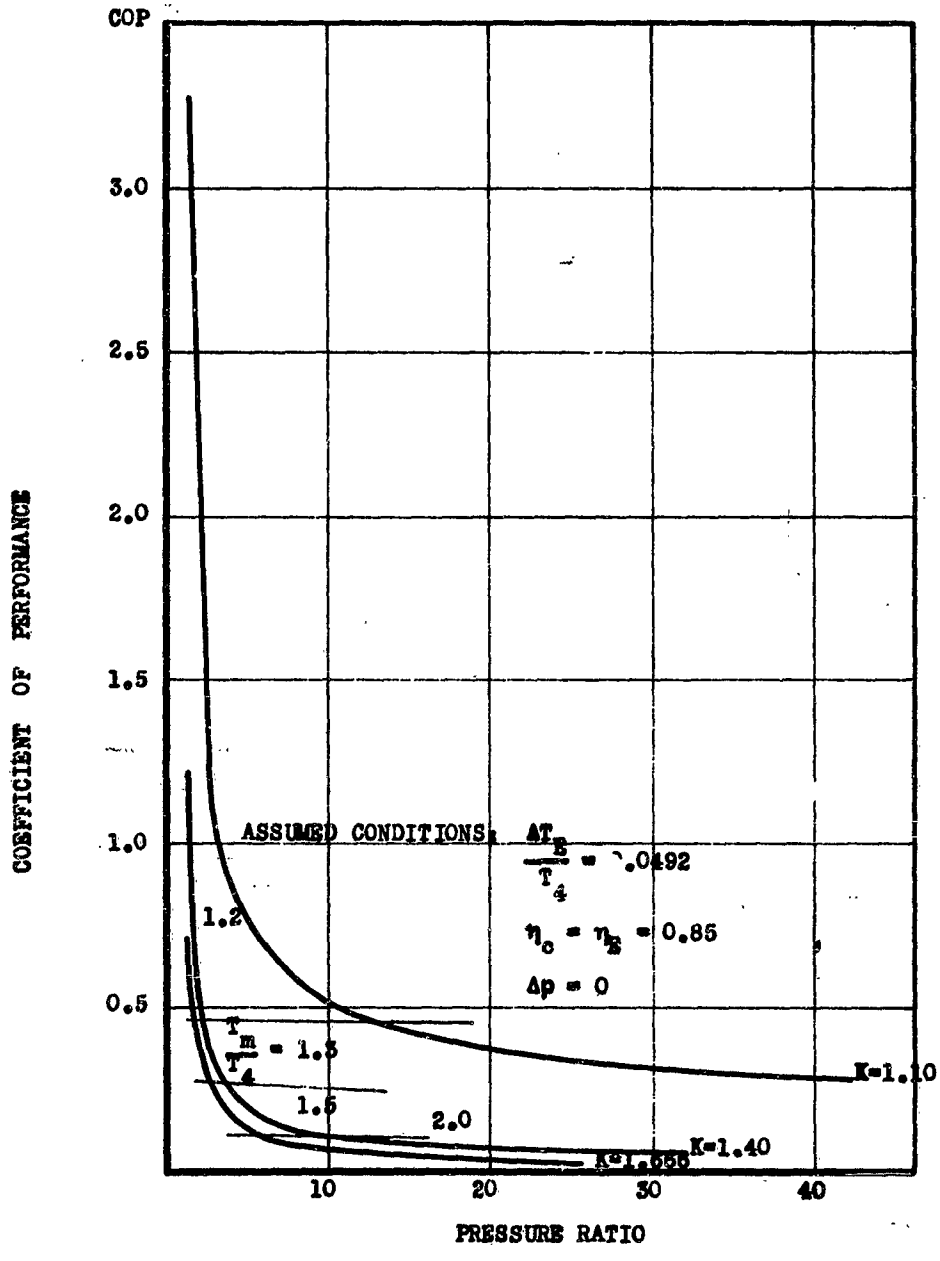

Figure 73. Relationship of Gas Cycle Coefficient of Performance to Pressure Ratio

Besides the flow rate, the specific heat also establishes the boundaries of practical application of the gas cycle using compressors and turbines. For this type of equipment, the energy input per unit mass rate of flow is given by relationships such as the head rise in the compressor:

$$H_{ad} = \frac{Jc_p T_{1nlet}\left[r^{(k-1/k)} - 1\right]}{\eta_c} \tag{77}$$

The head, H_{ad}, represents a temperature rise and cannot be taken above the limits set up by the physical properties of the material. It follows then that for a given inlet temperature T_1, the specific heat establishes a maximum value of the pressure ratio usable in the gas cycle.

Radiator Area

In this comparative study, it will be assumed for simplicity that the radiator rejects heat at the mean temperature T_m to outer space having a temperature of $0^{\circ}R$. The radiator area required for a cooling capacity Q is given by:

$$Q\left(1+\frac{1}{COP}\right) = A\sigma\epsilon T_m^4 \tag{78}$$

where Q = Cooling capacity, Btu/hr

σ = Stefan-Boltzmann Constant = 0.1714×10^{-8} Btu/(hr)(sq ft)$(^{\circ}R)^4$

A = Radiator area, sq ft.

ϵ = Emissivity, dimensionless

$T_m = \left(\frac{T\ inlet + T\ exit}{2}\right)_{Radiator}$, $^{\circ}R$

The area A* of a radiator required to handle the heat rejection rate Q at the turbine exit temperature T_4 is now defined as:

$$Q = A^*\sigma\epsilon T_4^4 \tag{79}$$

Using Equation 78, a nondimensional relation is now established:

$$\frac{A}{A^*} = \frac{1+\frac{1}{COP}}{(T_m/T_4)^4} \tag{80}$$

This dimensionless area ratio is shown in Figures 74 and 75 superimposed on various values of pressure ratios, COP and k. For a typical pressure ratio of 6, a gas with a value of k = 1.1; however, the radiator area is smaller by 35 per cent. For a large number of gases with k = 1.4, operation

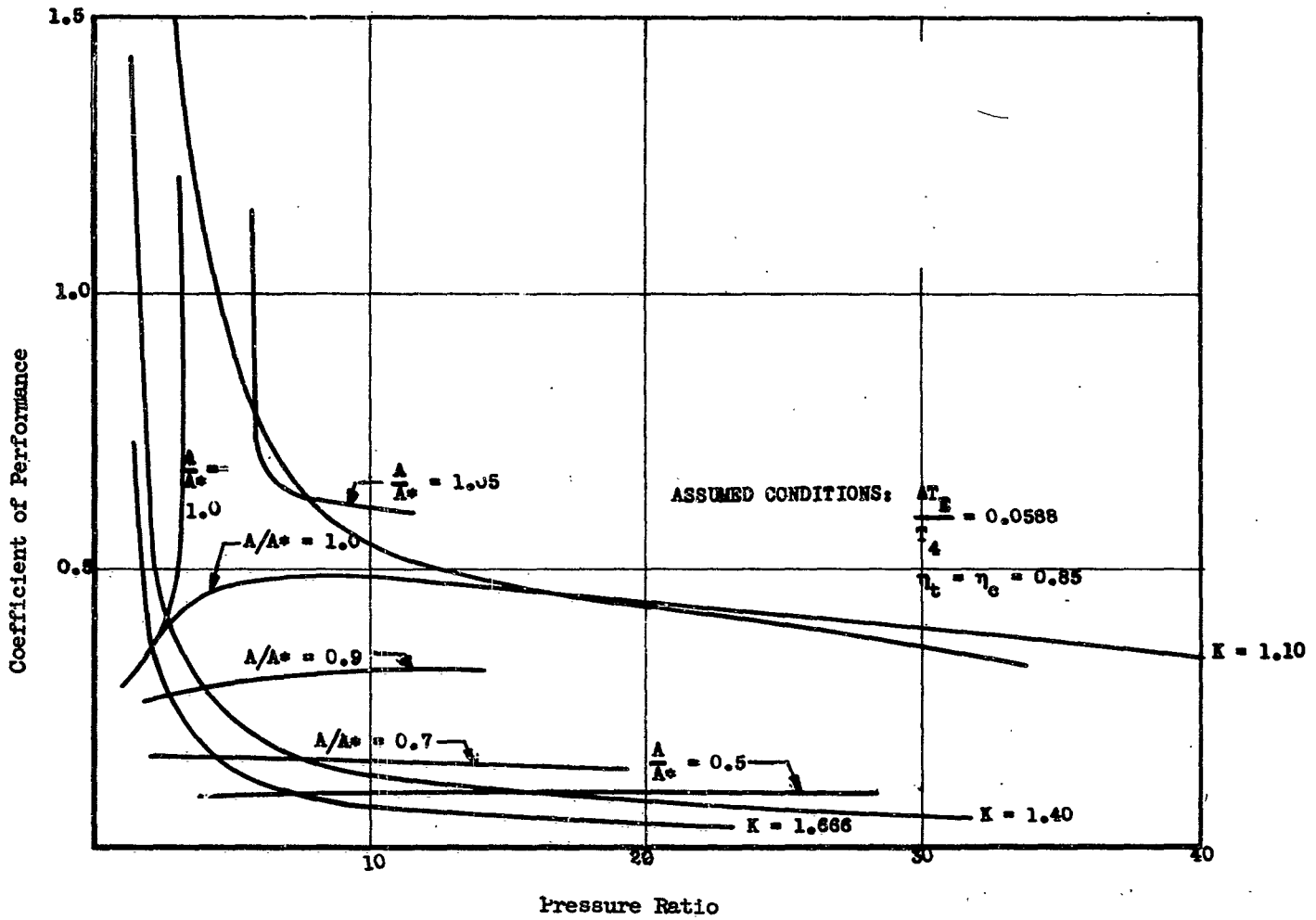

Figure 74. Radiator Requirements of Gas Cycle Systems

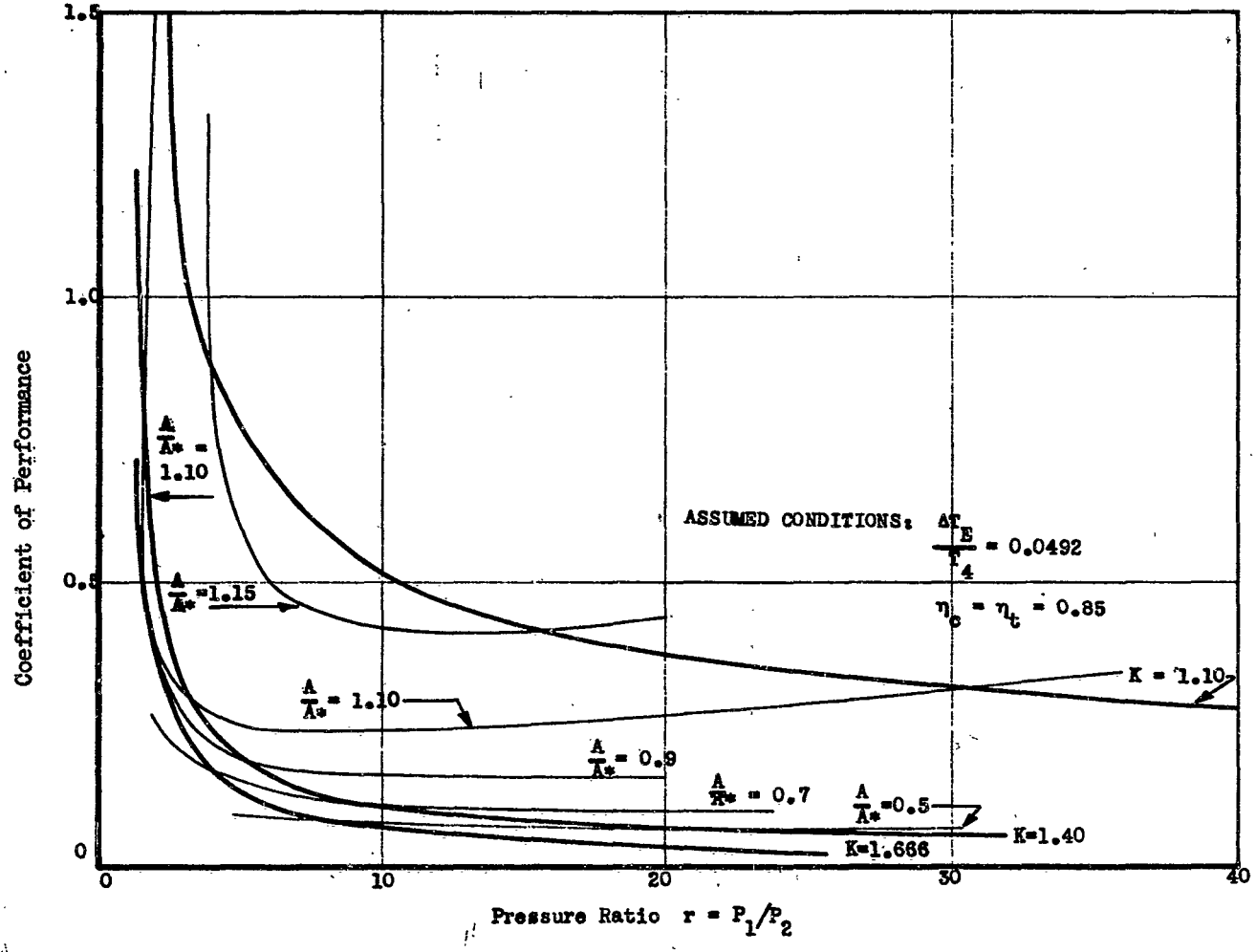

Figure 75

Radiator Requirements of
Gas Cycle Systems

at a COP of 0.5 requires an increase in radiator area of 30 per cent over that of a system having a COP of 0.2 .

The variation of the radiator area with pressure ratios is presented in Figures 76 and 77. Starting with small pressure ratios, the radiator area increases as it must reject the mechanical energy input in addition to the cooling load. As the pressure ratio increases, the radiator temperature rises, permitting a higher rate of heat rejection with a consequent decrease in required area.

Fluids For Gas Cycle Systems

Among the fluids usable in a gas cycle, air has the most advantages. A major advantage is the possibility of non-toxic open cycle application in an environmental control system for human use. The components for the cycle are well developed and available today. Extensive studies of both air and hydrogen gas cycles may be found in Reference 47.

Hydrogen deserves consideration because its k value of 1.4 yields the same COP as air. Its high specific heat, however, dictates a lower flow rate for any given refrigeration load. The advantage of hydrogen lies then in a reduction in the size of the system components when large cooling requirements are encountered. One disadvantage is hydrogen's high combustibility.

Helium has an intermediate value in specific heat and a k value of 1.666. Although its COP is lower than that of other gases, helium has the advantage of being inert.

At the outer end of the spectrum, gases and vapors with K = 1.10, such as Freon 113 or 114 or benzol (C_6H_6), are capable of achieving a high COP. However, their low specific heat values would require larger components. They find use where the cooling load is small, since the system components can be large and still remain practicable. The temperature stability of these organic vapors may preclude their operation at high temperature.

System Components

Compressors

The selection of the compressor for gas cycles can best be made by applying the concept of specific speed, as introduced in the discussion of vapor cycles. The specific speed is defined by the relation

$$n_s = \frac{N\sqrt{V}}{6270\ (H_{ad})^{0.75}} \tag{81}$$

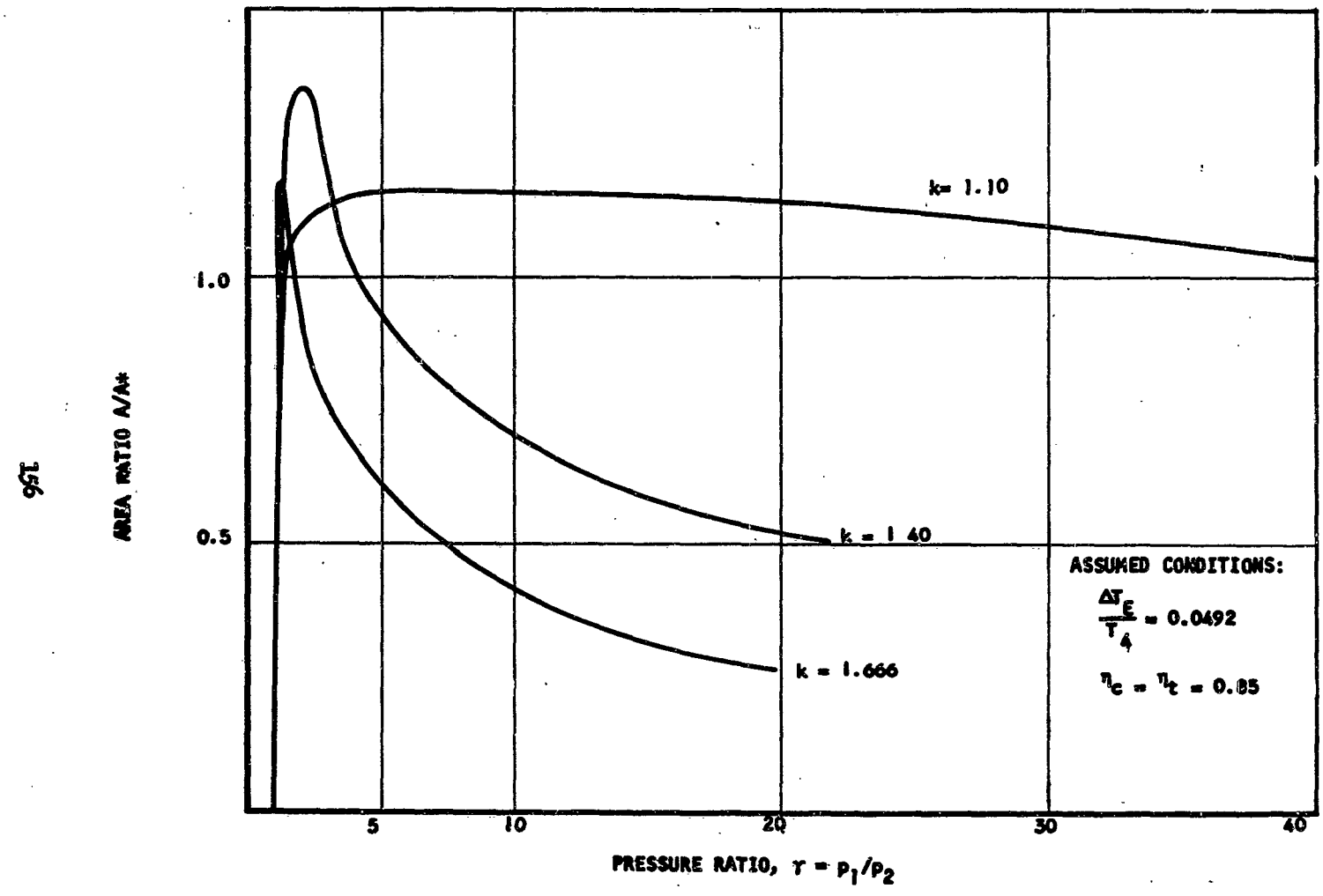

Figure 76. Relationship of Radiator Area Ratio to Cycle Pressure Ratio

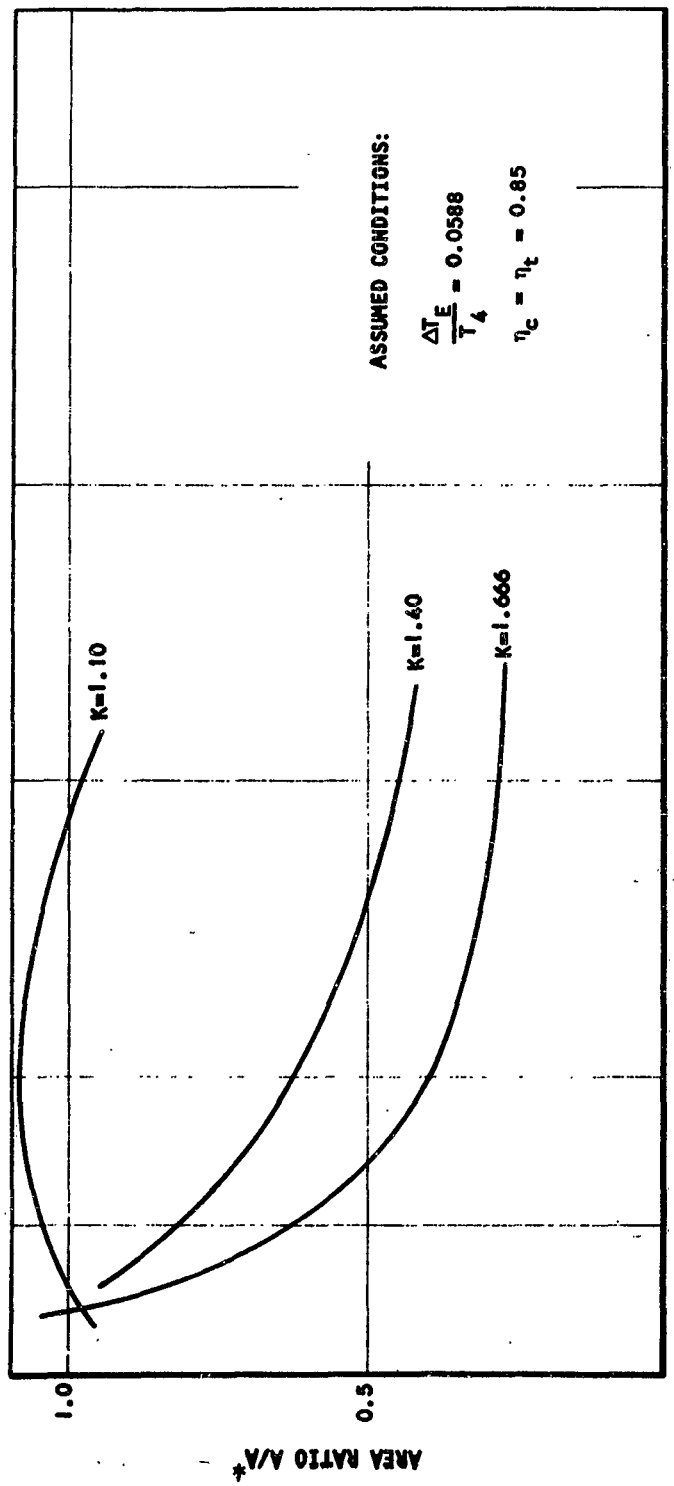

Figure 77. Relationship of Radiator Area Ratio to Cycle Pressure Ratio.

where n_s = Specific speed

N = rpm

V = Volumetric flow at compressor exit, cu ft/min

H_{ad} = Adiabatic head, ft

Theoretical and experimental work on compressors has led to associating each type of compressor with a range of specific speeds. This is shown in Table 21.

If the specific speed is now calculated as a function of the cooling load, the following auxiliary relations are applicable:

Perfect gas equation $\quad p\nu = RT$

Specific heat and k relationship $\quad Jc_p\left(\frac{K-1}{K}\right) = R$

Volumetric flow equation $\quad V = \frac{Q}{p} J\left(\frac{K-1}{K}\right) \frac{T_1}{\Delta T_E}$

Adiabatic head equation $\quad H_{ad} = Jc_p T_1 \left(T^{\frac{K-1}{K}} - 1\right)$

An expression for the specific speed is formed by combining these equations:

$$n_s = \frac{N \sqrt{\frac{Q}{P}} \sqrt{J\left(\frac{K-1}{K}\right)\left(\frac{T_4}{\Delta T_E} + 1\right)}}{6270 \left[Jc_p T_4 \left(1 + \frac{\Delta T_E}{T_4}\right)\left(r^{\frac{K-1}{K}} - 1\right)\right]^{3/4}} \qquad (82)$$

where N = rpm

Q = Btu/min

P = lb/sq ft

c_p = Btu/(lb)($^\circ$F)

Equation 82 indicates that the range of specific speed and consequently the type of compressor to be used depends upon the following factors:

a. The physical rotational speed
b. The operating pressure level of the cycle
c. The cycle pressure ratio

Table 21

Range of Suitable Specific Speeds For Various Compressor Types

COMPRESSOR TYPE	SPECIFIC SPEED	
	Maximum n_s	Minimum n_s
Axial	1.0	0.3
Mixed Flow	0.3	0.2
Centrifugal	0.2	0.06
Rotary	0.005	0.002
Reciprocating	0.005	0.0001

Table 22

Range Of Suitable Specific Speeds

TURBINE TYPE	SPECIFIC SPEED
Axial	.3 - .7
Radial	.15 - .3
Rotary	0.03 - .15

d. The adiabatic exponent or specific heat ratio, k
e. The specific heat, c_p
f. The temperature of the gas at the inlet to the source heat exchanger.

Since air is used most frequently in the gas cycle, calculation have been carried out for some typical values of these factors with air as the thermodynamic fluid. Figure 78 shows the type of compressor to be used for various cooling loads with a selected rotational speed of 40,000.

The requirement of low radiator area dictates an operation of the gas cycle between the pressure ratios of 5 and 10, according to Figures 74 and 75. Figure 78 shows that, within this range, a rotary or a piston compressor would be used for a larger cooling load. The previous speeds and pressure levels can be modified over a wide range to accommodate the type of compressor available to the system designer.

Turbines

Turbines for gas cycles are selected in the same manner as compressors--by using the concept of specific speeds. For turbines, the specific speed is also defined as

$$n_s = \frac{N}{6270} \frac{V}{(H_{ad})^{.75}} \tag{83}$$

where N = rpm

V = Volumetric flow rate of turbine exist, cu ft/min.

H_{ad} = Adiabatic head, ft

The range of specific speeds associated with different types of turbines is given in Table 22.

The turbine specific speed can be expressed in terms of the cycle variables and parameters and does not differ greatly from that of the compressor. For perfect gas operation in the gas cycle on Figure 70, the following relations may be established:

$$\begin{aligned} H_{ad\ (turbine)} &= H_{ad\ (compressor)} \times \frac{T_4}{T_1} \\ V_{exit\ (turbine)} &= V_{inlet\ (compressor)} \times \frac{T_4}{T_1} \\ n_{s\ (turbine)} &= n_{s\ (compressor)} \times \left(\frac{T_1}{T_4}\right)^{1/4} \\ &= \left(1 + \frac{\Delta T_E}{T_4}\right)^{1/4} n_{s\ (compressor)} \end{aligned} \tag{84}$$

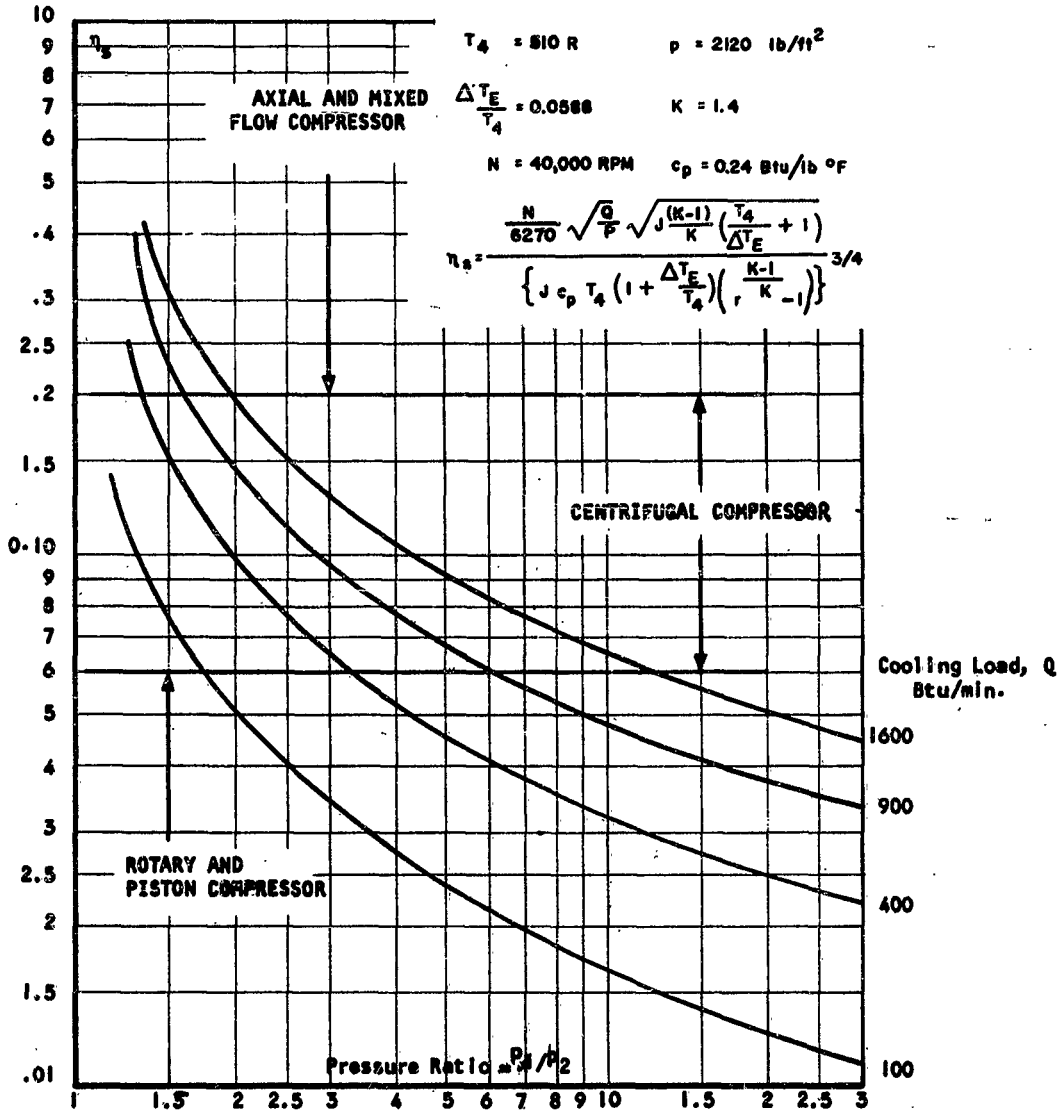

Figure 78. Compressor For Gas Cycle

Since the design temperature ratio $\frac{\Delta T_E}{T_4}$ is small in magnitude, the specific speed of the turbine is approximately the same as that of the corresponding compressor of the same cycle, or

$$n_s(\text{turbine}) \simeq n_s\ (\text{compressor})$$

The data presented on Figure 78 can be used to select the proper turbine for the typical cycle. For the range of specific speeds established by the previous table, it can be seen that a radial turbine can be used over the range of cooling loads of 400 to 1600 Btu/min.

Radiators and Heat Exchangers

A detailed calculation of the required dimensions of the radiator of the gas cycle system, where the temperature of the fluid changes from entrance to exit, can be made using the design methods presented in Reference 48.

The heat exchanger of the gas cycle cooling system allows heat transfer from the environment to the gaseous refrigerant. This transferred heat is the cooling load of the system. The heat exchanger is essentially a gas to gas exchanger for which numerous light-weight and compact types of construction, suitable for space applications, have been studied and produced in Reference 49.

Example of Gas Cycle Systems

Despite its low performance, various applications of gas cycle systems can be found in space vehicles. For instance, an open air cycle can be considered for emergency operation in a life support system.

For illustrative purpose, the performance and weight characteristics of such a system delivering various cooling capacities are presented in Table 23.

A low pressure ratio cycle (3:1) is selected as a numerical example to offer a good COP and simplify the problem of selecting the system compressor and turbine. Table 23 shows that the main weight of the system is in the radiator, which contributes between 65 per cent and 75 per cent of the total weight for the range of cooling capacity considered here. Even with an optimistic approach to the system, the specific weight is still a considerable number; 75 to 65 lb per ton of cooling capacity.

Further improvement in the specific weight of the above system is possible by operating at a much higher cycle pressure to yield a higher heat rejection temperature, but at the expense of higher energy consumption. From the viewpoint of integrating the cooling and power system, operation at a higher cooling radiator temperature may not lead to a lighter overall unit, as noted in the preliminary investigation of Reference 47.

Table 23

Weight and Performance Characteristics
Of A Gas Cycle Refrigeration System

Conditions of Operation:

An open system with air as working fluid
Turbine exhaust temperature, T_4 = 50°F
Compressor inlet temperature, T_1 = 80°F

SYSTEM CHARACTERISTIC	COOLING CAPACITY BTU/MIN			SOURCE OF DATA
	200	600	1000	
Cycle pressure ratio, r	3	3	3	----
Coefficient of performance	0.37	0.37	0.37	Figure 71
Power requirement, hp	12.72	38.16	62.75	----
Refrigerant (air) flow rate, lb/sec	0.464	1.390	2.22	
Radiator area, sq ft	182	486	910	Equations 79, 80 Emissivity = 0.9 Fin Eff'ness =0.6
Radiator weight, lb	52.5	157.5	262.5	0.02 in. thick Alum. = 173 lb/ft^3
Compressor and expander, lb	10	15	25	AiResearch data
Electric motor and gear weight, lb	15	35	50	AiResearch data
System total weight, lb	77.5	207.5	337.5	----
Specific weight, lb/ton (1 ton of refrigeration = 20 Btu/min) 77.5	77.5	69.2	67.5	----

ACTIVE TEMPERATURE CONTROL SYSTEMS WITH A VORTEX TUBE

The vortex tube has often been suggested for use in temperature control systems because of its extreme simplicity and its adaptability to small, localized cooling requirements. Actually an expansion refrigeration machine with no moving parts, it is simply a straight length of tubing into which compressed gas is admitted tangentially at one end. In the counter-flow design illustrated in Figure 79, cold gas emerges from one end of the tube and hot gas exhausts from the other.

While many theories (References 50 and 51) have contributed to the understanding of this system, a simple presentation of its mechanics is as follows: in expanding between the nozzle blades shown in Figure 80, the gas enters the tube to form a free vortex flow pattern. In the central core of this vortex, viscosity of the fluid modifies the free vortex velocity distribution shown in Figure 81a into a forced vortex distribution, as in Figure 81c. In the conversion, the velocity decreases in the center core and increases in the outer layer. Equivalent to a work transfer from the center to the outer layer, this results in the gas becoming cold in the center and hot on the periphery. Simultaneous with this tangential flow, a longitudinal flow pattern, shown in Figure 81d, is established. This permits the cold gas to exhaust at one end and the hot gas at the other end.

Nomenclature

T	Temperature
W_T	Inlet air flow
K	Adiabatic exponent of working fluid
r	Inlet pressure/cold end pressure
q	Rate of heat transfer of the tube to outer environment
d	Diameter hot tube
p	Pressure
μ	Cold gas produced as a fraction of entering gas
π	Hot end pressure/cold end pressure
ΔT	Temperature difference
η	Efficiency

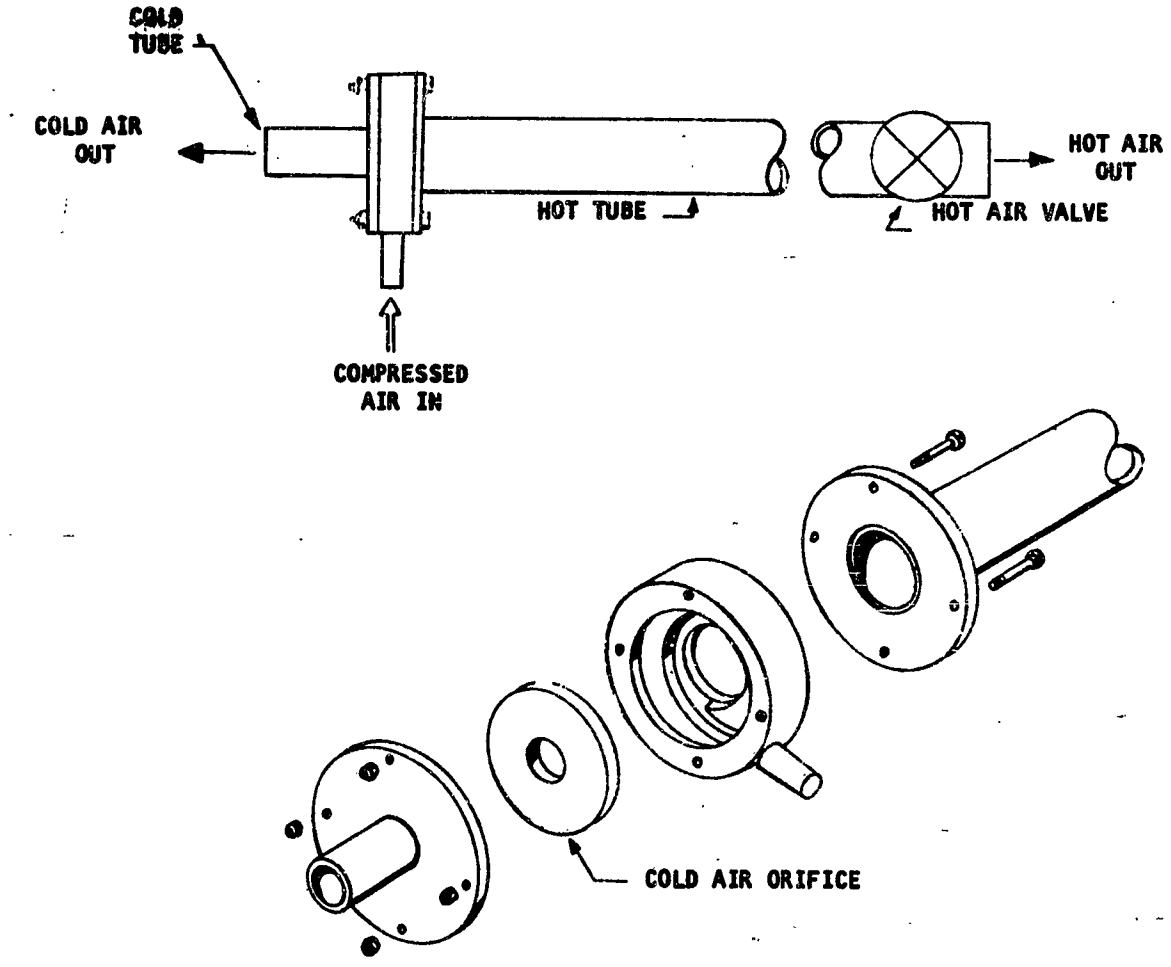

FIGURE 79.
VORTEX TUBE
LABORATORY MODEL

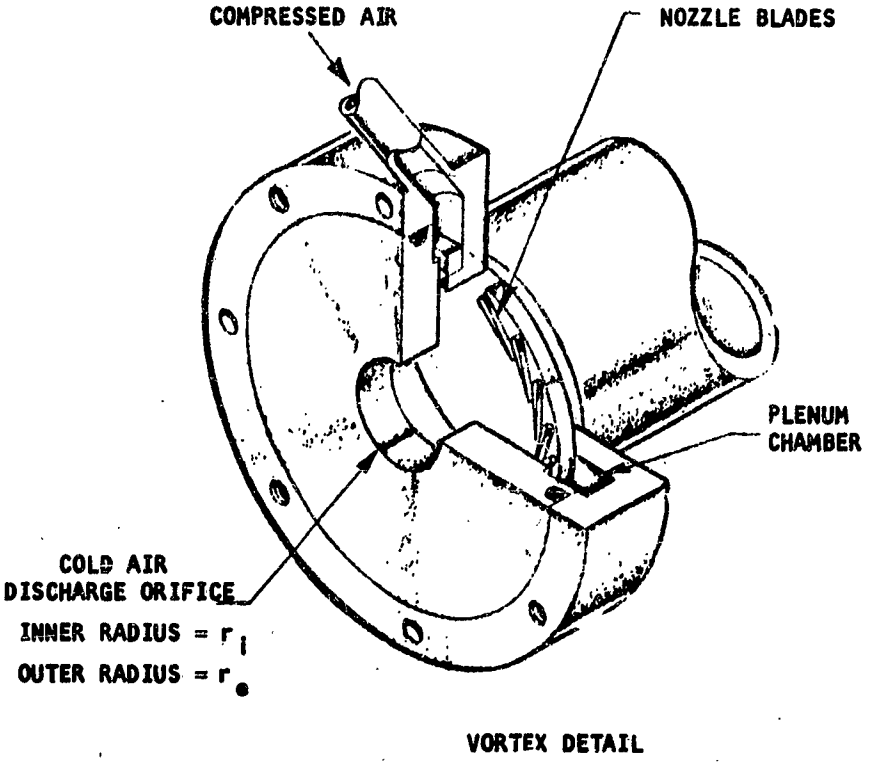

Figure 80.
Vortex Tube Nozzle Design

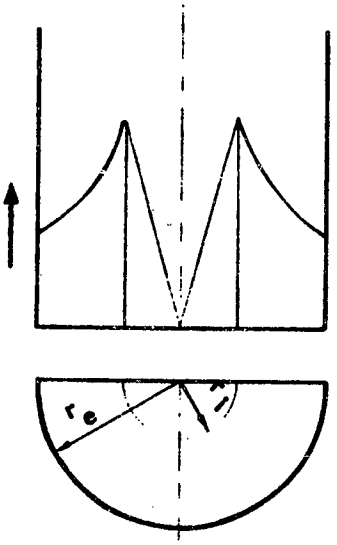

a.
Distribution of the Circumferential Velocity in a Tube

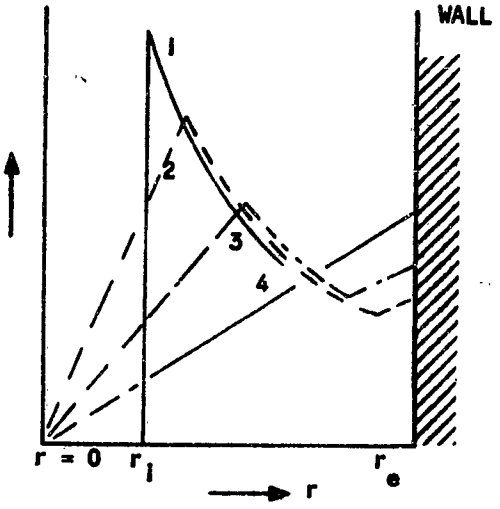

b.
Conversion of Irrotational To Rotational Flow

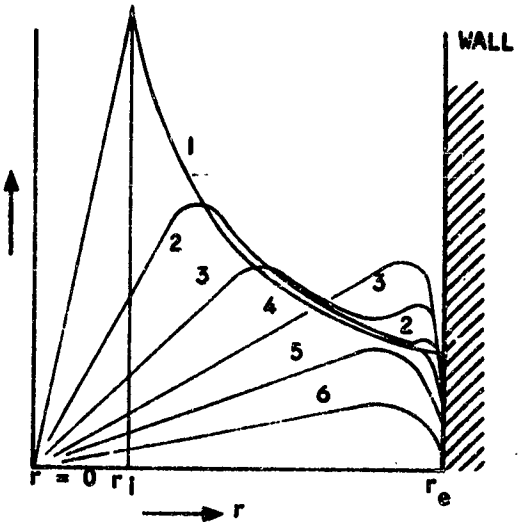

c.
Conversion of Flow Shown for 6 Intervals

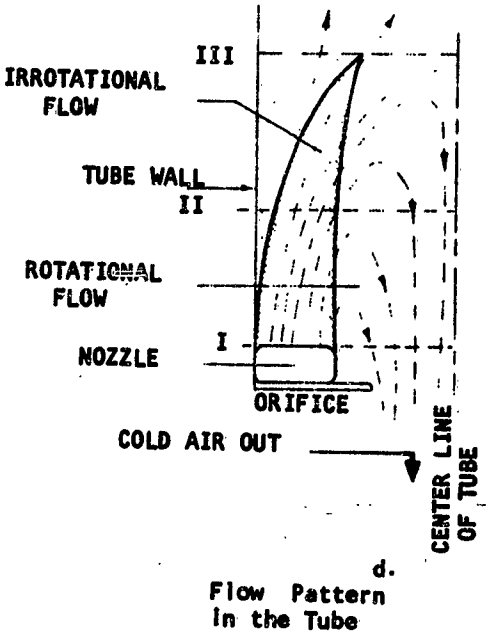

d.
Flow Pattern in the Tube

Figure 81. Vortex Tube Flow Patterns

Subscripts

1	Compressor inlet
2	Compressor exit
3	Inlet, vortex tube
4	Cold end, vortex tube
h	Hot end, vortex tube
c	Compressor
t	Turbine
E	Evaporator
C	Condenser

Characteristics of the Vortex Tube

Performance

Although theoretical analysis has been unsuccessful in predicting performance of this device, much experimental information has been obtained. The performance of a vortex tube of given design is governed by the following relationship:

$$\mu = f(T_3, r, \pi, q)$$

where μ = amount of cold gas produced, as a fraction of entering gas

T_3 = inlet gas temperature

r = inlet pressure/cold end pressure

π = hot end pressure/cold end pressure

q = rate of heat transfer of the tube to outer environment

In reporting an investigation of the vortex tube, Reference 52 gives the relationships of the cooling potential, $\Delta T_c = T_{in} = T_{cold}$, to μ for two pressure ratios. These are shown in Figure 82. A recent study (Reference 52) carried out with $q = o$, over a range of pressure ratios r between 2 and 10, shows that the best performance of an optimum geometric configuration is achieved when there is a back pressure at the hot end so

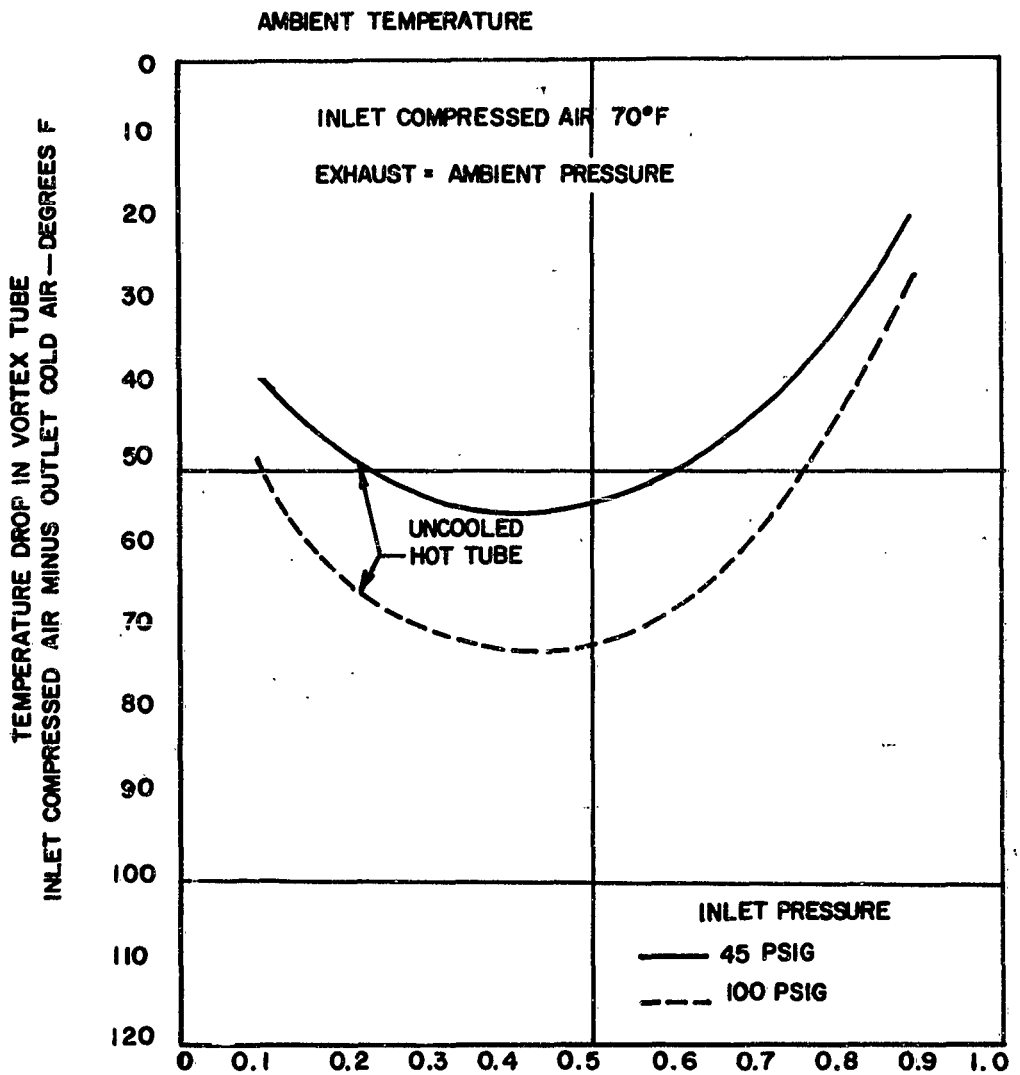

Figure 82

Performance of Vortex Tube
At Sea Level

that Π = 1.1 to 1.4. The optimum configuration requires a good flow stabilizer at the hot end with a tube length that has been obtained from experimental data.

The heating and cooling effects and the amount of cold flow in a vortex tube are obtained from a basic relation given by writing the energy conservation equation:

$$\mu = \frac{T_h - T_3}{T_4 - T_h} \qquad (85)$$

Size and Weight

Sizing the vortex tube for an active temperature control system is principally a question of determining the nozzle area that passes the amount of fluid to be processed and of using a proper hot tube diameter.

While the equations governing compressible flow give the nozzle area, the hot tube diameter is given by a design equation from Reference 52 as:

$$d = 1.2\sqrt{\frac{W_T}{P_i}} \qquad (86)$$

where d = Diameter of hot tube, in.

W_T = Inlet air flow, lb/min

P_1 = Inlet pressure, atmospheres

The cold tube diameter is determined by the continuity relationship for the amount of cold air μ produced. The hot tube length can be determined for the optimum operation with the stabilizer previously mentioned. According to Reference 52, this should be from 6 to 12 times the hot tube diameter. Figure 83 indicates the size of a typical vortex tube and its design condition.

Thermal Control Systems Using the Vortex Tube

As an expansion refrigerating device, the vortex tube can take the place of a turbine, particularly in a gas cycle. Since the cooling effect of the vortex tube is generally one-half that of a turbine, the coefficient of performance of a gas cycle using the vortex tube will not be as good as that of a corresponding conventional cycle.

The T-S diagram of Figure 84 shows the processes of a reverse Brayton cycle with a vortex tube for the hot and the cold gas. Neglecting the back pressure required for optimum operation, the hot gas, at the same pressure as the cold gas, is assumed to be cooled to the temperature T_1 to permit compression in the same compressor as the cold gas. Here an important

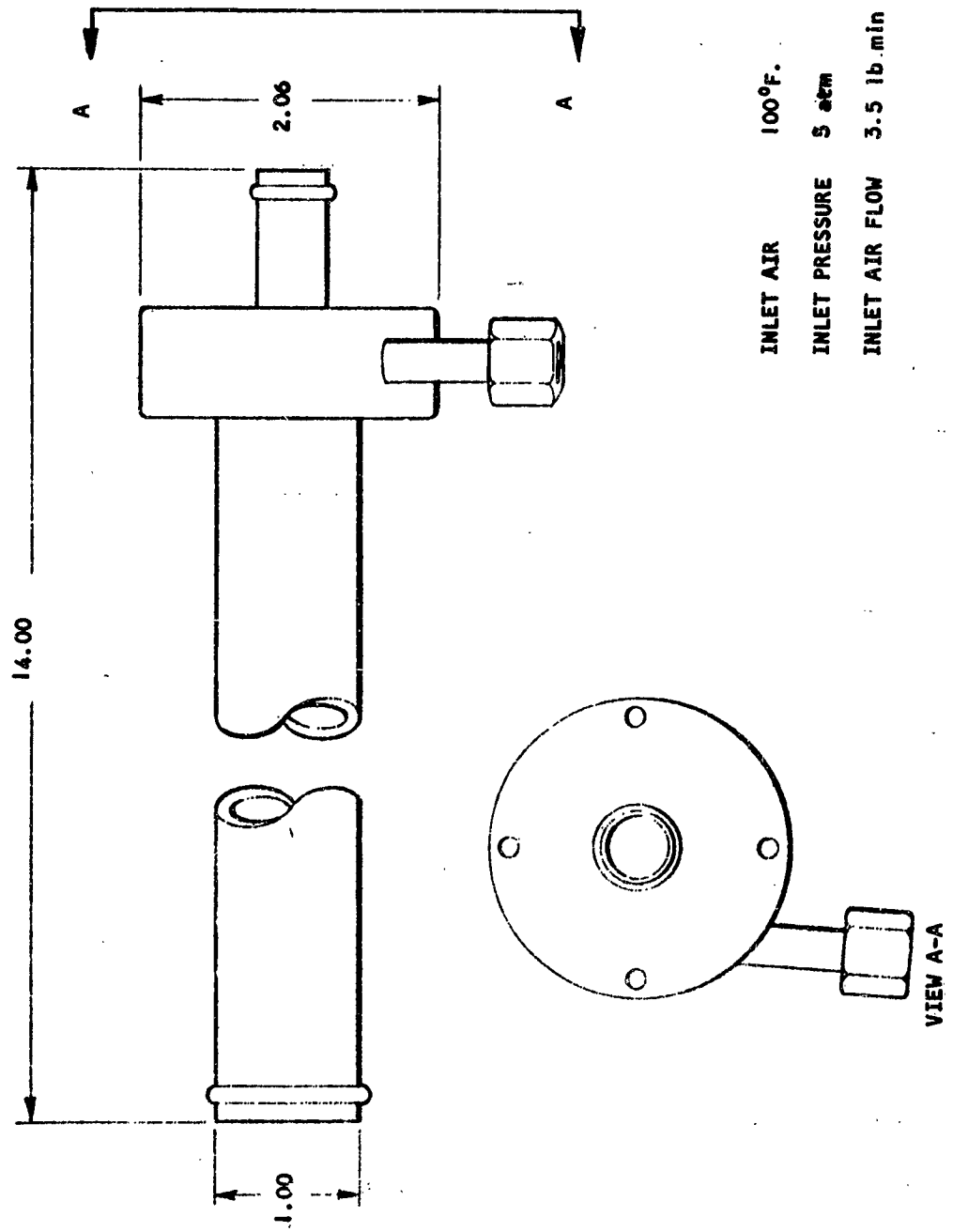

Figure 83. Typical Vortex Tube

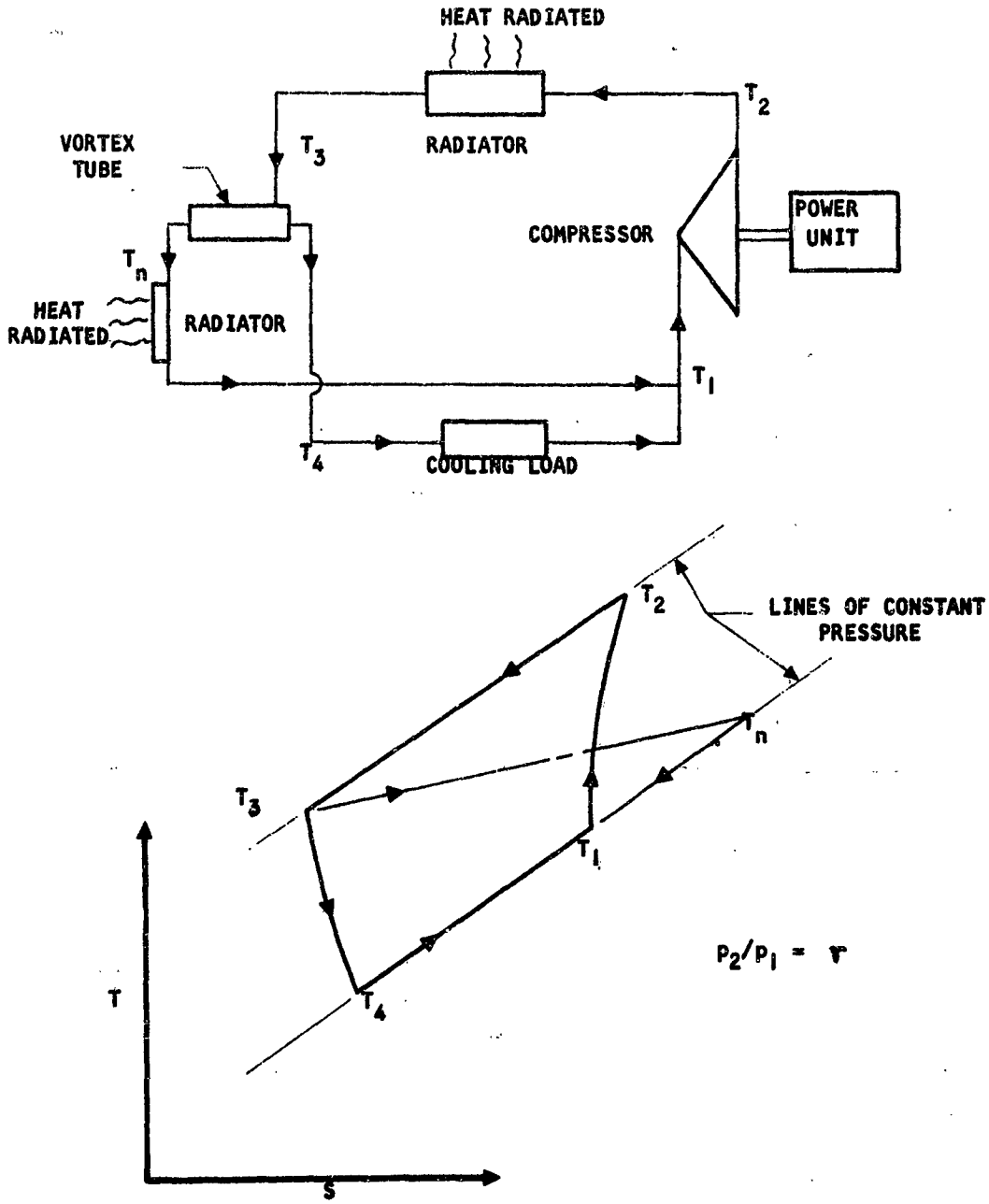

Figure 84. The Vortex Tube in a Brayton Cycle

difference between the vortex tube and turbine cycle appears. In a turbine, energy extracted from the cold gas goes into the shaft work used to drive the compressor, thus bettering the cycle performance. In the vortex tube cycle, energy from the hot gas is rejected to ambient along the Path T_2-T_3. Unless this energy is used profitably, such as for heating a thermoelectric refrigerator, the cycle performance will be low.

With the assumption of no pressure drop in heat exchange equipment (Paths T_2-T_3; T_h-T_1; T_4-T_1), the coefficient of cycle performance is calculated in the same way as for the gas cycle:

$$COP = \frac{\mu \, \Delta T_E / T_4}{\Delta T_C / T_4}$$

$$\frac{\Delta T_C}{T_4} = \left(1 + \frac{\Delta T_E}{T_4}\right) \frac{\gamma}{\eta_c} \qquad (86)$$

$$\gamma = r^{\frac{K-1}{K}} - 1 \, , \quad \mu = f(T_3, r, \pi, q)$$

where: COP = $\frac{\text{Heat extracted}}{\text{Cycle work}}$

ΔT_c = Temperature rise in the compressor, $^{\circ}R$

ΔT_E = Temperature rise in the compressor, $^{\circ}R$

T_4 = Cold air temperature of vortex tube, $^{\circ}R$

η_c = Compressor efficiency

The ratio $\Delta T_E / T_4$ is a design parameter of interest. The temperature T_3 entering the vortex tube is obtained from:

$$\frac{T_3}{T_4} = 1 + \frac{\eta_t \gamma}{(1+\eta_t)\gamma + 1} \qquad (87)$$

where η_t = cooling efficiency of the vortex tube defined on the same basis as a turbine:

$$\eta_t = \frac{T_3 - T}{T_3 \left(1 - \frac{1}{r^{\frac{K-1}{K}}}\right)} \qquad (88)$$

Figure 85 presents the variation of COP, T_3/T_4, as a function of the pressure ratio with practical values of the main parameters.

THERMOELECTRIC METHOD

The basic content of this discussion is taken from internal reports written by M. E. Stelzriede of S&ID.

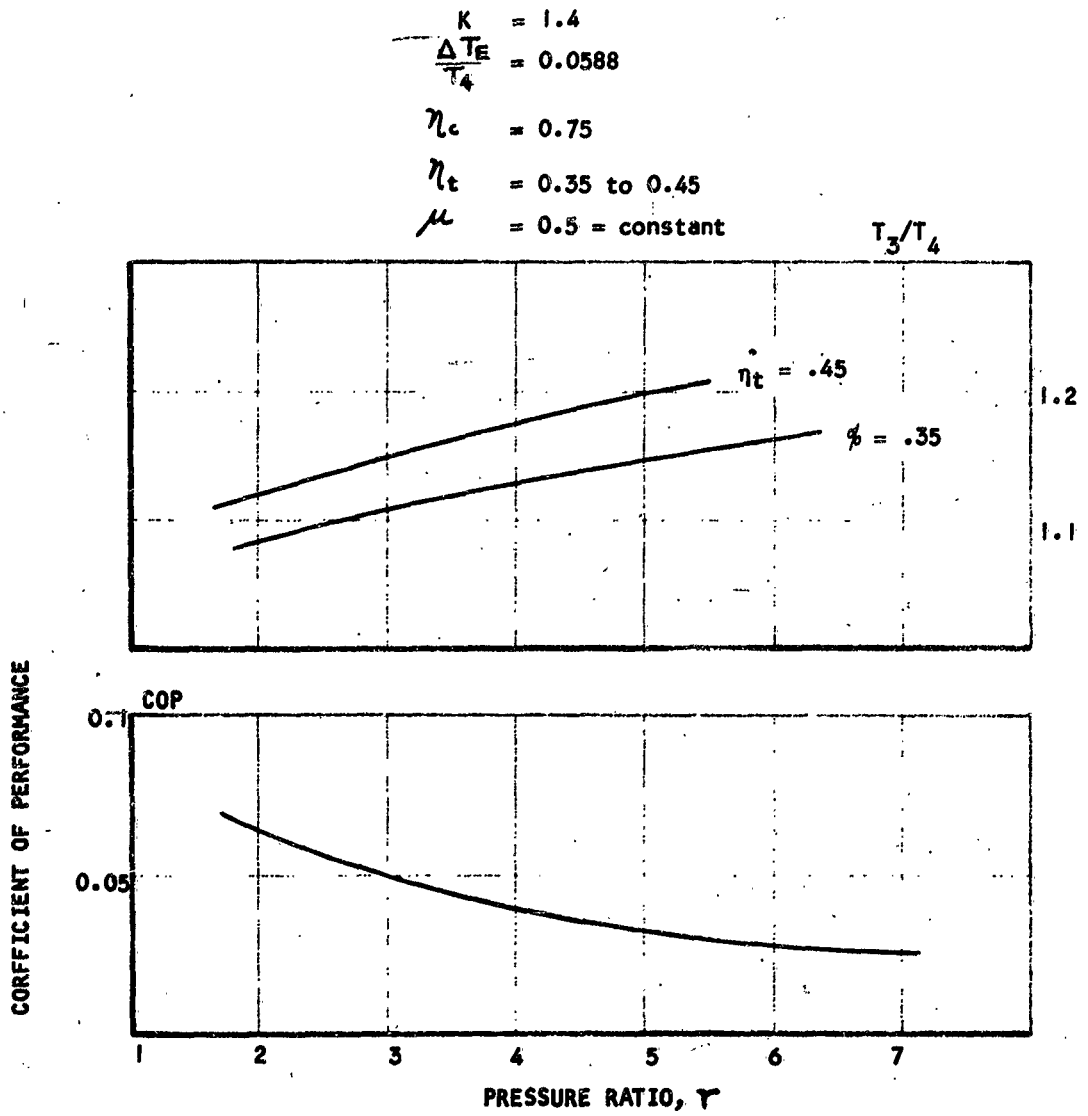

Figure 85. Performance of a Brayton Cycle Using a Vortex Tube.

Advantages and Disadvantages

Thermoelectric devices have a number of features which make their incorporation into the cooling and power generation systems of space vehicles appear attractive. Some of these features are the following:

1. Technical simplicity, compactness, lack of moving parts and lubrication requirements, and consequently a relatively high degree of reliability.

2. Freedom from noise and vibration.

3. Freedom from a requirement for consumable refrigerants and the related plumbing and leakage problems.

4. Freedom from toxic materials.

5. A minimum of maintenance and ground handling requirements.

6. The use of d-c power; if solar power or power produced by a thermoelectric generator is used, conversion from a-c to d-c is unnecessary.

7. Insensitivity to duration.

8. Adaptability to applications in weightless state.

9. Versatility; the same basic device can be used for heating, cooling, or power generation.

10. Design adaptability which permits Peltier devices to be incorporated into panels of component packaging.

11. Potential capabilities for miniaturization.

12. Usefulness over a wide range of ambient temperatures and in moderately corrosive environments.

13. Low mass production costs; most suitable materials are relatively inexpensive and readily obtainable in large quantities.

14. Simplicity of control; temperatures within small spaces can be held to close tolerances. Different areas can be selectively heated or cooled.

Generally speaking, most of these claims are justified. Many of the companies in the thermoelectric field tend to overemphasize these attractive features, however, and to minimize some of the limitations. This tendency is partly the result of the usual sales-department optimism which is manifest

with relation to any new product. It is also due partly to a lack of appreciation of the true potentialities of the devices at their present state of development.

The following list indicates some of the limitations of the Peltier cooling devices when used in primary cooling systems:

1. Power requirements are unfavorable; coefficients of performance using current materials are low compared with those of other cooling systems.

2. The ratio of weight to cooling capacity of practical Peltier cooling devices is high compared with other refrigeration systems, especially in the large capacity ranges.

3. Heat exchange at the hot and cold junctions may become the factor limiting the range of practicability for this type of system.

The current intense interest in manned space vehicles makes it urgent that all potential types of environmental control systems be explored to determine their place in craft of this kind. The main reason this study was initiated was to perform such an evaluation for thermoelectric cooling devices from the hard, practical viewpoint of a weapon system manager.

Nomenclature

a	Seebeck coefficient (volts per ^{o}K).
A	Total cross-sectional area of a cooler divided by the number of elements (square centimeters).
B	Active material volume proportionality factor.
F	Factor of merit of active thermoelectric material.
$\bar{I}$	Total current (amperes).
I_o	Current passing through each element (amperes).
k	Thermal conductivity of active thermoelectric material (watts per centimeter -^{o}K).
L	Length of thermoelement arm (centimeters).
m_o	Arm area ratio yielding maximum combined figure of merit.
M	Ratio of total voltage drop of thermoelement to $\bar{I}R$ portion.
N	Total number of elements in cooler.

N_e	Number of elements connected in a series branch.
N_r	Number of parallel rows of N_e elements each.
Q	Rate of heat flow (watts).
Q_o	Rate of heat removal from heat source (watts).
Q_1	Rate of heat rejection to heat sink (watts).
R	Total electrical resistance of two arms of thermoelement (ohms).
S	Total area of active material in refrigerator (square centimeters).
S_n	Area of n arm of thermoelement (square centimeters).
S_o	Area of both n and p arms of thermoelement (square centimeters).
S_p	Area of p arm of theremoelement (square centimeters).
T_a	Temperature of heat source (^oK).
T_b	Temperature of heat sink (^oK).
T_c	Cold junction temperature of Peltier cooler (^oK).
T_h	Hot junction of Peltier cooler (^oK).
ΔT	Temperature differential between hot and cold junctions (^oK).
v_o	Total voltage drop across one thermoelement (volts).
V	Supply voltage to Peltier cooler (volts).
V_m	Volume of active thermoelectric material (cubic centimeters).
W	Electrical power input to cooler (watts).
W_m	Weight of active thermoelectric material (grams or pounds).
Z	Figure of merit of thermoelectric material ($^oK^{-1}$).
Z_o	Optimum combined figure of merit of two.

Subscripts

n	n arm of thermoelement
p	p arm of thermoelement

γ	Specific weight (grams per cubic centimeters)
ϵ	Coefficient of performance (watts heat per electrical watt)
ϵ_c	Carnot, or ideal, coefficient of performance (watts per watt)
ϵ_o	Optimum, or maximum, coefficient of performance (watts per watt)
ρ	Electrical resistivity of thermoelectric material (ohm-centimeters)

Potential Applications

Peltier devices utilize a principle which has been known for a century and a quarter: that when an electrical current is passed through certain types of material a temperature differential between the two ends is produced. These devices are heat pumps and in this function are quite effective. The density of heat pumped, in watts/unit area, is enhanced by a temperature draw-down at the surface facing the cooled object or space, and a temperature build up at the surface toward which the heat is rejected. Consequently the heat flow density may be many times that which is typical of straight conduction through a solid material.

A Peltier heat pump, as any other type, refrigerates by transferring heat from a region where it is unwanted or not needed to another region where it is needed or where it may be disposed of. In a manned space vehicle its potential applications are most likely to be one of the following: (a) transferring excess heat from a mechanical or electronic component to the vehicle compartment; (b) transferring heat from one compartment to another, and (c) disposing of excess heat from within the vehicle to space.

Thermoelement Design for Peltier Refrigerators

In this section, a more detailed and logical technique of calculating performance capabilities and designing elements is presented.

The design equations are approximate, being based on several simplifying assumptions:

1. The thermal and electrical characteristics of the junctions between the active materials and the conducting strips are neglected.

2. It is assumed also that all heat flow occurs in the active material. Losses caused by heat back-flow from hot to cold plates between element arms, and heat losses from the sides of the cooler, are neglected.

3. The thermoelectric characteristics of the active materials are assumed to be independent of temperature within the range between the hot and cold junction temperatures.

Despite these assumptions, the answers are adequate for a first approximation required for preliminary design purposes. More precise values of the pertinent variables required for later stages of design can be obtained by digital computer techniques, using more exact relationships.

Design Problem Classes

At various times, the refrigeration system engineer may be faced with one of a number of types of problems relating to Peltier refrigerators. He may, for example, be required to analyze the theoretical performance of an existing component under certain temperature conditions. At another time he may be required to design a new cooler to meet certain specified conditions of weight and performance.

In the latter case, the relative emphasis placed on such factors as weight, power consumption, and cost will determine to a great extent the manner in which he applies the design equations. Reliability is always a consideration, and is, in fact, a strong point in favor of Peltier coolers. It may be necessary to design a cooler of a specified refrigeration capacity with relatively loose bound of available power to fit within certain space. In another situation, power may be most critical, with some weight and size penalty tolerable. Problems of this type lend themselves to ready solution by means of the equations discussed in this section.

In the unlikely situation where cost is the most critical factor, a cooler may be designed around thermoelectric slugs of a standard size and configuration.

Approach Used

The procedure outlined here covers a very general design problem: the synthesis of a design for an optimum-performance Peltier refrigerator to operate at or near room ambient temperature. It is assumed that any necessary variations in heat load can be handled by switching modules in and out of the circuit as required, keeping the current flowing in each element reasonably constant and near the design point. The element arms will be proportioned in such a manner as to minimize input power requirements, and consequently the design equations based on optimized performance can be used.

In the interest of overall optimization of the vehicle system, certain compromises must be made in the design of the refrigerator. Some of the compromises which enhance systems integration are discussed in this section.

Design Procedure

Within the framework of the general problem formulated for this discussion, the designer may wish to know general performance capabilities, volume and weight resulting from optimum design, or all details of the required design, including the number and configuration of elements and how they must be connected electrically. A complete solution may be determined through three steps which correspond to these considerations.

Determination of Optimum Performance. The maximum coefficient of performance with a Peltier refrigerator is capable of achieving in a given set of conditions can be determined by means of the following sequence of calculations. The equations are shown as they are given by Ioffe (Reference 56). Additional equations, such as those for the volume of active material, are developed in this report.

1. Selection of Temperature Range and Materials

The range from the cold junction temperature T_c to the hot junction temperature T_h across the active material (Figure 86), for specified source and sink temperatures T_a and T_b, depends on the current flowing, refrigeration rate Q_o, mode of heat exchange (conduction, convection, or radiation) at the two sides, and nature and area of heat transfer surfaces. Consequently the weight and complexity of the auxiliary thermal equipment, as well as the weight and performance of the active thermoelectric materials, must be considered in selecting a suitable temperature level.

Pending a more detailed analysis of the integrated vehicle system, the following general guide may be used during preliminary design to select a suitable range:

1. A low value of T_c and a high value of T_h favor efficient extraction of heat from the source and disposal to the sink, respectively, and thereby simplify auxiliary heat transfer equipment.

2. A high mean temperature, $(T_h + T_c)/2$, improves performance of the Peltier device.

3. An excessively high temperature boost, $T_h - T_c$, increases both the input power requirements and the weight of the active materials.

In the absence of any other specific temperature criterion, the error in the calculated performance of a cooler operating near room temperature will not be great (for first approximation, at least) if a cold junction temperature of 300 K and a temperature boost of 50 K are used. The accuracy of the performance parameters may be improved later by a more detailed analysis with more exact equations.

The best materials for refrigeration at moderate temperatures are n-type and p-type bismuth telluride. The quality of a material is judged on the

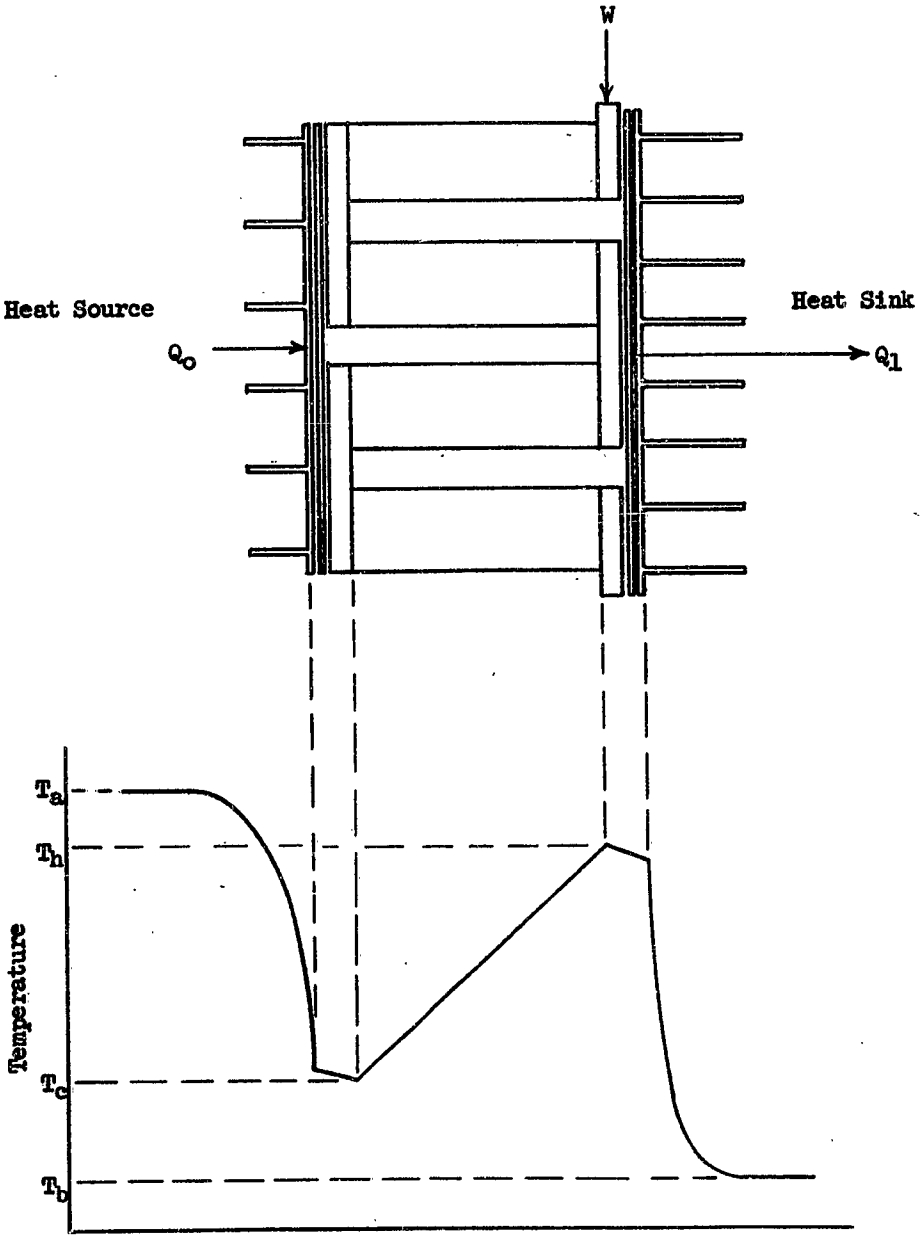

Figure 86. Temperature Profile Across Peltier Refrigerator

basis of its figure of merit

$$Z = \frac{a^2}{k\rho} \tag{89}$$

where

a = Seebeck coefficient (volts per ^{o}K)

K = Thermal conductivity (watts per centimeter -^{o}K)

ρ = Electrical resistivity (ohm-centimeters)

The figure of merit may be taken directly from published performance curves or determined from the other thermoelectric properties. Bismuth telluride having figure of merit values higher than 0.003 K^{-1}. However, it is thus far uncertain whether these results are repeatable.

2. Combined Figure of Merit

Because two different materials are normally used together in a cooler, it is necessary to compute an optimum effective or combined figure of merit. They may be expressed as

$$Z_o = \frac{(a_p - a_n)^2}{(\sqrt{k_p \rho_p} + \sqrt{k_n \rho_n})^2} \tag{90}$$

The subscripts in Equation 90 refer to the p-type and n-type materials. This optimum figure of merit can be achieved only by proportioning the cross-sectional areas of the two arms of the elements with respect to each other. The magnitude of the optimum combined figure of merit lies between that of the better and that of the inferior of the two individual materials.

3. M Factor

The total voltage drop v_o in each element is

$$v_o = (a_p - a_n)(T_h - T_c) + I_o R$$

where

I_o = Optimum current flowing

R = Total resistance of the two arms of the element

The ratio of the total unit voltage drop to the Joulean portion $I_o R$ under optimum conditions is a useful parameter in many design calculations. It can be shown to be $M = \frac{v_o}{I_o R} = \left[1 + Z_o \left(\frac{T_h + T_c}{2}\right)\right]^{1/2}$. (91)

3. Optimum Coefficient of Performance

The optimum, or maximum, coefficient of performance ϵ_o which can be achieved from two materials in the specified temperature range is

$$\epsilon_o = \frac{T_c}{T_h - T_c}\left(M - \frac{T_h}{T_c}\right) \qquad (92)$$

$$= \epsilon_c F$$

where

ϵ_c = Carnot or ideal coefficient of performance

F = Factor of merit

This optimum performance can be attained only after the elements have been proportioned geometrically for the level of current supplied.

The variation of ϵ_o is shown as a function of ΔT in Figure 87.

5. Power Input

The required power input can be found from the refrigeratior capacity and optimum coefficient of performance by

$$W = \frac{Q_o}{\epsilon_o} \qquad (93)$$

6. Disposal Heat

The heat to be discharged from the hot junction to the heat sink is the sum of that removed from the heat source plus the heat equivalent of electrical power supplied

$$Q_1 = Q_o + W = Q_o\left(1 + \frac{1}{\epsilon_o}\right) \qquad (94)$$

One of the factors determining the field of applicability of Peltier coolers is the ability to remove heat from the hot plate.

Determination of Quantity of Active Material. The required volume and weight of active material may be determined from the material characteristics and the junction temperatures without making a detailed element design.

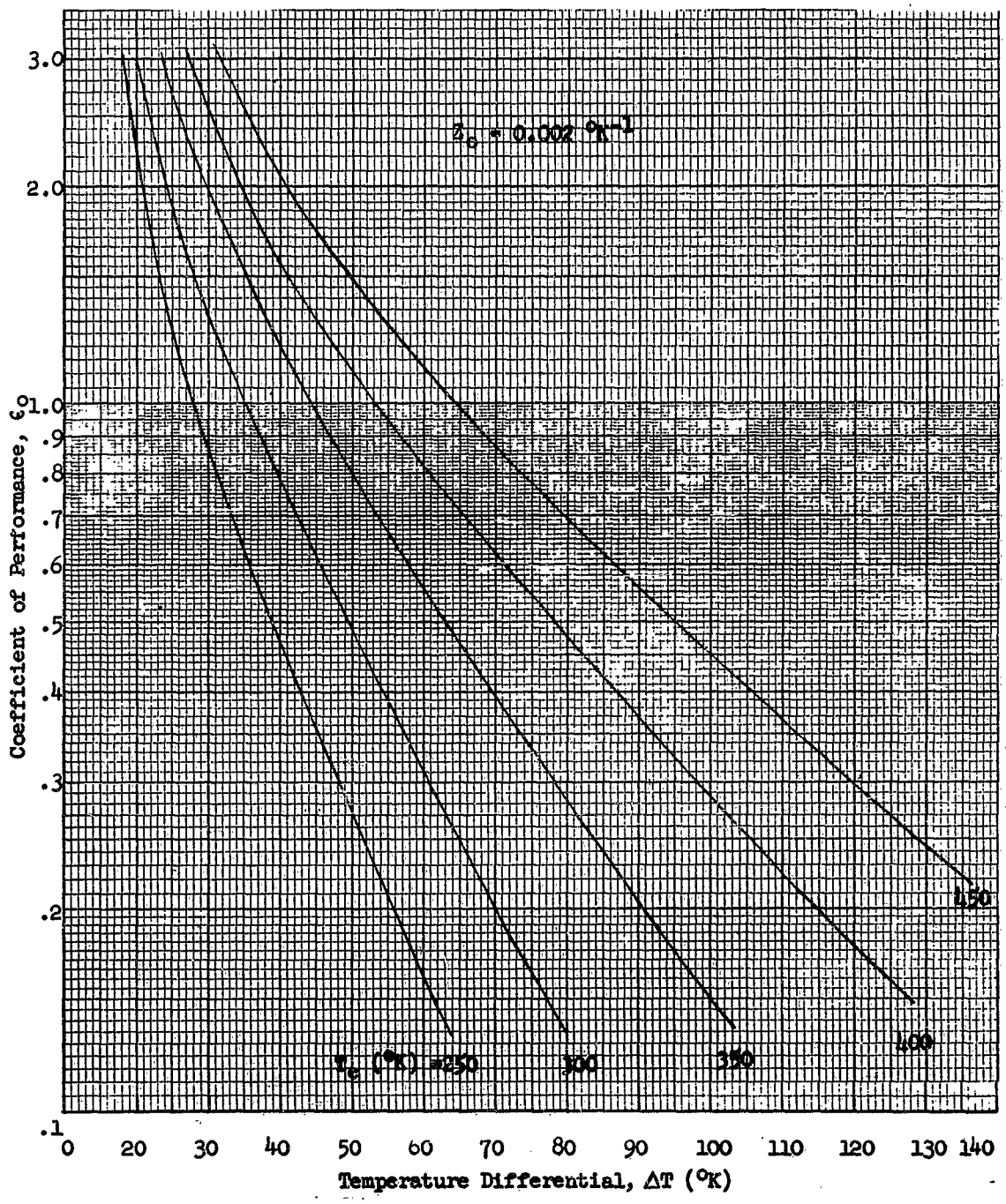

Figure 87. Peltier Coefficient of Performance as a Function of Temperature Differential

1. Element Arm Ratio

The ratio of the arm areas required to optimize the configuration of the element is

$$m_o = \frac{S_p}{S_n} = \sqrt{\frac{k_n \rho_p}{k_p \rho_n}} \tag{95}$$

2. Resistivity Factor

A factor joining the resistivities of the two element arms appears in many equations. It may be defined as

$$r = \rho_p + m_o \rho_n \tag{96}$$

3. Volume Proportionality Factor, B

The volume proportionality factor B collects into one term much of the influence of materials properties on the volume of active material. It is defined as

$$B = \frac{(a_p - a_n)^2}{r Z_o \left(1 + \frac{1}{m_o}\right)} = \frac{\left(\sqrt{k_p \rho_p} + \sqrt{k_n \rho_n}\right)^2}{r \left(1 + \frac{1}{m_o}\right)} \tag{97}$$

4. Minimum Acceptable Length

In order to establish the geometry of the elements, a value for either minimum total area or minimum acceptable element length is required. To keep the junction resistance below about 10 percent of that of the elements themselves, a minimum length of approximately 0.5 centimeter must be used.

5. Volume of Active Material

The volume of active material may be expressed in a form convenient for calculation

$$\frac{1}{Q_o}\left(\frac{V_m}{L^2}\right) = \frac{(T_h - T_c)(M - 1)}{2BM\, T_c \left(M - \frac{T_h}{T_c}\right)(T_h - T_c)} \tag{98}$$

6. Weight of Active Material

The weight of active material may be found by means of the expression

$$W_m = \gamma V_m \tag{99}$$

where

γ = Specific weight of active material (approximately 8.0 grams per cubic centimeter)

7. Modification of Hot and Cold Junction Temperatures

The junction temperatures may now be refined from the values originally assumed by making a three-way trade-off among active material weight, weight of power generator, and weight of auxiliary thermal equipment. With the new optimized temperatures, the previous solutions may be iterated to obtain closer approximations of performance.

Determination of Circuit Configuration. After the performance and the element configuration have been determined, the electrical arrangement of elements must be established. Outlined here are the factors to be considered in this aspect of device design.

1. Series Circuit

One arrangement of thermoelements for a Peltier refrigerator is a simple series circuit, (Figure 88). The total current passes through all elements and is equal to

$$I = I_o = \frac{W}{V} = \frac{Q_o}{\epsilon_o V} \tag{100}$$

where

V = Voltage supplied to refrigerator

The voltage drop across each element is

$$v_o = \frac{(a_p - a_n)(T_h - T_c)\,M}{M - 1} \tag{101}$$

To utilize the available voltage V, the total number of elements N must be

$$N = N_e = \frac{V}{v_o} \tag{102}$$

where

N_e = Number of elements connected in series

The total area of active materials in all elements has been determined by methods previously discussed. The area of material in one element is

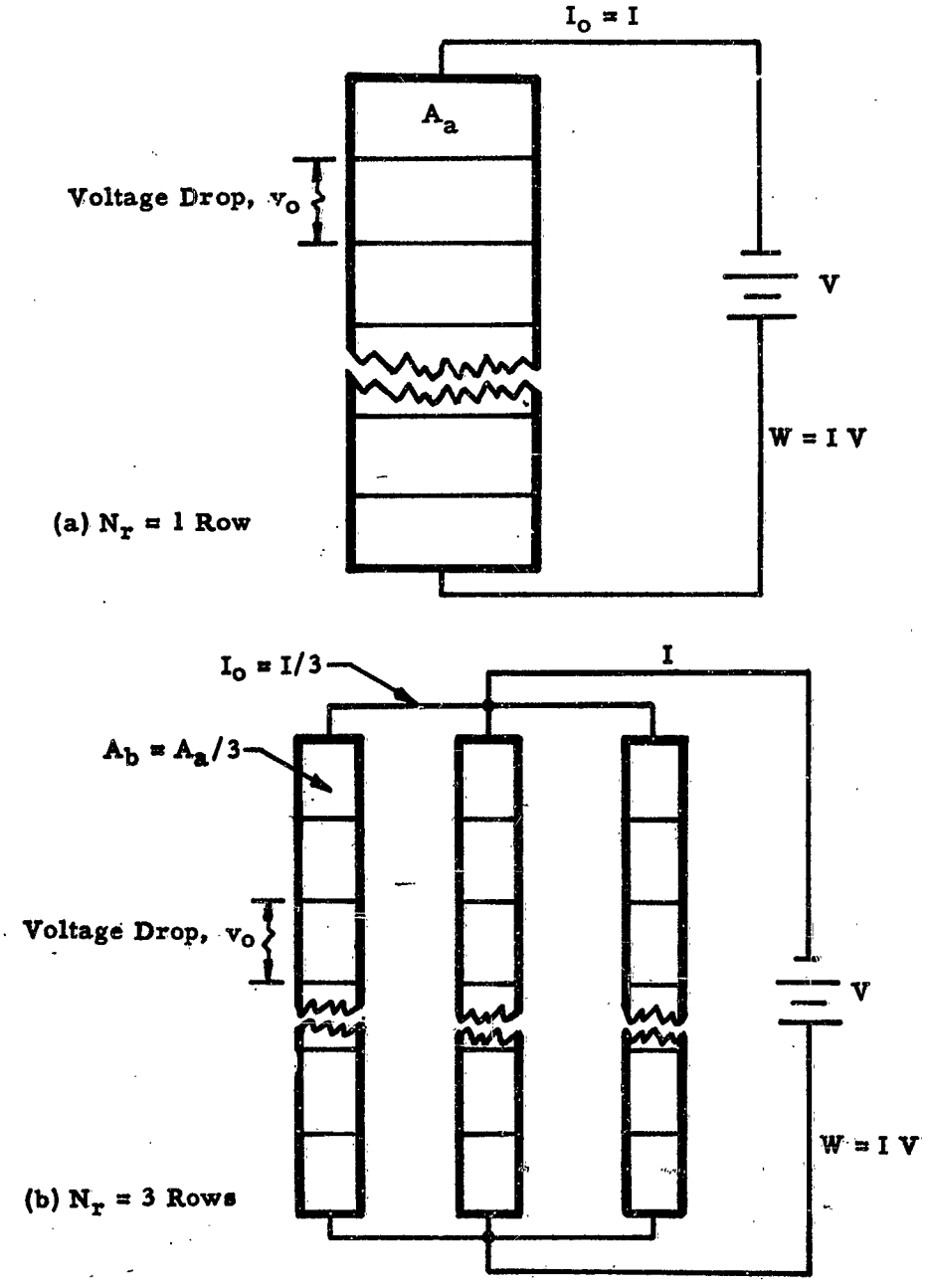

Total Thermoelement Area Same in Both Cases
Total Number of Elements Per Row, N_e, Same in Both Cases

Figure 88. Equivalent Series and Series-Parallel Thermoelectric Circuit Configurations

$$S_o = \frac{S}{N} \tag{103}$$

Areas of the individual arms of an element are

$$S_p = \frac{S_o}{1 + \frac{1}{m_o}} \tag{104}$$

$$S_n = \frac{S_p}{m_o} \tag{105}$$

Equations 100 through 105 are adequate for determining the configuration of elements for a simple series circuit. This arrangement provides for the smallest number but largest individual size of thermoelements.

2. Series-Parallel Circuit

In the equivalent alternate element layout (Figure 88) there are N_r parallel rows (in this case, $N_r = 3$), each containing N_e elements in series as before. The total number of elements is

$$N = N_e N_r \tag{106}$$

Because the number of elements in series is the same as in the simple series configuration, the unit voltage drop is the same. The total current is divided equally among the parallel branches, and consequently the unit current flowing through each element is

$$I_o = \frac{1}{N_r} \tag{107}$$

The total area at each element and the areas of the individual arms may be determined by Equations 103 through 105. The total area of all elements is unaffected by the manner of subdividing into elements. The effect of using a series-parallel circuit design is simply to use a larger number of smaller elements, while maintaining the same values for mass of material and current density.

It may be desirable to use a series-parallel arrangement for several reasons. For example, the larger number of elements can be more evenly spread over a larger area. This reason must be balanced against other equally important considerations, such as the fact that the use of a series circuit simplifies fabrication by reducing the required number of junctions.

Factors Controlling Active Material Volume

The equation for the volume of active material is

$$\frac{BV_m}{Q_o L^2} = \frac{(T_h + T_c)(M - 1)}{2M T_c \left(M - \frac{T_h}{T_c}\right)(T_h - T_c)} \qquad (108)$$

This equation has been solved by means of the digital computer, and the solution is presented graphically in various forms in this section. The curves given here show how the volume, and consequently the weight, of active material may be minimized by improving the material quality and by carefully selecting the temperature range. However, in many cases, the auxiliary theremal equipment rather than the active material may represent the most significant components of total weight. Hence, care should be taken in choosing the operating temperature range to ensure that the gross weight of the refrigeration system is not increased as a result of achieving economy of active material.

Cold Junction Temperature

Figure 89 is the solution of Equation 108 for a pair of materials having a combined figure of merit of $0.002K^{-1}$ as a function of cold junction temperature for temperature differentials up to 120 K. The envelope of these curves represents the minimum volume which can be attained by using the specified materials and still maintain optimum performance. The ΔT curve, which touches the envelope at any point, represents the temperature differential to be employed for corresponding cold junction temperature in order to achieve minimum weight. A series of such envelopes for pairs of materials having combined figures of merit from 0.001 to 0.005 K^{-1} is plotted in Figure 90. The temperature differentials yielding minimum volume are cross-plotted on these curves.

From Figure 90, it is apparent that the minimum volume which can be achieved decreases rapidly as the cold junction temperature increases. For example, the volume of materials, having a Z_o value of 0.003 K^{-1}, can be reduced 44 percent by increasing the cold junction temperature from 300 K (ΔT = 62 K) to 400 K (ΔT = 106 K). This latter example will be realistic only after future development. Even individual figures of merit, as high as 0.003, have not yet been consistently obtained. The highest temperature differentials which have been reported thus far are about 80 K.

Temperature Differential

The curve in Figure 91 shows $B V_m/L^2 Q_o$ as a function of the temperature differential. The materials selected have a combined figure of merit of 0.002 K^{-1} for various cold junction temperatures. The locus of minima represents the minimum volume which can be achieved for given temperature differentials. The interpolated value of T_c at any point on the locus

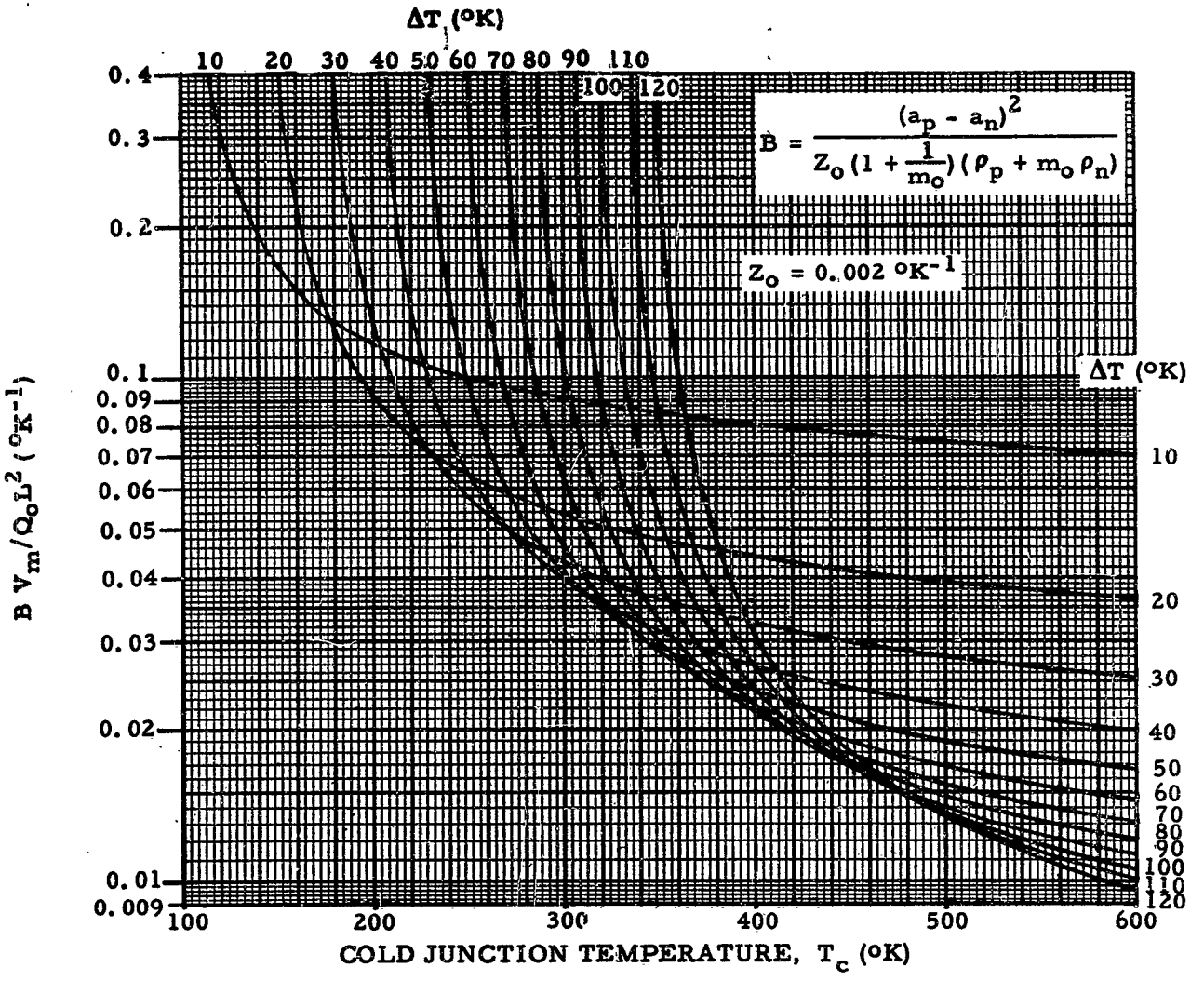

Figure 89. Volume of Active Thermoelectric Material as Function of Cold Junction Temperature

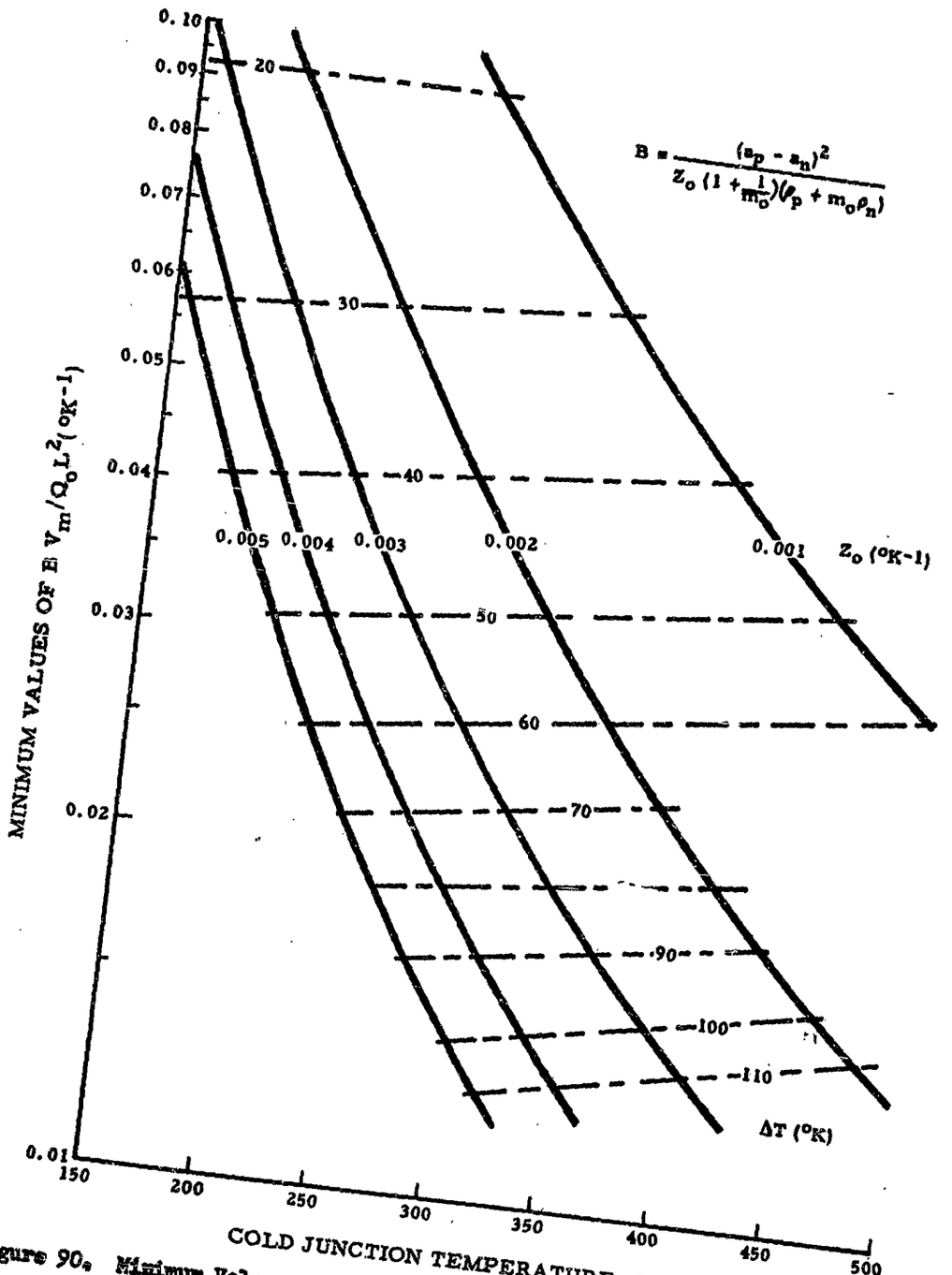

Figure 90. Minimum Volume of Active Thermoelectric Material Per Watt Refrigeration Capicity as Function of Cold Junction Temperature

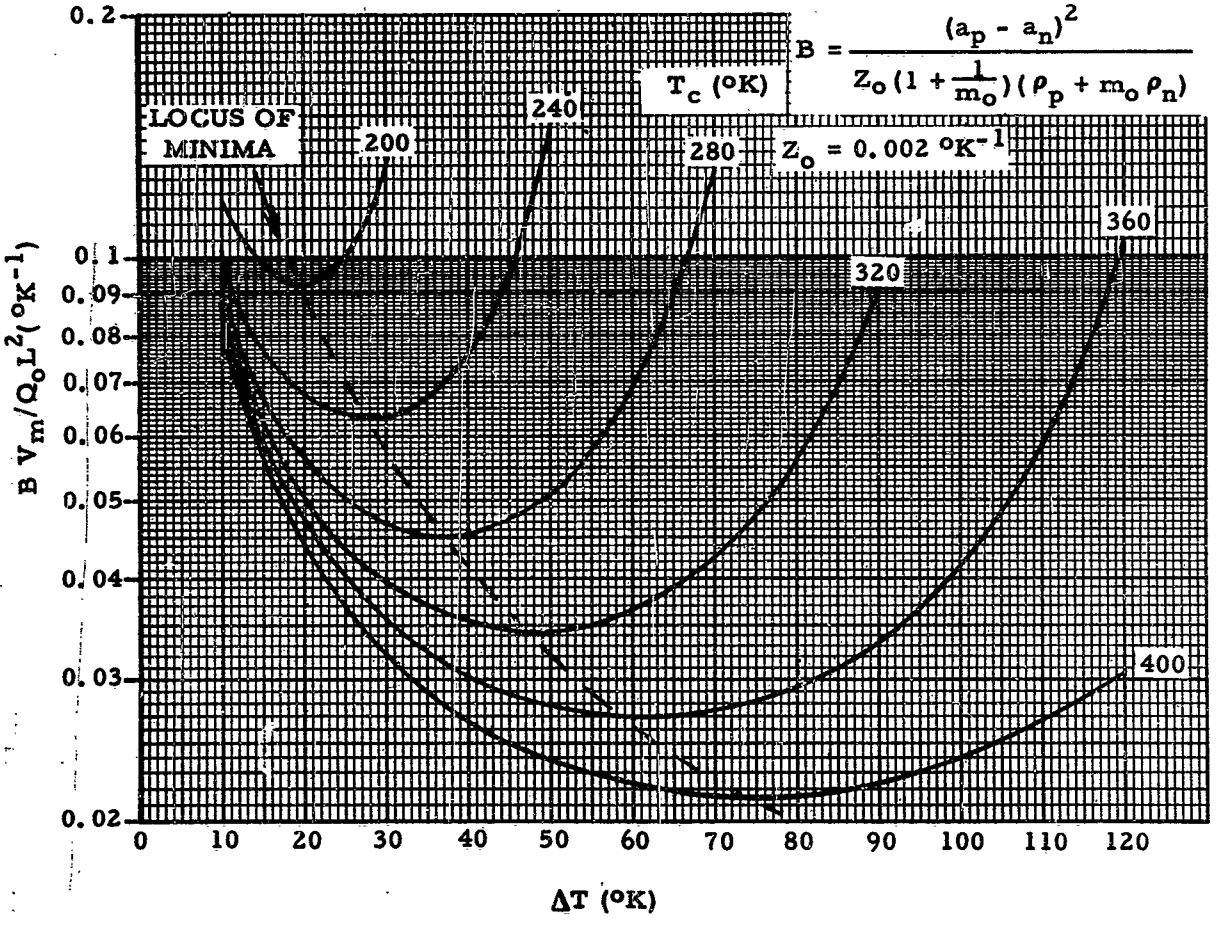

Figure 91. Volume of Active Thermoelectric Material as Function of Temperature Differential

represents the cold junction temperature for the corresponding value of temperature differential.

The method of balancing the weight of active material against weight of power generator may be obtained from Figure 91. For a case in which the cold junction temperature is 320 K, the weight of material increases as the temperature differential is decreased from the optimum value of 48 K. However, in making this change in differential, the coefficient of performance improves (Figure 87). Consequently, the weight of the power generator required to enable the cooler to pump heat at a specified rate decreases. The weight of heat exchanger at the heat sink side would also increase slightly because of this decrease in differential. The overall optimum differential would be the one which optimizes the sum of the weights.

The correlation between temperature differential and cold junction temperature for optimum material weight is presented in Figure 92. The optimum temperature differential is roughly proportional to the cold junction temperature.

Material Quality

As shown in Figure 93, for a constant cold junction temperature of 300 K, the volume may be reduced 28 percent by increasing the figure of merit from 0.003 to 0.004 K^{-1}. An increase in the cold junction temperature, coupled with an improvement in material, provides a greater advantage. For example, assume materials having a Z_o value of 0.0025 $K,^{-1}$ T_c of 300 K, and ΔT of 52 K. If these are replaced by materials having a Z_o value of 0.003$\frac{1}{4}$ $K,^{-1}$ T_c of 350 K, and ΔT of 93 K, the volume may be reduced by half.

CONCLUSION

Vapor Cycles

As an element of the active thermal control system for space vehicles, the vapor cycle system finds its application in meeting a requirement for large cooling capacity. Two general conclusions concerning its use are:

1. With the present state-of-the-art, the components of the vapor cycle can be made to operate in a zero-gravity environment by introducing some modifications to present designs for ground application. Within a condenser temperature range of 150°F to 250°F, a simple vapor cycle using Freon 11 appears most promising for space application. The evaporator of this zero-g vapor cycle would be of conventional design, using a heat transfer surface such as the plate fin or vortex type. The condenser would be of the radiator type using a tapered tube design. Other components of the cycle are common to that of high speed aircraft environmental control systems. This present-day approach is characterized by a specific weight on the order of 35 lb/ton of cooling capacity.

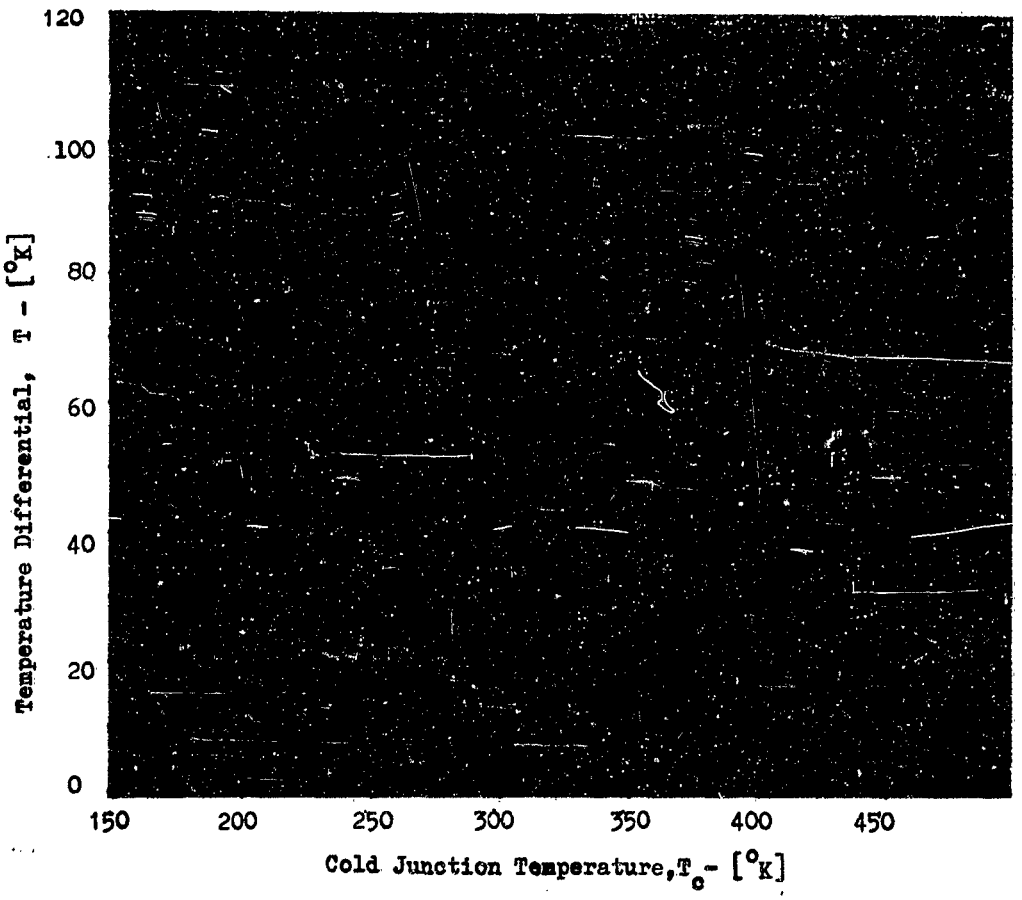

Figure 92. Optimum Temperature Differential as Function of Cold Junction Temperature (Based on Minimum Weight)

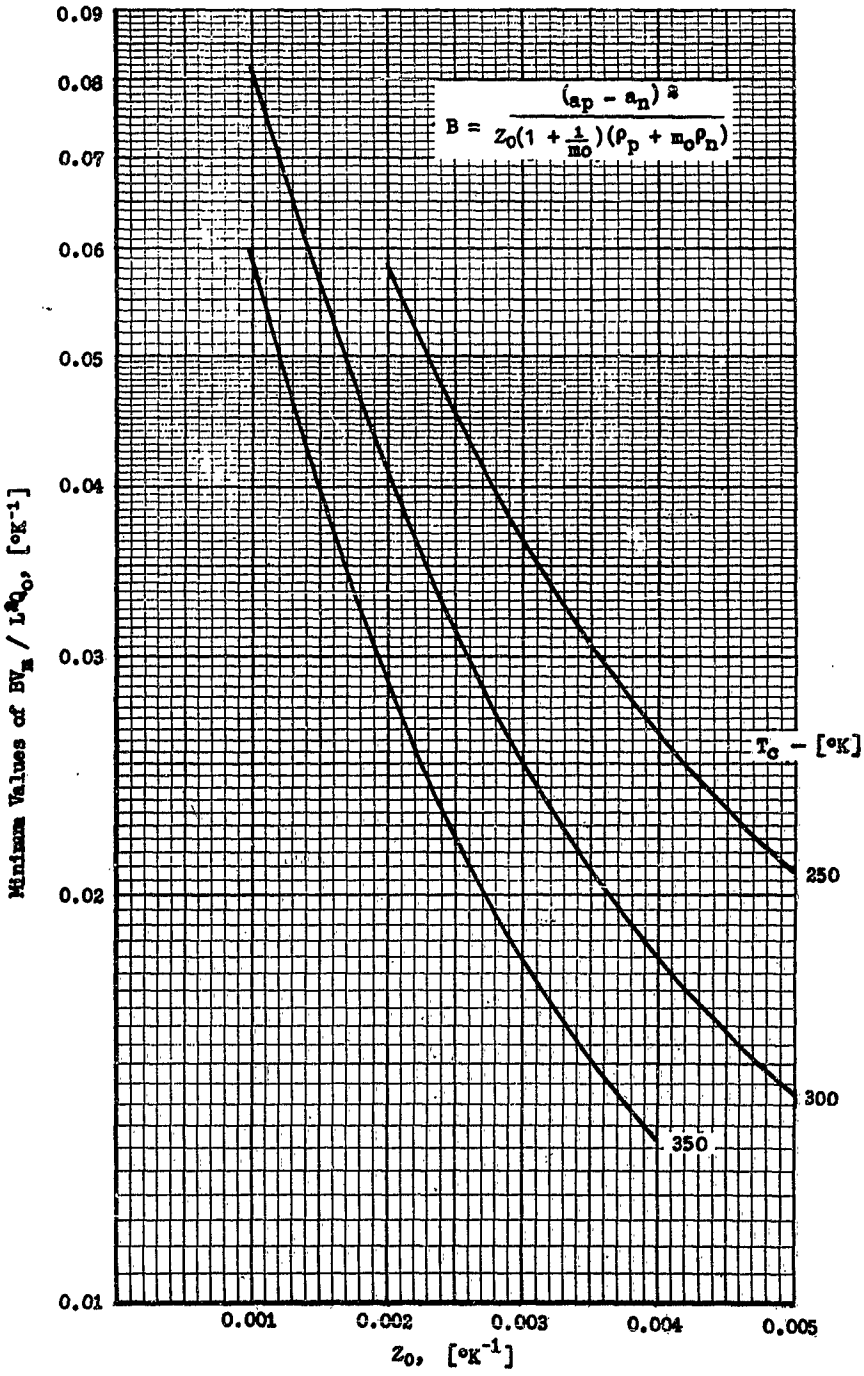

Figure 93. Minimum Volume of Active Thermoelectric Material as Function of Figure of Merit

2. To place the vapor cycle system in a more favorable position in the thermal control system, the most important step is to achieve a high COP at a temperature beyond 250°F. This approach is the most effective way to reduce the radiator weight that contributes largely to the system weight. It can be achieved by:

   a. A continuous search for high temperature refrigerants

   b. A development towards a quantum jump in performance of the compressor used in the system

   c. Advances in other components, such as high performance, light-weight evaporators and condensors.

Gas Cycles

As an element of active thermal control systems for space vehicles, the gas cycle system is characterized by a low coefficient of performance. Under favorable conditions, this performance is approximately one-half that of a vapor cycle. Among many usable fluids, gases with the lowest K values offer the best performance. As these gases do not lend themselves readily to an open cycle system, however, the many advantages of the gas cycle system are nullified.

Despite low performance, an application of the gas cycle system may be found in certain requirements, as, for example, in an emergency system to back up a malfunctioning vapor cycle. Its position in the emergency cooling spectrum lies between that of a passive cooling system and an extra vapor cycle system.

Vortex Tube

The results indicate a low COP compared to the gas cycle using a turbine. From the study of the variation of μ in Figure 44, the assumed value of 0.5 gives a realistic value of COP for the pressure value range of 2 to 3. At higher pressure ratios, it is smaller and the COP of Figure 85 represents optimistic values. It is seen then that, for best operation of the vortex tube, a low pressure ratio is preferred. From the system viewpoint, it may not be desirable because of the low temperature level at which heat is rejected to the outside environment. Thus, use of the vortex tube is beneficial if there is a heat transfer loop where the system can parasitically reject heat and also where the energy from the hot gas can be put profitably to work.

Thermoelectric Method

The initial surge of interest in semiconductors has tended to lead to overoptimism among people in the thermoelectric field regarding the place of Peltier cooling systems in space vehicles. The attractive aspects of

thermoelectric devices are balanced by an abundance of practical limitations.

It appears that at the current state of the technology other refrigeration systems, such as the vapor compression cycle, are better fitted to perform the primary refrigeration task for space vehicles. This conclusion is reached after considering relative weights, power requirements, and cost. In an unlikely situation where excessive weight and power requirements are not objectionable but reliability is of extreme importance, Peltier cooling could become competitive. For Peltier cooling to become generally competitive with other methods at reasonable temperatures, a major breakthrough in the materials field will apparently be required. In areas where heat pumping may take place at a very high temperature (presumably in an unmanned vehicle or in a portion of a manner vehicle distant from the passengers), thermoelectric systems may have a very definite application even at the present state-of-the-art.

The place of Peltier devices in the spot-cooling of temperature-sensitive electronic components having a low level of power dissipation from a small volume has already been proved. For this application the close-control capabilities of thermoelectric systems more than offset the disadvantages they may have with regard to weight, power and cost.

The use of Peltier heating during shady period on board the vehicle will also be limited. It cannot be used to pump heat inward from space during these periods because there is no significant external source from which heat can be pumped. On the moon it may, however, become feasible to pump heat into the vehicle from the moon's surface during the nights.

SECTION V. HEAT STORAGE METHODS

A heat storage method may be used aboard a space vehicle in preference to a cooling method for one of a number of reasons. These reasons include:

(a) The occurance of a peak heat load during a limited period, and in excess of the capacity of the disposal system.

(b) An increase in reliability and possible saving of weight over a cooling method.

(c) A desire to recover the heat for some purpose at a later date.

The purpose of such a method may be, therefore, to replace or supplement a cooling method.

NOMENCLATURE

C	Required Thermal Storage Capacity, Btu/hr
C_p	Specific Heat, Btu/lb°F
h	Heat Transfer Coefficient, Btu/$(ft)^2$(hr)(^oF)
k	Thermal Conductivity, Btu/(hr)(ft)(^oF)
Q	Heat Quantity, Btu
Q_f	Heat Quantity Stored as Heat of Fusion, Btu
Q_r	Heat Quantity that can be stored, Btu
Q_s	Heat Quantity stored as sensible heat, Btu
q	Rate of Heat Transfer (per unit length), Btu/(hr)
R	Radius, ft
R_f	Radius at which fusion fronts meet, ft
r	Radius of Fusion Front within Storage Cylinder at time Θ, ft

r_o Radius to edge of solid phase storage material outside, ft

r_2 Radius to edge of solid phase storage material, inside, ft

T Temperature, ^oR

T_o Maximum Temperature of Operation, ^oR

t Thickness of container wall, ft

W Weight, lb

x Distance from outside wall to fusion front at time Θ, ft

x_s Distance from centerline to container wall, ft

x_w Thickness of container wall, ft

λ Heat of Fusion, Btu/(lb)

ρ Density, $lb/(ft)^3$

Θ Duration of Latent Heat Transfer, hr

Θ_1 Duration of Latent Heat Transfer, Inside, hr

Θ_f Duration of Latent Heat Transfer, hr

Θ_r Duration of Total Heat Transfer, hr

Θ_s Duration of Sensible Heat Transfer, hr

Subscripts:

f Fusion

f Working Fluid

i Inside

m	Melting
o	Outside
s	Storage Material
w	Wall
1	First Material to be Compared
2	Second Material to be Compared

METHODS OF HEAT STORAGE

Because of the nature of heat energy, it can only be stored in some material. In space vehicles, this may be in a part of the structure or the equipment, in the fuel, or in a material especially provided for the purpose.

Storage in equipment or structure would be possible for relatively small quantities of heat and for relatively short periods of time. Heat storage in the fuel may be advantageous, especially if the fuel is to be vaporized and burned immediately. It may be argued, however, that this procedure is not heat storage but is an expendable coolant system. In any event, it could be applied only to those vehicles carrying fuel for space or reentry propulsion. The purpose of the present study is to explore the third means of storage, the use of materials serving no other function than to store heat.

HEAT STORAGE MATERIALS

Materials used for heat storage are selected on their ability to "soak up" or hold heat in one of several ways. The simplest method is to absorb heat without phase or chemical change, until the material reaches the temperature of the heat source. The amount of heat absorbed is, in this case, the product of mass, temperature and heat capacity.

A more effective material is one which has a fusion or melting temperature somewhere within the range of temperatures to be encountered. In such materials, a considerable amount of heat can be absorbed as heat of fusion, so that the capacity of a given quantity of material is increased without an increase in the operating temperature range.

The capacity of the system would be greatly increased if, after undergoing fusion and further temperature increase, the material could then be vaporized. It could then absorb an even greater quantity of thermal energy as latent heat of vaporization. However, the large increase in specific volume caused by vaporizing the material would be an inconvenience that could not ordinarily be handled aboard a space vehicle.

An endothermic chemical reaction between materials, at essentially constant temperature, can also serve to increase the ability of a system to absorb heat within a given temperature range. In cases where the stored heat is to be recovered later, it is necessary that these reactions be reversible, in other instances this may not be necessary.

Somewhat similar to the employment of chemical reactions between materials would be the use of endothermic dilutions. Here the addition of water to either a dry chemical or a concentrated solution is accompanied by an absorption of heat from the surroundings. This approach has received little if any attention and merits further exploration.

The Ideal Storage Material

A material which would be ideal for the storage of heat would have the following properties:

Thermal -

- High heat capacity
- High termal conductivity
- High boiling point
- High latent heat of fusion
- Melting point within the expected range of temperatures

Physical or Chemical -

- Stable or restorable to original composition
- Non-toxic
- Non flammable
- Non explosive
- Non Corrosive
- Low density
- In solid state at start

Other -

- High availability
- Low cost

It is obvious that no single material possesses all these desirable characteristics. In the following pages, the need for some of these properties is discussed and the search for materials approaching this paragon is described.

REVIEW OF HEAT STORAGE REPORTS

Two of the reports available on heat storage have been selected for close examination in the present report (References 57 and 58). They are comprehensive and summarize the results of studies of several thousand materials. In addition, they are of relatively recent publication.

These reports have two separate and distinct areas of study whose principal difference is the respective temperature range considered. The electronic cooling report (57) is concerned with temperatures of approximately 100 to 400°F, while the other (58) covers materials suitable for temperatures of 1200 to 3000°F. In the two following subsections, the contents of these reports are summarized. It is believed that in this way the most important aspects and problems of heat storage may be presented, as well as data on the properties of various heat storage materials. Observations on heat flow analyses are also included.

Heat Storage Cooling Of Electronic Equipment

Purpose and Scope of Investigation

The purpose of the investigation reported in Reference 57 was to study the cooling of electronic equipment in high speed air craft by the use of latent heat sinks, and to study the characteristics of materials suitable for such use. In these studies, operation of the heat sink was not expected to be continuous, but only during transient conditions of high ambient temperature, such as could result from aerodynamic heating. A similar situation in space vehicles may occur during relatively short periods of transmission of data accumulated over longer periods of observation.

The scope of the investigation included literature searches, experimental research and the analysis of the accumulated data. In the following discussions some of these results are examined and related to the present study.

Selection Of Materials

A literature search was made for materials having reversible solid liquid changes of phase occuring within the temperature range expected, and having "fairly reasonable" heats of fusion. This resulted in a list of almost 600 potentially suitable chemical compounds, most of which were organic. The number was quickly reduced by eliminating those which were toxic, scarce, costly, flammable or having other undesirable properties. The reduced list is seen in Table 24.

Compounds 1, 2 and 7 of Table 24 are shown to have two latent heats of fusion. This results from a double melting point which is characteristic of almost all glycerides. Tristearin, when moderately heated, will melt at 55°C while absorbing 46 gm-cal/gm. Upon further heating, it becomes solid again until reaching 72°C when it remelts with a latent heat of fusion of 55 gm-cal/gm.

The materials of this table have been listed in order of increasing melting temperatures. By selecting one with its melting point within the range of temperatures to be encountered, a heat storage capability equivalent to the latent heat of fusion may be obtained. The temperature above the melting point to which the material can be raised varies with the material and may be limited by evaporation, decomposition, or other change of property.

Other Sections Of Report

Other sections of Reference 57 cover the arrangement of heat storage devices, heat flow analyses, and the results of experimental work. The storage arrangements studied in this report were for high speed aircraft and are not directly applicable to spacecraft, except, perhaps, during reentry. In any event, this subject is considered from a space point of view later in the present report.

The heat flow analysis is made for three separate phases:

(a) from zero time until melting begins at time θ_1

(b) from time θ_1 until convection currents become important enough to be considered, at time θ_2

(c) from time θ_2 until the end of the transition of phase from solid to liquid.

TABLE 24 POSSIBLE COMPOUNDS FOR HEAT-STORAGE DEVICES

No.	Common Name	Chemical Symbol	Fusion Temp °C	Fusion Temp °F	Heat of Fusion gm-cal/gm	Heat of Fusion Btu/lb
1.	Tristearin	$(C_{17}H_{35}COO)_3C_3H_5$	56 72.5	133 162.5	45.6 54.5	82.1 98.1
2.	Heptadecanoic Acid	$C_{17}H_{34}O_2$	60	140	45.2 50.9	81.4 91.6
3.	Octcosance	$C_{28}H_{58}$	60.3	140.5	53.6	96.5
4.	Beeswax		61.8	143	42.3	71.6
5.	Hydrogenated Cottonseed Oil		62.3	144	44.3	79.7
6.	p-Chloroaniline	$H_2NC_6H_4Cl$	69	156	37.2	67
7.	Dotriacontane	$C_{32}H_{66}$	70	158	35.9 52.2	64.6 94
8.	Acetamide	C_2H_5ON	71	160	57.7	103.9
9.	Bromcamphor	$C_{10}H_{15}O\ Br$	77	171	41.6	74.9
10.	Durene	$C_{10}H_{14}$	79.3	175	37.4	67.3
11.	Methyl Bromobenzoate	$C_8H_2O_2\ Br$	81	178	30.2	54.4
12.	Dimethyl Tartrate	$(CHOH)_2$	87	189	35.1	63.2
13.	α-Naphtol	$C_{10}H_7OH$	95	203	38.9	70.0
14.	Glutaric Acid	$(CH_2)_3\ (COOH)_2$	97.5	207.5	37.4	67.3
15.	p-xylene Dichloride	$C_8H_8Cl_2$	100	212	32.9	59.2
16.	Catechol	$C_6H_4(OH)_2$	104.3	220	49.4	88.9
17.	Acetanilide	C_8H_9NO	115	239	36.3	65.3
18.	Succinic Anhydride	$(C\ H_2CO)_2O$	119	246	48.7	87.7
19.	Benzoic Acid	C_6H_5COOH	121.7	251	33.9	61.0
20.	Stilbene	$(C_6H_5CH)_2$	124	255	39.9	71.8
21.	Benzamideq	$C_6H_5CONH_2$	127.2	261	40.48	72.9
22.	Phenacetin	$CH_3CONHC_6H_4OC_6H_5$	137	279	32.68	58.8
23.	α-Glucose	$C_6H_{12}O_6$	141	286	41.7	75.1
24.	Acetyl-p-toluidine	$CH_3CONHC_6H_4CH_3$	146	295	43.0	77.4
25.	Phenalhydrazone Benzaldehyde	$C_6H_5CH_2NNHC_6H_5$	155	311	32.21	58
26.	Salicylic Acid	HOC_6H_4COOH	159	318	45.6	82.1
27.	Benzanilide	$C_6H_5CONHC_6H_5$	161	322	38.8	69.8
28.	Mannitol	$C_6H_{14}O_6$	166	331	70.3	126.5
29.	Hydroquinone	$C_6H_6O_2$	172.4	342	61.7	111.1
30.	p-Aminobenzoic Acid	$C_6H_4(NH_2)\ COOH$	188.5	371	36.5	65.7

A fourth phase would also have to be considered beginning at the time that all melting has been completed and continuing until the highest temperature is reached.

Differential equations were established for the first three phases, but no attempt was made to solve them because of their complexity. It was noted that the disregard of convection currents would be an assumption that would simplify these solutions. (In a zero-g field, this would be a necessary assumption). However, the investigators felt that an experimental determination of the protection time offered by a heat storage device would be " a much more rapid solution for preliminary engineering estimates".

The pertinent part of the experimental program covered transient heat flow during melting and the measurement of the time required for representative electronic equipment to reach a fixed percentage of the steady-state temperature. The conclusion reached was that the data obtained experimentally could not be predicted by known analytic methods. This serves to supplement the previous statement that experimental methods are much more rapid than analytic. The heat storage materials used in the study were beeswax and paraffin.

The conclusions reached by the authors regarding this entire program of study and test include: (1) that heat storage materials, such as beeswax and parrafin, cannot protect, adequately, representative electronic equipment during a step increase in ambient temperature from 50 to 400°F, for as short a period as 20 minutes. (2) that cooling methods exist that are more adequate and offer much better protection for the same weight (3) than an evaporative cooling system using water or a water-alcohol solution can absorb 10 to 20 times the heat absorbed in a latent heat sink, per pound of system weight. (4) the heat transfer rate for an evaporating fluid is 100 to 1000 times that into a storage system, during a step increase in temperature. It should be emphasized, however, that for space flight a direct comparison cannot be made between expendable and storage systems on the basis of heat transfer and absorption alone.

Heat Storage At Higher Than Electronic Equipment Temperatures

Purpose And Scope Of Investigation

The purpose of the study reported in Reference 58 is to determine and to analyze the potentialities of a number of thermal energy storage materials. The scope of the study was threefold:

(1) a literature search for heat storage materials and their physical properties; (2) a research program to obtain unavailable data on properties of these materials; (3) a thermal analysis of some heat storage systems. Another investigation of the physical properties at high temperature of some materials of construction is also reported but is not of interest in the present investigation.

This program differed from that on electronic cooling in that the range of temperatures was considerably higher, being from approximately 1200 to 3000°F. Also, the concept of an endothermic chemical reaction as a heat absorber was considered, as well as the more usual phase-change type of storage.

Results Of Literature Search

The purpose of the first part of the literature search was to study compounds which might be able to store thermal energy through heats of reaction. This may be referred to as the chemical storage of heat. The materials sought would be of liquid, as both reactants and products, in the desired temperature range of 1200 to 3000°F. Liquids were considered to be most desirable because they would have the least volume change and the best heat transfer characteristics, and because the design of such systems would be simpler. Another requirements was that the chemical reaction be reversible. In addition, it was desired that the storage capability be at least 400 Btu per pound of storage material.

The reactions believed by the authors to be most promising involved alkaline earth metals and halides of alkaline metals. However, the conclusion reached was that the reactions do not become thermodynamically favorable until vaporization of the volatile metal begins and that, therefore, this form of storage does not warrant further study.

Another part of the literature search covered peritectic reactions of binary alloys and of double salts compounds and eutectics. It was concluded that these reactions showed promise and should receive further consideration.

The method of heat storage having the most promise was concluded to be the use of latent heat of fusion of certain selected compounds. Table 25 lists fifteen materials having melting temperatures between 1200 and 3000°F, and heats of fusion greater than 300 Btu per pound. Some of the materials, such as lithium hydride and the other alkali metal halides, are reactive with most construc-

TABLE 25. HEAT OF FUSION OF POTENTIAL HEAT STORAGE MATERIALS

MATERIAL	Melting Temperature		Heat of Fusion
	°K	°F	BTU/lb
LiH	961	1270	1000*
Si	1683	2570	710
Be	1556	2341	560
VSi_2	1927	3009	489
$TiSi_2$	1813	2803	474
LiF	1121	1558	450
$CrSi_2$	1823	2821	446
MgF_2	1536	2305	390
$CoSi_2$	1599	2418	380
$MgSi_2$	1375	2015	361
CrSi	1873	2911	342
CaSi	1518	2272	338
CoSi	1733	2659	310
$Li_2O\ B_2O_3$	1033	1400	310
NaF	1268	1823	300-345

tion materials. The mixed oxide and binary metallic compounds do not have this disadvantage.

Theoretical Heat Transfer Analysis

The equations derived in this section of the report were intended to permit comparisons between potential heat storage materials. They are not considered to be adequate for determining an exact heat release rate at any time, but only an average rate for the period under consideration. One reason for this is the fact that poor heat conducting solids are expected to build up on the colder wall during heat release, so that the heat release rate will continuously vary.

The variables included in these analyses are the thermal conductivity, density and heat of fusion of the material, and the geometry of the material container. Three geometric forms were considered, cylindrical capsules, the annular space between concentric cylinders, and thin blocks which would conform to the shape of the working fluid reservoir. Heat transfer to and from the storage material is accomplished by means of this working fluid.

The following equations and definitions are either basic or easily derived, and are applicable to all geometric forms:

$$\Theta_r = \Theta_s + \Theta_f \tag{109}$$

$$Q_r = q_r \Theta_r \tag{110}$$

$$\Theta_s = W_s c_{p_s} (T_o - T_m) \tag{111}$$

$$\Theta_f = W_s \lambda \tag{112}$$

$$W_s = \frac{Q_r}{C} \tag{113}$$

$$T_o = T_m + \frac{Q_s}{W_s c_{p_s}} \tag{114}$$

$$\Theta_r = \Theta_s + \Theta_f \tag{115}$$

$$\Theta_s = \frac{Q_s}{q_r} \tag{116}$$

$$\Theta_f = \frac{Q_f}{q_r} \tag{117}$$

Equations were derived for each of the three geometries described. The important equations for the cylinder and block case are given here, but the reader is referred to the original report for details of their derivation.

Equations For Heat Storage Material Contained In Cylindrical Capsules. (See Figure 94a).

$$q = \frac{(T_m - T_f)}{\frac{\ln(R_o/r)}{2\pi k_s} + \frac{1}{2\pi(R_o + \frac{t}{2})k_w} + \frac{1}{2\pi(R_o+t)h_o}} \tag{118}$$

$$\theta_f = \frac{\lambda \rho R_o^2}{4k_s(T_m - T_f)} \tag{119}$$

$$\frac{\theta_{f2}}{\theta_{f1}} = \frac{\lambda_2 \rho_2 k_{s1}}{\lambda_1 \rho_1 k_{s2}} \tag{120}$$

Equations For Heat Storage Material Contained In Rectangular Blocks. (See Figure 94b)

$$q' = \frac{(T_m - T_f)}{\frac{x_s}{k_s} + \frac{x_w}{k_w} + \frac{1}{h_o}} \tag{121}$$

$$\theta = \frac{\lambda \rho x_s^2}{(T_m - T_f)} \left(\frac{1}{2k_s} + \frac{x_w}{k_w x_s} + \frac{1}{h_o x_s} \right) \tag{122}$$

For negligible film and wall resistances this becomes:

$$\theta = \frac{\lambda \rho x_s^2}{2k_s(T_m - T_f)} \tag{123}$$

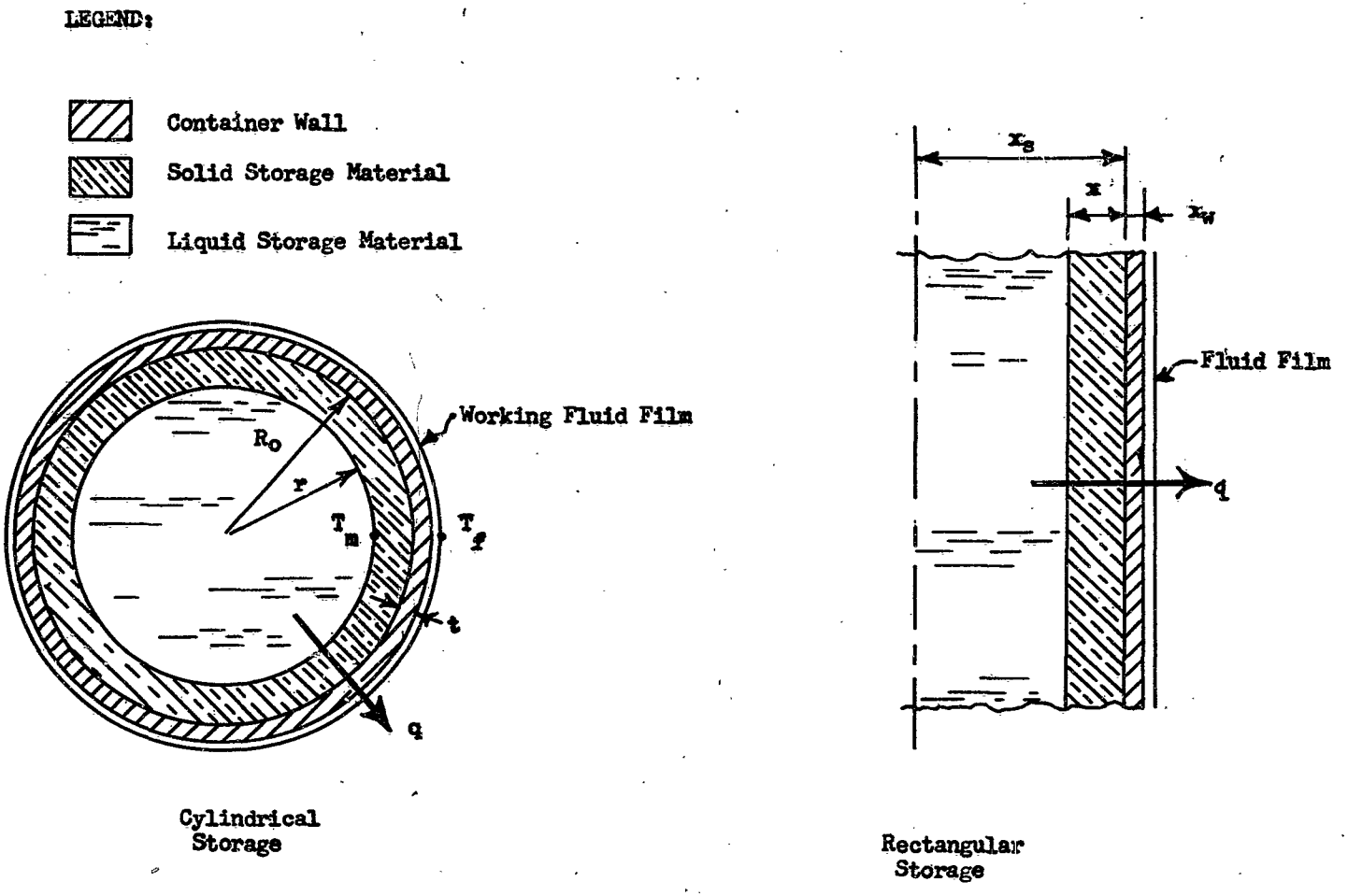

Figure 94. Dimensional Relationships in Heat Storage Analysis

CONCLUSION

The mass of the equipment and structure can serve as a heat storage medium. However, the use of materials with high heats of vaporization or fusion can give a higher heat storage capacity at a relatively low weight. Unfortunately, the problem of maintaining good heat transfer to the face of the heat storage material in a zero-gravity environment makes this method limited in usefulness. The expendable coolant method has many advantages over direct storage because of the forced convection boiling.

Equations for predicting, the rate of decomposition and heat storage of heat storage materials are complex and inaccurate. Therefore, direct experimentation is necessary for good measurements of decomposition time and heat storage capacity in most applications.

SECTION VI

COMPARISON OF TEMPERATURE CONTROL METHODS AND SYSTEMS

INTRODUCTION

The comparison of temperature control methods is desirable in order to select the ideal control method for a particular application. Of course, the variety and differences of the methods makes comparison fairly difficult, especially in the general case. Considering all of the parameters involved, the main criteria for comparison appear to be the following in order of importance:

1) Performance: control limits, maximum cooling load, response, adaptability;

2) Weight: weight of components, fluid, penalty weight of power requirements;

3) Volume: volume of tanks, components;

4) Surface area: surface area of radiator and power source;

5) Reliability: redundancies, mechanical and electrical failure, possible damage to vehicle equipment from malfunction;

6) Others: cost; corrosiveness, flamability, and toxicity of fluids; maintenance.

Some comparisons using these criteria are included in the first part of this section. Other parts of the section deal with (2) combinations of methods into control systems and comparison of these systems and (3) special considerations for control methods due to mission, equipment and vehicle requirements.

The first part of this section deals with comparison of methods. Various passive, semi-passive, and active methods are tabulated (Tables 26, 27, and 28) and described, and limitations and advantages of each method are discussed. Following these tables is a chart (Table 29) and curve (Figure 95) useful in comparing passive, semi-passive, or active methods in general. This table shows that the skin or radiator temperature and maximum heat load dissipation per unit area are useful in comparing the methods. In addition, this first part includes a discussion and curves of penalty weight and surface area for power requirements useful in evaluating the power requirement for fans, pumps, compressors, controllers, and heaters in terms of weight.

Table 26. Table Of Methods Of Passive Temperature Control

Method	Description	Limitations	Advantages
External Surface Coating 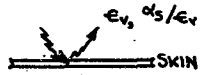	The choice of Surface coating properties ϵ_v and α_s allows a selection of vehicle skin temperature	1) Practical Surface limits; $\alpha_s/\epsilon_v = 0.2$ to 4.0 $\epsilon_v = 0.05$ to 0.97 2) The surface coating properties may change because of heat radiation, cosmic radiation, meteorite damage, or low vaccumm pressures in space.	1) Little additional weight to vehicle 2) Minimizes solar heat radiation effects to vehicle by use of low 3) Increase internal heat dissipation to space by use of high ϵ_v.
Internal Heat Transfer Thermal Conductivity 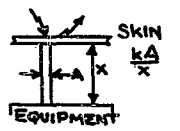	Variation of thermal conductivity, area, distance from skin, or all three influences the heat transfer from the internal equipment.	1) Practical Thermal conductivity limits are 0.02 lower and 200 $\frac{BTU}{ft.hr.^oF}$ upper. 2) Area and distance from skin variations are limited by physical dimensions of vehicle. 3) Joint Resistance at mounting surfaces may decrease the thermal conductivity.	1) Conductivity path can be an existing flange or insulation, thus, requiring no additional weight to vehicle.
Thermal Radiation 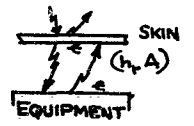	The choice of surface coatings and radiation area for the equipment compartment and the skin internal surface allows a selection of equipment temperature.	1) The combination of surface emissivities and view factors is limited from Fae = 0 to F_{ae}=1.0. Thus, radiation will need to be supplemented by conduction for heat loads above the F_{ae}=1 limit. 2) Mounting of skin and radiation shields can be a problem.	1) No additional weight to vehicle except for shields.
Solar Shield 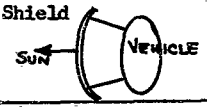	Shield protects vehicle from radiation. Solar cells can be placed on sun side of shield. Shields can also be used on shade side of vehicle as radiators.	1) Vehicle must always be orientated so that the shield faces the sun.	1) Keeps most solar radiation from vehicle. 2) Solar cells have good view of sun.

Table 27. Table Of Methods Of Semi-Passive Temperature Control

Method	Description	Limitations	Advantages
Variable external surface α_s and ϵ_v	α_s and ϵ_v are made to vary to control the skin temperature. Methods of varying and include shutters, rotating discs, and the proposed variable mercury surface.	1) Properties of surfaces are limited to: ϵ_v = 0.05 to 0.97 α_s/ϵ_v = 0.2 to 4.0 2) Variable surfaces will add weight to vehicle. 3) Surface coatings can change with heat radiation, cosmic radiation, meteorite damage, or low vacuum pressure in space. 4) Cannot be utilized on extensive solar cell areas.	1) Simple, reliable mechanical design. 2) One of lightest weight semi-passive control methods. 3) Malfunction of control method need not damage internal equipment. 4) Rotating disk and similar methods have been used successfully on satellites.
Variable internal thermal conduction paths.	Internal heat conduction is varied to control the internal compartment temperature. Variation methods include bimetallic conductivity paths which switch in or out, variable joint conductance, variable fluid conductives, and variable length conductivity paths.	1) Practical thermal conductivity limits are .02 to 200 Btu/ft.hr.$^{\circ}$F 2) Joint resistances may lower the thermal conducitivity. 3) Malfunction of control method can cause damage to equipment (overheating).	1) Simple mechanical design. 2) One of lightest weight semi-passive control methods.
Solar Shield	Shield protects vehicle from solar radiation. Shield can rotate or vehicle solar orientation can be controlled to keep shield in correct position. Solar cells can be placed on the shield. Other types of shields can be used with solar cells on the sun side and space radiators on the shade side.	1) Increases vehicle complexity, reliability of mission decreases. 2) Requires rotation of shafts (bearing problems) or orientation of vehicle. 3) Can be bulky and heavy.	1) Decreases solar radiation to vehicle 2) Allows solar cells to be always facing sun. 3) Allows radiator to always face space.

Table 27. Table Of Methods of Semi-Passive Temperature Control (Cont)

Method	Description	Limitations	Advantages
Fluid Controlled Flow (closed loop)	Gas or liquid flows between vehicle skin and equipment. Control valve or variable flow fan regulates flow rates to control the equipment temperature.	1) Weight is medium or high compared to other semi-passive methods. 2) Power is required for fans or pumps. 3) Malfunction of control system can cause damage to equipment (overheating or liquid leakage). 4) Probably the most complex semi-passive control methods.	1) Allows direct cooling of equipment and use of cold plates. 2) Ideal for combination with active systems.
Open Loop Fluid methods (expendable)	Fluid (Gas or liquid) is expelled from tank through equipment, cold plates and/or heat exchangers and is dumped overboard.	1) Very little cooling can be accomplished for a given weight since the specific heat of the fluids is too low.	1) Only useful for utilization of fluids to be dumped overboard. Such as liquid fuel cooling of a rocket nozzle.
Vaporizing liquid open loop (expendable)	Liquid is expelled from tank and vaporized in the equipment, cold plate, or/and heat exchanger and is dumped overboard.	1) Weight of method becomes a function of mission time and heat load and can be heavy for extended missions. 2) Tank sizes and expellant gas tank can become excessive. 3) Pressurized tanks can be dangerous.	1) Offers cooling at high heat loads without radiator skin temperature and area limitations. 2) Can be lighter than active methods dependent on mission time. 3) Liquid gases can be used for cryogenic cooling.
Vaporizing solid	Solid such as CO_2 is placed in container next to equipment to be cooled. As solid vaporizes, gas is dumped overboard.	1) Weight can become excessive for long mission times and high heat loads. 2) Volume requirements can be large.	1) Offers cooling without radiator skin temperature and area limitations. 2) Can be lighter than active control methods dependent on mission time. 3) Can be used for cryogenic cooling.

Table 28. Table of Methods Of Active Temperature Control

Method	Description	Limitations	Advantages
Vapor Cycle	Liquid expands at the expansion valve and boils in the cold plate or heat exchanger. The vapor is then compressed and cooled by the radiator. (More complex forms are possible).	1) Complex method with decrease in reliability. 2) Organic coolants are limited to below 500°F. 3) Power requirement of compressor is high.	1) Allows higher radiator temperatures. 2) Allows control of compartment temperature. 3) Allows compartment to be at lower temperature than surroundings.
Gas Cycle	Gas expands through the turbine and cools the equipment. Gas is then compressed and gives off heat at the radiator.	1) Less efficient, heavier, and requires more surface area than the vapor cycle.	1) Can use existing compartment gas for cooling in emergencies. 2) (3) of vapor cycle
Vortex Tube Gas Cycle (See Fig.43)	Vortex tube replaces turbine of gas cycle.	1) Less efficient than the turbine equipped gas cycle.	1) Useful if the energy from the hot gas can be put profitably to work. 2) (3) of vapor cycle.
Thermoelectric cooling	Electrical current causes lowering of temperature at the base of equipment to be cooled.	1) Weight and surface area requirements are much higher than vapor cycle. 2) High power requirements (low cop) compared to vapor cycle.	1) Reliability can be high since no fluid leakage problem is present. 2) Can dissipate large amounts of heat from small components. 3) (3) of vapor cycle.

Table 29 Comparison of Basic Space Vehicle Temperature Control Methods

Control System	Methods of Control	Limitations		Advantages	Disadvantages
		Internal Temperature	Maximum Skin Radiation Heat Dissipation		
Passive (No Moving Parts)	1) External skin surface characteristics (α_v, ϵ_v). 2) Internal heat transfer coefficient and area (UA). 3) Heat storage properties (ρ, C_p latent & fusion heats)	$T_B > T_V$	$\frac{q}{\epsilon_v A_v} = \sigma T_v^4$ a) for electronics: (T_B = 300°F) $\frac{q}{\epsilon_v A_v}$ max. = 200 $\frac{\text{watts}}{\text{ft.}^2}$	No mechanical moving parts	1) $T_B > T_V$ 2) Not recommended for manned vehicle. 3) No temperature control correction is possible for analysis errors unpredicted maneuvers, or missed orbits. 4) Temperature variations are uncontrolled.
Semi-Passive (Moving Parts and/or expendable coolant)	1) Variable external skin surface characteristics and area. 2) Variable internal heat transfer coefficient and area (UA) 3) Heat Storage Properties. 4) Electrical Heaters with thermostats. 5) Variable flow forced convection fluid internal heat transfer. 6) Expendable coolants.	$T_B > T_V$ (Except for expendable coolant)	$\left(\frac{q}{\epsilon_v A_v}\right)_{\text{max.}} = \sigma T_y^4$ (Except Expendable) a) Manned Vehicle: (120°F) $\left(\frac{q}{\epsilon_v A_v}\right)_{\text{max.}}$ = 56 $\frac{\text{watts}}{\text{Ft.}^2}$ b) Electronics: (300°F) $\left(\frac{q}{\epsilon_v A_v}\right)_{\text{max.}}$ = 200 $\frac{\text{watts}}{\text{Ft.}^2}$	1) Temperature control correction is possible. 2) Fluid forced convection allows cooling at critical components. 3) Temperature variations can be controlled	1) Power may be required for actuators, heaters, pumps or fans. 2) Mechanical and fluid systems may malfunction 3) Weight or system will usually be greater than passive system. 4) $T_B > T_V$ (Except for expendable coolant). 5) Response time for temperature changes may be slow.
Active (Heat Pumps)	1) All methods of semi-passive systems. 2) Evaporative cooling and heating cycles. 3) Electronically controlled electrical heaters & valves.	Limitations depend on evaporative cycles, heat load and fluid properties	$\frac{q}{\epsilon_v A_v}$ max. = σT_v^4 a) For organic coolants: $\frac{q}{\epsilon_v A_v}$ max. = 480 $\frac{\text{watts}}{\text{Ft.}^2}$	1) Close temperature control is possible. 2) Internal temperatures are independent of skin temperature. 3) Fluid flow allows cooling at critical components. 4) Temperature control correction is possible. 5) Higher heat dissipation for surface area rates can be obtained than for passive or semi-passive systems (except expendable) 6) Anticipation is possible for fast response to temperature change.	1) Power is required for compressors, fans, pumps, actuator and controls. 2) Mechanical, control and fluid systems may malfunction. 3) Weight of system usually is greater than for passive or semi-passive systems.

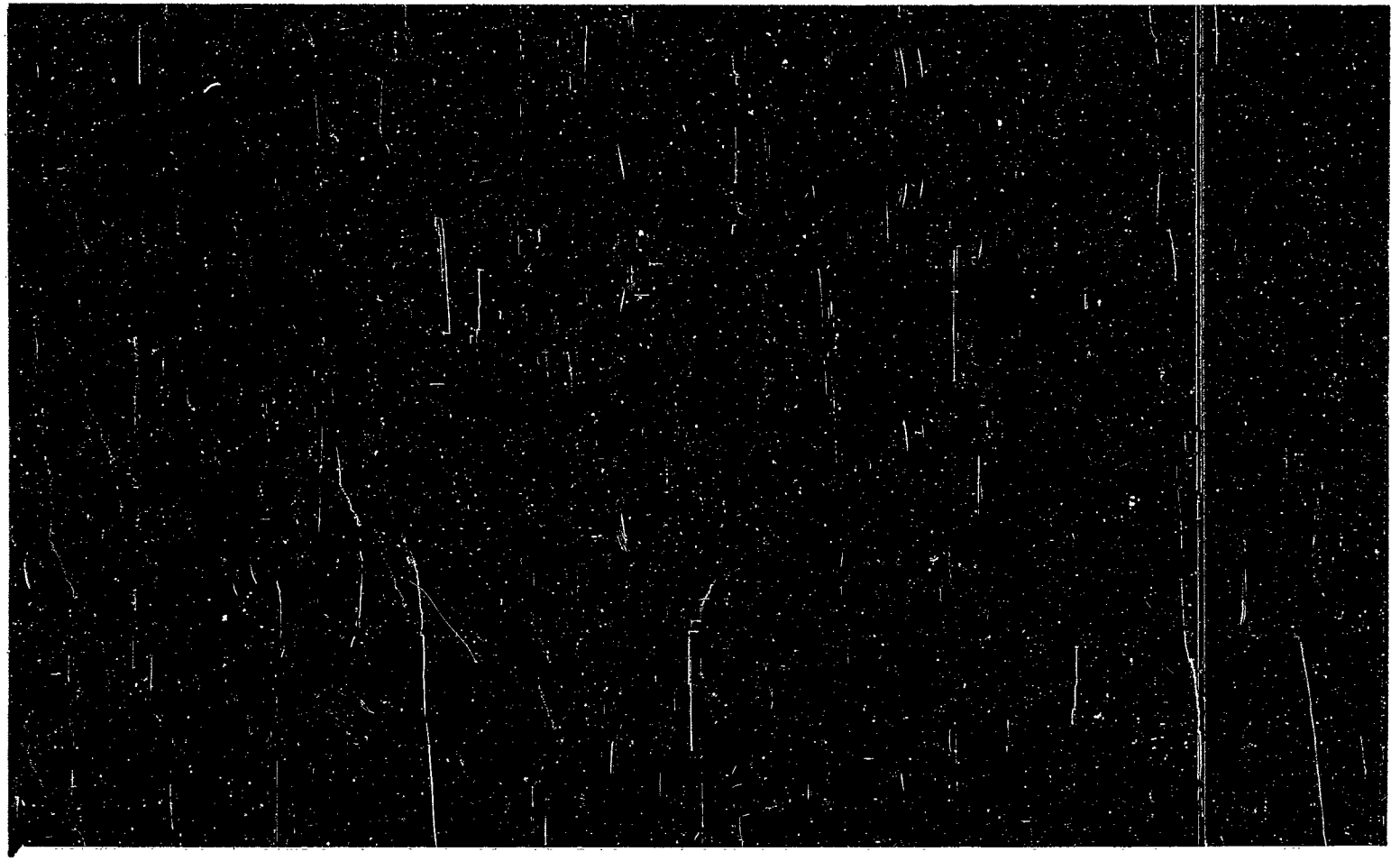

Figure 95 Maximum Heat Dissiptation Rates by Radiation from Vehicle Skin

Also included are weight, volume and area comparisons and discussions of reliability and other criteria. Expendable and recycle cooling, transport fluid loops and conduction and convection paths, and expendable heat sinks and space radiators are compared by use of weight parameters. Volume and area comparisons of these methods are also made. The reliability discussion includes relative reliabilities of methods, possible redundancies and affects of malfunctions. The discussion of other criteria includes fluid properties, cost, and maintenance considerations.

The second part of this section pertains to combination of methods into workable systems for space vehicles. Some of these combinations are broken down in terms of compartment loop, intermediate transport loops or heat transfer paths, and sink or space radiator loops. Comparisons of overall system performance, weight, volume, reliability, and other criteria is included for some of the more typical systems. Finally, this part includes an example vehicle problem with solution for choice of the methods and total control system by comparison of methods.

The third and final part of this section deals with the effects of mission, compartment and equipment requirements, skin and radiator temperature limits, and volume, weight and area allowances on the choice of control methods. For example, a long duration mission would usually eliminate the expendable control method, an extra hot or cold requirement would eliminate most of the usual coolants, and accurate control requirements can eliminate passive and sometimes semi-passive methods. Temperature limits and vehicle area, volume and weight allowances also affect the choice of control methods. As a result, some comparison of the affects of temperature and area requirements for various methods are included.

NOMENCLATURE

A	Area, sq ft
C_p	Specific Heat, Btu/(lb)(^oF)
D	Diameter (Hydraulic Diameter), ft
E	Electric Power, KW
H	Effective Latent Heat of Vaporization, Btu/lb (of system)
h	Film Heat Transfer Coefficient, Btu/(hr)(sq ft)(^oF)
h_r	Radiation Equivalent Heat Transfer Coefficient, Btu/(hr)(sq ft)(^oF)
HP	Power, ft-lb/hr

K_1	Core Flow Area/Core Face Area
K_2	Constant (See Equation 131)
K_3	Approximately 1 to 2 lb/sq. ft.
K_4	Constant (See Equation 134)
k	Thermal Conductivity, Btu/(hr)(ft)(^oF)
L	Latent Heat of Vaporization, Btu/lb
m	Mass Flow Rate, lb/hr
P	Power, ft-lb/hr
p	Pressure, psf (also psia)
Q	Volume Flow Rate, CFM
q	Heat Transfer Rate, Btu/hr
q_s	Power, But/hr
T	Temperature, ^oR
t	Time, hr
U	Over-all Conductance, Btu/(hr)(sq ft)(^oF)
V	Volume, cu ft
W	Weight, lb
X	Distance or Length, ft
α	Absorptivity, nondimensional
ϵ	Emissivity, nondimensional
ϵ	Effectiveness (Coefficient of Performance)
η	Efficiency
ρ	Density, lb/cu ft
σ	Stefan-Boltzman Constant, 0.1713 x 10^{-8} Btu/(hr)(sq ft)($^oR^4$)

Subscript:

B	Equipment or Compartment
C	Compressor or Pump
co	Core, Heat Exchanger

CP	Cold Plate or Heat Exchanger
E	Expulsion System
EX	Expendable System
Fr	Freon
f	Fluid
H	Hardware
P	Power
Pr	Pressure Regulator
r	Radiator
RE	Refrigeration System
S	Solar
t	Tank
v	Vehicle Skin

WEIGHT AND AREA PENALTIES FOR TEMPERATURE CONTROL METHOD POWER REQUIREMENTS

In order to compare temperature control methods, a common comparison parameter must be considered. Frequently, this parameter becomes the weight comparison of methods. Consequently, it becomes desirable to determine the weight of power generation and storage equipment required to furnish power to the fans, pumps, compressors, controllers, and heaters. This weight can then be included in the total weight of the control method for comparison to other methods.

Figure 96 and Figure 97 show some typical weight penalties for additional power requirements. The weight penalty sometimes varies as a function of the vehicle power requirements - i.e., the weight penalty for adding 100 watts to a 50 watt vehicle may be much higher than 100 watts to a 5000 watt vehicle. The solar cell and battery weight curve is based on S&ID power supply data. The fuel cell weight is based on proposal data. The fuel cell weight should be higher since battery storage will be required. Also, fuel cells require about 0.82 LB/KW HR of fuel (hydrogen and oxygen). Thus, the weight of a fuel cell power supply is a function of time. If the curve presented in Figure 96 is used, 0.82 LB/KW HR should be multiplied times the time and power requirement and included in the total fuel cell system weight. (Frequently, the water generated from the fuel cell reaction

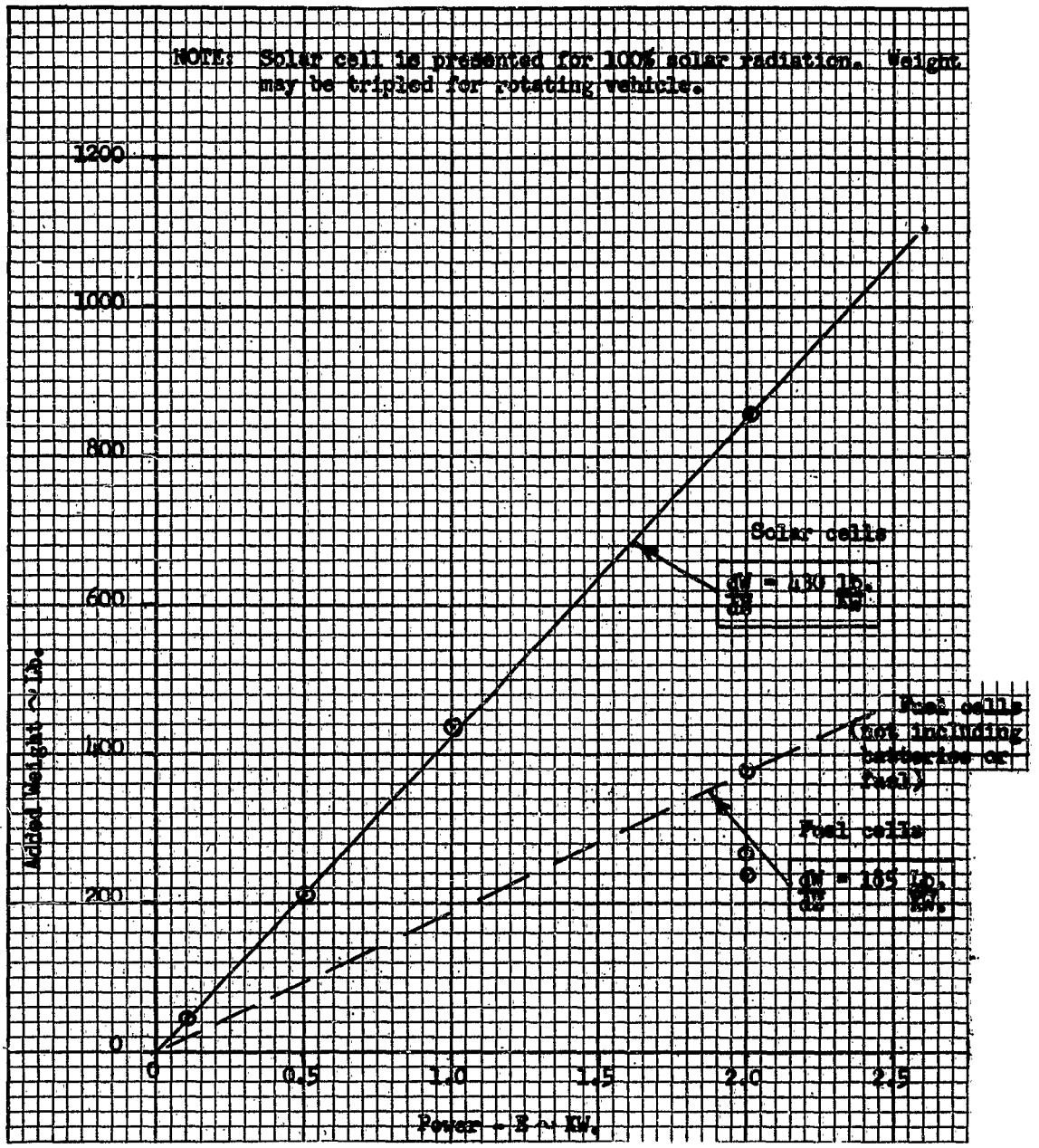

Figure 96. Weight Penalty For Additional Power For Solar Cells With Batteries And For Fuel Cells (115V., 3ø, 400cps)

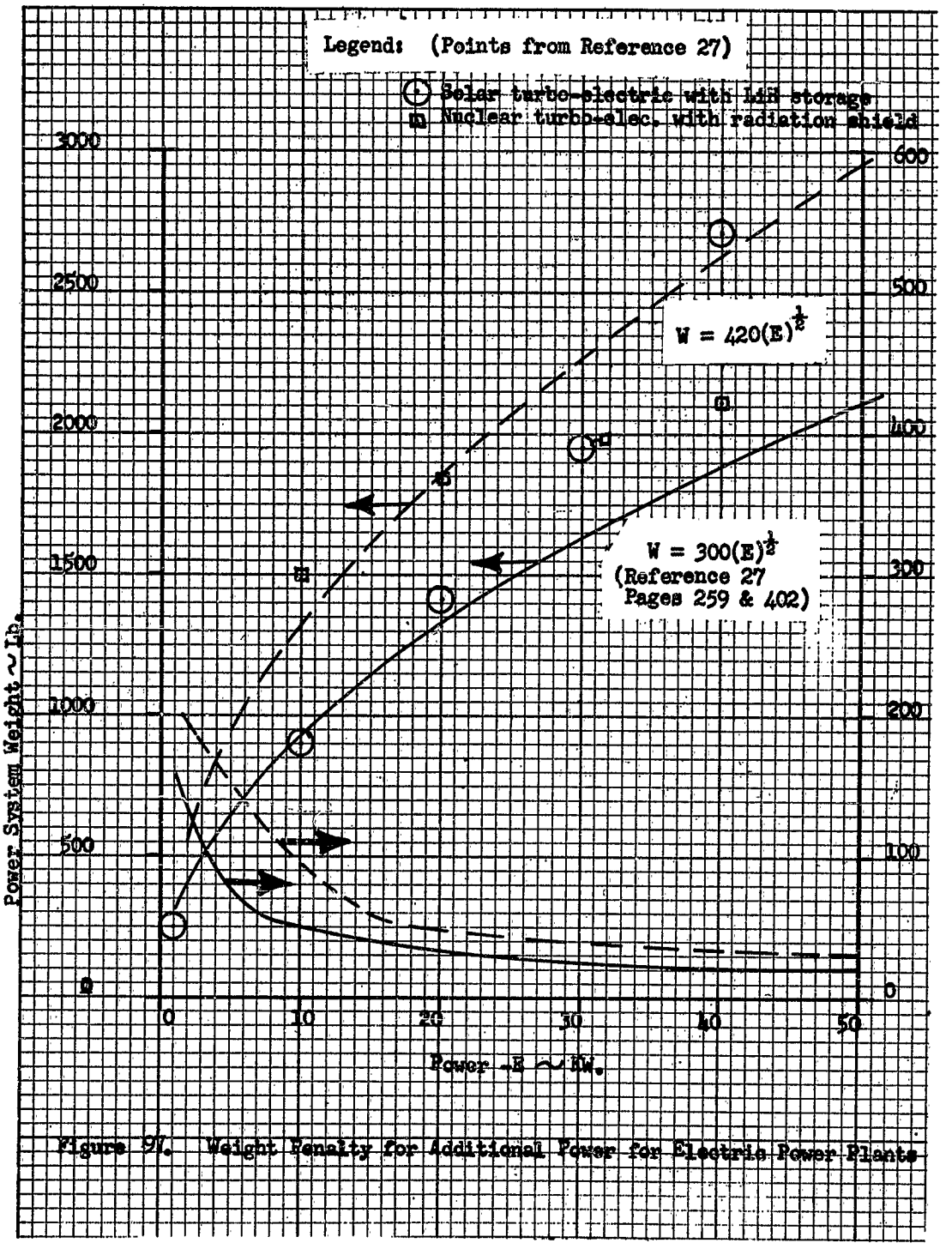

Figure 9V. Weight Penalty for Additional Power for Electric Power Plants

can be utilized for cooling or drinking purposes thus eliminating the 0.82 LB/KW HR fuel weight penalty. Also sometimes normal boil-off from engine fuel tanks can be utilized cutting down fuel cell weight requirements).

Figure 97 shows a curve of weight versus power requirements based on solar-turboelectric and nuclear power plant data plus storage (as presented in Reference 27). Other data available indicates that structural weight considerations might raise the weight to the dashed curve shown. Note that actual weight penalty for adding a small amount of power ΔE to a system is really a product of the slope of the weight versus power curve multiplied by the added power ΔE. $\left(\frac{\partial W}{\partial E} \times \Delta E = \Delta W\right)$.

Figure 98 shows the surface area requirements for a solar cell power source. This curve is useful in estimating surface area including radiator and power requirements. Such a consideration is necessary for valid comparisons of temperature control methods. Radiator area can be estimated from Figure 99.

WEIGHT ESTIMATE EQUATIONS FOR TEMPERATURE CONTROL METHOD COMPARISONS

The following equations (Table 30) for estimating the weight of components have been found from a literature search and some simplified analyses.

COMPARISON OF STRAIGHT VAPOR CYCLE AND COMPOSITE PELTIER SYSTEM

To evaluate the composite system alongside a conventional vapor cycle system it is not necessary to resort to an extremely detailed comparison; a very gross comparison is sufficient. The advantage demonstrated by a Rankine cycle system in several important respects becomes quite apparent. The comparison described here is based on a refrigeration load of 10KW in both cases.

The composite cycle consists of the Peltier evaporator discharging heat to the transport fluid, which is Freon 113 at 130°F (or 328°K). The single stage compressor operates over a pressure ratio of approximately 5:1 and feeds vapor to the radiaor at 245°F. The Rankine cycle roughly follows the path 1-2-3-4-1 as shown in Figure 100. (No superheat is assumed in this case). The pressure, enthalpy, and temperature of the fluid at beginning and end of each step of the cycle are also tabulated in Figure 100.

In the straight vapor cycle, on the other hand, a conventional heat exchanger replaces the Peltier evaporator. The existing compressor stage is kept as second stage, while a first stage is added to raise the pressure from 2.7 to 18.7 and thus simulate the gas temperature and pressure conditions at which the Peltier evaporator delivers vapor to the compressor stage, for a common basis of comparison. The cycle follows the path 1-2'-3'-4-1 in Figure 100. As far as the general system configuration is concerned, the Peltier evaporator is replaced by a conventional heat exchanger and a first stage of compression.

NOTE: Curve is for 100% solar radiation. Area requirements for rotating vehicles may be tripled.

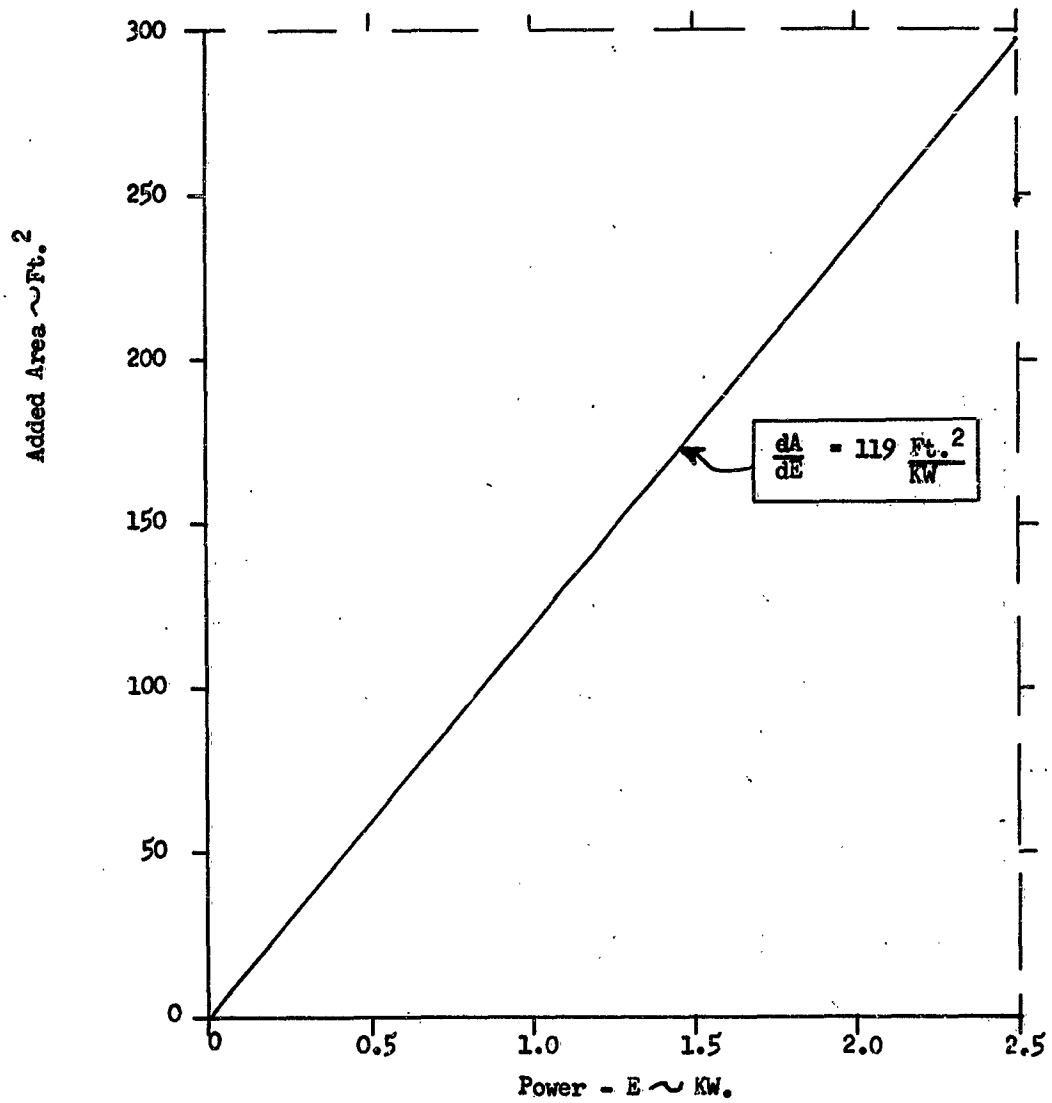

Figure 98. Surface Area Penalty for Additional Power for Solar Cells

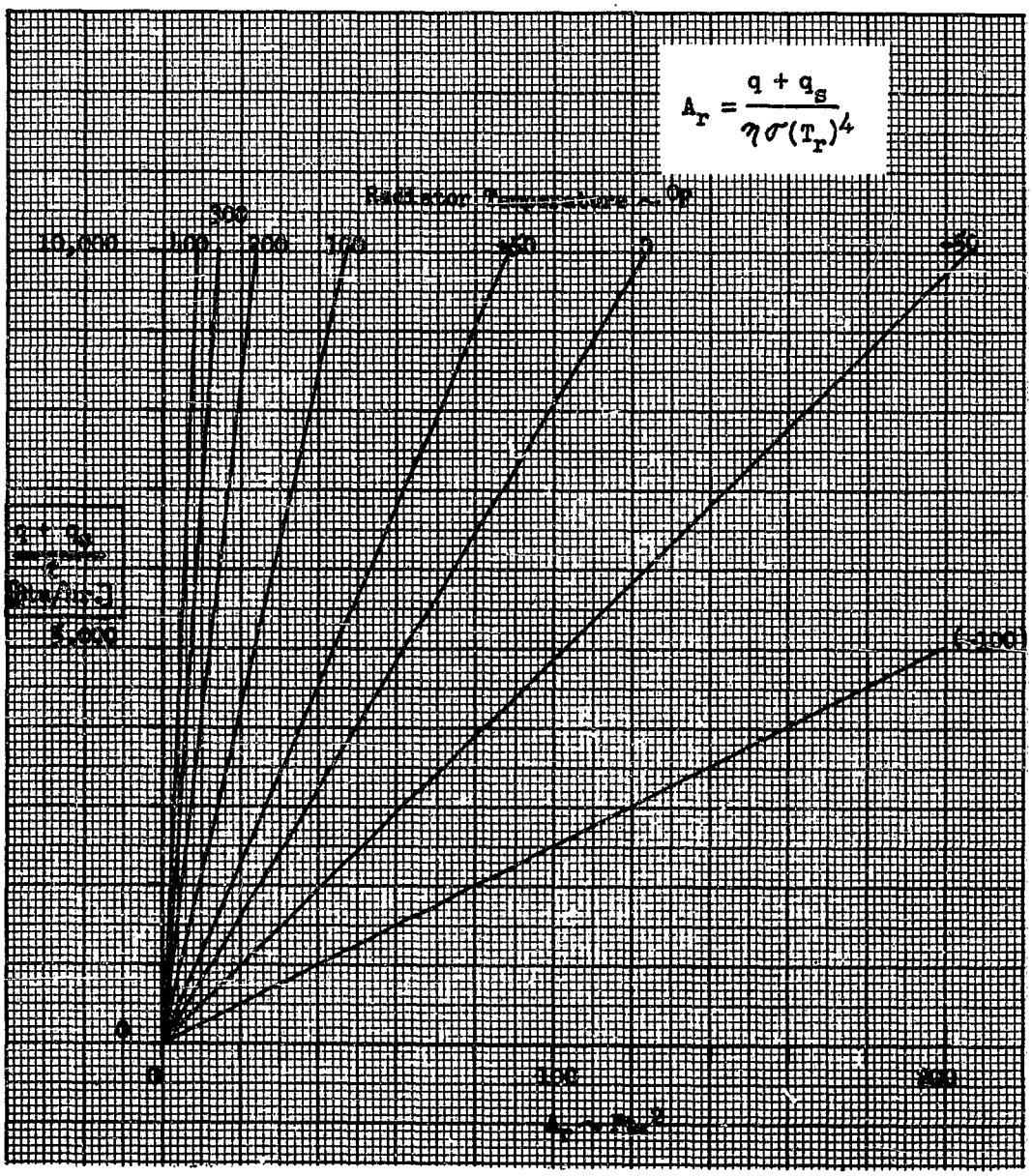

Figure 99. Radiator Area Estimate Curve
(Minimum Area Requirements)

Table 30. Weight Estimate Equations

Component	Weight Equation (lb)	
Blower (23)	$W = 3.24(\Delta p) + 0.011\ (Q)$	(Eq. 124)
Pump (23)	$W = 5.61(Q)^{0.75}$	(Eq. 125)
Motor (23)	$W = 2 + 4.5HP \quad 0 < HP < 1$ $W = 5 + 1.5HP \quad 1 < HP < 10$	(Eq. 126)
Fluid in Pipe	$W = \frac{\pi}{4}\rho_f (D)^2 X$	(Eq. 127)
Storage Tanks	$W = K_o \sqrt{\frac{q\ \Delta t}{\rho\ L}}$ (see Figure 21)	(Eq. 128)
Piping	W = (constant for AN tubing at D)(1.5)(X) 1.5 - accounts for brackets, etc.	(Eq. 129)
Heat Exchanger (25)	$W = 1.48\ \rho_{co}(V_{co})^{0.882} + K_1 \rho_f V_{co}$ $K_1 = \frac{\text{core flow area}}{\text{core face area}}$	(Eq. 130)
Cold Plate	$W = K_2(q/h\Delta T)$	(Eq. 131)
Power Source (23)	$W = (dW/dE) \times (q_g/3410)$ (dW/dE) = penalty slope, lb/kw (See power penalty curves)	(Eq. 132)
Power Source APU Generator	W = 5.1 HP + 7.5 (HP-hr)	(Eq. 133)

Table 30 (Cont.)

Component	Weight Equation (lb)
Space Radiator	$W = K_3 A_r$ (Space side) (Eq. 134) $W = K_4 \frac{q + q_s}{h \Delta t}$ (Fluid side) (Eq. 135) (Use larger value)
Compressor & Motor	$W = 19 + 0.7(HP)$ $0 < HP < 100$ (Centrifugal) (Eq. 136) $W = 5 + 9(HP)$ $0 < HP < 100$ (Reciprocating) (Eq. 137) (From Section IV, Table 15)

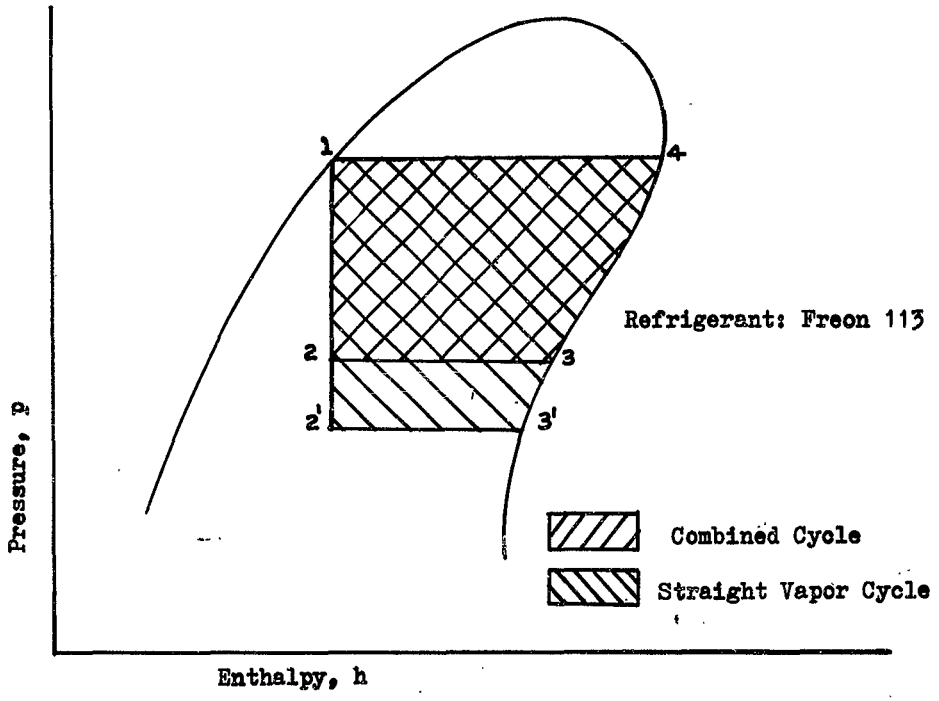

Fluid Properties

T_1=245°F
p_1=93.5 psia
h_1=62 Btu/lb

T_4=245°F
p_4=93.5 psia
h_4=113 Btu/lb

T_2=130°F
p_2=18.7 psia
h_2=62 Btu/lb

T_3=130°F
p_3=18.7 psia
h_3=98 Btu/lb

T_2'=40°F
p_2'=2.7 psia
h_2'=62 Btu/lb

T_3'=40°F
p_3'=2.7 psia
h_3'=84.6 Btu/lb

Figure 100. Rankine Refrigeration Cycles For Freon 113 And Compound Thermoelectric Methods

Weight of Evaporator

For the purpose of this comparison it was assumed that the film heat transfer coefficients in the heat exchanger were 15 BTU/hr-ft^2-°F for air and 150 BTU/hr-ft^2-°F for Freon. The area on the air side was assumed to be six times that on the Freon side. With the air temperature dropping from 100°F to 50°F, and with a Freon temperature of 40°F, the log mean temperature difference in the exchanger is 28°F.

The product UA_{Fr} of the overall heat transfer coefficient times the Freon surface area may be calculated to be 56.4 BTU/hr-°F. The required area on the Freon side is 22.6 ft^2 and on the air side 135.6 ft^2. A heat exchanger having a total heat transfer area of 158 ft^2 would weigh approximately 15.4 lb, including the fins on the air side.

The weight of thermoelectric material alone for the conditions assumed has been previously computed (Section IV) at 35 lb/KW, or 350 lb for 10KW, excluding the junction plates and fins. The complete Peltier evaporator would be almost 25 times as heavy as the straight Freon exchanger. The weight of the thermoelectric material was based on an arbitrary length of one centimeter. At the current state of the art the area corresponding to this length, approximately 0.164 cm^2 or 0.4 cm square appears to be a minimum, and thus the total weight cannot be readily reduced below the 350 lb specified.

Compressor Power

The amount of heat transferred to the refrigerating fluid in the case of the straight Freon system is simply 10KW or 570 BTU/min. In the case of the Peltier evaporator, the electrical power which is applied to pump the 10KW of heat has been seen to be also converted to heat and must be carried away by the Freon. Thus, the total heat transferred to the refrigerant in this case is

$$Q = 570 + \frac{570}{\epsilon} = 570 + \frac{570}{0.312} = 2400 \text{ BTU/min}$$

At 40°F the refrigerant absorbs heat at the rate of 84.6 - 62.0 = 22.6 BTU/lb in the straight vapor cycle evaporator. The amount of refrigerant required for the vapor cycle is 570/22.6 = 25.2 lb/min. The compressor adds 113 - 84.6 = 28.4 BTU/lb and the compressor input power is, therefore, assuming 70 percent efficiency:

$$P_{RE} = \frac{25.2 \times 28.4}{0.7 \times 42.4} = 24.2 \text{ hp}$$

In the composite cycle, on the other hand, the evaporator transfers heat at the rate of 90 - 65 = 36 BTU/lb at 130°F. The amount of refrigerant required is 2400/36 = 66.7 lb/min. In compressing the vapor from 18.7 psia to 93.5 psia, the compressor adds 113 - 98 BTU/lb to it. The compressor input power for the composite cycle is then:

$$P_{COMP.} = \frac{66.7 \times 15}{0.7 \times 42.4} = 33.7 \text{ hp.}$$

It is noted, therefore, that the compressor for the straight vapor cycle requires almost a third less power than that for the composite cycle and is consequently much lighter.

Radiator Area

The amount of heat which must be removed from the refrigerant in either cycle is 113 - 62 = 51 BTU/lb. In the vapor cycle, therefore, the heat removed is 51 x 25.2 = 1290 BTU/min. In the composite cycle it is 51 x 66.7 = 3400 BTU/min. The radiator area requirement is proportional to the heat to be dissipated and consequently the radiator for the composite cycle is about 2.6 times as large as for the straight vapor cycle. This item of comparison is extremely significant, inasmuch as the design of radiators and their facilities for storage during boost is critical at the current state-of-the-art.

Fan Power for Forced Convection

The cross-sectional area of the thermoelectric material is small compared to the required air and Freon heat exchange areas. The composite evaporator must, however, be designed to allow for the full 135 ft^2 of area on the Freon side. The air side heat exchange area will also be of the same order of magnitude as in the straight vapor cycle exchanger. The rates of airflow will not be much different. Since it can be shown that fan power is but a small portion of the total power, this component of power may be considered equal in the two cases without introducing a great deal of error.

It is instructive to determine the order of magnitude of power required to drive the fan. An airflow of 47.4 lb/min is required to remove 10KW of heat with an air temperature drop of 50°F. The volume of a rectangular plate and fin heat exchanger having a total area of 158 ft^2 is about 0.45 ft^3. The exchanger may be arbitrarily proportioned at 0.5 ft in the direction of airflow and 1.0 x 0.9 feet in cross section. The total pressure drop across the exchanger is about 0.08 psi. The input power required, assuming 0.60 efficiency, is about 0.35 hp, or 260 watts.

Overall Coefficient or Performance

The overall coefficient of performance of each system is the ratio of the heat removed from the compartment to the total power consumption of the system. In the composite system, power is consumed by the thermoelectric materials, by the compressor and by the air fan:

$$\epsilon_{comp.} = \frac{10{,}000}{\frac{10{,}000}{0.312} + 39.7 \times 746 + 260} = 0.174 \ \frac{\text{WATTS}}{\text{WATT}} .$$

The straight vapor cycle uses power only for the compressor and the fan:

$$\epsilon_{RE} = \frac{10{,}000}{24.2 \times 746 + 260} = 0.545 \ \frac{\text{WATTS}}{\text{WATT}},$$

The overall coefficient of performance for the straight vapor cycle is thus seen to be more than three times as great as for the composite Peltier-vapor system.

Summary of Comparison

The preceding paragraphs have compared the straight vapor cycle with the composite system in several respects. The results are summarized in Table 31.

Table 31. System Comparison for 10KW Cooling Capacity
(Peltier vs Vapor)

	Straight Vapor Cycle	Composite Peltier-Vapor Cycle System
Evaporator Weight (lb)	15.4 (total, including fins)	350 (thermoelectric material only, excludes junction plates, insulation, fins, etc.)
Compressor Input Power (hp)	24.2	33.7
Radiator Area (ft^2)	A (240 at 200°F Min.)	2.65A (635 at 200°F Min.)
Air Fan Power (hp)	0.35	0.35
Overall Coefficient of Performance	0.545	0.174

It is seen that in all important respects the straight vapor cycle shows a decided advantage over the one containing the Peltier evaporator. The basic reason is that the Peltier evaporator requires the use of electrical power to transfer heat. This power is not only employed at a low utilization efficiency but also completely degenerates to heat and adds to the heat load of the second stage. The property of thermoelectric m materials by means of which it concentrates the heat flow into a small flow area cannot be used effectively because adequate heat transfer areas at the air and Freon sides must still be maintained.

The comparison as it was made here is conservative in that assumptions were made which favor the Peltier system. A realistic appraisal, in which more nearly optimum conditions were chosen for the Rankine cycle, would probably yield even more striking results than those shown here. For cooling very small volumes having low heat output, however, the Peltier system begins to be competitive with a vapor cycle.

WEIGHT COMPARISON OF EXPENDABLE COOLING METHODS TO RECYCLE COOLING METHODS WITH A SPACE RADIATOR

Figure 101 offers a visual comparison of the expendable and recycle cooling methods. From these sketches, the weight of the expendable method is a total of the weight of the expulsion system W_E, the weight of the fluid W_f, the weight of the tank W_t, the weight of the valve W_v, the weight of the controlled compartment heat of change or cold plate (if used) W_{cp}, the weight of the tubing and fittings (hardware) W_H, and the weight of the pressure regulator W_{pr}. Similarly, the recycle methods weight is the sum of W'_v, W'_{cp}, W'_f, W'_H, the weight of the pump or compressor W'_c, the weight penalty for the pump power W'_p, and the weight of the space radiator W'_r. For the trade-off point where both methods weigh the same.

$$W_{Ex.} = W_E + W_f + W_t + W_v + W_{cp} + W_H + W_{pr} = W_{RE} = W'_v + W'_{cp} + W'_f + W'_H + W'_c + W'_p + W'_r \tag{139}$$

Also, the heat load rejection must be the same so that

$$\frac{qt}{H} = W_{RE} \tag{140}$$

where q = heat load BTU/HR,

t = time HR, and

$$H = \frac{W_f L}{W_{EX}} = \frac{\text{useable heat of vaporization(or enthalpy diff.)}}{\text{Expendable system weight}} \text{ BTU/LB}$$

But

$$W_{RE} = W_{EX} \quad \text{or} \quad W_{RE} = \frac{qt}{H} = \left(\frac{qt}{W_f L}\right) W_{EX}$$

$$\text{or} \quad \frac{W_{RE}}{W_{EX}} = \frac{qt}{W_f L} = 1.0 \tag{141}$$

Furthermore, $q = \eta \sigma A_r T_r^4$ for the recycle method radiator. Substitution into equation 141 yields

$$t = \left(\frac{W_f L}{\eta A_r}\right) \frac{1}{\sigma T_r^4} \tag{142}$$

η = Recycle system efficiency including radiator effectiveness.

T_r = Radiator temperature (°R).

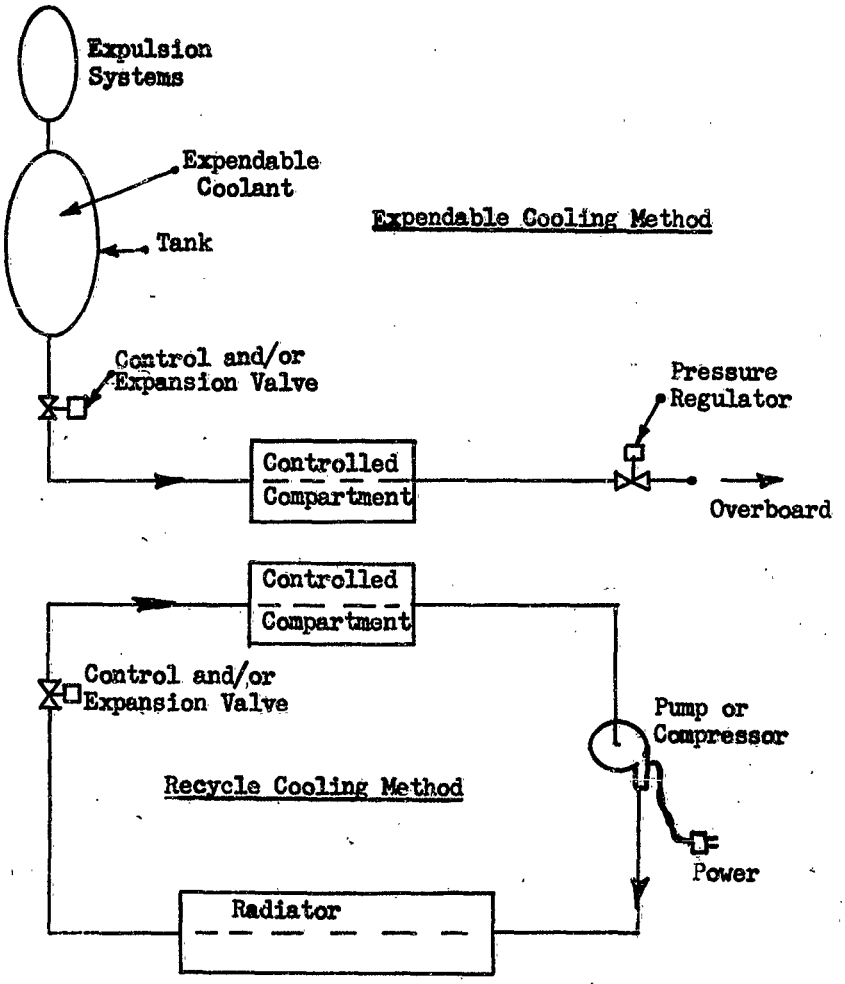

Figure 101. Sketches of Expendable And Recycle Methods

This equation can be used to compare expendable methods with recycle methods where $\left(\frac{W_f L}{\eta A_r}\right)$ is a constant dependent on the two methods compared. A curve of T_r versus t for various $\frac{W_f L}{\eta A_r}$ ratios is presented in Figure 102.

Example

Use of Figure 102 can be illustrated by a comparison of a known Freon 21 method to an expendable ammonia method.

The known Freon 21 method has a coolant capacity of 1000 watts with a 600 watt compressor and a 200°F radiator. The minimum radiator area for this method is

$$\frac{q+q_c}{\sigma T_r^4} = \frac{1600 \times 3.41}{0.173 (6.6)^4} = 16.6 \text{ (ft.)}^2 .$$

and the method efficiency is $\eta = \frac{1000}{1600} = 0.625$.

The weight of this method (including power penalty) is 260 lb. as shown in Figure 103.

Using Figure 21 with $W_{EX.} = W_{RE.} = 260$ lb.

and $W_{EX.} \approx W_f + W_t$ shows that $W_f \approx 175$ Lb.

calculating K with L = 300 BTU/lb. for ammonia stored to 5000 psi yields

$$K = \frac{W_f L}{\eta A_r} = \frac{175 \times 300}{0.625 \times 16.6} = 5070.$$

Referring to Figure 102 with K = 5070 and Tr = 660°R, gives t = 11 hours (which agrees with the value shown in Figure 103).

SURFACE AREA AND TOTAL WEIGHT COMPARISONS OF SEMI-PASSIVE AND ACTIVE RECYCLE COOLING METHODS

The comparison estimates of weight, radiator area, and power requirements made in Section VI for active control methods are all based on a 40 or 50°F compartment temperature. This temperature is the ideal temperature for control of a manned vehicle as reported in Reference 25.

For practical comparison the power penalty weights and areas from Figures 96 through 99 have been added to the tabulated values for the Freon 11 vapor cycle, air gas cycle and Peltier cycle in Section VI. In addition, area and weight values for a semi-passive 60% ethylene glycol-water cycle have been calculated. These areas and weights are plotted versus cooling capacity in Figures 104 and 105.

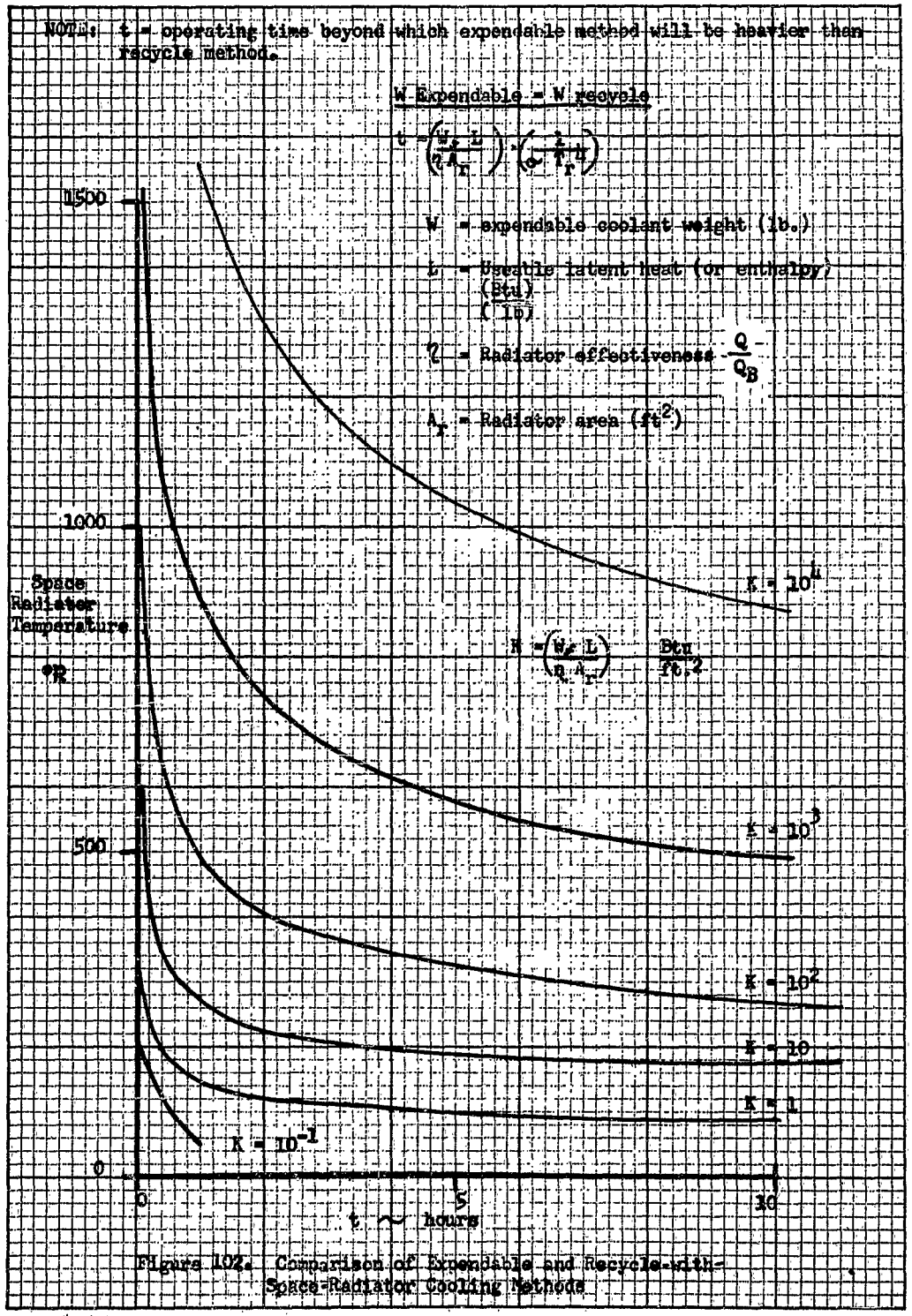

Figure 102. Comparison of Expendable and Recycle-with-Space-Radiator Cooling Methods

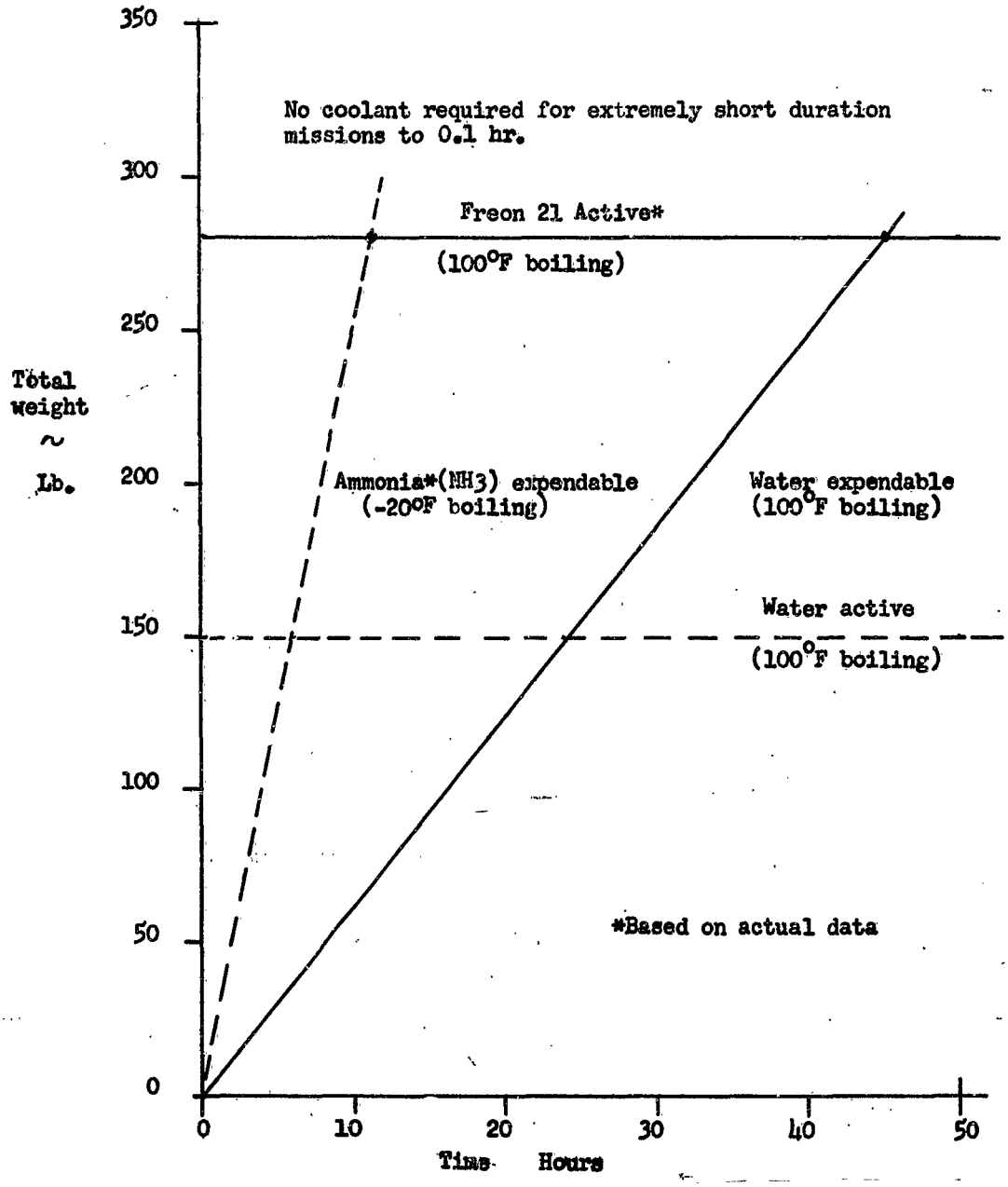

Figure 103. Comparison of Cooling Method Weights for 1000 Watt Load with 200°F Radiator

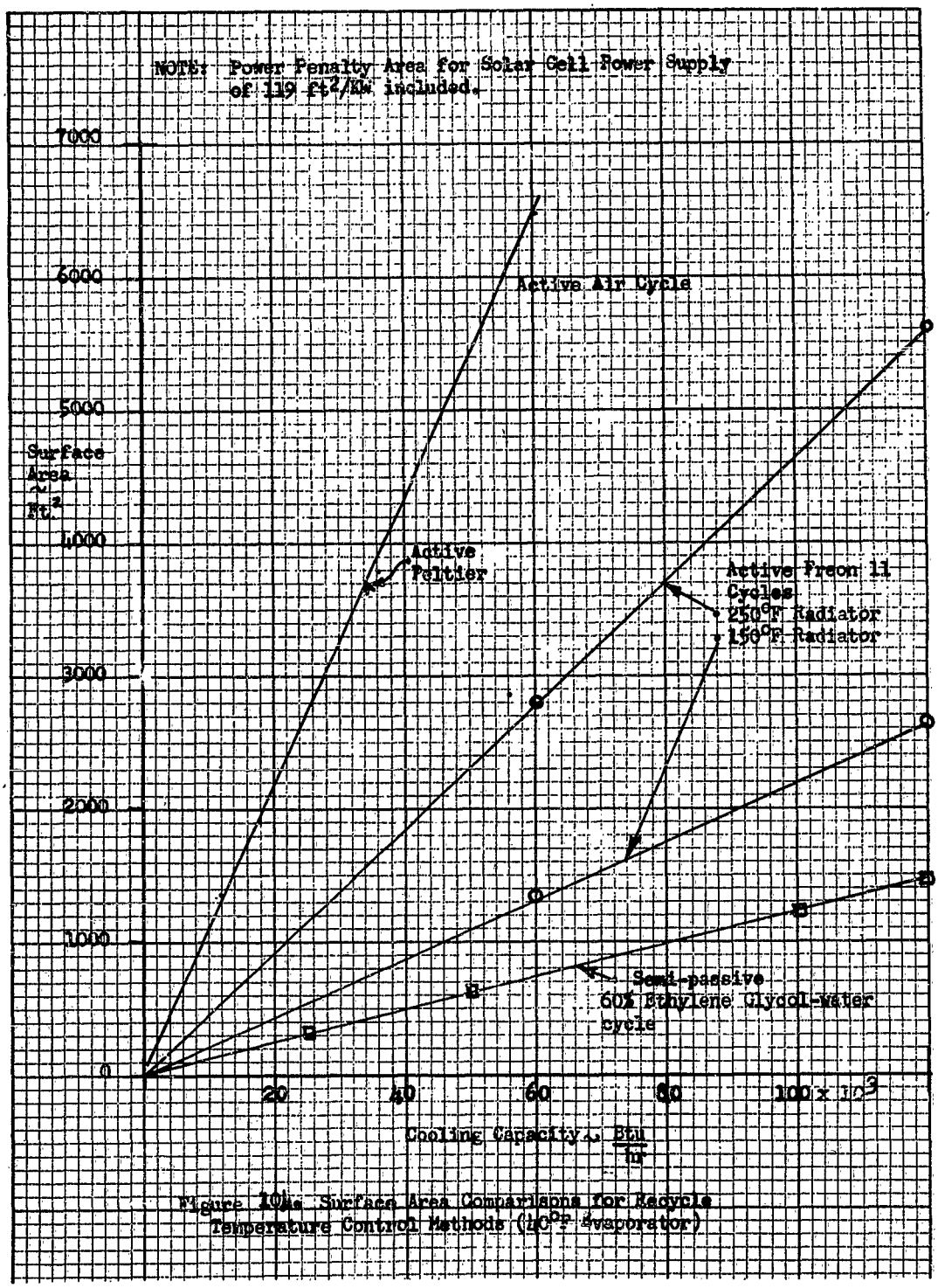

Figure 10. Surface Area Comparisons for Recycle Temperature Control Methods ($\Delta C^{o}p$ Evaporator)

NOTE: Power Penalty Weight Included From Figures 96 and 97 .

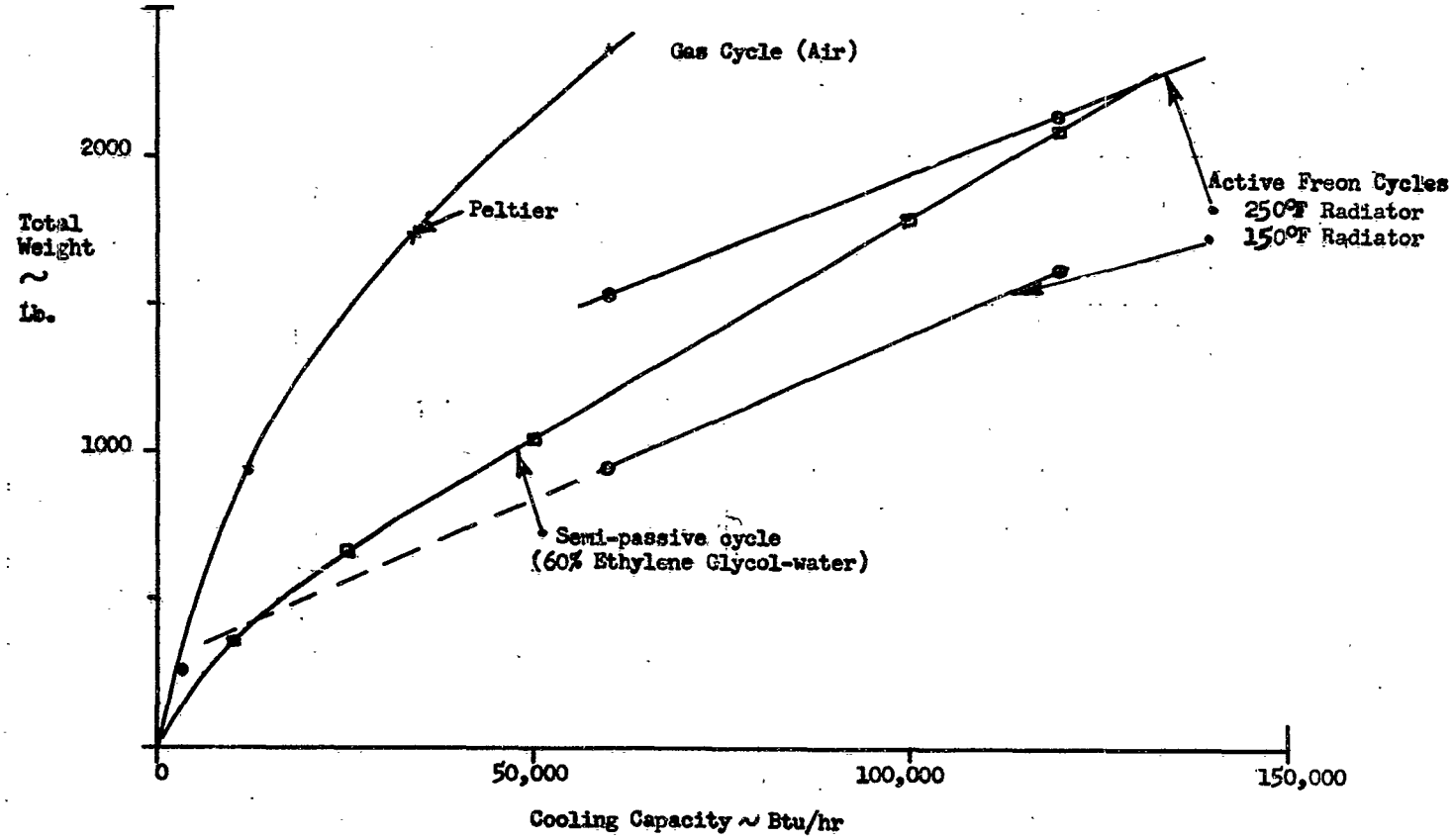

Figure 105 Total Weight Comparisons of Recycle Temperature Control Methods

TEMPERATURE CONTROL SYSTEMS

In most space vehicles with internal heat generation, a combination of temperature control methods is required for optimum design.

The most complex temperature control systems are usually encountered on manned re-entry vehicles where an air circulation semi-passive look is required in the cabin, a liquid semi-passive or active loop is required to control the air temperature and cool electronic equipment, and an expendable method is required to cool the vehicle during re-entry. Several systems for manned or large electronic compartments are shown in Figure 106. The coolant fluids indicated on this figure are the optimum fluids indicated in Sections III and IV. Comparisons of weight and surface area requirements of active and semi-passive liquid loops Figure 104 and 105 indicates that the semi-passive loop will usually be chosen unless an extremely large cooling capacity is required. The semi-passive liquid loop is almost always chosen over the passive heat transfer control for large compartments with heat dissipation since modulation of compartment temperature is possible and liquid to air heat exchangers and liquid cold plates can be used.

For small equipment compartments most of the methods discussed in the previous section can be considered depending on heat dissipation and temperature requirements. Several temperature control systems for small compartments are shown on Figure 107.

SPECIAL CONSIDERATIONS IN COMPARING TEMPERATURE CONTROL METHODS

The comparison of temperature control methods becomes more complex when the special considerations of an actual vehicle are included. Some of these special considerations are type of mission, compartment temperature requirements, skin and radiator temperature limitations, and vehicle weight, volume and surface area restrictions. Table 32 lists these considerations with some of the parameters and effects on comparison of methods.

This table illustrates only a few special considerations. Other considerations sometimes become even more important. For example, in one case, an electronics manufacturer chose a relatively inferior coolant semi-passive liquid in order to insure a high dielectric constant and no flamability, In this case, the prime consideration was reliability. This coolant required heavier heat exchangers, cold plates, and lines, more pump power and higher line pressure drops. But the manufacturer was willing to overlook these penalties to be assured that, should a liquid line leak slightly, no electronic equipment would be impaired.

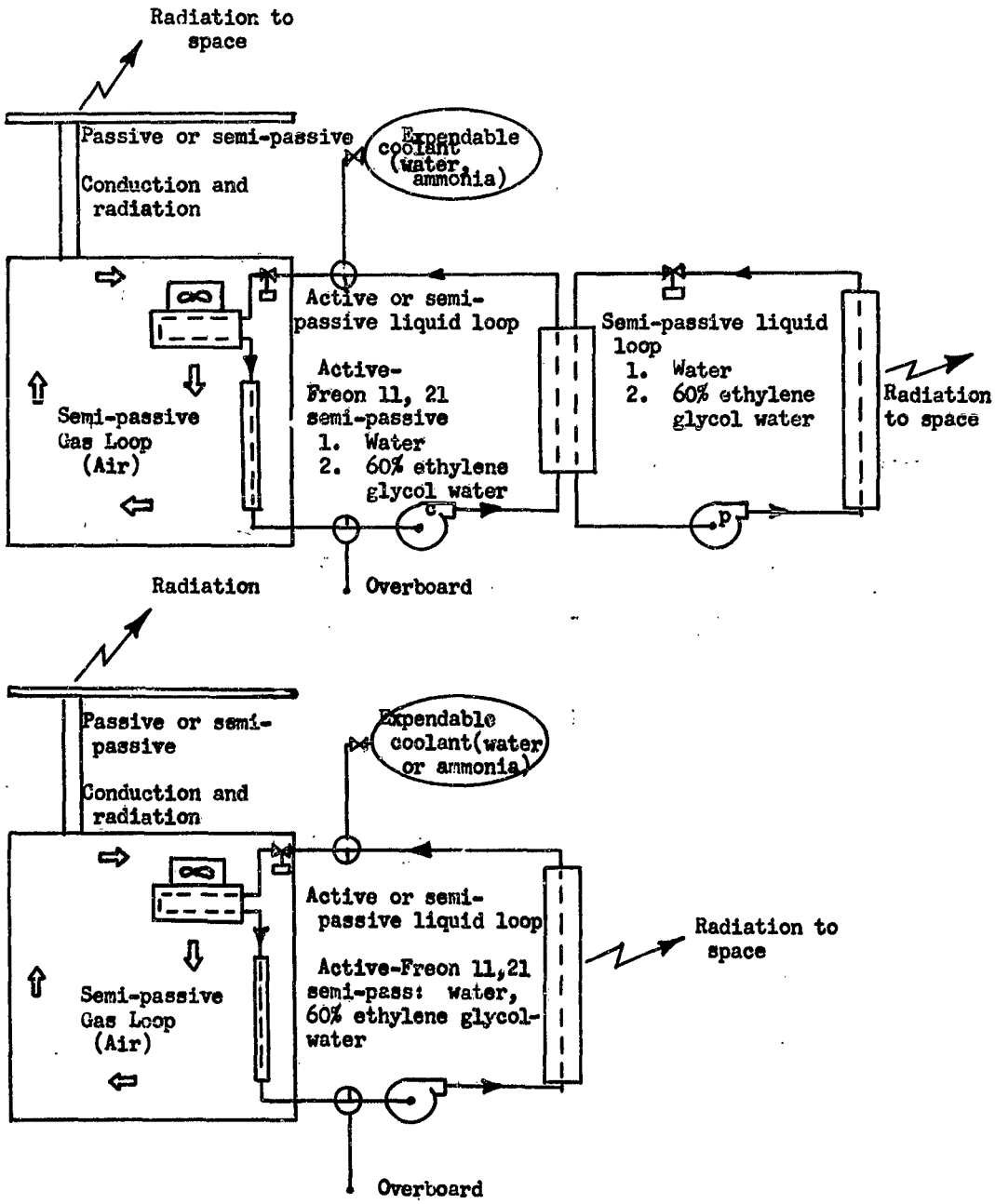

Figure 106. Temperature Control Systems for Manned or Large Electronic Compartments

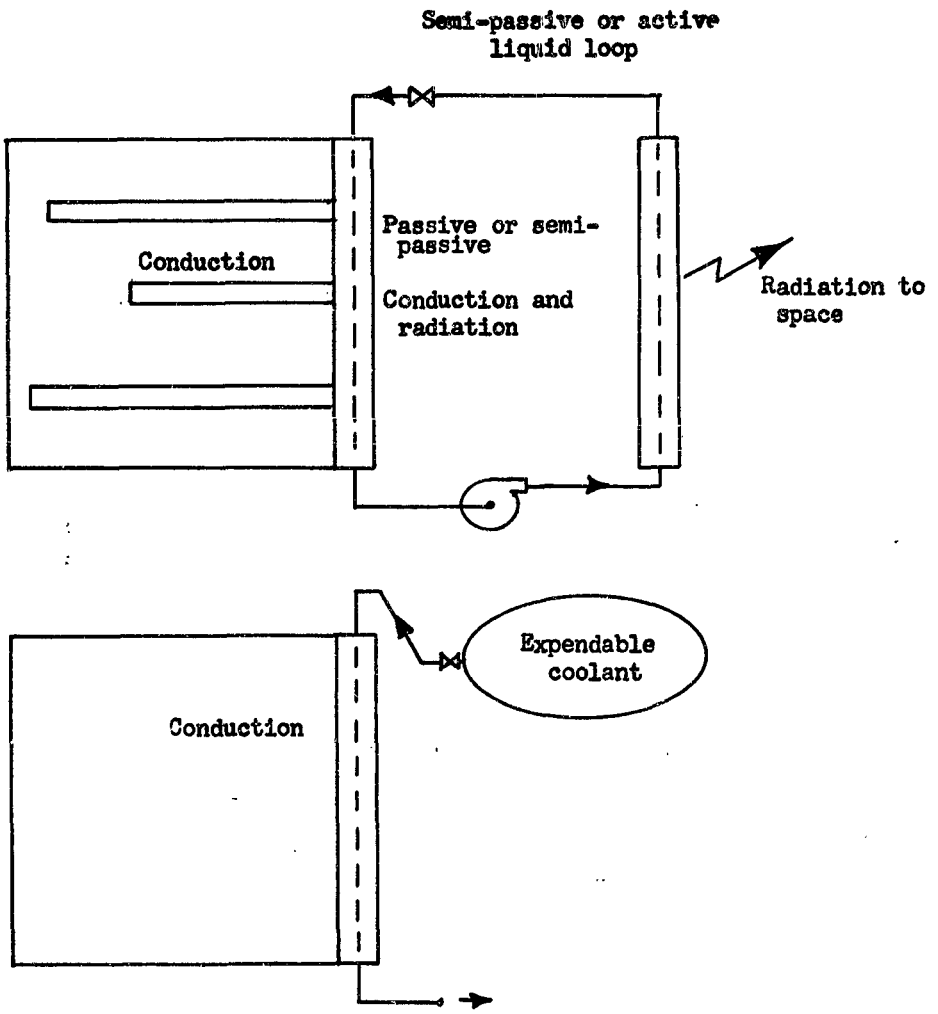

Figure 107. Temperature Control Systems for Small, Heat Dissipating Compartments

TABLE 32 - SPECIAL CONSIDERATIONS IN COMPARING TEMPERATURE CONTROL METHODS

Special Consideration	Parameter	Effect on comparison of methods
Mission	Time	Total time of mission affects comparison of expendable methods to others and of fuel cells versus solar power sources.
	% Sunlight	Radiator and solar power source efficiencies are a function of % sunlight.
	Rotation	Rotation affects radiator and solar power source efficiencies. Skin and radiator temperatures will fluctuate for slow rotation rates.
	Skin Temperatures	If the skin or radiator temperature is greater than the compartment temperature, an expendable or active method must be used.
Temperature Control	Control Band	Complex active or semi-passive method may be necessary for close control.
	Response Rate	A complex active or semi-passive may be required for fast response to changes in heat load or external conditions.
Radiator and Skin Temperatures	Design Temperatures	Material design and coolant temperature maximums limit the maximum heat dissipation per square foot of surface.
Vehicle Physical Restrictions	Volume, Weight, and Area	Vehicle volume, area, and weight will usually be limited by booster shape and thrust. Thus, volume, area, or weight may become a prime consideration in choice of method.
Control Method Component Location	Torque	Location of fans, pumps, and compressors in vehicle is important. Poor location can cause torque influence on the vehicle orientation.

This example case and the table are important in illustrating the fact that optimization of a coolant method cannot be done by arbitrary weighting of all the parameters affecting a choice. Weighting of the parameters must usually be done in consideration with the particular requirements of each vehicle. Reference 3 of this program is a study of integration and optimization of environmental control systems.

CONCLUSION

General results obtained from comparison of methods in this section are summarized in Table 33 and Figure 108. Table 33 shows the relative position of passive, semi-passive, and active methods for different comparison parameters. Figure 108 establishes the usualy boundaries for the basic methods relative to temperature and heat load. (Note that boundaries for heat load on this figure are fairly arbitrary.)

Figures 103, 104, and 105 are specific comparisons of methods for use in controlling a 40 to 50°F compartment such as a manned compartment. Results from Figure 103 indicate that the expendable method will be lighter than an active method for missions up to 44 hours with a 1000 watt heat load. Figure 105 indicates that a semi-passive liquid cycle will be lighter than an active vapor cycle for heat loads up to 12000 BTU/hr. Interestingly, Figure 104 indicates that no trade-off exists in surface area requirements. The lighter active Freon 11 vapor cycle requires more surface area than a heavier Freon 11 vapor cycle and the semi-passive cycle always requires less surface area than the active Freon cycles.

The specific comparison used in this section indicates that surface area and weight estimates for various methods for use in space vehicles are affected significantly by power penalties. A considerable amount of error is introduced by the rough data on power penalties and component weights. A detailed study of power penalties of weight, volume, and area is recommended as a necessity for valid comparisons between methods. Also, component weight estimate equations are in error when compared to off-the-shelf hardware. Evidently very few components are actually optimized for minimum weight and volume. Thus, optimization of components is necessary before any meaningful equations for prediction for component weights and volumes can be derived and used.

Table 33. Rating of Methods

Method Parameter		Passive	Semi-Passive		Active
			Expendable	Other	
Weight *		1	1 - 4 Time-Dependent	2 (3) for high heat load	3 (2) for high heat load
Surface Area*		2	None 1	3	4
Volume		1	1 - 4 Time Dependent	2	3
Reliability		1	2	2	3
Control	Band	4	2	3	1
	Response	4	2	3	1

*Includes power penalties. 1 - best

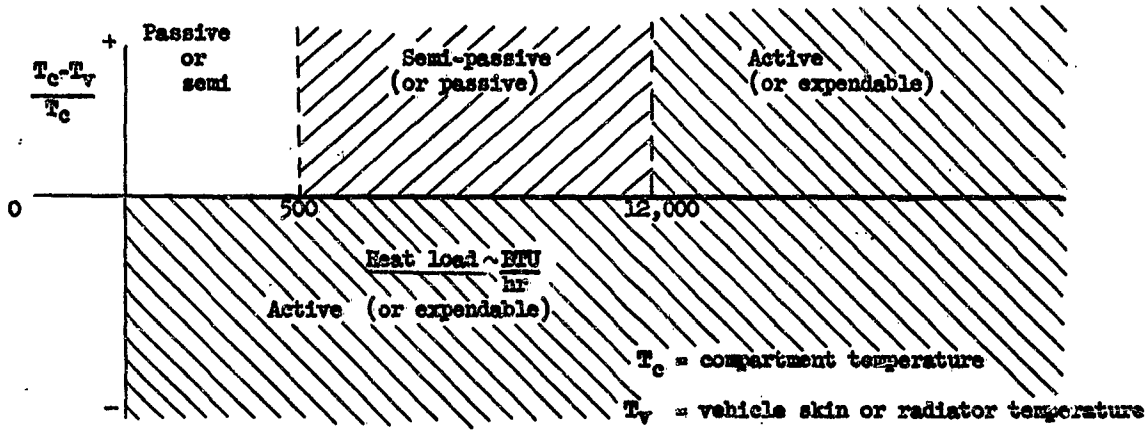

Figure 108. Temperature Control Methods As a Function Of Temperature And Heat Load

SECTION VII

THERMAL CONSIDERATIONS OF SPACE VEHICLE EQUIPMENT

This section is presented to give the environmental systems designer a familiarity with the thermal characteristics of the many components and systems he is called upon to support, and to emphasize, by example, the necessary role of the thermal engineer in arriving at optimized equipment design.

The heat generation characterists of typical equipments are discussed and, where possible, the thermal circuits describing the modes and paths for rejection of the generated heat are presented. The temperature limits of equipments are then categorized showing present state-of-the-art, the nature of the limitation (materials processes, etc.), and the approaches and promising methods of improving the temperature limitations.

Having considered the heat generation characteristics and temperature limitations, the basic methods of controlling the thermal effects are investigated. These are categorized as:

(1) Decreasing the heat generating rates
(2) Developing components for higher operating temperatures
(3) Protecting from generated heat
(4) Removing generated heat

A practical design problem follows illustrating the application of some of the techniques.

NOMENCLATURE

English Letter Symbols

A heat transfer area normal to flow, ft^2

A_f fluid flow area, ft^2

C flow stream capacity rate, $w\ c_p$, Btu/hr-^oF

c_p specific heat at constant pressure, Btu/lb-^oF

c_v specific heat at constant volume, Btu/lb-^oF

D diameter, ft

e	base of the natural logarithms (2.7183)
f	coefficient of friction, dimensionless
F	failure rate
G	mass velocity, w/A_f, lb/hr-ft^2
g	gravitation constant, ft/hr^2
h	heat transfer coefficient, Btu/hr-ft^2-^oF
HP	horsepower
I	current, amps
k	thermal conductivity, Btu/hr-ft-^oF
L	length, ft
M_N	molecular weight
N	nth number in a series
P	pressure, lb/ft^2
q	heat load, Btu/hr
R	thermal resistance to heat flow, ^oF hr./Btu
T	temperature, ^oR
t	temperature, ^oF
t	thickness, ft
U	overall heat transfer coefficient, Btu/hr-ft^2-^oF
V	volume, ft^3
W	weight, lb
w	flow rate, lb/hr

Δ difference

μ viscosity, lb/hr-ft

ρ density, lb/ft^3

Σ summation

γ ratio of specific heats C_p/c_v

Subscripts

1 initial conditions

2 secondary conditions

0 out

R rejected or radiator as noted

T total

TEMPERATURE LIMITS OF EQUIPMENT

For orbital flight, few high temperature problems are anticipated with mechanical equipment due to the generally high levels of permissible temperatures. Mechanical equipment such as valves and gears can be exposed to temperatures in the neighborhood of 500°F. Hydraulic equipments are presently capable of withstanding temperatures in the order of 400°F, with 1000°F the target temperature for the near future. During re-entry this is not necessarily the case and environmental protection will be required. However, the major emphasis of this discussion is concerned with the more critical electrical and electronic components.

One of the primary problems facing the electronic designer in the thermal design of electronic equipment is the determination of the maximum temperatures which electronic parts can withstand. The maximum temperature is usually limited by the thermal coefficients of the electrical characteristics of the part and their effect on electronic performance, the degree of reliability and life desired, and the temperature which the part can survive without outright failure. The thermal effects on electronic performance are considered to be peculiar to the circuits involved and indirectly related to the heat removal

problem. Therefore, a discussion on the thermal coefficients of electrical parameters is not considered a subject of this report. It is realized that the degree of cooling can alter the electronic performance by lowering the temperature spread and, in some instances, special cooling means will be required for this purpose. However, in most electronic equipment, the life, reliability and survival temperatures are the primary thermal factors.

Much remains to be accomplished in the determination of temperature vs. life or reliability for electronic parts. In general, such information is difficult to obtain. A reasonable collection of material on the maximum survival temperatures of electronic and electrical component parts is available. A considerable amount of this data is in terms of ambient temperature which is inadequate in the design of densely packaged electronic equipment. It is anticipated that the parts manufacturers will ultimately rerate their products and also assist in determining their compatibility with coolant fluids.

A list of the temperature limits of several representative electrical and electronic components which are representative of the present state-of-the-art are shown in Table 34. The particular detailed part or reason for the temperature limitation is indicated where known.

In the 150-200°F (66-93C) group are listed the 28-volt d-c overvoltage and differential reverse current relays. The purpose of these relays requires pickup and dropout within a relatively narrow tolerance and the effect of elevated temperatures is to cause operation outside the tolerance band before an actual material failure occurs. This limitation may apply to other relays limited by critical pickup and dropout values.

The bulk of items charted are in the range of 200-250°F (93-121C). The temperature limitation of a majority of these items is due to bearings, rectifiers, and capacitors. The temperature limitation of the bearings presents a serious problem because of their widespread use and the fact that the generation of electric power by dynamic generators depends on the proper operation of these bearings. If the bearing limitation can be cleared, an immediate uprating to the 400-450°F (204-232C) group is possible if Class H insulation is used. Class H insulation according to AIEE (American Institute of Electrical Engineers) standards may be a silicone elastomer, MICA, glass fiber, asbestos, etc., with suitable binding substances such as appropriate silicone resins. Limiting temperatures are listed at 180°C for these materials, but some upgrading is permissible as indicated.

The uprating of rectifiers and capacitors is extremely important as these are components of many equipment items. The rectifier problem may be solved through a new approach, while the solution of the capacitor problem is to obtain acceptable capacitance tolerance over a

Table 34

Component Temperature Limits

Equipment Components	Components Temperature Limited by	Temperature Limits °F
Transistors, Germanium		10-125°F
Batteries	Plate Materials	100-150°F
Potentiometers		-65-185°F
Relays - Over Voltage	Resistance and	150-200°F
Relays - Reverse Current	Reluctance Changes	
Generators - A.C.	Bearings	200-250
Generators - D.C.	Bearings	
Motors - A.C.	Bearings	
Motors - D.C.	Bearings	
Inverters	Rect. & Bearings	
Rectifiers-Metallic	Base Material	
Regulators - A.C.	Rectifiers	
Regulators - D.C.	Rectifiers	
Terminal Strips	Insulation	
Terminal Strip Covers	Material	
Capacitors	Dielectric	
Current Limiters	Resistance	
Switches - Toggle	Economics	200-250
Transistors, Special	Silicon	265°F Max.
Foam Plastic Sandwich		300°F Max.
Relays - Power	Solder	300-400
Relays - Control	Solder	
Relays - Gen. Field Cont.	Solder	
Porcelin, Silver Capacitors		390°F Max.
Transformers	Insulation	415°F Max.
Valves	Insulation	400-450
Connectors	Insert Material	
Switches - Unit	Spring	
Wiring	Insulation	450-500
Solenoids	Insulation	
Resistors - Wirewound	Insulation	
Subminiature Tubes	Surface Temp.	500°F Max.
Vacuum Tubes	Envelope Temp.	500°F Max.
Bonding Resins		575°F Max.
Clamps - Cushion	Insulation, Cushion	500-800
Ceramic Tubes		750°F

wide temperature range.

Note that toggle switches are listed on Table 34 as limited to the 200-250°F (93-121C) group by "economics". This means the switches may be capable of, and probably are, operating at higher temperature but for lack of economic demand have never been tested. The lack of demand is probably due to the cool atmosphere resulting from the requirements of the manned compartment in which switches are usually mounted. Additional testing may permit immediate uprating in temperature where required.

Generally used control and power relays are limited in the 300-400°F range by solder used in internal wiring. There are high temperature solders available but often the use of the higher temperature solder presents severe production problems. Mechanically attached terminations may be the solution. If the solder limitation is removed, insulation will be the limiting material with an upper temperature limit of 400-450°F.

Insulation limits the majority of the remaining equipment in Table 34. Upgrading beyond the 400-500°F Class H insulation range may be one of the major problems except in cases where bulky inelastic and inorganic insulations are acceptable. For want of a satisfactory higher temperature insulation, it is entirely possible that the 400-500°F (204-260C) range will prove to be a plateau of temperature upgrading.

In general, most of the presently used equipment is not designed for the new space era and much remains to be done, designwise, to "off-the-shelf" items to reach their thermal optimum.

In actual practice, many equipment items are rated on a steady state basis which does not necessarily conform to space vehicle usgae. For example, assume that a 200°F rating is based on the assumption of a full 200°F for full life. If, however, the normal application does not subject the component to a 200°F steady state continually but only for relatively short periods, with normal steady state operation at 150°F, then the component is rated too conservatively with regard to actual usage and life requirement. The rating of the 200°F component might be upgraded to 400°F is short enough and repeated exposure to 400°F is infrequent. Based on this fact, additional testing may permit upgrading the operating temperatures of current equipment. Operating life may often be sacrificed to gain higher operating temperature; however, the choice between life length and operating temperature must be made carefully and must be based on intended usage (see next part on thermal de-rating). This illustrates that rating method must be compatible with space vehicle usage.

In each of the above cases, reference is made to limiting hot spot temperature. However, it is important to realize that a high maximum hot spot temperature does not guarantee an effective high temperature

component. For example, a 600°F insulation operating temperature is of no value in a transformer design if the 600°F hot spot is so isolated from the cooling medium that the surface must be cooled to 200°F in order to keep the hot spot at 600°F. Higher operating temperatures cannot be substituted for good thermal design.

It is apparent that many difficult problems must be solved before the ultimate in equipment uprating is reached. It must be remembered that the goals of increased performance and reliability are not only desirable but are often manditory in space applications.

The immediate uprating of equipment operating temperature is not possible. In the interim, the space vehicle must suffer a large cooling penalty must always be held to a minimum and much can be done to arrive at more effective cooling, even with presently available materials and components. In accomplishing this aim, there are two major considerations: (1) Choosing the most effective cooling system and (2) Choosing the most thermally efficient equipment available. The choice of a cooling system and the best thermal equipment are integrally related and both must be considered jointly. However, the most important problem appears to be the design of electric equipment which is as thermally effective as possible. A further discussion of the progress of certain programs in uprating the temperature ratings of electrical and electronic equipment is included herein under the subject of "Methods of Controlling Thermal Effects".

HEAT GENERATION BY SPACE VEHICLE EQUIPMENT

This portion of the section discusses the heat generation of typical equipments and presents illustrative thermal circuits showing the complexity of the heat flow paths from the components to a sink.

The temperature variation of the internal structure with changes in envelope temperature may differ greatly among different types of components. For example, the plate structure of a vacuum tube transmitting heat to the tube's envelope principally by radiation undergoes a much smaller temperature change than the envelope because the rate of heat transfer is a function of the difference of the fourth-power of the absolute temperatures. In contrast, the innermost windings on a transformer may change in temperature almost as much as the surface when the cooling conditions are changed because heat is transmitted to the surface principally by conduction. If a low-loss component, such as a condenser, were mounted in such a way that it received heat by radiation from adjacent high temperature components, both its surface and internal temperatures would rise until the heat gained by radiation was offset by the heat lost from the surface by convection and conduction. Its internal temperature would approximate the average surface temperature. Regardless of the type of component, the surface temperature thus furnishes a reasonable indication of the internal thermal conditions

which determine whether or not a component will fulfill its design functions (Reference 59).

Electronic Equipment

Vacuum Tubes

The modes of heat generation and removal within a vacuum tube are complex. A simplified thermal analogous circuit is shown in Figure 109. A high temperature emitting surface is necessary to maintain proper electronic emission. Heater temperatures range from 1000° to 1300°C and cathodes operate in the neighborhood of 750°C (Reference 60). Tube structures are designed so that the thermal resistance from the heater and cathode to the envelope and leads is as great as possible in order to reduce the heater power to a minimum. However, for circuit purposes, most tubes are provided with low inductance leads to their internal elements. These leads can conduct heat from the cathode and a compromise between the thermal and electrical requirements must be made by the vacuum tube manufacturers.

Much of the heat dissipated in vacuum tubes appears at the plate. Almost all the heat produced at the filament, cathodes, control grid and screen grid is transmitted by radiation through the vacuum into this plate. The remainder of the heat produced by tube elements, other than the plate, is radiated to the inside surface of the tube envelope and/or conducted into the tube pins by metallic conduction paths along the tube element leads. The plate is heated not only by the heat received from the other elements but also by its normal dissipated energy. Plate temperatures in vacuum tubes, other than transmitting types, normally range from 350°C to 400°C. Almost all of the energy dissipated by the plate is transmitted by radiation through the vacuum and is absorbed by the glass envelope. Due to its transmission characteristics, glass begins to be a poor transmitter of infrared radiation at 2.5 microns. Thus, glass is essentially opaque to radiation from sources near 400°C, and only 6% of the energy radiated from the plate is transmitted directly through the glass envelope. The remaining 94% of the heat radiated from the plate is absorbed by the glass. The glass is heated and reradiates part of this energy at a lower temperature level and convects or conducts the remainder to the environment. Some heat from the plate is conducted along the plate lead through the tube pins. When plates operate at temperatures of the order of 750° to 850°C (cherry red), as in tantalum element transmitting tubes, the majority of radiation from the plate passes directly through the glass.

These modes of heat rejection from within a vacuum tube result in a concentration of heat in the glass envelope adjacent to the plate and to some extent at the base of the tube. If a tube is mounted vertically and operated in free air, a small hot spot, due to conduction through the leads, will appear at the base and the envelope will have a definite hot

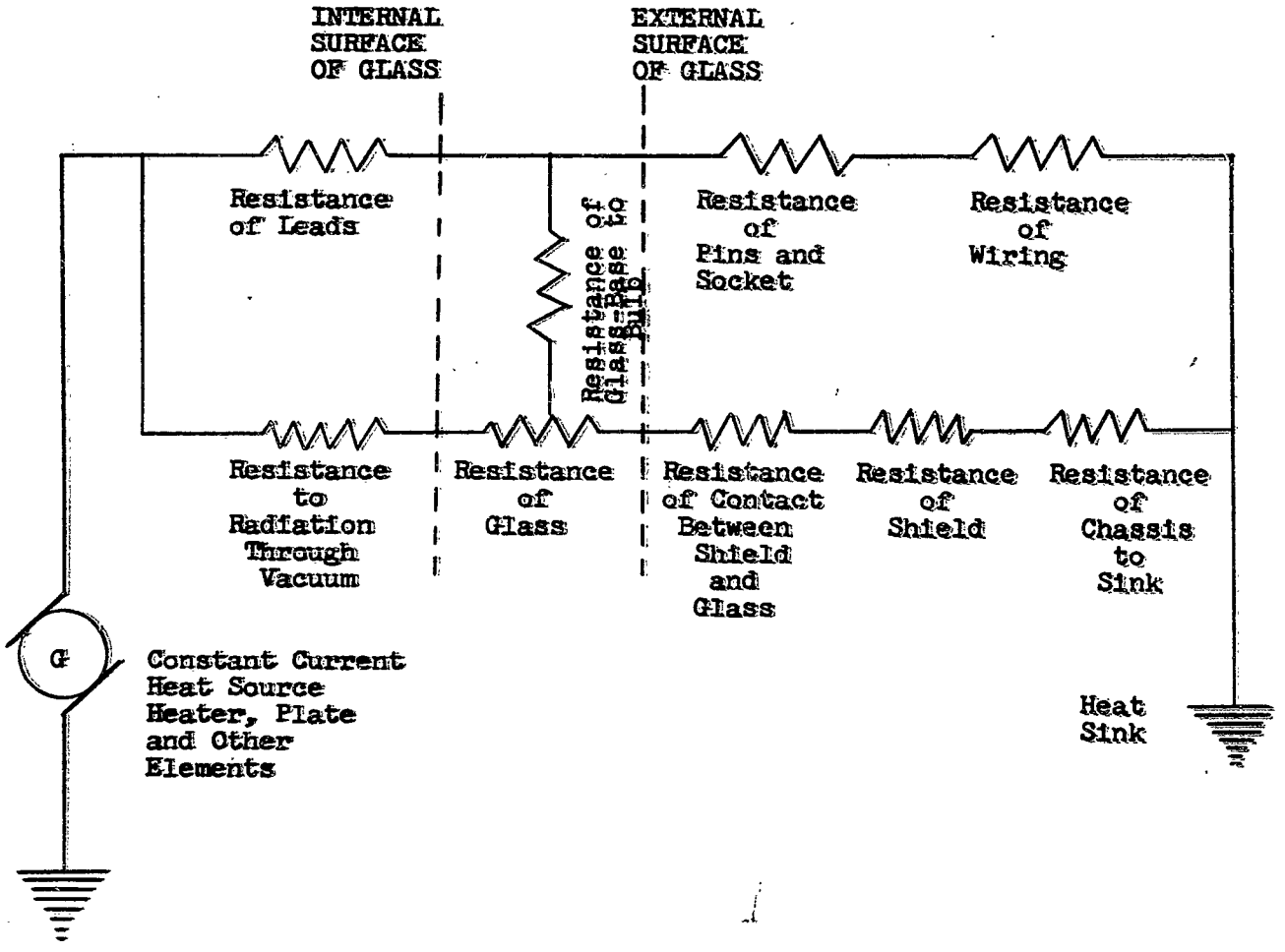

Figure 109 Simplified Thermal Analogy of a Vacuum Tube

spot at approximately two thirds its height, opposite the plate, due to radiation through the vacuum. Glass is also a relatively poor heat conductor and marked temperature gradients will appear in the envelope and adjacent to the upper and lower edges of the plate structure. It is desirable to cool vacuum tubes in a manner that will reduce such gradients in the evelope. Large temperature differences can cause severe mechanical strains which lead to envelope breakage.

It can be concluded that vacuum tubes must be cooled primarily by removing the heat from the envelopes. A portion of the heat can be removed through the pins or leads at the base. A study of the magnitude of heat removal which can be obtained by tube pin cooling is indicated in Reference 60.

Semiconductor Devices

Although semiconductor devices generate less heat than comparable equipments such as vacuum tubes due to higher electrical efficiency, units such as power transistors, semiconductor diodes, and similar devices generate large quantities of heat per unit of mass. In transistors the power is usually dissipated in the semi-conducting collector and base material and to some extent in the junction, as in the case of junction transistors. The heating occurs locally inside the device and must be removed through conduction in the case and the leads. Figure 110 is a schematic of an equivalent circuit of heat dissipation (Reference 61). Included in the circuit shown is a fin which is usually required for adequate heat dissipation adding to longevity of these devices. The techniques and methods applied for heat removal will be discussed in a subsequent part of this section.

The power handling capabilities of a transistor are largely dependent upon the maximum temperature which the material or junction can withstand. The maximum voltage and current ratings are also limiting factors, but in many cases the maximum temperature ratings will be exceeded first. The maximum junction temperature is that at which the reverse saturation current becomes large enough to cause thermal runaway, or the temperature at which the density of the thermally excited carriers becomes great enough to prevent transistor action.

Electrical Equipment

Transformers

The thermal analogy of a transformer is displayed in Figure 111. The heat flows out of a transformer structure to the environment as follows: In the usual power transformer, the coil and core are close fitting, and together present a more or less unified exterior surface which is composed of the exposed surface of the coil plus the exposed surface of the core. Heat flow to these surfaces from the interior of

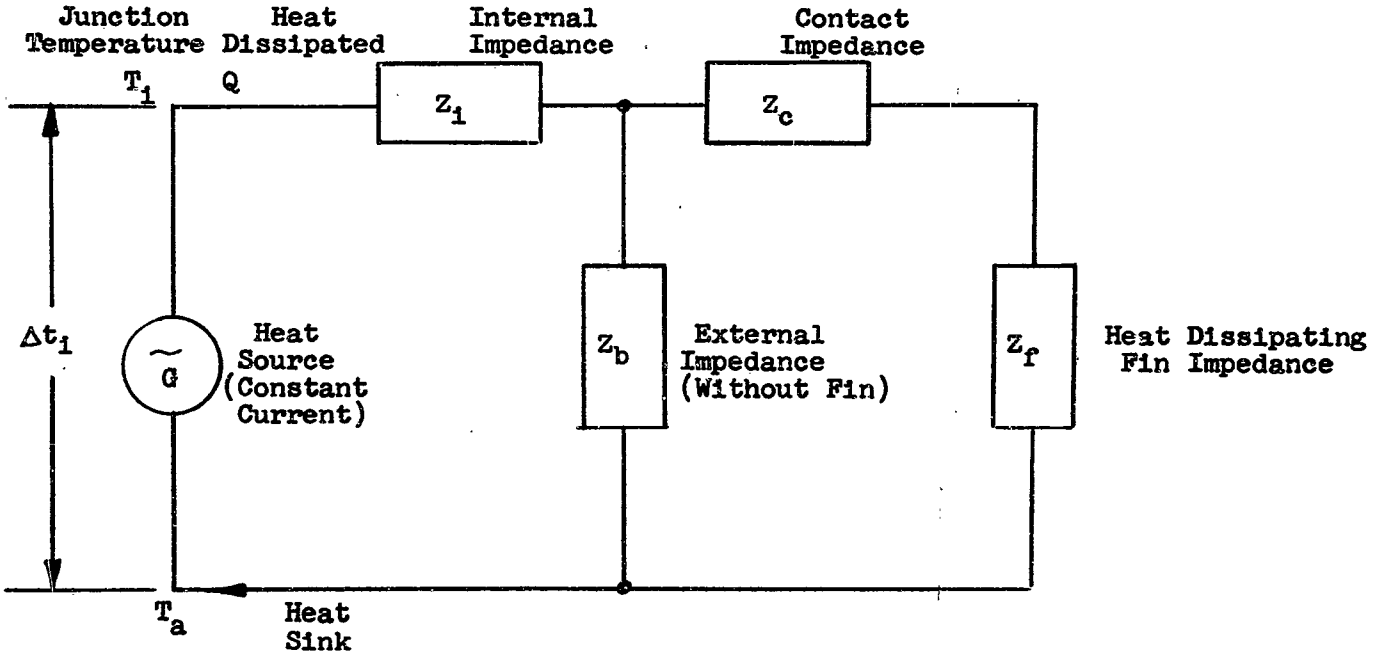

Figure 110 Semiconductor Equivalent Circuit of Heat Dissipation

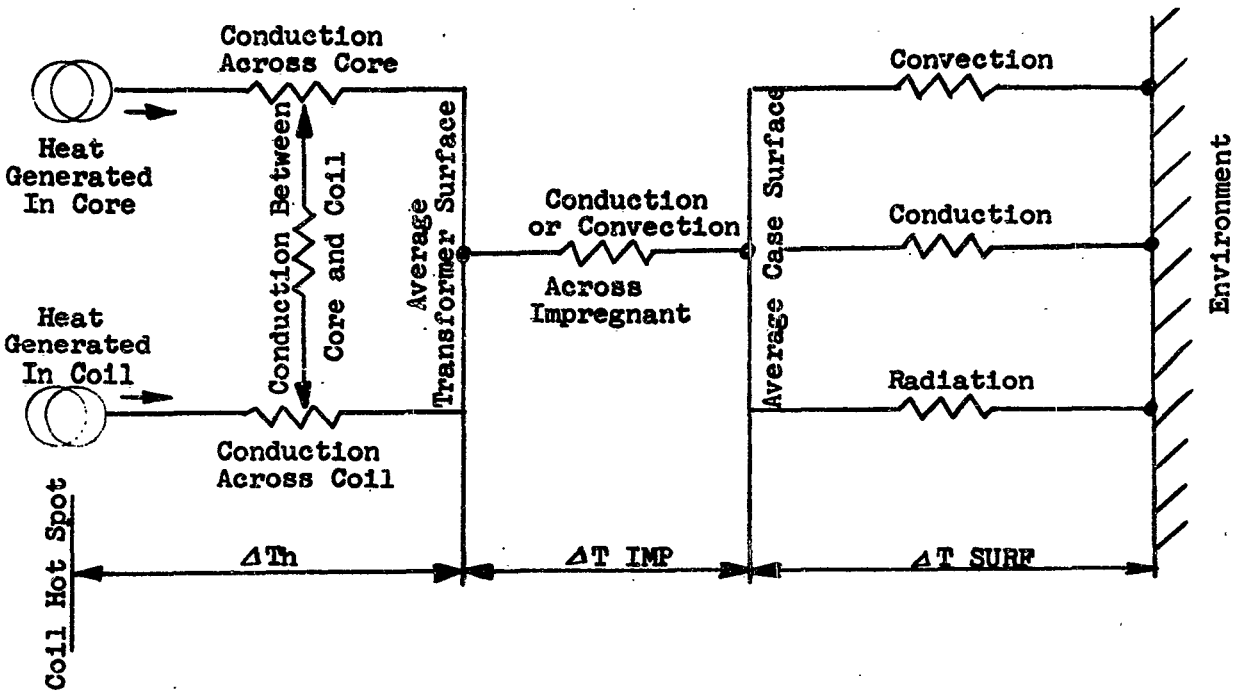

Figure 111 Heat Flow Analogue of A Transformer

transformer is primarily by conduction. The losses in the core and coil are not generated at a point but are distributed uniformly. This causes the interior flow paths to be quite complicated. However, with regard to the circuit external to the core and coil, the paths may be represented as single resistance connecting the source of heat with the transformer surface. Included in the circuit is provision for conduction between the core and the coil. When an impregnant is used, another thermal resistance is added to the circuit. Heat transfer from the outside surface to the environment can take place by all three modes (radiation, convection, and conduction), through the mountings.

The most important temperature in a transformer is the coil hot spot temperature. The largest temperature is usually between the coil hot spot and the core. If the maximum hot spot temperature is exceeded, the coil insulation is in danger of breakdown with subsequent failure of the transformer and possible damage to the connected equipment.

Connectors

The electrical connector like many other electrical and electronic components is a heat generating device. The total power transmitted through the connector and the length of exposure at a thermal environment must be established, as limiting operation parameters for each connector used. The limits of operation are defined in Reference 62 as the means of control to safeguard the physical properties, as well as the electrical and environmental integrity of the connector unit. The connectors referred to here are basically miniature multi-contact electrical connectors which conform to specification MIL-C-26500 (USAF).

The temperature gradient across the connector is a function of the heat generated within the unit or the total amount of current flowing through the contacts. The surrounding air conditions affect the heat transfer rate and thus the temperature gradient from the metal shell to the region of air turbulence. The thermal resistance of the interface is a function of the velocity of the airstream; therefore, a higher velocity airstream will result in a lower temperature difference between the interface and the bulk temperature of the airstream. This of course implies that for space vehicle application, these connectors will be used with equipment located within pressurized, environmentally controlled compartments where forced circulation of air or cooling gas will be utilized.

In steady state heat transfer condition or continuous connector operation, the heat generated within the connector is equal to the heat transmitted from the unit. The temperature rise within the connector is to be proportional to the power loss, which may be expressed by Joule's Law as:

$$q = \frac{\sum_{x=1}^{n} N_x I_x^2 R}{L} \qquad (143)$$

Heat conducted from the connectors may be expressed as Fourier's Law as:

$$q = \frac{kA\ (\Delta T)}{L} \tag{144}$$

where $T = t_c - t_a$, the temperature difference between the hottest contact and the ambient temperature.

T_1 = temperature rise generated by the full rated current I_f through all contacts N_T

For known connectors

ΔT is the temperature rise which results from various current combinations.

q then is proportional to q_1 the known heat generation, established by test.

so that

$$\frac{\Delta T}{\Delta T_1} = \frac{q}{q_1}$$

by substitution

$$\Delta T = \frac{q\,\Delta T_1}{q_1} = \frac{\sum_{x=1}^{h} N_x I_x^2 R}{N_T I_f^2 R}\,\Delta T_1$$

$$= \Delta T_1 \frac{\sum_{x=1}^{h} N_x I_x^2}{N_T I_f^2} \tag{145}$$

also

$$\Delta T = \frac{\Delta T_1 \left[N_1 I_1^2 + N_2 I_2^2 + \ldots + N_h I_h^2\right]}{N_T I_f^2} \tag{146}$$

Reference 62 indicates that theoretical calculations of temperature rise due to generated heat within the connector are within five percent of test data for the particular connectors in question. Utilization of Equation 146 is dependent upon the accuracy of data for ΔT_1. Ordinarily this data is obtained by tests of similar connectors for various current loads and ambient temperatures utilizing natural convection and forced

convection cooling. For space vehicle application this data must be presented in a manner to indicate forced convection cooling. Other parameters of gaseous pressure, cooling gas velocities, and coolant gas temperatures must be introduced in order to present the type of information which will be useful to the environmental control systems engineer.

Mechanical Equipment

Fundamentally, the most important properties in determining the amount of heat generated by any piece of mechanical equipment not containing the prime moves are the power input and the energy conversion efficiency of the equipment. For example, a highly efficient piece of equipment may show an efficiency of 90 to 95 percent so that the heat generated is low but all the input energy is ultimately converted to heat which has to be dissipated by the environmental control system.

If the equipment is a type of space vehicle power supply system which utilizes a combustion process and operates according to a standard thermodynamic cycle, the losses will be considerably greater. The heat energy generated may be several times the energy required by the equipment utilizing the generated power. If all of the equipment is in a sealed insulated compartment, the total energy released must be dissipated or removed by an environmental control system except for the quantity which may be "dumped" overboard by the exhaust system of the heat engine. It can readily be seen that for space vehicle applications, all equipment should be highly efficient and at the same time designed to require as little power as possible commensurate with the desired function.

Depending upon the mechanical equipment in question, heat may be generated in several different ways, but principally the heat will be generated by the mechanical inefficiency through friction, and through the thermal inefficiency of the energy conversion method employed.

Friction

Considerable heat can be generated by mechanical equipment due to the rubbing of two metallic surfaces together during rotational or translational motion of the component parts.

When friction occurs in the vacuum of space it may be considerably greater than it would be in a similar situation at sea level. Figure 112 taken from Reference 63 shows a comparison of average friction data for 19 metal pairs. The vacuum data was taken as soon as the pressure in the environmental chamber reached 3×10^{-6} mm Hg or less.

It can be readily seen that in areas of a space vehicle where there are unpressurized compartments including externally mounted equipment such as rotating antennas, solar cells, space radiators, and attitude controls, greater heat generation rates can occur due to increased

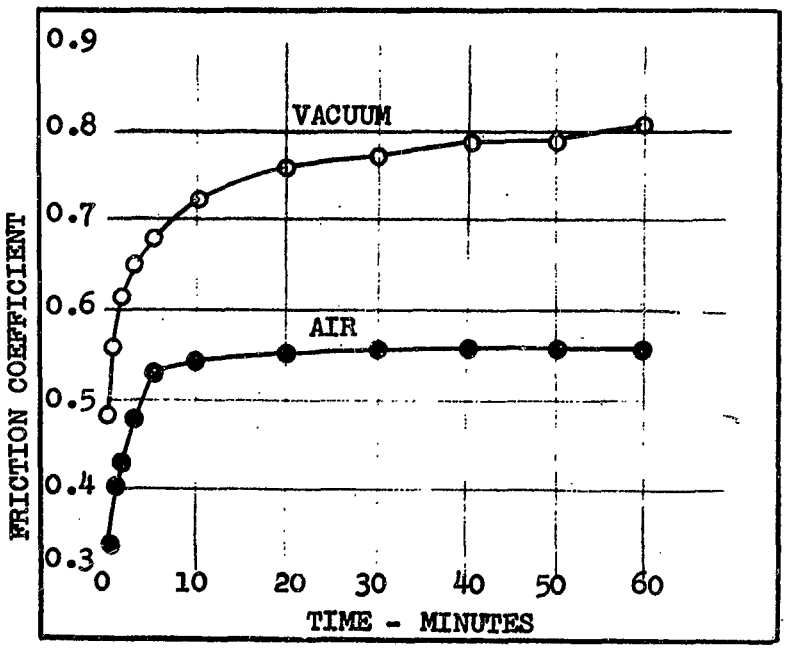

Figure 112 Average of Friction Data for 19 Metal Pairs-
Vacuum Data for Chamber Pressure of 3×10^{-6} MM.Hq.

friction if no lubricants are used or if the lubricants have evaporated due to the vacuum of the space environment. Much work remains to be done in exploring the friction phenomena in the space environment and the corresponding temperature and heat generation problems associated with and as a result of these phenomena.

METHODS OF CONTROLLING HEAT GENERATION

There are principally four methods for controlling the thermal effects of heat generating or thermally sensitive equipment:

(1) Decreasing heat generation rates
(2) Developing of components for higher operating temperatures
(3) Protecting from generated heat
(4) Removing Generated Heat

These methods are discussed in detail in this and the following two parts of the section. The methods for decreasing heat generation rates and some of the current programs for the development of components for higher operating temperatures are discussed in this part.

Heat generation in equipment may be decreased by (1) increasing the efficiency of energy conversion devices or substituting energy conversion devices of higher efficiency such as microminiaturized electronic equipment, (2) systems integration, (3) programming heat generating equipment for conservation of power, and (4) special devices such as low temperature thermionics, etc.

Several programs have been or are presently being conducted to develop components for higher operating temperatures. Two of the current programs discussed here to illustrate the direction that must be followed in order to eventually attain equipment which will operate at higher temperature levels are the "Hotelec" program (Reference 64) and the "Timms" program (Reference 65). Integral with the programs to develop equipment for higher operating temperatures are the programs being conducted to develop new materials which will aid component and systems design. An alternate method to the development of equipment operating temperatures is the use of one of the various techniques of thermally de-rating the equipment. Some discussion is devoted to this subject to define the various meanings of de-rating and to show some approaches to the thermal rating of a typical electrical component part.

Microminiaturization Designs

The requirements of space vehicles for extremely small electronic units which are light weight and highly reliable has accelerated the development of microminiaturized components and systems.

There are basically five major approaches to microminiature concepts which can be separated (Reference 66) as follows:

(1) High density packaging
(2) 2-D circuitry
(3) Micromodule
(4) Integrated circuitry
(5) Functional circuitry.

These five may be further reduced for the purposes of this discussion to two basic philosophies. The first is the micromodule concept which places a single component on a small plate (wafer) and then combines these plates to form standard circuits. A goal of 500,000 parts per cubic foot has been set for the component density of this concept. The second approach utilizes an entire circuit on one small plate (substrate). The IBM thinfilm effort exemplified this concept with component densities up to 5×10^{-6} parts per cubic foot. An outgrowth of the second type is the solid-circuit or moletronics where all components are an integral part on a single active element. Each concept has certain advantages and disadvantages depending upon its utilization but they all have the advantages of lower weight and volume, and higher reliability.

Unfortunately the inherent thermal characteristics of ultrasmall devices is to have a high power density (heat dissipation/unit volume of the equipment) which is exactly opposite to the desired characteristics from the standpoint of cooling requirements. The introduction of transistor devices to replace tubes initially reduced the power density, but further developments have raised the power density to two or three orders of magnitude higher than comparable vacuum tubes.

An examination of the cooling requirements of these miniaturized units has raised the importance of heat transfer to a prime level. Each concept must be evaluated for the best methods of dissipating generated heat or the overall gains in volume and weight reduction may not be reached.

Presently there are four areas of development that may alleviate the severity of the present thermal problems without affecting component density or reliability: (1) power reduction through use of pulse logic, (2) lower signal levels, (3) use of solid or molelectronic circuits, and (4) development of high temperature components (Reference 67).

The area which has been applied to the best advantage is the pulse logic rather than D-C logic. Since the pulse logic does not require continuous application of power to the circuit applications result in considerably less power dissipation. This mode of operation has been the foremost method applied toward the minimizing of heat generation within microminiaturized components to the present time.

Since the amount of power dissipated within a circuit is a direct function of signal levels, another method of retarding the power trend is the radical reduction of these levels. However, there are limitations below which the level cannot be decreased, the principal one being the necessity of having an adequate signal-to-noise ratio so that the signal is easily distinguishable. Since the emphasis has been to maintain present signal levels this technique has been somewhat neglected.

The final concept is directed toward the development of components for operation at higher temperatures, primarily in the 500 to 600°C range.

Energy Conversion

The demand for space vehicle power is increasing rapidly for which two types of power sources are receiving the greatest interest: (1) chemical energy (either converted directly to electrical energy or converted to thermal energy and then to electrical energy) and (2) solar energy. The majority of the development work on conversion systems is being conducted on four devices: (1) fuel cells, (2) thermoelectric converters, (3) thermionic converters, and (4) solar cells. The electrical output of these devices is low-voltage d-c, with the exception of the thermionic device, which may be developed to produce a-c.

Table 35 presents the available data on the various conversion systems, which includes possible growth potentials of some of the systems.

It appears that fuel cells will become a major power-conversion device for missions not exceeding about two weeks because of their high conversion efficiency.

In order to reduce waste heat to a minimum it may be desirable to utilize more than one power source, each having its desirable characteristics for different power requirements. For example, a fuel cell power source could be utilized for low continuous power operating a water recovery system, while an expansion engine APU could be utilized for a short period for supplying flight systems during re-entry or for high power surveillance radar equipment for short periods during orbital flight.

Integration of Equipment

Two qualifications or criteria for integration are duality of of function and replacement of function. By this definition it is possible to reduce the heat generated by equipment through the integration of equipment to increase efficiency of operation over that of the unintegrated equipment. An example of converting waste heat into useful energy through integration is a secondary power system which may derive energy from the heat generating components of the vehicle. In this case

Table 35

Conversion Systems For Electric Power

Conversion Systems	Efficiencies Percent	Current Densities Amp/ft^2	Power Densities Watts/lb
Fuel cells	60 to 80 (Ref. 68)	400	80 to 100*
Thermoelectric Converter	20*to 35*		100*
Thermionic Converter	17 to 40*	4500 to 18000*	75
Solar cells	15 to 20*		

* Represents anticipated results from future development.

consideration of increased radiator weight resulting from reduced transport fluid temperatures would tend to reduce any overall gains made by the integration.

Conservation of Power (Programming Operation)

By systematically planning the operation of the various equipment carried aboard a space vehicle the total heat load and the maximum possible peak load at any given time may be reduced. Pre-mission planning for equipment operation must include primary mission function, mission duration, power available, power usage, priority of equipment function, priority of data, and safety.

In order to reduce the equipment heat load generated at a given time the following methods may be applied:

(1) Turn off equipment when not in use (minimize standby operation of communication equipments, etc.)
(2) Program equipment operation for series operation rather than simultaneous operation (in other words don't turn on everything at once). This will aid in reducing size of power supply system.
(3) Intermittent use of equipment to utilize system mass for natural heat lags.

In order to minimize the overall heat load that may be generated the following methods may be used:

(1) Optimize equipment operation in terms of mission function.
(2) Restrict data transmittal to indicate changes of sufficient magnitude only.

By careful programming of equipment, operation benefits may be realized in terms of power conservation, reduction in the size of the power system required, reduction in system complexity, and possible reduction in overall vehicle size and weight.

Low Temperature Thermionics

By using low-temperature thermionic converters where possible, high temperature problems are reduced resulting in decreased heat generation. Also, life of the materials can be prolonged and system reliability enhanced. Test cells have already shown conversion efficiencies up to 15% and densities of 5 watts per square centimeter at the relatively low temperature of 1200°C. This operating temperature is far lower than that of other converters, whose emitters usually work at 1800°C. Low temperature thermionic converters will enable solar power to be fairly easily stored and used. For example, heating for cells operating in the 1800°C range is extremely difficult. Therefore, earth orbiting satellites

using thermionic cells would have to store electrical energy for darkside operations. On the other hand if the emitter is operated off a 1200°C source an extremely simple and lightweight beryllium heat storage unit could energize the cell during dark periods. Lower temperature also means that solar mirrors serving thermionic arrays would not have to be as accurately oriented as they would for higher temperature operation.

METHODS OF PROTECTION FROM GENERATED HEAT

Space vehicle equipment components which differ in temperature sensitivity cannot be packed into the same environment without risk of early failure of the more sensitive elements unless some method of segration or shielding is used to protect them. Some of the methods discussed in the following chapter which may be applied, are as follows:

Segration of heat generating and non-generating, and segration of critical and non-critical (temperature sensitivity) equipment.

Arrangement (relative positioning) of equipment for best utilization of a cooling medium.

Locally applied insulation and the use of heat baffles.

Protection by the use of closures

Also discussed in this chapter is the relationship of reliability to system design and arrangement for cooling. A technique for arrangement of components where the reliability factors are known is given and suggestions for further studies to develop computer programs for optimum cooling arrangement are made.

Protection By Separation and Spacing

Major thermal benefits can be achieved through the proper placement of electronic parts within assemblies. In general, it is desirable to locate the heat sources as near as possible to the coolest surface. This will provide the shortest thermal path from the source to the sink, together with the minimum gradient. In order to obtain maximum heat transfer, heat producing parts cooled by radiation and conduction should always be mounted with their major axes parallel to cooled surfaces.

When it is necessary to group heat producing parts together for an assembly to be used in a space vehicle an attempt should be made to group components of like temperature sensitivity together for optimum utilization of the coolant flow.

For the purpose of illustrating the desirable utilization of a coolant by equipment compartment arrangement, four heat sources with step-wise temperature levels are shown in Figure 113 taken from Reference 69. The equipment and areas selected as an illustrative example

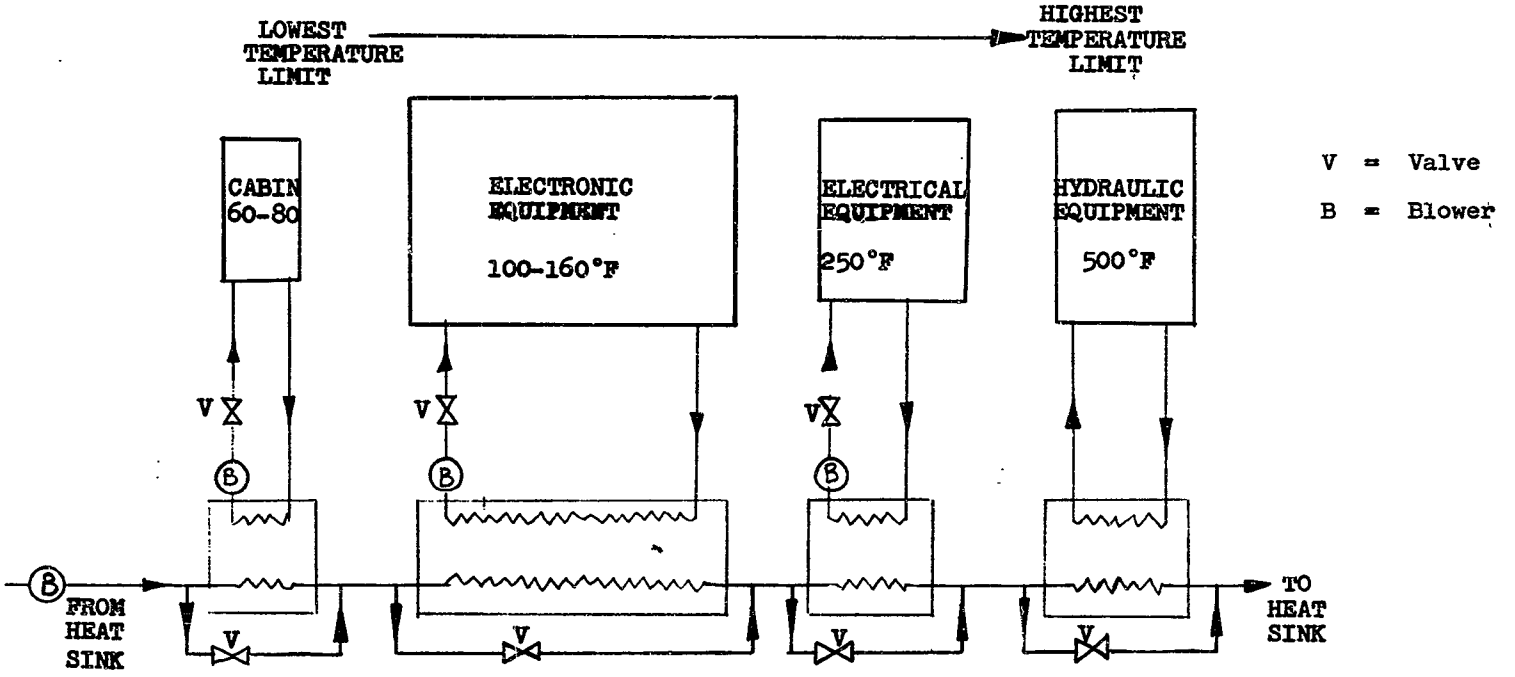

Figure 113. Environmental Control With Separate Coolant Loops

all generate heat at different rates and must be maintained at or below maximum allowable operating temperatures. The arrangement of these heat sources in the cooling circuit influences the degree to which the heat sink capacity is utilized as well as the reliability, weight and pumping power consumption of the environmental control system (ECS). The temperatures shown are basically compartment ambient temperatures; the maximum temperature indicated is the outlet temperature of the cooling fluid from the compartment. The primary system cooling fluid can be either liquid or gas as separate heat exchangers are indicated for each loop. Figure 114 shows a combined parallel - series fluid loop.

The advantages and disadvantages of each of the typical examples shown have been determined from analysis in Reference 69. These analyses provide a convenient means of studying the effect of coolant heat capacity rate and outlet temperature on required compartment heat transfer surface area and blower power consumption when no specific information is known on vehicle electronic and electrical equipment characteristics and arrangement.

Figure 115 indicates three levels of detail in which the series cooling technique may be used. For the purposes of this report the primary concern will be the electronic component (or general component) level, and possibly the "black box" level where a secondary cooling loop is utilized.

Certain advantages may also be realized by arrangement of equipment for parallel supply of coolant. With parallel system a manifold supply duct of some type is usually used to simultaneously supply coolant to different assemblies, compartments, or components at the same inlet temperatures. This concept is particularly advantageous to modular cooling and microminiaturized "card" assemblies where each unit in the assembly dissipates approximately the same quantity of heat and is subjected to the same temperature limits and cooling conditions.

Relative to the component level, techniques have been developed (Reference 70) whereby the reliability of components has been used to determine the best arrangement of the components in a "package" relative to coolant usage. This technique describes how the arrangment of equipment groups can be optimized to give the maximum system reliability, from a thermal design standpoint. The penalties due to a non-optimum arrangement can be evaluated allowing trade-offs with other design considerations. The study pertains only to series airflow over equipment, however, similar techniques can be devised which will apply to equipment cooled by parallel supply systems.

The average air temperature passing over the nth equipment group, compartment, or heat exchanger downstream from the primary cooler or heat sink loop, depends on the airflow rate, the heat dissipated by the intervening equipment and part of the dissipation from the nth equipment. Mathematically the average air temperature is

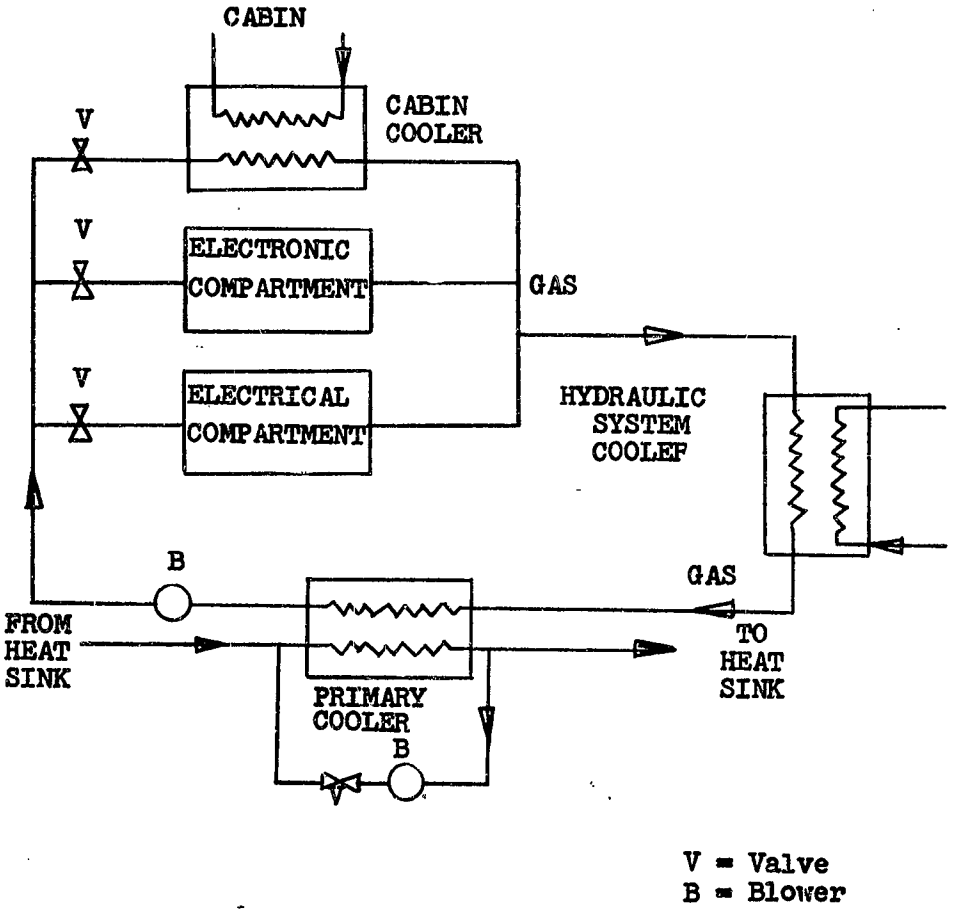

Figure 114 Parallel and Series Arrangement

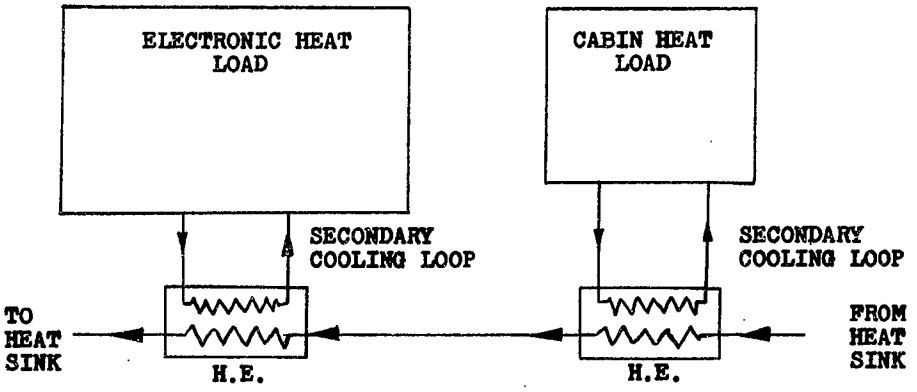

SERIES COOLING BY COMPARTMENT

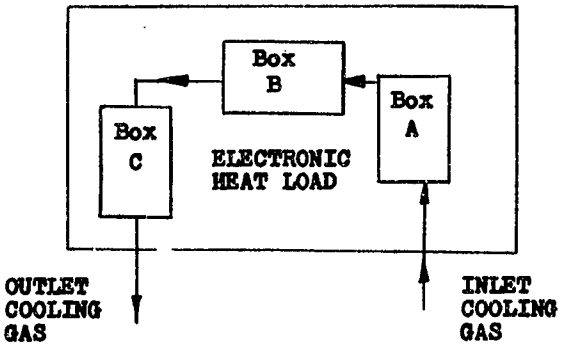

SERIES COOLING BY "BLACK BOX"

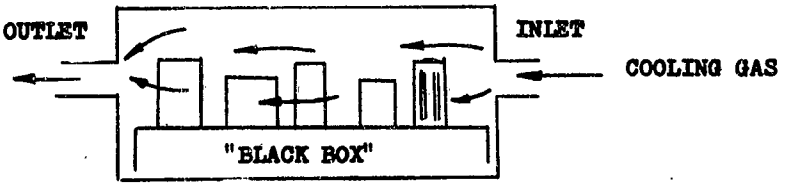

SERIES COOLING BY ELECTRONIC COMPONENT

Figure 115. Separation By Temperature Level And Arrangement For Best Coolant Utilization

$$T_n = T_{h_2} + \frac{1}{Wc_p}\left[\sum_{i=1}^{n-1} q_i + \frac{q_n}{2}\right] \tag{147}$$

where

T_n = average air temperature at the nth equipment

T_{h_2} = heat exchanger exit temperature

W = air flow rate, lbs/min

C_p = specific heat capacity, Btu/lb.$^{\circ}$F

q_i = heat dissipation of any group

q_n = heat dissipation of group "n"

also

$$T_n = T_{h_2} + \frac{1}{W}\left(\frac{q_T}{c_p}\right) A_n \tag{148}$$

$$A_n = \sum_{i=1}^{n-1}\left(\frac{q_i + \frac{1}{2}q_n}{q_T}\right) \tag{149}$$

q_T = Total heat removed by heat exchanger (primary) or heat sink loop.

A_n = Cumulative fraction of total heat load up to equipment "n"

T_n = can be plotted versus A_n values of zero to 1 at various values of W. In order to determine air temperature at the equipment group the (A_n) abscissa is divided proportionately to (q_g/q_T) for each group. The average temperature is the midpoint of each section.

Reliability is defined as the probability, P_r that given equipment will operate satisfactorily for a specified time τ

Equation:

$$P_r = e^{-\tau/m} \tag{150}$$

m = mean-time to failure

Failure rate F in failures/million hours is related to m as $F = \frac{10^6}{m}$.

Variation of part failure rate due to one failure source appears to vary exponentially with absolute temperature

$$\text{or} \quad F = F_{oe}^{r\,(T-T_o)} \tag{151}$$

$$dF = FrdT$$

Experimentally the rate usually increases with the temperature of the component. Part failure rate coefficients must be established by experimental data (r_i = failure rate coefficient).
For variation of equipment group failure rate with temperature, calculate the group failure rate at several temperatures based on $n_i f_i$

where

n_i = number of parts of (i) type

f_i = failure rate of part (i)

The temperature coefficient of failure of the group (r_g)

$$r_g = \frac{1}{Fg} \frac{d\,Fg}{dT} \tag{152}$$

For determining equipment arrangement, layout the equipment groups in the order of decreasing failure rate, with the high failure rate at the cool end as shown in Figure 116.

Select an inlet Temp. T_{n2} and an airflow (W)

Compute the average air temp. for each equipment group (Fg)

Compute group failure rate temp. coef. (rg)

Then compute Fg x rg for each group.

Calculate air temp. rise due to each equipment group

$$\delta T_g = \frac{q_g}{WC_p} \tag{153}$$

If two groups say A and B are interchanged (A is initially upstream of B) group A will get warmer cooling air by an amount T_B and suffer an increase in failure rate by $F_A \times r_A \times T_B$. The failure rate of group B decreases $F_B \times r_B \times \delta T_A$. The interchange is desirable if

$$F_B \times r_B \times \delta T_A > F_A \times r_A \times \delta T_B \tag{154}$$

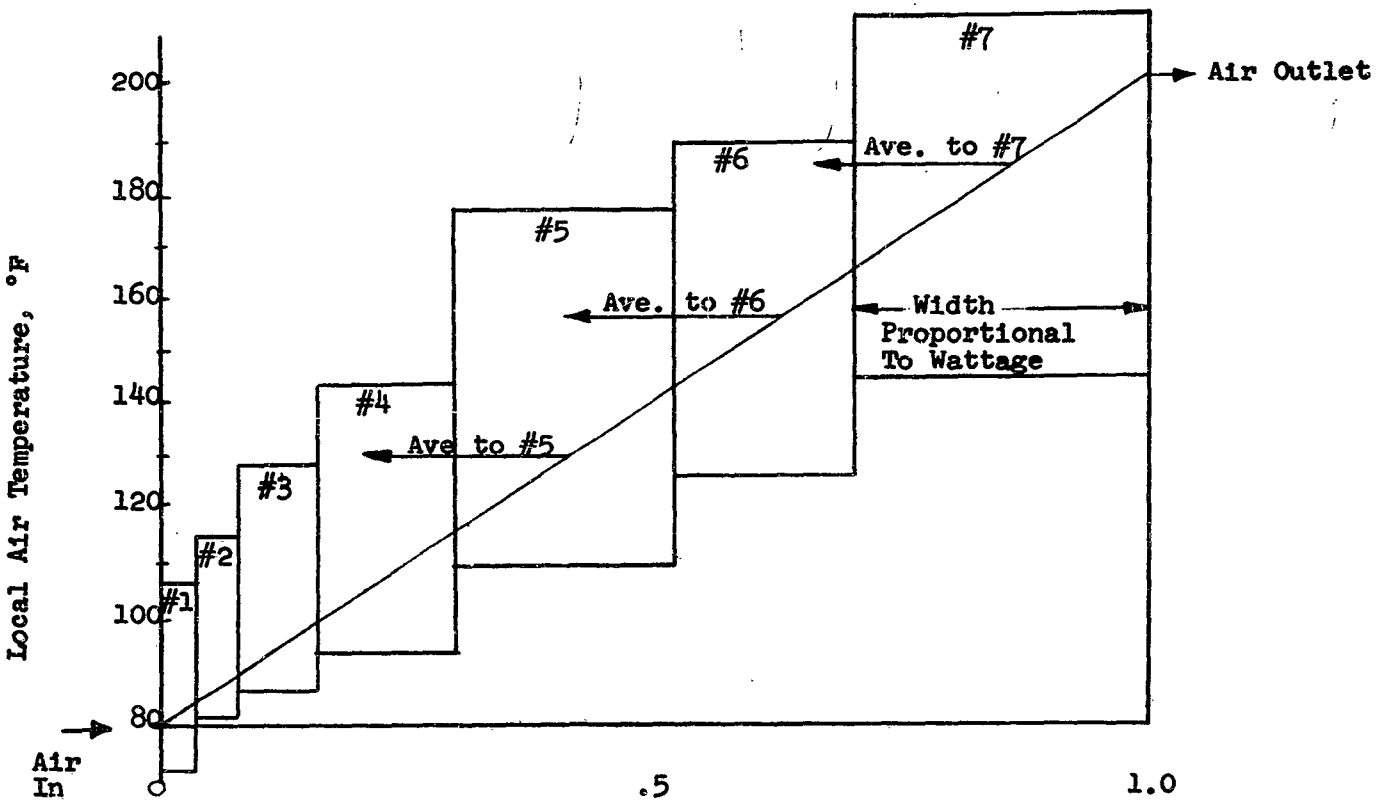

Figure 116 Determination of Local Air Temperature of Equipment Groups

Beginning with the cold end the products of $F_g \times R_g \times \delta T_g$ can be computed and the desirable interchanges made. If any equipment group moves very far it may be necessary to re-evaluate the F_g and R_g at its new temperature. When the procedure is completed the calculated best arrangement will be obtained.

In order to quickly determine the equipment components best arrangement graphically, the blocks representing the fraction of the heat load (q_g/q_t) for each component of a module may be constructed as transient paper cutouts as suggested by F. W. Thunberg of Autonetics in an internal report. It may prove worthwhile to set up the method for computer solution whereby the program for determining arrangement can be linked with programs to determine the necessary reliability coefficients.

Protection By Shielding

Various shielding techniques may be used to protect space vehicle equipment from generated heat. The generated heat may come from various sources, but in the main it will be from the equipment item, from other equipment, or from the vehicle during re-entry flight. The type of shielding utilized for protection may consist of locally applied insulation, heat baffles, or some type of closure or encapsulating method. The type of shielding used will depend upon the specific equipment of equipment component in question and the location of the equipment item in the space vehicle. The equipment carried in a manned space vehicle will be located (1) in the protected environmentally controlled crew compartment, (2) in a specially protected compartment, (3) in an unprotected compartment, or (4) externally on the vehicle. In the first two cases protection or shielding other than on a small component basis (i.e., tube shields, plastic embedment) is accomplished by the compartment and environmental control system. In an unprotected compartment equipments can be shielded by use of baffles, locally applied insulation, or by encapsulation. Externally mounted equipment may utilize the same shielding techniques and be retracted or jettisoned prior to re-entry of the vehicle. Proper thermal design of external equipment will facilitate the temperature control of such equipment, since direct radiation of generated heat to space can be accomplished from this location.

Locally Applied Insulation

The application of a type of insulating material or method to an equipment item may be done as a protective measure against generated heat. Local insulation of equipment is a type of shielding as opposed to a heat removal technique, although cooling systems invariably utilize insulation in one form or another, in some part of the system.

The chassis of an electronic equipment assembly may be insulated to protect the internal components from externally generated heat. At the same time such insulation would assure that nearly all of the internally generated heat could be removed by a coolant flowing through the unit, thus providing protection from the introduction of undesirable heat into a space vehicle crew and equipment compartment.

Equipment located in areas which are remote relative to the cooling system may be protected by insulation from the heat generated by adjacent equipment or from heat generated during re-entry.

Various insulators of low thermal conductivity are used for purposes of insulation of equipment. A few are listed as follows:

Fibrous insulation
Honeycomb
Foam plastics
Ceramics
Powdered metals
Vacuum

A more detailed discussion of insulation is included in Sections II and III.

Application to Temperature Control

It was previously mentioned that insulation is often used with a cooling system to attain a protective system which more nearly approaches the optimum. Figure 117 illustrates several methods by which close temperature control may be attained by variable conduction. By varying the quantity of gas in an insulating material, the conductance of the insulation can be varied and controlled to an extent. If it is desirable to dissipate more heat due to increasing component temperatures the pressure of the gas within the insulation may be increased to increase the overall conductance of the insulation system. The converse may be done when the component temperature decreases. Section III, Variable Conductance shows the variation of the conductance of typical insulation materials with pressure. Although the data are for air, other cases of higher conductance could be utilized which would expand the range in which control can be attained.

Heat Baffles

(a) Tube Shields

Tube shields remove heat from the vacuum tubes which they enclose. They also act as an electrical shield around the tube to reduce interaction due to stray fields.

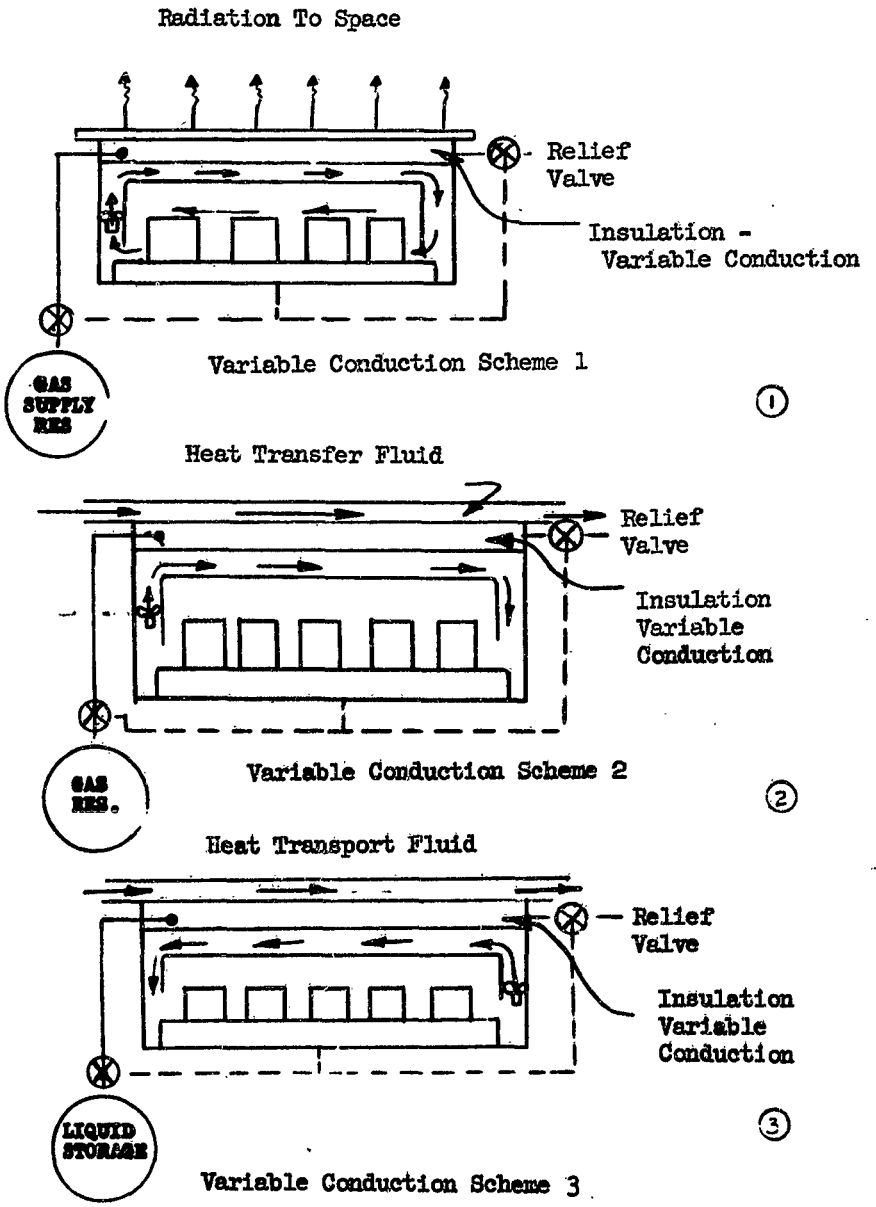

Figure 117 Variable Conduction Temperature Control Systems

There are three heat transfer paths from a bare tube:

(1) Radiation from the envelope to surfaces which the envelope "sees"
(2) Forced convection from the envelope to the environmental air or gas surrounding the tube.
(3) Conduction along the tube lead-wires.

In order to be effective in removing heat from the envelope there must be a minimum of contact resistance between the tube shield, its base, and the chassis or mounting surface. The mounting surface should be of metal and be brazed or bonded to the shield. In addition the tube shield should fit as close as possible to the tube envelope to reduce the air gap to a minimum. It is also advisable to have a highly absorptive inner surface of the shield. Depending upon the surrounding components, the outside of the shield can be polished to reflect heat or left dull and blackened (same as the inner surface) for absorption of heat. Several types of tube shields are illustrated in Figure 118 taken from Reference 71.

(b) Subminiature Tube Shields

The wrap-around shield is the most commonly used subminiature tube shield in current electronic equipment. The shield consists of a cylinder of springy metal which is forced to fit and wrap around a miniature tube envelope. Heat is transferred by radiation, direct conduction and gaseous conduction.

Other types of shields are:

(1) Fuse clip type
(2) Slotted aluminum cylindrical tube
(3) Metal tube blocks

A summary chart of subminiature tube shields is shown in Figure 119 taken from Reference 72. The chart indicates the various types of tube shields in common usage and shows the relative order of merit of each type of shield.

Fluid Shields

A closed loop circulating system may be used as a shield against aerodynamic heating during re-entry for almost any item of equipment located near the external skin of a space vehicle. In this system the coolant is passed between the skin and the equipment to be cooled, as shown in Figure 120.

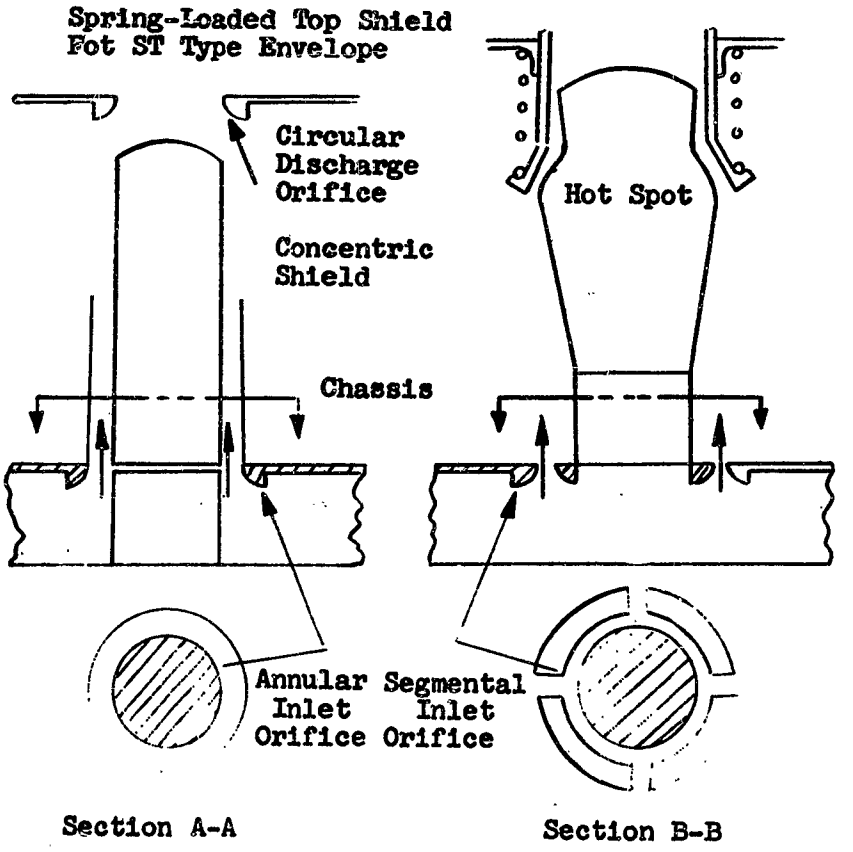

Figure 118 Orifices and Shields

	TUBE SHIELD DESCRIPTION	°C ENVIROMENTAL TEMP	°C TUBE BASE	°C TUBE ENVELOPE (NEAR PLATE)	°C TEMP. RANGE OVER TUBE ENVELOPE	REMARKS (H.S. = HOT SPOT) LOCATION	RELATIVE MERIT IN ORDER OF EFFECTIVE COOLING
1	PLAIN WRAP-AROUND (COPPER)	23	128	103	——	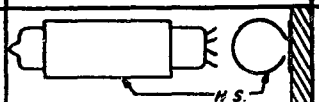	E
2	SLOTTED WRAP-AROUND WITH BASE CLIP (COPPER) C.A.L.	24	71	88	96 —— 61	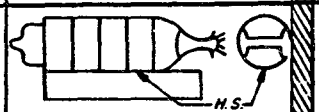	C
3	FUSE CLIP WITH WRAP-AROUND AL.	26	88	82	82 —— 60	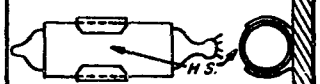	C
4	FUSE CLIP (NO COVERING)	23	86	139	140 —— 56	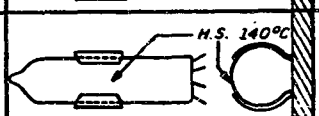	D
5	SLOTTED CYLINDRICAL SHIELD (SCREW BASE) (AL.)	20.5	88	49	44 —— 41	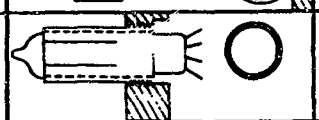	A
6	METAL BLOCK (AL.)	24	82	RESULTS EFFECTED BY CONVECTION COOLING THIS TECHNIQUE PRODUCED THE LOWEST TEMPERATURE			B
7	NO SHIELD TUBE VERTICAL IN AIR	24	103	163	163 ——	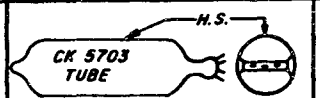	F

Figure 119 Summary of Subminiature Tube Shield Evaluation

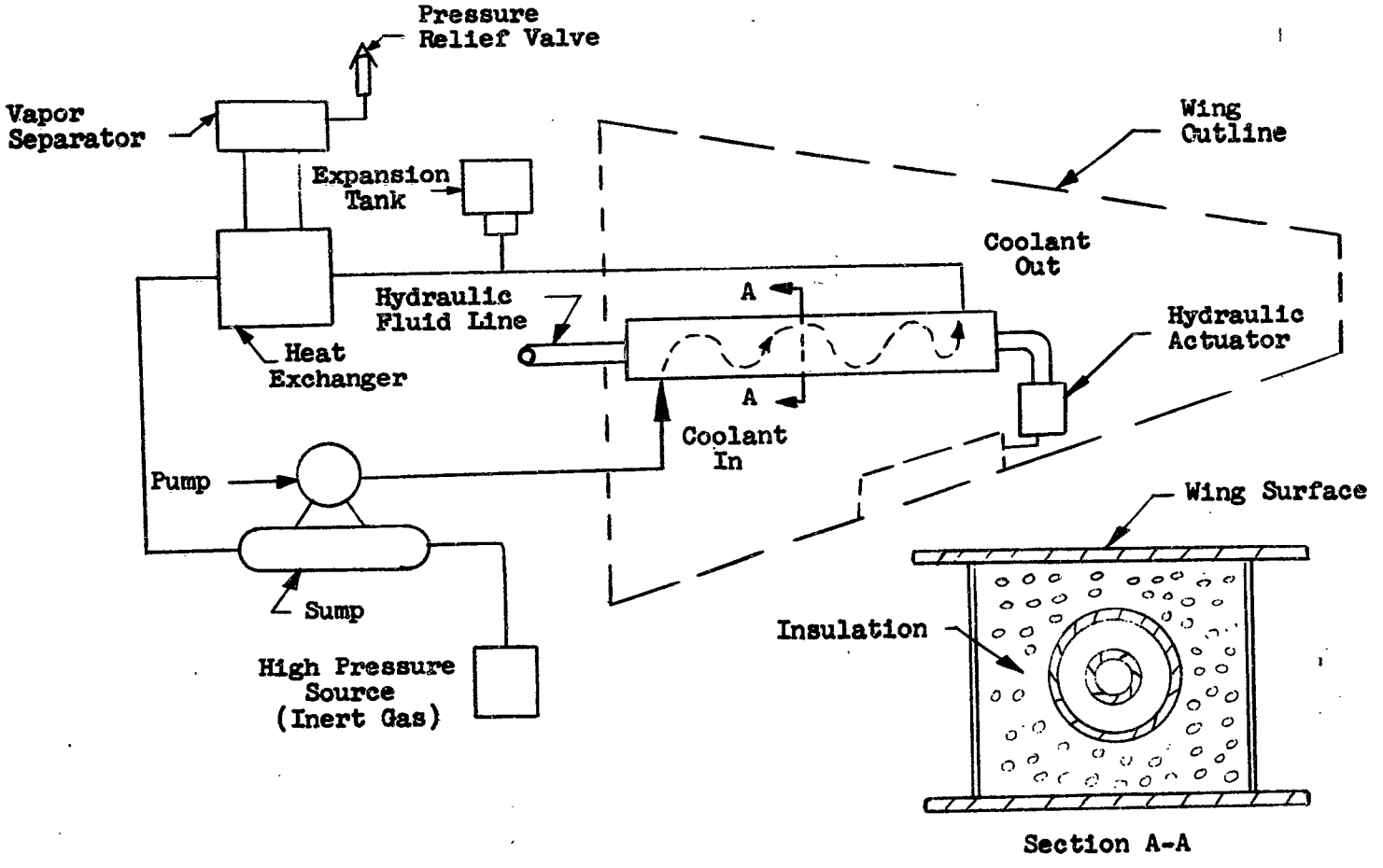

Figure 120 Equipment Cooling System Circulation Tyoe (Closed Loop)

(a) Semi-Conductor Heat Dissipators

The useful life of any semi-conductor device is dependent upon the temperature to which it is subjected. The closer to the manufacturer's recommended temperature the device can be operated, the better its chances for long life. When stating electrical characteristics, the manufacturer usually specifies a 25°C mounting base temperature (Reference 73). With an increase in temperature above this figure, the efficiency decreases in a direct linear relation to the temperature.

The power handling capabilities of a transistor are largely dependent on the maximum temperature which the material or junction can withstand. The maximum voltage and current ratings are also limiting factors, but in may cases the maximum temperature ratings will be exceeded first. The maximum junction temperature is that at which the reverse saturation current becomes large enough to cause thermal runaway, or the temperature at which the density of the thermally excited carriers becomes great enough to prevent transistor action.

The methods for using "Dissipators" to dissipate heat from transistors by natural heat transfer such as described in Reference 73, will not be adequate for space vehicle electronic equipment. The conduction and radiation of heat from the transistor to the dissipator will of course help the situation, but ultimately a forced convection process utilizing liquids or gases as heat transfer media will be required.

(b) Other Applications

Shielding techniques are particularly useful for equipment located in unpressurized areas of a space vehicle. Since the vacuum of space eliminates possible heat transfer by convection and the conduction of heat through structural supports can be minimized by good design, only radiation remains as a source of employed to protect equipment components from the radiant heat. For example polished copper has a monochromatic reflectivity of approximately 95 percent for most wavelengths. Commercial aluminum has a monochromatic reflectivity which ranges from 10 to 95 percent depending upon wavelength. Properly used radiant heat shields fabricated from these materials offer good protection for minimum weight and complexity

Closures

In this report "closures" refers to the potting or plastic embedment of electronic components and to the lithium package protective cooling systems for remotely located mechanical or hydraulic components. However, "closures" might also include the "black box" enclosures or chassis of an electronic assembly. The chassis plays an important role in the thermal protection of the components within it. First of all the chassis will shield the components from external heat sources particularly radiant heat. Secondly and probably most important the chassis is often used as

an important integral part of the equipment cooling system. The chassis either facilitates cooling by confining the cooling air or aids the dissipation of heat directly through cold plate heat exchangers and conductive paths incorporated in integral design concepts. A more complete review of these methods of cooling is given in the next part.

(a) Metal Fusion Systems

In the metal fusion system of thermal protection equipment is encased with a metal whose melting point is at or below the operating temperature limit of the quipment. The effective heat sink capacity of the metal thus includes its heat of fusion and temperature limits will not be exceeded until sufficient heat has been absorbed to liquefy the encasing material. (1) it is completely enclosed, requiring no resupply of coolant material, (2) it is self-regulating, has no moving parts, and requires no power supply, (3) it may be designed to have a high degree of reliability. (See Figure 120)

The selection of a material for a fusion system depends on the temperature to which the equipment must be cooled. If the temperature of a hydraulic line using conventional hydraulic fluid is limited to 400°F then it is required that the melting point of the coolant be equal to or below 400°F. It is also required that the coolant material have as large a heat of fusion as possible. Reference to Section V shows some materials which melt at or below 400°F. Many other properties as a function of temperature and properties of mixtures such as NaK-44, NaK-56, and NaK-78 are shown in Reference 58.

If the system selected is a fusion system and the metal is not to be vaporized then it may be possible to eliminate the vapor separator and any lines to or from the unit. The major problem in determining both the feasibility and the weight of a metal fusion system lies in calculating the weight and volume of the coolant material that is necessary to control the temperature of the component being cooled, for the entire high temperature period of a space mission. In most cases the severest problem will be during re-entry. For example, to determine the weight and volume of lithium coolant needed for thermally protecting a hydraulic line it is necessary to write a series of simultaneous heat balance equations on the various elements of the system. The equations and analysis for this type of system have been worked out in detail and may be found in Reference 58.

(b) Potting

Thermal protection may be afforded to electronic assemblies through the use of cast-resin compounds for heat dissipation. A review of the literature indicates that the common terms of casting resin; embedment, encapsulation, and potting are best defined by Reference 75 as follows:

Casting Resins: A generic term for all resins used for the purpose of embedment, encapsulation, potting and impregnation of circuit sub-units and components.
Embedment: A component part or circuit sub-unit completely cast with a block of resin. Only a temporary mold is used, which is discarded after casting and cure has been accomplished.
Encapsulation: Casting resin applied by means of dip coating or other surface application method followed by cure. The cured resin follows the configuration of the part.
Potting: Embedment where the mold in the form of a can or other container remains as an integral part of the unit.

The cast resin compounds of the electronic assemblies may be used in two ways (1) the thermal conductivity ability of the resin material may be used to obtain an improvement in the overall heat dissipation characteristics of a given device or equipment where heat removal is a problem (2) the resin material may be used to shield the components of the assembly from thermal and other effects of the surrounding environment including vibration, acceleration and possible atmospheric hazards such as low pressure, contaminants in the atmosphere, moisture and possible electrical arcing at low pressure levels. At the same time other equipment is protected from the possible contaminants and fire hazards which might otherwise be produced by the encapsulated components.

Excessive hot spot surface temperatures of components can be avoided by the various techniques through the diffusion of the heat from the component surface through the plastic material. Most applications of potting or embedment should be limited to electronic equipment having low heat concentrations. This is due primarily to the temperature drop from the surface of the component to the surface of the potting or embedment material which is enclosing the component. The heat generated by the component is removed from the surface of the plastic. If the plastic is very thick or the component has a high heat concentration a relatively high temperature difference will prevail with correspondingly high component temperatures. Potting and embedment techniques are best used with components which operate on an intermittant basis whereby the heat storage ability of the resin material and components first stores, then dissipates the heat in a transient manner.

The key to the reduction of a high ΔT between the electronic component and the surface of the resin material is high thermal conductivity. Since most unfilled casting resins show only minimal differences in thermal conductivity the development of high thermal conductivity in resins depends upon the thermal characteristics of the powders. The thermal conductivity of some representative fillers and of some epoxy-resin embedding compounds containing fillers are shown in Table 36.

Table 36

Casting Resin Filler Thermal Conductivity Data

THERMAL CONDUCTIVITY OF FOUR REPRESENTATIVE FILLER MATERIALS	
Filler	Thermal Conductivity Cal/cm. sec. °C
Mica	0.0012
Sand	0.0028
Aluminum	0.497
Copper	0.918

THERMAL CONDUCTIVITIES OF EPOXY-RESIN EMBEDDING COMPOUNDS USING VARIOUS FILLERS		
Filler	Percent Filler in Compound by Weight	Thermal Conductivity of Filled Compound Watts/in.°C
Copper Powder (Venus A, U.S. Bronze)	90	0.040
30 Mesh Aluminum	80	0.064
Fine Mesh Aluminum	40	0.022
Course Grain Sand	70	0.025
Tabular Alumina	80	0.026
325-Mesh Mica	45	0.013
325-Mesh Silica	55	0.019
Hollow Phenolic Spheres	15	0.003
Unfilled Epoxy-Resin		0.005
Unfilled Urethane Foam (5 lbs/Ft3 Density)		0.0001

The application of cast-resin materials as a protection meth dissipation of generated heat has to be weighed against the use o sinks or forced cooling of the unenclosed components. For space the components enclosed by one of the casting techniques, and loc within a compartment must rely on some method of removing the hea the surface of the resin material other than free convection. E individual application must be evaluated in terms of the local en conditions, the component function, and desired reliability.

METHODS OF REMOVING GENERATED HEAT

The methods of controlling thermal effects which have been d in the preceding parts have been concerned principally with the r and delay of heat dissipating requirements. Except for isolated however, these methods do not eliminate the necessity for heat re systems although they may substantially reduce their size.

This section is primarily concerned with the flow of heat fr equipment subsystem and/or components. The succeeding elements i heat flow path to the ultimate sink are of concern only from the point of compatibility and integration problems.

For heat removal considerations, the equipment to be cooled necessarily specifically defined. The equipment may be simply re by a "box" that dissipates heat at a predescribed rate while maint a surface temperature within design limitations.

Convection

The most common expression for convection as offered by Newt simply $q = hA (T_h - T_c)$ where

- q - heat transfer rate, BTU/sec.
- h - heat transfer coefficient, BTU/sec.-ft.^{2} - F°
- T_h - temperature of hot surface or fluid
- T_c - temperature of cold surface or fluid

The simplicity of the above equation is contrasted by the difficul analytically predicting the heat transfer coefficient, h, without reference to a particular combination of surface relationships and properties, and then only after a considerable amount of laborator testing and correlation. The non-dimensional relationships of Nus Reynolds, Stanton, etc., are assembled to allow considerable exten predictable data with limited emperical background. Nevertheless lack of techniques applicable to any conceivable combination of po parameters, the additional unknowns presented by unfamiliar enviro of space and the high degree of reliability required, demands that testing programs be conducted even after the most skillfully devel mathematical analysis.

Convection is here considered to be only forced convection. The fluid may be (1) gaseous, (2) liquid, or (3) both (change of phase). The choice will be dictated by the application in question. In general the decision will tend towards satisfaction of the following considerations:

1. The gaseous transport fluid has distinct advantages: (a) compatibility with the heat transfer surface is easily attainable; high dielectric strength, little or no tendency for chemical reaction, etc., (b) the use of surrounding cabin atmosphere is highly desirable to eliminate contamination and leakage problems, (c) packaging is simplified in that little consideration need be given to minimizing fluid passageways to reduce fluid volume as added weight of gas is very small. The primary disadvantage of gaseous transport fluids is their relatively low values of specific heat and density necessitating high circulation rates and consequently high pumping power unless large temperature differences are allowed.

2. A liquid transport fluid has, in general, the capability of removing relatively large quantities of heat from high concentrated areas. By present standards, and considering existing off-the-shelf equipment, liquids can fulfill practically all heat removal requirements from the thermodynamic standpoint (cold plate). The high density and specific heat qualities of many liquids lend themselves well towards minimization of power and piping penalties. Liquids are generally good to excellent in heat transfer qualities and presents no added problems due to space environment (zero g).

The use of liquids for convection heat transfer presents a number of problems that must be considered in any application: (a) the fluid choice must be a compromise among numerous desirable fluid properties such as boiling and freezing points, thermal conductivity, specific heat, density, viscosity, dielectric strength, etc., (b) storage capability and associated weight penalty, (c) fluid leakage as related to seals and fluid make-up requirements, and (d) special equipment packaging considerations to minimize fluid volume requirements.

3. The change-of-phase (liquid to gas) fluids are attracting more attention as potential solutions to the newly created heat removal problems of micro-miniaturized electronics. The trend towards tight packaging and high heat dissipation per unit volume demands a fluid capable of receiving and transporting large quantities of heat from exceedingly small spaces, and with minimal power requirements. It can be stated that the change-of-phase fluid will take over, from the standpoint of the heat flux density parameter, where liquids begin to falter just as liquids present a progressive step in the area of gas limitations. The primary advantages of 2-phase fluids are (1) high heat hold capacity (latent heat of evaporation) thus reducing flow rates considerably and (2) good heat transfer coefficients especially when nucleate boiling can be accomplished. In addition, fluids meeting temperature and dielectric strength requirements are generally available. The major potential handicap with any multi-phase

fluid is separation and control under zero-g conditions of space travel. Although this presents a serious problem, considerable effort is being expended to overcome these limitations. Many of the disadvantages of liquids are likekise applicable, i.e., storage, leakage, control.

Conduction

Conduction for homogeneous materials is probably the best known and most accurately predictable means of transferring heat. Basically, conduction paths may be divided into two categories; (1) equipment structure and (2) specifically designed conductors.

The equipment structure provides an excellent medium through which heat may be dissipated and exemplifies an ideal dase of integration where a single item is utilized as an aid towards two or more solutions.

In previous paragraphs, several means were described for methods of control of generated heat which included the thermal isolation of certain types of equipment. This is readily accomplished by the use of insulating materials for housing and mounting. For the predominant case however, it will be desirable to incorporate all possible means of heat disposal. This will include such things as thermally conductive component boards, structural mounts and electrical leads. Where additional conductive heat transfer is desirable, conductors may be designed into the package.

Joint Resistance

In the transfer of heat by conduction, the thermal resistance across the mounting surfaces can decrease the overall heat transfer. This decrease in heat transfer becomes particularly important when considering cold-plate mounted components where the small change in heat transfer can cause the junction temperature to operate 10°F higher or more. Some methods of decreasing joint resistance are discussed in Section II.

For cold-plate mounted components, a spacer with high electrical resistance and low thermal resistance is required. Two new methods of decreasing joint resistance have been used:

1) RTV rubber between component, washer, and cold-plate and,

2) Special washer with high dielectric and low thermal resistance.

RTV rubber has been used successfully by Nortronics Division of Northrop Corporation.

North American Aviation, Inc. (Autonetics Division) has instituted a program for the development of dielectric spacer material to increase the ratio of electrical to thermal resistances. A newly developed washer (spacer) material which may be classified as a breakthrough in material development has resulted. It consists of 30% (by weight) of 0.002" diameter glass balls bonded into a single layer solid by Epoxy 907 which constitutes the remaining 70% finished material. This is sandwiched between two layers of 0.020" thick dead-soft aluminum (110 S-0) and bonded to same. As an alternate, a single layer of aluminum may be used; the washer would then be bonded to the electronic element during the packaging phase. The dielectric layer thickness of 2 mils is fixed by the glass ball diameter (state-of-the-art); however, the aluminum thickness is limited only by physical considerations (see Figure 121).

Preliminary tests have been conducted on glass epoxy and comparisons made with other materials (Table 37), including Beryllium oxide (ceramic). The latter is an excellent electrical dielectric while being favorable for thermal conductivity. The major disadvantage of Beryllium oxide, other than brittleness, is its extremely high cost. Its sinclusion in Table 6 signifies its importance and shows it should not be neglected from consideration in the T & A study. Along with the above mentioned glass-epoxy and BeO, the often discussed mica and anodized aluminum are also compared for electrical and thermal resistance. It should be emphasized that these are comparative values only due to the nature of the preliminary tests and are not to be used as absolute values for design purposes.

From the summary of the preliminary test data shown in Table 37, it can be seen that Beryllium oxide is by far the best material although, in addition to extremely high cost, it is quite brittel and requires a form of grease or smear gasket for maximum usefulness. Based on these test results, the glass-epoxy has great promise. As a complete sandwich (between two layers of aluminum), the dead-soft aluminum provides a smear-gasket, with a good thermal bond between the aluminum and glass-epoxy joint. Used with a single sheet of aluminum this epoxy joint is made direct to the heat source or heat sink. More extensive tests of this nature, are planned. This is expected to provide more data on joint resistance in general. Table 38 shows the results of a series of laboratory tests designed to indicate the magnitude of thermal resistance of the materials investigated as compared to mechanical joints with no electrical insulation.

The wide application of joint heat transfer or joint resistance, is described in a later section of this report. It will suffice here to identify its importance with vehicle and component structure, fluid circuitry hardware, especially designed conductors, and all mechanisms

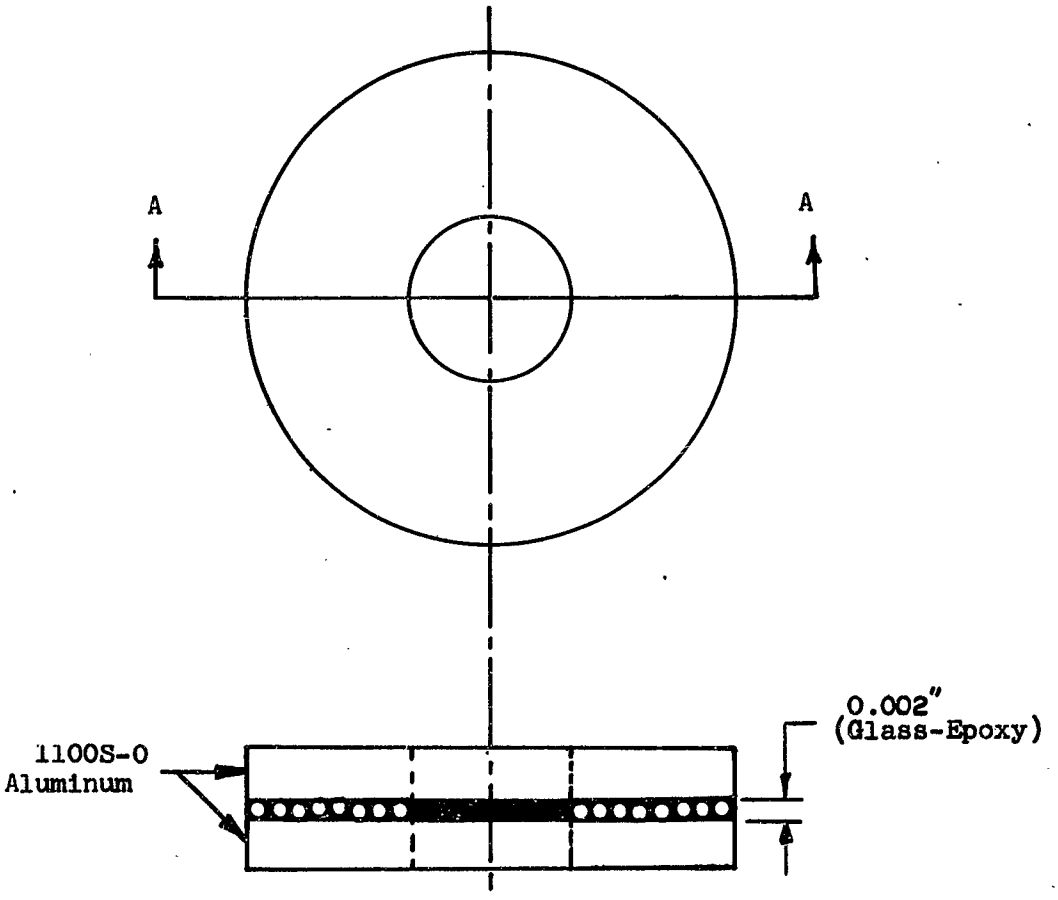

SEC A-A

Figure 121 Electrical Separation Washer Using Glass Balls as Dielectric Material

Table 37

Comparative Thermal and Electrical Resistances of Various Electrical Insulating Materials (Washers)

Resistance	Type of Washer			
	Mica(0.002")	BeO	Glass-Epoxy	Anodized Aluminum
Thermal (°F/watt)	2.61	1.7	1.5	2.6
Electrical (megohms)	150×10^3	$.250 \times 10^4$	150×10^3	Range from $(100\text{-}750) \times 10^3$

Table 38

Effect of Electrical Insulators on Thermal Resistance of Typical Component Mounting Joint (Reference sketch below)

Run No.	Washer "A"	Washer "B"	Temperature Gradient (°F/watt)
1	Bare Al.	(2) Mica (.006)	1.05
2	Bare Al.	None	0.94
3	Mica (.006)	(2) Mica (.006)	2.61
4	Anodized Aluminum	(2) Mica (.006)	2.55
5	None	(2) Mica (.006)	1.17

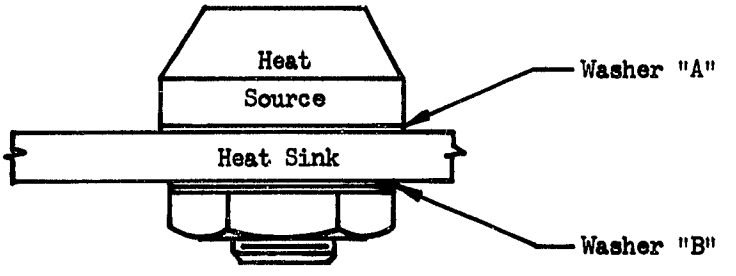

in general regardless of the primary purpose of the equipment. The high degree of reliability and minimization of weight and volume required for space vehicles demands accelerated programs in the field of joint resistance to (1) further improve methods of efficient transfer of heat across joints and (2) produce better predictability of results.

Radiation

Although radiation is almost always present in equipment cooling, the amount of heat transfer by this mode is usually small compared to conduction and forced convection because of the low radiating temperature and temperature differences. One of the exceptions, radiation heat transfer from the skin to the equipment during re-entry is high but can be decreased by use of insulations and reflective foils.

Calculation of radiant heat transfer between equipment is fairly complex but can be simplified by use of radiosity networks as shown in Section VIII and more extensively in Reference 18. For equipment attached directly to the skin, the radiation heat transfer to space as developed in Passive (Section II) and Semi-Passive (Section III) Temperature Control Methods can be used.

Combined Heat Paths

The distinction in methods of heat transfer is made for the purpose of providing evaluation methods. It must be remembered however, that invariably all three basic modes of heat exchange are present simultaneously to some degree. Where temperature differences and/or absolute temperature ranges are small, radiation would be in the beneficial direction providing some small degree of design safety factor while being insignificant relative to inclusion in design calculations. On the other hand, a problem of heat containment such as described before under "Protection From Generated Heat" might require that even this small heat loss be considered. Similarly, a sealed package designed to conduct heat from the individual components to the package housing may find a small convective contribution due to free convective forces of a contained gas or other fluid. Even a mission primarily in zero-g environment will at times be in an acceleration field or a victim of maneuvering, rotational, or other forces.

Combined modes of heat transfer may be purposely integrated into a heat removal loop for optimization considerations. They may operate in parallel or in series with each other or a combination of the two. A typical example of the combined use of conduction and convection with each as primary contributors, is the so-called cold plate.

A cold plate is merely a simple plate-fin-type heat exchanger providing an interchange between conductive and convective paths arranged in series. As shown schematically in Figure 122, heat conducting plates form passageways for fluid flow. The components to be cooled are connected through good heat conducting paths to the plates. The fluid passages may be independently designed for optimum convective heat transfer to the fluid through consideration of flow resistance, extended surface application, choice of fluid, etc.

Basically, the cold plate provides a physical barrier between elements, maintaining a heat flow path with minimum temperature gradient. At the same time it provides means for contamination prevention, pressurization and hermetic sealing, and can serve as a structural member. The coolant and cold plate surface design are specifically selected for optimum heat transfer and power requirements without regard to the nature of the primary equipment to be cooled.

Heat transfer from the component to be cooled to the cold plate surface is likewise independent of the intermediate or ultimate means of heat disposal. Components are thus generally mounted directly on the cold plate which serves as the structural support and mounting plate. This geometric relationship highly favors conductive heat flow from the component. The heat removal aspects of component design are thus greatly simplified for many types of equipment but some complication does arise.

The vacuum tube, still an important piece of electronic equipment by present state-of-the-art, will serve to exemplify the advantages and disadvantages of the cold plate as an aid to heat removal. The geometry of the vacuum tube is generally the same regardless of the package in which it it used. Only the orientation within the package will differ because of the cooling techniques involved. Figure 123 shows schematically, three possibilities for the exchange of heat between the tube and coolant. Figure 123a typifies a standard commercial type installation which will be considered for comparative purposes. Within an enclosed box, a forced gas stream would pass over such components in a random path. The fluid flow characteristics can be specified only at the inlet and outlet connections with an unpredictable flow pattern surrounding each tube, putting severe limitations on the success of analytical solutions. Each change in tube orientation and/or flow passage must be tested to determine the Fanning Friction and Colburn Modulus factors for flow and thermal resistance respectively. Additional complications will result from protective envelopes around the tube such as electronic grounding shields which would restrict air flow from contacting the tube.

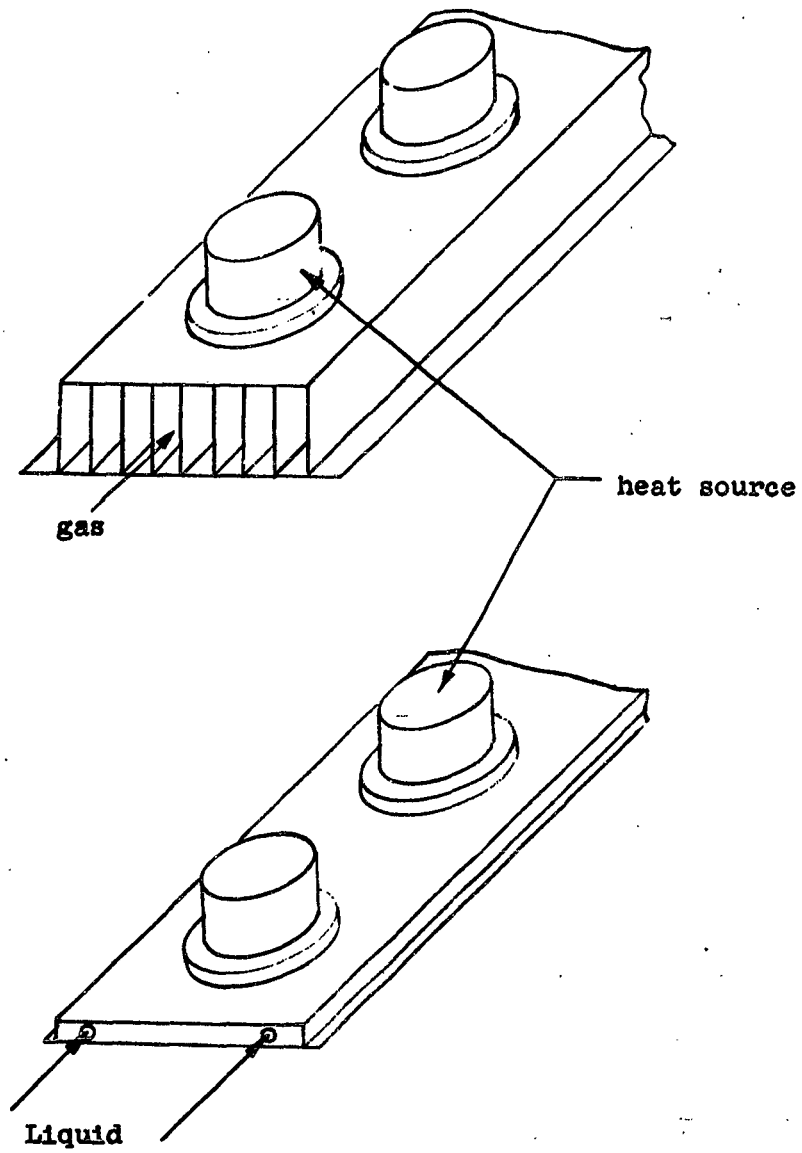

Figure 122 Schematic Diagram of Cold Plate for Gas or Liquid Transport Fluid

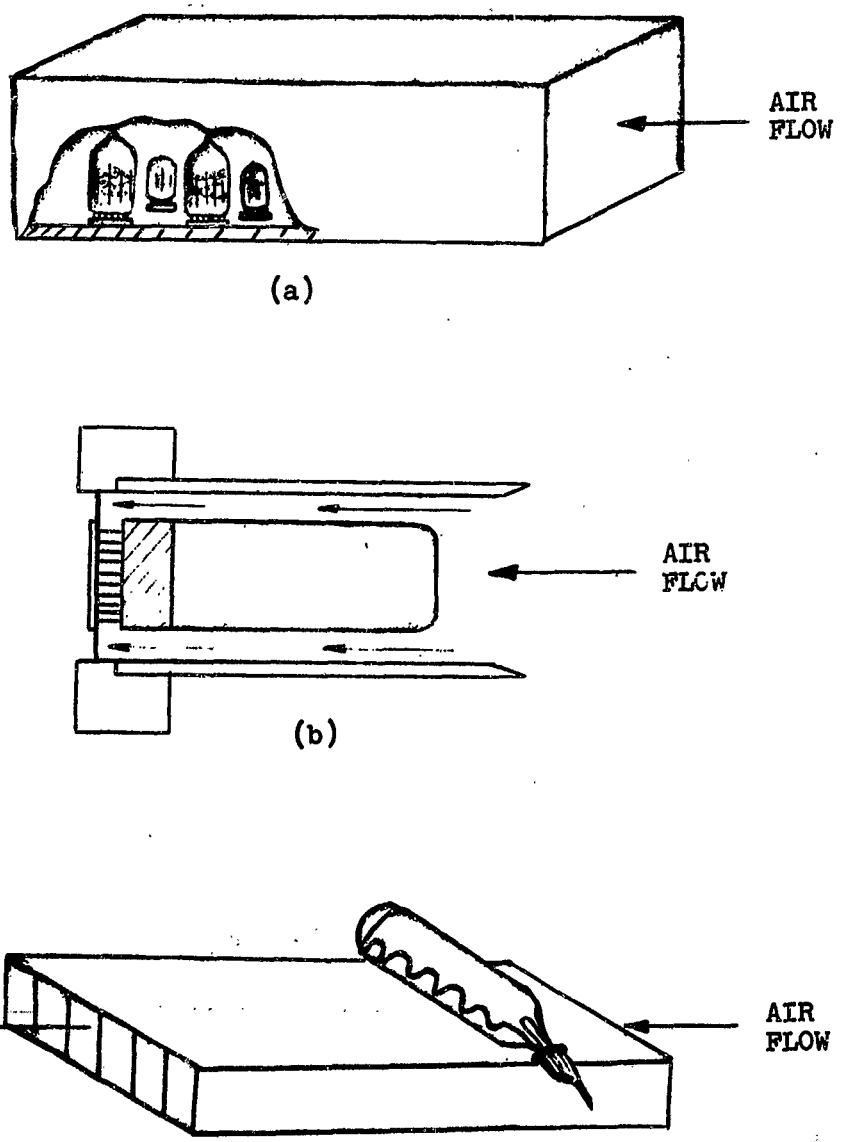

Figure 123 Schematic Showing Three Fluid Flow Arrangements for Vacuum Tube Cooling

A more realistic approach to direct air cooling of the vacuum tube is the use of chimney cooling as shown in Figure 123b. Here an attempt is made to control the airflow, and therefore the heat transfer characteristics, by properly selecting flow and sizing the annular space, or chimney, surrounding the tube. Not only is heat removal better predicted quantitatively, but control is more precise in obtaining the desired tube envelope temperature.

Another method of temperature control for the vacuum tube is utilization of the cold plate as described above (see Figure 123c). Probably the greatest single advantage of cold plate design as applied here is the physical separation of coolant and heat generating device allowing (1) use of the best fluid as selected by consideration of all portions of the thermal exchange system and (2) the ability to design for optimum heat trransfer to and from the cold plate independently. The additional benefits relative to mounting, structural integration, etc., also hold true for this example. However, close attention must be given to the physical design of the system to assure maximum conductance between tube and plate.

The mandatory consideration of maximum vehicle reliability dictates in flight component replacement capabilities. In the case of the vacuum tube-cold plate assembly under consideration, this requirement is satisfied by a spring-clip arrangement as shown in Figure 123c. Optimization of the clip material, material thickness and width relative to weight addition and heat conduction is routine provided a method has been devised to evaluate the joint resistance between tube and clip and between clip and cold plate. As outline previously, the surface has barely been scratched in this area, an all important "missing link" in heat transfer.

Thermoelectric Cooling

The reader is directed to Section IV of this report for a discussion of Peltier cooling, its current state-of-the-art, and future potential. It is significant, however, to indicate here that recent developments in the construction of thermoelectric coolers have resulted in improved units suitable for use in electronic equipment. One of the more promising uses of thermoelectrics, even in its present state of development, is in the area of spot cooling.

Spot Cooling

Spot cooling pertains to the cooling of temperature-limiting components parts located within local areas of an electronic package. By cooling the local areas containing temperature-limiting components, the equipment cooling requirements can be reduced or contrariwise, customary convection, conduction,

or radiation cooled equipment can be operated in higher temperature environments when local problems are handled by thermoelectric heat removal. Since thermal reversal of thermoelectric element is simply a matter of current reversal, the spot cooler can be used alternately as a heater and cooler, thereby providing heat input as required locally and might be applied in addition to temperature control.

An investigation of thermoelectric spot cooling in electronic equipment is presented in Reference 76 where the following conclusions were reached.

1. The spot cooler can efficiently pump 5 watts wover a 30°C temperature difference. The COP is 0.6 for this condition.

2. The spot cooler can maintain a 46°C temperature difference under no-heat-load conditions.

3. The use of spot cooling can increase the operational temperature environment of self-cooled equipment.

4. Spot cooling can reduce the cooling requirements of remotely-cooled equipment or eliminate the need for remote cooling.

5. The largest benefits from spot cooling can be obtained in applications where the limiting components dissipate a small portion of the equipment heat.

DEVELOPING COMPONENTS FOR HIGHER OPERATING TEMPERATURES

Importance of Development

The development of high temperature equipment for space vehicles will provide many advantages that would otherwise be lost with low temperature conventional equipment. Since a stored heat sink will be heavy and impractical for long duration missions, radiation will be the primary mode of heat transfer in space. The fourth power law in the radiation heat transfer equation dictates that the higher the operating temperature, the higher the net heat transferred. In other words, the higher the operating temperature, the lower the radiator area required for a specified heat load.

Electrical Equipment

The need for increasing temperature capabilities of airborne and first generation space vehicle electrical, electronic, and mechanical equipment has been constant. In response to this need the maximum temperature capabilities of this equipment have increased in recent years and will increase significantly in the next few years to meet the requirements of future generations of space vehicles.

One of the most significant areas where work has been conducted to develop higher temperature capabilities has been with electric generation and distribution equipment. Much of this work is described in References 64 and 65. This referenced work was accomplished under an Air Force sponsored program which has become known as Project Hotelec. The major purpose of this project was to develop airborne electric generation and distribution components capable fof operating successfully in a 600°F ambient environment. The system under development is a basic 115/200 volt, 400 cycle 3 phase alternating current system. It is built around a 40 KVA generator with all other components aimed at operating from this type generation system. As shown in Figure 124 all major components are included. Generation equipment consists of generator, voltage regulator, paralleling equipment, protective panel, constant speed drive and transformer rectifier. Wire, contactor, fuses, and circuit breakers were to be developed as being representative of distribution equipment. Motors were also included.

Progress made in the past fifteen years in the development of equipment to operate at higher temperature levels is indicated on Figure 125. An extrapolation of the state-of-the-art indicates the future trend based on past results. This figure also shows the accelerated developments intended for the Hotelec program.

The program consists of three major areas pertaining to development of equipment and materials as follows:

(1) Materials

(2) Subcomponents

(3) Major Component Design

There is no clear distinction made between what is classified as a material and what is classified as a component of sub-component. However, for the following discussion, insulation, conductors, and magnetic steel will be the materials; resistors, capacitors, transformers, rectifiers, tubes, and magnetic amplifiers will be the sub-components; generators, motors, wire, circuit breakers, terminals, etc., will be major components.

Materials

(a) Electrical Insulation

In equipment designed to operate in a 600°F ambient, insulation will include both inorganic and organic materials but the majority of insulation applications require the higher temperature capacility of inorganic materials. In the temperature region from 600 to 700°F certain

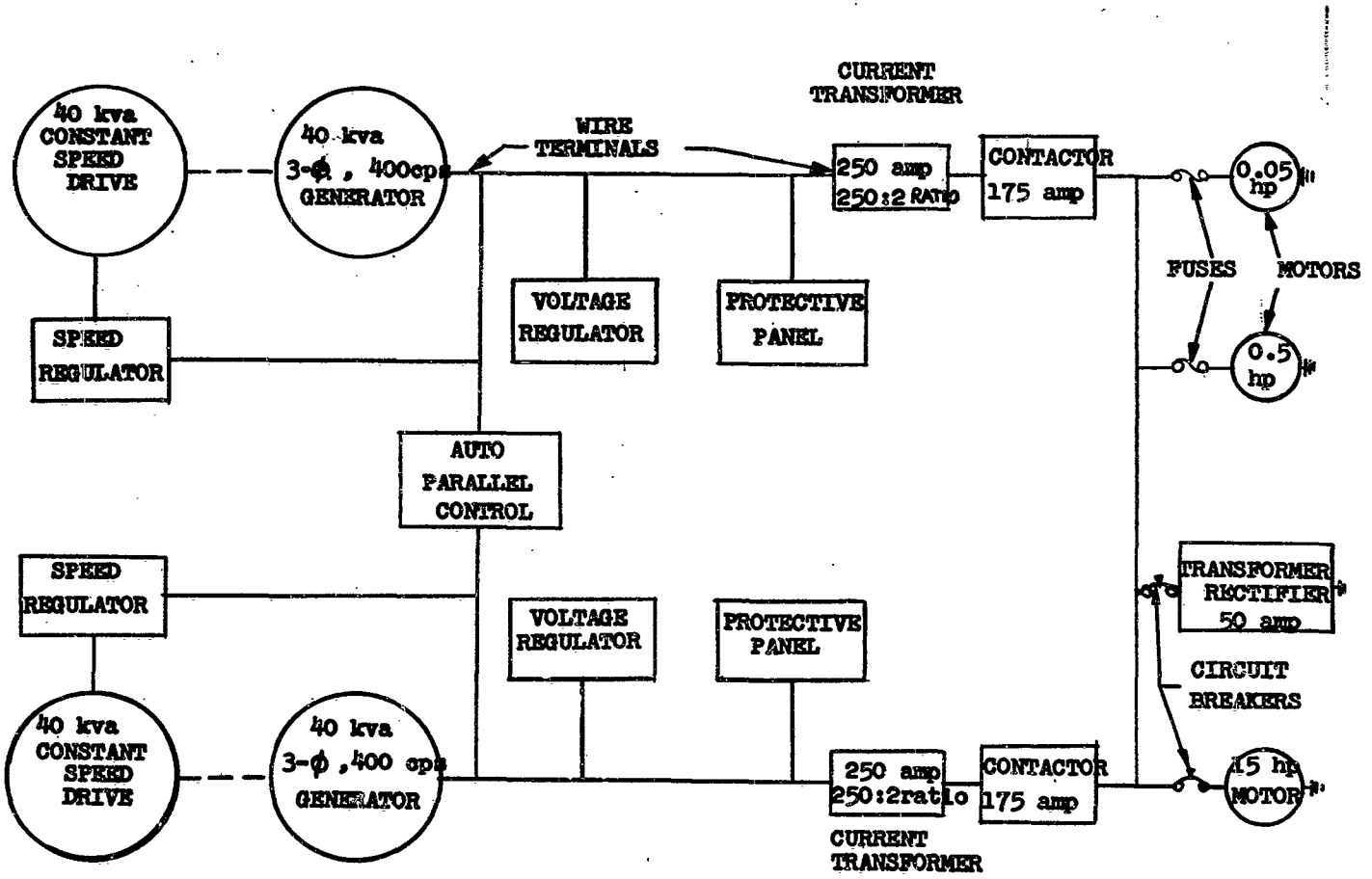

Figure 124 Basic Parallel Electrical System

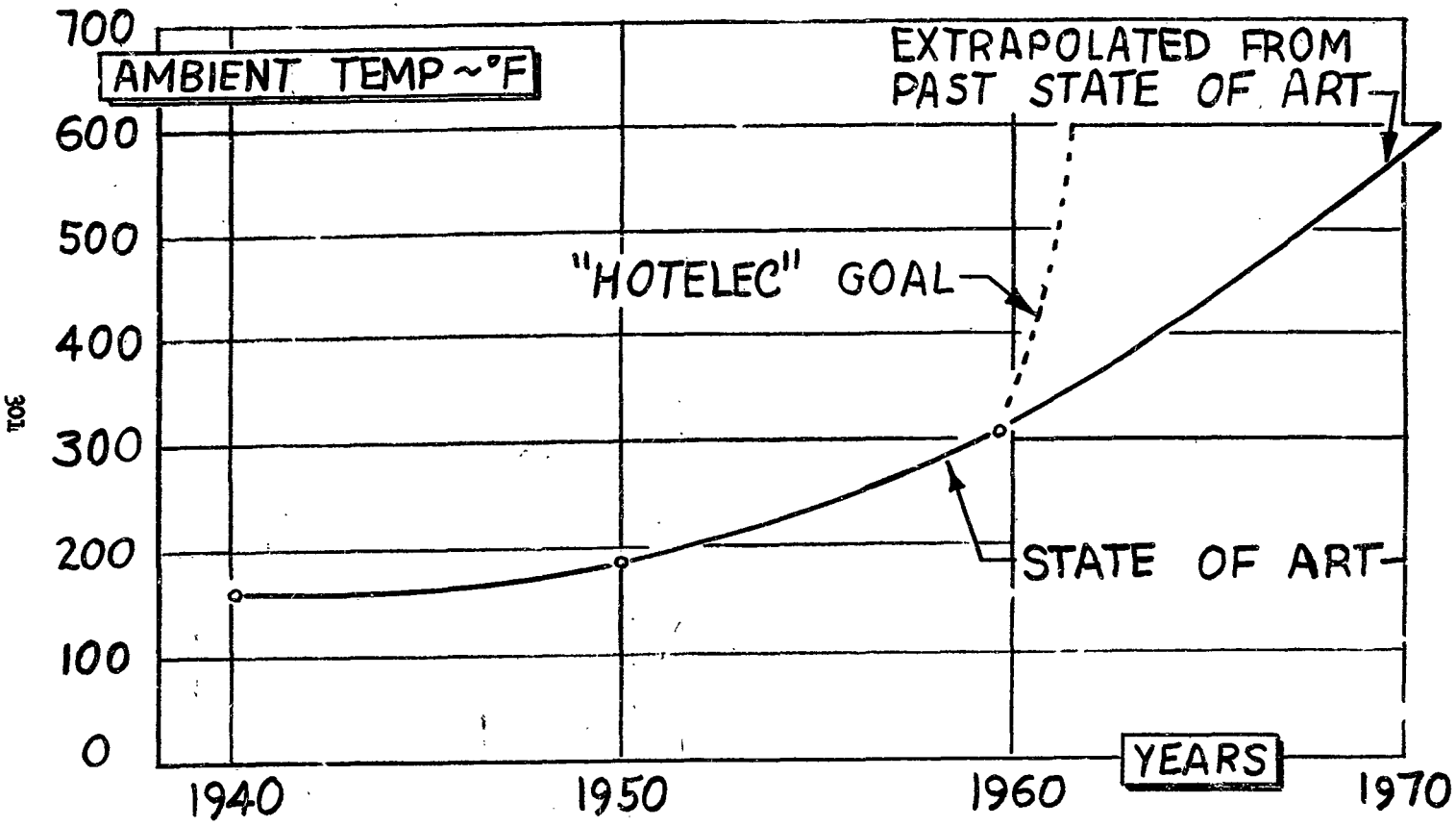

Figure 125 State of Art of Electric Generation and Distribution Equipment

applications can utilize the more conventional resins and polymers such as silicones and teflons. Above this temperature range inorganic materials are required. Most applications in the Hotelec program have fallen in the inorganic range.

Silicone and teflon insulations have been found to be capable of withstanding higher temperatures for longer periods of time than common knowledge indicates. For example, polytetrofluorethylene has been repeatedly and successfully tested for periods of time up to 500 hours at temperatures of 650°F without significant degradation of the material. The condition of the material after test indicates that considerably longer life can be expected. Softening of the material does occur at these temperatures and mechanical stress must be avoided, particularly cut through type stress. Similarly certain silicone resins are capable of at least 500 hour life at 600°F. Higher temperature capability results if the resins are highly filled with inorganic materials, particularly with the solventless type silicone resins. In general, these type materials have found limited but useful applications in the components being developed.

The inorganic materials are usually required to meet the hot spot temperatures up to 1000°F found in power requipment designs. In organic insulations, the field is narrowed to a relatively few choices by a combination of mechanical and electrical requirements. The materials most generally used and found useful in this temperature range from 700 to 1000°F are Mica, glass, quartz, alumina, refractories such as magnesium oxide or zirconium oxide, mixtures of the above in the form of cements and to a limited extent asbestos.

Two important deficiencies of inorganic insulation have become evident. One is lack of resiliency; the other is porosity, which makes moisture proofing difficult. The lack of resiliency in inorganics requires that very special attention be devoted to prevent cracking of insulation under mechanical or thermal stresses. Particular attention must be paid to matching thermal coefficients of insulator and insulated elements and to special mechanical designs that take into account the limited tensile strength of the insulations. These problems are not so severe for fixed applications, such as motors, generators and transformers, where lack of flexibility and porosity can be designed around. Flexible, moisture proof, insulated wire capable of withstanding 1000°F without a metal jacket is one the most difficult insulation problems.

(b) Conductors

Only two practical conductors have evolved for the applications being considered; silver and copper. While silver is in many respects an ideal conductor for high temperature its high cost and high density make

it undesirable where large quantities are required. Although copper has a severe oxidation problem in the temperature range of 600 to 1000°F it has been generally adopted. Much time and effort has been devoted to establishing the best method of protecting the copper against oxidation with minimum increase in resistivity. The performance of several protected copper conductors are shown on Figures 126 and 127. It should be noted that the curve shown for 10 percent nickel coating is only applicable to the most perfect platings of the non-porous type.

(c) Magnetic Steel

In general the magnetic steels currently in use are only slightly affected at the elevated temperatures. The silicon and coblat steels will fins wind application at high temperature. The effects of temperatures are small, especially in the region of ordinary design, which, fortunately, is near the cross over point in the B-H curves, just below saturation. Temperature will probably cause less than a 5 percent change in flux density for a given magnetizing force. Nickel-iron magnetic materials generally have low Curie temperatures and are considerably more affected by temperature. They are usually not usable in the temperature range above 600°F. This is particularly unfortunate for saturable reactor designs which ordinarily utilize these materials. However, some of the newest cobalt-vanadium iron magnetic materials demonstrate equally good or better square loop characteristics and will supplant the iron-nickel alloys in high temperature design.

Electrical Subcomponents

Nearly all of the complete spectrum of electrical sub-components are needed to construct an electrical generation and distribution system. Resistors, capacitors, transformers, voltage reference tubes, magnetic amplifiers, vacuum tubes and many others are needed and considerable time in this program has been devoted to the developing, constructing and testing of high temperature versions of these fundamental electrical building blocks.

(a) Resistors, Capacitors and Transformers

These three fundamental subcomponents are well along in the high temperature development cycle. Considerable work has been done on them prior to this program under various military and private development programs and their performance is generally satisfactory for their intended usage. This is shown graphically for resistors in Figure 128 in which the important parameters are plotted against temperature. However, in each area further development is highly desirable to minimize the effect of temperature and bring about reduction in size.

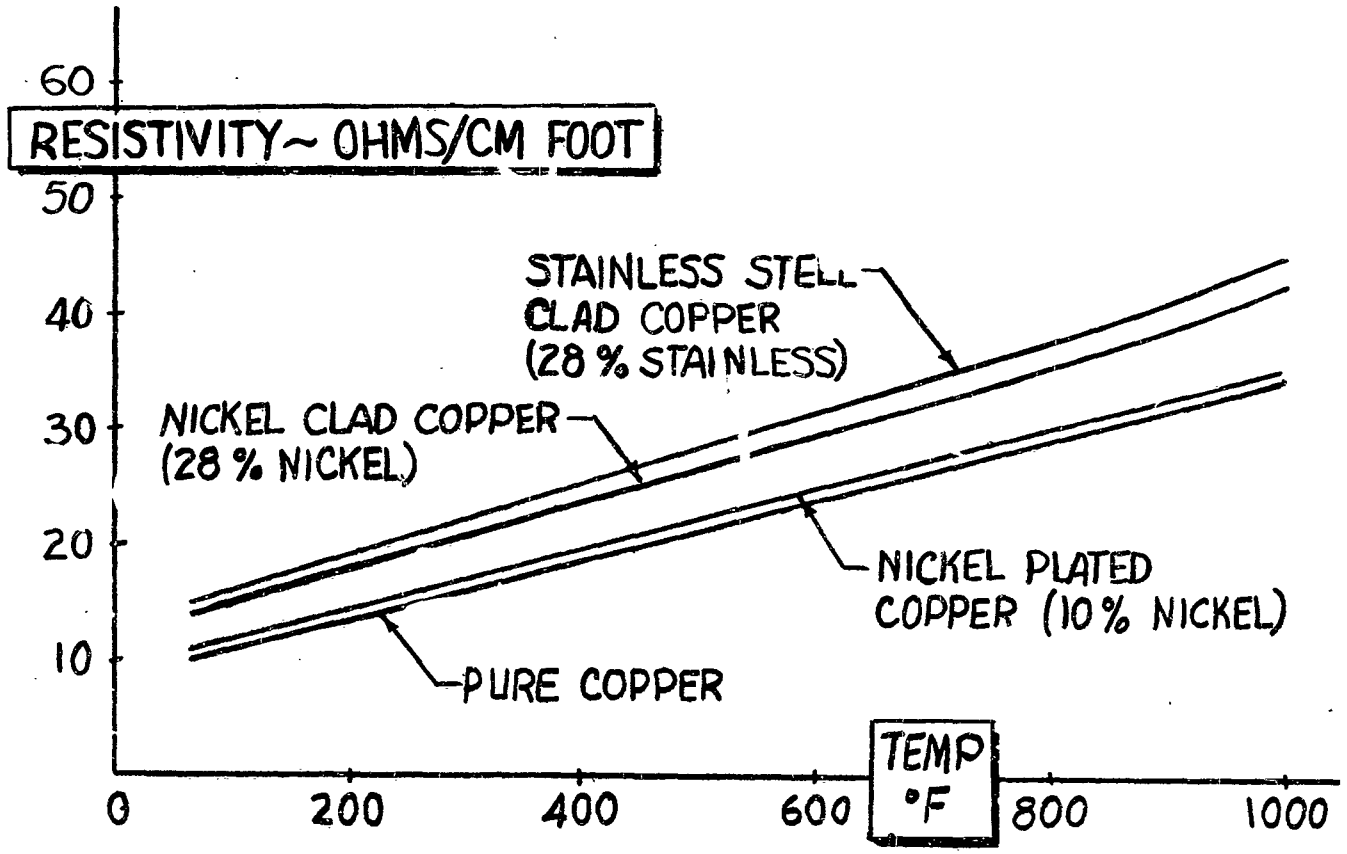

Figure 126 Conductors - Resistivity vs Temperature

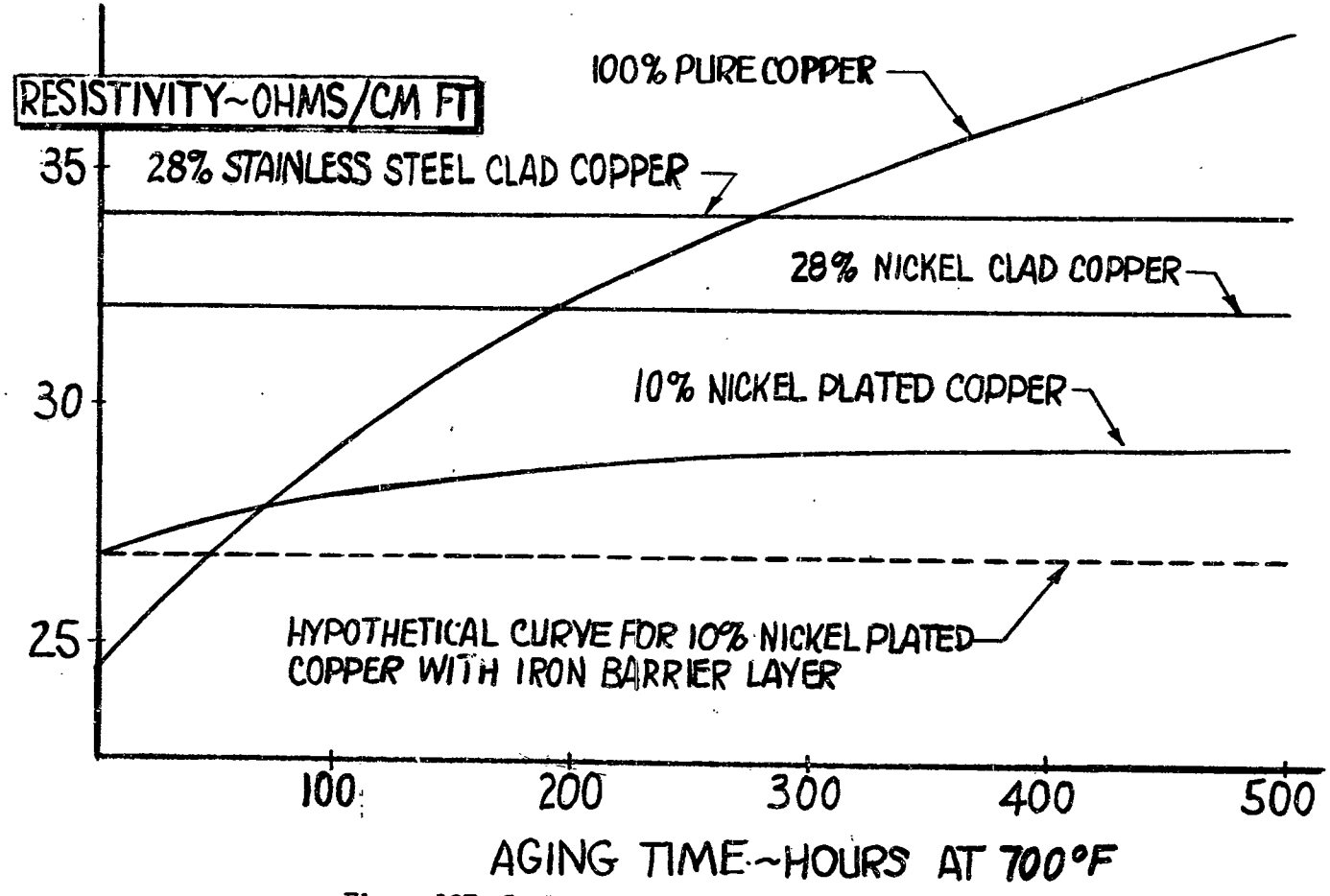

Figure 127 Conductors - Resistivity vs. Aging Time

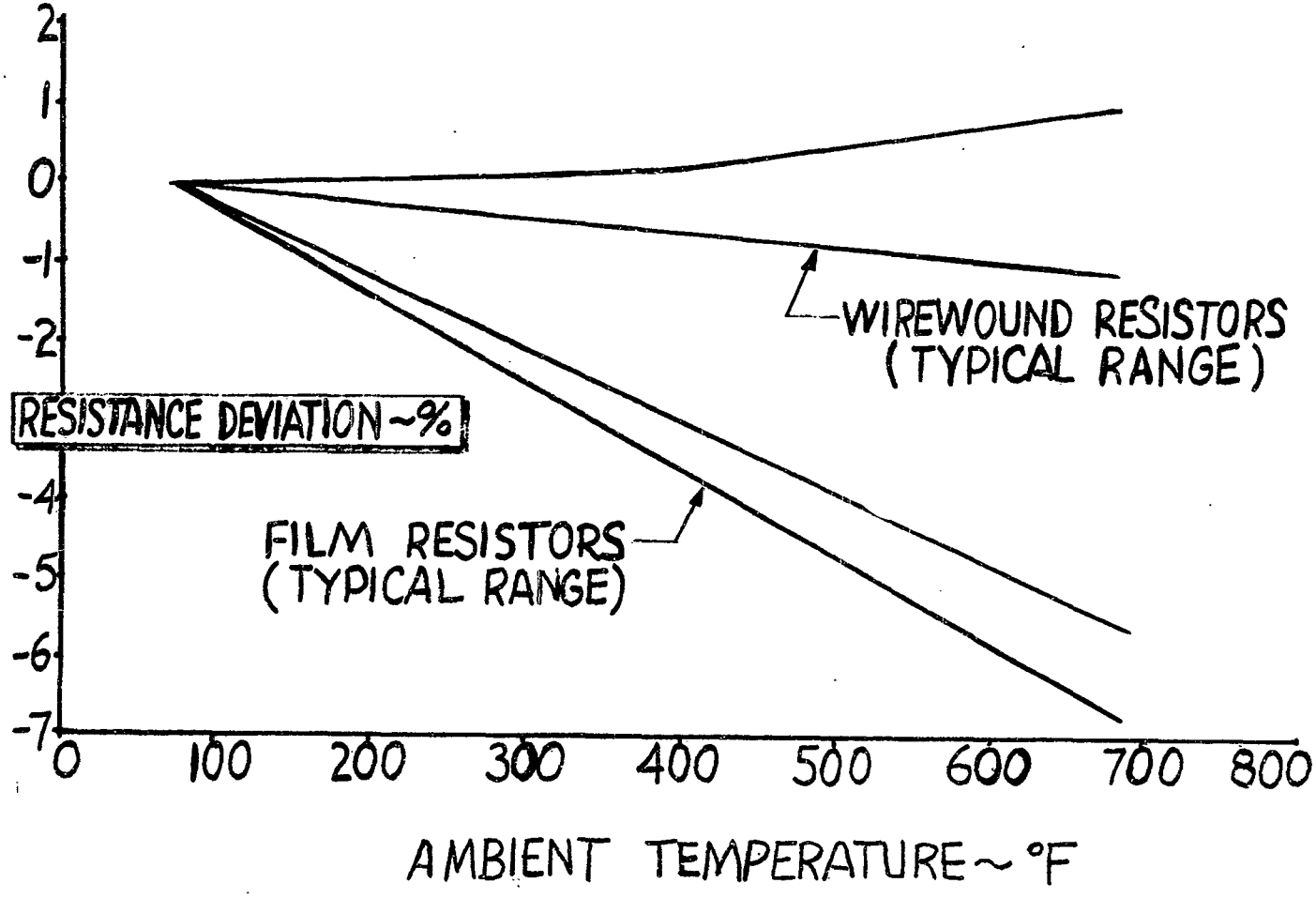

Figure 128 Resistor Operating Characteristics

Two types of resistors are available for use at high temperature: wire wound and film types. Of these two, the film types are more compact although less accurate. They will generally be utilized in applications of low wattage (under 2 watts) in which a temperature effect of less than 5 percent is not required. They are especially well adapted to very high resistance areas in which the wire wound types become very bulky. Wire wound types will be utilized to meet the requirements of high accuracy and high power.

High temperature capacitors are available from several sources which utilize mica as the dielectric material. These units have very usable performance over a temperature range from 200 to 450°F. Approximately a five percent change in capacitance can be expected over the temperature range and the megohm-microfarad product will decrease to a range of 0.1 to 1 at the upper temperature extreme of 842°F (450°C). This type of capacitor is characterized by a large volume; ten to fifteen cubic inch per microfarad. This is considerably larger than low temperature types available and certainly an undesirable penalty.

The most important transformer problem is the mechanical one of reducing size and weight. Transformers are available which have been operated successfully for 1000 hours at 1000°F. However, all currently available transformers depend on a sealed metal can to provide moisture protection and mechanical strength. These types are suitable for the specific programs under consideration but as an area of future improvement an open type design of lighter weight construction would be desirable. The major problem is finding a suitable impregnating and potting compound which is capable of withstanding mechanical and thermal stresses and of preventing the entrance of moisture at lower temperatures.

Reference 77 is a report on the Air Force WADC sponsored work to develop electronic power transformers capable of operation in a 500°C ambient temperature and in intense nuclear radiation (10^{11} fast neutrons/cm^2/sec and 10^{12} gamma protons/cm^2/sec.). Initial work involved evaluations of basic materials and combinations of materials in transformers, and development of ceramic processes and supporting members. The use of ceramics as encapsulating material was found to be rather limited because of their inability to resist moisture. Later work included studies of transformer operation in air up to 500°C and in a radiation environment. The breakdown potential of air was found to be significantly affected by high temperature. The chief effect of the radiation environment was to create an extra internal source of heat, thus increasing the temperature rise. Material development studies revealed that aluminum phosphate solution could be useful as a coil impregnant to impart strength to insulations. Also included in this work were weight reduction studies on standard hermetic construction designs and design optimization studies.

(b) Rectifiers

Rectifiers capable of operating in a 600°F ambient are definitely feasible in the form of gas rectifiers. However, as at low temperature, gas rectifiers represent large bulky components undesirable in airborne equipment. In addition, they are relatively inefficient because of heater power requirements and high forward voltage drop. Again, as at lower temperatures, semiconductor rectifiers would be advantageous if high temperature versions retain the desirable features of small size, low forward voltage drop, and high efficiency.

(c) Generator System

This system includes the generator, voltage regulator, protection panel and reactive load division circuits for parallel operation. The generator design is new and unique. It is called the "Inductor-Lundell" design and features a rotor that does not require windings. The flux is generated on the stator, hence eliminating the need for electrical current flow on the rotor and with it, the need for slip rings or rotating rectifiers. This windingless motor has distinct advantages for high speed operation and increased reliability at high temperature. Excellent rotor balance can be achieved and the normal high stress on rotor windings and insulation is eliminated. Rotor cooling problems are also eliminated. Three developmental versions of this generator design have been constructed utilizing class H insulations. Operation of these machines have verified design calculations and proven feasibility.

(d) Motors

Three sizes of motors are being developed: a small 0.05 hp, a medium sized 0.5 hp, and large 15 hp. All are of the induction type. High temperature breadboard versions of these have been constructed and successfully operated to demonstrate feasibility of the design. Prototype units are being constructed for complete qualification testing. The most difficult development area has been that of bearings. The .05 and 15 hp motors utilize ball bearings while the 0.5 hp which operates with highest bearing temperatures utilizes a journal bearing.

(e) Wire

Three types of wire are being developed:

(1) Type I -600°F ambient, 650° conductor
(2) Type II -600°F ambient, 600° conductor
(3) Type III -850°F ambient, 1000° conductor

Reference 78 concerns an experimental study made of the dielectric properties of ceramic materials and the fabrication of these materials into a form and substance suitable for capacitor dielectrics and wire insulation. Both commercial and laboratory prepared ceramic specimens were evaluated at 500°C for dielectric constant, dissipation factor, resistivity dielectric strength and aging effects. A "slurry" (combination of a ceramic and an inorganic binder) containing AL_2O_3 with mono-aluminum phosphate and additions of Nalcoag showed the most promise both for capacitors and wire.

(f) Circuit Breakers

A magnetic trip design with toggle type actuator was chosen for development under the HOTELEC Project. The unit possessed the design feature of an all hermetic sealed case. The terminals are sealed by metal seals to the case and the toggle is sealed by a small bellows arrangement. The major development area concerns the design of a time delay element.

(g) Terminals

Terminals capable of matching the 1000°F maximum conductor temperature are also under development. One new concept is called the "washer" type; another is an insulated post type. In both cases potential problems with high voltage drop across the crimp and bolted joints have been avoided by the use of special platings and optimum crimps.

The development of electronic components for utilization in space vehicles depends on the ingenuity of the components designer and the availability and development of new materials which exhibit the required physical or chemical characteristics. In a very real sense electronic and other equipments must operate in new environment.

In many locations on a space vehicle it will not be possible to afford the construction of regions of optimum local environment. Regions of relief from high temperature, high vacuum, and other effects will be obtainable only at great expense to the mission.

Electronic Equipment

An electronic component which has been developed for ultra high temperature operation, radiation tolerance, mechanical ruggedness, and is microminiature in size is the thermionic integrated micromodule (TIMM) unit. By utilizing radical approaches to materials, processing, joining, and circuit design these units have been fabricated to operate at 580°C.

At the heart of the TIMM's system is a heaterless ceramic vacuum tube in which cathode emission is developed by the high operating temperature. For operation in the same high temperature environment, resistors, capacitors, and inductors with similar ceramic structures have been developed. All of these components are assembled and sealed with interconnections into a monolithic stacked structure which serves a single electronic function.

It has been stated that the advantages of the TIMM's units are as follows:

(1) A large number of tubes and components can be joined together to form strong structures with a minimum number of interconnections.

(2) A very high component density is possible. In a thermally insulated enclosure, the densely packed components contribute their heat losses to sustain the operating temperature.

(3) Operating at a controlled high temperature, the components of the TIMM system require less temperature compensation and can operate with larger temperature coefficients.

(4) A built in bias eliminates the need for external bias voltages or cathode bias resistors and also makes possible direct coupling between circuits.

(5) All of the materials in the TIMM circuit are radiation tolerant and operate at a high level of thermal excitation.

Several types of circuits have been investigated which utilize the inherent characteristics of the TIMM units as follows:

(1) Nor
(2) Flip-Flop
(3) Clock
(4) Delay Line Driver
Delay Line Receiver
(5) Temperature Controller

The various uses of the TIMM components for the above listed circuits and systems are described in Reference 65.

Electronic Materials

The importance of electronic materials in the development of electronic components for operation at higher temperature levels cannot be overemphasized, and major breakthroughs in research will be required

to furnish the building blocks of future electronic components. Reference 79 summarizes some of the materials research for electronic components and a summary chart of this data is shown in Table 39. Materials considered here are for use above 200°C and are limited to magnetic, ferroelectric, dielectric and insulating, conductor, semi-conductor and a few miscellaneous materials.

While electronic design is concerned with many products which are sensitive to the properties of their thermal environment and constituent materials, no area is currently as sensitive to these parameters as the solid state field and semi-conductor devices in particular (Reference 80).

Semi-conductor devices are very sensitive to temperature change. An example of the temperature effects for one device, a silicon strain gage, may be seen in Figure 129 from Reference 81. Temperature effects on resistance values of unbonded units and on gage factors for units bonded to 17-4PH steel are shown. Although the semi-conductor strain gages show great potential, they presently use compensating electrical bridge networks to overcome the temperature sensitivity of the materials utilized.

Reference 82 described two main sources of material problems as follows:

(1) "Functional Multiplicity" arises when a material is expected to perform two or more functions.

(2) "Qualitative Multiplicity" arises when two or more materials must stand in proximity or in contact with one another.

Problems in qualitative multiplicity are seldom found alone, but are usually linked with the problems of functional multiplicity.

Problems arise in functional multiplicity when there is, for example, a high ambient temperature and an imposed maximum weight limitation. A solution to the problem will require a detailed knowledge of strength-weight ratios and thermal conductivities as functional of temperature for the various materials which appear to be applicable.

Problems arise in qualitative multiplicity where, for example, ease of bonding, low electrical resistance and high mechanical reliability stand coequal (i.e., a soldered connection). In general solutions to problems arising from qualitative multiplcity are more difficult to come by, but an approach as described in Reference 82 called microanalogy is a help.

Tubes

Included in this category are small vacuum diodes and triodes, small gas diodes and voltage reference tubes. Vacuum tubes capable of

Table 39

Electronic Component Materials Temperatures

Material Type	Temperature Levels			Remarks
	Investigation Level °C	Operating Level °C	Usable Max °C	
Alnico 5	800	250 to 650	700	20% Loss in Total Energy in Magnets at 700°C
Barrium Ferrite	450	-40 to 250	250	Coersivity is good (H_c -2500 at Room Temp. Coersteds)
Ferro Electric Materials				
Lead Titanate	490	-60 to 250	250	Curie Temp. 220 to 490°C Freq. Dependent up to 250°C
Lead Meta-Niobate	+250°C		+250°C	
Dielectric and Insulating Materials				
Lead Barium-Titanate		-65		25 to 50% variation in dielectric constant at range indicated
Silicon Monoxide			200	Used on Substratun of nicket-iron as a capacitor
	300		200	With Aluminum foil substrates

TABLE 39 (cont'd)

Material Type	Temperature Levels			Remarks
	Investigation Level °C	Operating Level °C	Usable Max °C	
Teflon			200	As a dielectric for capacitors
Zirconium Dioxide (ZrO_2)			500	Substrate of Aluminum
Beryllium Oxide (BeO)				Being investigated
Magnesium Oxide (MgO)				Being investigated
Mica		340 to 370		Bonded to Glass
Fluor-Phlogopite		420 to 480		
Conductor Materials				
Chromium & Titanium			250	Good stability
Nitrides, Borides, Silicides, Carbides, Transition Metals in Groups III, IV, and V	250			Resistivity Spectrum 10^{-5} to 10^{-1} Ohms-con.
Chromium Silicide	300			With additives

TABLE 39 (cont'd)

Material Type	Temperature Levels			Remarks
	Investigation Level °C	Operating Level °C	Usable Max °C	
Molybdenum & Tantalum		250 to 300		
Noble Metals	500			Oxide Films for Resistors
Copper Alloys		-65 to 600		Conductive Wire 16 to 40 AWG 1000 hrs at 600°C
Semi-Conductor Materials				
Silicon		-65 to 200	300	Short Time Operation at 300°C
Germanium		-65 to 100	125	Short Time Operation at 125°C
Indium Phosphide	300 to 400			Temp. Investigation Above Silicon Temp. Level
Gallium Arsenide				
Silicon Carbide				
Diamond				Investigated as semi-conductor
Miscellaneous Materials				
Ceramics and Inorganic Powders	300°C +			Potting Compounds
Silicon Rubber			300	Electronic Component Projection

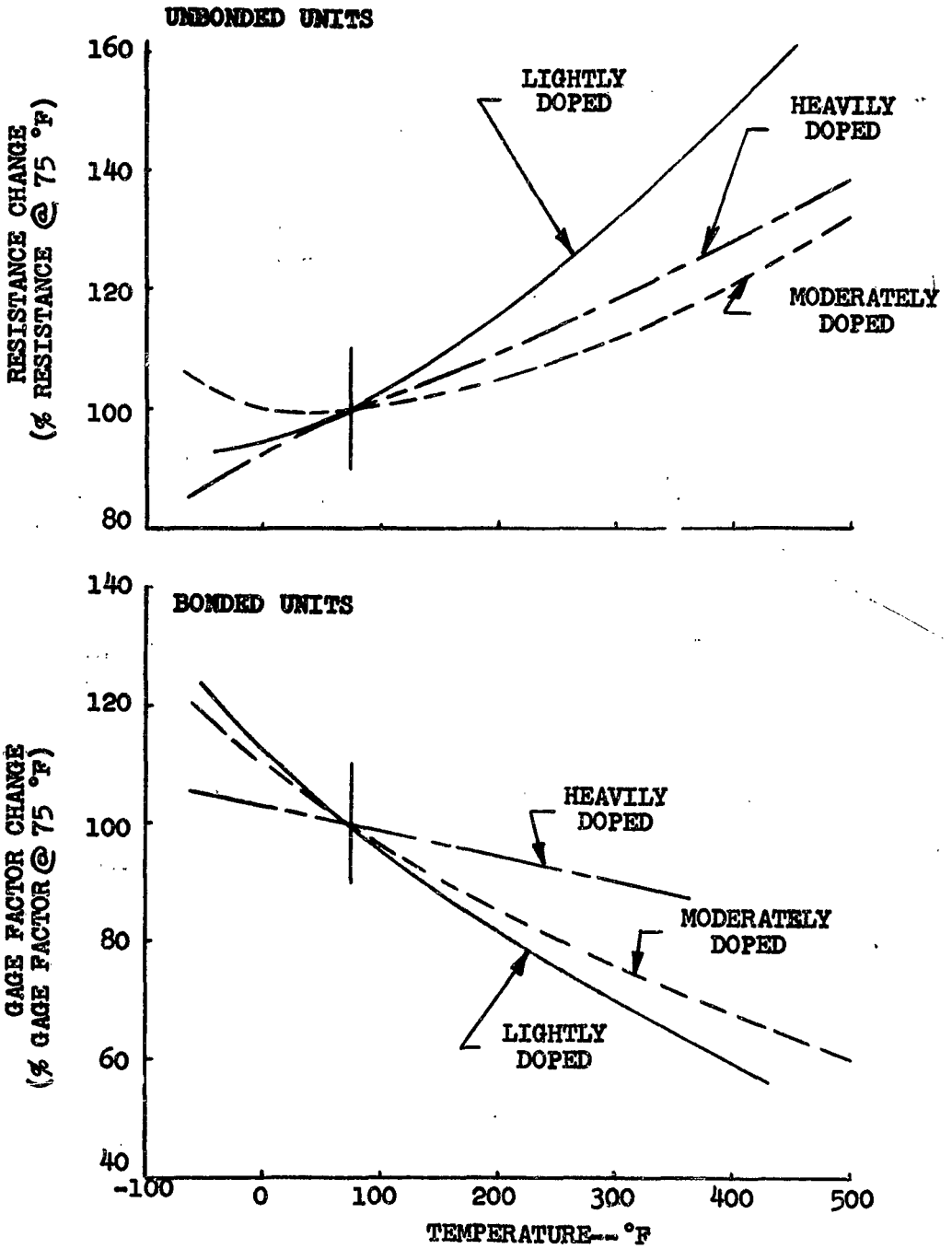

Figure 129 Semiconductor Temperature Sensitivity

operating up to at least 650°F ambient are readily available from several sources. Typical types have been operated for 500 hours and longer at 650°F with success.

The tubes most widely used in this program have been of a planar construction. This stacked construction utilize ceramic "washers" to separate the tube elements with seals at each junction between ceramic and metal. A very rugged construction results. The next section of this chapter discussed the development of this type of "stacked disk" unit which is known as the TIMM's unit.

One of the most important developments of this program is the construction of a saturable reactor which when coupled with high temperature rectifiers and other high temperature components will form a magnetic amplifier. While there are many difficult portions of this development, the key area is obtaining and packaging a magnetic material with the proper characteristics over the temperature range. The nickel-iron alloys generally utilized are not satisfactory because of significant temperature effects on characteristics which are primarily due to relatively low Curie temperatures. One of the most satisfactory materials appears to be a cobalt-iron alloy which demonstrates excellent square loop characteristics, high flux densities and high Curie temperatures. Major problems are in obtaining consistent material parameters from developmental batches of material and in proper packaging of cores to protect against mechanical stress and thermal effects.

Mechanical Equipment

Hydraulic and Pneumatic Components

High temperature problems are expected to continue in the areas of hydraulic and pneumatic system design for the next several years until more is known about the space environment. In the period during which operational hardware will be developed for the B-70, the supersonic transports, and the Dyna-Soar many problems will be solved. Nuclear radiation effects will increase in importance over the coming years because of progress on spacecraft secondary power systems more than as a result of the development of nuclear-powered aircraft. Designers of components connecting with or on the outer surface of space vehicles will have to deal with the unique problems of the space environment, which combines high levels of cosmic, solar and X-radiation and electromagnetic and gravitational fields with an ultra-high vacuum.

The vacuum (10^{-12} mm Hg at 760 miles) will probably be a more important factor than temperature considering externally mounted equipment in the space environment, and will influence the effects of all the other factors.

Current hydraulic systems are limited by component availability to a maximum operating temperature of 400°F (X-15 airplane system). The B-58 system operates just below that level; the hydraulics for the B-70 and supersonic transport will run between 400 and 700°F; and the Dyna-Soar's requirements will range basically from 700 to 1200°F, with excursions to 1500°F.

One company is working on a Phase II Air Force contract for a 1000°F hydraulic system. The Phase I contract, covering the selection of a fluid, ending with the choice of a polyphenyl ether. It has been reported that NaK-77 liquid sodium-potassium alloy was rejected because of handling dangers, very poor lubricating qualities, and great corrosiveness, among other drawbacks (Reference 6).

Under development are axial-piston, variable-displacement type pumps which will operate with a 700°F inlet temperature and 600°F ambient. Data have been obtained which indicate that good results have been obtained with MLO 7243, a dewaxed mineral oil, at inlet temperatures up to 600°F. The low temperature limit of the fluid is around 20°F. Among MLO 7243's other properties are excellent lubricating qualities, lack of toxicity, and good radiation resistance.

Other components under development in the 1000°F program are servo, relief, and check valves, actuators, seals and fittings. Not even reservoirs are available off-the-shelf for this temperature. Servo valves and actuators, located close to control surfaces for design reasons, will be subjected to severe thermal conditions. They will have to withstand ambient temperatures as high as 1500°F. Dynamic seals are a major problem. Possibly two-stage seals will be used in which the inner seal acts as a controlled leak and the outer seal works against a greatly reduced pressure.

It has been predicted that the hydraulics systems of space vehicles will be more complicated than present systems not only because of the high temperatures (produced by aerodynamic heating on reentry) but also because of a greater demand for flight control power and for reliability.

The profusion of hydraulic systems (and especially of pumps) on glide reentry space vehicles makes the use of accessory gear boxes for direct drive likely in order to simplify the installation and facilitate the integration of the flight vehicle power systems.

The power needs of a typical glide reentry vehicle are estimated at about 150 hp for flight controls (divided into two systems). This estimate includes power for electrical requirements as well as hydraulic. For comparison the total maximum pump power of a current jet transport is 80 hp. The ambient temperature during reentry will be such that cooling or thermal protection will be required to maintain the hydraulic systems

at the operable temperature level. The vehicle must provide the necessary thermal protection and/or heat sinks for the high temperature periods.

Many of the worst problems of hydraulic systems at high temperatures do not exist in pneumatic systems. Research is not necessary to find a compatible fluid, and a cooling system will not be needed. Air works just as well at 1000°F as it does at 100°. Pneumatic actuation systems under development will be shortly in a position to challenge hydraulic systems for use in aircraft and space vehicles due to recent advances in system stability and in offsetting the effects of compressibility as well as the development of efficient positive-displacement air motors for reliable high temperature operation.

Some of the advantages of air over hydraulic fluid obviously do not apply for hot-gas systems. Gas generators and fuel supplied are needed, and there is a serious problem of contamination. Solid particles in the gas stream clog small passages and orifices. Considerable progress is being made on these problems with cleaner-burning fuels and valves and other components that can operate in spite of contamination.

Most applications for hot-gas systems have been in one-shot, short-term APU's for missiles. Researchers are now working on equipment suitable for longer missions. Units have been produced utilizing a solid-propellant hot-gas system that have run for 32 minutes, driving a 30-kva generator and losing no power through contamination. The propellant has the slowest burning rate yet achieved. Other research work is being done on a burn-rate control for solid-propellant gas generators.

Thermal Derating

One of the ways of obtaining equipment which will operate at high temperatures is by "thermally derating" the equipment. It has been recognized in the past throughout industry that thermal derating of electronic components was necessary for high temperature service. A number of manufacturers established derating "bench marks" for particular components. However, little is known in these matters of the characteristics of the majority of electronic components, especially in terms of long life and reliability. However, the ultimate purpose of the derating of components is to meet some equipment design requirement by using components that are readily available without resorting to expensive special units. The term "derating" may have any one of three general meanings (Reference 83):

(1) The under-rating of power in applications where the ambient temperatures are above those specified for full load.
(2) The under-rating of temperature to permit power loads in excess of the rated values.

(3) The under-rating of both ambient temperature and power in an attempt either to obtain smaller changes in parameter values over the life cycle, or to reduce failure rates.

Problems involved in derating are not restricted to any particular type of component. While the terms used here apply only to resistors, as an example to illustrate the principles, the problems described are general.

Derating of Power

Some general observations may be made in discussing derating of power in resistor applications. First, derating practices vary between resistor manufacturers and also between different sizes of resistors made by the same manufacturer. Second, many derating concepts are frequently confounded because only end-points are considered. Finally, end points are not properly defined either in military specifications or in company standard practices. Very little data are ever demanded or supplied regarding intermediate points on the derating curve, so that it is necessary to accept or assume a straight-line curve, which may not be entirely accurate.

Specific practices on the derating of a resistor are illustrated in the applicable MIL specification and/or catalog material for that resistor. When the 1000-hr load-life requirement is based on the maximum ΔR (performance degradation) during the life test, that same definition applies to every point along the derating curve. In fact, empirical derating curves are determined by finding the wattage loading at various ambient temperatures which produces the ΔR required by the specification for the 1000 hr requirement at rated stress.

It is essential to note that inherent in any derating curve is the associated reliability or failure-rate level. A conservative manufacturer, for example, may derate to 150°C because the quality at this end point equals that at the lower ambient temperature of the load-life test. A less conservative manufacturer, in order to rate his product for 170°C, may do so simply by making a small sacrifice in reliability or failure rate, on the assumption that this cornercutting is rarely checked in practice.

A conventional derating curve is shown in Figure 130. Several possible interpretations can be made of a straight-line curve such as this. It can be assumed, for instance, that the average change in parameter value at Point A is the same as that at point B, C and D. Similarly, it can be assumed that the distributions of values around the averages at each of these points are equal. These appear to be useful interpretations, but they make no provision for including random excessive excursions.

The curve in Figure 131 may also be interpreted to mean that the failure rate at each point is the same. This interpretation becomes valid when one is concerned with reliability, but it has the limitation that a

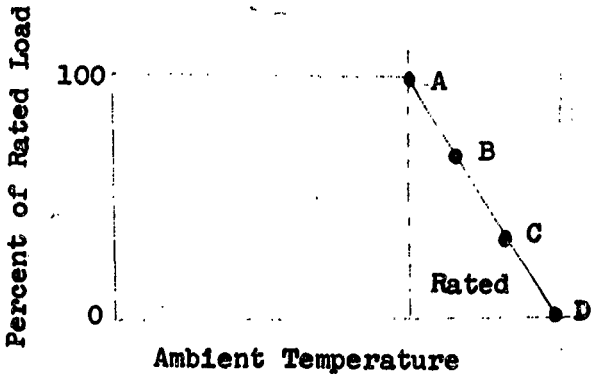

Figure 130. Conventional Derating Curve

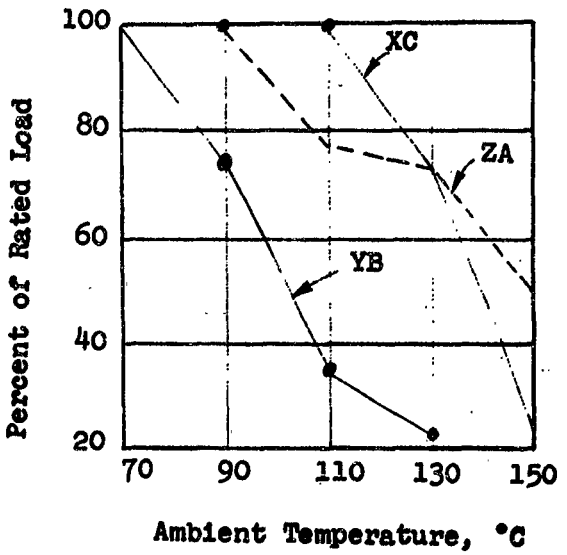

Figure 131 Derating Curves From Three Manufacturers
(Based on Maximum Deviation From
Nominal 20 percent During 2000 Hour
Of Life For at Least 90 percent Confidence)

line which indicates uniform failure rate is uniquely related to a definition of failure.

Any examination of specific test data on a group of competitive products will demonstrate the differences in viewpoint among manufacturers. It also will point up the questionable nature of the straight-line derating curves obtained from three manufacturers as indicated in Reference 83.

Derating of Temperature

There is little data to indicate that resistor power can be increased at lower temperatures as a result of derating the units. The amount that a resistor may be over-rated at a reduced temperature may be determined by standards of resistance change, or by failure rate. Any temperature derating based on linear concepts fails due to the complexity of the problem, which includes hot spots and thermal shock. In the rating of resistors or any electrical component an understanding of the temperature stresses is necessary before proper derating of the unit may be accomplished.

CONCLUSIONS

This section has reviewed the considerations for controlling the thermal effects, methods of protection, and methods of heat removal for possible space vehicle equipment. A thorough survey of the literature was made including direct contact with a number of organizations who have had experience related to this study.

Studies performed in connection with this report have led to a number of conclusions as follows:

1. Microminiaturization and high density packaging is an increasing cooling problem, but certain design considerations help relieve the situation. As a result, emphasis should be directed towards lower powered equipment.

2. Increased efficiency of energy conversion devices will help reduce heat loads. Programming of the equipment use will be necessary to reduce or minimize heat loads. Development of equipment for higher operating temperatures and the development of new materials and new ways of using old material will be required. However, there is a trade if the weight of this equipment increases.

3. The use of closures appears to offer good possibilities for protection and cooling of equipment in the space environment. They also provide side effects in protection from sparking contamination, fire hazards, and vibration.

4. Equipment operating at significantly different operating

temperatures or requiring special conditions should be separated for better utilization of the coolant flow available.

5. Standard shielding techniques can be used for radiation protection, but "chimney effects" etc., normally utilized in a 1 - "g" environment, cannot be relied upon for convective cooling under space conditions.

6. The basic modes of heat transfer (conduction, convection, and radiation) are generally applicable for space although there are some limitations such as natural convection at zero-g. Although one mode of heat transfer is generally predominant in the overall cooling effect, two, or sometimes all three modes play an important role in the overall thermal balance.

7. Thermoelectric cooling in an otherwise passive or semi-passive temperature control system can be useful for spot cooling of critical components.

8. Optimum arrangement can be obtained if reliability data is known on the various equipment items being environmentally controlled.

PROBLEM AREAS

The problem areas which came to light in the preparation of this section are summarized as follows:

1. Thermal resistance across a joint made up of two or more conductors can be appreciable relative to the overall resistance of the conductor. This resistance is primarily a function of pressure normal to the joint and surface roughness. Temperature also effects the joint resistance to the degree of the change in thermal conductivity of the material with temperature. A great deal of analyses and experimentation is still required before reliable data and techniques are available.

2. Materials used to aid heat transfer must be acceptable for utilization in the space environment. For example, the "space grease" used to aid conduction across a joint must withstand radiation and hard vacuums unless located within a pressurized enclosure.

SECTION VIII
METHODS OF ANALYSIS

Two types of analysis are usually required for defining the temperature control requirements of space vehicles -- (1) a heat transfer and thermodynamic analysis and (2) a dynamic response analysis. Consequently, a development of the theory, equations, and some examples was felt to be a necessary addition to this report. As a result, this section is divided into two parts; the first part is on methods of thermal analysis and the second part is on dynamic response of control methods.

The first part on methods of thermal analysis discusses (1) heat transfer and temperature equations for passive and semi-passive temperature controlled vehicles with examples, (2) methods of analysis of transient heat transfer problems, (3) analog networks, and (4) heat transfer computer programs. A more detailed description of the method of analysis for design of space vehicle temperature control systems will be included in Part II of this report.

The second part on dynamic response discusses analysis techniques and design considerations for the dynamic response of temperature control methods. An example of the set-up for solution by Laplace transform loop and electronic analog network is included. This part has not been expanded since a detailed treatment of dynamic response will be given in Part II of this report.

NOMENCLATURE LIST

A	Area, (sq. ft.)
a, α	Thermal Diffusivity, sq. ft./hr.
b	Vehicle Skin Thickness, ft.
c	Specific Heat, Btu/lb. (^{o}F)
c	Electrical Capacitance, Farad
D	Diameter, ft.
E	Rate of Radiation, Btu/hr (sq.ft.)

E_R	Rate of Radiation, Reflected Solar, Btu/hr. sq.ft.
E_P	Rate of Radiation, Direct from Plane and Atmosphere, Btu/hr. sq.ft.
E_B	Blackbody Radiation Rate Per Unit Area, Btu/hr. sq.ft.
e	EMF, Voltage, Volts
e,ϵ	Surface Emissivity
F,$\mathcal{F}$	Radiation View Factor
f	Fluid Friction Factor
G	Internal Heat Generation, Watts
g	Gravity Constant, $(lb_f)(ft)/(lb_m)(sec)^2$
h	Film Heat Transfer Coefficient, $Btu/(hr)(ft)^2(^oF)$
h_r	Equivalent Radiation Film Coefficient, $Btu/(hr)(ft)^2(^oF)$
i	Electrical Current, Amps
J	Radiosity; Sum of Emitter, Reflected, and Transmitted Radiation Flux Per Unit Area, $Btu/(ft)^2(hr)$
K	Thermal Conductivity, $Btu/(hr)(ft)(^oF)$
L	Electrical Industance, Henries
l	Fluid Flow Equivalent Length, ft.
M	Mass, lb.
m	Mass Flow Rate, lb./hr.
p	Pressure, psf (psi)
q	Heat Transfer Rate, Btu/hr
q_e	Electrical Charge, Coulomb
R	Radius, ft
R	Electrical Resistance, Ohm

r, ρ	Surface Reflectivity
S	Solar Constant, Btu/$(ft)^2$(hr)
T	Temperature, $^oR(^oF)$
$\dot{T}$	Rate of Temperature Change, ^oR/hr (^oF/hr)
t	Time, hr.
U	Overall Heat Transfer Coefficient, Btu/$(ft)^2(^oF)$(hr)
V	Velocity, ft/sec
v	EMF (VOLTS), Volt
X	Length of Thermal Conductance Path, ft.
X	Distance in Body From Surface, ft.
Z	Electrical Impedance
α	Absorptivity
α, (a)	Thermal Diffusivity, $(ft.)^2$/(hr)
α_n	Phase Displacement of Nth Harmonic in the Lumped Mass, Radians (Degrees)
β_n	Phase Angle of Nth Harmonic of the Surrounding Fluid, Radians (Degrees)
ϵ, (e)	Emissivity
μ	Amplification Factor
ϕ	Phase Lag Between Fluid Temperature and Surface Temperature, Radians (Degrees)
μ	Viscosity, lb/(ft)(hr)
w	Rotational Velocity, Rev/hr
w_n	Harmonic Frequency (n signifies one Harmonic of Fourier Series), Rad/hr

ρ	Density, $lb/(ft)^3$
ρ, (r)	Reflectivity
σ	Stefan-Boltzmann Constant, 0.173×10^{-8} $Btu/(ft)^2(hr)(^oR)^4$

Subscripts

a	Ambient
B	"Blackbox" Equipment or Compartment
f	Fluid
f,v	Fluid to Skin
I	Insulation, Conduction Path
i	Internal, Initial
i,v	Internal to Skin
m	Mean or Average
n	Number in Series (1,2,3,4,...)
nm	Amplitude of Nth Harmonic
o	Out, Outside, Initial

P	Planet
R	Reflected Solar From Planet
S	Solar
TSV	Total Space Vehicle
V	Vehicle Skin
Vi	Vehicle Skin Segments
V,V_i	Vehicle Skin Segment to Other Vehicle Skin Segments Stored

METHODS OF THERMAL ANALYSIS

General Heat Transfer and Steady-State Temperature Equations for a Space Vehicle Skin

The general equation for heat transfer on a section of the vehicle skin can be expressed as:

$$q_{\Delta v} = q_{\alpha v} + q_s + q_R + q_p + q_I + q_{vi} \qquad (156)$$

The meanings of the various "q" terms are listed in Table 40 and illustrated by Figure 132.

The general heat transfer equation as presented can be made as complicated or as simple as desired. For instance the view factors for radiation from the sun and the planet can include complex trigonometric relationships as a function of orbit and spin or the orbit function can be simply assumed as "1" or "0" dependent upon whether the vehicle skin segment sees the sun or planet. Values of F_R and F_p for various shaped space vehicles are presented in Ref.18 .

The general equation can be set up for IBM solution by iteration over intervals of time. However, for a quick estimation and check, simplification for hand solution is desirable. A list of "q" terms and conditions for their elimination is given in Table 41.

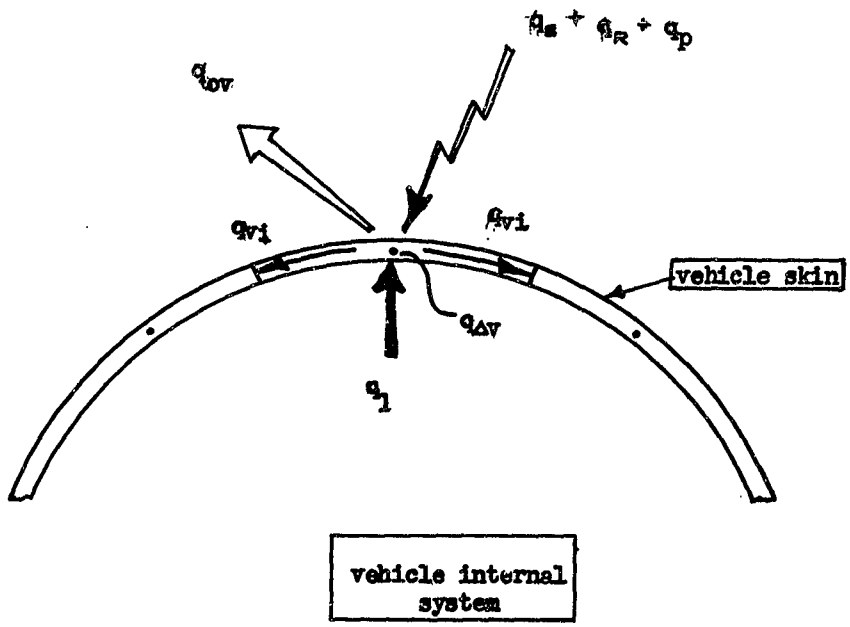

heat balance

$$q_v = q_v + q_s + q_R + q_p + q_I + q_v$$

Figure 132. Heat Transfer Balance for a Space Vehicle Skin

Table 40. Definition of "q" Terms

q_i	Definition	Heat Transfer Expression
q_v	Stored Heat in Vehicle Skin	$A_v(bpc)_v \Delta T_v$
q_{ov}	Radiation out from Skin	$-\epsilon_v \sigma A_v T_v^4$
q_s	Direct solar radiation	$\alpha_s A_v F_s S$
q_R	Reflected Solar Radiation from planet	$\alpha_R A_v F_R E_R$
q_p	Direct radiation from planet and planet atmosphere	$\alpha_p A_v F_p E_p$
q_I	Internal heat transfer to skin	$\left(\frac{kA}{x}\right)_{z,v}(T_z-T_v)+(hA_2)_{z,v}(T_z-T_v)+(UA)_{s,v}(T_{s_i}-T_v)$
q_{vi}	Heat conduction to other skin segments	$\left(\frac{kA}{x}\right)_{v,v_i}(T_{v_i}-T_v)$

Table 41. Elimination Of "q" Terms

q	Condition for Elimination (q=0)
$q_{\Delta v} = 0$	All other "q" terms are constant with time ie steady-state, or equilibrium.
$q_{\Delta v} \approx 0$	b→0 Very thin vehicle skin
$q_s = 0$	1) Skin segment does not see sun or 2) Space vehicle on shade side of planet
$q_R = 0$	1) Skin segment does not see planet, or 2) Space vehicle on shade side of planet, or 3) Space vehicle not in orbit around planet
$q_p = 0$	1) Skin segment does not see planet, or 2) Space vehicle not in orbit around planet
$q_I = 0$	1) Equilibrium, no internal heat generation, or 2) Insulated skin with no internal heat transfer
$q_I = G$	Equilibrium, q_1 = internal heat generated = constant or zero
$q_{vi} = 0$	All skin segments are at equal temperatures
$q_{vi} \approx 0$	Thin skins with long conductivity paths

For the steady-state condition, Table 41 shows that $q_v = 0$ and $q_I = G$.

Substituting in the general equation, (Eq.156) and allowing $q_{vi} = 0$,

$$0 = q_{ov} + q_S + q_R + q_p + G \tag{157}$$

Substitution for q_{ov} from Table 40 yields the following equation for T_v.

$$T_v = \sqrt[4]{\frac{q_S + q_R + q_p + G}{\epsilon_v \sigma A_v}} \tag{158}$$

Further substitution for the other q-terms shows

$$T_v = \sqrt[4]{\left(\frac{\alpha_s}{\epsilon_v}\right)\frac{F_s S}{\sigma} + \left(\frac{\alpha_R}{\epsilon_v}\right)\frac{F_R E_R}{\sigma} + \left(\frac{\alpha_p}{\epsilon_v}\right)\frac{F_p E_p}{\sigma} + \frac{G}{\epsilon_v \sigma A_v}} \qquad (159)$$

The value of the equilibrium solution is very limited since the conditions for steady-state do not, in general, exist. The temperature control system designed from the steady-state conditions will have somewhat higher requirements than are really necessary. However, the steady-state conditions do indicate maximum possible variations in internal environment for changes in external environment. Should the space vehicle, then by accident or design, assume a planetary orbit of 100% sunlight or 100% shade or a solar orbit at constant distance from the sun; the steady-state calculations will be justified. Furthermore, the steady-state solutions do not require knowledge of masses and specific heats of materials used in the vehicle construction. This is an advantage for predicting temperature control requirements in advanced proposals without detailed knowledge of fabrication and materials.

For a space mission where the vehicle assumes an orbit around the sun, the vehicle skin will approach steady-state temperature for the condition of no tumbling or rotation about the flight path. A calculation with constant solar radiation shows that steady-state conditions can used for cylindrical vehicles with $\left(\frac{\rho b c}{\epsilon}\right)_v \omega > 66$ where w is the rotation rate of the vehicle about the longitudinal axis and no tumbling is present. Figure 133 presents a curve of the effect of axial rotation, w, on the skin temperature variation of the solar orbiting vehicle.

Equation 158 and 159 are general solutions for the one-dimensional steady-state condition and can be used to estimate steady-sate passive, semi-passive, and active temperature control system skin temperatures.

General Heat Transfer Equation for an Instrument Inside The Space Vehicle

The heat transfer equation for internal heat transfer to the instrument can be written:

$$q_{\Delta B} = q_{OB} + G \qquad (160)$$

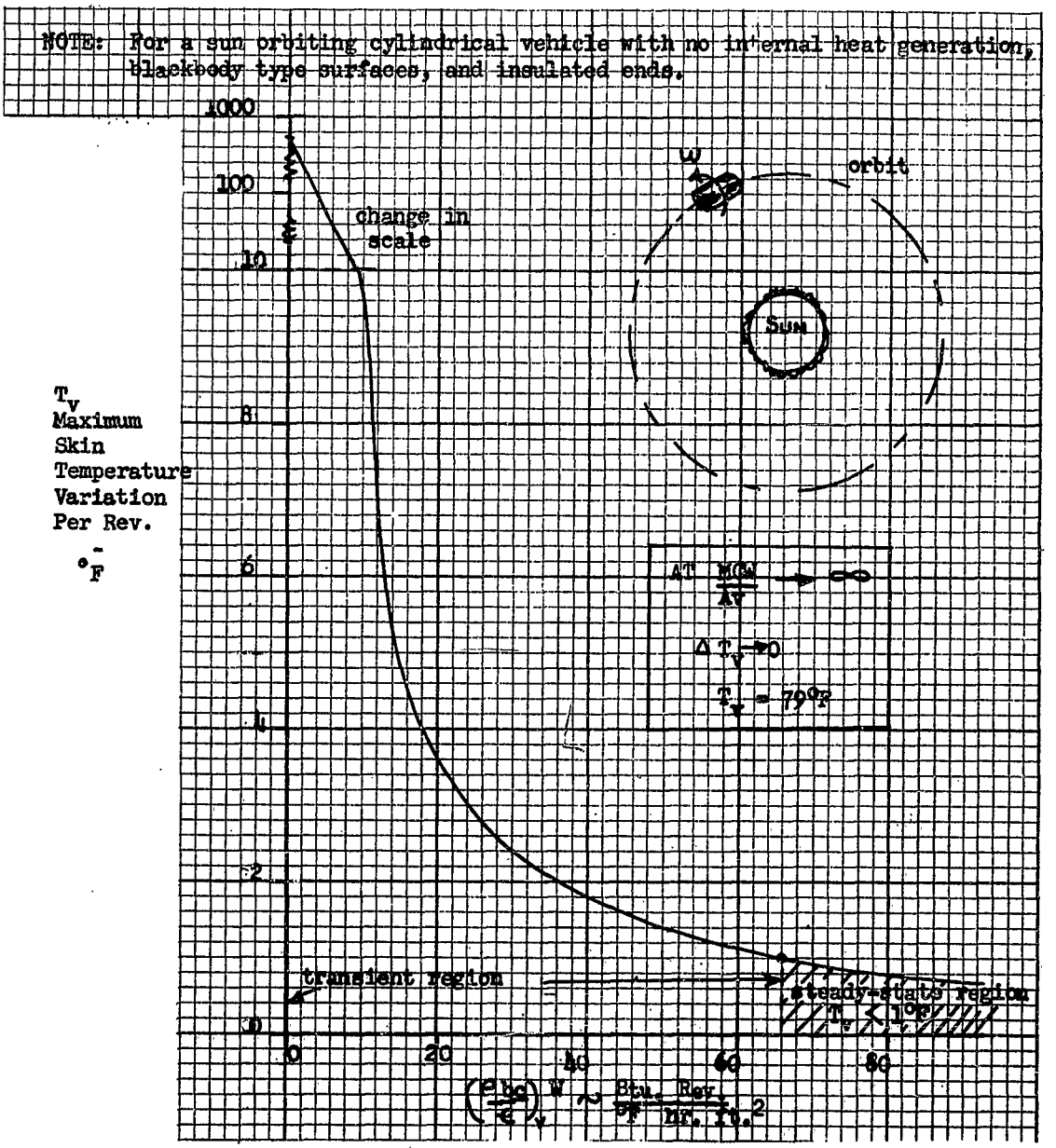

Figure 133. Effect of Axial Rotation and Skin Heat Storage On The Skin Temperature Variation

This equation can be very complex dependent upon the configuration of the instrument and the modes of heat transfer.

"q" terms for the instrument are defined in Table 42 and illustrated in Figure 134.

Table 42. Definition Of Instrument "q" Terms

q	Definition	Heat Transfer Expression
$q_{\Delta B}$	Stored heat in instrument	$M_B C_B \Delta T_B$
q_{OB}	Heat transfer from instrument	$\left(\frac{kA}{x}\right)_{B,O}(T_O - T_B) + (h_{B,O}A)(T_O - T_B) + (\bar{h}_{B,E}A)(T_{E_2} - T_B)$
G	Heat generated in instrument	G

Terms can be eliminated from the equation if the conditions of Table 43 are met.

Table 43. Conditions For Eliminating Instrument q Terms

q	Condition for Elimination
$q_{\Delta B} = 0$	Steady-state, all q terms are constant with time
$q_{\Delta B} \approx 0$	Negligible instrument mass, $m \rightarrow 0$
$q_{\Delta B} = 0$	Steady-state, no heat generation
$G = 0$	No heat generation

If the instrument "black box" is small, assumptions of (1) uniformily distributed mass and heat transfer, and of (2) infinite instrument internal thermal conductivity can be made for simplification of the calculations. These assumptions are justifiable only for rough estimates or very small instruments. Other more detailed solutions with consideration for the instrument internal configuration and cooling system are presented in Section VII of this report.

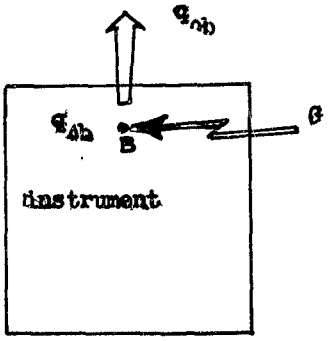

Heat Balance: $q_{Ab} = q_{ob} + G$

Figure 134. Heat Transfer Balance for an Instrument Inside a Space Vehicle

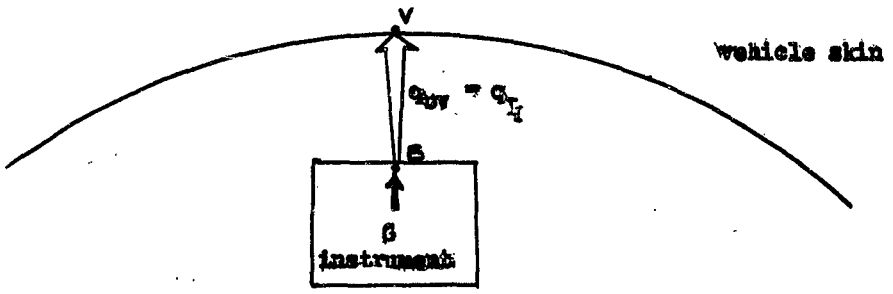

Heat balance: $q_{bv} = q_I = G$

Figure 135. Steady State Heat Balance for Instrument in Space Vehicle

Substituting into the equation (Eq. 160), the values for the q terms, $q_{\Delta B} = 0$ for steady-state and

$$q_{OB} = -G = \left(\frac{kA}{x}\right)_{B,O}(T_O - T_B) + (hA)_{B,O}(T_O - T_B) + (UA)_{f,B}(T_{f_2} - T_B) \quad (161)$$

However, for the steady-state conditions, $q_I = -q_{OB} = G$ since all internal heat at steady-state will ultimately be transferred to the skin (see Figure 135). Also, $\left(\frac{kA}{x}\right)_{B,O}(T_O - T_B)$ and $(hA)_{B,O}(T_O - T_B)$ can be combined to form $(UA)_{B,O}(T_O - T_B)$. Further simplifications can be made since the condition implies no heat storage term in the heat conduction or fluid transfer medians so that subscripts become B = I and O = V.

Substitution of these considerations yields the following equation for the instrument temperature.

$$T_B = \frac{(UA)_{B,V}T_V + (UA)_{f,B}T_{f_2} + G}{(UA)_{B,V} + (UA)_{f,B}}$$

$$\text{or} \quad T_B = T_V + \frac{(UA)_{f,V}(T_V - T_{f_1}) + G}{(UA)_{B,V}} \quad (162)$$

$$\text{or} \quad T_B = T_V + \frac{\dot{m}_f c_f (T_{f_1} - T_{f_2}) + G}{(UA)_{B,V}}$$

Passive Temperature Control Estimates For Space Vehicles

Solar Orbits

For the space vehicle in interplanetary travel, the vehicle can be considered to be in the sun 100% of the time (see Figure 136). Also, the reflected solar radiation and planetary radiation terms are zero (or negligible). Consequently, the equilibrium skin heat transfer equation (Eq. 157) reduces to

$$0 = q_{ov} + q_s + G \quad (163)$$

or, substituting terms and rearranging,

$$\frac{G}{\epsilon_V A_V} = \sigma T_V^4 - \left(\frac{\alpha_s}{\epsilon_V}\right) F_s S \quad (164)$$

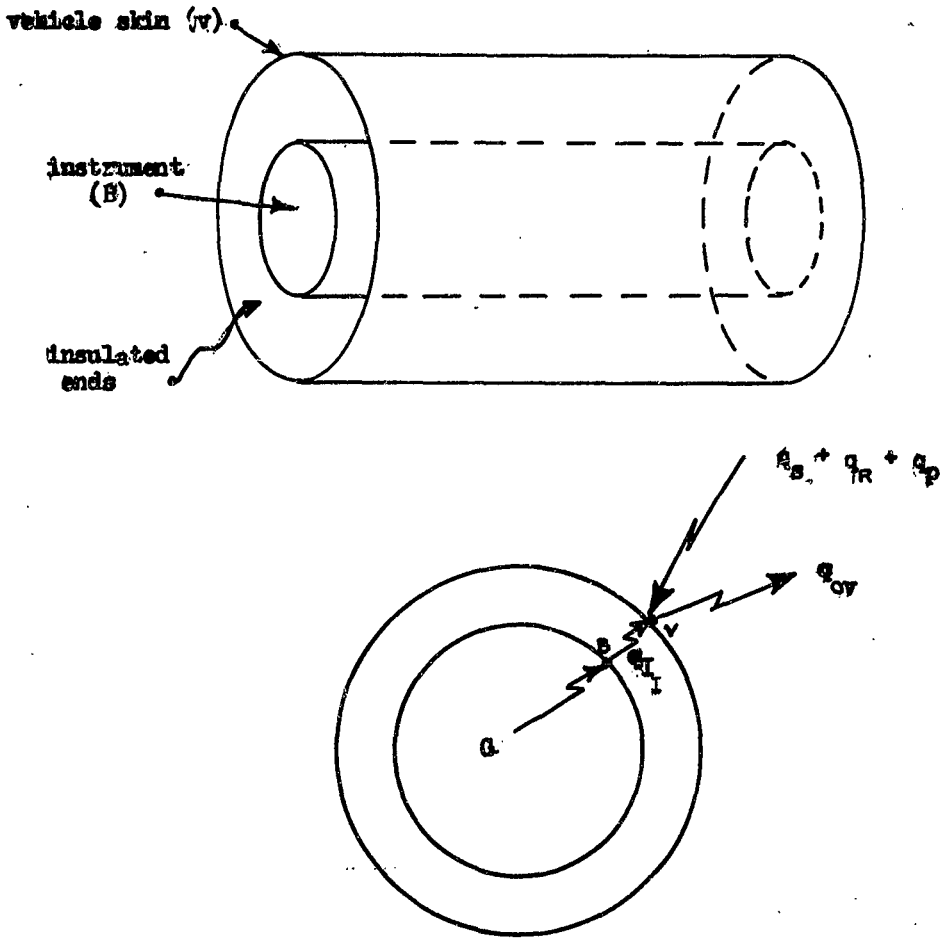

Heat Balance: $q_{ov} + q_{\overline{s}} + q_{\lambda} + q_p + q_I = 0$

$q_{\Sigma} = 0$

Figure 136. Steady State Heat Balance for Simple, Rotating Space Vehicle

This equation shows that for a given internal heat generation rate, G, the outside surface conditions, α_s/ϵ_v and ϵ_v can be varied to some extent to influence the skin temperature T_v. Conversely, for specific values of heat generation rate and skin temperature, the surface conditions are limited to one value of α_s and ϵ_v. The values of α_s and ϵ_v may be obtained by patterned areas of different coatings if one coating with values α_s and ϵ_v is not available. Note that the solar constant S varies with distance from the sun (see Figure 11, Page 26, Reference 18).

Plots of Equation 164 for $\frac{G}{\epsilon_v A_v}$ versus T_v with various values of α_s/ϵ_v are given in Figures 137, 138, 139 and 140 for a flat-plate, cylinder, and sphere. These figures can be used for quick estimates of skin temperature, maximum internal heat dissipation, or skin outside surface α_s and ϵ_v requirements.

The temperature equation for a heat generating instrument for an equilibrium passive system is

$$T_B = T_v + \frac{G}{(UA)_{B,V}}$$

OR

$$T_B - T_v = \frac{G}{(UA)_{B,V}} \quad . \tag{165}$$

Equation 165 shows that the temperature of the instrument can be controlled in a passive system at equilibrium by variation of $(UA)_{B,V}$. Consequently, the relationship $\frac{1}{(UA)_{B,V}} = \frac{1}{\left(\frac{kA_1}{x}\right)_{B,V} + (hA_2)_{B,V}}$ shows five ways in which $(UA)_{B,V}$ can be altered. (166)

1) Vary $X_{B,V}$ (conductance path length),

2) Vary $k_{B,V}$ (Thermal conductivity),

3) Vary $A_{1_{B,V}}$ (Area of conductance),

4) Vary $A_{2_{B,V}}$ (Area of radiation), and/or

5) Vary $h_{B,V}$ (heat transfer coefficient).

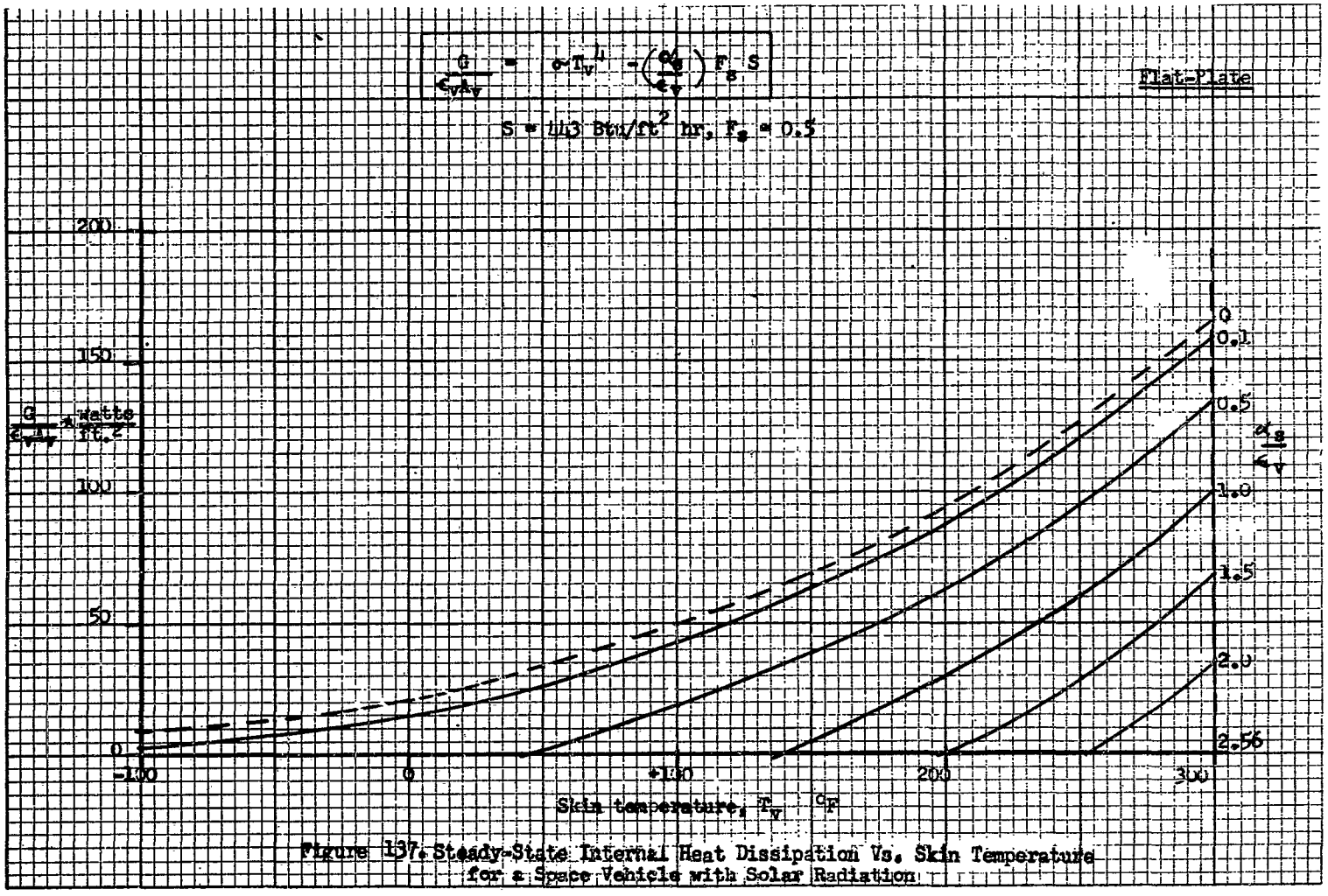

Figure 137. Steady-State Internal Heat Dissipation Vs. Skin Temperature for a Space Vehicle with Solar Radiation

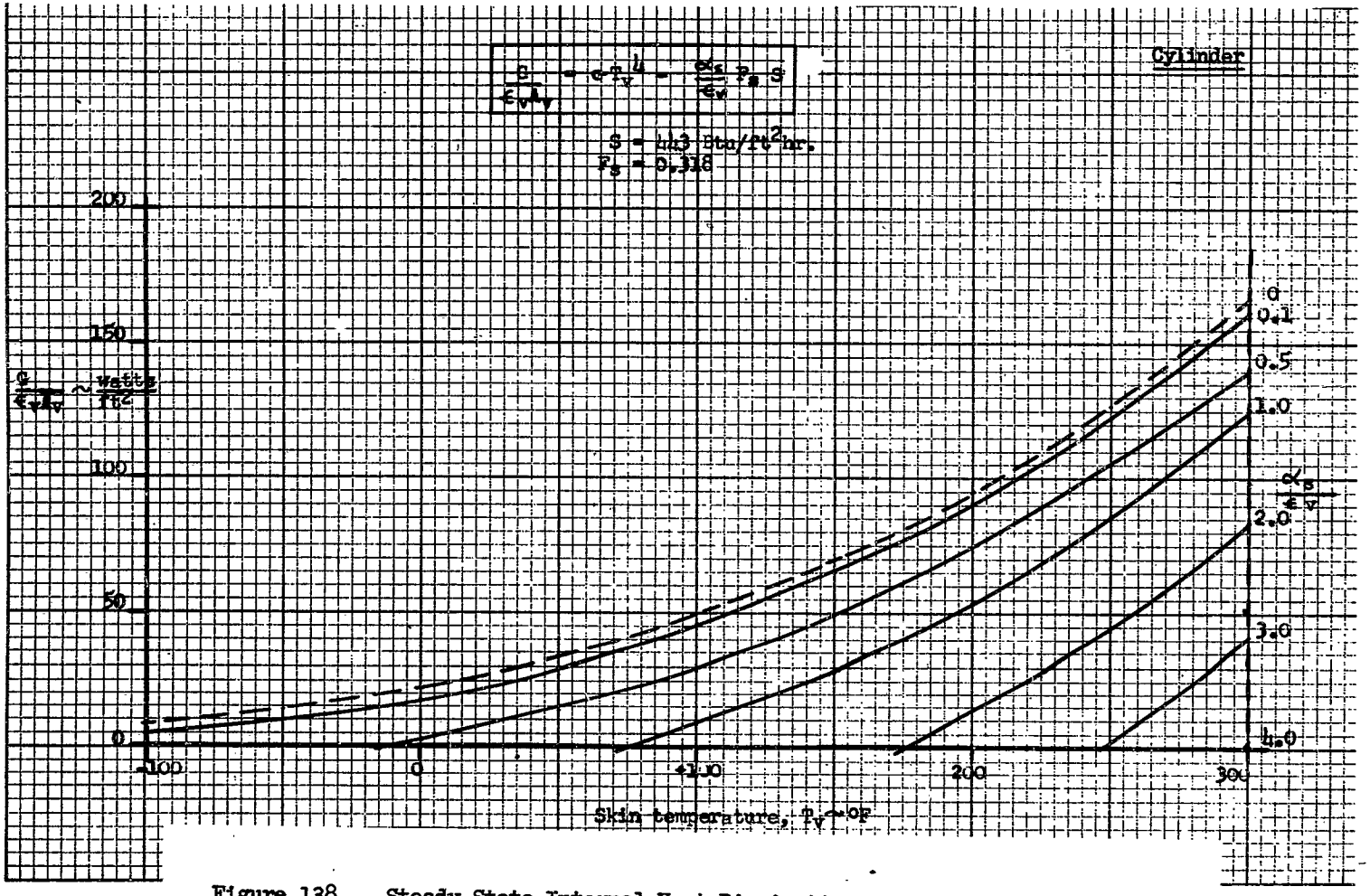

Figure 138. Steady-State Internal Heat Dissipation vs. Skin Temperature for a Space Vehicle with Solar Radiation

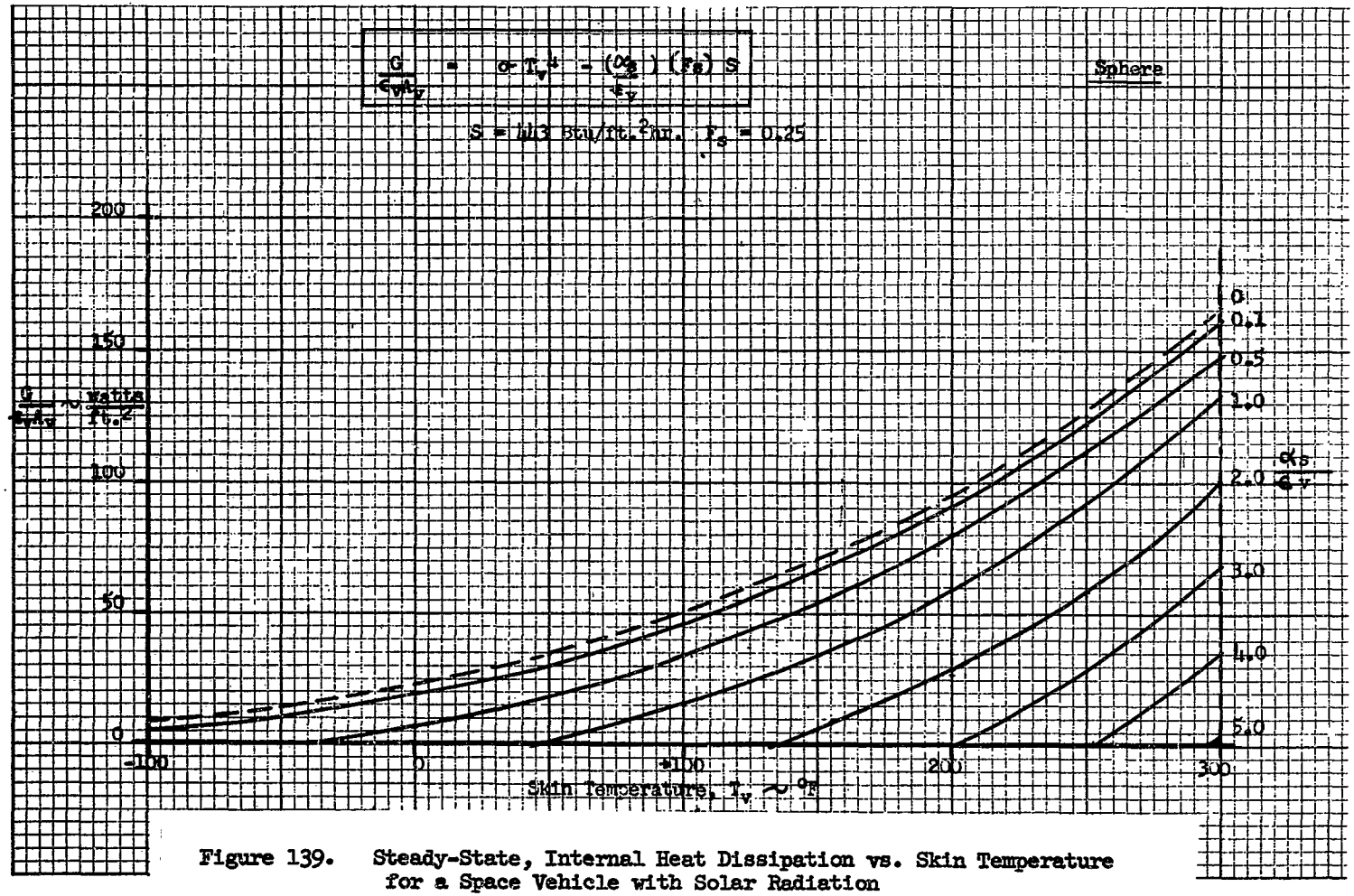

Figure 139. Steady-State, Internal Heat Dissipation vs. Skin Temperature for a Space Vehicle with Solar Radiation

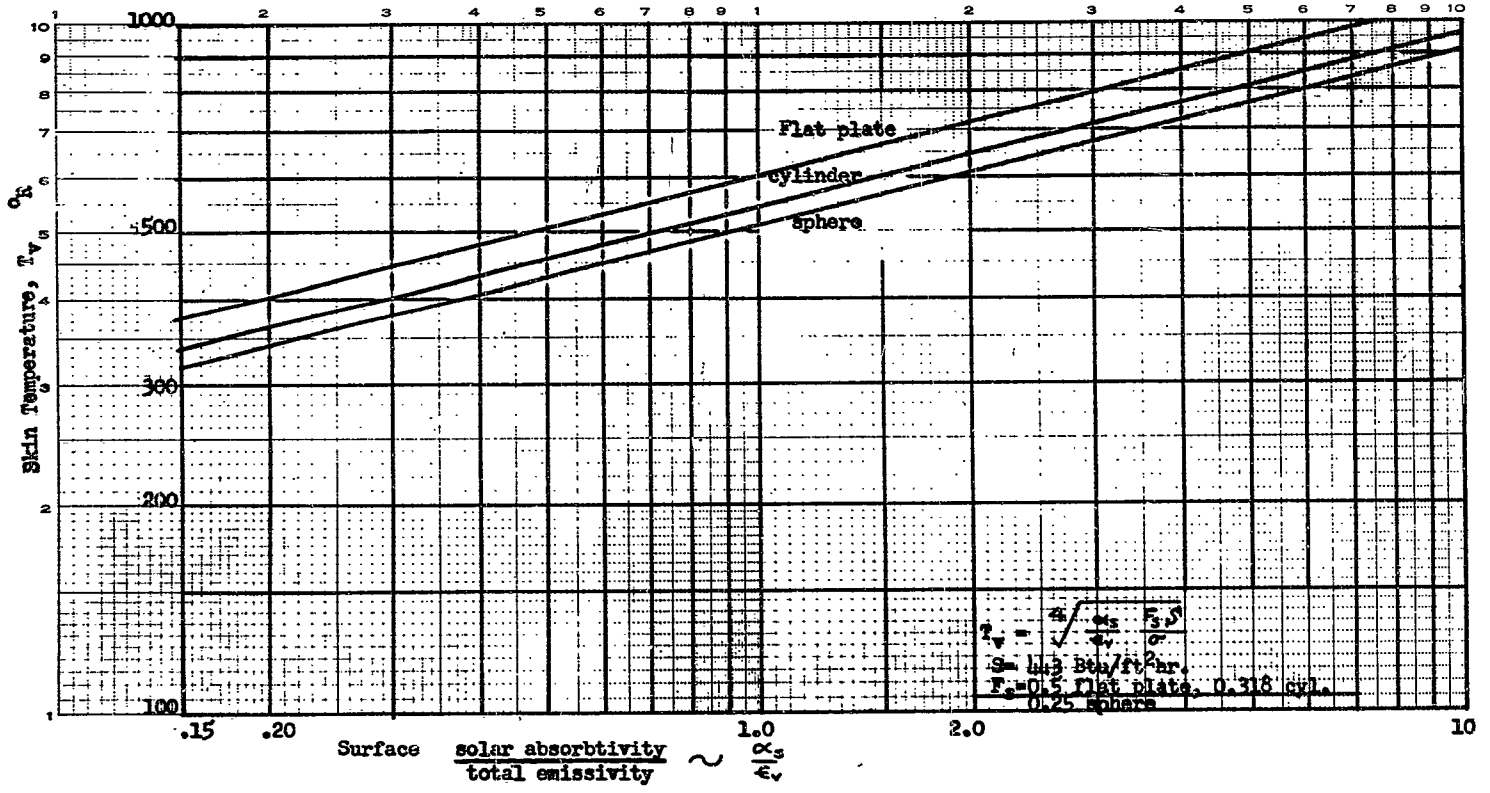

Figure 140. Steady-State Skin Temperature for a Space Vehicle with Solar Radiation and no Internal Heat Source

$h_{B,V}$ is considered to be a heat transfer radiation coefficient

$$h_r = h_{B,V} = \mathcal{F}_{B,V}\, \sigma (T_B^2 + T_V^2)(T_B + T_V) \qquad (167)$$

Values of $h_r/\mathcal{F}$ are presented for various T_B and T_V values in Figure 141. Also Figures 142 and 143 are useful in estimating $U_{B,V}$. $\mathcal{F}_{B,V}$ can be calculated by using equations or data presented in Reference 18.

Planetary Orbits

For planetary orbits, the equation for heat transfer is given by adding heat transfer for solar reflected radiation and planetary radiation to the equation 164 for the solar orbit. Note that all three radiation terms (solar, solar reflected, and planetary) become variables as a function of orbit and time.

The skin temperature equation 159 shows that for the planetary orbit with internal heat dissipation both the external skin surface black-body type emissivity ϵ_V and the ratio α_s/ϵ_V are important. Whereas, for the shadow condition, the emissivity, ϵ_V, is more important.

The internal heat transfer is the same as discussed for the solar orbit. Figure 144 gives some skin temperatures as a function of α_s and ϵ_V for an earth orbit with no internal heat generation.

Example Solution Of Passive Temperature Control System

Problem Definition

A space vehicle is to orbit around the earth in a 100 mile altitude circular orbit for a long period of time. The orbit will be 50% in sunlight and 50% in earth shadow. Then, the vehicle is to change course and form an orbit about the Sun. A blackbox of electronic instrumentation is to be carried in the vehicle.

The space vehicle is spherical of 2 ft. diameter with a fast rotation about its orbital axis relative to the orbit cycle. The electronic instrumentation must dissipate a constant 100 watts and must be controlled at 75°F ± 75°F. The blackbox is a sphere of 1 ft. diameter.

Design a passive temperature control system for the vehicle to control the instrumentation at 75°F ± 75°F.

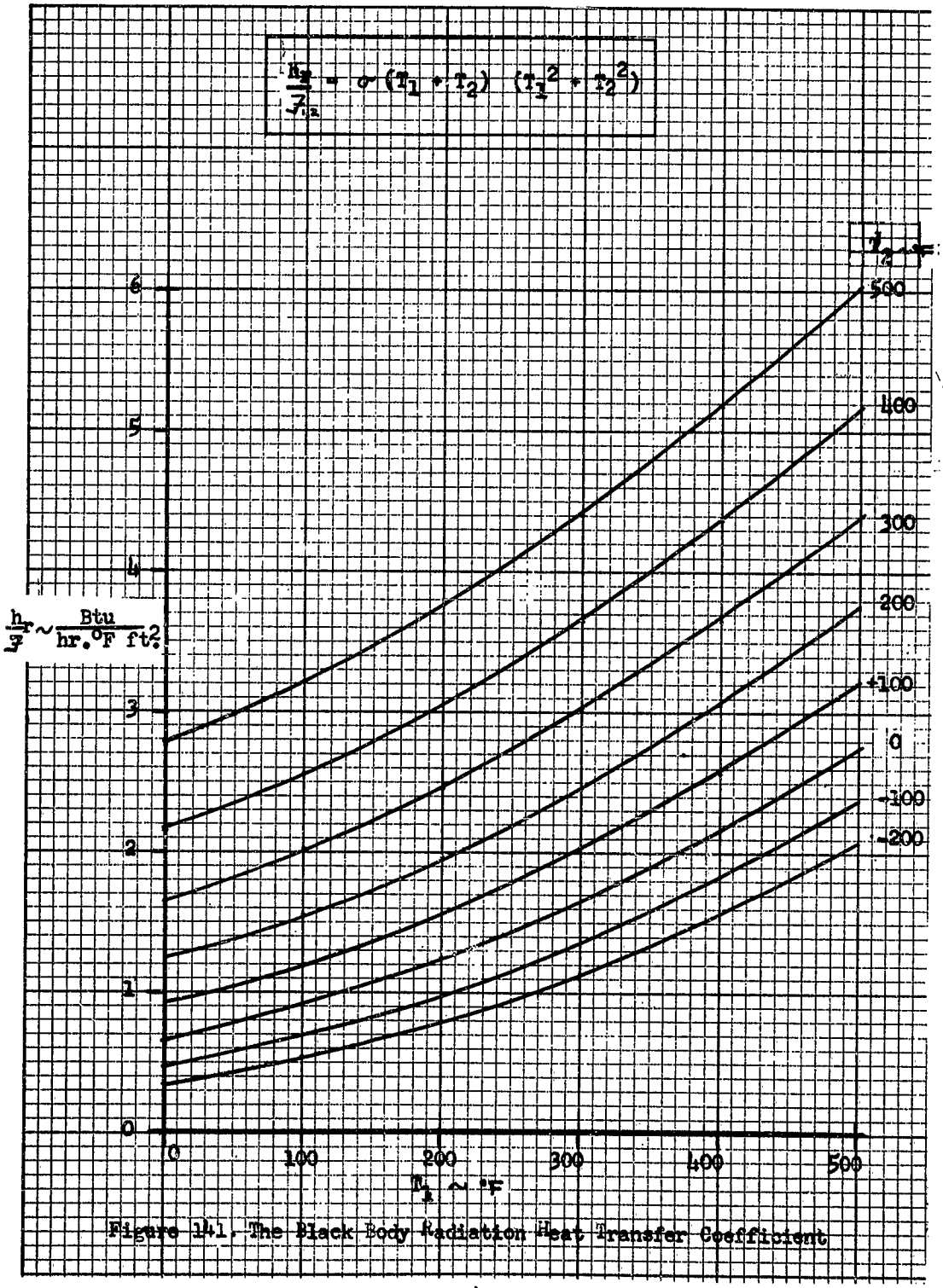

Figure 141. The Black Body Radiation Heat Transfer Coefficient

$$UA = \frac{1}{\frac{1}{B_1} + \frac{1}{B_2} + \frac{1}{B_3}}$$

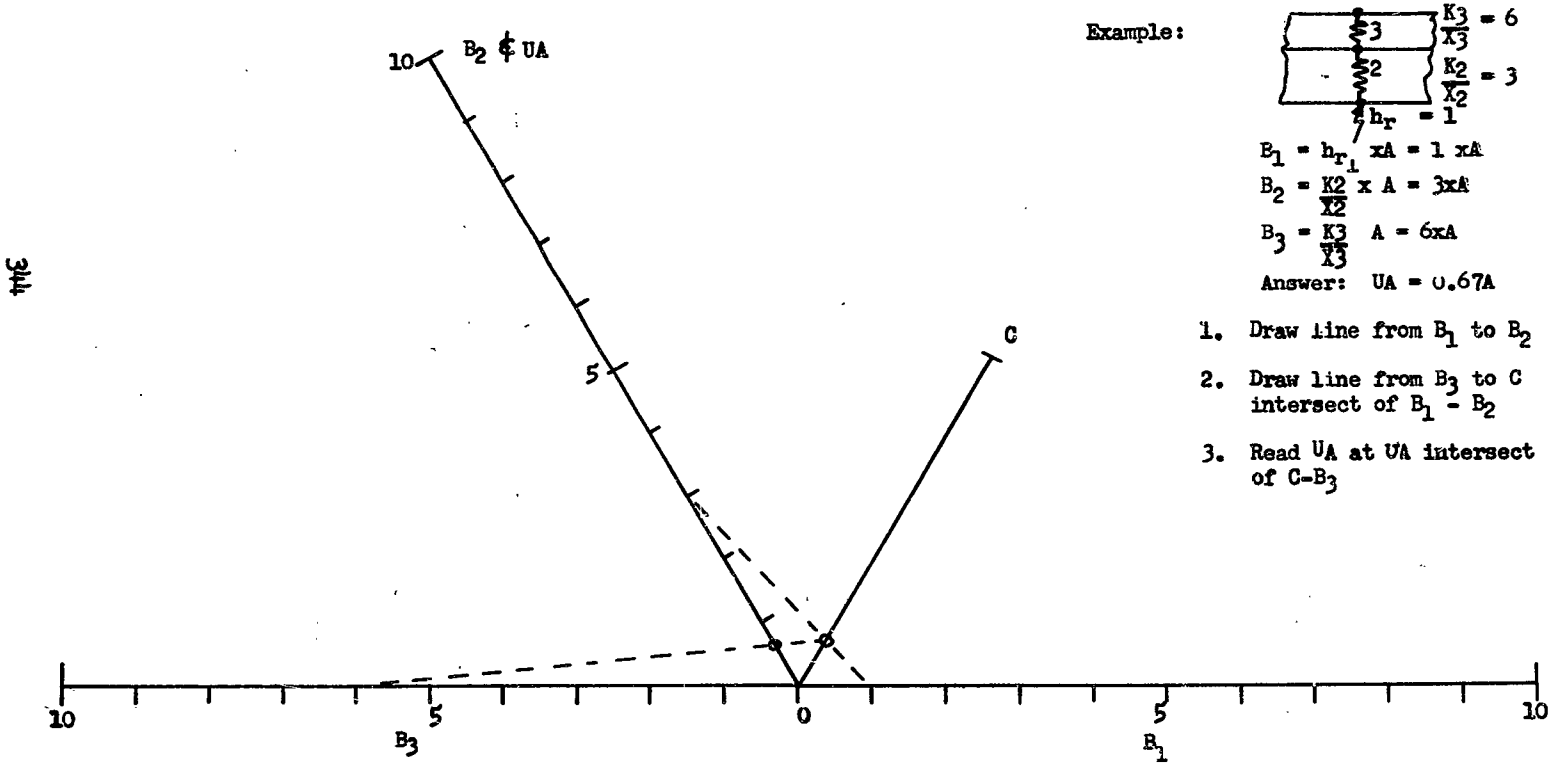

Example:

$B_1 = h_{r_1} xA = 1 xA$

$B_2 = \frac{K2}{X2} x A = 3xA$

$B_3 = \frac{K3}{X3} A = 6xA$

Answer: UA = 0.67A

1. Draw line from B_1 to B_2
2. Draw line from B_3 to C intersect of $B_1 - B_2$
3. Read UA at UA intersect of C-B_3

Figure 142. Overall Heat Transfer Coefficient Calculation Aid

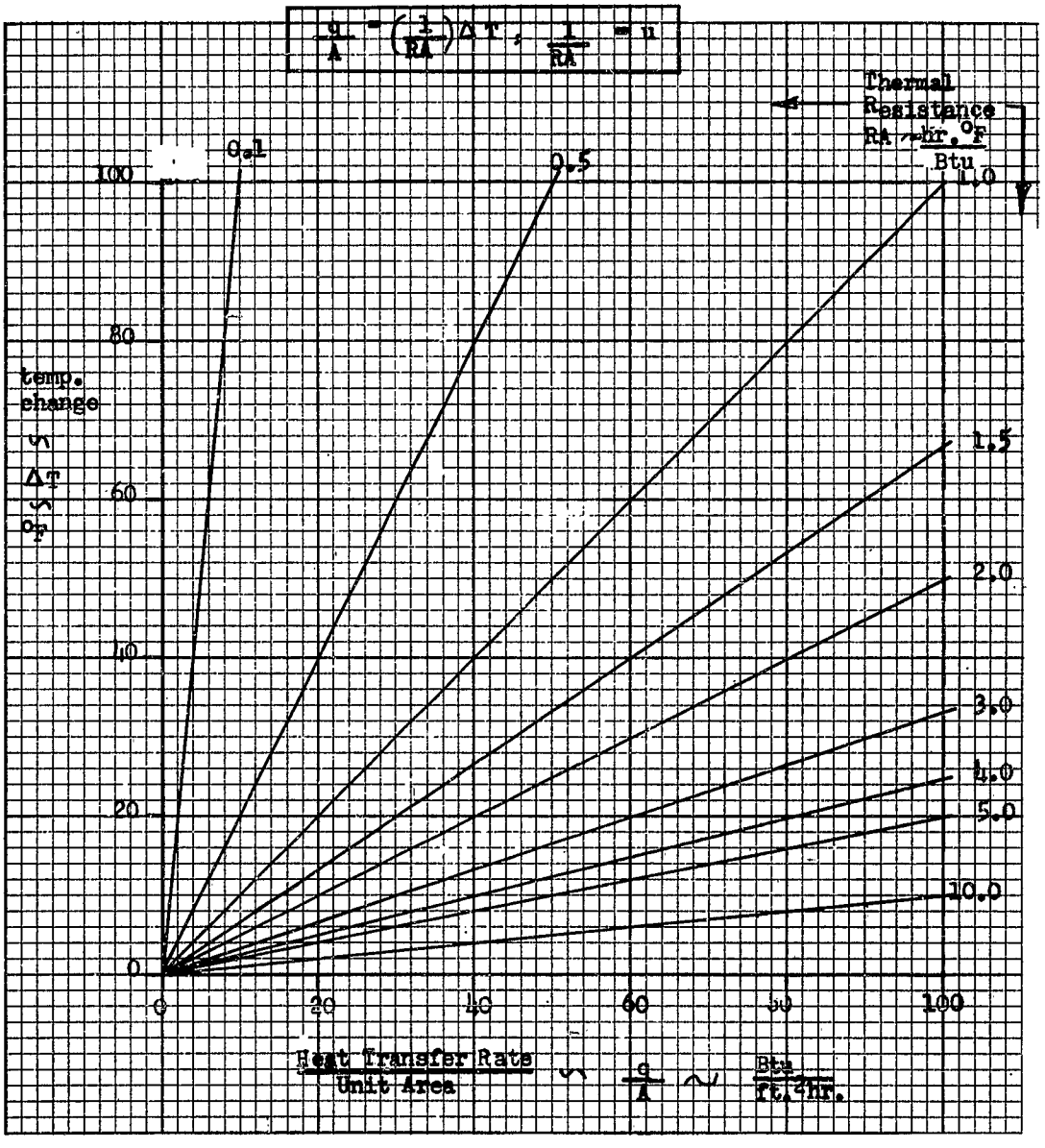

Figure 143. Temperature Change vs. Heat Transfer For Various Thermal Resistance Values

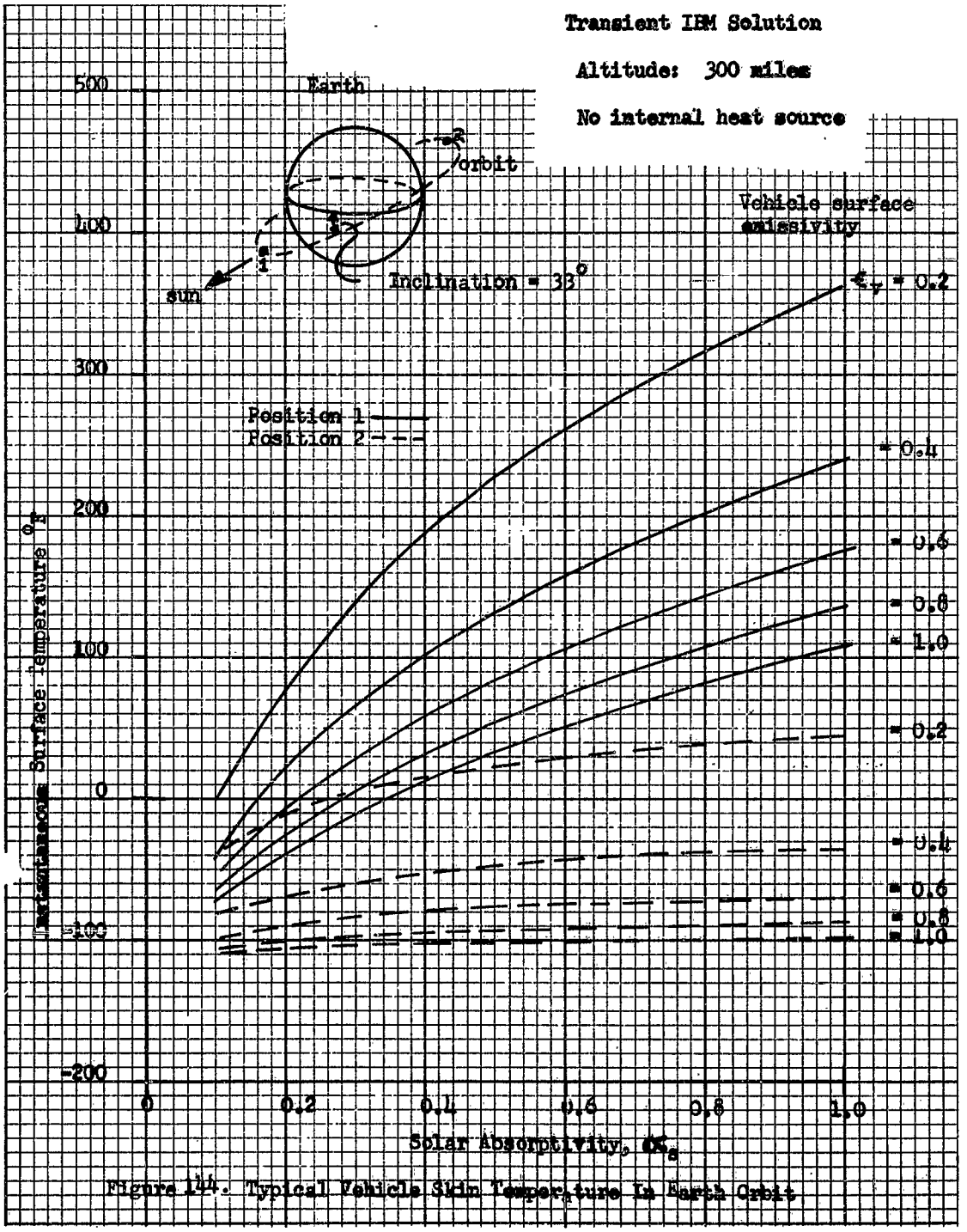

Figure 144. Typical Vehicle Skin Temperature In Earth Orbit

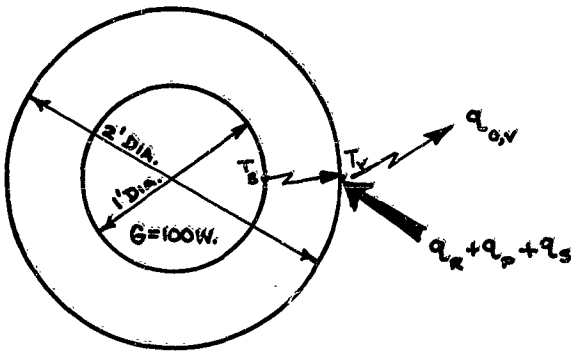

Figure 145. Example Problem Vehicle Sketch

Assumptions for Solution

1) The vehicle skin assumes an average temperature with no temperature variation. (This assumption is fairly valid for the fast rotating satellite).

2) The "blackbox" instrumentation is assumed to have an average temperature, T_B, at the case. (Valid only for a "blackbox" of uniform density, uniform heat generation, and uniform heat dissipation. These conditions can be approached but are limited by mounting problems and high heat dissipating components.)

3) The vehicle is considered to attain equilibrium in space. (Valid for a long time space orbit).

4) The vehicle is considered to attain equilibrium at a point facing the sun in the earth orbit and at a point in 100% earth shadow. (The equilibrium condition is not likely due to mass thermal storage during the orbit. However, the equilibrium conditions will give maximum and minimum values of temperature which are theoretically possible. The resulting change in satellite temperature will be greater than the actual satellite change in temperature as a function of orbit period, orbit path, vehicle thermal capacity, and vehicle insulation).

5) Radiation from the earth and atmosphere is considered to be grey-body type radiation. (The actual radiation distribution from the earth is hard to predict and appears to be at most wavelengths although not ideally grey-body radiation).

6) Reflected solar radiation from the earth and atmosphere is assumed to have the same wavelengths as the incident solar radiation. (The actual reflection may be at different wavelengths due to atmospheric effects).

Step-Wise Methods Of Solution Of Problems

1) Assuming 100% internal heat conduction, pick a value of $(UA)_{B,V}$ where $U_{B,V}=(\frac{k}{x})_{B,V}$, such that the thermal conductivity is attainable preferably between 0.1 and 100 Btu/ft°F hr.) Use this $(UA)_{B,V}$ in Equation 162 to calculate a skin temperature (T_V). (Note: 100% conduction is first approximation due to almost certain conduction from instrumentation mounting to the skin so that 100% heat radiation is not attainable).

2) Using T_V from (1), estimate the external surface requirements and α_s/ϵ_V from Figure 139. (137 for flat-plates, 138 for cylinders).

3) Using ϵ_V and α_s/ϵ_V from (2) calculate the vehicle skin temperature in the earth orbit at 100% sunlight and at 100% earth shadow using Equation 159 and the geometric factors presented in figures in Section V of Reference 18. (Use Figure 140 if G = 0).

4) Compare the three calculated skin temperatures from (1) and (3) and obtain the maximum difference in temperature. Check this temperature band with the required control band. If the calculated band is within the required band, proceed to step (5). If not, go back to step (1) and pick another $(UA)_{B,V}$ and start over.

5) Find the average temperature difference between the skin temperatures and the instrumentation temperature. (T_B-T_V average). Remember that the instrument temperature can be considered to be at the high limit for the highest T_V and at the low limit for the lowest T_V.

6) From this minimum (T_B-T_V) from (5), calculate the required internal heat transfer coefficient, $(UA)_{B,V}$ by use of equation

7) Using $(UA)_{B,V}$ from (6); estimate internal surface coating requirements for 100% radiation heat transfer from the instrumentation to the skin. Use Figure 141 to obtain $h_r/\mathcal{F}_{B,V}$.

8) Using $(UA)_{B,V}$ from (6), estimate the conductivity requirement for 100% heat conduction from the instrumentation to the skin.

9) Compare (7) and (8), if neither solution is feasible, go back to (1) and choose another value of $(UA)_{B,V}$. If (7) is feasible but (8) is not, the design is possible but not desirable -- a new value could be chosen for $(UA)_{B,V}$ in (1). If (7) and (8) are feasible, the design is possible and a combination of conduction and radiation can be used to arrive at an optimum design using the required $(UA)_{B,V}$ from (6).

10) If (9) is successful, the following temperature control conditions have been obtained.

(a) Skin external surface condition ϵ_V, α_s/ϵ_V (2)

(b) Overall $(UA)_{B,V}$ requirements --(6)

(c) 100% radiation surface requirements -- (7)

(d) Maximum instrument temperature band -- (4)

(e) Possible vehicle skin temperatures -- (1) and (3)

Numerical Solution Of Example Problem

Using the stepwise solution of the problem, the following solution to the example was obtained.

1) Estimate to pick T_V :

(a) Set $U_{B,V} = \left(\frac{k}{x}\right)_{B,V}$

$$x = R_V - R_B = 1 - 0.5 = 0.5 \text{ Ft.}$$

(b) Choosing $k_{B,V} = 0.5$ Btu/(ft)(°F)(hr.)

(c) Calculating $A_{B,V}$ for 100% conduction for a sphere:

$$A_{B,V} = 4\pi \frac{(R_V^2 - R_B^2)}{\ln\left(\frac{R_V}{R_B}\right)^2} = 6.8 \text{ Btu/(hr.)(°F)}$$

(d) $(UA)_{B,V} = \left(\frac{kA}{x}\right)_{B,V} = \frac{0.5 \times 6.8}{0.5} = 6.8\ (ft)^2$

(e) From Equation 162:

$$T_V = T_B - \frac{G}{(UA)_{B,V}} = 75 - \frac{100(3.4)}{6.8} = 24°F$$

2) Estimating ϵ_V and α_s/ϵ_V from Figure 139 for $T_V = 50°F$ and $G = 100$ watts:

(a) Estimating $\epsilon_V = 0.8$

(b) $\frac{G}{\epsilon_V A_V} = 10$ watts/$(ft)^2$ $(A_V = \pi D^2 = 12.6 (ft)^2)$

(c) Reading Figure 139 for $T_V = 24°F$ and $\frac{G}{\epsilon_V A_V} = 10$:

$$\frac{\alpha_s}{\epsilon_V} = 0.5 \quad (T_V = 20°F)$$

3) Calculation of T_V for 100% sunlight and 100% shadow in earth orbit:

(a) Estimating Earth radiation to vehicle:

$$E_p = \frac{(1 - \text{ALBEDO PLANET})}{4} S \qquad (164)$$

where albedo = a = 0.35 (Table #4, p. 31, Ref. 18)

$S = 443$ Btu/$(ft)^2$(hr) (Figure 11, p. 26 Ref. 18)

for the 100 mile altitude = (Figure 34, p. 82, Ref. 18)

$$J_p = \frac{q_p}{\pi R_V^2 E_p \alpha_p} = 1.5$$

Solving for q_p , $q_p = \alpha_p (1.5) \pi R_V^2 E_p = 339\,\alpha_p$ Btu/hr.

But $$\frac{q_p}{\epsilon_V A_V} = \frac{\alpha_p A_V F_P E_P}{\epsilon_V A_V} = F_P E_P$$

Since $\alpha_p = \epsilon_V$ from assumption (5)

or $$F_P E_P = \frac{q_p}{\epsilon_V A_V} = \frac{339}{4\pi R_V^2} = 26.9 \text{ Btu/(hr.)(ft.)}^2$$

(b) Estimating Earth solar reflection to vehicle:

$$J_R = \frac{q_R}{\pi S a R_V^2 \alpha_s} = 1.7$$

(For altitude = 100 miles, solar angle, $\theta_S = 0^o$)

Figure 43, Page 98, Reference 18

or $q_R = \alpha_s \pi R_V^2 S a (1.7) = 830\,\alpha_s$ Btu/hr.

$$\frac{q_R}{\alpha_s A_V} = F_R E_R = \left(\frac{\alpha_s}{\alpha_s}\right) \frac{830}{4\pi R_V^2} = 66.2 \text{ Btu/(hr)(ft.)}^2$$

(c) Estimating direct solar radiation to vehicle:

$$F_S = \frac{\pi R_V^2}{4\pi R_V^2} = \frac{\text{Vehicle Solar Radiation Area}}{\text{Vehicle Surface Area}} = \frac{1}{4}$$

$$F_S S = \frac{443}{4} = 110.8 \text{ Btu/(hr)(ft.)}^2$$

Calculating T_V for $\alpha_s/\epsilon_V = 1.0$ and $\epsilon_V = 0.8$: (Eq. 159)

$$T_{V\ \text{SUNLIGHT}} = 155.6 \sqrt[4]{88.5 + 26.9 + 10} = 518^\circ R = 58^\circ F$$

$$T_{V\ \text{SHADOW}} = 155.6 \sqrt[4]{26.9 + 10} = 386^\circ R = -74^\circ F$$

4) Maximum temperature change of skin:

From (1) and (2), the skin temperature can vary from $-74^{\circ}F$ to $58^{\circ}F$ maximum.

For equilibrium $\Delta T_V = \Delta T_B = 58+74 = 132\ ^{\circ}F.$

(This is within the required $150^{\circ}F$ band for ΔT_B)

5) $(T_B - T_V)$ average

T_V average from (1) and (2) = $\frac{58-74}{2} = -8\ ^{\circ}F.$

T_B average = $75^{\circ}F$ (design point)

$(T_B - T_V)$ average = $(75 + 8) = 83^{\circ}F$

6) Required $(UA)_{B,V}$:

Using Equation

$$(UA)_{B,V} = \frac{G}{T_B - T_V} = \frac{341}{83} = 4.11 \ \text{Btu/(hr)(°F)}$$

7) Required internal surface coatings for

from (6) for 100% radiation heat transfer:

$$(UA)_{B,V} = (h_r A)_{B,V} = 4.11$$

From Hottel the combined emissivity and geometric factor for concentric spheres is (Reference: Jacot (107)

$$\mathcal{F}_{B,V} = \frac{1}{\frac{1}{F_{B,V}} + \left(\frac{1}{\epsilon_B} - 1\right) + \frac{A_B}{A_V}\left(\frac{1}{\epsilon_{V_{INTERNAL}}} - 1\right)} = \frac{1}{\frac{1}{\epsilon_B} + \frac{1}{4}\left(\frac{1}{\epsilon_V} - 1\right)} \quad (169)$$

From Figure 141 for $T_B = 75°F.$, $T_V = -8°F$:

$$h_r/\mathcal{F} = 0.82 \ \text{Btu/(hr)(°F)(ft)}^2$$

Substituting:

$$(UA)_{B,V} = (h_r A)_{B,V} = \mathcal{J}_{B,V}\left(\frac{h_r}{\mathcal{J}}\right) A_{B,V} = \frac{0.82 \times 6.8}{\frac{1}{\epsilon_B} + \frac{1}{4}\left(\frac{1}{\epsilon_{V\ \text{INTERNAL}}} - 1\right)} = 4.11 \ \frac{\text{Btu}}{\text{hr.}(^\circ\text{F})}$$

Rearranging: $\frac{1}{\epsilon_B} + \frac{1}{4}\frac{1}{\epsilon_{V(IN)}} - \frac{1}{4} = \frac{0.82 \times 6.8}{4.11} = 1.36$

If $\epsilon_B = \epsilon_{V(IN)}$ (all internal coatings, the same)

$$\frac{5}{4}\frac{1}{\epsilon_B} = 1.36 + \frac{1}{4} = 1.61$$

$$\epsilon_B = \frac{1.25}{1.61} = 0.77$$

8) For 100% conduction:

$$k_{B,V} = \frac{(UA)_{B,V}}{A_{B,V}} X_{B,V} = \frac{4.11 \times 0.5}{6.8} = 0.302 \ \text{Btu}/\text{ft}(^\circ\text{F})(\text{hr.})$$

$k_{B,V}$ is in the range 0.1 to 100 $\frac{\text{Btu}}{(\text{Ft})(^\circ\text{F})(\text{hr.})}$ and thus is attainable for present materials.

Note: $A_{B,V}$ can be altered by use of insulated and conduction paths.

9) Comparison of 100% Radiation and 100% Conduction:

100% radiation heat transfer is possible with internal surfaces at ϵ=0.77. Also, 100% conduction or a combination or radiation and conduction is practical (although $k_{B,V}$ is smaller than originally picked).

10) Summary of design example results:

a) Skin external surface conditions -- $\epsilon_V = 0.8$

$$\frac{\alpha_s}{\epsilon_V} = 0.5$$

b) Overall $(UA)_{B,V}$ requirements $(UA)_{B,V} = 4.11 \ \frac{\text{Btu}}{(^\circ\text{F})(\text{hr.})}$

c) 100% Radiation surface requirements: $\epsilon_B = 0.77$

d) Maximum Instrument Temperature Band:

$$\Delta T_B = 132\,^\circ F$$

e) Possible vehicle skin temperatures:

Solar orbit:		$T_V = 20\,^\circ F$
Earth Orbit:	(100% sunlight)	$T_V = 58\,^\circ F$
	(100% shadow)	$T_V = -74\,^\circ F$

11) Actual possible internal construction to achieve
If the inside sphere is mounted to the skin by two circular flanges and the rest of the space between sphere surfaces is evacuated (with radiation shields), the thickness of the flanges can be calculated as follows:

Average Radius of Flange: $R_{AVG.} = \frac{R_V - R_B}{\ln(R_V/R_B)} = \frac{1-0.5}{\ln 2} = 0.725$ Ft.

$$A_{B,V} = b \times 2\pi \times R_{AVG} \times 2 = b \times 2\pi \times 0.725 \times 2 = 9.1 \times b \text{ ft}^2$$

$$(UA)_{B,V} = \left(\frac{k_{B,V}}{x_{B,V}}\right)(A_{B,V}) = \frac{k_{B,V} \times b(9.1)}{0.5} = 4.11.$$

Solving for $k_{B,V}b$

$$k_{B,V}b = \frac{4.11 \times 0.5}{9.1} = 0.226 \text{ Btu/(hr)(°F)}$$

For steel, $k \approx 10$ Btu/(ft)(°F)(hr)

Solving for b (FLANGE THICKNESS): $b = \frac{0.226}{10} = 0.0226$ ft. $= \underline{0.27 \text{ in.}}$

Thus, two circular steel flanges of thickness 0.27 inches and conductivity $10 \frac{\text{Btu}}{(\text{ft})(^\circ\text{F})(\text{hr})}$ can fulfill the $(UA)_{B,V}$ requirements.

Note: These flanges would affect the localized vehicle skin temperatures so that the assumption (1) of uniform skin temperature is in error. The example only indicates that a solution is feasible, a more complex IBM Program must be used for detailed analysis and final design requirements.

Semi-Passive Temperature Control System Estimates

The equations and curves developed previously for the passive system are directly applicable to the semi-passive system. However, in order to obtain better control of temperature, the possibility of variation in surface conditions and internal heat transfer from or to the instrumentation to the skin is introduced. These variations can be used to compensate for changes in external and internal heat transfer rates in order to keep instrument temperatures within a specified temperature tolerance band. Many methods are available through use of mechanical, chemical, or electrical systems to cause variations in the surface coatings and/or internal heat transfer rate. Some of these methods are illustrated in this report. Figure 146 shows change of UA with T_V.

Basically, the method used in estimating temperatures, coating requirements, and overall internal heat transfer coefficients for the passive system can be used in estimations for the semi-passive system. However, optimum coatings and internal coefficients can now be chosen for each external condition.

Example Steady-State Solution Of A Semi-Passive Temperature Control System

Problem Statement

For the purposes of comparison, the problem will be the same as stated in the passive example. However, the electronic instrumentation will be limited to a $75 \pm 1^{\circ}F$ band instead of $75 \pm 75^{\circ}F$.

Stepwise Method Of Solution Of Problem

All steps are the same as in the passive example except in step 3 use the skin temperature T_V from 1 instead of ϵ_v and α_s/ϵ_v from 2 and calculate the required surface conditions. If the surface conditions are outside the obtainable surface coatings variation in $(UA)_{B,V}$ must be included in the design. Then $(UA)_{B,V}$ must be picked for each equilibrium point to allow a practical choice in surface coating.

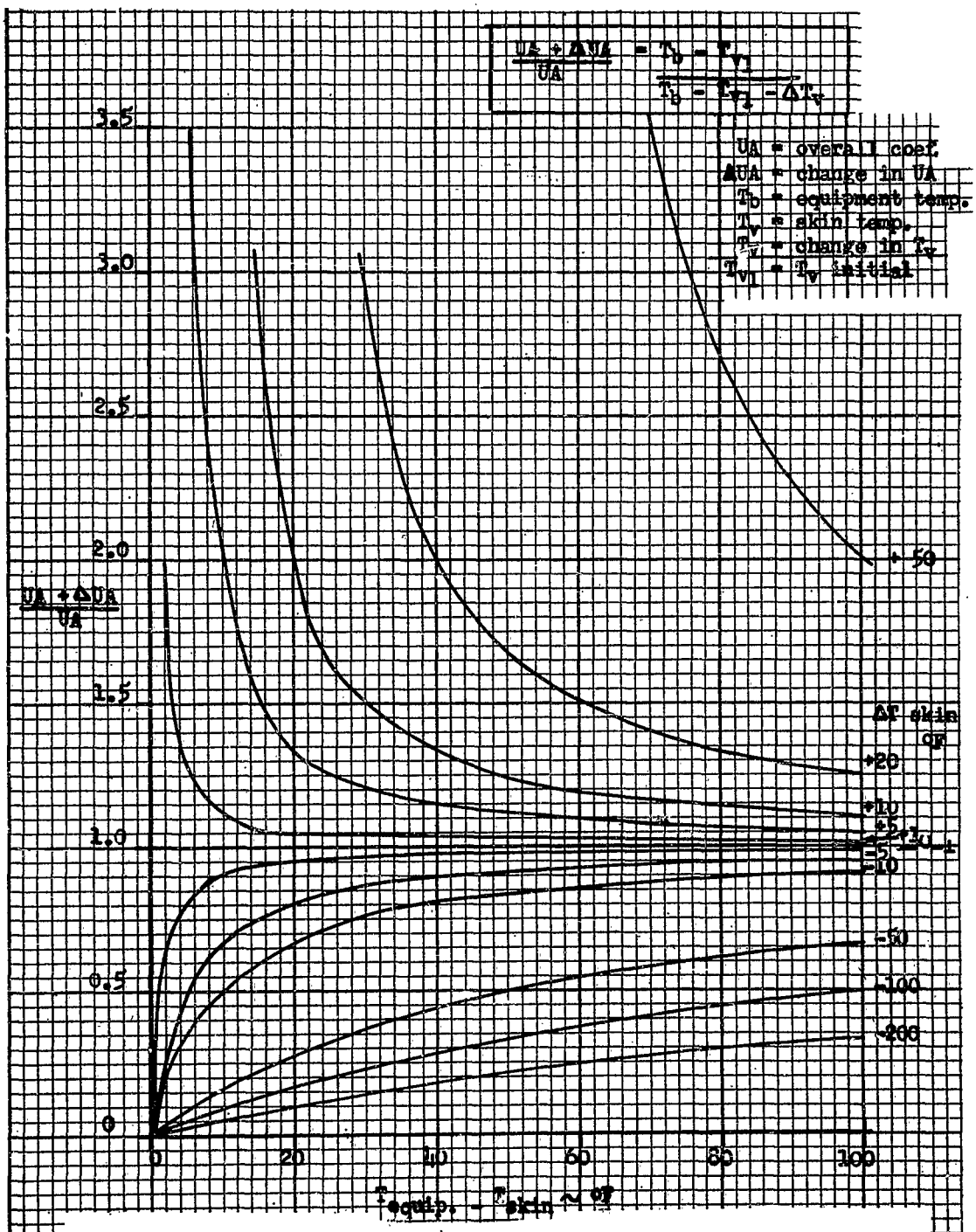

Figure 146. Relationship Between Overall Heat Transfer Coefficient And Skin Temperature For Constant Equipment Temperature And Heat Load

Numerical Solutic Of Example Problem

1) Estimate to pick T_v:

$$K_{B,V} = 0.5 \ \text{Btu/(°F)(ft)(hr)}$$

$$A_{B,V} = 6.8(ft)^2 \ , \ (UA)_{B,V} = 6.8 \ \text{Btu/(hr)(°F)}$$

$$T_V = 24°F.$$

2) Estimating ϵ_v and α_s/ϵ_v for space :

T_v - [illegible]°F and G = 100 watts

From Figure [illegible] 139

$$\epsilon_v = [illegible] 0.8 \ , \ \frac{\alpha_s}{\epsilon_v} = 0.5$$

3) Calculation of ϵ_v [illegible] and α_s/ϵ_v for 100% sunlight and 100% shadow in earth or [illegible]it at 100 mile altitude:

(From the previous [illegible]xample)

$F_p E_p$ = 26.9 Btu/hr ft^2

$F_R E_R$ = 66.2 Btu/hr ft^2

$F_S S$ = 110.8 Btu/hr ft^2

Substituting into Equation

with $\frac{\alpha_s}{\epsilon_v} \approx \frac{\alpha_R}{\epsilon_v}$

and rearranging:

$$\alpha_s = \frac{\epsilon_v (\sigma T_v^4 - F_p E_p) - G/A_v}{F_s S + F_R E_R} \qquad (170)$$

Thus, α_s is defined if ϵ_v is chosen.

Substituting numbers:

$$\alpha_s = \epsilon_v \frac{[\,0.173(4.84)^4 - 26.9\,] - 7.95}{110.8 + 66.2}$$

or

$$\alpha_s = 0.41\,\epsilon_v - 0.045 \qquad \text{For 100\% Sunlight}$$

For $F_S S = 0$ and $F_R E_R = 0$:

$$\epsilon_v = \frac{G}{A_v(\sigma T_v^4 - F_p E_p)} \qquad \text{or} \quad \epsilon_v = \frac{7.95}{68.1} = 0.117 \qquad (171)$$

For 100% Sunlight, if $\epsilon_v = 0.8$:

$$\alpha_s = 0.41(0.8) - 0.045 = 0.283$$

$$\frac{\alpha_s}{\epsilon_v} = \frac{0.283}{0.8} = 0.359$$

For 100% Shadow:

α_s not important
$\epsilon_v = 0.117$

4) Required internal coatings for $(UA)_{B,V}$:

All numbers are the same as in the passive example except $(UA)_{B,V} = 6.8$ instead of 4.11 and $h_r/J = 1.10$.

$$\text{or} \quad \frac{1}{\epsilon_B} + \frac{1}{4}\frac{1}{\epsilon_{v(IN)}} - \frac{1}{4} = \frac{1.10(6.8)}{6.8} = 1.02$$

$$\text{and} \quad \epsilon_B = \frac{1.25}{1.10 + 0.25} = 0.92$$

5) Summary of design example results:

The desired control can be obgained by variation of the skin surface condition as follows:

a) Space with Solar Radiation:

$$\epsilon_V = 0.8 \; , \quad \frac{\alpha_s}{\epsilon_V} = 0.5$$

b) Earth orbit; 100% sunlight:

$$\epsilon_V = 0.8 \; , \quad \frac{\alpha_s}{\epsilon_V} = 0.36$$

c) Earth orbit, 100% shadow:

$$\epsilon_V = 0.12 \qquad \frac{\alpha_s}{\epsilon_V} = \text{ANY VALUE}$$

For 100% conduction;

$$k_{B,V} = 0.5 \ \text{Btu}/(\text{ft})(^\circ\text{F})(\text{hr})$$

$$(UA)_{B,V} = 6.8 \ \text{Btu}/(^\circ\text{F})(\text{hr})$$

For 100% Radiation: $\epsilon_{V(IR)} = \epsilon_B = 0.92$

Skin Temperature; $T_V = 24^\circ\text{F}$

Instrumentation Temperature = 75°F

Instrumentation Temperature Band = 0°F *

* Steady-state (actual band depends on control response and actual coating and $(UA)_{B,V}$ values).

Practical Solutions To The Example Problem

Variable Skin Surface Coating. If the proposed mercury-glass variable radiation surface presented in Section III is considered, then $\alpha_s = 0.07$ and $\epsilon_V = 0.10$ to 0.93 might be values to expect.
For 100% shadow: $\epsilon_V = 0.117$ as before.
For 100% sunlight; From step #3

$$\alpha_s = 0.07 = 0.41 \epsilon_V - 0.045$$

$$\text{or} \quad \epsilon_v = \frac{0.07 + 0.045}{0.41} = 0.28$$

For space:

Eq. 170 reduces to

$$\alpha_s = \frac{\epsilon_v \sigma T_v^4 - G/A_v}{F_s S} \tag{172}$$

and

$$\alpha_s = 0.07 = \frac{95\epsilon_v - 7.95}{110.8}$$

or

$$\epsilon_v = \frac{110.8(0.07) + 7.95}{9.5} = 0.165$$

Thus the proposed mercury control surface can be used. With α_s held constant at 0.07 and ϵ_v varying from 0.117 to 0.28. This system would adapt to the actual transient conditions.

Variable Internal Heat Transfer Coefficient. A variable internal heat transfer coefficient might be obtained by putting two conduction paths and a radiation path in parallel from the instrumentation to the skin. The radiation path could be used to obtain the $(UA)_{B,V}$ required for the earth orbit on the shadow side, one conductivity path plus the radiation path could be used for the space orbit. Two conductivity paths plus the radiation path could be used for the 100% Sun, earth orbit. Conductivity paths could be engaged or disengaged by metallic or bimetallic expansion (See Figure 147).

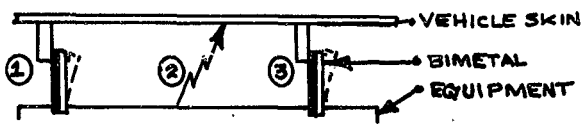

Figure 147. Variable Conduction Sketch (Example Problem)

Using the skin temperatures calculated in the passive example and Equation 165 without fluid flow,

$$(UA)_{B,V} = \frac{G}{(T_B - T_V)}$$

For 100% Sun, earth orbit:

$$(UA)_{B,V} = \frac{341}{75 - 58} = 20.1 \text{ Btu/(hr)(ft.)}^2$$

For 100% earth shadow:

$$(UA)_{B,V} = \frac{341}{75+74} = 2.3 \text{ Btu/(hr)(ft)}^2$$

For Solar, space orbit:

$$(UA)_{B,V} = \frac{341}{75-24} = 6.8 \text{ Btu/(hr)(ft)}^2$$

For parallel conduction paths $(UA)_{B,V}$ can be expressed as

$$(UA)_{B,V} = \left(\frac{kA}{x}\right)_1 + (h_r A)_2 + \left(\frac{kA}{x}\right)_3 \qquad (173)$$

For the 100% earth shadow, the conduction paths can be open and

$$(UA)_{B,V} = (h_r A)_2 = 2.3 \text{ Btu/(hr)(ft)}^2$$

A solution can be obtained for the required internal surface coating, by using the equation developed previously:

$$\frac{1}{\epsilon_B} + \frac{1}{4}\left(\frac{1}{\epsilon_{V(IN)}}\right) - \frac{1}{4} = \frac{(h_r) A_{B,V}}{(UA)_{B,V}} \qquad (174)$$

For $\epsilon_B = \epsilon_{V(\text{INTERNAL})}$:

$$\epsilon_B = \frac{1.25 (UA)_{B,V}}{(h_r) A_{B,V}} + 0.25$$

From Figure 141 for $T_B = 75°F$, $T_V = -74°F$

$h_r \approx 0.70$ Btu/(hr)°F(ft)^2 For blackbody radiation

Substituting:

$$\epsilon_B = \frac{1.25 \times 2.3}{0.70 \times 6.8} = 0.61$$

For solar, space orbit: $T_V = 24°F$, $T_B = 75°F$

$$(UA)_{B,V} = (h_r A)_2 + \left(\frac{kA}{x}\right)_1 = \left[\frac{h_{r(75-24)}}{h_{r(75+74)}}\right](h_r A)_2 + \left(\frac{kA}{x}\right)_1 = 6.8 \text{ Btu/°F(hr)}$$

From Figure 141

$$h_r \approx 0.92 \text{ Btu/(ft)}^2\text{(°F)(hr.)}$$

Substituting:

$$\left(\frac{kA}{x}\right)_1 = (UA)_{B,V} - \left[\frac{h_{r(75-24)}}{h_{r(75+24)}}\right](h_r A)_2 = 6.8 - \frac{0.92}{0.70} \times 2.3 = 3.77 \text{ Btu/°F(hr)}$$

For 100% sun, earth orbit: $T_V = 58°F$, $T_B = 75°F$

$$\left(\frac{kA}{x}\right)_3 = (UA)_{B,V} - \left[\frac{h_{r_{75-58}}}{h_{r_{75+74}}}\right](h_r A)_2 - \left(\frac{kA}{x}\right)_1$$

$h_{r(75-58)} = 1.0$ Btu/(ft)²°F(hr) FROM FIGURE 141

or $$\left(\frac{kA}{x}\right)_3 = 20.1 - \frac{1.0}{0.70} \times 2.3 - 3.77 = 14.0 \text{ Btu/°F(hr.)}$$

For an aluminum conduction path:

$$k \approx 100 \text{ Btu/(ft)(°F)(hr.)}$$

Also, $x = 0.5$ ft.

Thus, $$A_1 = 3.77 \left(\frac{x}{k}\right)_1 = \frac{0.5}{100} \times 3.77 = 0.019 \text{ (ft.)}^2$$

and $$A_3 = \frac{0.5}{100} \times (14) = 0.07 \text{ (ft)}^2$$

Solution. The desired control temperature of the instrumentation can be achieved by providing internal radiation coatings with $\epsilon = 0.61$ and two aluminum conductivity paths of area 0.019 ft^2 and 0.07 ft^2. The conductivity paths would have bimetallic connectors such that path (1) would be disconnected below $T_B \approx 74.5^oF$ and path (3) would be disconnected below $T_B \approx 75.5^oF$. Since the bimetallic connectors will connect or disconnect at set instrumentation temperatures, this control system adapts to the actual transient condition with a pulse modulated control action.

The conduction paths would not have to be one strip. Ideally paths (1) and (3) could consist of a number of conduction strips at spaced intervals. These spaced strips then would be able to correct the instrumentation case temperature at 75 ± 1°F at all points on the sphere. Also, the radiation path (2) could be replaced by a constant conduction path which could be used as a flange between the skin and instrumentation.

Variable Internal Forced Convection (Recirculating Liquid. The heat dissipated by the electronic instrumentation can be transported to the skin by use of a recirculating fluid.

This system has advantages over the radiation and/or conduction temperature control system since the fluid can be directed to the electronic components in the instrumentation which require cooling. Also, the case temperation need no longer be the controlling heat transfer temperature--a much hotter component temperature can be used.

Disadvantages of this system are the additional weight of the system, the power requirements of the pump, and the decrease in reliability. The weight of the system can be prohibitive due to the fluid, heat exchangers and cold-plates, flow control valve, lines and pump. The power requirements for the pump can be high for long lines, high flow rates, or high pressure drops. And the reliability decreases because of possiblities of fluid leaks and pump or control valve malfunction.

For the example problem if the exchanger or cold plate average fluid temperatures are defined as

T_{f1} = fluid temperature at vehicle skin
T_{f2} = fluid temperature in instrumentation

then an estimate of the system requirements can be obtained by the following reasoning.

If the exchangers are ideal and the flow is slow, $T_{f_1} \rightarrow T_V$ and $T_{f_2} \rightarrow T_B$. Thus the mass flow requirement becomes

$$(\dot{m}c)_f (T_{f_2} - T_{f_1}) = G = (\dot{m}c)_f (T_B - T_V) \quad (175)$$

or $\dot{m}c = \frac{G}{T_B - T_V}$. For a given fluid, c is known specific heat and $\dot{m} = \frac{G}{c(T_B - T_V)}$

In this problem, $(T_B - T_V)$ varies from (a) 149°F to (b) 17°F. The change in flow would be $\frac{\dot{m}_a}{\dot{m}_b} = \frac{(T_B - T_V)_b}{(T_B - T_V)_a} = \frac{17}{149} = 0.114$.

For a maximum flow at 0.2 GPM, the minimum flow requirement would be 0.114 x 0.2 = 0.0228 GPM. This would establish the control valve requirements, i.e., proportional or pulse modulated control from 0.0228 GPM to 0.20 GPM.

If $\frac{1}{4}$" tubing was used at 50 feet equivalent flow length where "equivalent" includes additional length to account for bend and valve losses, the flow pressure drop can be calculated as

$$\Delta p = \rho f \frac{L}{D} \frac{V^2}{2g} \quad (176)$$

The friction factor, f, is a function of Reynold's number and pipe surface roughness and is given in curves in most fluid flow books (see Figure 148.) The "gravity constant" in the equation is not a function of external gravity and, therefore, is not affected by the zero-gravity condition.

For the example problem, a typical coolant fluid has the properties $\rho = 110$ lb./cu.ft., $\mu = 3.6$ lb/(hr)(ft), and $c = 0.25$ Btu/(lb.)(°F).
For the $\frac{1}{4}$" tube in aluminum, $D_{inside} = 0.18" = 0.015$ ft., flow area = 1.77×10^{-4} ft.^{2}, and weight = 0.0276 lb/ft (from Reference 84 Perry's Chemical Engineers' Handbook, Page 425).

To find V

$$V = 0.00222 \times \left[\frac{GPM}{\text{Flow Area}(ft^2)}\right] = \frac{0.00222 \times 0.2}{1.77 \times 10^{-4}} = 2.5 \text{ ft./sec.} \quad (177)$$

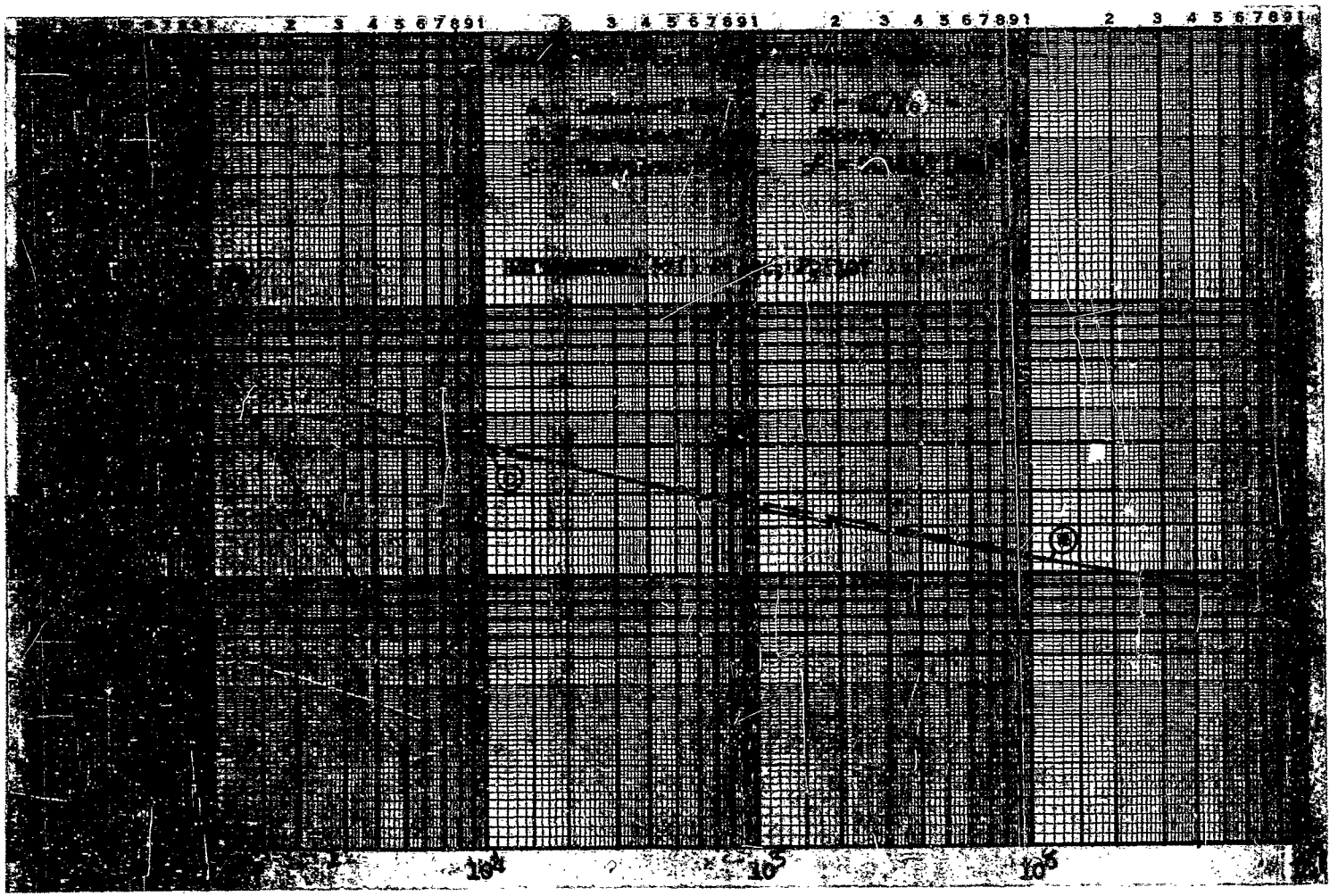

Figure 148. Smooth Tube Fluid Flow Friction Factor

For f:

Reynold's number $= \frac{\rho V D}{\mu} = \frac{110 \times 2.5 \times 0.015 \times 3600}{3.6} = 4100$

From figure 148:

For a smooth pipe with $R_e = 4100$,

$$f = 0.04.$$

Evaluating the pressure drop,

$$\Delta P = \rho f \frac{L}{D} \frac{V^2}{2g} = \frac{110 \times 0.04 \times 50 \times (2.5)^2}{0.015 \times 2 \times 32.2} = 1430 \text{ PSF} = 10 \text{ PSI}$$

$$\text{PUMP POWER} \approx 1.36 \text{ VA } \Delta P = 1.36 \times 2.5 \times 1.77 \times 10^{-4} \times 1430 = 0.86 \text{ WATTS} \quad (178)$$

Thus the pump requirements can be set at 0.2 GPM at 10 PSID head pressure. Such a pump is available and weighs 0.8 lb with 7.5% efficiency, power required is about $\frac{0.86}{0.075} = 11.5$ WATTS.

Summary of fluid system:

Valve: Control from 0.022 to 0.20 GPM at fluid temperatures from -74 to +380F.

Pump:	Maximum flow:	0.20 GPM
	Head Pressure:	10 PSI
	Power Required:	12 watts
	Weight:	0.8 lb

Tubing: $\frac{1}{4}$" O.D. Aluminum:

50 ft. at 50 x 0.0276 = 1.38 lb.

Heat Exchangers or Cold plates:	Not included, depend on design. (see Kays & London or AiResearch Handbook (Ref. 85 and 86) for heat exchanger designs).

Radiators: See Reference 48

Fluid: Line volume = $1.77 \times 10^{-4} \times 50 = 8.85 \times 10^{-3}$ ft^3
Weight = 110 x volume = $110 \times 8.85 \times 10^{-3} = 0.97$ lb

System Requirements

Weight = 3.65 lb (8 oz valve) or higher depending on Heat Exchanger and cold plate weight.

Power = 11.5 watts

Simplified Transient Heat Transfer Analysis

In many applications, the equilibrium analysis is only an approximation useful for estimates of maximum possible temperature variations, temperature control requirements, and vehicle mean skin temperature. The more complex transient analysis is the only way to obtain valid predictions of temperature variations and exact temperature control requirements for most space vehicles.

Most space vehicles can be expected to have variations in external heat loads due to planet, solar, and reflected solar radiation and variations in internal heat dissipation. As a result, the general transient analysis needs to take into consideration the temperature changes and control response requirements for transient heat transfer in the vehicle with variable external and internal heating loads.

Several IBM programs are available for quick solution of highly complex transient heat transfer problems. These programs should be used when possible since they lead to a minimum of engineering time and allow a more detailed analysis. However, many simplified transient analyses have been in use many years. Some of these analyses are Schmidt plots, numerical analysis, classical mathematical approaches using Bessel functions, reiterative stepwise solutions, and passive and electronic differential analog systems. These analyses are the basis for the IBM programs and are useful for simple transient problems and for a basic understanding of the IBM program concepts.

This section shall attempt to show the method of setting up the general transient equations of problems for solution by reiterative stepwise hand solutions, by differential analog, or by IBM program. Also, classical mathematical methods and assumptions will be shown for the single node lumped system and one-dimensional heat conduction problems.

Node Transient Heat Transfer Equations

In general, the smallest number of nodes needed to describe the transient heat transfer are three nodes as shown in the sketch. The therm "nodes" is used in the analog and program language to denote points about which heat transfer equations are formed and heat storage terms have been considered lumped together.

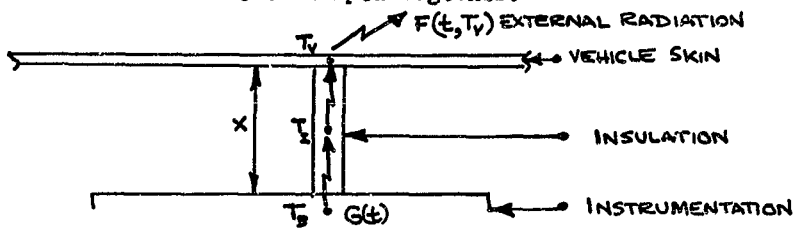

The heat balance about the three node points becomes:

$$\text{SKIN:} \quad m_v c_v \dot{T}_v = F(t,T_v) + \frac{2k_I A_I}{x_I}(T_I - T_v) + \mathcal{J}\sigma A_r (T_B^4 - T_v^4)$$

$$\text{INSULATION:} \quad m_I c_I \dot{T}_I = \left(\frac{2k_I A_I}{x_I}\right)(T_B + T_v - 2T_I) \qquad (179)$$

$$\text{INSTRUMENTATION:} \quad m_B c_B \dot{T}_B = G(t) + 2\frac{k_I A_I}{x_I}(T_I - T_B) + \mathcal{J}\sigma A_r (T_v^4 - T_B^4)$$

These equations can be rearranged to the form

$$\dot{T}_v = \frac{F(t,T_v)}{m_v c_v} + \frac{2k_I A_I}{x_I m_v c_v}(T_I - T_v) + \frac{\mathcal{J}\sigma A_r (T_B^4 - T_v^4)}{m_v c_v}$$

$$\dot{T}_I = \frac{2k_I A_I}{x_I m_I c_I}(T_B + T_v - 2T_I) \qquad (180)$$

$$\dot{T}_B = \frac{G(t)}{m_B c_B} + \frac{2k_I A_I}{x_I m_B c_B}(T_I - T_B) + \frac{\mathcal{J}\sigma A_r (T_v^4 - T_B^4)}{m_B c_B}$$

$F(t, T_V)$ is a function of time and skin temperature with variations in external heat transfer and $G(t)$ is the variation in internal heat dissipation with time.

The equations presented in equation set 180 are solvable by electrical differential analog using $F(t, T_V)$ and $G(t)$ as input functions. Reiterative methods are possible for IBM or hand solution by setting $\dot{T}_V \approx \frac{\Delta T_V}{\Delta t}$, $\dot{T}_I \approx \frac{\Delta T_I}{\Delta t}$, $\dot{T}_B \approx \frac{\Delta T_B}{\Delta t}$ and solving all three equations at a simultaneous interval of Δt.

For simple periodic, ramp, or constant forms of $F(t, T_V$ and $G(t)$, the three equations can be solved by stepwise solution by use of a Friden or other calculators.

Also, for hand or IBM calculations, the time interval t must be smaller than the smallest time constant of the skin, insulation, and instrumentation. The time constant can be calculated from the formula

$$\Delta t_c = \frac{mc}{2UA} \quad .$$

where UA is the overall heat transfer to a node and mc is the node heat storage. The term UA can become extremely complicated for combined forms of heat transfer and is somewhat arbitrary in most cases except for pure convection, conduction, or radiation heat transfer. The time constant is the largest value of t which can be used in a stepwise solution without introducing large oscillations in the step intervals which will invalidate the solution.

The previous equations in Equation Set 180 have not indicated that nature of the thermal properties included. In general, for analog and hand solutions all properties are considered constant with temperature. However, in the actual case, most thermal properties vary to some extent with temperature. Also, for the semi-passive control system the internal and external properties may be controlled as functions of time, temperature, or both. Consequently, the only method for obtaining accurate predictions for even the simple 3-node problem at present is by IBM program.

Some Classical Approaches To Transient Heat Transfer Analysis

Most engineering applied math books and advanced heat transfer books have some examples of mathematical approaches to transient heat transfer problems (References 26, 29, 87, 88 and 89 are examples). The usual solution ends up with some form of Bessel functions or a transient chart such as a Heisler Chart. The solutions presented are generally very limited since boundary conditions such as initial temperatures and heat inputs are very restricted in order to obtain a solution.

Two classical approaches to the solution of transient heat transfer are (1) the solution with lumped mass and specific heat with instantaneous thermal response (infinite conductivity) and (2) the solution of the one dimensional Fourier heat conduction equation with instantaneous temperature changes at the surface with external heat transfer changes. Both solutions have rather limited applications but are useful in certain cases. For instance, the first solution could be used to estimate the average temperature of a low heat dissipating space vehicle subject to variations in external heat radiation with time. The second solution can be useful in estimating maximum temperature gradients in insulations, flanges, windows, and other conduction paths.

Perhaps in the near future, or in Phase IV of this study, an IBM program can be developed for more complicated boundary conditions and two and three dimensional cases.

Case I; Lumped Heat Storage, Large Thermal Conductivity.

The heat balance for Case I is

$$q_\Delta = q_s + q_R + q_P + q_{ov} = \Sigma q \qquad (181)$$

where $q_\Delta = (Mc\dot{t})$ total space vehicle (TSV).

Substituting:

$$(Mc)_{TSV}\dot{T}_{TSV} = \alpha_s A_V F_S S' + \alpha_R A_V F_R E_R + \alpha_P A_V F_P E_P - \epsilon_V \sigma A_V \mathcal{F} (T)_{TSV}^4 \qquad (182)$$

a) For $\Sigma q = q_s + q_R + q_P + q_{ov} = C$ (CONSTANT)

$\dot{T} = \text{Constant} = C_1$

Or $\int_1^2 dT = \int_1^2 C_1\, dt$

And $\Delta T_{1,2} = C_1\, \Delta t_{1,2}$.

b) $\Sigma q = f(t)$,

$$\Delta T_{1,2} = \frac{1}{(Mc)_{TSV}} \int_1^2 f(t)\, dt .$$

c) For $q=f(T)$:

$$\int_1^2 \frac{dT}{f(T)} = \Delta t_{1,2}$$

Example.

For a body suddenly immersed in a fluid

$$hA(T_f - T) = \rho V c \frac{dT}{d\tau}$$

or

$$\int_1^2 \frac{dT}{T_f - T} = \int_1^2 \left(\frac{hA}{\rho V c}\right) d\tau$$

solving

$$\frac{T_f - T}{T_f - T_i} = e^{-\left(\frac{hA}{\rho V c}\right)t} \qquad (183)$$

where T_f = Fluid Temperature

V = volume

T_i = Initial Body Temperature.

This solution is the basis for the time constant used in setting the calculation time interval in stepwise solution by hand and IBM programs. The time constant is $t_c = \frac{\rho V c}{hA}$ which is the value $\frac{T_f - T}{T_f - T_i} = e^{-1} = 0.37$.

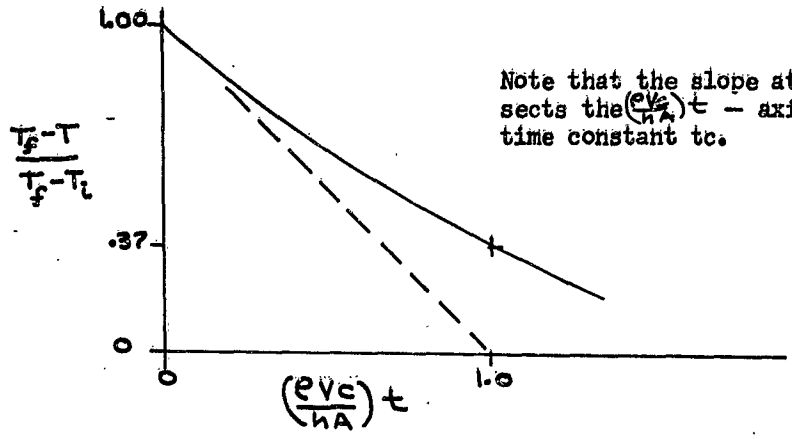

Figure 149. Temperature vs. Time For Body Suddenly Immersed In A Fluid

d) For $\Sigma q = KT^4$

$$(mc)\dot{T} = KT^4$$

$$\text{or} \quad \dot{T} = \frac{dT}{dt} = \left(\frac{K}{mc}\right)T^4$$

Separating variables and integrating

$$\int \frac{dT}{T^4} = \int \left(\frac{K}{mc}\right) dt + C$$

$$\text{or} \quad -\frac{T^{-3}}{3} = \left(\frac{K}{mc}\right)t - \frac{T_i^{-3}}{3}$$

where $T_1 = T$ initial

Rearranging

$$\frac{T}{T_i} = \sqrt[3]{\frac{3}{1 - (T_i)^3\left(\frac{K}{mc}\right)t}} \qquad (184)$$

This is the temperature change with time of an object or skin section with no internal heat dissipation radiating to absolute zero space. A curve of this function is shown on Figure 150. Note that this solution does not have an easily definable time constant as shown in c).

e) For $\Sigma q = K_1(t) + K_2 T^4$

$$mc\,\dot{T} = K_1(t) + K_2 T^4$$

$$\text{or} \quad \dot{T} = K_3(t) + K_4 T^4$$

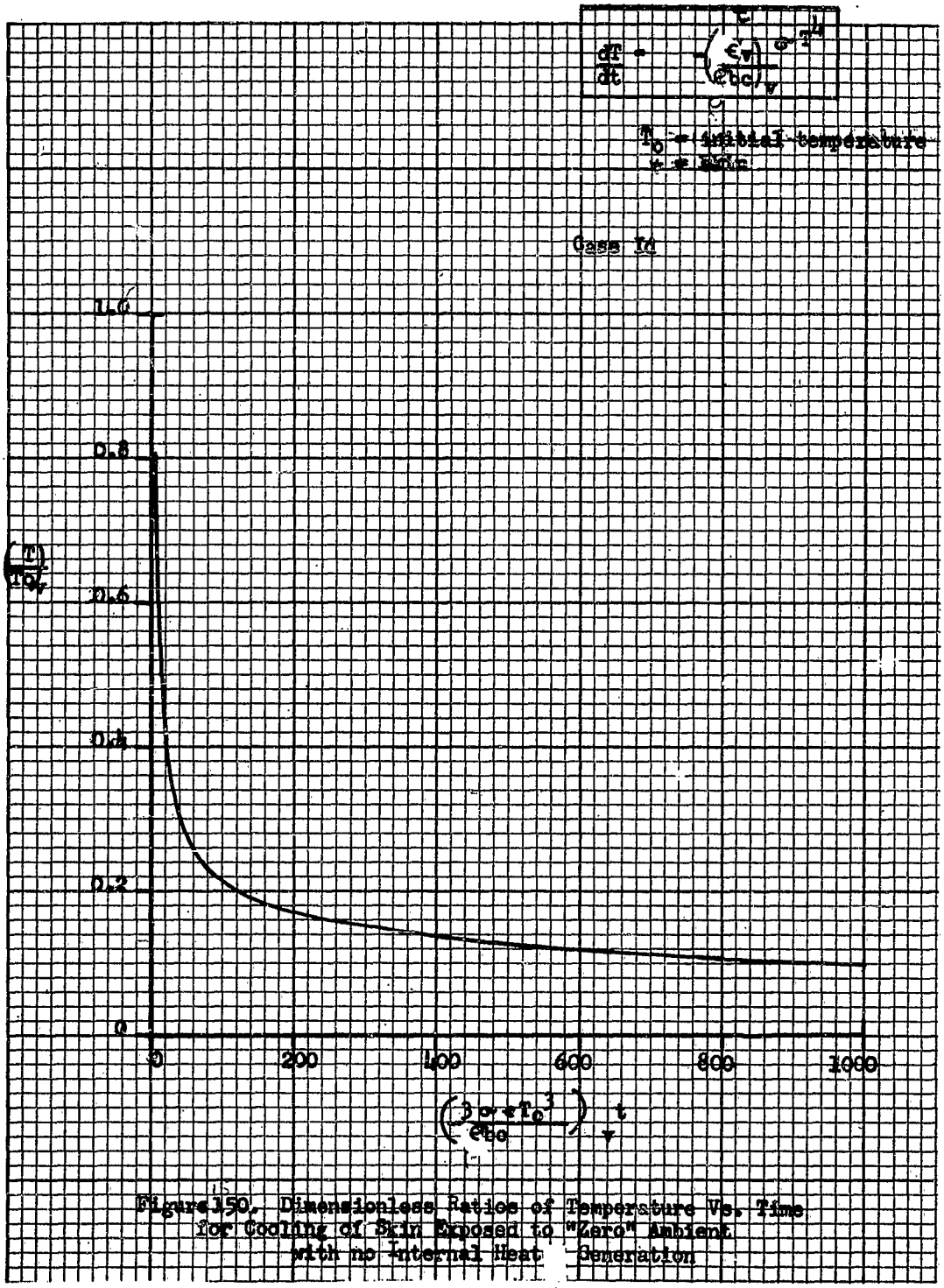

Figure 150. Dimensionless Ratios of Temperature Vs. Time for Cooling of Skin Exposed to "Zero" Ambient with no Internal Heat Generation

Where $K_1(t)$ is some Fourier series relationship with time. This form for Σq is the most usual for satellite vehicles. However, because of the T^4 term, it is difficult to solve. The simplest solution is to let $\dot{T} = \Delta T / \Delta t$ and using $K_3(t)$ for each $t_i + \Delta t$ to solve by step-wise numerical integration. The equation can be integrated directly for K_3 constant.

Let $$\dot{T} = \frac{q}{\rho c b} - \left(\frac{\epsilon \sigma}{\rho c b}\right) T^4 = K_3 - K_4 T^4$$

Separating variables $$\int_{T_o}^{T} \frac{-dT}{K_4\left(T^4 - \frac{K_3}{K_4}\right)} = \int_{t_o}^{t} dt$$

Integrating and Rearranging

$$\left(\frac{3 \epsilon \sigma T_o^3}{\rho c b}\right) t = -\frac{3}{4}\left(\frac{T_o}{T_f}\right)^3 \left\{ \log\left[\frac{(T - T_f)(T_o + T_f)}{(T_o - T_f)(T + T_f)}\right] + 2\left[\tan^{-1}\left(\frac{T_o}{T_f}\right) - \tan^{-1}\left(\frac{T}{T_f}\right)\right]\right\}$$

(185)

Steady-state Temperature $$= T_f = \left(\frac{K_3}{K_4}\right)^{1/4} = \left(\frac{q}{\epsilon \sigma}\right)^{1/4}$$

(See Figure 151. for plotted results)

f) Periodic Heat Transfer: $\Sigma q = hA\left[T_{am} - T + \sum_{n=1}^{n} T_{anm} \cos(\omega_n t - \beta_n)\right]$

The variation in temperature versus time for any periodic function can be expressed by:

$$T_a = T_{am} + \sum_{n=1}^{n} T_{anm} \cos(\omega_n t - \beta_n) \qquad (186)$$

where T_a is the surrounding fluid temperature, T_{am} is the mean temperature, and T_{anm} is the temperature amplitude of the nth harmonic (see Reference 90).

$\omega_n = \frac{2\pi n}{t_o}$ the circular frequency of the nth harmonic (radians/hour)

t_o = period of the first harmonic or fundamental (hours), and

β_n = phase angle of the nth harmonic.

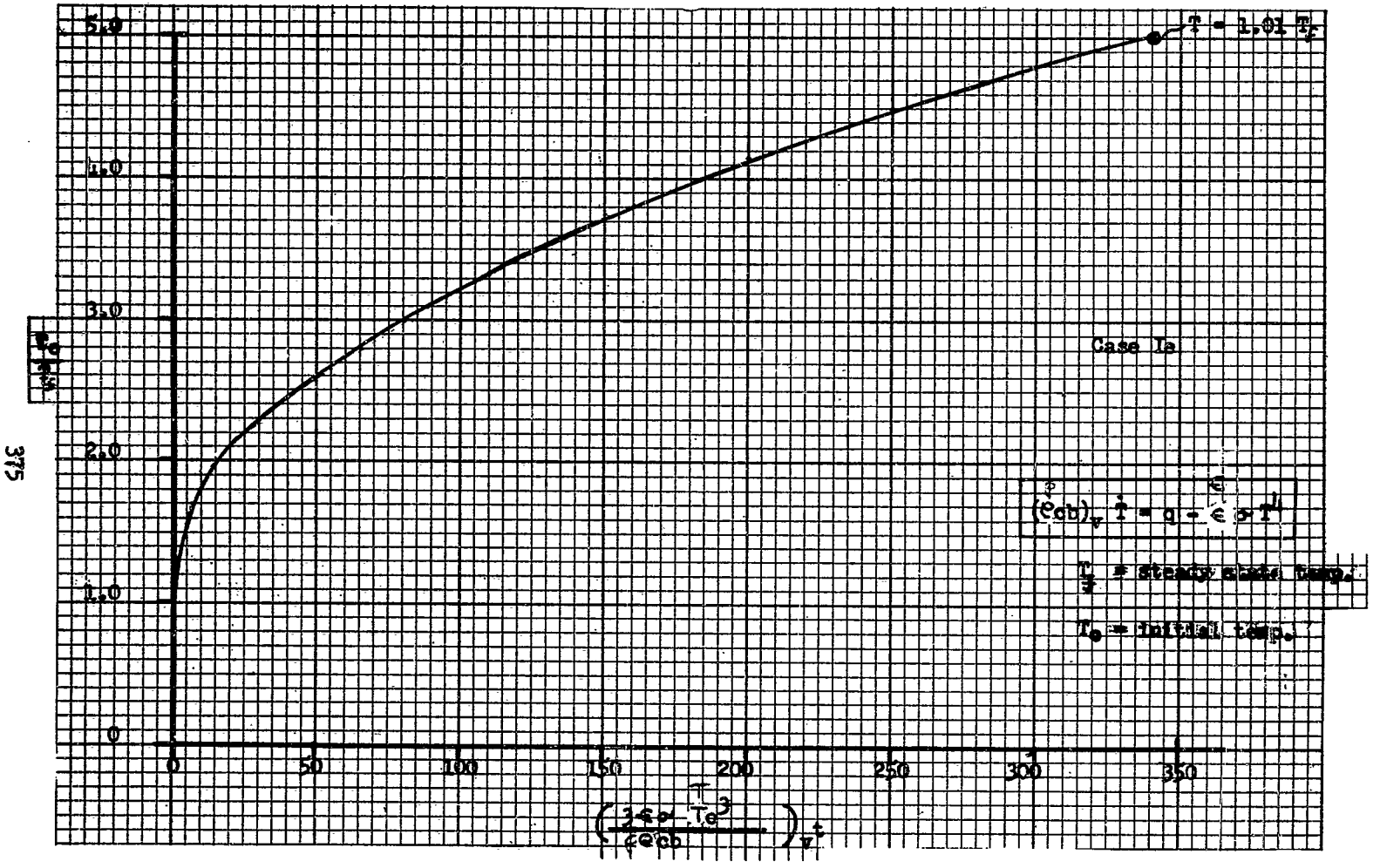

Figure 151. Dimension Less Ratio Of Temperature vs. Time for Cool Down To Steady-State Of Skin Exposed To Zero Ambient With Internal Heat Generation

Substitution of Equation 186 into the form $q_\Delta = \Sigma q$

gives the equation

$$\left(\frac{mc}{hA}\right)\frac{dT}{dt} = T_{am} - T + \sum_{n=1}^{n} T_{anm}\cos(\omega_n t - \beta_n) \qquad (187)$$

Considering an nth harmonic only

$$\frac{dT_n}{dt} + \left(\frac{hA}{mc}\right)T_n = T_{anm}\left(\frac{hA}{mc}\right)\cos(\omega_n t - \beta_n) \qquad (188)$$

The solution consists of two terms, a transient term and a steady state periodic term. For large times, (i.e. long time in orbit), the transient term approaches zero and only the steady-state periodic therm will need be considered. The temperature fluctuation of the lumped mass will have the same frequency as the driving function, the fluid temperature. However, the amplitude T_{nm} will be less and there will be a phase displacement α_n. The solution for the nth harmonic is of the form

$$T_{hm} = T_{anm}\cos\alpha_n = \frac{T_{anm}}{\left[1 - \left(\frac{mc}{hA}\omega_n\right)^2\right]^{1/2}} \qquad (189)$$

and

$$T = T_{am} + \sum_{n=1}^{n} T_{anm}\,\frac{\cos(\omega_n t - \beta_n - \alpha_n)}{\left[1 - \left(\frac{mc}{hA}\omega_n\right)^2\right]^{1/2}} \qquad (190)$$

where $\tan(\alpha_n) = \left(\frac{mc}{hA}\right)\omega_n$.

The previous relationships can be shown by use of the vector diagram (Figure 152).

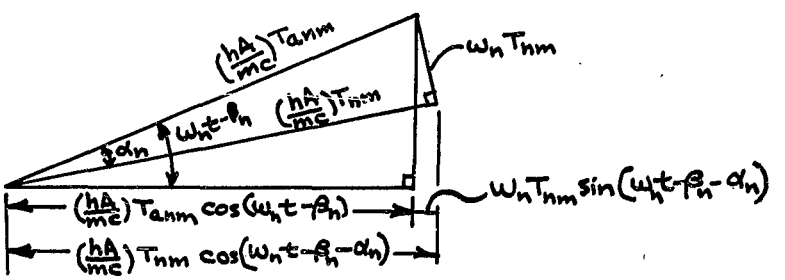

Figure 152. Vector Relationship of Periodic Heat Transfer Temperatures

Note that the amplitude of the fluctuations in the temperature of the lumped mass, $\frac{1}{\left[1+\left(\frac{mc}{hA}\omega_n\right)^2\right]^{1/2}}$ decreases with increasing m or ω_n.

A plot of $\frac{1}{\left[1+\left(\frac{mc}{hA}\omega_n\right)^2\right]^{1/2}}$ versus $\left(\frac{mc}{hA}\right)\omega_n$ shows that

amplitude decreases to 0.015 at $\left(\frac{mc}{hA}\right)\omega_n = 66$.

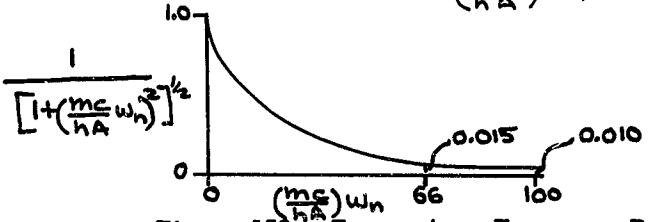

Figure 153. Temperature-Frequency Relationship For Periodic Heat Transfer

Thus, in any space vehicle with low internal heat dissipation where the product $\left(\frac{mc}{hA}\right)\omega_n > 66$, the mass can be considered at a constant temperature and the mass will assume the mean temperature of the periodic driving temperatures.

Case II. Instantaneous Temperature Response at Surface. For the case of instantaneous temperature response at the surface, the heat transfer to a conducting body can be written as the one-dimensional Fourier equation,

$$\frac{\partial T}{\partial t} = a\,\frac{\partial^2 T}{\partial x^2} \quad \text{where} \quad a = \frac{k}{\rho c} = \text{Thermal Diffusivity} \qquad (191)$$

This equation can be solved easily for constant heat inputs and step-changes in surface temperature. Such solutions have been carried out for plates, cylinders and spheres and plotted as Heisler charts or in similar charts. The temperature can be obtained for any time and distance from the surface by looking at values on these charts. However, these limited boundary conditions are not very useful for most conduction problems in space with varying boundary conditions and a non-linear T^4 radiation away from the surface.

One solution which can be of use in space vehicle analysis is that for periodic heat transfer for semi-infinite solid. This solution or a slight modification can be used to predict the effects of periodic heat transfer due to rotation of the vehicle or changes in radiation in a planetary orbit. The solution can also be used to predict at what value of thickness of material the periodic temperature changes will be effectively damped out.

If the Fourier conduction equation is used with the cyclic ambient fluid temperature variation as described in Equation 180 and transient results are ignored (long time), the equation for temperature becomes

$$T = T_{am} + \sum_{n=1}^{n} \frac{T_{amn} e^{-x\sqrt{\frac{\omega_n}{2a}}} \cos\left(\omega_n t - \beta_n - x\sqrt{\frac{\omega_n}{2a}} - \phi_n\right)}{\left[1 + \sqrt{\frac{2\omega_n k^2}{ah^2}} + \frac{\omega_n k^2}{ah^2}\right]^{1/2}} \qquad (192)$$

where $\phi_n = \tan^{-1}\left(\frac{1}{1 + \sqrt{\frac{ah^2}{2\omega_n k^2}}}\right)$ = phase lag between fluid temperature and surface temp.

x = distance in body from surface (ft)

$\frac{1}{\left[1 + \sqrt{\frac{2\omega_n k^2}{ah^2}} + \frac{\omega_n k^2}{ah^2}\right]^{1/2}}$ = temperature amplitude reduction factor from fluid to surface of body.

$e^{-x\sqrt{\frac{\omega_n}{2a}}}$ = temperature amplitude reduction factor from surface to depth x.

$x\sqrt{\frac{\omega_n}{2a}}$ = phase lag from surface to depth x.

Observe that if the surface temperature variation is given as

$$T_o = T_{om} + \sum_{n=1}^{n} T_{onm} \cos(\omega_n t - \beta_n) \tag{193}$$

the result is

$$T = T_{om} + \sum_{n=1}^{n} T_{onm}\, e^{-x\sqrt{\frac{\omega_n}{2a}}} \cos\left(\omega_n t - \beta_n - x\sqrt{\frac{\omega_n}{2a}}\right) \tag{194}$$

A study of this equation reveals a damped temperature wave travelling into the solid with a wave velocity $2\sqrt{\frac{\pi n a}{t_o}}$ ft/sec and a wave length of $2\sqrt{\frac{\omega}{2a}}$ feet. It is also apparent that the higher frequencies decrease much more rapidly with depth. A plot of the temperature amplitude of the nth harmonic divided by the surface amplitude as a function of $x\sqrt{\frac{\omega_n}{2a}}$ yields the following curve (Figure 154).

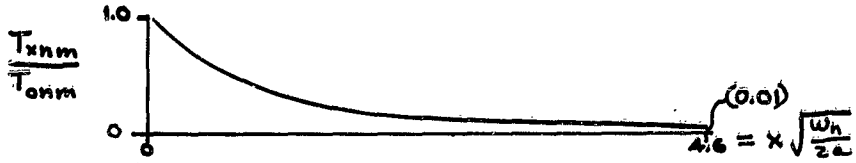

Figure 154. Temperature Amplitude vs. Distance at One Frequency

Thus, the amplitude becomes $\frac{T_{onm}}{100}$ at a value of $x\sqrt{\frac{\omega_n}{2a}} = 4.6$.

At this point the amplitude could be considered damped and

$$x = \frac{4.6}{\sqrt{\omega_n/2a}} = 4.6\left(\frac{2k}{\rho c}\right)^{1/2}\frac{1}{(\omega_n)^{1/2}} \tag{195}$$

From this relationship, $x = \frac{k}{\sqrt{\omega_n}}$ for a known material where K = a constant, $4.6\left(\frac{2.5}{\rho c}\right)^{1/2} = 6.5\sqrt{a}$. In other words, a material with a thermal diffusivity (a) or a fast rotation rate (w_n) will cause the distance of penetration of the periodic temperature variation to decrease.

Equation 195 or Figure 155 can be useful in estimating the distance at which uniform or low heat dissipating equipment should be mounted from the surface (skin) to achieve a desired maximum instrumentation temperature amplitude.

Solution Of One Dimensional Heat Conduction Problem By Method Of Finite Differences. The stepwise solution for transient heat transfer problems can be simplified by setting the calculation time interval Δt equal to a product of a simple constant and the time constant t_c.

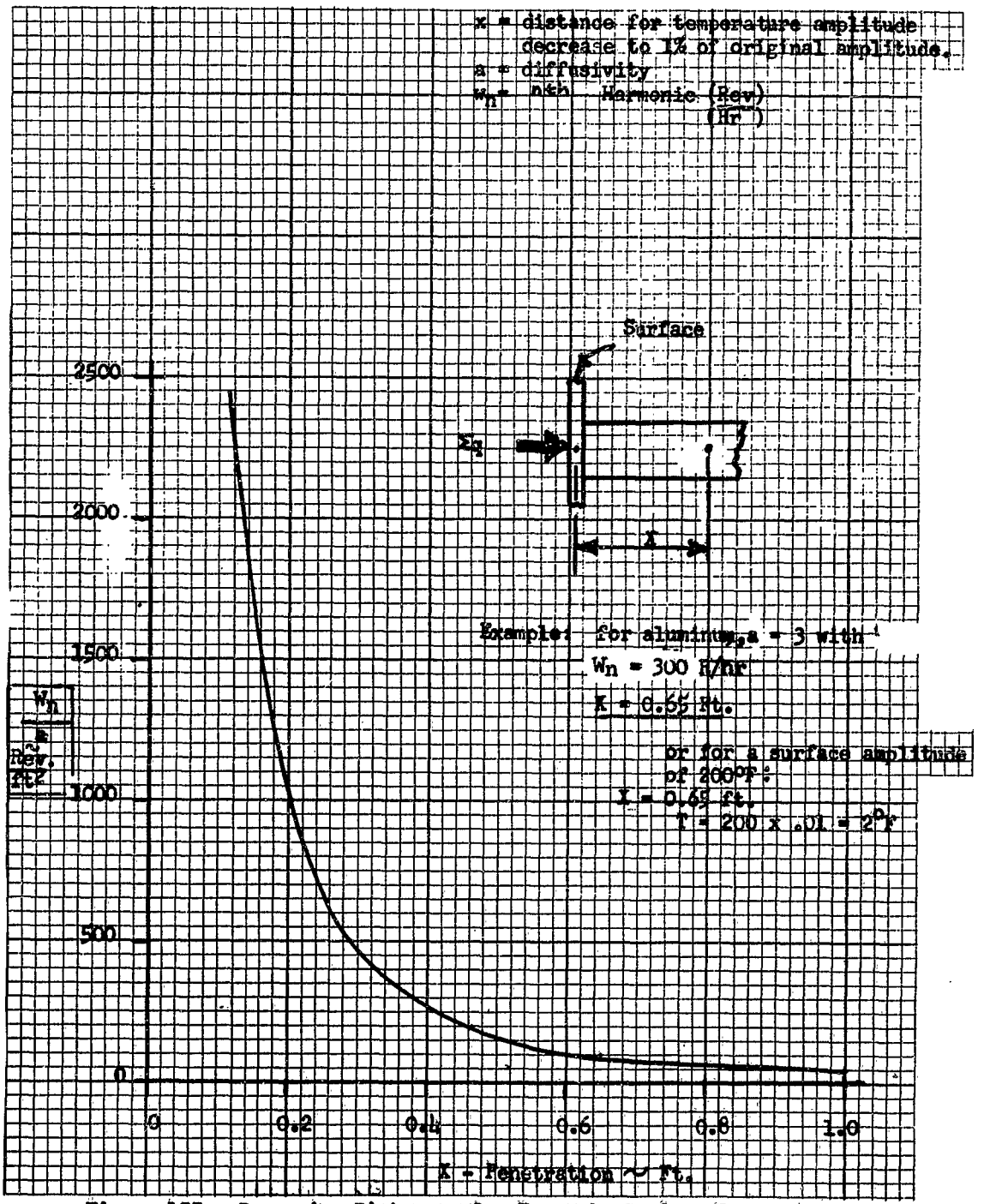

Figure 155. Dampening Distance of a Harmonic Surface Temperature In a One-Dimensional Conduction Path

For example, consider a one dimensional conduction path (Figure 156).

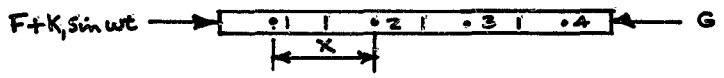

Figure 156. One Dimensional Heat Path Sketch

This could be a heat transfer path from the vehicle skin to the internal equipment with $F + K_1 \sin \omega t$. the external heat radiation and G the internal heat dissipation. If x = the distance between nodes and k = conductivity, A = conduction area, M = mass, c = specific heat of node, then the time constant $t_c = \frac{Mc\,x}{kA}$.

Thus, the calculations interval can be set as $\Delta T = \frac{t_c}{2}$ and the heat transfer equations for the inner nodes becomes

$$\frac{\Delta T_2}{\Delta t} = \frac{kA}{xMc}(T_1 + T_3 - 2T_2), \quad \Delta T_2 = T_2' - T_2 = \frac{T_1+T_3}{2} - T_2$$

$$\text{or} \quad T_2' = \frac{T_1+T_3}{2}; \quad \text{in general} \quad T_n' = \frac{T_{n-1}+T_{n+1}}{2}. \tag{196}$$

A numerical table can be set up of nodes versus time in intervals Δt and the temperatures can be solved easily. A graphical solution can also be solved and is known as a Schmidt plot. However, the table is more effective for Fourier series solutions or wave solutions where alternate cooling and heating causes temperatures to fluctuate such that the lines on a graphical solution would overlap and come back into each other thus confusing the plotter. Further extensions of the method of Schmidt plots are shown in Jacob's (Ref. 89) and Giedt (Ref. 26).

Electrical Analog Networks

Before the digital programs were developed, complicated transient heat transfer problems were solved by use of electrical analog networks. These electrical networks were studied by the programmers for the digital programs. As a result, the view point of most heat transfer programs reflects an electrical analog network. For example, the Lockheed program uses the passive thermal-electrical analog network, the North American Aviation AESOP Program uses the differential analyzer approach, and the S&ID program uses a combination of

Table 44. Differential Analyzer Operations

	Math Function	Symbol	Circuit	Electrical Function	Remarks
1		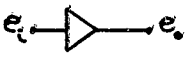		$\frac{e_o}{e_i} = -\infty$	High gain amplifier
2	Multiplication by a constant	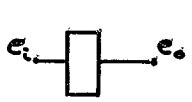		$\frac{e_o}{e_i} = -\frac{R_f}{R_i}$	also $\frac{e_o}{e_i} = -\frac{Z_f}{Z_i}$
3	Integration	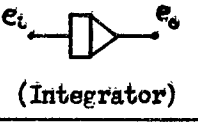 (Integrator)	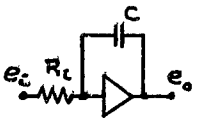	$\frac{e_o}{e_i} = -\frac{1}{RCS}$ For $RC=1$: $e_o = -\int_0^t e_i\,dt$	$Z_f = \frac{1}{CS}$, $S \equiv \frac{d}{dt}$ ($S=2\pi f$ for sine wave)
4	Multiplication by adjustable constant	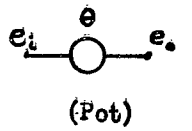 (Pot)	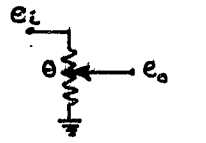	$\frac{e_o}{e_i} = \theta$	
5	Summing with multiplication by constants	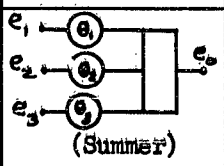 (Summer)	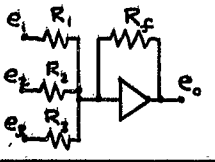	$e_o = -R_f \sum_{n=1}^{\infty} \frac{e_n}{R_n}$	
6	Multiplication with two variables	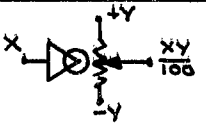			
7	Arbitrary function generator	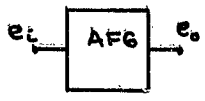		$e_o = f(e_i)$	$f(e_i)$ can be any single-valued function.
8	Division	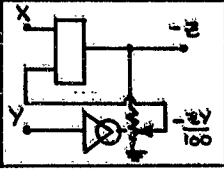		$\frac{z}{100} = x - \frac{xy}{100} = 0$ $z = 100\frac{x}{y}$	

Table 45. Analogous Electrical-Thermal Quantities For a Passive Analog Network

	Electrical	Thermal
1	Charge = q (coulomb)	Heat = Q (Btu)
2	Voltage - (volt)	Temperature = T (^{o}F, ^{o}R)
3	Resistance = R (ohm)	Resistance = R(hr ^{o}F/btu)
4	Current = i (ampere)	Heat Flow = q (btu/hr.)
5	Capacitance = C (farad)	Heat capacity = V_pC_p (Btu/^{o}F)

the passive network and the Oppenheim radiosity network.

Electrical analog networks are useful in arranging heat transfer terms for problem solution. Consequently, the typical network arrangement of a passive electrical analog solution, an electronic differential analyzer solution, and a radiosity electrical analog solution are presented here.

Electronic Analog Computer. D-C Analog Computers are relatively simple electronic devices commonly in use to solve a wide variety of problems in applied mathematics. With the building blocks of the computer the functions of addition, subtraction, multiplication, division, and integration can be used to construct a mathematical model of the equations to be solved (Table 44). The variables of the problem are related to the mechanized equations in terms of properly scaled voltages that are continuously recorded as the problem solution progresses, on some convenient output device.

Passive Network Computer. The Passive Network Computer is limited in the variety of problems it can solve, and is generally classified as a special purpose computer. It differs basically from electronic analog computers in that its elements (resistors, capacitors, inductors) and the machine variables (voltage, current, charge) bear a direct analogy to the coefficients and variables in the problem being solved. In other words, the variables in the mechanization obey a set of physical laws in the same manner that the variables of the problem obey a different set of physical laws. For example, the force equation for a mass-spring-damper system is

$$M\ddot{r} + B\dot{r} + K\int \dot{r}\,dt = F(t) . \qquad (197)$$

The voltage equation for a series L-R-C circuit is $L\dot{I} + RI + \frac{1}{C}\int I\,dt = E(t)$ The analogous quantities are evident. Table 45 lists some electrical-thermal analog equivalent quantities.

The Oppenheim Radiosity Network. Enclosure consisting of four surfaces:

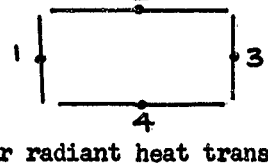

Radiosity network for radiant heat transfer between surfaces:

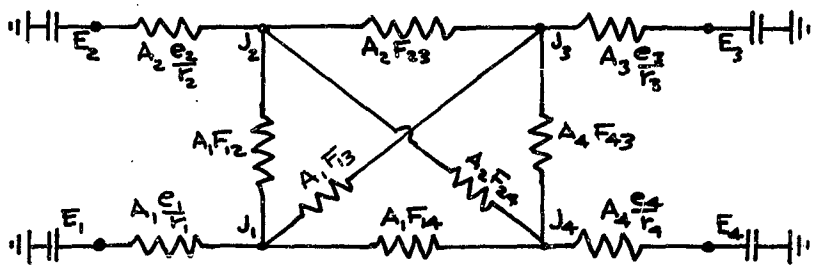

Figure 157. Radiosity Network

A = Surface Area (Ft^2)

E_b = Blackbody Radiation , Btu/(sq.ft.)(hr.)

F = Shape Factor

J = Radiosity, Sum of Emitted, Reflected, and Transmitted Radiation Flux Per Unit Area , Btu/(sq.ft.)(hr.)

e - Surface Emissivity

r - Surface Reflectivity

A more complete presentation of the radiosity network is included in Reference 18 and in Oppenheim's original paper (Ref. 30).

One Dimensional Heat Flow Problem. To demonstrate the use of analog computers (both active and passive) in solving thermodynamic problems, a basic one dimensional heat flow problem will be considered. From a previous discussion, it was seen that the equation for the rate at which a homogeneous medium (with no internal heat sources) stores heat is given by

$$c_p \rho \, dx \cdot dy \cdot dz \frac{\partial T}{\partial t} = dx \cdot dy \cdot dz \, K \frac{\partial^2 T}{\partial x^2} \qquad (198)$$

Since analog computers can only handle equations with time derivatives, it will be necessary to convert equation 7 into its finite difference form. Thus, instead of solving for temperature at all stations x, solve only for the temperatures at stations x 1,2, ...N. Let these stations be spaced at equal intervals, Δx, as indicated in Figure 158. The length of this interval affects the accuracy of the solution. When the medium is sectioned into a number of elements, the assumption is made that, for any instant of time, the temperature throughout the element is the same. Also, in replacing derivatives with finite differences, the accuracy of the approximation is increased by keeping the interval small.

The heat flux vector $K\frac{\partial T}{\partial x}$ at the N + $\frac{1}{2}$ station can be approximated by

$$K\left.\frac{\partial T}{\partial x}\right|_{N+\frac{1}{2}} = \frac{K_{N+\frac{1}{2}}}{\Delta x}\left(T_{N+1} - T_N\right) \tag{199}$$

The limit of this equation as $\Delta x \to 0$ is simply the partial x derivative at that point. Similarly, the $\frac{\partial}{\partial x}\left(K\frac{\partial T}{\partial x}\right)$ term for the Nth element can be approximated by

$$\left.\frac{\partial}{\partial x}\left(K\frac{\partial T}{\partial x}\right)\right|_N = \frac{1}{\Delta x}\left[K\left.\frac{\partial T}{\partial x}\right|_{N+\frac{1}{2}} - K\left.\frac{\partial T}{\partial x}\right|_{N-\frac{1}{2}}\right] \tag{200}$$

Equations 198 and 200 result in

$$c_p V \rho \frac{dT_N}{dt} = A\Delta x \cdot \frac{1}{\Delta x}\left[\frac{K_{N+\frac{1}{2}}}{\Delta x}(T_{N+1}-T_N) - \frac{K_{N-\frac{1}{2}}}{\Delta x}(T_N - T_{N-1})\right]$$

$$= \frac{K_{N+\frac{1}{2}}}{\Delta x}A(T_{N+1}-T_N) - \frac{K_{N-\frac{1}{2}}}{\Delta x}A(T_N - T_{N-1}) \tag{201}$$

where V is the volume of the element, and A is the surface area normal to the heat flux. Since the medium is homogeneous, and the dimensions of each element are the same, equation 10 reduces to

$$\frac{dT}{dt} = \frac{K}{c_p \rho \Delta x^2}\left[T_{N+1} - 2T_N + T_{N-1}\right] = K'\left[T_{N+1} - 2T_N + T_{N-1}\right] \tag{202}$$

This is the desired form of the equations when presenting them for analog solution. That is, explicity solve for the highest ordered derivative.

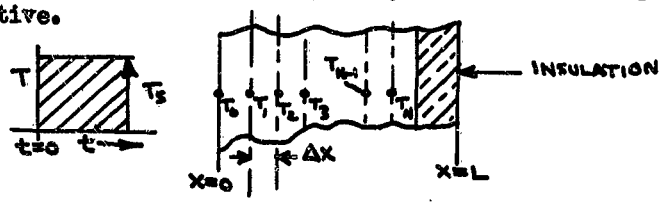

Figure 156. One-dimensional Transient Heat Transfer Example

For a given heat flow problem, it is always necessary to stipulate spacial boundary conditions either on the temperature T or the heat flux $K\frac{\partial T}{\partial x}$, as well as the initial temperature distribution throughout the medium. Consider that the infinite slab of Figure 158 be bounded on one side by insulation such that there is no heat flow past the wall. It may be required to determine the transient decay for some initial temperature distribution when the other boundary is maintained at zero temperature, or it may be required to determine the temperature - time history for the chosen points when, initially, the medium has the same temperature throughout and then is subjected at the other boundary to a step input. Let us consider the latter case.

Equations To Be Solved.

$$\begin{aligned} T_o &= T_s \\ T_1 &= K' (T_2 - 2T_1 + T_o) \\ T_2 &= K' (T_2 - 2T_1 + T_1) \\ T_n &= K' (T_{n+1} - 2T_N + T_{N-1}) \end{aligned} \qquad (203)$$

Boundary Conditions. When the specified boundary condition is on temperature, this condition occurs at a full station. If it is on heat flux, this condition occurs at a half station. Therefore, the step input occurs at the point T_o, and the zero flux occurs at the $N + \frac{1}{2}$ station.

$$T(0,t) = T_s \quad , \quad K\frac{\partial T}{\partial x}(L,t) = 0$$

Initial Conditions.

$$T(x,0) = T_c \text{ for all } x$$

The lowest temperature existing in the problem is generally considered zero voltage in the machine. If $T_C = 300^oF$, this would correspond to zero voltage. The step input to the circuit will result in a transient voltage rise at each point, which when converted to temperature, is added to the initial 300^oF.

Non-Homogeneous Medium Unequally Spaced Points. The heat conduction problem encountered most frequently in heat transfer work involves medium whose elements have dissimilar conductivities and dimensions. When solved for the time derivative of temperature, equation becomes, for this case,

$$\dot{T}_N = \frac{K_{N+1,N} A_{N+1,N}}{W_N S_N X_{N+1,N}} \left(T_{N+1} - T_N\right) - \frac{K_{N,N-1} A_{N,N-1}}{W_N S_N X_{N,N-1}} \left(T_N - T_{N-1}\right) \quad (204)$$

where $W_N = \rho_N V_N$ (Lb.)

and $A_{N+1,N}$ is surface area normal to heat flux vector and common to the elements N + 1 and N.

The equivalent thermal conductance between typical temperature points is given by

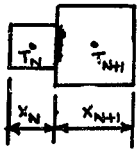

$$U_{N,N+1} = \frac{K_{N+1,N} A_{N+1,N}}{X_{N+1,N}} = \frac{1}{\frac{X_N}{2K_N A} + \frac{X_{N+1}}{2K_{N+1} A}} \quad (205)$$

Combining all terms in the coefficients into one symbol, equation (204) becomes

$$\dot{T}_N = U'_{N,N+1}\left(T_{N+1} - T_N\right) - U'_{N-1,N}\left(T_N - T_{N-1}\right) \quad (206)$$

where

$$U'_{N,N+1} = \frac{U_{N,N+1}}{C_N W_N} \quad \text{and} \quad U'_{N-1,N} = \frac{U_{N-1,N}}{C_N W_N}$$

The mechanization of Figure 160 is the general case for N temperature points. Whereas the mechanization for the case of homogeneous medium and equally spaced points required one amplifier per temperature point, the present case requires three amplifiers per temperature point, However, in the latter case, the heat flux times a constant, $\frac{A_{N+1,N}}{C_N W_N}$, can be recorded for each element, in addition to the temperature.

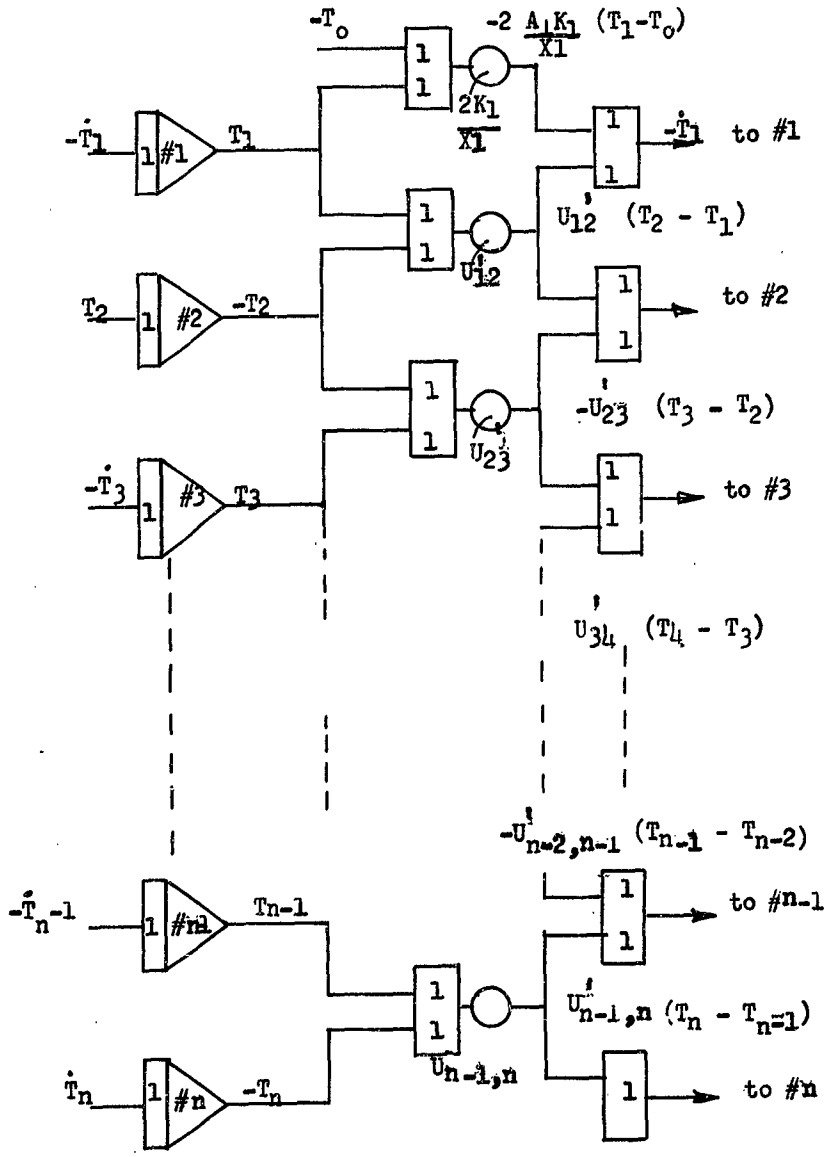

Number of Amplifiers Approximately 3X No. of Points

Figure 160. Electronic Analog Mechanization - General Case for Heat Transfer

One Dimensional Mechanization For Homogeneous Slab And Equally Spaced Points. In this mechanization, the operational amplifiers are performing a number of functions:

1. Sum three inputs
2. Multiply one input by constant factor, 2.
3. Integrate the sum
4. Invert the sign of the input

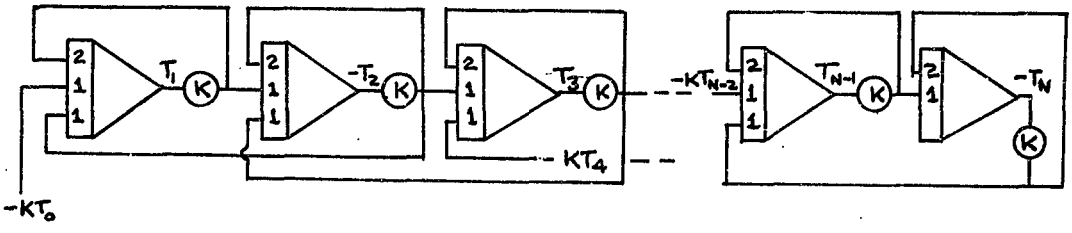

Figure 159. One-Dimensional Electronic Analog Mechanization For Homogenious Slab And Equally Space Points

One Amplifier per point is required

Passive Network Mechanization. The direct analogies between thermal and electrical quantities, as previously outlined, lead to a single mechanization for both one dimensional problems just considered. The circuit is indicated below:

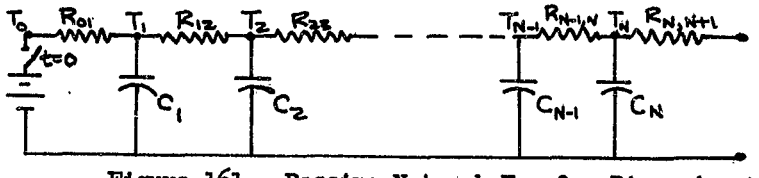

Figure 161. Passive Network For One-Dimensional Heat Transfer

Homogenious Medium:

$$R_{01} = \frac{\Delta X}{2KA} = R_{N,N+1} \qquad C_{1,2,..} = c_p \rho V$$

$$R_{12} = R_{23} = \cdots = R_{N-1,N} = \frac{\Delta X}{KA} \tag{207}$$

Non-Homogenious Medium.

$$R_{01} = \frac{X_1}{2K_1 A_{01}} \qquad C_1 = c_{p_1} \rho_1 V_1$$

$$R_{12} = \frac{X_1}{2K_1 A_{12}} + \frac{X_2}{2K_2 A_{12}} \qquad C_2 = c_{p_2} \rho_2 V_2 \qquad (208)$$

$$\vdots \qquad\qquad \vdots$$

$$R_{N-1,N} = \frac{X_{N-1}}{2K_{N-1} A_{N-1,N}} + \frac{X_N}{2K_N A_{N-1,N}} \qquad C_N = c_{p_N} \rho_N V_N$$

$$R_{N,N+\frac{1}{2}} = \frac{X_N}{2K_N A_{N,N+\frac{1}{2}}} \quad \left(\text{Not required this case since } K\frac{\partial T}{\partial x}\Big|_{N+\frac{1}{2}} = 0\right)$$

Simulation Of Radiation On Electronic Analog Computer. Many problems in thermodynamics involve the transfer of radiant energy. The Stephan-Boltzman equation for the net radiant exchange between two radiators is

$$q = \sigma F_E F_A A\left(T_1^4 - T_2^4\right) \qquad (209)$$

where q = heat rate
A = area
σ = Stephan-Boltzman Constant
F_A = shape factor
F_E = emissivity factor

The use of a servo-multiplier in taking integral powers of a variable was indicated in Table 44. This is precisely the method by which temperatures are raised to the fourth power. There is, however, one modification from the equipment standpoint that is required to prevent potentiometer loading effects. As indicated in Figure 162, amplifiers are used to isolate the follower-pots from each other.

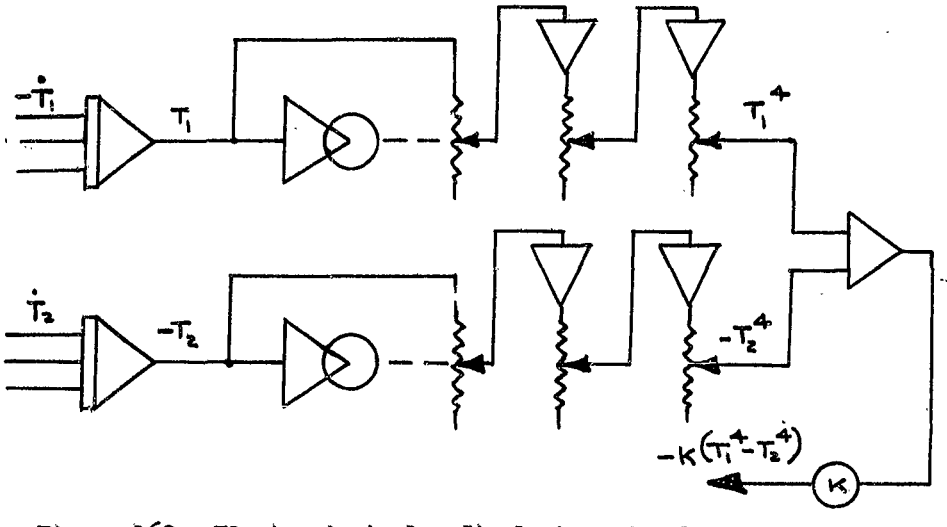

Figure 162. Electronic Analog Simulation of Radiation

Radiation between two temperature points is calculated and the term is fed back to be summed and integrated with other terms in the heat flow equation for the particular point. Simulation of radiation is expensive of equipment. For interfacial radiation, each point requires one servo-multiplier, two and one half amplifiers and one potentiometer.

Simulation Of Radiation On Passive Network Computer. To represent rate of heat loss due to radiation on a passive network computer, current must be drawn away from a temperature point N according to the relation

$$i_{NR} = K v_N^4 \qquad (210)$$

Since only the first power of voltage is available at any point in the analogy, and since current dissipation can only be brought about by changing load, the expression is mechanized by loading the point N with a resistance that varies according to the relation $R=1/Kv^3$. For such a resistance, current flow according to Ohm's Law (current=voltage/resistance) will be a function of v^4.

The variation of resistance is approximated in a stepwise fashion so that the current characteristic is approximated by straight line segments, as indicated in Figure 163A shown below.

The biased diode circuit of Figure 163B is designed to yield such a current characteristic. As the temperature (voltage) at the nodal point increases beyond the voltage at which a diode is "back biased", conduction through the diode takes place so that the diode resistor-loads the point. Each diode conducting causes an effective paralleling of resistance, thus increasing the current drain on the circuit.

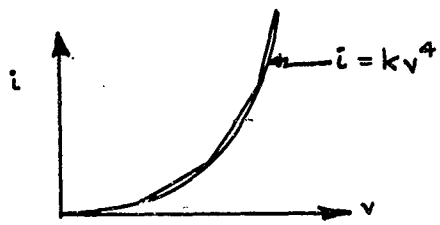

Figure 163A

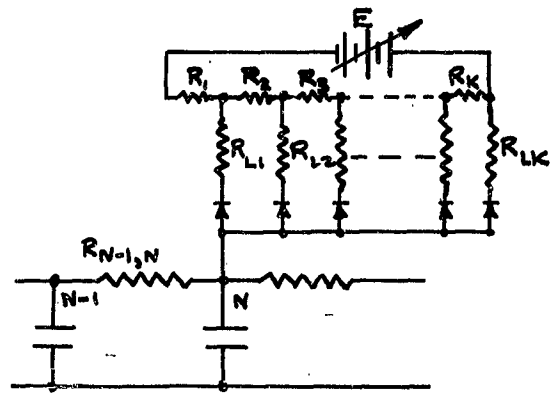

Figure 163B

Figure 163. Passive Network Simulation of Radiation

Using this method, it is impossible to simulate interfacial radiation. This is true because the voltage source E and bias resistors R_1, R_2 . . . .RK would become active parts of the circuit in any new mechanization that attempts to account for radiation current between 2 points in the circuit. Therefore only terms involving radiation to space can be handled.

It should be mentioned that non-linear resistors (such as thyrite and metrosil) with a current characteristic $i = Kv^x$ are currently being investigated at some research centers. Their use is extremely limited because of two major reasons. The exponent x is generally less than 4, impairing accuracy. Secondly, the limited range of voltage over which the radiation holds, in addition to the generally low power rating, dictates a voltage and current scaling that is impractical when simulating terms other than radiation. If these limitations are overcome in the development of non-linear resistors, mechanizing any type of radiant energy transfer would be a simple matter.

Transient Heat Transfer Computer Programs

A number of programs are available for transient heat transfer analyses. These programs have almost always been developed using the analog networks as a model. Table 48 summarizes three of the programs in current use at this company. The references shown on the table give detailed information on problems which can be solved by the program and methods of entering the IBM data. Program decks for these programs are available to ASD and Air Force contractors.

Other programs are being developed in support of this contract. These programs can be used for computing view factors for radiant heat transfer to 3-dimensional bodies, for integrating monochromatic test data to obtain total emmissivity and solar absorbtivity values, for optimizing fluid loops, and for heat exchanger design.

The IBM programs could be improved if some method of integration and differentiation without employing stepwise solution could be used. Such a program might be arranged by combining digital computer systems with electronic differential analyzer components. The use of the differential $\dot{T}$ in place of the approximation $\Delta T/\Delta t$ would eliminate the necessity of computing a time constant and errors introduced by stepwise solution.

The ultimate program would eliminate the node concept since the node is an arbitrary lumping of thermal and physical properties about a point. (The choice of too large nodes can cause large errors in results). Such a program might be devised by using the methods developed in the mathematical treatment of transient heat transfer. Bessel functions, matrices, and series approximations could be part of the program.

Summary Of Methods Of Heat Transfer Analysis

Some of the more important methods of heat transfer analysis are included in Table 46, 47 and 48. Table 46 is a list of some of the equations developed for the passive and semi-passive and mathematical analyses. Included on the table are region of application, limitations, and advantages of the equations. Table 47 is a list of analog networks with descriptions and applications. Table 47 is a list of analog networks with descriptions and applications. The last table, Table 48, summarizes three heat transfer analysis programs currently being used. A description of the electrical analog used for a model and description of regions of application, limitations and advantages are included.

Table 46. Table of Heat Transfer Equations For Quick Estimates

	TYPE OF EQUATION	EQUATIONS	REGION OF APPLICATION	LIMITATIONS	ADVANTAGES
EQUILIBRIUM	PASSIVE, SEMI-PASSIVE	Skin Temperature: $T_v = \sqrt[4]{\frac{\alpha}{\epsilon}\left(\frac{F_{s1}\sigma}{\sigma}\right) + \frac{\alpha}{\epsilon}\left(\frac{F_{s2}\sigma}{\sigma}\right) + \frac{\alpha}{\epsilon}\left(\frac{F_{s3}\sigma}{\sigma}\right) + \frac{G}{\epsilon\sigma}}$ Instrumentation Temperature: $T_B = T_v + \frac{G}{(UA)_{B,v}}$	Steady state heat transfer or constant orbit with $\left(\frac{Mc}{A}\right)_v \omega > 66$	1) Not good for prediction of temperatures or heat transfer with changes in heating or orbit with time.	1) Rapid calculation of extreme temperatures and heat conditions, 2) Quick estimate of system feasibility
	ACTIVE	Active Cycle Equations= Depend on Cycle and Coolant	Estimates of active system requirements for fairly constant heat loads and vehicle paths	1) Doesn't give system transient response rates. 2) Not good for prediction of transient temperatures or heat transfer.	1) Rapid estimates of active system extreme requirements.
TRANSIENT, NON-IEM	STEPWISE OF NUMERICAL	$\dot{T} \approx \frac{\Delta T}{\Delta t} = \frac{\Sigma q}{Mc}$	Transient temperature estimates of one or two node or one dimensional problems with heat terms which can be linearized.	1) Limited to one to three nodes except for one-dimensional heat conduction becomes tedious for a large number of steps (for small time intervals or/and long times). 3) Errors in stepwise solution.	1) Quick estimates of heat storage effects of vehicle skin and instrumentation. 2) Less accurate but more adaptable lumped mass integration.
	LUMPED MASS	$Mc \frac{\partial T}{\partial t} = \sum_{n=0}^{\infty} q_n$	Quick estimates of mean transient temperatures in instrumentation mass or in total spacecraft with low internal heat dissipation.	1) Requires simple heat transfer boundary conditions for integration, stepwise solution is more adaptable. 2) Doesn't show actual temperature gradients.	1) Quick estimates of average instrumentation temperatures. 2) Estimates of heat effects.
	ONE-DIMENSIONAL FOURIER CONDUCTIVITY	$\frac{\partial T}{\partial t} = \alpha \frac{\partial^2 T}{\partial x^2}$	Estimates of transient temperatures gradients in heat conduction paths (flanges, windowns, insulation, fuel tanks at "0"g.)	1) Requires simple heat transfer boundary conditions and transient changes. 2) Can only be applied to conduction paths	1) Quick estimates of maximum temperature gradients.

Table 47. Table of Electrical Analog Networks for Transient Heat Transfer

NETWORK	DESCRIPTION	APPLICATIONS
Passive Element Thermal Analog	Uses Resistors and Capacitors to simulate heat transfer resistance and heat storage respectively. Voltage is temperature, current is heat transfer rate. Radiation is simulated with an effective convective resistance. $(1/h_r A)$.	1) Transient heat transfer problems where the heat transfer, resistance and heat storage don't change much with temperature or time or are constant.
Differential Analyzer	Solves differential equations of form used in node heat transfer description with heat storage ($\dot{T} = \sum q/mc$). Can include T^4 radiation terms and variations in thermal properties with time or temperature. Number of nodes is limited by size of differential analyzer system available.	1) To check errors in IBM program Δt stepwise solutions (eliminates time interval requirement as possible error in analysis). 2) Transient heat transfer problems with limited T^4 radiation terms.
Radiosity Analog	Uses resistors to simulate resistance to radiant heat flux transfer. Uses $E = \sigma T^4$ as input voltage. Assumes gray body radiation.	1) Calculation of the net heat transfer in an enclosure where the radiation effects are appreciable.

Table 48. Table of IBM Programs For Heat Transfer And Temperature Estimates

PROGRAM	METHOD OF SOLUTION	REGION OF APPLICATION	LIMITATIONS	ADVANTAGES
S&ID: ISOS LOCKHEED THERMAL ANALYZER WITH RADIOSITY	Electrical analogs of thermal network and radiosity network, stepwise $\dot{T} \approx \frac{\Delta T}{\Delta t}$	1) Any transient heat transfer problem with an equation form which can be linearized. 2) Heat radiation problems 3) Other problems which can be set up similar to thermal analog.	1) Stepwise solution requires estimate of time constant 2) Arbitrary selection of node points can cause large computation errors.	1) Excellent for multi-node conduction, convection, and radiation problems. 2) Program can be used for other problems in addition to heat transfer. 3) Easy set-up or problem for solution.
NAA: AESOP	Differential equation form, stepwise $\dot{T} \approx \frac{\Delta T}{\Delta t}$	1) Any transient heat transfer problem with an equation form which can be linearized. 2) Any linear differential equation.	1) Estimates of radiation view factors becomes difficult for multi-radiation problems. 2) Stepwise solution requires estimate of time constant 3) Arbitrary selection of node points can cause large computation errors.	1) Excellent for multi-node conduction & convection heat transfer with some radiation. 2) Differential type equations can be used for other problems in addition to heat transfer (fluid flow, hydraulics). 3) Heat transfer properties can vary with temperature.
LOCKHEED: THERMAL ANALYZER	Electrical analog of thermal network, linearized radiation resistance $\dot{T} \approx \frac{\Delta T}{\Delta t}$	1) Any transient heat transfer problem with an equation form which can be set up similar to thermal analog.	1) Estimates of radiation view factors can become difficult for multi-radiation problems. 2) Stepwise solution requires estimate of time constant. 3) Arbitrary selection of node points can cause large computation errors.	1) Excellent for multi-node conduction & convection heat transfer with some radiation. 2) Program can be used for other problems in addition to heat transfer.

DYNAMIC RESPONSE OF TEMPERATURE CONTROL METHODS

Dynamic response is an important consideration in semi-passive or active temperature control methods with fluctuations in heat load or fluid flow rate. In many cases, fast response in the order of milliseconds to a minute will be required to keep the control temperatures within the required temperature band. In such cases, the method usually requires an electronic (or pneumatic) control circuit to anticipate changes, to sense the magnitude of the change and to take corrective action (by controlling a valve to change the fluid flow rate or other thermal regulation). The analysis of the rate of response and control characteristics of a complete system then becomes a combined problem in electronics and heat transfer.

Discussion of Analysis Techniques

Two types of analysis are in general use for solution of dynamic response problems -- the use of linearized open-loop and closed-loop Laplace transform methods and the use of the electronic analog. Also, a proprietary computer program has been developed. The use of the Laplace transform or analog analyses depends on the description of the electronic and thermal components in terms of their response characteristics.

Many text books are available on automatic controls and servomechanisms. These books define the characteristics of the electronic or pneumatic control circuit fairly well. However, very little data appears on the characteristics of the thermal components. Consequently, some approximations are necessary to define the characteristics of the thermal components. One usual approximation is to define most thermal components in terms of mass thermal storage. This can be expressed as a simple Laplace term of the form $\frac{1}{\tau_c(s+1)}$ where τ_c is the time constant of the component.

The disadvantage of this assumption becomes apparent in the consideration of a variable flow fluid coolant problem. In this case, the forced convection coefficient will usually be a function of flow rate and will affect τ_c since $\tau_c = \frac{WC_p}{2h_A}$. Thus, in cases where h varies considerably with flow rate or other parameters, an analog or computer analysis necessary. In this approach, the temperature control method and electronic control circuit can be approximated as closely as time, money, and manpower permits. Of course, the final result is usually a series of test for control response of the actual control method after manufacture.

Design Considerations

Design considerations for dynamic control include choosing the thermal and electronic control components, locating the control components, and decreasing the thermal response lag in thermal control components.

The choice of components is difficult since almost all components can be either on-off or proportional actuated. For example, valves can be solenoid (on-off) or variable flow (proportional) and temperature sensors can be thermoswitches (on-off) or wire resistance sensors (proportional). Similar choices exist in controllers. The final choice between on-off and proportional components usually must be the result of a detailed dynamic response analysis. However, the big difference between on-off and proportional control is usually cost and availability. In general, the proportional control is more expensive and must be custom designed. For instance, many good solenoid valves are available at competitive prices. On the other hand, proportional valves usually must be custom designed and developed at high prices including engineering design and development cost.

The location of control components such as valves, sensors, and anticipators is also important. The sensor must be located with care in order to obtain a good measurement of the controlled surface or fluid. In a fluid such as air, a wire resistance grid may be desirable in order to obtain an average air temperature. Similarly, the anticipator must be located to sense the change in temperature of a fluctuating high heat dissipating source or other temperature driving function. The sensors and anticipators must also be coupled together and the choice of how much anticipation and how much sensing is required must be decided by use of a dynamic response analysis. The location of the valve or other control servo-mechanism must be within a short distance of the sensor. Otherwise, a time lag in response to control demand is possible and the control valve may be out of phase with the sensor resulting in oscillation of the control circuit and loss of temperature control.

The final major design consideration is the decreasing the thermal lag time in control components. For fast response of the temperature control system, consideration of the time constant relationship leads to the following conclusions for design considerations.

(1) Mass of components should be decreased to decrease response lag.

(2) Fluid flow area of components should be increased to decrease lag, and

(3) Fluid forced convection coefficient should be increased to decrease lag.

Dynamic Response Analysis Example

The following dynamic response analysis was undertaken by the United Control Corporation (Reference 91) for temperature control of an astronertial guidance compartment. This analysis illustrates the consideration of on-off control versus proportional control and the set up of Laplace loops and electronic analog networks.

Statement Of Problem

A block diagram of the basic system is shown in Figure 164. As shown there are two equipments requiring temperature control to within ± 10F within the compartment, both being cooled from a common cooling air source. The cooling air temperature is controlled in turn by an FC-75 fluid control valve which modulates the fluid flow through an air to fluid heat exchanger. The FC-75 fluid temperature control is maintained at 41 ± 9°F by an external independent control system. This study assumes there is no problem due to the coupling of the two temperature control systems, since the heat load on the compartment cooling system is but a small part of the total load on the external cooling system.

Controller Types

Two types of controllers for the temperature control requirement were studies, viz.:

1. A linear rate servo, consisting of a linear 400 cycle amplifier driving a size 8 servo motor which drives a tachometer generator and the reduction gearing to the control valve. The output rotational speed of the gearing is directly proportional to the magnitude of the input signal.

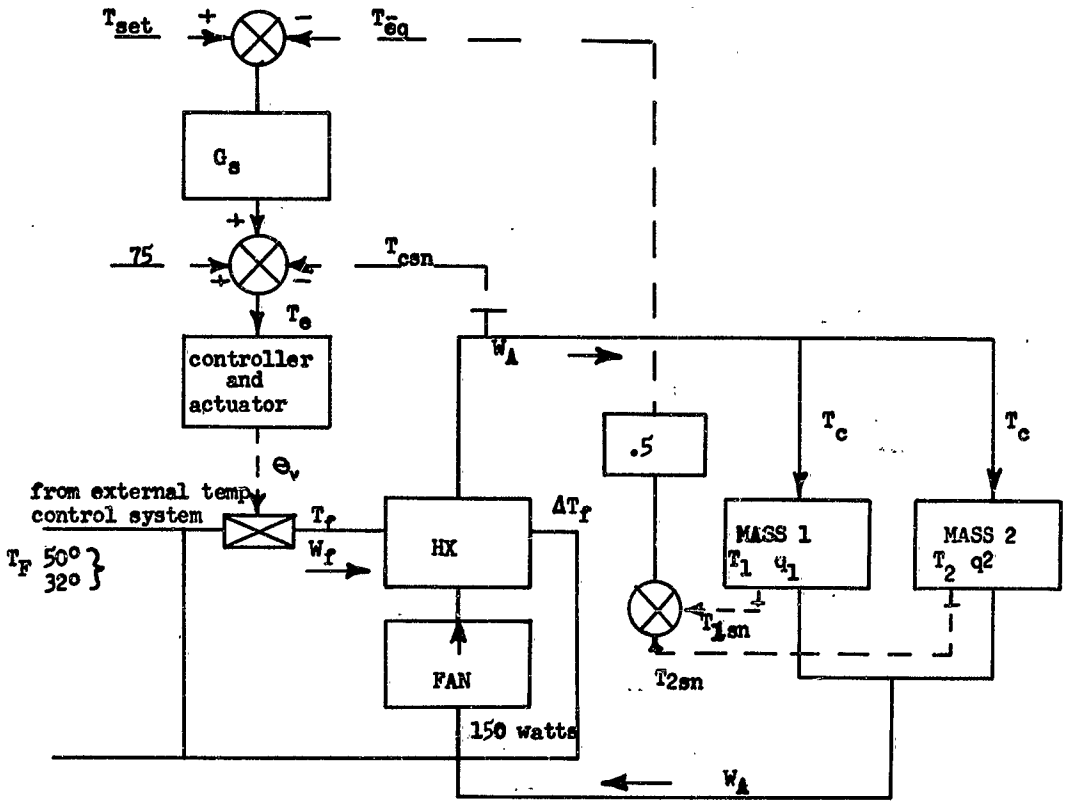

(UCC, Ref. 91)

LEGEND:

T_{set}	- Selected temperature	ΔT_f	- Rise of FC-75 temp. in HX
T_F	- FC-75 fluid temp.	T_{csn}	- Cooling air sensor temp.
T_C	- Cooling air temp.	W_f	- FC-75 fluid flow rate
T_1	- Temp. of mass No. 1	W_A	- Air flow rate, constant
T_2	- Temp. of mass No. 2	Θ_V	- Control valve position
T_{1sn}	- No. 1 sensor temp.	G_s	- Static Gain = T cooling / T equipment
T_{2sn}	- No. 2 sensor temp.	⊗	Electrical summing point
T_{eq}	- Average of T_{1sn} & T_{2sn}	HX	Heat Exchanger
T_e	- Error signal to controller	q1,q2	Heat source in equipment

Figure 164. Block Diagram of Temperature Control System for Dynamic Response Analysis

2. An on-off pulse-width modulation servo, similar in operation to a relay servo but utilizing all solid state components. The servo consists of a high gain DC magnetic amplifier, a solid state AC output stage directly coupled to an induction motor then through reduction gears to the control valve. A negative feedback single time constant network is employed to obtain pulsing action. The pulsing action obtains an average valve speed proportional to the magnitude of the input error.

The three sensors for each system will match either controller. Time constants assumed for the three sensors are 2 seconds, 2 seconds, and 1 second for the two equipment sensors and the cooling air sensor respectively.

Stabilization Technique

Both controllers ultimately do the same thing, i.e., modulate the control valve position to obtain cooling as required. Both make use of the cooling air temperature for stabilization and thus are type zero or droop systems. Figure 165 illustrates how the temperature of the cooling air is made to vary proportional to the average temperature error at the equipment.

As shown, the primary control effort is always applied to the equipment temperature with secondary control being on the cooling air temperature where it leaves the heat exchanger.

Since any change in the cooling air temperature will lead, in time, a corresponding change in equipment temperature, sensing and feeding back cooling air temperature is phase lead feedback which is required in all control systems for stability. System damping is thus proportional to the inverse of the static gain, G_s. For a block diagram of the system dynamics, see Figures 166 and 167. Figure 168 is a block diagram of the analog computer network for this system.

Steady-State Accuracy, Droop

Figure 165 indicates that there is a fixed relationship between the equipment temperature and the cooling air temperature. Thus, as the equipment heat load varies, the steady-state temperature will change also, the amount of which being proportional to the inverse of

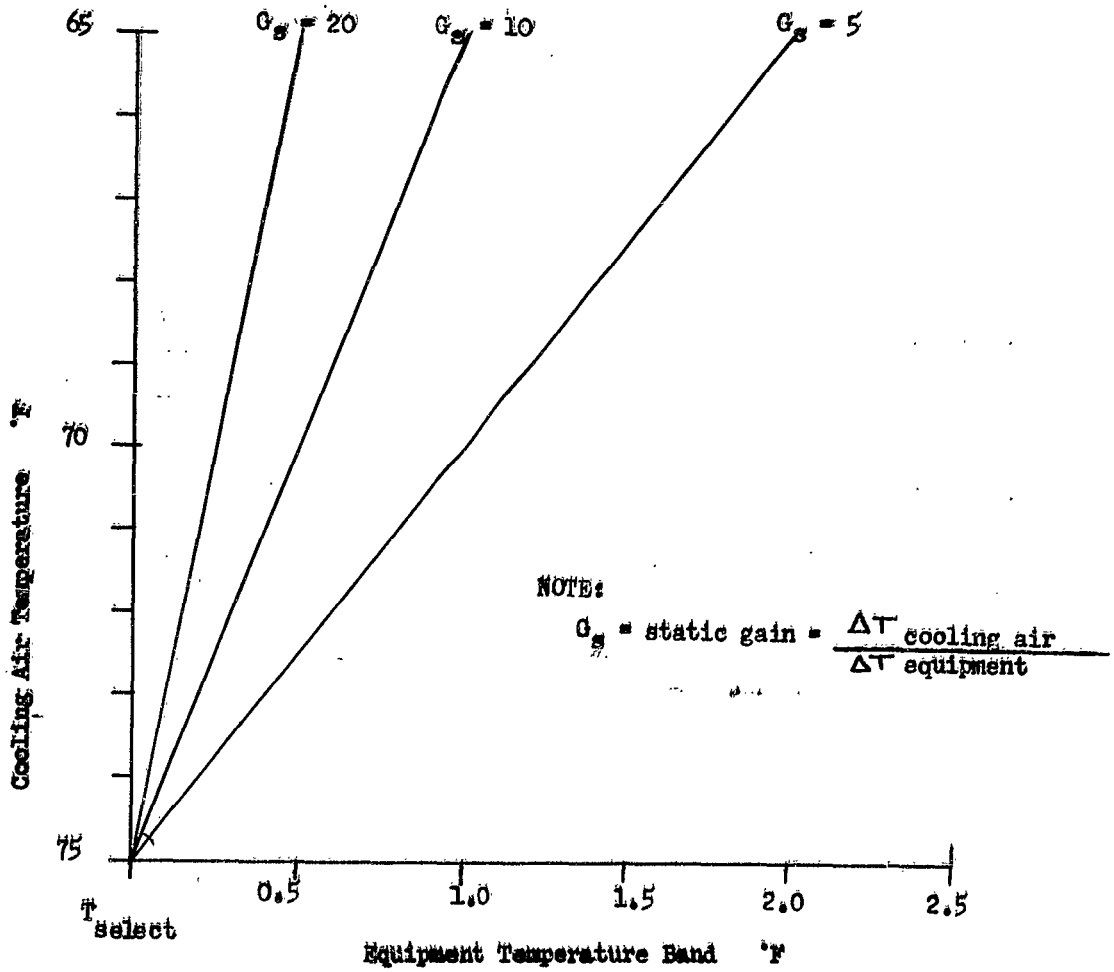

Figure 165. Cooling Air Temperature vs. Equipment Temperature Steady-State Characteristics (From United Control Corporation. Ref. 91)

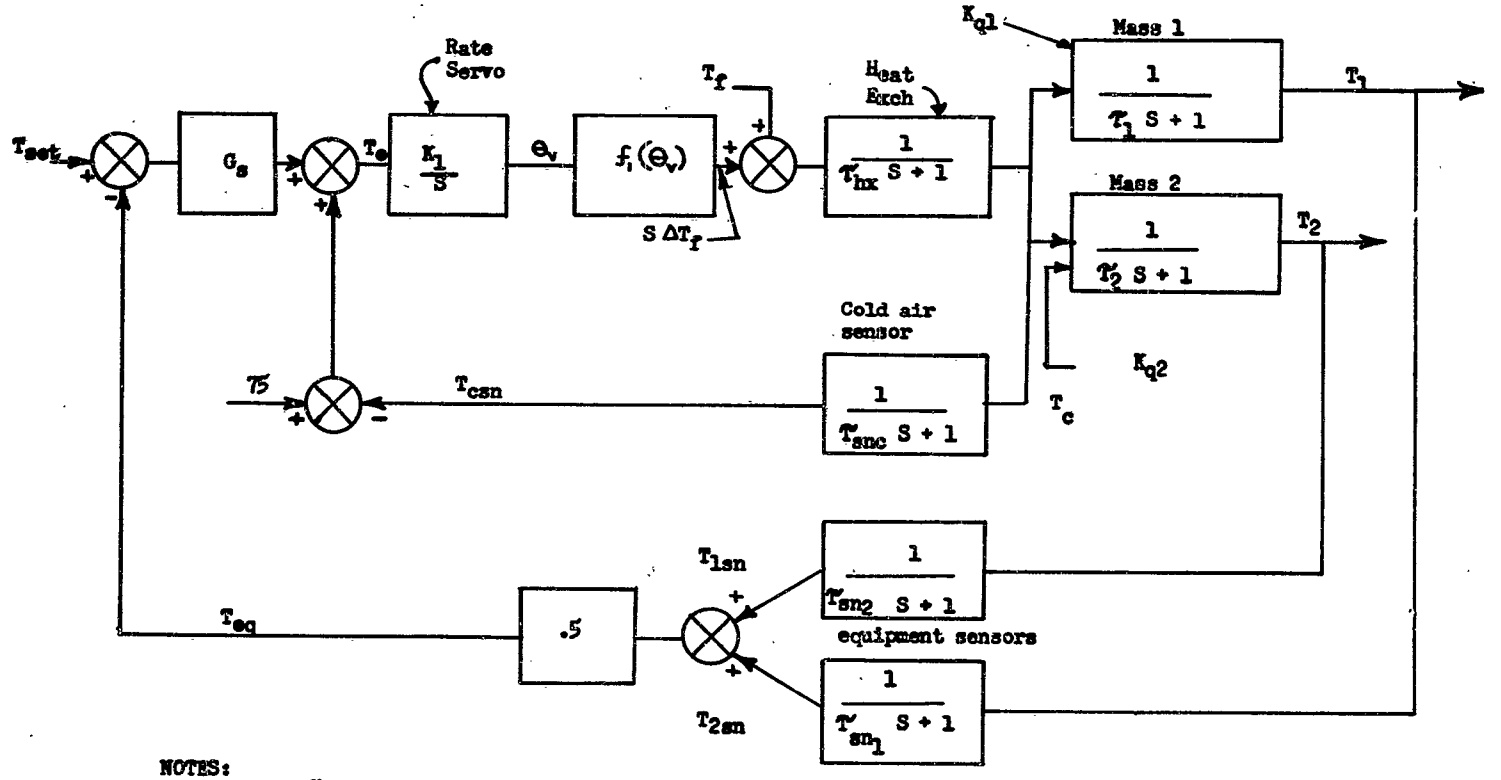

Figure 166. Temperature Control System Dynamics, Linear Servo (United Control Corporation, Reference 91)

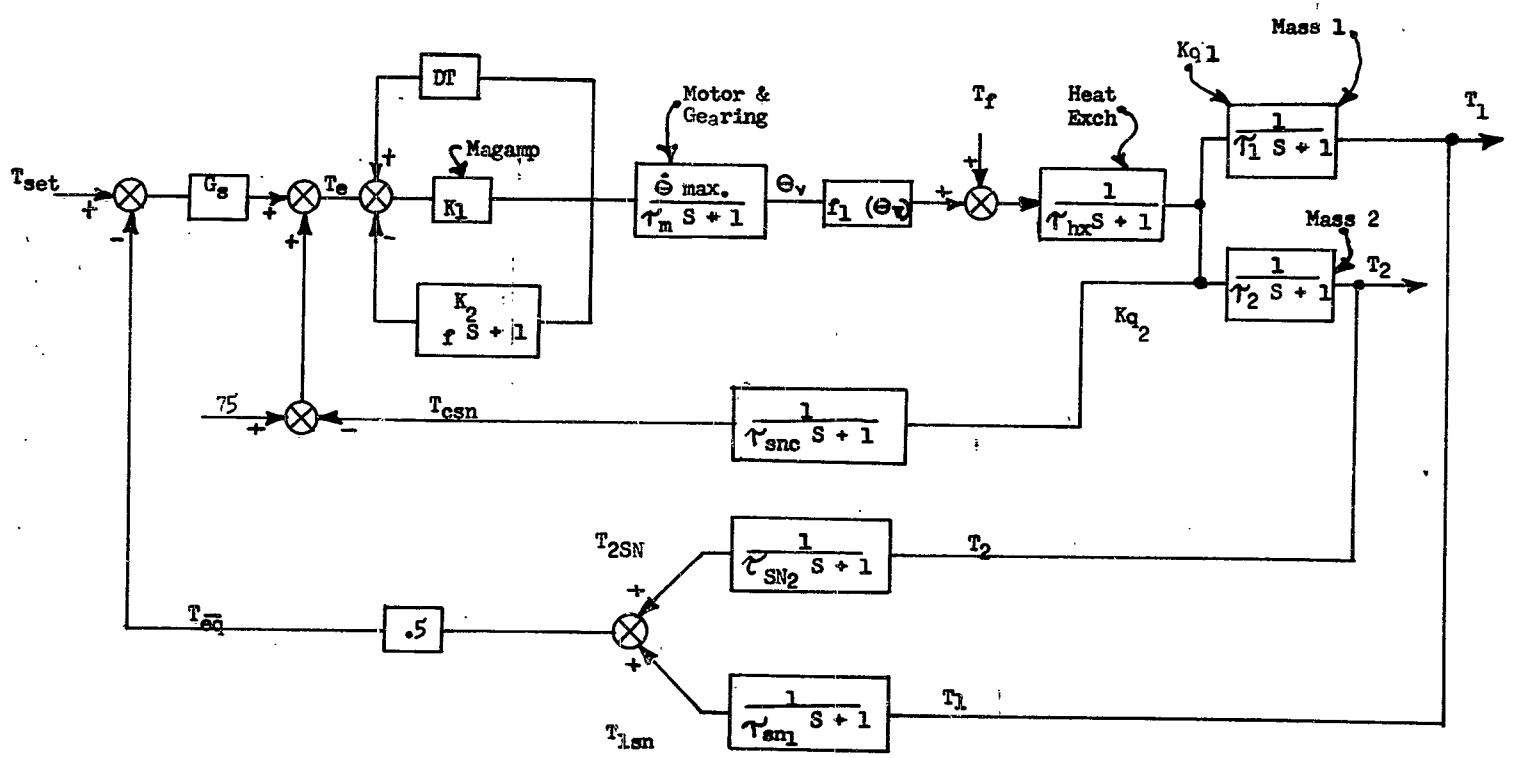

NOTES:
1 - see Fig.164 for definition of symbology
2 - S = Laplacian operation
3 - τ = time constant, seconds

Figure 167. Temperature Control Systems Dynamics, On-Off Servo (United Control Corporation, Reference 91)

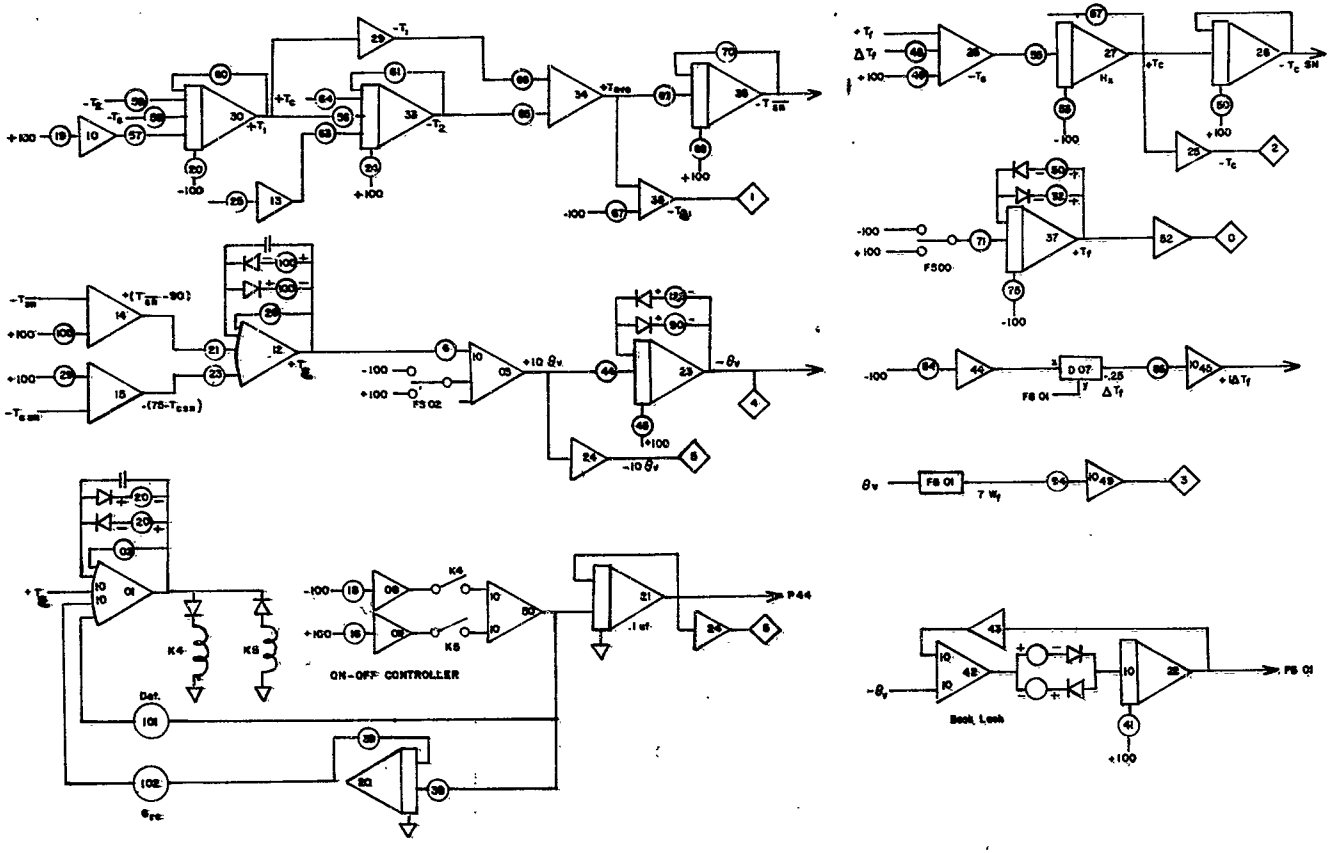

Figure 168. Analog Computer Circuit Diagram, Dyanmic Response Example Temperature Control System (Reference 91)

the static gain. For a given constant heat load, the equipment temperature can be adjusted to any desired level (within the extremes of the cooling system authority). Thus, if load is constant, droop is constant and the effective droop may be adjusted to zero.

Absolute Vs. Relative Steady-State Accuracy

Equipment temperature control within ± 1°F about some set (adjustable) point is much easier to obtain than ± 1° about a fixed absolute value. The reason for the above fact is seen by a consideration of the equipment tolerances which are involved. Reasonable tolerances available in hardware are the following:

Equipment:	Tolerance
1. Sensors, each, (equipment)	
Calibration	± .4°
Drift with age	± .1°
2. Sensor, (cooling air)	
Calibration	± .2°
Drift with age	± .05
3. Controller	
Calibration	± .15°
Drift with age	± .05°
Total, maximum	± 1.45°F

While it is probable that the above tolerances would not all be of the same polarity to result in the worst possible error, such a case is possible, thus in a large production run it may well occur. In the light of the above data, it is recommended that the equipment temperature be adjusted in place for each compartment, i.e., base the system accuracy of ± 1°F about a given set point which is obtained by in-place adjustment.

Conclusions And Recommendations From Computer Study

The most severe transient applied to the system is a 10°/min. ramp on fluid temperatures. This results in an equipment temperature transient of about 1° maximum for the on-off system and about 3° maximum for the linear system.

1. The use of a simple type zero or droop system appears well suited to this application, assuming no large variations in heat load occur.

2. Sensing the cooling air temperature and using it for droop stabilization is superior to a simple valve position feedback system which cannot automatically adjust for variations in fluid supply temperature.

3. A slowly moving control valve (low gain system) is required to allow the system to come to rest and thus obtain best life and steady-state accuracy.

4. System stability is reduced as the time constant of the heat exchanger is increased.

5. System gain is dependent upon the steady-state control valve position, gain increasing as the valve closes.

6. Control accuracy is proportional to static gain, while damping or stability varies inversely with static gain, G_s.

7. The linear system requires a higher reduction gear ratio than does the on-off system since it must use cooling airflow temperature only for stabilization. The R-C feedback net effectively provides increased stabilization for the on-off system.

8. Required droop, or change in equipment temperature with load is greater for the linear system.

While both the controllers discussed above are workable, the on-off system provides better control and appears to present fewer manufacturing problems. Use of the on-off system is therefore recommended.

SECTION IX

CONCLUSIONS

This report has presented methods of temperature control, comparisons of these methods, equipment thermal considerations, and techniques for analyses of the heat transfer and dynamic response. Section VI in particular should be noted since summary tables of control methods and comparison are included in this section. Conclusions are presented in the last pages of each of the sections. Consequently, only a few of the more important conclusions are reviewed in this section. Also, included is a discussion and recommendations for the major problem areas encountered during preparation of this report.

MAJOR CONCLUSIONS

The major conclusions from this report are listed below.

1. Power penalty requirements of weight, surface area, and volume are major considerations in comparisons of temperature control methods.

2. Definition of regions of application of passive, semi-passive and active methods is possible by use of compartment and skin temperatures and compartment heat load (see Tables 29 and 33 and Figures 95 and 108).

3. Thermal control requirements of space vehicle equipment can be reduced if equipment heat transfer design is improved and higher temperatures components are developed.

4. IBM computer solutions are necessary and should be used for accurate estimates of temperatures and heat transfer rates for most transient and/or complex heat transfer problems.

PROBLEM AREAS AND RECOMMENDATIONS

During this study program, problem areas in temperature control have been uncovered in regards to surface coatings, fluids, power penalties, dynamic response, control hardware, and equipment design. These problem areas are discussed under each subject and recommendations are made.

Surface Coatings

Space vehicle surface coatings encounter three unusual conditions in space which are not usually found on earth (1) hard vacuum (10^{-12} mm. or less), (2) cosmic ray and meteorite bombardment, and (3) direct solar radiation. These three conditions can and do lead to deterioration of many surfaces and coatings. Much research is being done on coating problems at the present time. However, recommendations is made that more testing should be directed towards the combined effects of hard vacuum with cosmic ray and meteorite bombardment and solar heating on the surface emissivity and solar absorptivity.

Fluids

Fluids are affected in space primarily by the zero gravity condition and possibly by deterioration due to cosmic ray effects. Since the zero gravity condition has not been encountered on earth, predictions of fluid behavior on the basis of existing forced invection or boiling data is questionable. This becomes apparent when it is realized that most forced convection and boiling film coefficient equations for heat transfer are based on test data. Although the present recommendation is made that extensive testing of fluid behavior (especially forced convection boiling) should be conducted in a space environment to verify the present theory and to eliminate use of over conservative values of film coefficients.

Power Penalties

The power penalties can be a major contribution to the temperature control system weight, surface area and volume. Also, the state-of-the-art of many power supply systems is changing at a rapid rate. Thus, a detailed study of space vehicle power supplies and their associated weights, surface areas and volumes with a prediction of future possibilities becomes a necessity for comparison of temperature control methods.

Dynamic Response

Dynamic response theory has been well developed by electronic engineers. Unfortunately, most literature on the subject is written around electrical or pneumatic control systems. More data is needed on the characteristics of temperature control methods and components. Also needed is a computer program for fast, accurate analysis of dynamic response.

Control Component Hardware

In the design of aircraft and missiles, a lack of off-the-shelf temperature control systems hardware has been apparent. This lack is even more apparent when space vehicles are considered. Virtually all components in the system need improvement and optimization. Major improvements are needed in compressors, proportional valves, quick disconnect self-sealing couplings, fittings, radiators, heat exchangers, and cold plates. In essence, all attempts at system optimization are fruitless if only a few unoptimized components are available off-the-shelf. Therefore, recommendation is made for funding of hardware sub contractors for research and development of a series of optimized temperature control components. The efficiency of fans, pumps and compressors also needs to be improved to cut down the power penalties.

Equipment Design

Equipment design for cooling of components and compartments has improved noticeably in the last few years. The integration of temperature control with the electronic and design considerations has become a prerequisite for decreasing weight and increasing reliability. Improvements in equipment design still are needed especially in the area of small components such as power transistors where temperature control and cold plate design considerations appear to have taken second place to case of manufacturer.

Three main improvements which should be considered in equipment design are (1) increase operating temperatures so that higher temperature radiation can be used, (2) increase efficiencies so that power and coolant requirements decrease, and (3) consider heat transfer by designing components for efficient cooling and for less variation in performance with temperature.

SECTION X

REFERENCES

1. Kilpatrick, B. K., Parks, C. H. and Watanabe, D, "Environmental Control System Selection for Unmanned Space Vehicles"; Space and Information Systems Division of North American Aviation, Inc.; ASD TR 61-164 Part I

2. "Environmental Control Systems Selection for Manned Space Vehicles"; Los Angeles Division of North American Aviation, Inc.; ASD TR 61-240 Part I Volume I; 9 October 1961.

3. Glasser, S. P. and Stelzriede, M. E., "Integration and Optimization of Space Vehicle Environmental Control Systems"; Space and Information Systems Division of North American Aviation, Inc.; ASD TR 61-176 Part I

4. Weills, N. D. and Ryder, E. A.; "Thermal Resistance Measurements of Joints Formed Between Stationary Metal Surfaces", Trans. of ASME, April, 1949, p. 259.

5. Brunot, A. W. and Buckland, F. F.; "Thermal Contact Resistance of Laminated and Machined Joints", Transactions of ASME, April 1949, p. 253.

6. "Research and Development Handbook", Space and Aeronautics 1960-1961 Edition.

7. Fenech, H; "Thermal Conductance of Metallic Surfaces in Contact", M. I. T. Thesis, 1957.

8. Groff, W. J.; "Thermal Conductance Across Metal Joints", Machine Design, Sept. 15, 1960, p. 166.

9. Barzelay, M. E., Tong, K. N., and Holloway, G. F.; "Thermal Conductance of Contacts in Aircraft Joints", TN 3167, March 1954.

10. Barzelay, M. E., Tong, K. N. and Holloway, G. F.; "Effect of Pressure on Thermal Conductance of Contact Joints", NACA TN 3295, May 1955.

11. Barzelay, M. E. and Holloway, G. F.; "Effect of an Interface on Transient Temperature Distribution in Composite Aircraft Joints", NACA TN 3824, April 1957.

12. Barzelay, M. E. and Holloway, G. F.; "Interface Thermal Conductance of Twenty-seven Riveted Aircraft Joints", NACA TN 3991, July 1957.

13. Fried, E. and Costello, F. A.; "Interface Thermal Contact Resistance Problem in Space Vehicles", ARS Journal, Vol. 32, No. 2, pp. 237-243, February 1962.

14. Verschoor, J. D. and Greebler, P.; "Heat Transfer by Gas Conduction and Radiation in Fibrous Insulations", Transaction of the ASME, Vol. 74, pp. 961-968, August 1952.

15. Christensen, E. H.; "Thermal Insulation of Space Vehicles"; Astronautics Division of General Dynamics Corporation, Report AZJ-55-005.

16. Rowley, F. B., Jordan, R. C.; Lund, C. E. and Lander, R. M.; "Gas is an Important Factor in the Thermal Conductivity of Most Insulating Materials"; the American Society of Heating and Ventilating Engineers; Paper No. 1445; January 1952.

17. "Juno II Summary Project Report. Volume I, Explorer VII Satellite"; NASA TN D-608;

18. Stevenson, J. A. and Grafton, J. C.; "Radiation Heat Transfer Analysis for Space Vehicles"; Space and Information Systems Division of North American Aviation, Inc.; ASD TR 61-119; October 1961.

19. Deleted

20. "Truflex Thermostat Metals"; Metals and Controls Division of Texas Instruments Inc., General Plate Plant, Attleboro, Mass.; April 1959.

21. Gross, A. and Sackleh, F. J.; "Thermal Control of an Orbital Vehicle"; Flight Accessories Laboratory, Wright Air Development Division.

22. Tupper, J. S.; "An Approach to Equipment Cooling Problems in an Orbital Space Vehicle"; Society of Automotive Engineers, Inc.; SAE Paper 58-87B; October 1958.

23. Schroeder, F. E., Towe, E. E., Lake, P. H. and Wunderman, R. L.; "Study of Equipment Cooling Systems"; Boeing Airplane Company; WADC TR 59-253; November 1959.

24. Mackay, D. B.; "Methods for Removing the Heat Produced by Electronic Equipment in High-Speed Flight" from "Cooling Of Airborne Electronic Equipment, Volume II"; Second Conference at Ohio State University; 23 June 1953.

25. Shaffer, A. (Editor); "Analytic Methods for Space Vehicle Atmospheric Control Processes"; AiResearch Manufacturing Division of the Garrett Corporation, Los Angeles, California; ASD 61-162 Part I; October 1961.

26. Giedt, W. H.; "Principles of Engineering Heat Transfer"; D. Van Nostrand Co., Inc., New York, 1958

27. Heldenbrand, J. L.; "Selection of the Closed System Atmosphere"; A Selection from the Closed Circuit Respiratory Systems Symposium, WADD 60-574.

28. Acker, R. M., Lipkis, R. P. and Vehrencamp, J. E.; "Temperature Control System for the Atlas ABLE-4 Lunar Satellite"; ASME Paper 60-AV-46; June 1960.

29. McAdams, W. H.; "Heat Transmission"; McGraw-Hill Book Co., Inc. New York; 3rd Edition 1954.

30. Oppenheim, A. K.; "Radiation Analysis by the Network Method"; ASME Paper No. 54-A-75; Transactions of the ASME, p. 725-735, May 1956.

31. Mason, J. L., Burriss, W. L., Connally, T. J., "Vapor Cycle Cooling for Aircraft," WADC TR 53-338.

32. "Engineering Study of Vapor Cycle Cooling Equipment for Zero-Gravity Environment," edited by Kymus Ginwala, Northern Research and Engineering Corporation, WADD TR 60-776.

33. Deleted

34. Mason, J. L., Whitnah, G. R., Larson, E. M., "Study of Vapor-Cycle Refrigerants for High Performance Aircraft," WADC TR 56-93.

35. Silverman, M. D., Heston, B. C., Rudolph, P. S., "Radiation Damage to Freon," Oak Ridge National Laboratory CORNL Central File No. 56-8-198 (Memorandum to G. H. Jenks and E. G. Bohlman, August 17, 1956).

36. Gambill, W. R., and Grene, N. D., "Boiling Burnout with Water in Vortex Flow," Chemical Engineering Progress, Vol. 54, October 1958, pp. 68-76

37. "Study of Liquid Feed Control to a Wick Type Boiler," South Wind Division, Stewart-Warner Corporation, Indianapolis, Indiana (Unpublished report, 1958, as mentioned in Reference 32).

38. Gilmour, C. H., "Nuclear Boiling Accumulation," Chemical Engineering Progress, Vol 54, October 1958.

39. Miles, J. "The Hydrodynamic Stability of a Thin Film of Liquid in Uniform Shearing Motion," Journal of Fluid Mechanics, Vol. 8, Part 4, August 1960, p. 593.

40. "The 300 KW Nuclear Dynamic Space Power Generating System," Second Quarterly Technical Report, Contract AF 33(616)-7379. AiResearch Report SY5213R, AiResearch Manufacturing Division, Phoenix, Arizona.

41. Haire, A. M., Hays, L. G., and Collins, J. L., "Radiator-Condenser for Space Environment," WADD TR 61-20.

42. Kreith, P., "The Influence of Curvature on Heat Transfer to Incompressible Fluids," ASME Vol 77, 1955, pp. 1247-1256.

43. Tang, K. K., Chang, K. T., and Mason, J. L., "Liquid Transfer Media for Airborne Thermal Systems," ASME Aviation Conference, 1959.

44. Moseley, D., Lt., "Vapor Cycle Cooling Systems for Space Vehicles," WADD TN 60-161.

45. Barger, J. P., Rohsenow, W. M., Treadwell, K. M., "A Comparison of Refrigerants When Used in Vapor Compression Cycles Over an Extended Temperature Range," ASME Transactions, Vol 79, No. 3, April 1957, P. 681.

46. Aerospace Applied Thermodynamics Manual, SAE, Sec 3, P. B-59.

47. Moseley, Lt. T. D., "Gas Cycle Cooling Systems for Space Vehicles," WADD Technical TN 60-66.

48. Mackay, D. B. and Bacha, C. P.; "Analysis and Design of Space Radiators"; Space and Information Systems Division of North American Aviation, Inc.; ASD TR 61-30 Part I; 1 April 1961.

49. Mason, J. L., "Vapor-Cycle Cooling for Aircraft," WADC TR 53-338.

50. Fulton, C. D., "Ranque's Tube," Refrigerating Engineering, May 1950.

51. Kassner, R., and Knoernschild, E., "Friction Laws and Energy Transfer in Circular Flow," USAF Wright-Patterson Air Force Base, Technical Report No. FTR 2198-ND, GS, No. 78.

52. Green, F. H., "The Use of Vortex Tubes for Localized Cooling," AiResearch Manufacturing Company, VT-28-R.

53. Meterin, V. I., "Investigation of Vortex Temperature Lyne Compressed Gas Separations," Zhurnal Tekhnicheskoi Fiziki, Vol. 30, No. 9, pp. 1095-1103.

54. Deleted

55. Deleted

56. Ioffe, A. F.; "Semiconductor Thermoelements and Thermoelectric Cooling"; Infosearch, Ltd., London; 1957

57. Kaye, J., Fand, R. N., Nance, W. G. and Nickerson, R. J.; "Final Report on Heat-Storage Cooling of Electronic Equipment"; WADC 56-473, ASTIA AD 97255; 1956.

58. Wilson, H. W., Beahm, K. W. and Cooper, W. J.; "Determination and Analysis of the Potentialities of Thermal Energy Storage Materials"; ASD TP 61-187; 1961.

59. Robinson, Walter and Zimmerman, R. H., "The Thermal Evaluation of Air-Cooled Electronic Equipment", Ohio State Univ. Res. Foundation WADC AFTR TR. No. 6579, dated Sept. 1952.

60. Welsh, J. P.; "Design Manual of Natural Methods of Cooling Electronic Equipment", Cornell Aeronautical Laboratory, Inc. Report No. HF-845-D-8, Naushipe 900, 192, dated Nov. 1956.

61. Luft, Werner, "Taking The Heat Off Semi-Conductor Devices", Electronics, June 12, 1959.

62. Stephanson, C. Dean, "Thermal Characteristics and Time-Temperature Studies of Miniature Electrical Connectors Conforming to MIL-C-26500A (USAF)," Amphenol Connector Division; presented WESCON Meeting August 1961.

63. Beller, William; "Friction Research Grinds to A Halt", Missles and Rockets, 29 Aug. 1960.

64. Pierro, John J., "A 600°F Airborne Electrical System", SAE Report No. 102V, North American Aviation, Inc. "Hot Elec" Project.

65. Broderick, E. J. and Barrows, W. A.; Part I; Bell, R. E., Bach, Hanna, J, Musbach, M. W., Part II, "Developments in the TIMM (Thermionic Integrated Micromodule) System", Presented at WESCON Meeting August 1961.

66. Bierman, Howard and Haavino, Robert; "Guidelines to Micro-Miniature Designs", Electronic Design 9 November 1960.

67. Kammerer, H. C., "Thermal Design for Micro Miniaturized Circuitry", ASME Paper 61-AV-5, 17 April 1961 IBM, Federal Systems Division.

68. Randall, Eric; "Unconventional Power Sources", Electro-Technology August 1961, International Telephone and Telegraph Corp.

69. Knights, A., Jennings, A, and Forte, M.; "Study of Integrated Cryogenic Fueled Power Generating and Environmental Control Systems", WADD(no number), May 1961, Walter Kidde and Co., Inc.

70. Deleted

71. Welsh, James P.; "Design Manual of Methods of Forced Air Cooling Electronic Equipment", Naushipe 900, 194, June 1958, Department of the Navy.

72. "Guide Manual of Cooling Methods For Electronic Equipment", Nauships 900, 190, 31 March 1955, Department of the Navy.

73. Burke, F. P.; "Dissipating Heat from Transistors", Electronic Equipment Engineering, July 1959, International Electronic Research Corp.

74. Deleted

75. Harper, C. A.; "Thermally Conductive Cast Resin Compounds for Heat Dissipation", Electrotechnology, April 1961, Air Arm Division, Westinghouse Electric Corporation.

76. Collins Radio Co., "The Application of Thermoelectric Spot Cooling to Electronic Equipment", CTR-224.

77. Hachs, H. B. and Fraser, J. E.; "Ultra High Temperature (500°) Power Transformers and Inductors", WADC TR-59-348, dated July 1959.

78. Goldberg, M. E., Hamre, H. G. and Noble, R. D.; "Electronic Component Parts Research For 500°C Operation", WADC TR-57-362, July 1958.

79. Ballard, Dr. James W.; "Electronic Materials at Elevated Temperatures", WADC TN-57-211, May 1957.

80. Javitz, Alex E., and Barken, Harold E.; "The Design Analysis of Materials", Electro-Technology, dated May 1961.

81. Stambler, Irwin; "Semiconductor Strain Gages", Space/Aeronautics, dated November 1961.

82. Letaw, Harry Jr.; "The Electronic Materials Frontier", Astronautics, May 1958, Research Division, Ratheon Mfg. Co.

83. Isken, J. R.; "Derating, Its Meaning and Limitations", Electro-Technology June 1961, International Resistance Company.

84. Perry, J. H. (Editor); "Chemical Engineers' Handbook"; McGraw-Hill Book Co., Inc., New York; 3rd Edition 1950.

85. Kays, W. M. and London, A. L; "Compact Heat Exchangers"; National Press; 1955.

86. Walters, F. M. and Mueller, R. D.; "Design Manual, Electronic Equipment Environmental Conditioning"; AiResearch Manufacturing Division of the Garrett Corporation, Los Angeles, AiResearch Report L-5909-R; 15 July 1960.

87. Wylie, C. W., Jr.; "Advanced Engineering Mathematics"; McGraw-Hill Book Co., Inc., New York; 2nd Edition, 1960.

88. Sokolnikoff, I. S. and Sokolnikoff, E. S.; "Higher Mathematics for Engineers and Physicists"; McGraw-Hill Book Co., Inc., New York; 2nd Edition 1941.

89. Jacob, Max; "Heat Transfer, Volume I"; John Wiley and Sons, Inc., New York; 1949.

90. "Mechanical Engineering 124, Syllabus"; California Book Co., Ltd., Berkeley, California; 1955.

91. Douthwaite, G. K., "Evaluation of Temperature Control System for Skybolt Missile (Nortronics)"; United Control Corporation, Seattle, Washington; UCC Engineering Report 1764; 7 Sept. 1960.

92. **Deleted**

93. Deleted

94. Deleted

95. Deleted

96. Glasstone, S.; "The Elements of Physical Chemistry"; D. Van Nostrand Co., Inc., New York; 1946.

97. Jacob, M.; "Heat Transfer, Volume II"; John Wiley and Sons, Inc., New York; 1957.

APPENDIX A

CRYOGENIC COOLING OF LARGE HEAT LOADS FOR SPACE VEHICLE APPLICATIONS

Prepared by

H. Monteros

AiResearch Manufacturing Company
A Division of The Garrett Corporation
Los Angeles 9, California

TABLE OF CONTENTS

SECTION I
INTRODUCTION

This report was prepared by the AiResearch Manufacturing Company of Los Angeles as a part of the space vehicle thermal and atmospheric control system study (T and A). It was prepared at the request of the Space and Information Systems Division of North American Aviation Inc., in support of the T and A Study Report No. 7, Part II, entitled: "Temperature Control Systems for Space Vehicles". The study deals with the cooling of large heat loads at cryogenic temperature aboard space vehicles.

The heat loads considered cover the range from 0.2 to 20 kw, and the temperature levels of interest are those attainable by boiling of liquid nitrogen, liquid neon, and liquid helium.

The cooling systems investigated are the Simple Joule-Thomson Expansion Systems, the Cascaded Joule-Thomson Expansion Systems, the bypass expander systems and the Stirling Cycle System.

In order to estimate the weight and power requirement of each proposed system, the characteristics of its components must be known. To this end, system components are first investigated and their characteristics and performance are determined. Among these are space radiators, compressors and motors, turbo-expanders, and heat exchangers. After this preliminary study, thermodynamic cycles are analyzed and compared. Finally, systems characteristics are given based on realistic assumptions. There are many parameters involved in a complete analysis of each system; for example, variation of the efficiency of turbomachinery with flow rate, system power requirement as a function of heat exchanger effectiveness and weight, etc. Optimization as to system weight and power requirements could be accomplished for these parameters, however, this would only be feasible with the extensive use of computer programs and is outside the scope of this study. Basic data is given for all system components, and general system analysis methods are presented, such that if desired the data included in this report can be used to perform system analysis for any particular application.

SECTION II
FLUIDS

Fluid Properties

In many applications, cryogenic cooling is produced by evaporation of a liquid refrigerant, the coolant temperature being regulated by control of evaporation space pressure. This gives very accurate average temperature control. The temperature range attainable with a given fluid in such a case corresponds to the range between coolant triple point and critical point. The coolants considered in this report are nitrogen, neon, and helium. Selected properties for these fluds, taken from References I, and II are given in Table I. The temperature range attainable by each in the liquid state is plotted in Figure I. Slight variations in the evaporation space pressure will produce only slight variations in the temperature of the boiling liquid. Figure 2 shows the saturated vapor pressures of the three coolants under consideration versus the temperature indicating the stability of an evaporative refrigeration system.

The nature of this report requires extensive cycle analyses for each working fluid in each proposed system. The thermodynamic data used for these analyses was obtained from References 2 through 5 for nitrogen, from Reference 6 for neon, and from the National Bureau of Standards for Helium.

Normal criteria used in the choice of refrigerants are:

(a) Toxicity

(b) Explosiveness

(c) Availability

(d) Ease of Handling

(e) Corrosiveness

(f) Fluid Stability

(g) Refrigeration effect per unit weight

TABLE 49

PROPERTIES OF NITROGEN, NEON, AND HELIUM

FLUID	NORMAL BOILING POINT (14.696 PSIA) TEMP., °R	DENSITY SAT. LIQ. LB/FT³	DENSITY SAT. VAP. LB/FT³	LAT. HT. OF VAP. λ BTU/LB	CRITICAL POINT °R	CRITICAL POINT PRESS. PSIA	TRIPLE POINT °R	TRIPLE POINT PRESS. PSIA
N_2	139.2	51.0	0.285	85.9	227.3	492.9	113.6	1.86
Ne	48.9	75.2	0.59	37.1	79.88	394.5	44.23	6.26
He	7.59	7.8	≈ 1	8.93	9.36	33.21	3.92*	0.735*

*λ-POINT

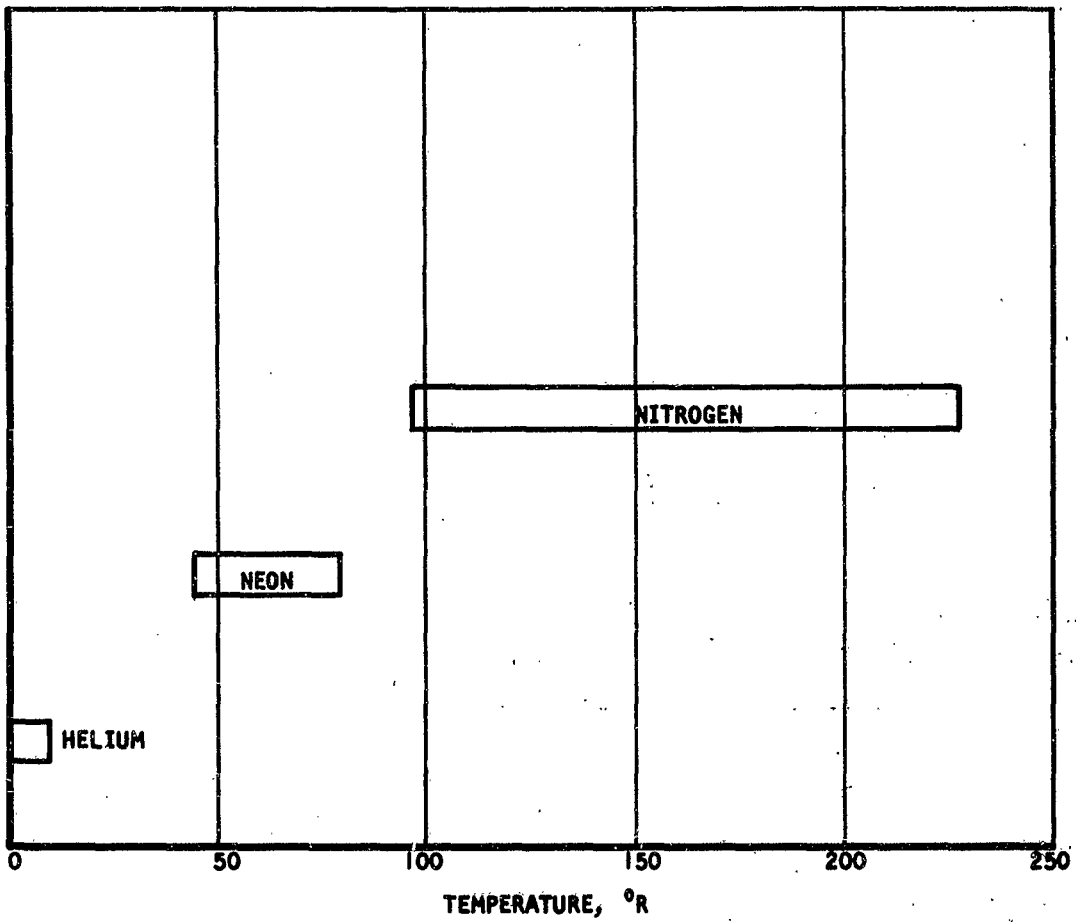

Figure 169. Liquid Temperature Range of Low Boiling Point Fluids

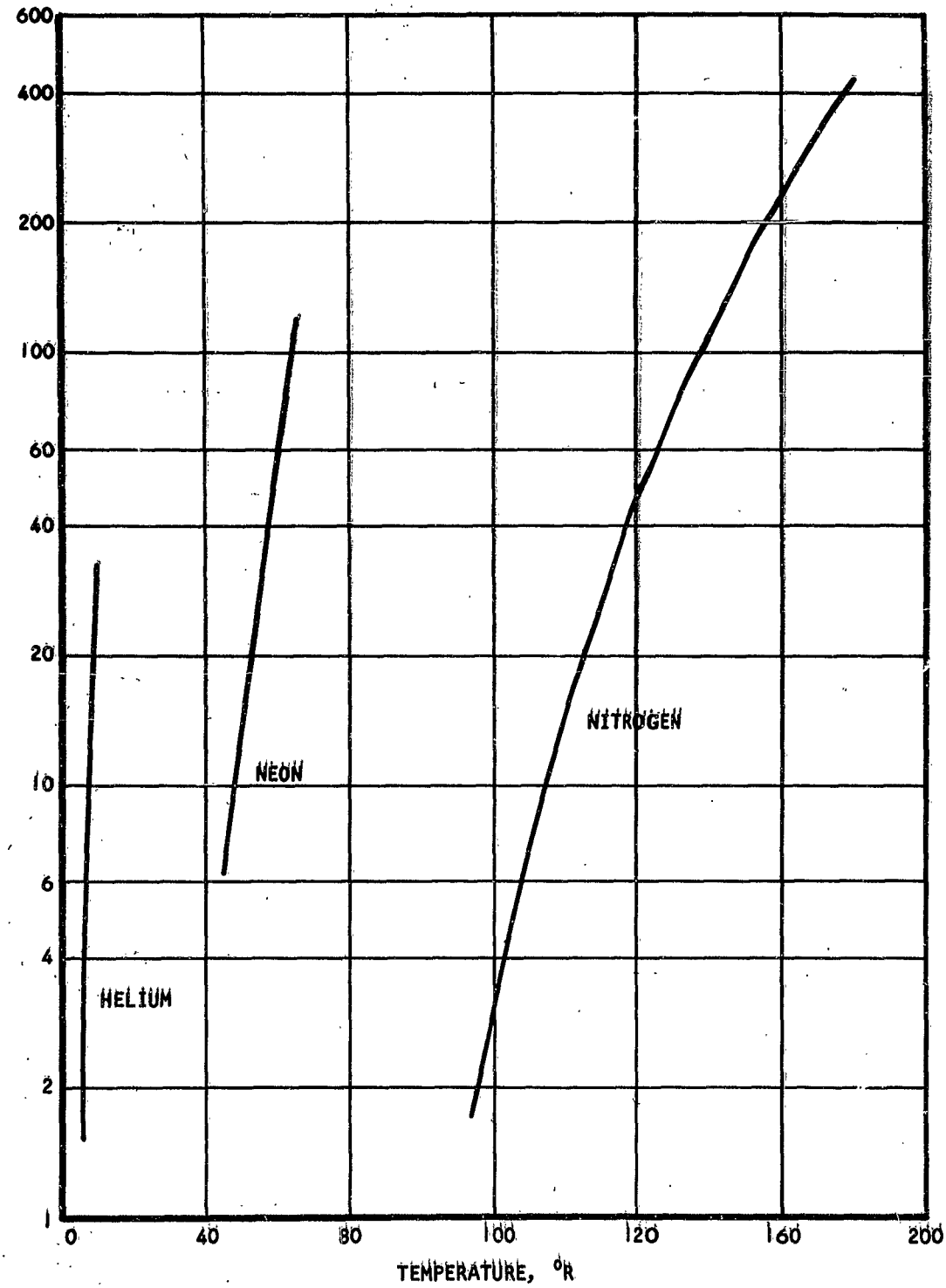

Figure 170. Vapor Pressure of Cryogenic Liquids

Availability and ease of handling are relatively insignificant problems for space vehicle applications. Nitrogen, neon, and helium, being inert gases, can be used without further restriction. The refrigeration effects of interest here are determined by the refrigeration temperature level and specific refrigeration capacity.

Long duration applications with high cooling loads require sophisticated refrigeration systems. Considerable care is required here in system selection in cases where power is limited or heat rejection is a problem.

Fluid Contamination

Another area requiring considerable attention in the design of closed cycle refrigerators is contamination. Extreme care must be taken when charging the system to prevent the introduction of foreign materials into the system together with the working fluid. In addition, all materials "gas off" and exert vapor pressures. Initial degassing must be performed in order to remove adsorbed substances. After degassing, most metals will exert negligible vapor pressures. On the other hand, organic materials such as plastics, rubbers, and lubricants produce significant quantities of vapors which, over a period of time, can freeze and clog the system. This can be avoided by employing gas-bearing machinery throughout the system. This method will also alleviate the problem of leakage since the system may then be completely sealed.

In addition to gaseous contaminants, the system can be contaminated by solid materials generated within the system itself by the normal wear of the moving parts. Solid contaminants can completely disrupt the operation of systems utilizing Joule-Thomson expansion valves by blocking the expansion orifice. Solid contaminants also form in the high-pressure passages of the heat exchangers acting as fractionating columns to freeze out impure gases. Eventually, blockage or severe restriction occurs at distinct locations within the heat exchangers. Contaminant freeze-out is of more concern in helium liquefying systems, since all other fluids in the system would be frozen. Safeguards against solid contaminants must be employed by introducing suitable filters in the system lines and by minimizing the possibility of their occurrence by careful design of the system moving parts.

SECTION III

RADIATORS

Heat rejection from a space vehicle over long-duration operation necessitates the use of radiators, since the only practical means of effecting continuous heat rejection in a space environment is by radiation. It is outside the scope of this report to make a thorough investigation of radiators; however, a brief outline of radiator design considerations is in order.

The design of actual hardware to be used in radiator systems for space applications is not well developed due to the many requirements that must be met by such systems, e.g., low weight, high reliability, operation in vacuum environment, capability of continued operation despite many possible collisions with meteoroids.

Among several schemes of radiator design guarding against meteoroid hazards, one of the most promising is the armored-tube and fin type. The following discussions are concerned with this type of radiator and are based on single-phase flow of the heat transport fluid through the radiator panels.

Design Considerations

In any extended surface radiator configuration, heat is transferred by forced convection from the flowing fluid to the conduit walls, through the conduit walls either to the outer conduit surface or to the extended surfaces via some type of fin, and by radiation to the space environment. The largest thermal resistance in the process by far is in the radiation process. Hence, the thermal design of a radiator is primarily concerned with its radiative properties.

The net radiant heat flux from an element of surface area may be expressed as:

$$dq_{R\ net} = dq_R - dq_{in} \tag{211}$$

where dq_R is the radiant heat flux from the element and dq_{in} is the radiant heat flux from the environment. By the Stefan-Boltzmann law:

$$dq_R = \sigma \epsilon_T T^4 dA \tag{212}$$

where σ = Stefan-Boltzmann constant = 0.1712×10^{-8} $\frac{Btu}{hr\text{-}ft^2\text{-}{}^\circ R^4}$

ϵ_T = emissivity for thermal radiation

The absorbed heat flux, dq_{in}, comes from four sources for a vehicle orbiting around a planet

a) direct solar radiation, dq_S

b) solar radiation reflected from the planet, dq_P

c) thermal radiation from the planet, dq_{PT}

d) reflected and thermal radiation from other parts of the vehicle itself or another vehicle, dq_V

This can be expressed algebraically by

$$dq_{in} = dq_S + dq_P + dq_{PT} + dq_V \tag{213}$$

The direct solar radiation may be expressed as

$$dq_S = \alpha_S \, S \, F_S \, dA \tag{214}$$

where α_S = absorptivity for solar radiation of the surface

S = solar constant = 443 Btu/hr ft^2 at the earth's orbit

F_S = solar view factor

Assuming that the planet concerned is the earth, the solar radiation reflected from the planet can be expressed as

$$dq_P = \alpha_S \, a \, S \, F_{E(SR)} \, dA \tag{215}$$

where a = earth's albedo (normal value: 0.35)

$F_{E(SR)}$ = view factor for reflected solar radiation

The thermal radiation from the earth is similarly given by

$$dq_{PT} = \alpha_T \, E_T \, F_{E(TR)} \, dA \tag{216}$$

where α_T = absorptivity for thermal radiation of the surface

E_T = thermal radiation constant of the earth

$F_{E(TR)}$ = view factor for thermal radiation

The solar view factor, F_S, is the cosine of the angle between the sun vector and the normal to the element of area. For the geometry shown in Figure 14, the value of F_S is found to be

$$F_S = \sin\gamma \sin\theta_S \cos\phi_C - \cos\gamma \cos\theta_S \tag{217}$$

The view factor for reflected solar radiation, $F_{E(SR)}$, is also a function of the various angles involved and of the distance to the earth. Plots of $F_{E(SR)}$ for the geometry of Figure 14 are shown in Figures 15, 16, 17, and 18. The dependence of $F_{E(SR)}$ on ϕ_C (see Figure 18) is not great, and for values of ϕ_C between the plotted values of 0° and 180°, linear interpolation should be sufficient.

The view factor for thermal radiation, $F_{E(TR)}$, is plotted in Figure 19.

In order to relate the thermal radiation constant of the earth, E_T, to the solar constant, S, we may equate the thermal radiation of the entire planet to the absorbed radiation. Thus, from steady-state energy balance, the following expression is obtained

$$4\pi R^2 E_T = (1 - a)\, S\, \pi R^2 \tag{218}$$

where R is the radius of the earth. Now, summing all dq terms and substituting the value of E_T from Equation 8, the value of $dq_{R\ net}$ (see Equation 1) becomes

$$dq_{R\ net} = \left[\sigma\epsilon_T T^4 - \alpha_S SF_S - \alpha_S\, a\, SF_{E(SR)} - \alpha_T \frac{(1-a)}{4} SF_{E(TR)}\right] dA \tag{219}$$

An effective sink temperature, T_S, can now be defined such that

$$dq_{R\ net} = \sigma\epsilon_T (T^4 - T_S^4)\, dA \tag{220}$$

Equating Equations 9 and 10, the explicit expression for T_S is found

$$T_S = \left\{\frac{1}{\sigma}\left[\frac{\alpha_S}{\epsilon_T} SF_S + \frac{\alpha_S}{\epsilon_T}\, a\, SF_{E(SR)} + \frac{(1-a)}{4} SF_{E(TR)}\right]\right\}^{1/4} \tag{221}$$

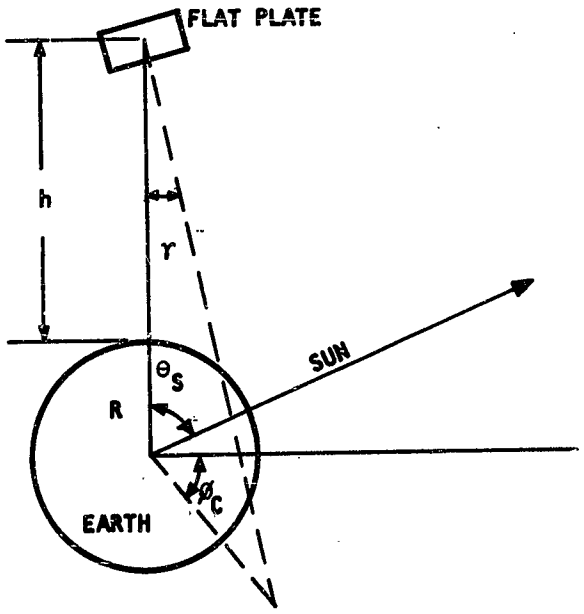

Figure 171. Special Coordinate Scheme for Flat Plate View Factors

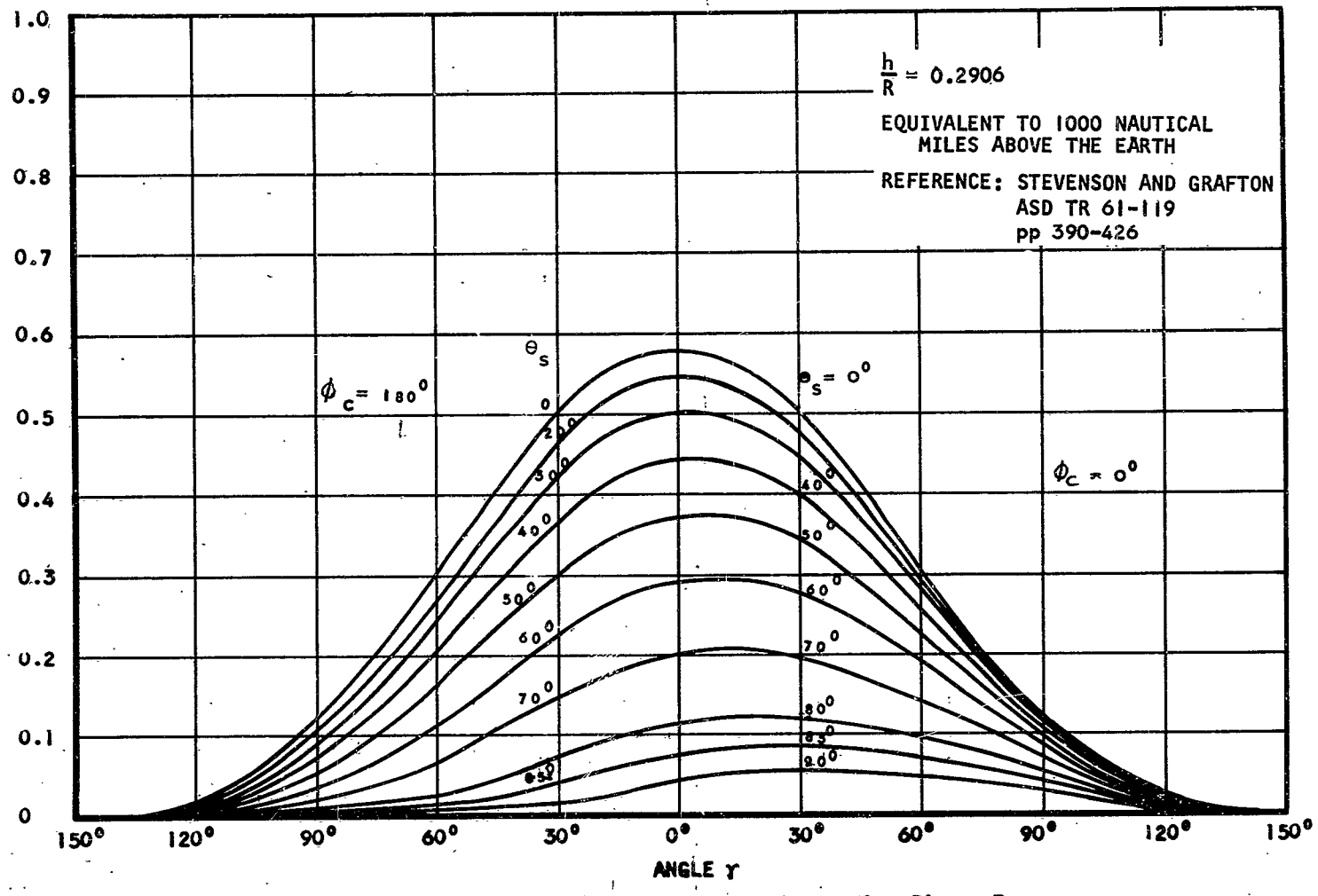

Figure 172. Reflected Solar View Factor for a Flat Plate, $F_{E(SR)}$

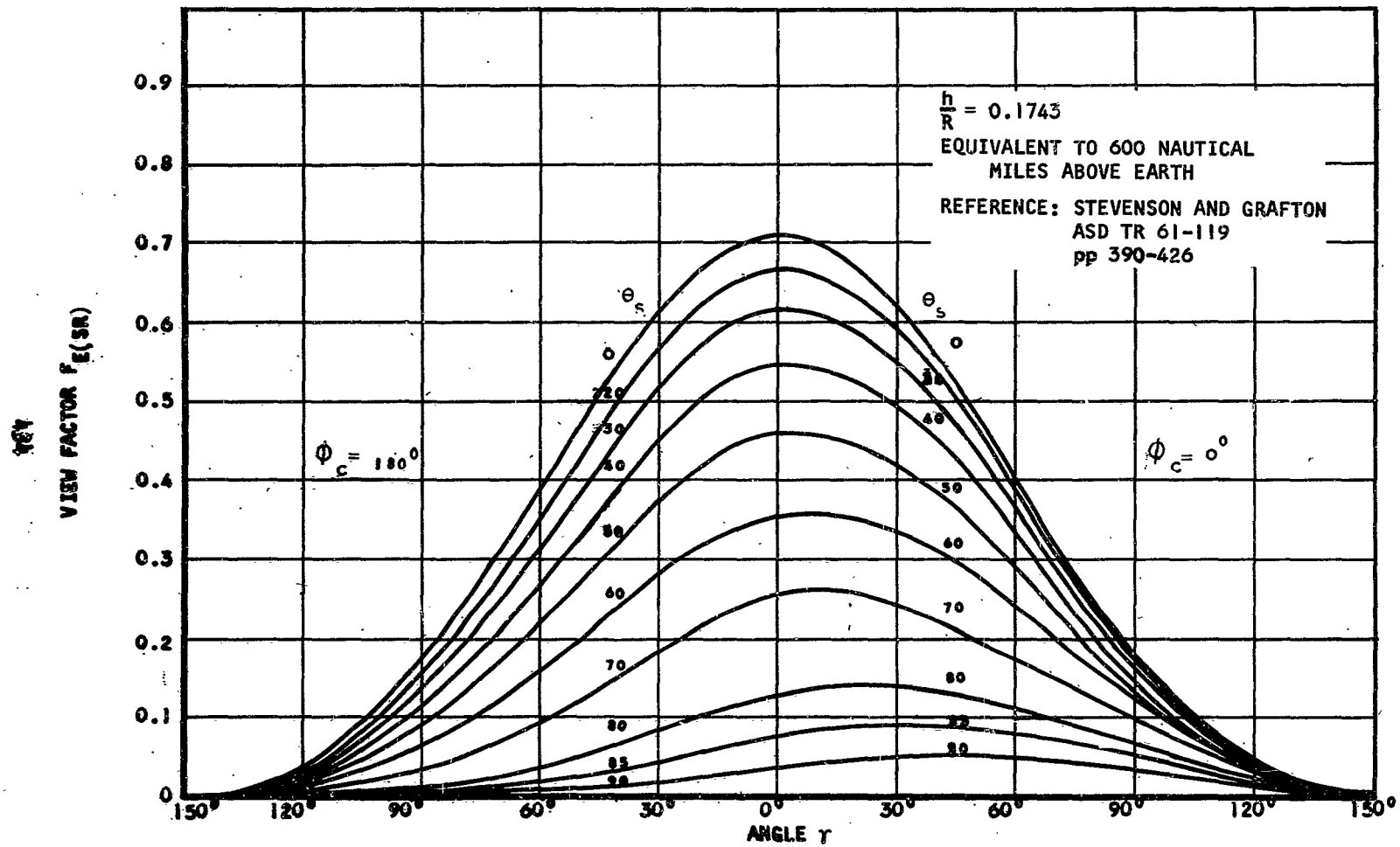

Figure 173. Reflected Solar View Factor for a Flat Plate, $F_{E(SR)}$

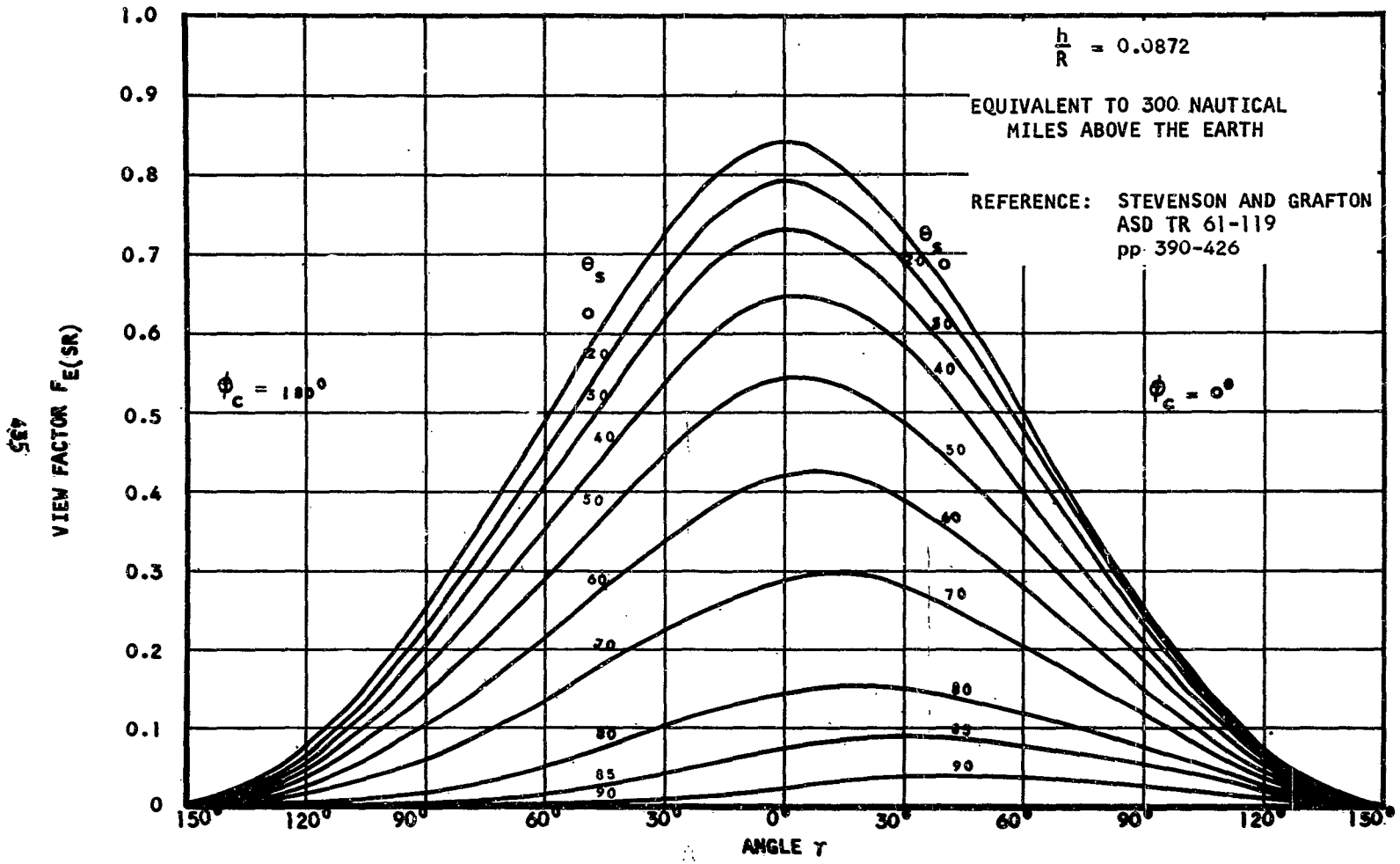

Figure 174. Reflected Solar View Factor for a Flat Plate, $F_{E(SR)}$

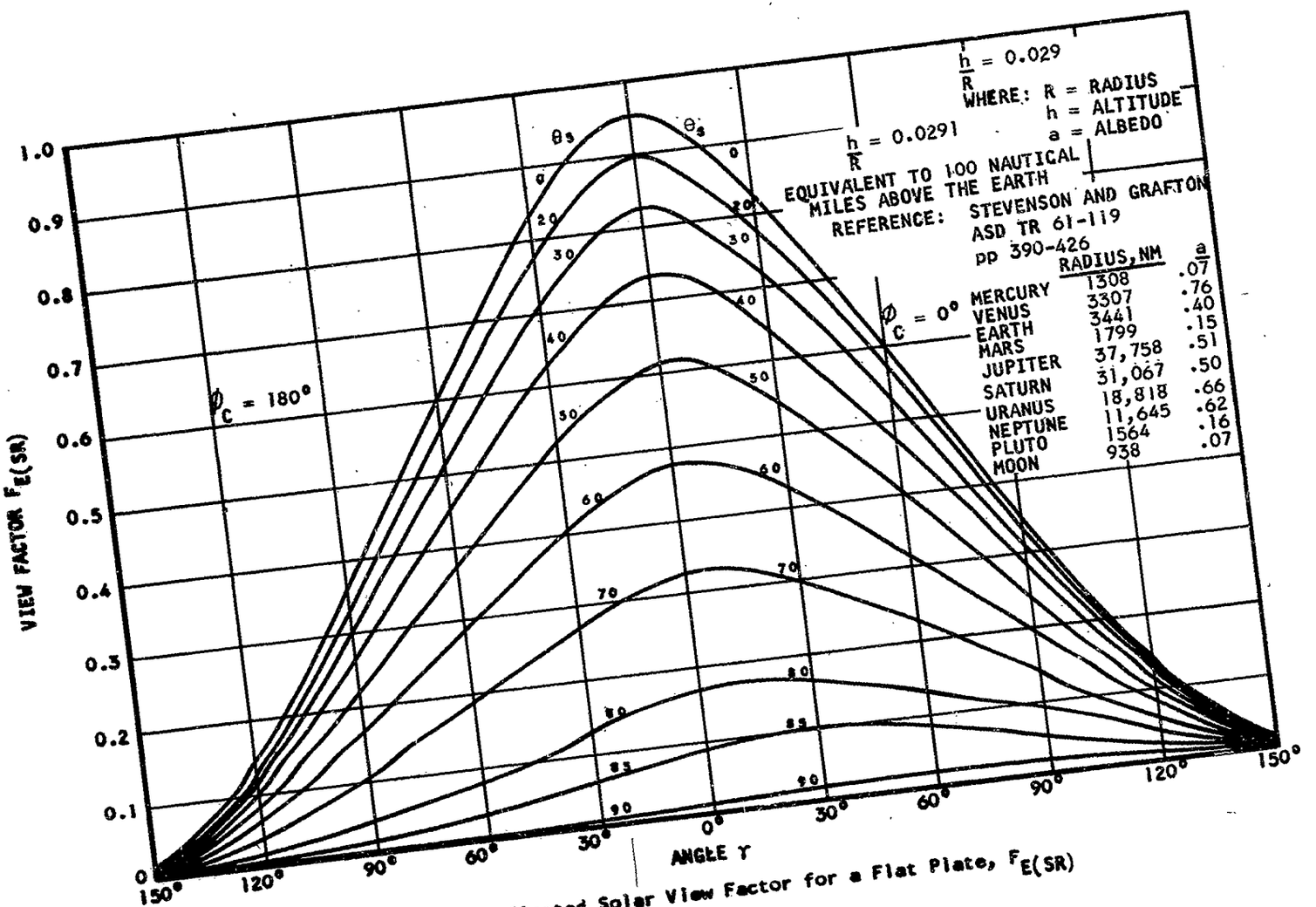

Figure 175. Reflected Solar View Factor for a Flat Plate, $F_{E(SR)}$

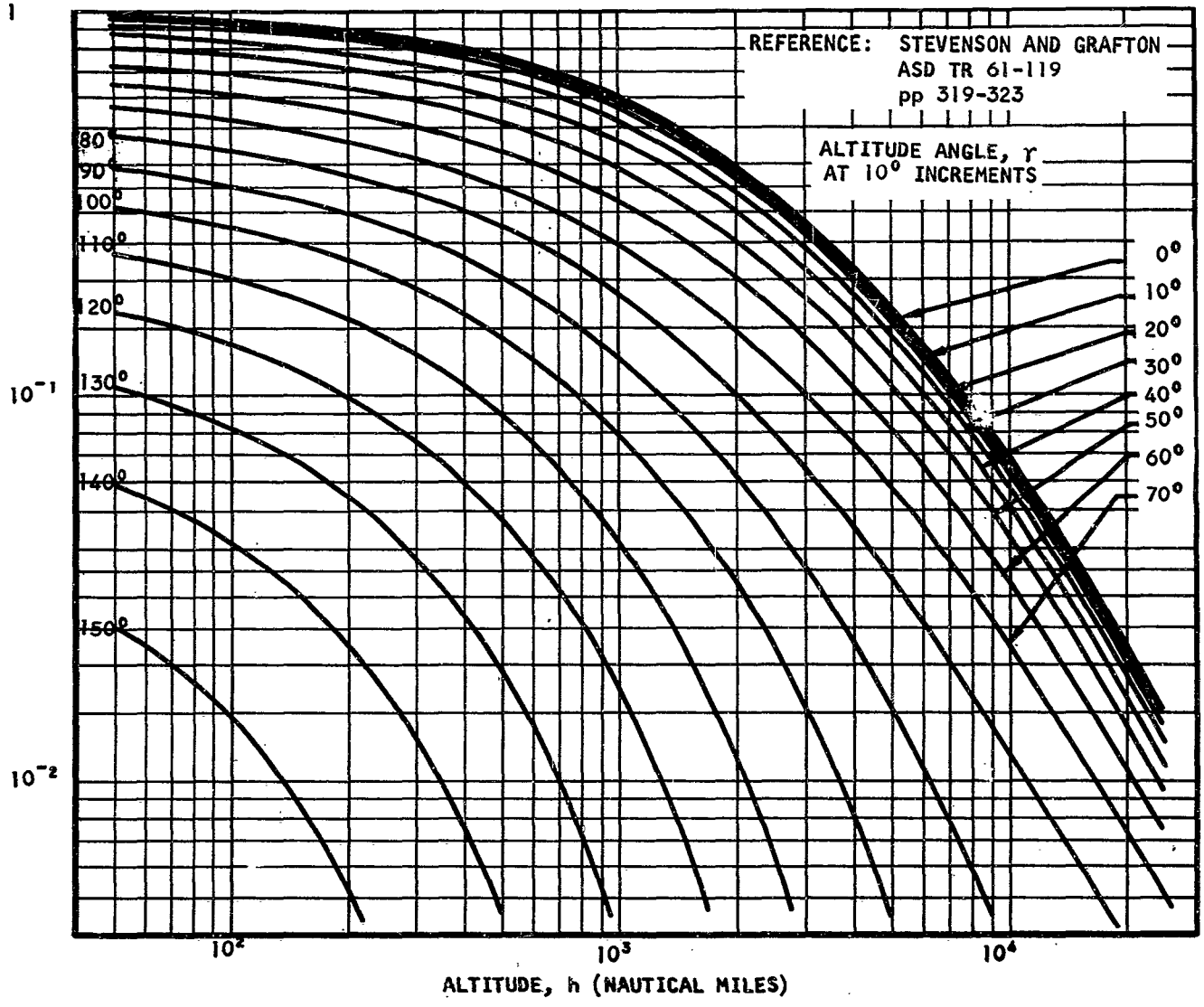

Figure 176. View Factor for Earth Thermal Emission Incident to a Flat Plate, $F_{E(TR)}$

It should be noted that T_S, the effective environmental sink temperature, is not a true temperature of a part of the physical system. It is merely a quantity, having the dimensions of temperature, defined by Equation 10. T_S would be the equilibrium temperature of a planer surface if it were completely insulated from all heat inputs except those due to radiation on one side only.

Surface Emissivity and Coatings

The evaluation of the equivalent sink temperature, T_S, depends on the ratio of the radiator surface solar absorptivity to thermal emissivity corresponding to the specific radiator temperature. Therefore for low sink temperatures and relatively high heat rejection rates, it is desirable to have spectrally selective coatings applied to the radiator surface to control energy flux. There are many materials in which total emissivity varies with temperature; these can be used to achieve the proper energy balance. Selective radiation surfaces can be fabricated by depositing multi-layers on the surface; for example, a gold smoke film has the property of being almost completely transparent to radiation above 2 microns. Using a heat source of 120°F, about 97 per cent is transmitted whereas only 20 per cent of the visible spectrum is transmitted with 2 to 3 per cent reflection.

A polished copper surface may be assumed to have a 75 per cent reflectivity in the visible range and 98 per cent in the infrared range. Thus, if the gold smoke film were deposited on this copper surface, 92 per cent of the radiation above 2 microns and only 5 per cent of the visible radiation would be reflected due to double absorption. However, at elevated temperatures, the structure and optical properties of the film are affected and stability becomes a factor.

Considerable effort is being directed toward development of organic coatings which will have high thermal emittance at relatively low temperatures (70-300°F), and low absorptivity for solar radiation. These coatings must be characterized by high resistance to ultraviolet and nuclear radiation, good thermal stability, and high molecular weight to minimize boiloff losses.

Preliminary work indicates that organic coatings can be developed with thermal emissivities greater than 0.95. At the present time, no organic coating can be recommended which will meet all the environmental requirements. Some work has shown that organic coatings which are sensitive to ultra-violet may be successfully protected.

White and black paints can also be used to obtain the proper spectral surface. One advantage that paints have over ceramic coatings is that they can be applied in the field. These paints consist of a silicone or acrylic base with a white or black pigment. Typical values are:

White paint - Thermal emissivity, 0.85-0.87
Solar absorptivity, 0.17-0.30

Black paint - Thermal emissivity, 0.92-0.95
Solar absorptivity, 0.9

Since pure metals are generally reflective at temperatures from 100-1200°F, they are not suitable for radiator coatings.

Metallic oxides have relatively high emissivities in the infrared region and low absorptivities in the solar radiation region. A summary of radiative characteristics and some physical properties of various oxides is given in Table 2.

TABLE 50

RADIATION CHARACTERISTICS OF METAL OXIDES

Material	Specific Gravity	Total Normal Emissivity 125°F	750°F	Solar	Remarks on Application and Stability
Al_2O_3	3.5-3.9	.98	.79	.16	Good
ZrO_2	5.49	.95	.77	.14	Good
MgO	3.65-3.75	.97	.84	.14	Fair, too soluble
ZnO	5.606	.97	.91	.18	Fair to bad, too soluble in water
CaO	3.40	.96	.78	.15	Bad, decomposes in water
ThO_2	9.69	.93	.53	.14	Good
Y_2O_3	5.096	.89	.66	.26	Fair

Some tests have indicated that an emissivity of at least 0.85 at 100-200°F can easily be obtained for some of these oxides using flame spraying. The values of 0.93-0.97 at low temperatures listed above can only be obtained under ideal conditions.

From the values listed above it can be seen that reasonable values for the ratio of the solar absorptivity over the thermal emissivity, α_S/ϵ_T, are in the neighborhood of 0.15.

Radiator Area

Using Equation 10 to represent the net radiant heat exchange at the surface, the one-dimensional heat flow in a thin extended surface may be expressed as (see Figure 20).

$$\sigma\epsilon_T (T^4 - T_S^4)\, dX = K \frac{d^2T}{dL^2} (\delta\, dX) \qquad (222)$$

where K = thermal conductivity of the fin material
δ = fin thickness
X = coordinate parallel to the fluid conduit
L = coordinate in the direction of heat flow

The above equation has been integrated numerically in References 8, 9, and 10 for various types of fins. The results are given in terms of a "fin effectiveness", η_F, which is the ratio of the actual net heat radiated from the fin to the net heat flux that would be radiated if the fin were at a constant temperature, T_R, equal to the fin temperature at its root. The results of References 8, 9, and 10 have been compared and are presented in Figure 21. The radiant heat flux from one side of a fin is then

$$q_{R,net} = \sigma\epsilon_T \eta_F (T_R^4 - T_S^4) A_F \qquad (223)$$

assuming a constant fin root temperature in the direction of the flow. This temperature drops from one end of the fluid conduit to the other. The fin root temperature, T_R, must be determined from the bulk fluid temperature, T_L, within the conduit wall and from the type of flow within the conduit.

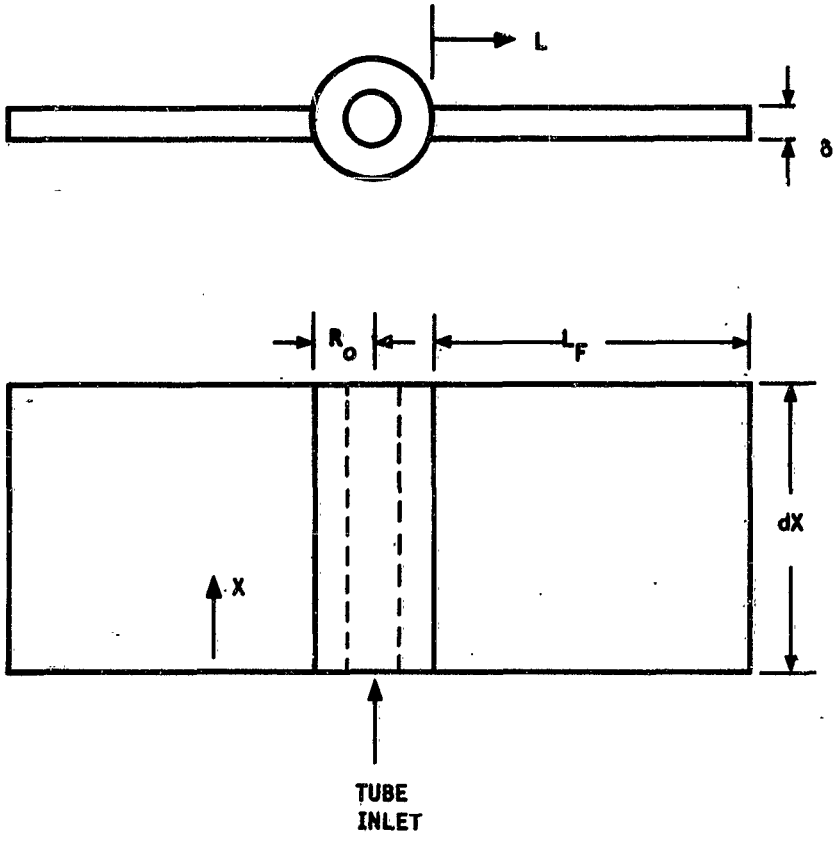

Figure 177. Coordinates for One-Dimensional Heat Flow

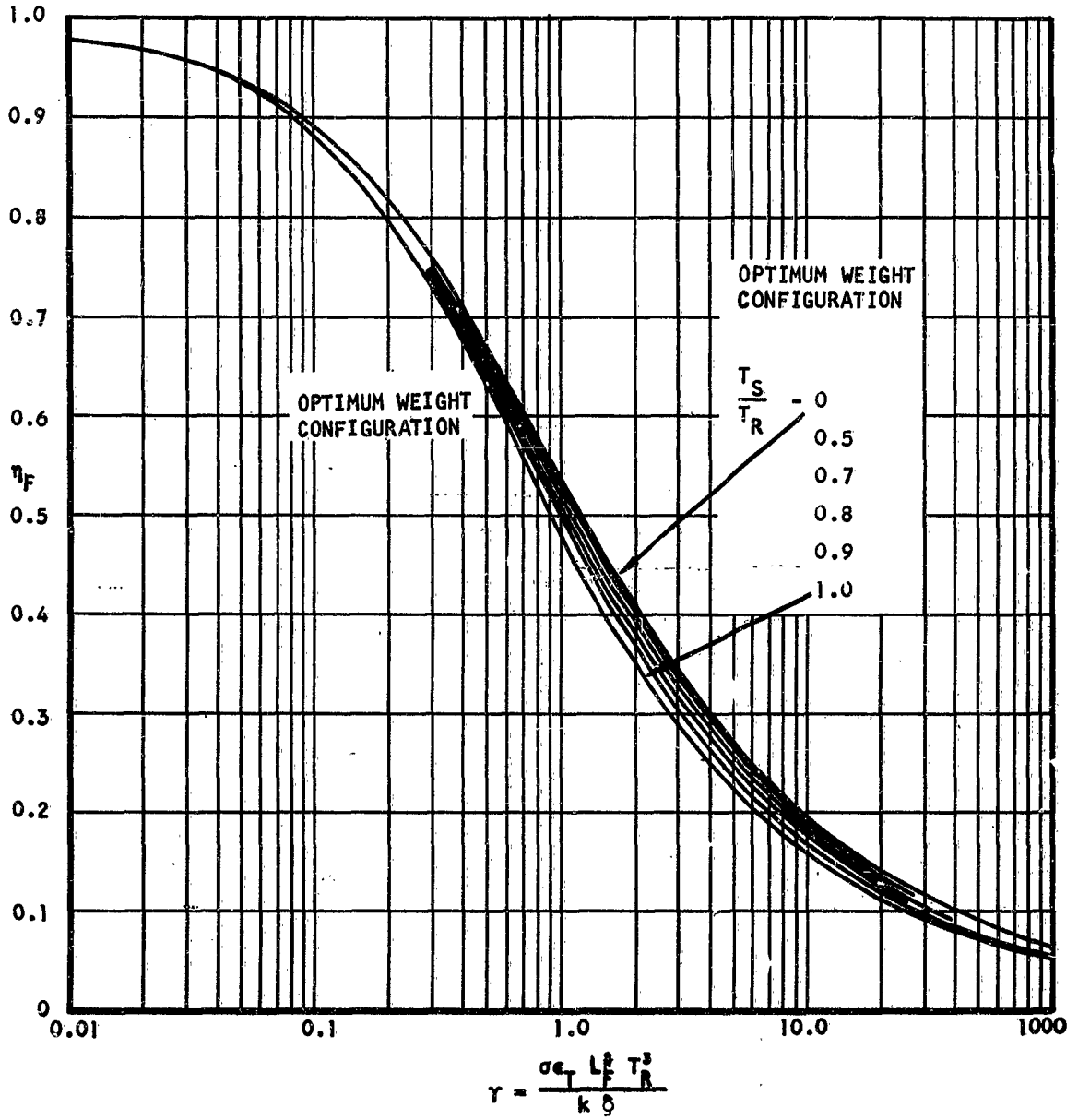

Data taken from: Bartas and Sellers, Trans. ASME, Series C, Journal of Heat Transfer 82, 73-75 (1960)
S. Lieblein, NACA TN D-196
D. B. Mackay, ASD 61-30, NAA SID 61-66

Figure 178. Radiation Fin Effectiveness η_F, for Rectangular Fins

For the simple case of a flat radiator panel, the geometric view factors and the effective sink temperature will remain constant over the entire surface. For a tube segment of length, dX, the element of surface area is

$$dA = (2 R_0 + 2 L_F)\, dX \tag{224}$$

where R_0 = outside tube radius

L_F = fin length

Assuming that the tube surface area has an effectiveness of 1.0, we can write

$$dq_{R,\ net} = \sigma \epsilon_T (2 R_0 + 2 \eta_F L_F)(T_R^4 - T_S^4)\ dX \tag{225}$$

We also have the relation

$$dq_{R,\ net} = -w C_p\, dT_L \tag{226}$$

where C_p = heat capacity of the fluid

w = fluid flow rate

T_L = bulk fluid temperature

Assuming that the bulk fluid temperature is sufficient to represent the thermal conditions at any point and also assuming steady-state conditions. Combining the two expressions,

$$\sigma \epsilon_T \eta_0 (T_R^4 - T_S^4)\, dA = -w C_p\, dT_L \tag{227}$$

where η_0, the overall effectiveness, is defined by

$$\eta_0\, dA = (2 R_0 + 2 \eta_F L_F)\, dX \tag{228}$$

The rigorous analytical integration of Equation 17 has not yet been accomplished. In order to have some basis for estimating the performance characteristics of the thermodynamic cycles studied in this report, the following simplifying assumptions are made:

(1) $T_R = T_f$

(2) $\eta_F = 1.0$

These assumptions permit the analytical integration of Equation 17 and predict the maximum possible heat rejection from the panel. The integrated expression is

$$A_{R,\,min} = \left[\zeta\,(\tau_{outlet}) - \zeta\,(\tau_{inlet})\right] \frac{w\,C_p}{\sigma \epsilon_T\, T_S^3} \qquad (229)$$

where $A_{R,\,min}$ = minimum radiator area, total

$\tau = T_R/T_S$

$\zeta\,(\tau) = \frac{1}{4} \ln\left(\frac{\tau+1}{\tau-1}\right) + \frac{1}{2} \arctan \tau$

For the purpose of this study it is necessary to choose a value for T_S, the effective sink temperature, in order to arrive at some reasonable value for the radiator area. T_S will vary widely according to the geometry of the system. As an example, referring to Figure 14, assume

h = 300 nautical miles

$\phi_c = 90^\circ$

then T_S will vary from 0°R to 490°R depending on what values θ_S and γ assume. Since the assumptions made in deriving Equation 19 lead to overly optimistic results, a relatively high value of 400°R for T_S was chosen. Values of $A_{R,\,min}/wC_p$ as a function of inlet temperature are plotted in Figure 22.

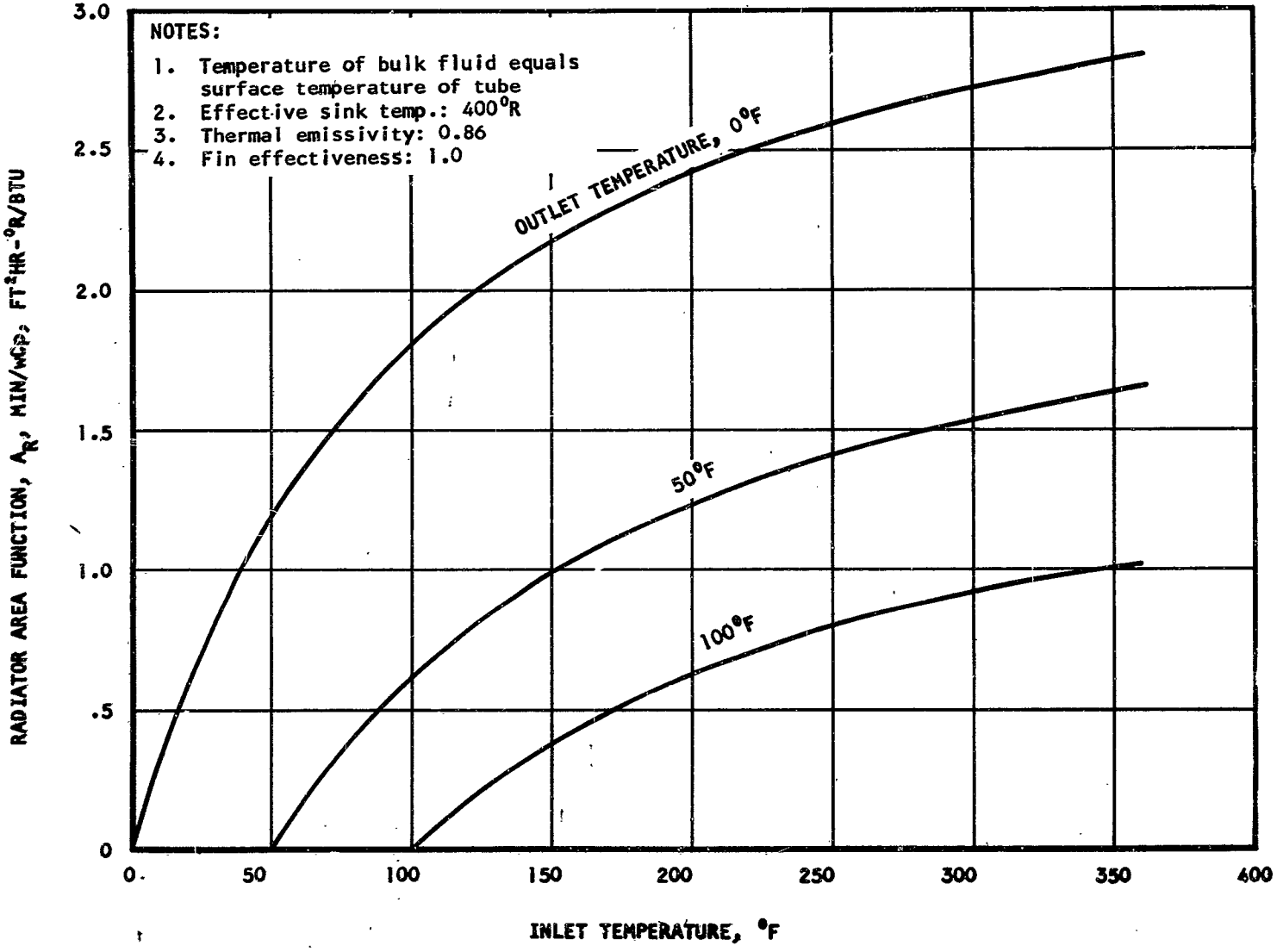

Figure 179. Radiator Area Function

The rate of heat rejection, Q, is given by

$$Q = w C_p (T_{inlet} - T_{outlet}) \qquad (230)$$

$(T_{inlet} - T_{outlet})$ as well as T_{outlet} should be chosen with the entire vehicle temperature control system in mind. For the purpose of this study, T_{outlet} was chosen to be 50^0F and $(T_{inlet} - T_{outlet})$ was chosen to be 120^0R. Therefore, the radiator area A is given by

$$A = 31.3\ Q, Ft^2 \qquad (231)$$

where Q is in kw.

Radiator Weight

The weight of the radiator per unit area will depend primarily on the amount of meteoroid shielding and on the equivalent sink temperature. In order to achieve a minimum equivalent sink temperature, orientable radiators may be employed. However, this approach requires additional components and may prove unfeasible when very large radiators are involved. Typical fixed radiator weights are in the range 1/2 to 3/4 lb per square foot. For the purpose of this study, a weight of 3/4 lb will be assumed.

SECTION IV

COMPRESSORS AND EXPANDERS

The compressors and expanders that are most suitable for low temperature refrigeration systems used in space applications are turbomachines of the centrifugal types. They are selected on the basis of the requirements for high pressure ratios encountered in optimization of the refrigeration cycles. Their high performance and reliability also make them attractive for space vehicle installation.

Compressors

The centrifugal compressors considered in this study are of the multi-stage type. Interstage cooling is used to minimize the power consumption and also to reduce the number of stages necessary for the high pressure ratios In view of the latest developments in high-speed motor technology, the compressors are assumed directly driven by high-speed electric motors at the compressor design speed. This approach leads to a lightweight compact construction as compared to gear driven compressors. Also, the motor-compressor assembly is well suited to the incorporation of gas bearings in the design. This contributes greatly to the elimination of the problems of working fluid contamination and leakage in closed cycle systems.

As the flow rates and pressure ratios considered in this study cover a wide range, it is understood that the parameters describing the compressors correspond to attainable values in the present state-of-the-art.

A. Power Requirements and Characteristic Dimensions

The basis for the calculation of the compressor power requirement is the wealth of experimental data available on centrifugal compressors, References 12 and 13. In general, the efficiency of these compressors can be expressed by the functional relationship:

$$\eta_c = f(n_s, (\rho/\rho_i), Re, M) \qquad (232)$$

where

η_c = compressor efficiency

n_s = compressor specific speed

ρ/ρ_1 = density ratio across the compressor

M = compressor Mach number

Re = compressor Reynolds number

The compressor Mach number is generally determined from impeller stress considerations and also from the attractiveness of a supersonic design. In general, it limits the attainable pressure ratio. A reasonable value is taken here to ensure a good performance and also to facilitate the matching of the various stages of the multistage design.

The density ratio parameter is one that depends essentially on the nature of the refrigerant, be it nitrogen, neon, or helium. As the pressure ratio across each stage is held within reasonable limits, the density change is not large, and the previous functional relationship (Equation 22) is reduced to:

$$\eta_c = f(n_s, M, Re) \qquad (233)$$

Within a range where Reynolds number and Mach number are not effectively contributing to any change in compressor performance, the above relation is reduced to:

$$\eta_c = f(n_s) \qquad (234)$$

Attainable performance of centrifugal compressors as a function of specific speed can be found from the data of Reference 12. As the flow rate decreases to small values, the compressor diameter reduces to a size where a penalty in performance is suffered due to manufacturing tolerances.

The attainable efficiency as a function of specific speeds is used to derive the power requirements shown on Figures 23, 24, and 25. The The calculations leading to these plots are based on the following assumptions:

	Nitrogen	Neon	Helium
First Stage			
Inlet Temperature, °R	560	560	560
Inlet Temperature to Various Stages (Intercooling Effect), °R	565	565	565
Inlet Pressure, psia	14.7	14.7	14.7
Tip Speed, ft/sec	1500	1500	1500
Mach Number	1.27	.99	.44
Backward Blade Angle, deg	30-45	30-45	30-45

B. Compressor Weight

The weight of the compressor is calculated using the data on high-speed compressors built by AiResearch for airborne applications. An analytical expression approximating these data points is given by

$$W = \lambda + D^3 \left[\phi Z + \psi p_1 (r - 1) Z^n\right] \qquad (235)$$

where

W = compressor weight, lb

P_1 = inlet pressure, psia

Z = number of stages

D = diameter of compressor wheel, in.

r = compressor pressure ratio

λ, ϕ, ψ, n are constants given as

$\lambda = 3.9$

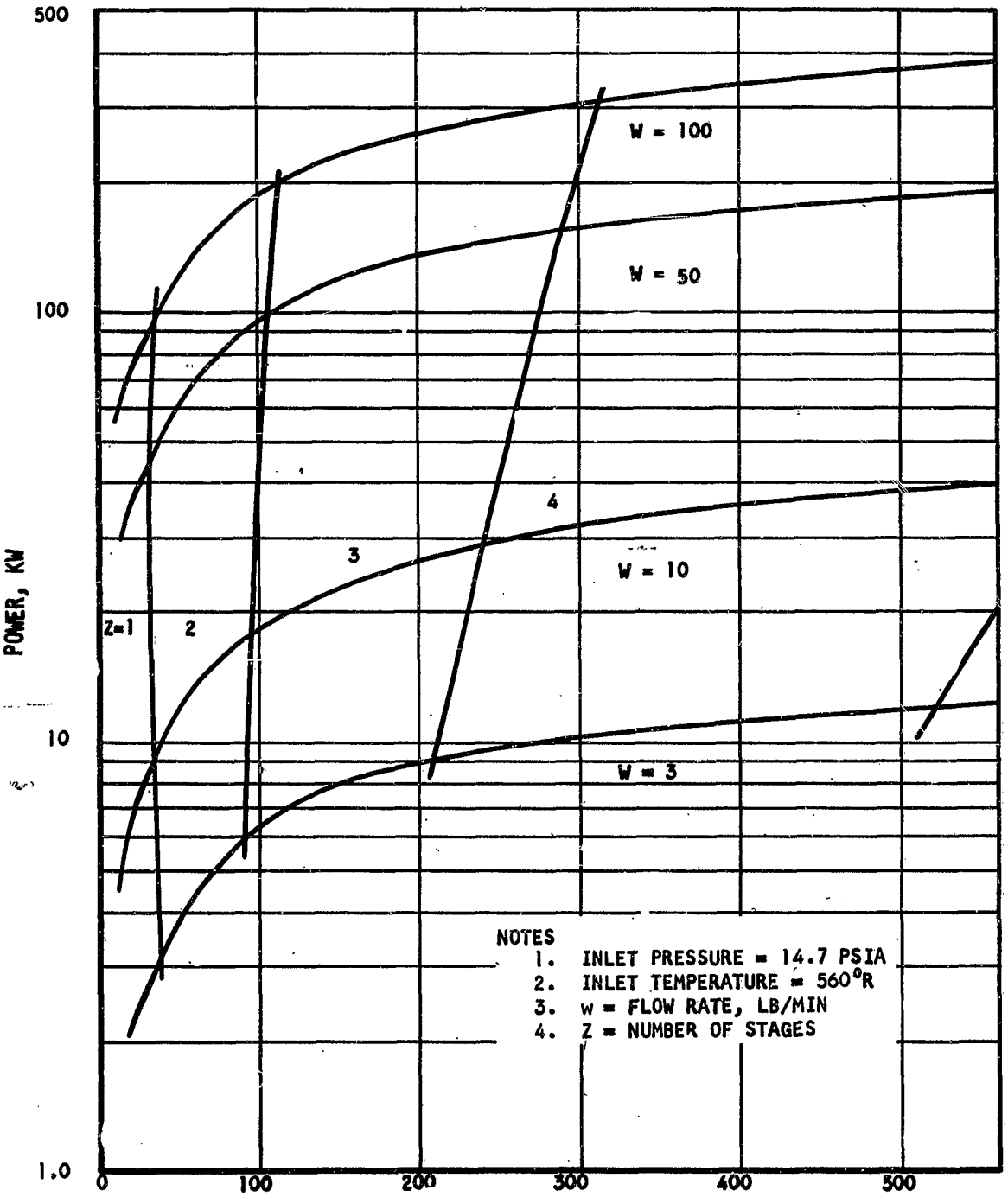

Figure 180. Nitrogen Compressor Power Requirement

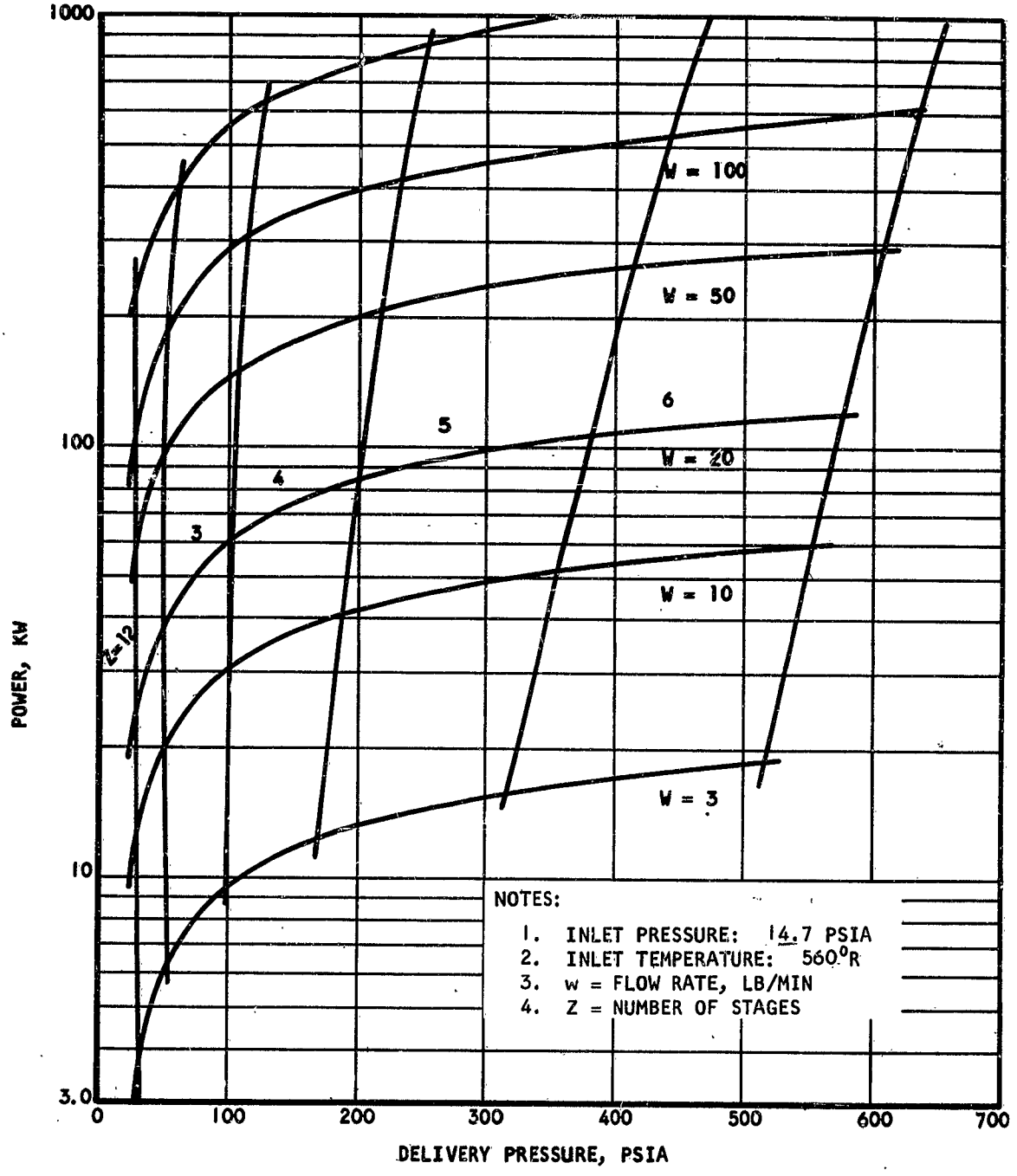

Figure 181. Neon Compressor Power Requirement

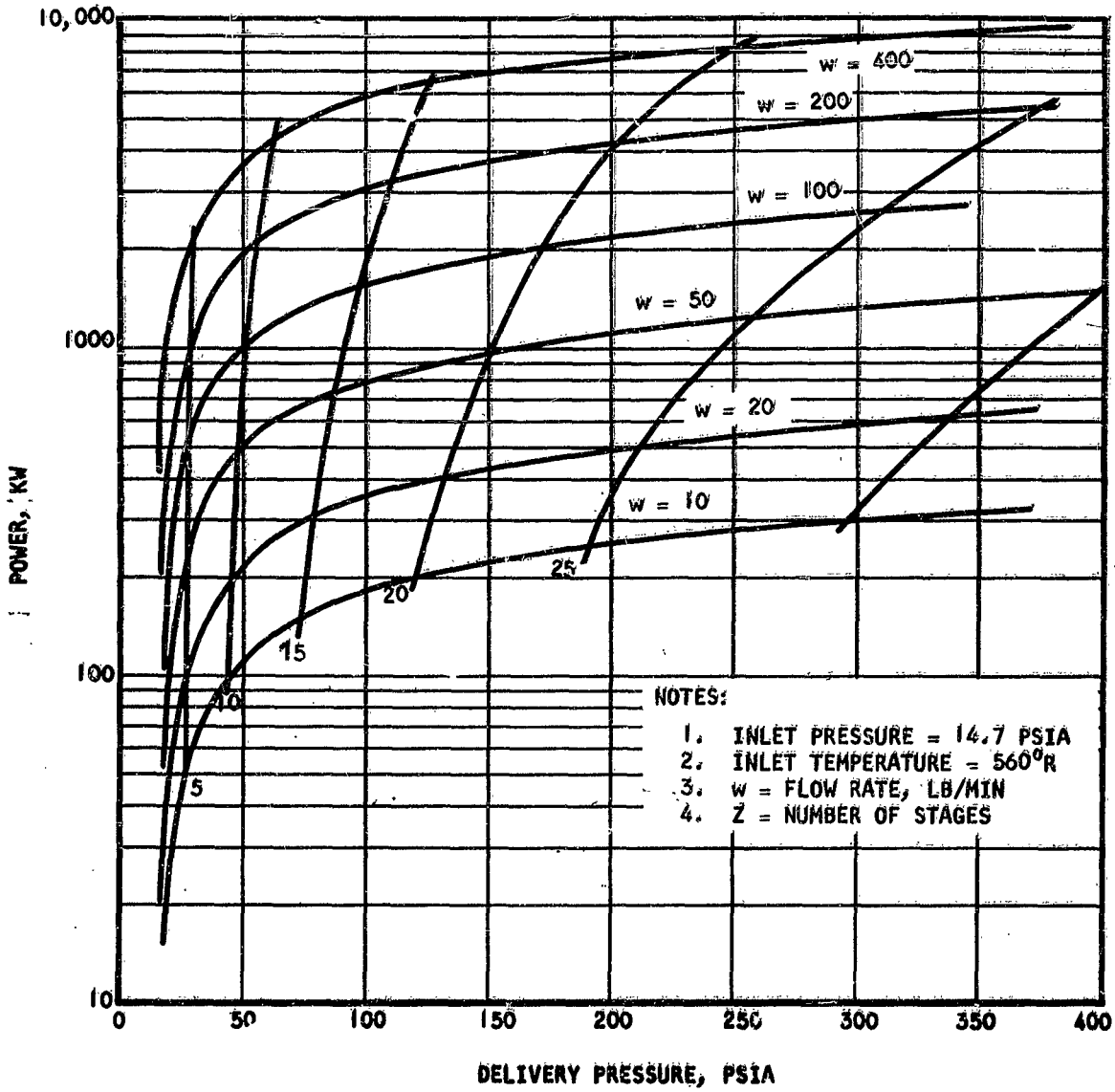

Figure 182. Helium Compressor Power Requirement

$\phi = -0.028$

$\psi = 0.0021$

$n = 0.26$

The impeller diameters as functions of the flow rates are plotted in Figure 26.

C. Electric Motors

In the present state-of-the-art, the maximum speed of motors in the sizes considered in this study is on the order of 100,000 rpm. In some cases, therefore, gears would have to be used to accomodate the high compressor operating speeds. As an alternatative, the compressor design speed could be reduced to match that of the motor. The direct drive feature with gas lubricated bearings is very attractive in refrigeration systems of the type considered, since it makes possible the design of a closed system without any leakage or working fluid contamination by lubricants. One method of driving the compressor at its own speed is by means of a magnetic coupling, the motor and gearing being physically located outside the sealed system.

The efficiency of high speed motors in the 10 kw range or above is taken in this study as 85 per cent. This value is commonly attained and apresents the state-of-the-art. High speed motor weight is taken in this study as 0.8 lb per kw; this value is somewhat optimistic for motor sizes lower than 20 kw. However, most motors considered in this study deliver power in excess of this value.

D. Intercooling and Aftercooling

Most of the heat input into the refrigeration systems under consideration is introduced into the working fluid during the compression process. This occurs at a temperature above ambient. Removal of this heat between the compressor stages greatly improves the compressor efficiency. Removal of the compression heat after the last compressor stage, on the other hand, improves the cycle performance. In this study, the working fluid is

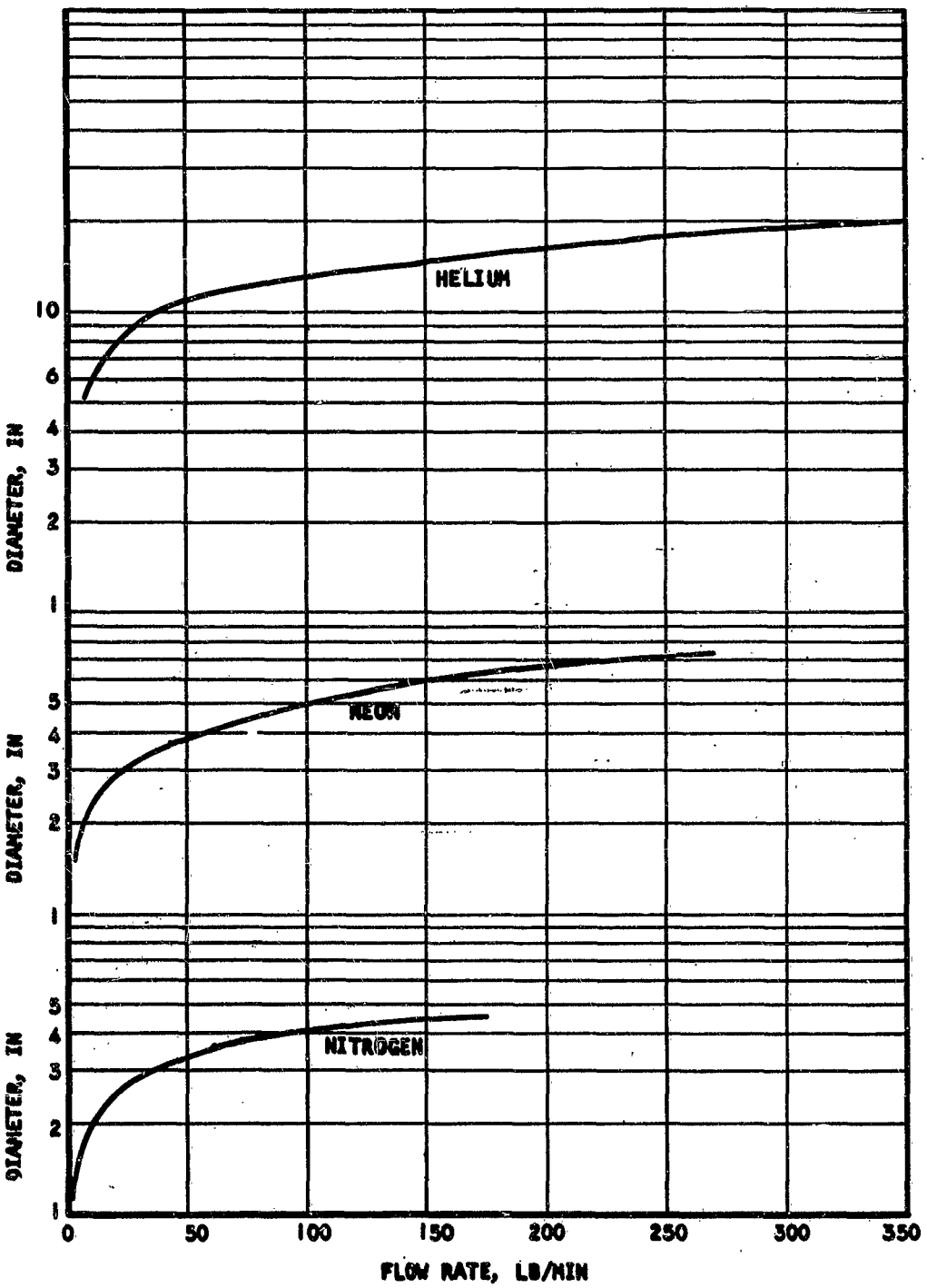

Figure 103. Compressor Impeller Diameter

assumed to leave the compressor aftercooler at a temperature of 100°F. Generally, cooling at this temperature level does not impose a high weight penalty on the vehicle thermal management system. Also, as will be seen later, the refrigeration systems of interest are not overly sensitive to compressor (aftercooler) delivery temperatures.

Studies of space vehicle thermal management systems have shown the desirability of integrating all the vehicle heat sinks and heat loads into a single system. The heat load of the refrigeration systems discussed in this report is, therefore, assumed to be dumped into the vehicle heat transport fluid which, in turn, is cooled in the vehicle radiator.

Turboexpanders

Because of their low weight and high intrinsic reliability, radial flow, turboexpanders are well suited for use in refrigeration systems of the type considered in this report; this, in itself, is enough to recommend them in preference to the reciprocating type expanders. In addition, rotating assemblies can easily be supported by gas bearings which are attractive from the working fluid contamination and leakage viewpoint.

A survey of the literature was made in an effort to determine the efficiency and the weight of existing radial flow turbines. It was found that in the range of flows considered in this report, turbine efficiencies between 0.70 and 0.90 are common. It is felt that with careful design and close control of manufacturing tolerances, turbine efficiency on the order of 0.85 can be achieved even at the lower flow rates. This value is used in this report to characterize the various cooling systems considered.

An estimate of the weight of radial flow turbine is given in Figures 27 through 30, for nitrogen, neon, and helium. These plots were also obtained from data gathered from the published literature and AiResearch's own experience in turbomachinery.

The power produced in the expansion process can be used as part of that necessary to drive the compressor. This can be done by direct coupling of

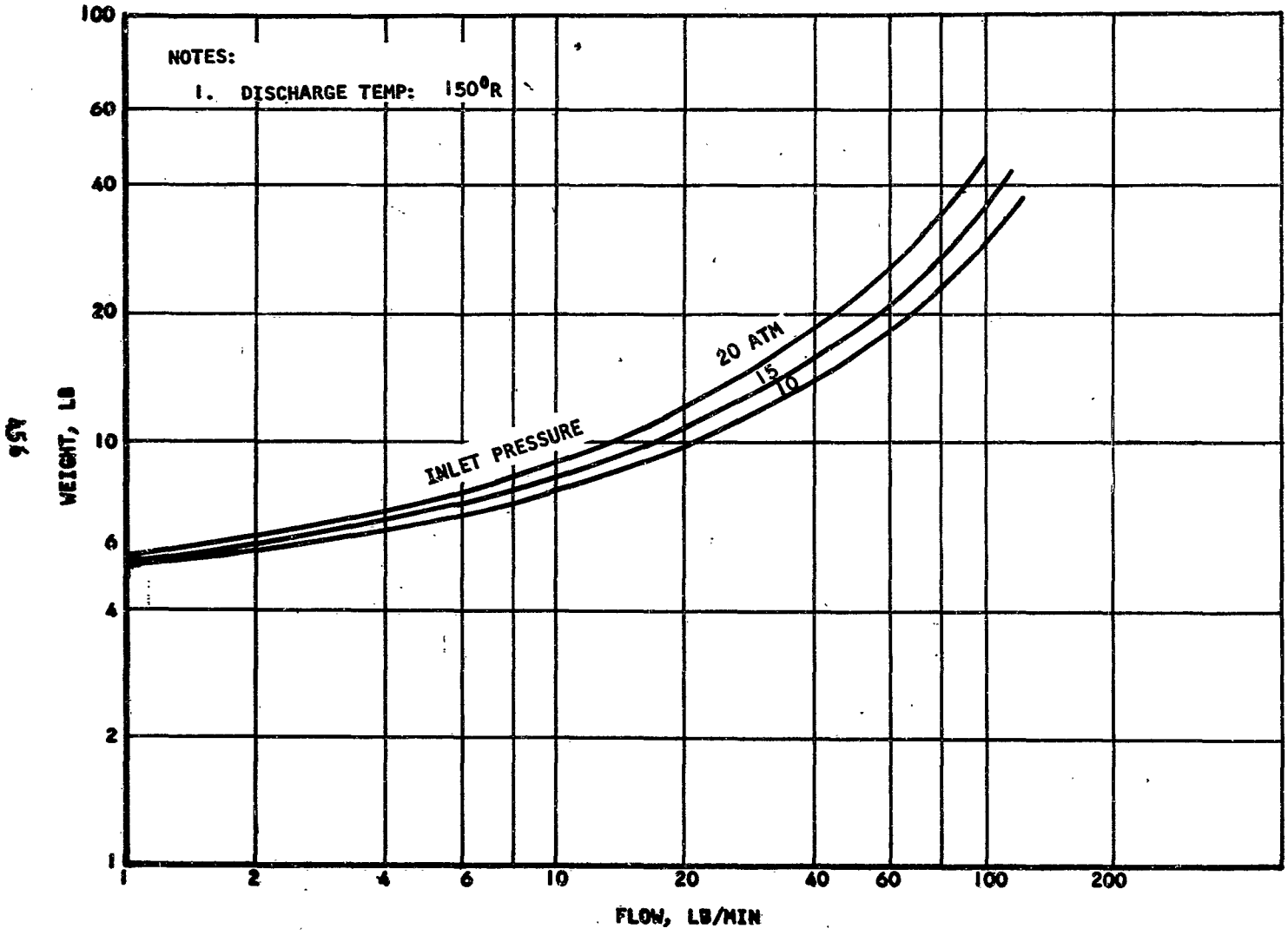

Figure 23. Nitrogen Turbo-Expander Weight

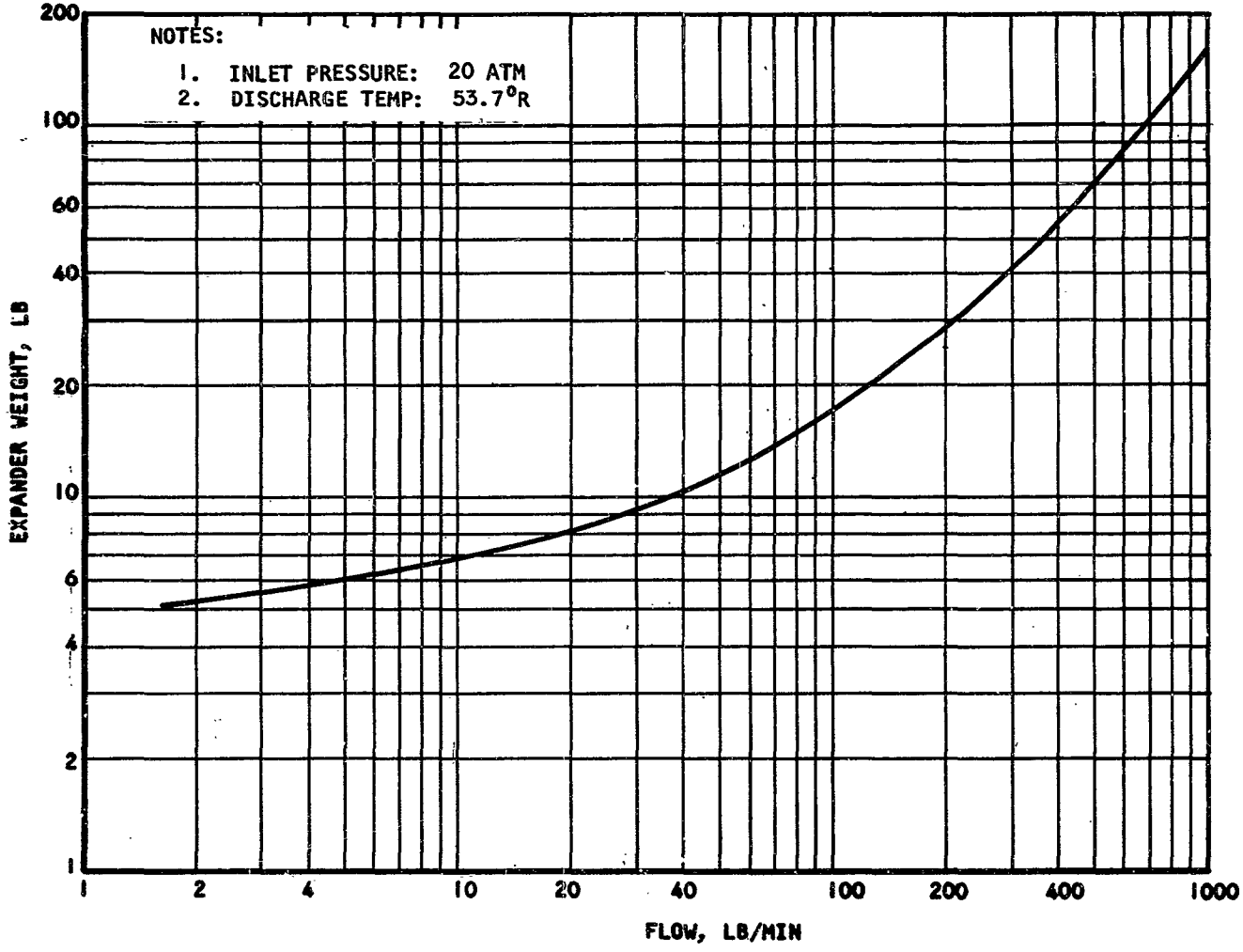

Figure 185. Neon Turbo-Expander Weight (A)

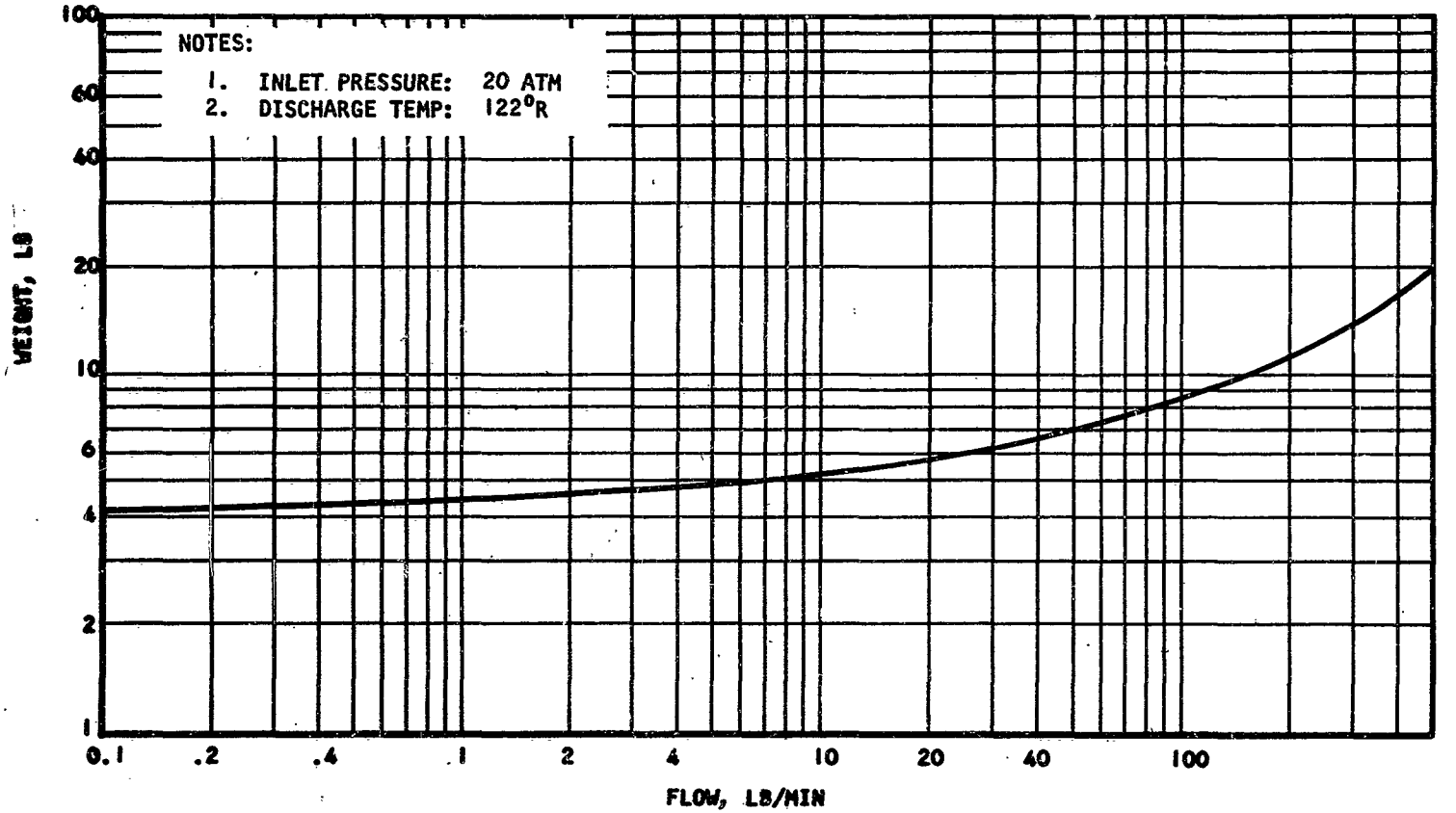

Figure 186. Neon Turbo-Expander Weight (B)

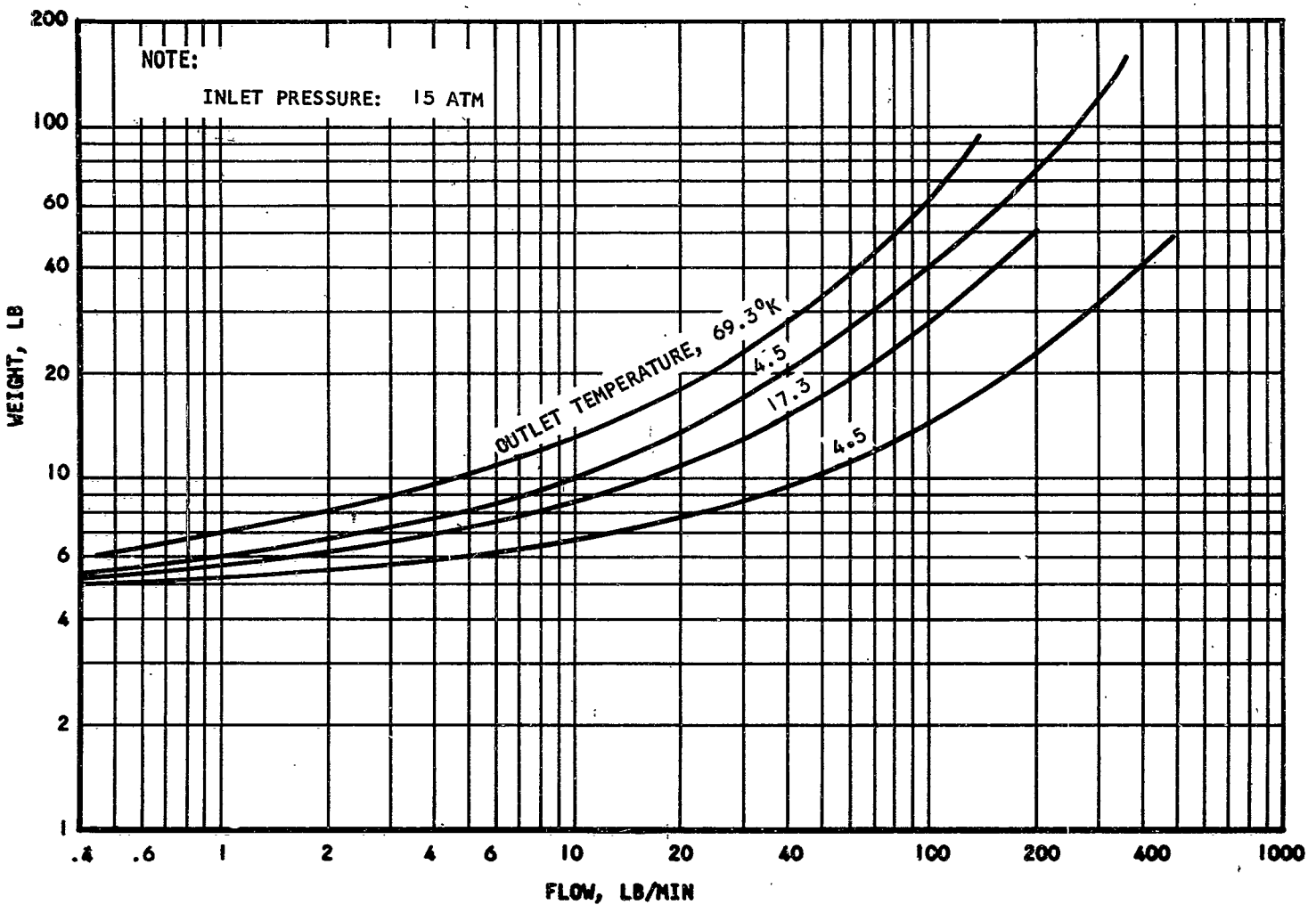

Figure 187. Helium Turbo-Expander Weight

the compressor and turbine, although this method leads to complex motor-compressor-turbine speed matching and to packaging problems. An alternate method is to use the turbine to drive a generator or alternator, the electrical power thus produced being, in turn, used to drive the compressor. The losses in the electrical machines make this last method less efficient than the direct drive approach. The best turbine loading method in any particular application can only be determined by careful weight, packaging and power tradeoff studies. In this report, the power requirements of the systems analyzed are determined on the basis of full utilization of the turbine power.

SECTION V

HEAT EXCHANGERS

Heat exchangers contribute a large portion of the fixed weight of cryogenic refrigeration systems. The weight of these exchangers is a direct function of their effectiveness or NTU requirement; on the other hand, the system power requirement is an inverse function of the system heat exchanger effectiveness. Optimum system design for a particular application can only be the result of a comprehensive tradeoff study of the system fixed weight and power requirement.

In this section of the report, the assumptions used in the analyses of the refrigeration systems under consideration are discussed, and parametric data leading to heat exchanger weights is presented.

Typically, in the refrigeration systems considered, the low pressure fluid is used to cool the hot high pressure fluid from the compressor; the weight estimates given in this section are all based on the low pressure or cold side of the heat exchanger. These heat exchangers are all of the plate-fin type.

Heat Exchanger Effectiveness

Figure 31 is a schematic diagram of a refrigeration system. An overall heat balance of the system can be expressed by

$$Q_I + Q_L = Q_R + Q_W \tag{236}$$

where the terms are defined in Figure 31. The heat balance in the lower part of the system can be written as

$$Q_W = Q_L + Q_F \tag{237}$$

where Q_F is the heat entrained by the outlet gas. Q_F can be defined by

$$Q_F = W_F (h_1 - h_2) \tag{238}$$

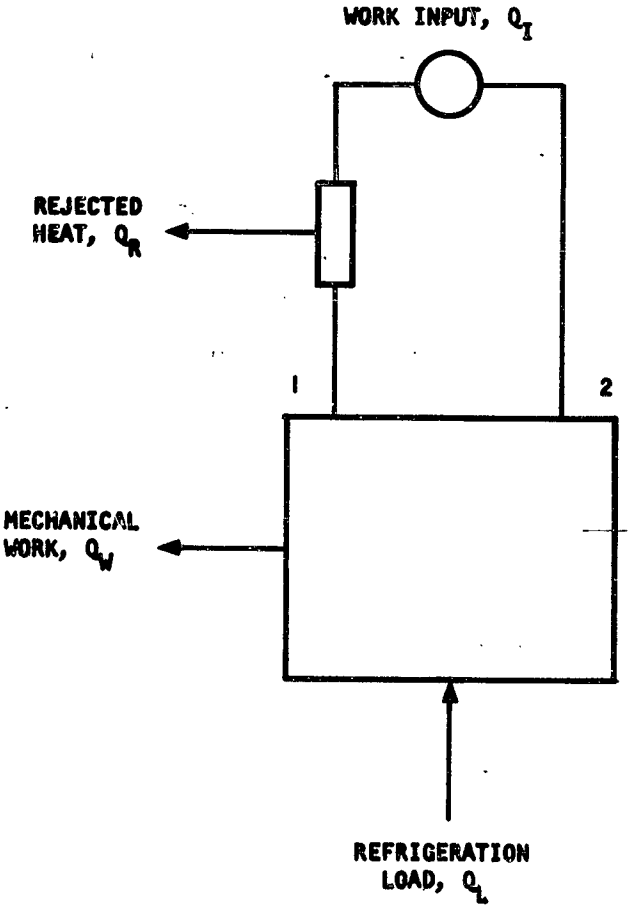

Figure 188. Refrigeration System Heat Balance

where w_F: working fluid flow

h_1, h_2: working fluid enthalpy at inlet and outlet

For a given refrigeration load, the amount of work to be done by the working fluid depends on the difference in enthalpy of the working fluid between Point 1 and Point 2 (see Figure 31). If the working fluid behaves as a perfect gas at the temperature level of the system inlet and outlet, Equation 28 can be written

$$Q_F = w_F c_p (T_1 - T_2) \qquad (239)$$

This assumption is not far from reality at temperature levels on the order of 500 to 600°R. Q_F becomes zero if the effectiveness of the last system heat exchanger is unity ($T_1 = T_2$). When this condition is realized, the mechanical work to be extracated from the working fluid is reduced to a minimum (see Equation 27), and the power input to the system is also reduced to a minimum (see Equation 26). On the other hand, a heat exchanger effectiveness of unity could only be achieved with an infinitely large heat exchanger.

Effectiveness above 0.90 in heat exchangers in which the capacity rate (wc_p) ratio is near unity can only be achieved in multipass cross-counterflow or in pure counterflow heat exchangers. In this study, because of the high effectiveness requirements, all the heat exchangers are assumed to be of the counterflow type.

In counterflow heat exchangers with capacity rate ratios of unity, the NTU can be calculated from the effectiveness by the relation

$$NTU = \frac{\epsilon}{1 - \epsilon}$$

where ϵ is the heat exchanger effectiveness. It can be shown (Reference 14) that the volume of a heat exchanger, hence, its weight, is proportional to $(NTU)^{3/2}$. As an illustration of the weight variation of a heat exchanger as

a function of its effectiveness, Figure 32 is shown where $(NTU)^{3/2}$ is plotted versus ϵ. This plot shows that the weight increases very rapidly as the heat exchanger effectiveness increases above 0.90. An effectiveness increase of 0.01, from 0.90 to 0.91, corresponds to a weight increase of approximately 19 per cent. For this reason, in this study of refrigeration systems, the upper limit of regenerator effectiveness (with capacity rate ratio of unity) was taken as 0.9, corresponding to a NTU of 9. This value of the NTU was also taken as an upper limit for the design of coolers and precoolers in which the capacity rate ratio is different from unity.

Heat Exchanger Weight

Based on the heat exchanger design method developed in Reference 14, the core weight of nitrogen, neon, and helium heat exchangers suitable for use in cryogenic refrigeration systems was calculated. The calculations were based on the assumptions discussed in the following paragraphs.

1. As mentioned previously, counterflow pattern is assumed.
2. The same plate fin surface is used on the high and low pressure sides of the heat exchangers. A single sandwich is used on the high pressure side and a triple sandwich on the low pressure side. This arrangement was found to be about optimum for pressure ratios around 15:1.
3. Since the temperature effectiveness of the heat exchangers designed is generally very high, the average fluid temperature on both sides of the exchanger is approximately the same; it follows that the fluid transport properties can be assumed to be the same on both sides. These properties are evaluated at average fluid temperature.
4. The fluid pressure drop in the heat exchanger is taken as a certain percentage of the fluid pressure. An allowance of 15 per cent is made on the total pressure drop to account for the inlet and outlet manifold pressure losses.
5. The heat transfer surface friction factor, f, and Colburn's modulus are assumed to be straight line functions of the Reynolds number on log-log plots, i.e.,

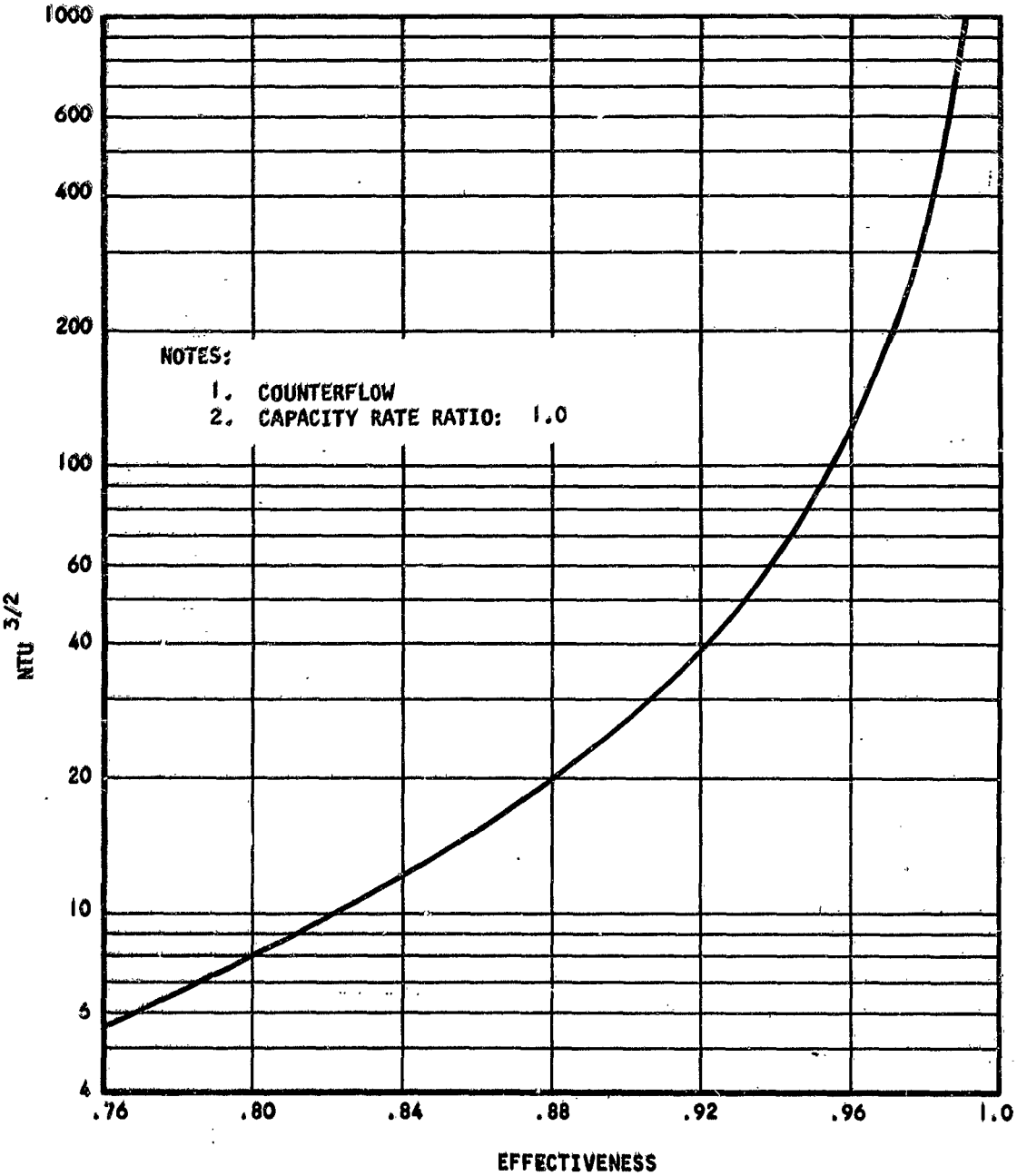

Figure 189. Heat Exchanger Weight Function

$$f = A\,Re^{a} \text{ and } j = BRe^{b}$$

where a, A, b, and B are constants.

6. The same heat transfer surface is used for neon and nitrogen. This surface is very restrictive and is defined as follows:

   a. 20 rectangular fins per inch, 0.100 in. high, 0.004 in. thick, with 1/8 in. offset.

   b. Fin material: aluminum

   c. Core density: 27.56 lb/ft^3

   d. $f = 3.91\ Re^{-.621}$

      $j = .878\ Re^{-.6}$

   This fin is much too restrictive for use in helium refrigeration systems. It was found to yield large heat exchanger face areas which present serious manifolding problems. A less restrictive heat transfer surface was, therefore, selected for the purpose of estimating the weight of helium heat exchangers. This surface is defined below:

   a. 12 rectangular fins per inch, 0.178 in. high, .004 in. thick, with 0.178 in. offset.

   b. Fin material: aluminum

   c. Core density: 20.91 lb/ft^3

   d. $f = 7.69\ Re^{-.732}$

      $j = 1.491\ Re^{-.681}$

The results of these calculations is given in Figure 33 for nitrogen and neon, and in Figure 34 for helium. In these plots, the heat exchanger volume function ($V/w\,\zeta$) is given as a function of the cold side NTU requirement for various cold side pressure drops. Here, the function ζ is a fluid properties parameter which can be read from Figure 35 for nitrogen, neon and helium. Figures 33 and 34 are given for regenerators in which the capacity rate ratio is

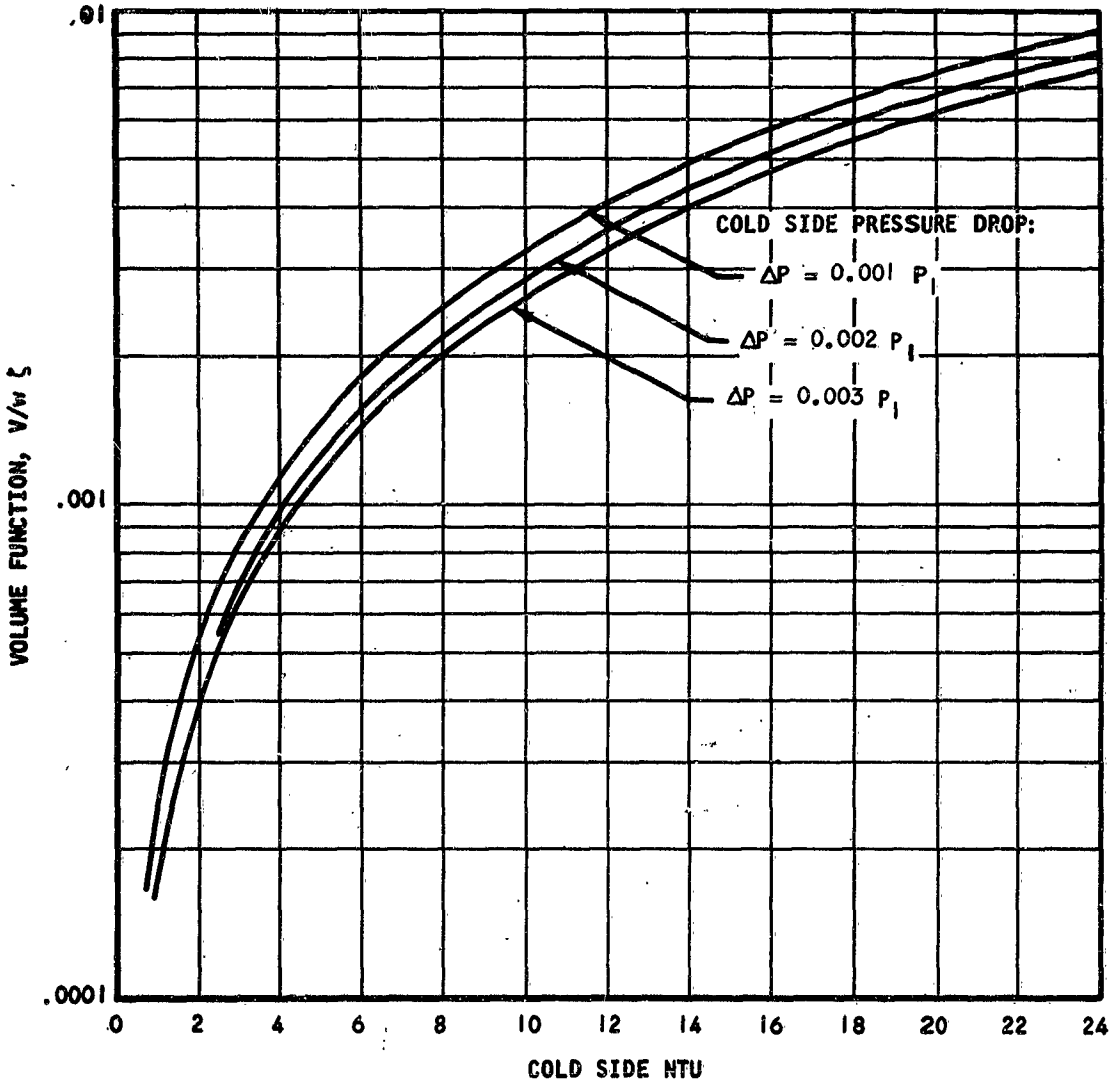

Figure 190. Heat Exchanger Volume Function
(Al Fin: 20 Rect., .100 in. high.
1/8 in. offset, .004 in. thick).

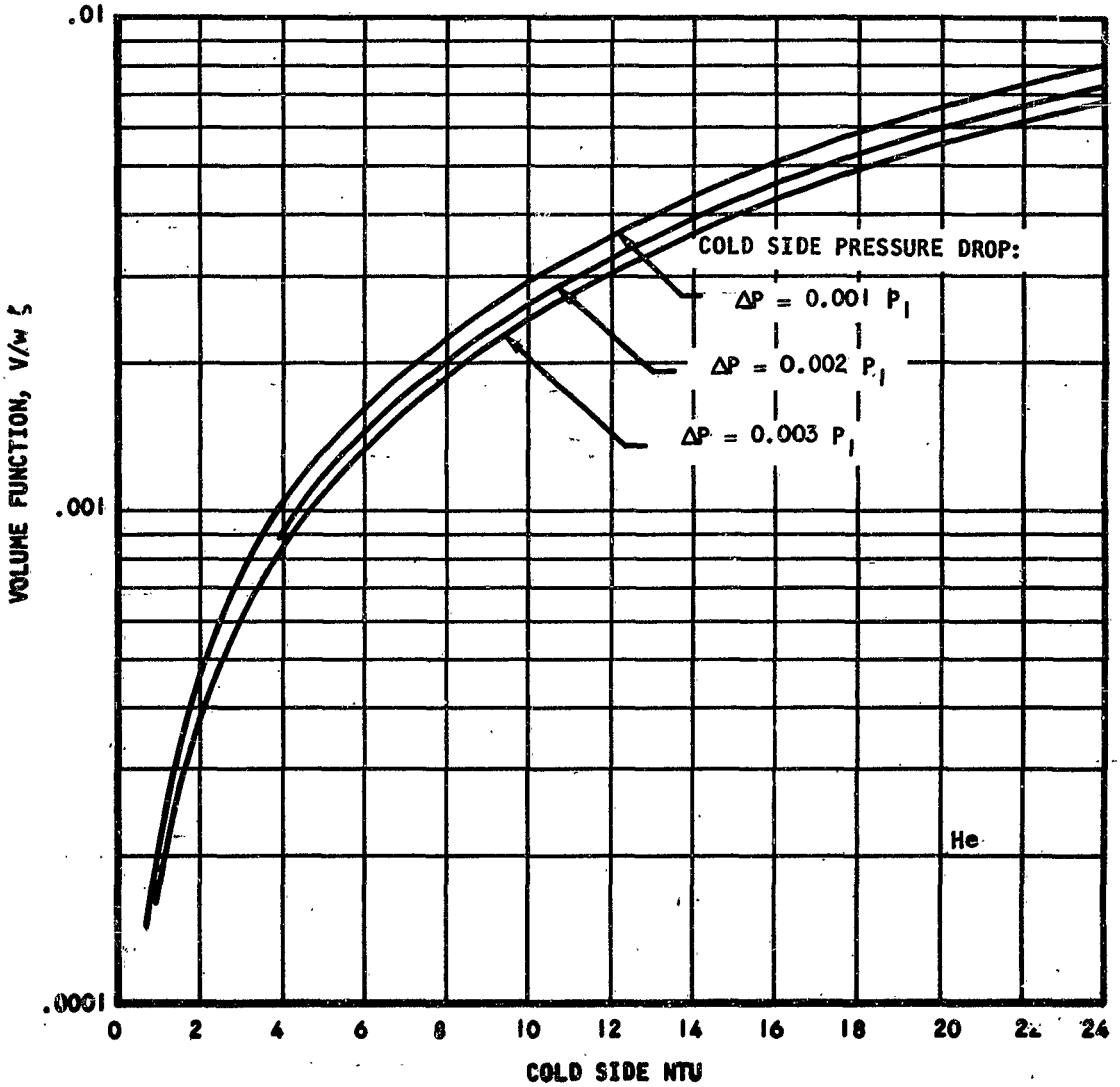

Figure 14. Heat Exchanger Volume Function
(Al Fin: 12 Rect., .178 in. high,
.178 in. offset, .004 in. thick)

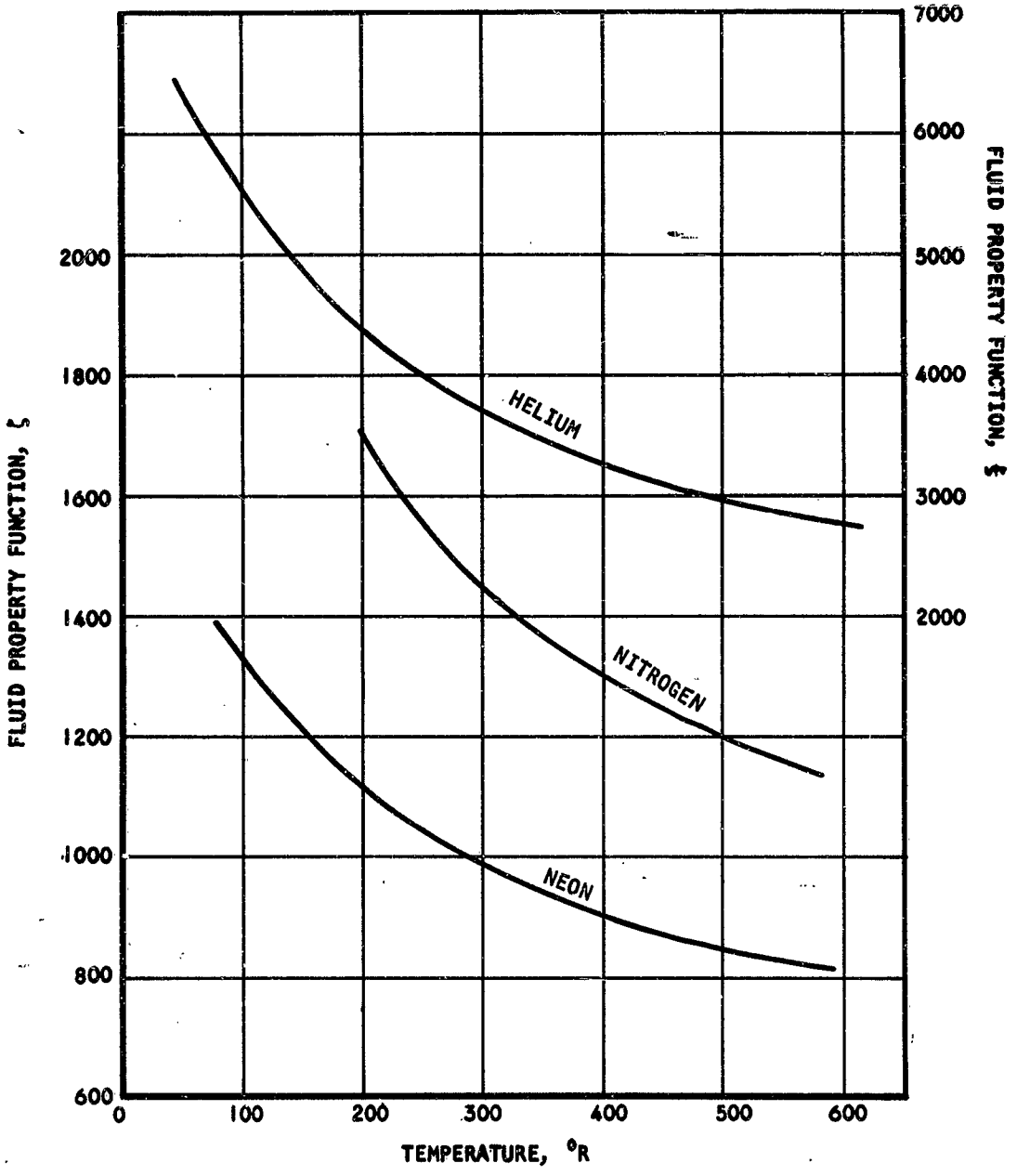

Figure 192. Fluid Property Function

unity. Because the low pressure side of the exchanger is controlling, a flow reduction on the high pressure side corresponds to only a relatively small reduction in core volume and weight.

From these plots, the heat exchanger core volume can easily be found, knowing the average fluid temperature, the NTU based on the cold side, the flow on the cold side of the heat exchanger and the allowable pressure drop. The core weight is easily calculated knowing the core density. The total heat exchanger weight, including side plates, manifolds, etc., is found from Figure 36.

These curves are used in the system analyses for the purpose of estimating the heat exchanger weights.

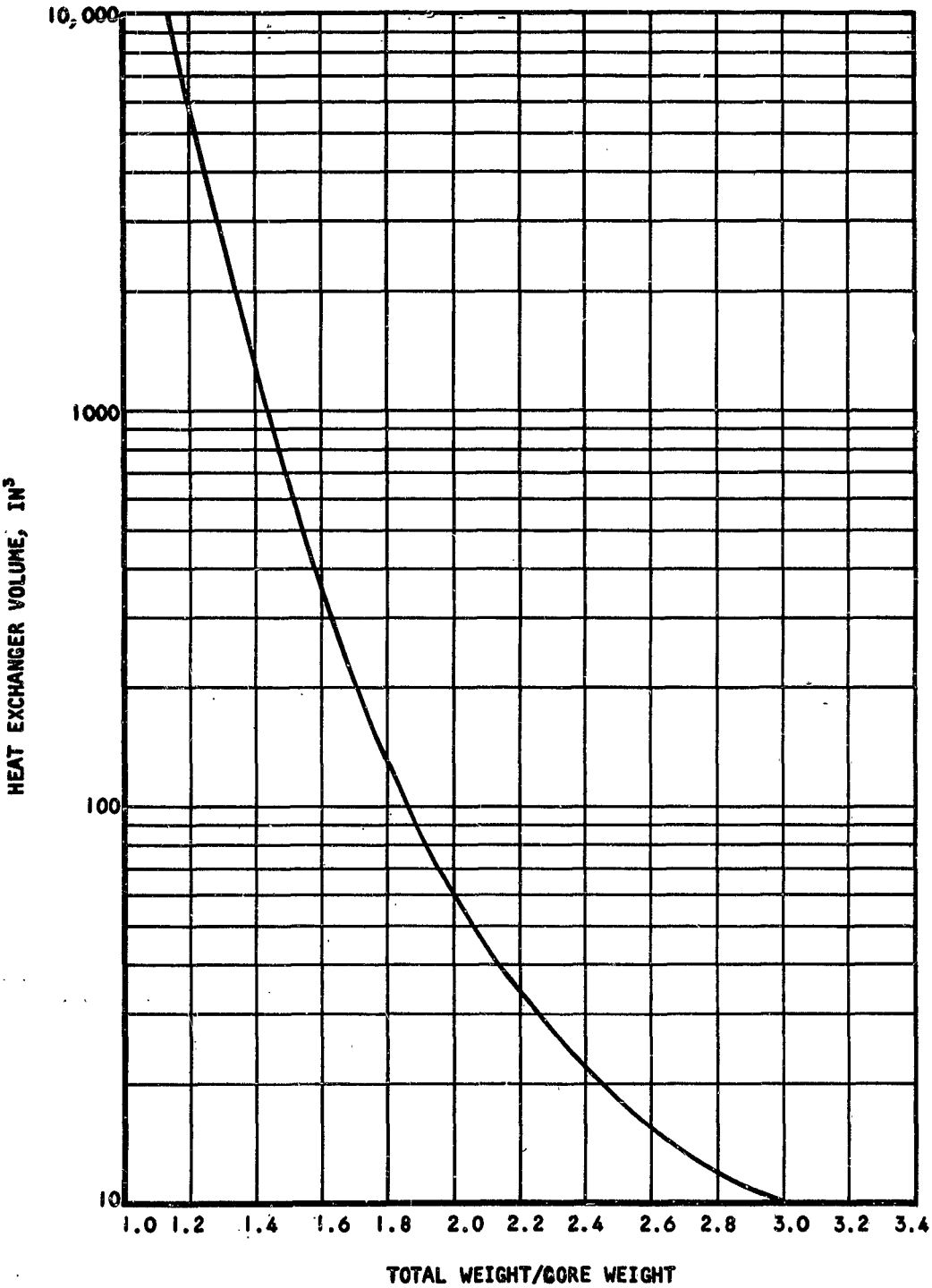

Figure 193. Heat Exchanger Total Weight To Core Weight Ratio

SECTION VI

THERMODYNAMIC CYCLES

In this section, various thermodynamic cycles are analyzed and compared. The analyses are performed assuming ideal components in order to avoid obscuring the essential features of each and to provide a common basis for comparison. General design criteria are developed for actual systems, and the most promising cycles are considered further in subsequent sections of this study.

The cycles considered are:

(a) Joule-Thomson expansion cycle
(b) Cascaded Joule-Thomson expansion cycle
(c) Bypass expander cycle
(d) Stirling cycle

Ideal Work Requirements

Long duration applications of cryogenic cooling, particularly those with high cooling loads, require sophisticated refrigeration systems. In cases where power is limited or heat rejection is a problem, one must exercise considerable care in selecting a cooling system.

In order to appreciate the necessity for a high cooling system efficiency, the ideal Carnot cycle, which has the theoretically maximum efficiency, can be examined. In this case, the coefficient of performance, COP, can be expressed by

$$COP = \frac{Q_2}{Q_1 - Q_2} \qquad (240)$$

where Q_1 = heat rejected at temperature T_1

Q_2 = heat absorbed at temperature T_2

$(Q_1 - Q_2)$ is the work input to the cycle. From the definition of the absolute temperature scale,

$$\frac{Q_1}{Q_2} = \frac{T_1}{T_2} \qquad (241)$$

Combining these equations and definitions, the following expression is obtained:

$$P_I = H_2 \left(\frac{1}{COP}\right) \qquad (242)$$

where P_I = power input, kw

H_2 = heat load, kw

A plot of $\frac{1}{COP}$ is shown in Figure 37 for the case of heat rejection at a temperature of 540°R as a function of cold end temperature. The coefficient of performance of the Carnot cycle, providing refrigeration at the normal boiling point of the three fluids considered (nitrogen, neon and helium), is also indicated in Figure 37.

It can be seen that refrigeration at liquid helium temperature requires, ideally, 70 kw input power per kw cooling load.

Also, since the rate of heat rejection, H_o, is given by

$$H_o = H_2 \left(\frac{1}{COP} + 1\right) \qquad (243)$$

The cooling system radiator must eliminate heat at the rate of 71 kw per kw of cooling load. In the load ranges under consideration, this introduces formidable problems when it is realized that no real cooling cycle attains the theoretically maximum efficiency.

Joule-Thomson Expansion Cycle

The simplest of the gas refrigeration cycles makes use of the isenthalpic expansion of pressurized gas. The basic method of coolant production is illustrated in Figure 38, which shows schematically a cycle flow diagram and a plot of the fluid thermodynamic behavior on a temperature-entropy diagram.

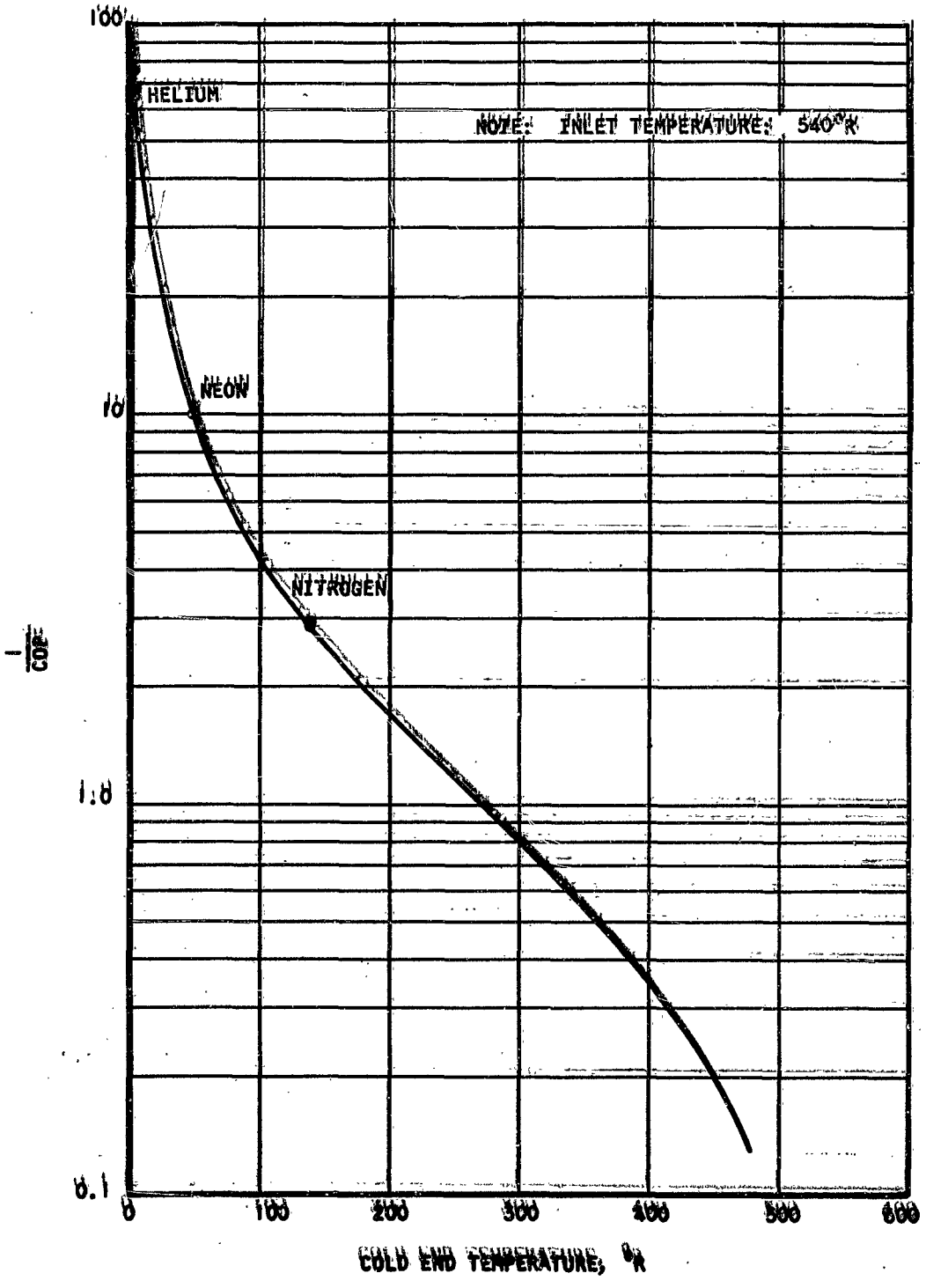

Figure 34. Ideal Work for Refrigeration

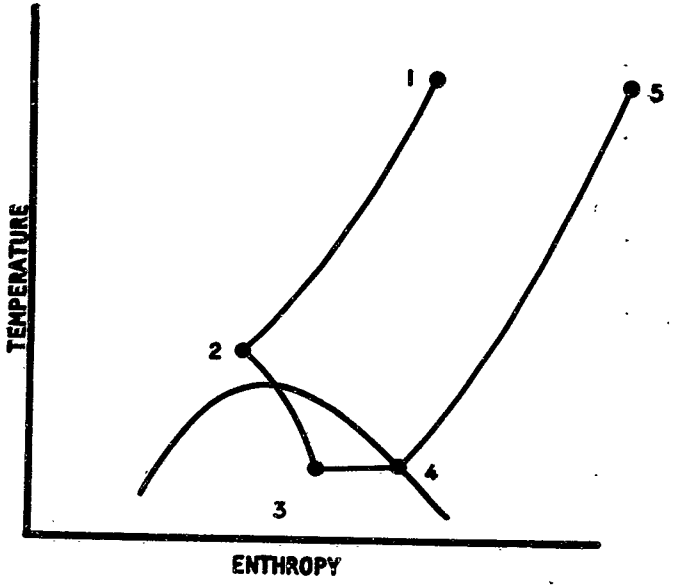

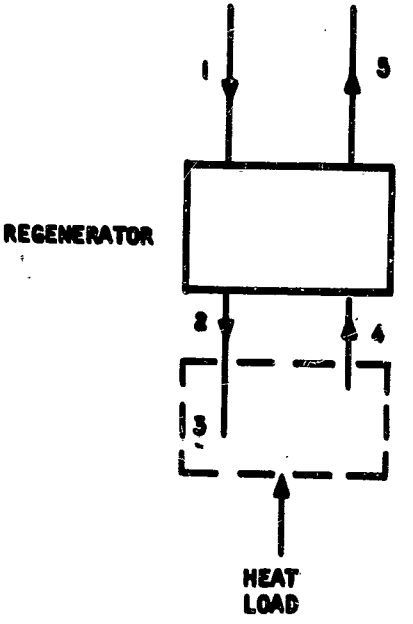

Figure 195. Steady-state Operation of Joule-Thomson Expansion System

In order to avoid obscuring the essentials of the system operation, ideal components are assumed throughout the following discussions; specifically, the assumptions made are:

(a) The cold gas produced by the evaporation of the liquid is assumed to enter the regenerator as a saturated vapor.

(b) The regenerator effectiveness is assumed to be 1.0.

(c) Perfect intercooling is assumed between compressor stages.

(d) Perfect aftercooling is assumed after the compression process.

(e) The heat leaks into any lines or chambers are all assumed to take place within the cooling cell as part of the cooling load.

(f) Negligible pressure losses are assumed throughout the system.

(g) The assumed pressure level in the cooling cell is 14.7 psia.

The steady-state operation of this simple system, referring to Figure 38, is as follows. High pressure gas (1) passes through a heat exchanger where it is cooled to T_2. The cold high pressure gas (2) is then expanded through an orifice (2-3). In this process, some of this gas is liquefied if the pressure, P_2, is above the critical pressure, and the temperature, T_2, is not too far above the critical temperature of the fluid. The stream leaving the orifice (3) is passed over the object to be cooled; here, it picks up heat, leaving the cooling space as a saturated vapor (4). This stream is then directed back through the heat exchanger, where it cools the incoming high pressure gas. The low pressure stream leaving the heat exchanger (5) is recompressed, cooled and recirculated. In addition to the heat input to the working fluid from the equipment cooling load, a large amount of heat is introduced into the cycle during the compression process. As mentioned previously, this added cooling load to the radiator system will not be taken into account in this section.

Starting of the Joule-Thomson cycle is as follows. First, the gas enters the expansion orifice at ambient temperature and is cooled slightly. This gas, in flowing back through the heat exchanger, cools the next element of gas entering the system. The Joule-Thomson orifice inlet temperature falls continuously until liquid formation conditions stabilize. The rate of pull-down

depends upon the ambient temperature level, gas pressures, the thermal capacity of the heat exchanger, and the conditions at the cold end of the system.

The cycle steady-state working relations are derived below, using the assumption that all extraneous heat leaks are part of the cooling load. The heat exchanger energy balance is given by

$$h_1 - h_2 = h_5 - h_4 \tag{244}$$

where h is the enthalpy at the point indicated. Expansion across the Joule-Thomson orifice is isenthalpic; thus,

$$h_2 = h_3 \tag{245}$$

The fluid enthalpy rise across the cooling load is

$$h_4 - h_3 = (q_c \times 56.9)/w \tag{246}$$

where h = fluid enthalpy, Btu/lb

q_c = cooling load, kw

w = fluid flow, lb/min

Combination of Equations (34), (35), and (36) yields the following expression for coolant flow rate in terms of inlet and outlet enthalpies:

$$\bar{w} = \frac{56.9}{h_5 - h_1} \tag{247}$$

where $\bar{w}$ = coolant flow per kw cooling load, lb/min per kw

Conditions necessary for this cycle to operate are readily apparent, considering Equation 37 and the starting cycle. With a perfect regenerator, the temperature at Point 5 would equal the inlet temperature, T_1. Cooling is thus possible only if the enthalpy at Point 5 is higher than the enthalpy of the high-pressure inlet gas; i.e., the inlet gas is below its Joule-Thomson inversion temperature. Thus, nitrogen can be used in simple Joule-Thomson cycles at ambient inlet temperatures, but neon and helium must be precooled.

Figure 39 shows the nitrogen flow required per kw cooling load as a function of inlet gas pressure for several values of compressor delivery temperature.

Cascaded Joule-Thomson Expansion Cycles

As noted previously, liquefaction of neon or helium cannot be accomplished at ambient regenerator inlet temperatures without precooling. The object of the precooling is to lower the gas temperature at the regenerator inlet below its Joule-Thomson inversion temperature. In the case of neon, nitrogen appears to be an attractive precooling agent, due to the fact that its normal boiling point is well below the neon inversion temperature. Helium can also be liquefied by Joule-Thomson expansion provided its temperature is lowered below approximately $90^{\circ}R$.

Cascaded Neon Joule-Thomson Expansion Cycle

One simple precooling scheme is to employ two simple Joule-Thomson expansion systems in a cascade fashion. The heat load to the upper (nitrogen) loop comes from cooling the working fluid (neon) in the lower loop below its inversion temperature before it enters the last regenerator.

Figure 40 is a schematic diagram of such a system. The cooling capacity of a nitrogen-closed cycle Joule-Thomson expansion system is used to precool the neon, which is also circulated in a closed loop. The nitrogen loop is similar to the one previously described with the exception that the cooling envelope heat load is replaced by a neon-nitrogen boiler where the nitrogen is vaporized by absorbing heat from the neon.

The neon is compressed and circulated through a regenerator, where it is cooled. The high pressure gas from this regenerator (7) is circulated through a nitrogen boiler, where its temperature is dropped to that of the evaporating nitrogen (8). Then the neon gas flows through a second regenerator (8-9) and is expanded isenthalpically (9-10). The gas is partially liquefied in the process. The liquid neon is vaporized by the heat load, and the cold low pressure gas is exhausted from the cooling envelope (11) through the two regenerators in series. The neon gas is then compressed and, after cooling, cycled again.

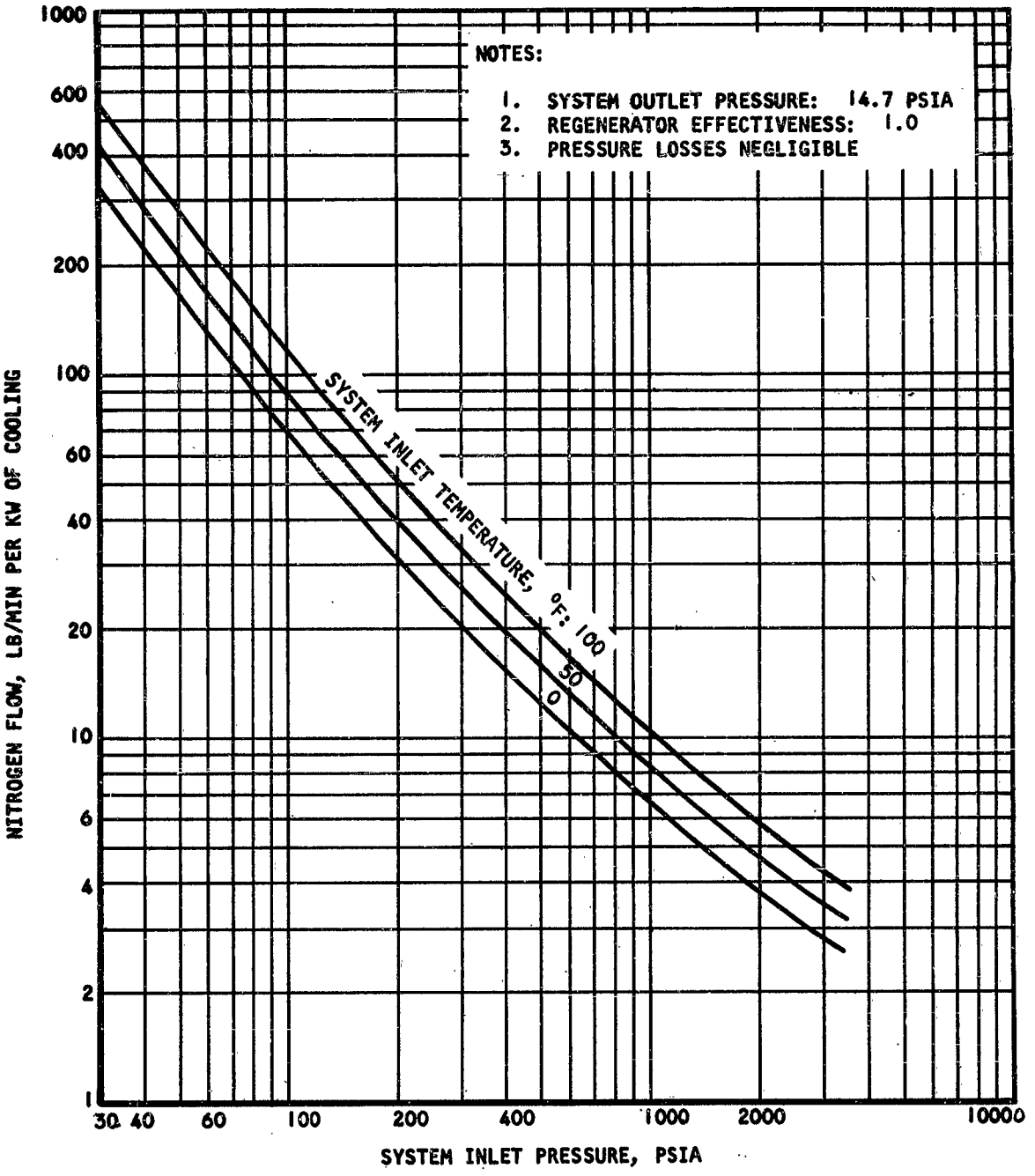

Figure 196. Nitrogen Flow in a Simple Joule-Thomson Expansion System

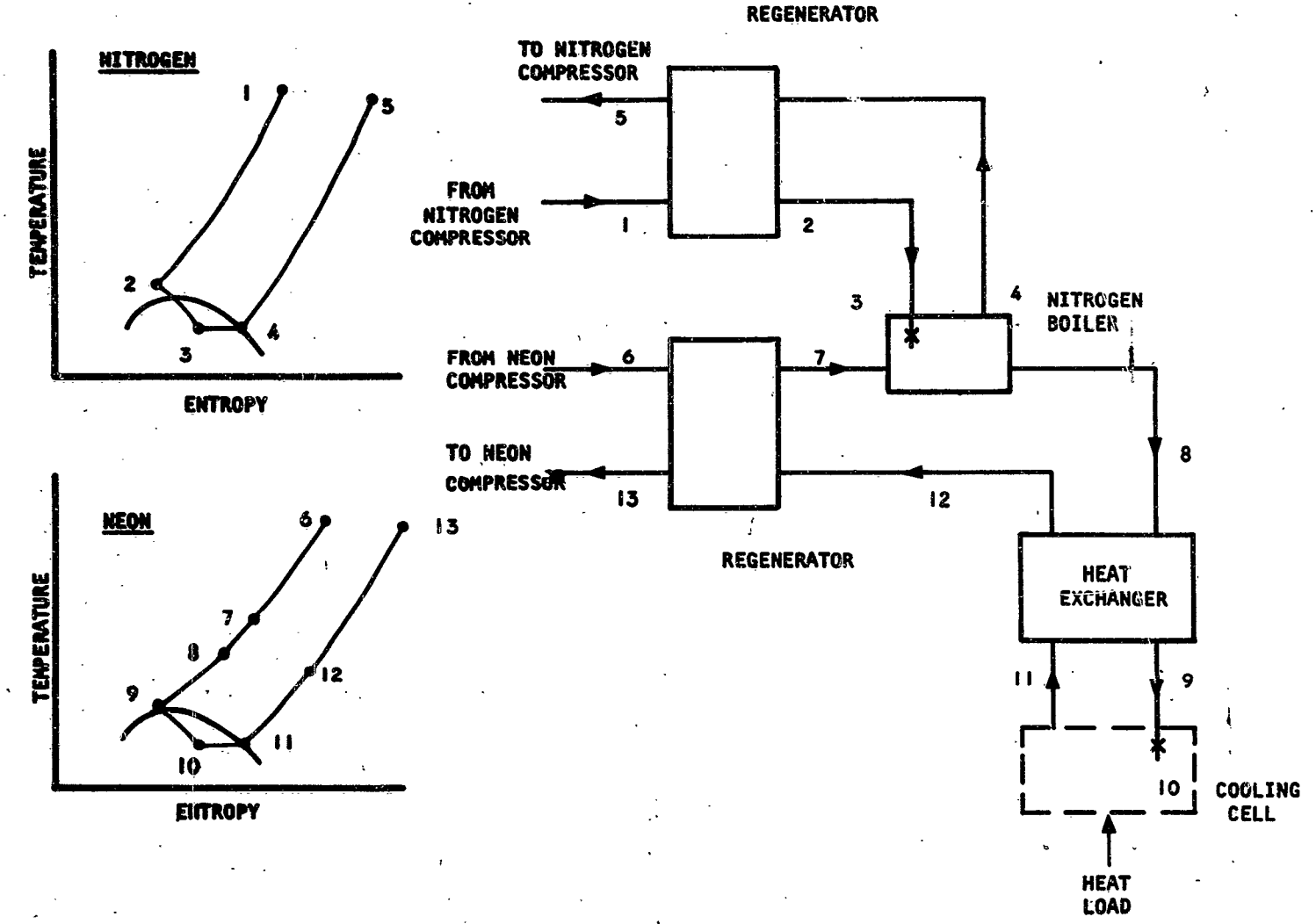

Figure 197. Precooled Neon Joule-Thomson Expansion System

The two regenerators in the neon loop are essential for operation of the compressor at near ambient temperatures while still achieving liquefaction of the neon. Precooling to liquid nitrogen temperature, if followed immediately by isenthalpic expansion, would produce refrigeration without liquefaction. In the regenerator introduced between the neon-nitrogen boiler and the Joule-Thomson expansion orifice, the neon is cooled below the boiling nitrogen temperature so that expansion through the orifice will result in partial liquefaction of the neon.

In analyzing the cycle, the same assumptions are made as for the nitrogen Joule-Thomson expansion system discussed previously. In addition, the boiler effectiveness is assumed to be 1.0; i.e., the temperature of the neon at the boiler outlet (8) is assumed equal to the boiling temperature of nitrogen at 14.7 psia.

Based on the above assumptions and referring to Figure 40, the following equations can be written.

For the neon loop: $h_6 - h_7 = h_{13} - h_{12}$ (248)

$$h_8 - h_9 = h_{12} - h_{11} \quad (249)$$

$$h_9 = h_{10} \quad (250)$$

$$\frac{56.9}{\bar{w}} = h_{11} - h_{10} \quad (251)$$

where the symbols have the same significance as in the simple Joule-Thomson expansion cycle analyzed previously and $\bar{w}$ is the neon flow rate in lb/min per kw cooling load.

Substituting and rearranging,

$$\frac{56.9}{\bar{w}} = h_{11} - h_{10} = h_{12} - h_8 \quad (252)$$

hence, $$\bar{w} = \frac{56.9}{h_{12} - h_8} \quad (253)$$

The neon flow rate given by Equation 43 is plotted in Figure 41 as a function of the neon compressor delivery pressure.

The heat load on the nitrogen cooling loop can be written as

$$h_7 - h_8 = (h_{12} - h_8) + (h_6 - h_{13}) \qquad (254)$$

As can be seen, the load on the nitrogen loop is a function of both the cooling envelope heat load and the neon compressor delivery parameters. In other words, given a fixed envelope cooling load, the cooling load which the nitrogen loop "sees" will be a constant factor times the envelope cooling load, which constant factor will depend on the neon compressor delivery parameters. These constant factors are plotted in Figure 42 versus neon compressor delivery pressure for neon compressor delivery temperatures of 0° and 100°F. Once the cooling load on the nitrogen loop is determined, the nitrogen flow rate can be determined, knowing the nitrogen compressor delivery parameters, from Figure 39.

Cascaded Helium Joule-Thomson Expansion Cycle

Hydrogen or neon may be used to provide the temperature level required in this case, but since both of these gases require precooling themselves, this implies a three-stage Joule-Thomson cascaded system: a nitrogen loop cooling a nitrogen-neon boiler, a neon loop cooling a neon-helium boiler, and finally the helium loop cooling the load. Such a system is shown schematically in Figure 43.

It can readily be seen that this system is similar to the system described for cooling at liquid neon temperatures with the addition of one more cooling loop and boiler.

The determination of the helium flow rate proceeds in the same fashion as the determination of the neon flow rate in the previous section. The helium flow rate thus determined is plotted as a function of helium compressor delivery pressure in Figure 44.

As before, the cooling load, which the neon loop "sees", is a function of the primary cooling load and the helium compressor delivery parameters.

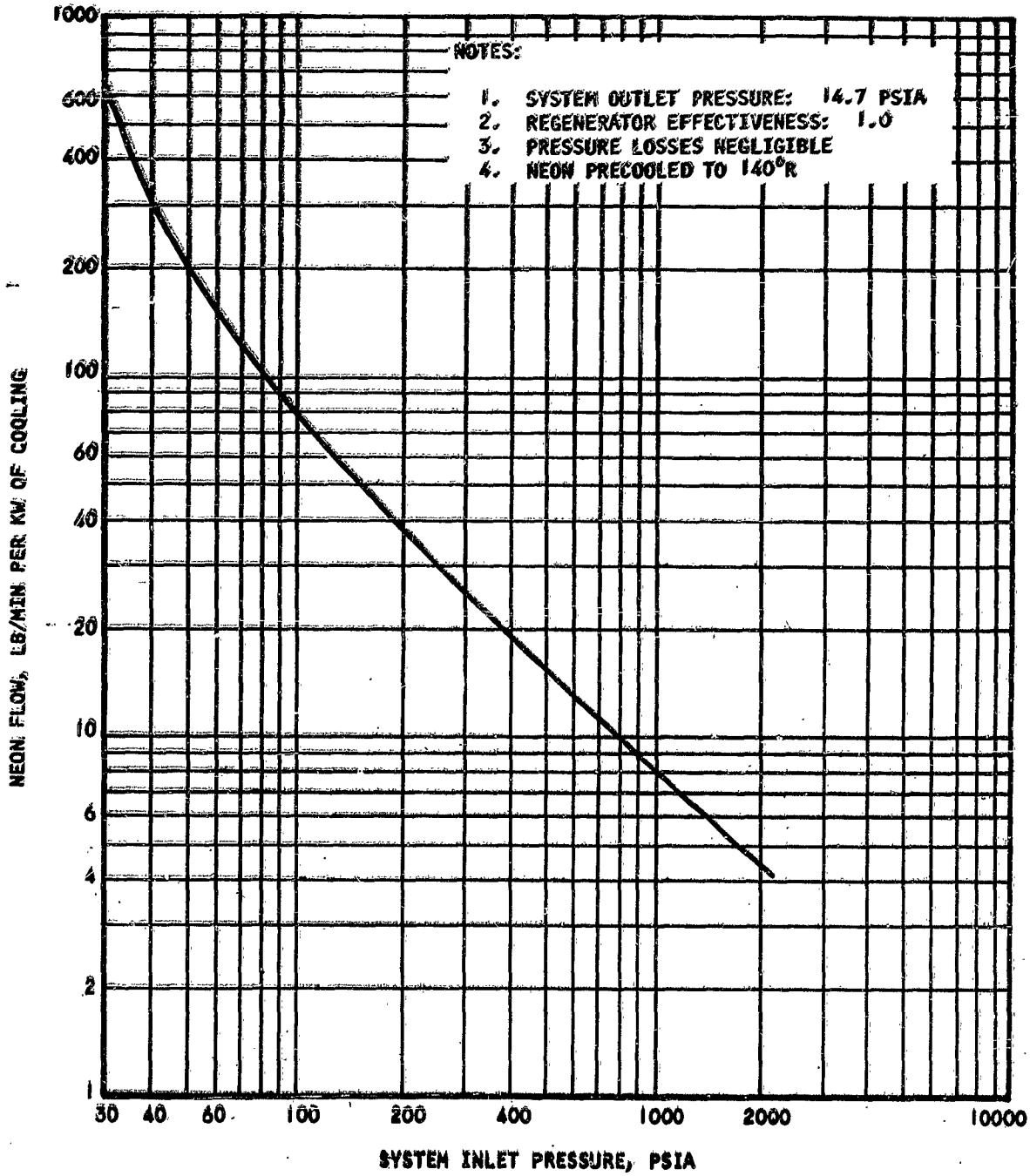

Figure 198. Neon Flow in a Cascaded Joule-Thomson Expansion System with Nitrogen Precooling

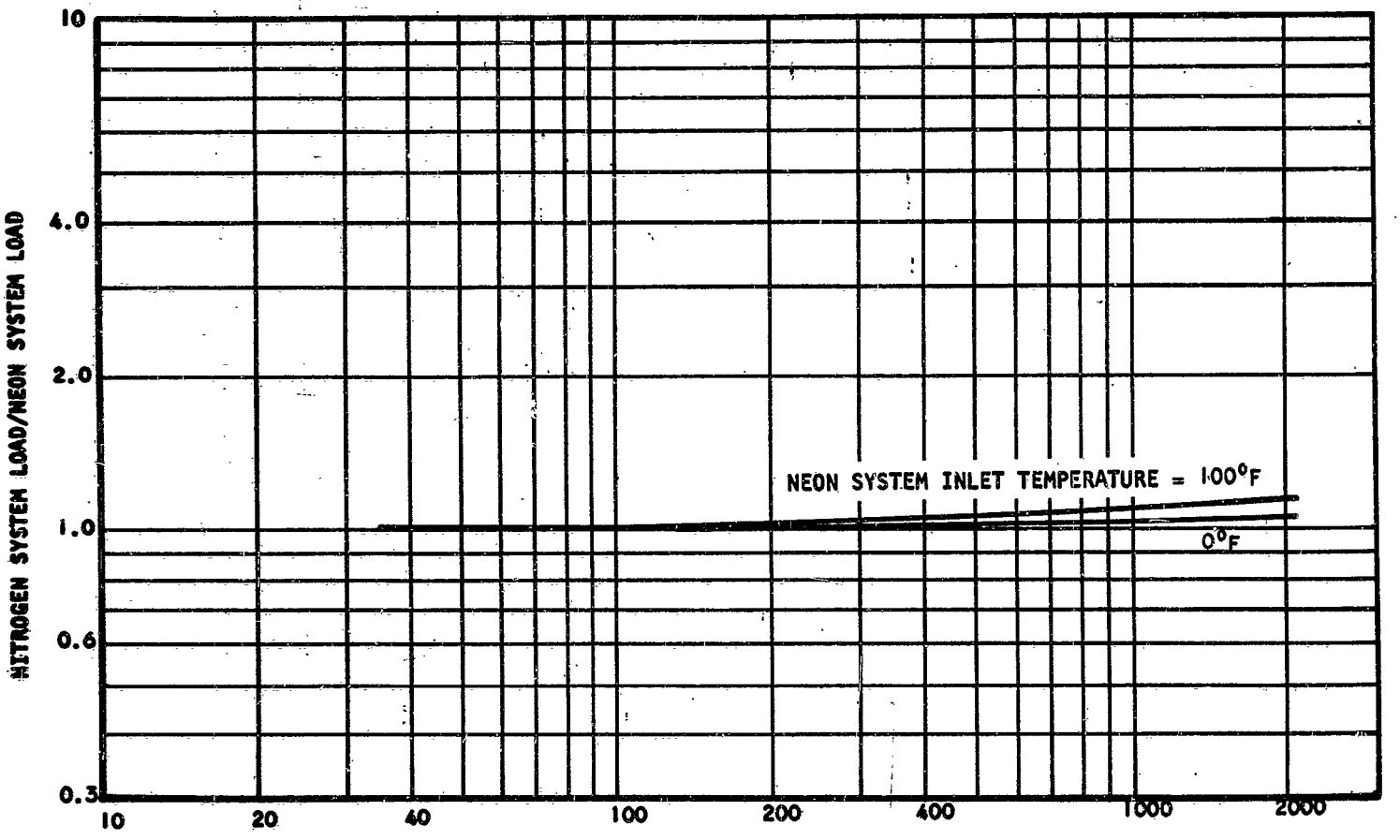

Figure 199. Nitrogen System Precooling Load Function

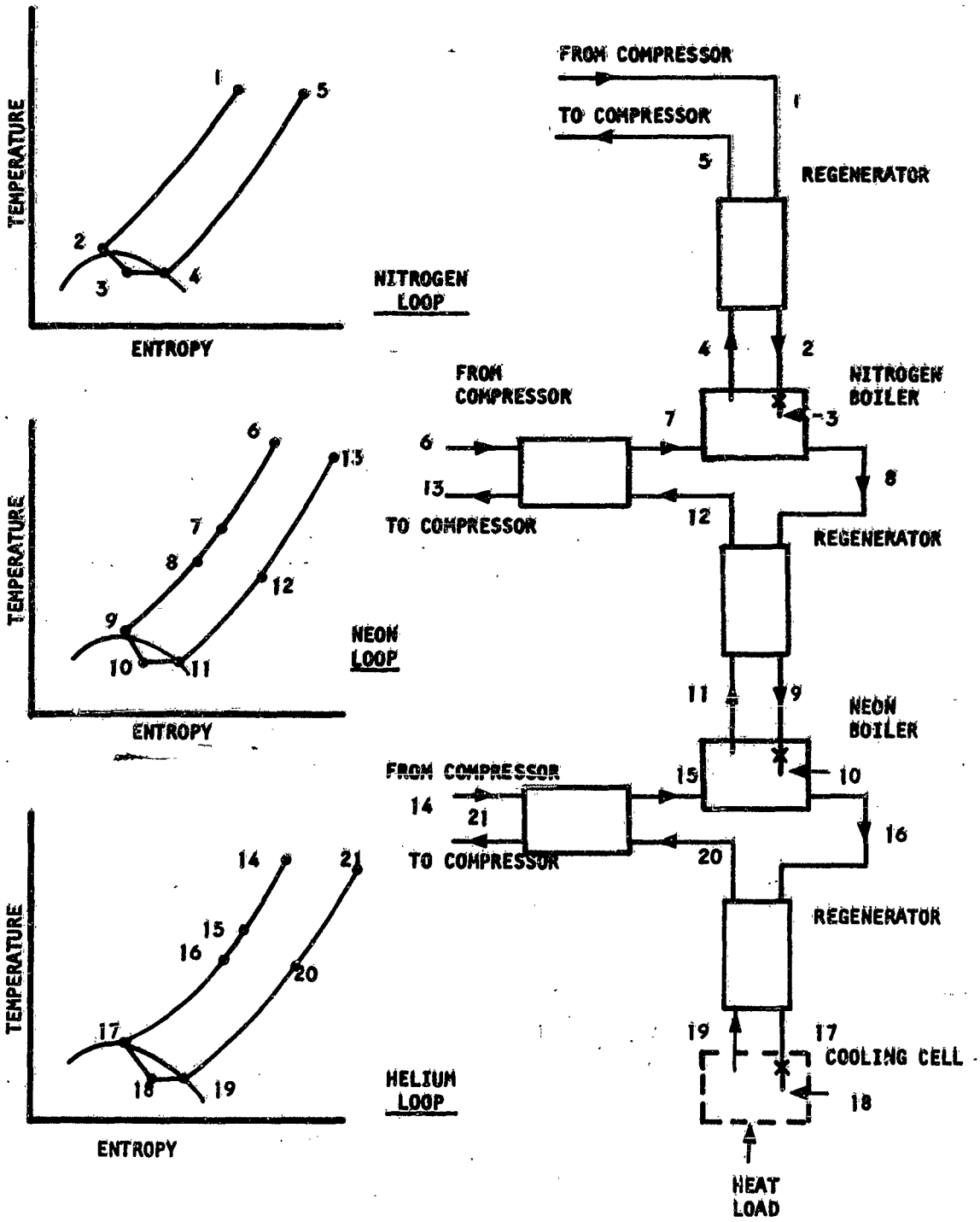

Figure 200. Precooled Helium Joule-Thomson Expansion System

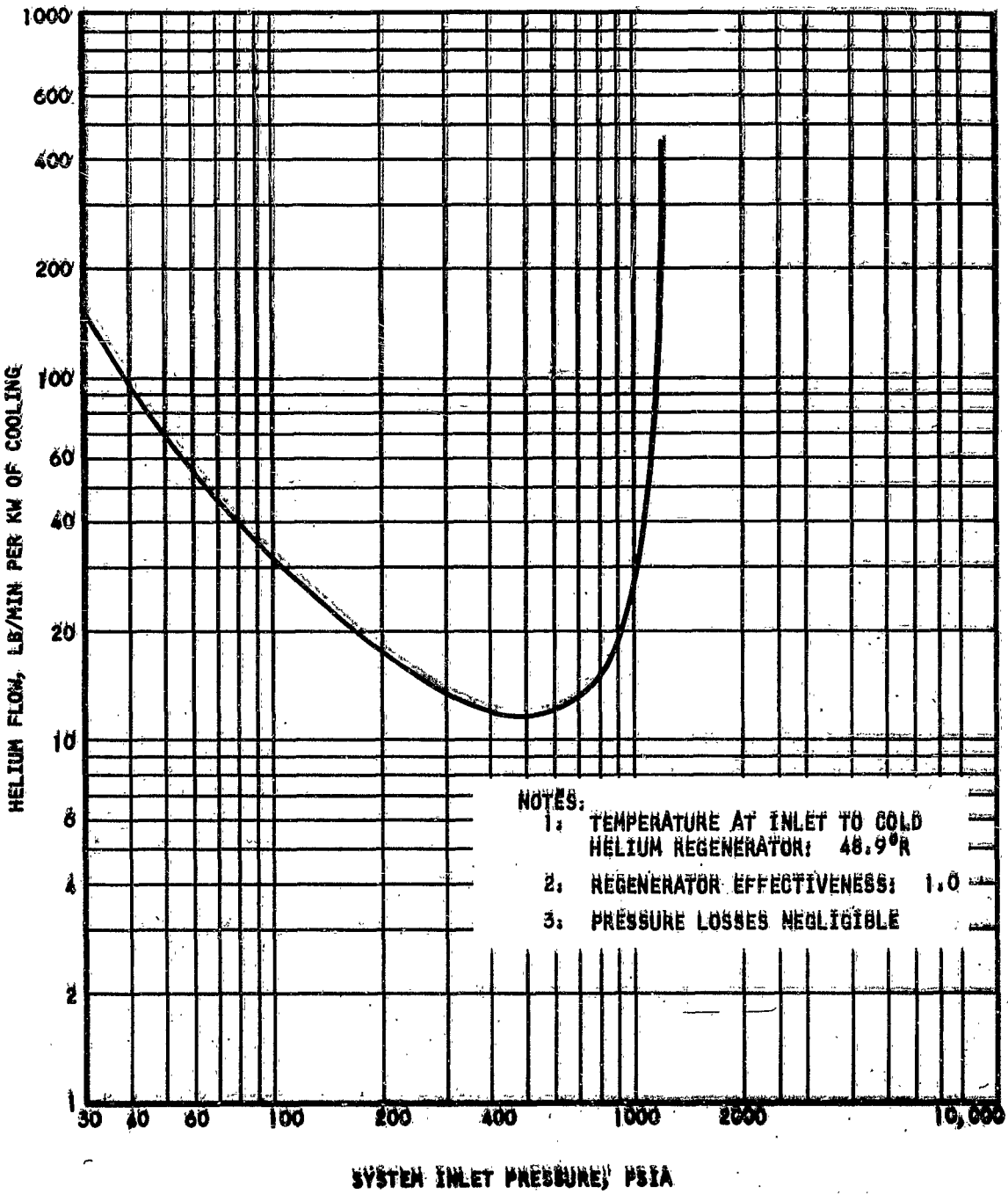

Figure 201. Helium Flow in a Cascaded Joule-Thomson Expansion System With Neon Precooling

This function is plotted in Figure 45 for helium compressor delivery t tures of 260°K and 300°K.

In order to determine the total system fluid flow rate, it is fir necessary to pick the helium compressor delivery pressure and temperat This will determine the helium flow rate and also the cooling load on neon loop. Given the cooling load on the neon loop, the neon compress delivery parameters will determine the neon flow rate and also the coo load which the nitrogen loop "sees". Once this is determined, the nit compressor delivery parameters will determine the nitrogen flow rate.

As an example, assume the helium compressor delivers helium at 26 and 220 psia. From Figure 44, we see that the helium flow is 16.4 lb/ per kw cooling load. The cooling load on the neon loop is 1.7 kw per cooling load. Assuming a neon compressor delivery pressure of 220 psi and temperature of 0°F from Figure 41, we have 57.8 lb/min neon flow p cooling load at the helium cooled envelope. From Figure 42, we have 1 per kw cooling load which the nitrogen loop "sees". Assuming the nitr leaves its compressor at 0°F and 220 psia, from Figure 39 we get a nit flow rate of 49.3 lb/min nitrogen per kw cooling load at the helium co envelope. If we assume a cooling load of 10 kw at the helium cooled lope, we have

164 lb/min helium

578 lb/min neon

493 lb/min nitrogen

as the required fluid flow for the system.

Bypass Expander Cycle

A much more efficient expansion cycle than the simple Joule-Thomso just described makes use of an operating principle similar to the one by Collins for liquid helium production. In this type of cycle, only of the gas is used for cooling. The portion of the gas not used for co is first passed through a mechanical expander where energy is extracted it by production of work. The cool low pressure gas issuing from the expander is then used to lower the temperature of the high pressure gas

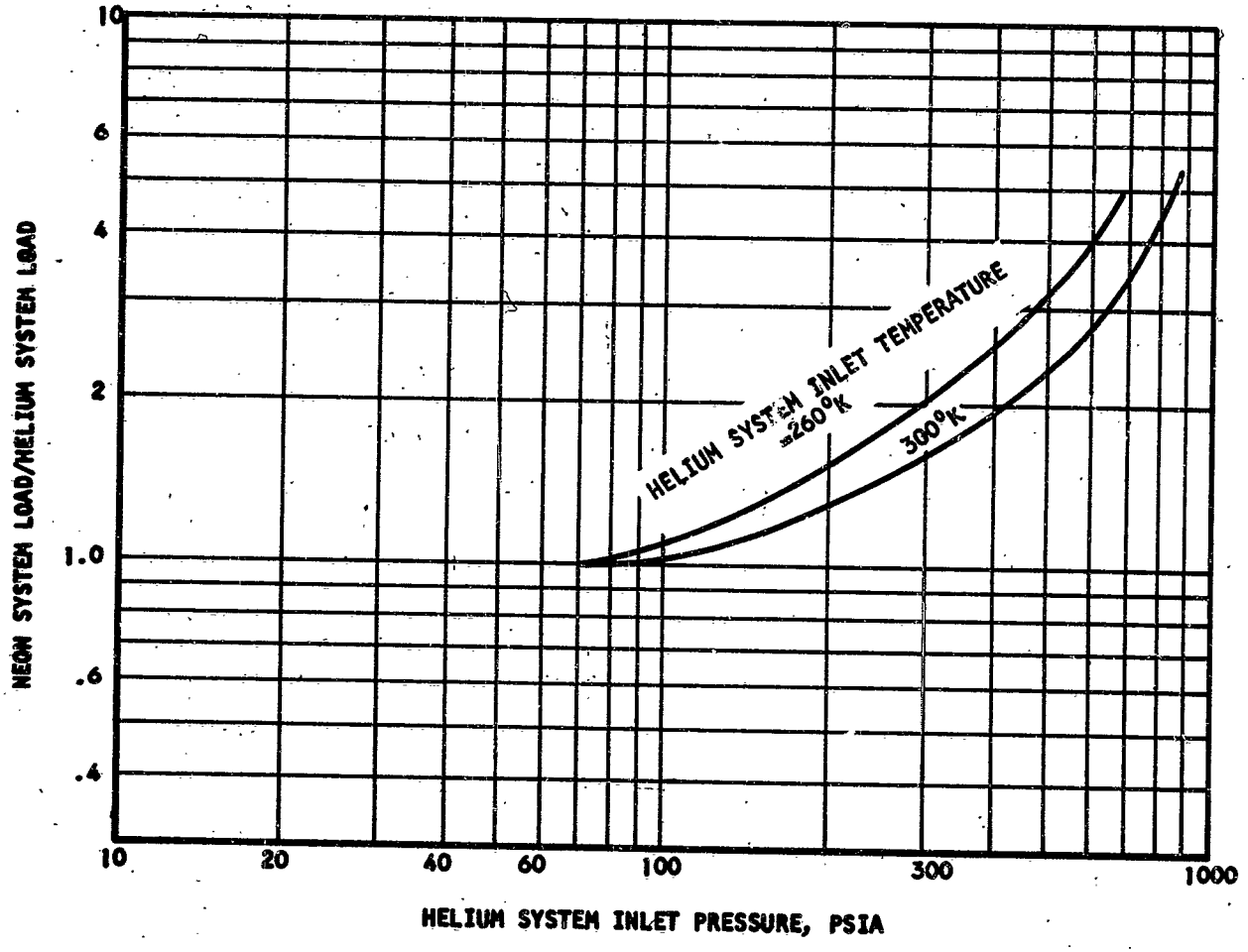

Figure 202. Neon System Precooling Load Function

It is interesting to note that this cycle can conceivably be made to approach ideal reversible behavior due to the fact that the expansion engines aim at isentropic expansion of the gas. Given a sufficient number of expanders, the reversibility of the cycle is limited only by the inefficiencies of the expanders and by the imperfections in the heat exchange mechanisms.

In order to make the most efficient use of this cycle, the energy produced in the expansion device should be used to drive the compressor. For example, a turbine type expander could be used to drive an alternator. The electrical power thus produced could in turn be used as part of the input to a motor which would drive the gas compressor.

This bypass expander cycle is shown schematically in its simplest form in Figure 46, which also shows the working fluid behavior on a temperature-entropy diagram. Operation of the cycle is as follows:

The gas discharged from the compressor (1) flows through a hot regenerator, (1) - (2), a precooler, (2) - (3), and a cold regenerator, (3) - (4), in series. The working fluid is cooled in these three heat exchangers and partly liquefied before being expanded isenthalpically through an orifice (4) - (5). The liquid produced provides refrigeration by boiling, (5) - (6). The working fluid is exhausted from the cooling envelope as a saturated vapor and passed through the three heat exchangers (6) - (7), (7) - (8), (8) - (9), where it cools the incoming gas. A portion of the high-pressure gas from the hot regenerator is tapped off and cooled to a relatively low temperature by expansion in a work extraction device, (2) - (7). The exhaust from the expander re-enters the cycle between the cold regenerator and the precooler, mixing with the gas exhausted from the cooling envelope. By increasing the flow in the expander relative to the total flow, a high degree of precooling can be achieved, and condensation of the working fluid can be obtained in the precooler as well as in the cold regenerator. In this manner full advantage is taken of the cooling capacity of the expander. No liquefaction occurs in the expander although gas exhausts from it at a temperature lower than the dew point of working fluid at the high-pressure level.

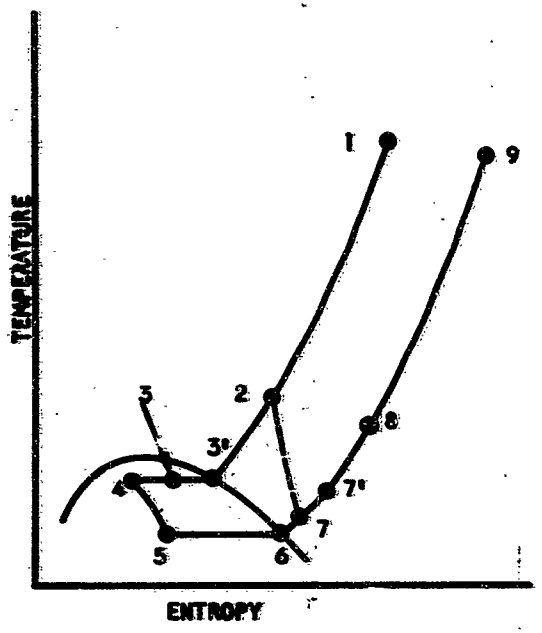

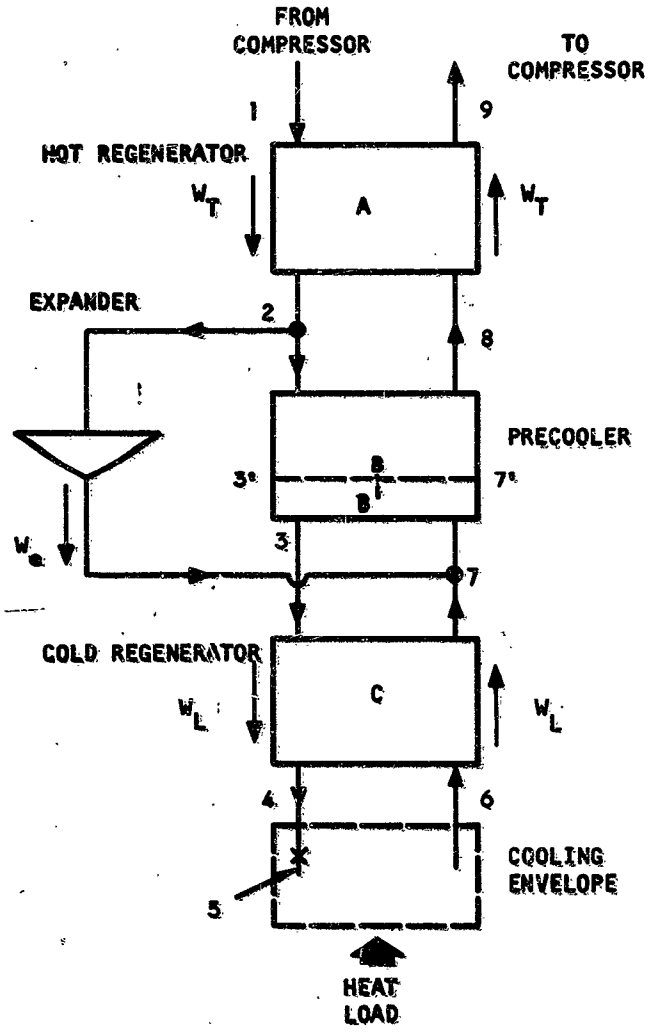

Figure 203. Bypass Expander System

As before, in order to keep the salient characteristics of the cycle from being obscured, the following simplifying assumptions are made in the analysis:

(a) The condensing portion of the regenerator downstream of the expander has an effectiveness of unity, i.e., the temperature at Point 3' is equal to that at Point 7'.

(b) The fluid is exhausted from the cooling envelope as a saturated vapor.

(c) The heat leaks in the system, which result in a net increase in the enthalpy of the working fluid, are all assumed to take place at the location of the equipment heat load and to contribute to the evaporation of the working fluid.

(d) The pressure losses in the lines and heat exchangers are assumed to be negligible.

(e) The hot regenerator has an effectiveness of unity, i.e., the temperature at Point 1 is equal to that at Point 9.

(f) The cold regenerator is a condenser.

An additional assumption is that all expanders have an efficiency of 0.65. The following equations form the basis for the cycle analysis:

$$h_1 - h_2 = h_9 - h_8, \text{ hot generator heat balance} \qquad (255)$$

$$w_L(h_2 - h_3) = w_t\,(h_8 - h_7), \text{ precooler heat balance} \qquad (256)$$

$$h_3 - h_4 = h_7 - h_6, \text{ cold regenerator heat balance} \qquad (257)$$

$$h_4 = h_5, \text{ J-T expansion process} \qquad (258)$$

$$h_6 - h_5 = \frac{q}{w_L}, \text{ refrigeration capacity of the working fluid} \qquad (259)$$

$$P_1 = P_2 = P_3 = P_4 \tag{260}$$

$$P_5 = P_6 = P_7 = P_8 = P_9 \tag{261}$$

An additional restriction is placed on the cycle by the second law of thermodynamics: The heat removed from the cold fluid during the liquefaction process = $w\ (h_3' - h_4)$ cannot cause heating of the low pressure gas flow to a temperature higher than the liquefaction temperature, T_4. Hence, the minimum value of h_4 is reached when $T_3' = T_7'$.

The heat balance in the precooler can be subdivided to express this condition:

$$w_L(h_2 - h_3') = w_t\ (h_8 - h_7'), \text{ cooling portion of the precooler} \tag{262}$$

$$w_L(h_3' - h_3) = w_t\ (h_7' - h_7), \text{ condensing portion of the precooler} \tag{263}$$

From the cold regenerator heat balance equation and the isenthalpic expansion condition, the refrigeration capacity of the working fluid is found to be

$$\frac{q}{w_L} = h_6 - h_5 = h_7 - h_3 \tag{264}$$

An expression for h_3 can be found from the overall precooler heat balance

$$h_3 = h_2 - \frac{w_t}{w_L}\ (h_8 - h_7) \tag{265}$$

then

$$\frac{q}{w_L} = (h_7 - h_2) + (h_8 - h_7) \tag{266}$$

Substituting the value of h_8 from the hot regenerator heat balance equation, we get a new expression for the refrigeration capacity of the cycle

$$\frac{q}{w_L} = \left(\frac{w_t}{w_L} - 1\right)(h_2 - h_7) - \frac{w_t}{w_L}(h_1 - h_9) \qquad (267)$$

or

$$q = w_e (h_2 - h_7) - w_t (h_1 - h_9) \qquad (268)$$

These equations show that the refrigeration capacity of the cycle is the difference between the expander work and the enthalpy difference between the gas at inlet and outlet of the hot regenerator.

The equation describing the heat balance in the condensing portion of the precooler indicates that more liquid is produced when $h_7' - h_7$ is increased. Hence, since the second law of thermodynamics fixes 7', the maximum cooling capacity of the cycle occurs when points (6) and (7) of Figure 46 coincide. Then points (3) and (4) will also coincide, and the expression for the refrigeration capacity of the cycle is

$$\frac{q}{w_L} = \left(\frac{w_t}{w_L} - 1\right)(h_2 - h_6) - \frac{w_t}{w_L}(h_1 - h_9) \qquad (269)$$

h_6 is fixed by the exhaust pressure of the system; hence, the refrigeration capacity will increase with h_2, which depends on the expander inlet pressure. However, the net refrigeration effect at the low-temperature level reaches a constant value as h_2 increases, as will be seen, due to the fact that $(h_1 - h_9)$ also increases when the expander inlet pressure is increased.

The maximum refrigeration capacity corresponds to the condition $h_6 = h_7$; however, the analysis of the cycle was conducted for an expander outlet temperature at point (7) slightly higher than that of the saturated vapor. This provides some margin in regard to the production of liquid in the expander itself and also corresponds to more realistic operating conditions for the cycle. If liquefaction occurs inside the expander, its efficiency drops considerably (see Reference 15).

Assuming that the hot regenerator effectiveness is unity reduces $(h_1 - h_9)$ to a minimum with a corresponding increase in refrigeration capacity of the cycle.

As noted previously, the operation of the cycle is restricted by the second law of thermodynamics. This restriction, in effect, fixes the minimum value of the nitrogen enthalpy at the Joule-Thomson expansion orifice for optimum operation. This minimum value of the enthalpy is dependent on the temperature of the fluid exhausting from the mechanical expander, on the high and low fluid pressure levels, and also on the ratio of the flow to the cooling envelope to the total fluid flow, w_L/w_T.

The values of the enthalpy of the nitrogen at the Joule-Thomson expansion orifice versus the cooling envelope flow to total flow ratio are plotted in Figure 47. The total nitrogen flow versus the same flow ratio is plotted in Figure 48. The minimum values of the nitrogen enthalpy, consistent with the second law, were calculated and these points are also shown in both plots as the line of optimum operating conditions. Figure 48 also shows the total system flow for a system inlet temperature of $0^{\circ}F$ and pressure of 30 psia. As can be seen, the total system flow is not too greatly sensitive to the system inlet temperature; therefore, complete plots for the other system inlet temperature were not made.

Decreasing the flow ratio below the value defined by the optimum condition curve produces more liquefaction in the portion of the total flow which goes to the cooling envelope. However, the decreased flow ratio also results in less fluid going to the cooling envelope, an effect which negates the previously mentioned increase in refrigeration capacity and, hence, the refrigeration capacity of the cycle remains approximately constant.

The same analysis that was conducted for the bypass expander cycle using nitrogen as a working fluid can also be performed using neon instead of nitrogen. The system schematic and cycle temperature-entropy diagram are identical to those used for nitrogen.

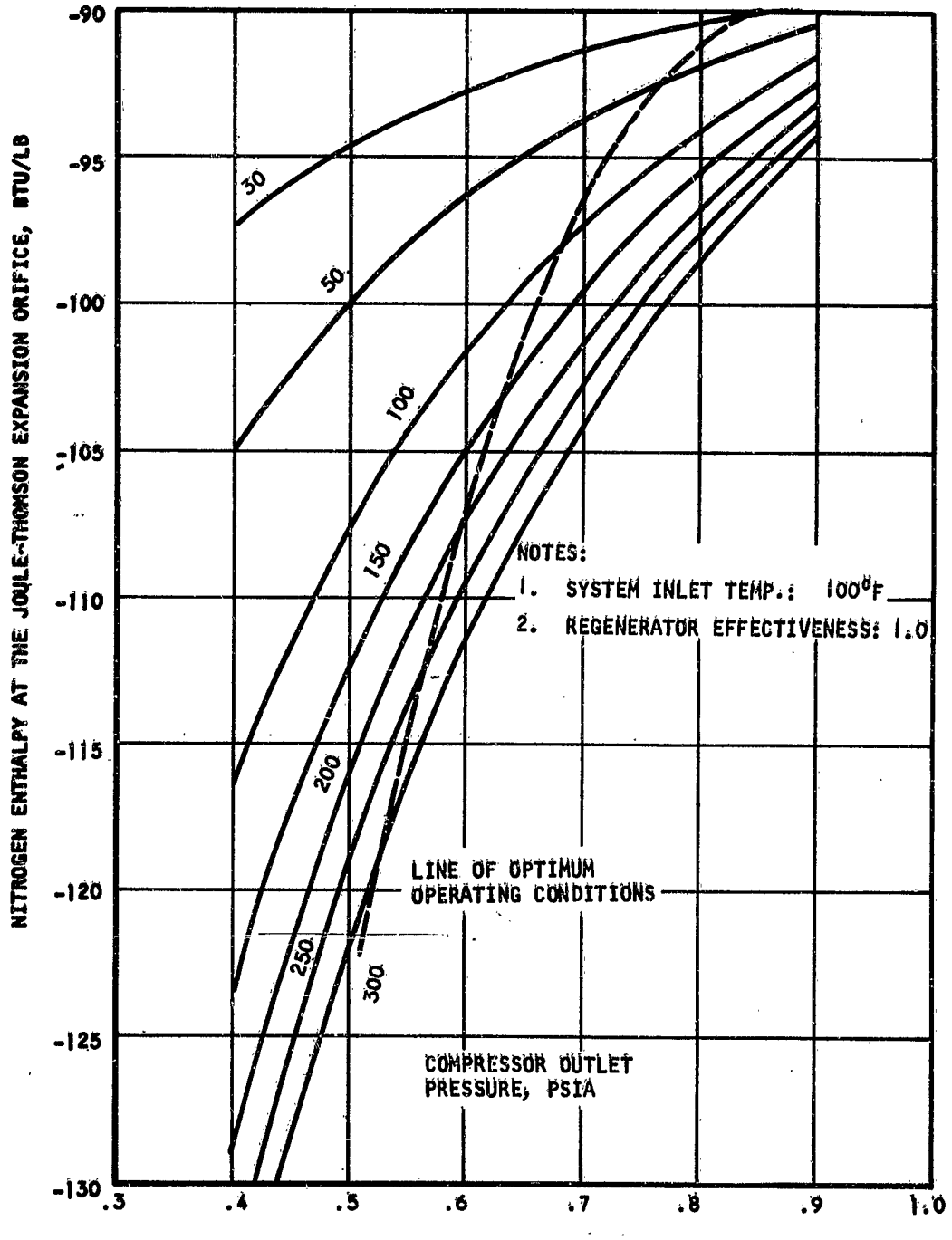

Figure 204. Nitrogen Enthalpy at the Joule-Thomson Expansion Orifice

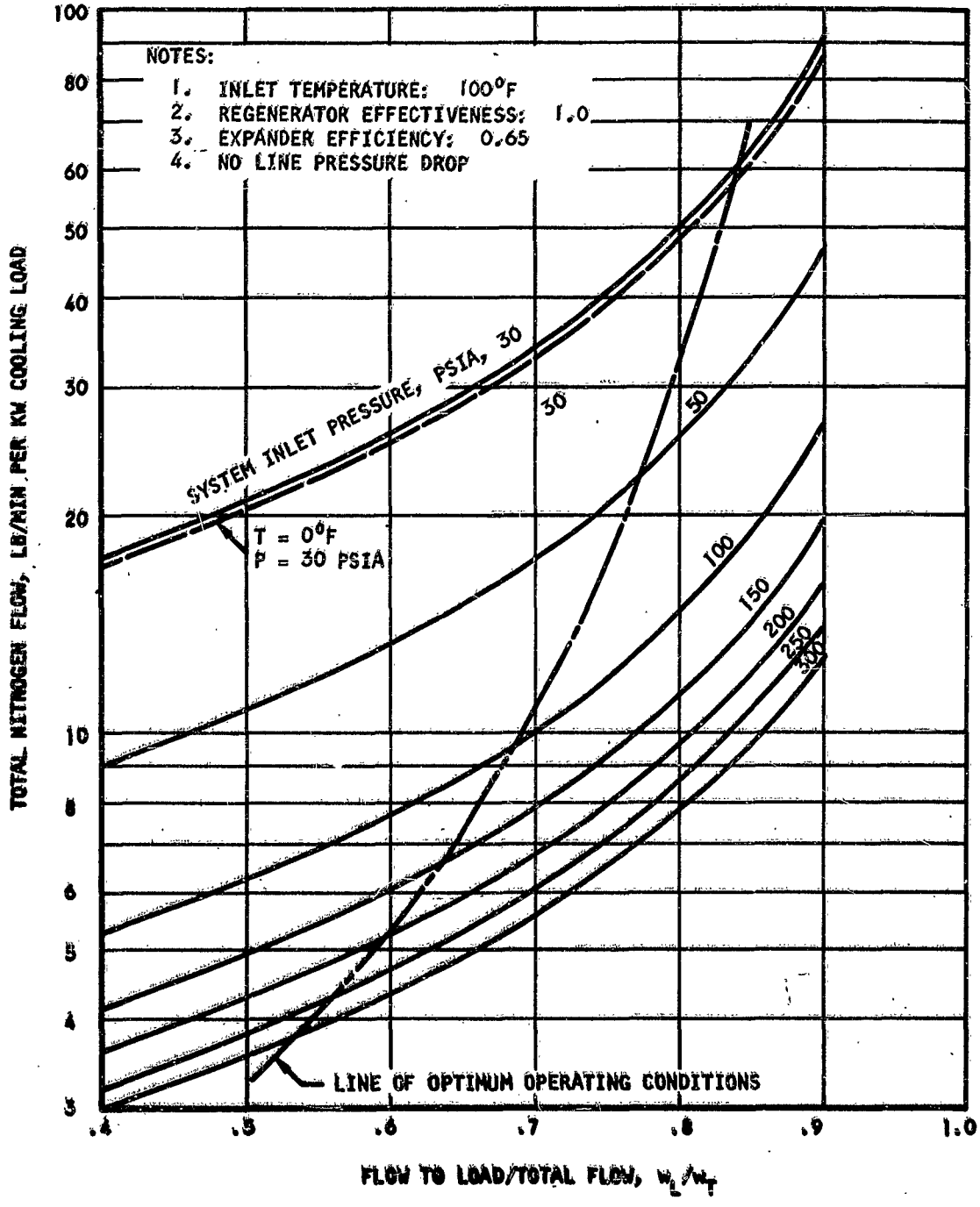

Figure 205. Nitrogen Bypass Expander System Total Flow

Calculations of the neon enthalpy at the Joule-Thomson expansion orifice, as a function of the cooling envelope flow to total flow ratio, were carried out. The results are shown in Figure 49. The system total flow values, as functions of the same parameter, were also calculated and the results plotted in Figure 50. The line of optimum operating conditions, as defined in the analysis for nitrogen, is shown on both plots for neon. As before, the system inlet temperature was taken to be 100°F.

The single bypass expander, using helium as a working fluid, was also analyzed. It was found that making the simplifying assumptions mentioned at the beginning of this section leads to a violation of the second law of thermodynamics, since the temperatures of the hot and cold fluids would have to cross in the heat exchanger. Consequently, no idealized cycle plots will be presented here, but the cycle will be analyzed with non-ideal components, and the results will be presented in a following section.

Summary of Ideal Isenthalpic Expansion Systems

The preceding sections have dealt with refrigeration systems having one common feature: refrigeration by means of isenthalpic expansion of the working fluid. In addition, all components were assumed to be ideal, with the exception of the expanders used in the bypass expander cycles. These expander efficiencies were taken to be 0.65 which is, perhaps, overly pessimistic, considering the large flow rates involved. In order to compare the systems, the required fluid flow rates can be calculated for each system operating under the same conditions. These conditions were arbitrarily taken to be:

1. System inlet pressure is 300 psia
2. System inlet temperature is 100°F
3. Cooling load is 10 kw
4. System outlet pressure is 14.7 psia

Under these conditions, for refrigeration at liquid nitrogen temperatures, the simple Joule-Thomson system requires a flow of 330 lb/min (Figure 39), whereas the bypass expander system requires 38 lb/min (Figure 48).

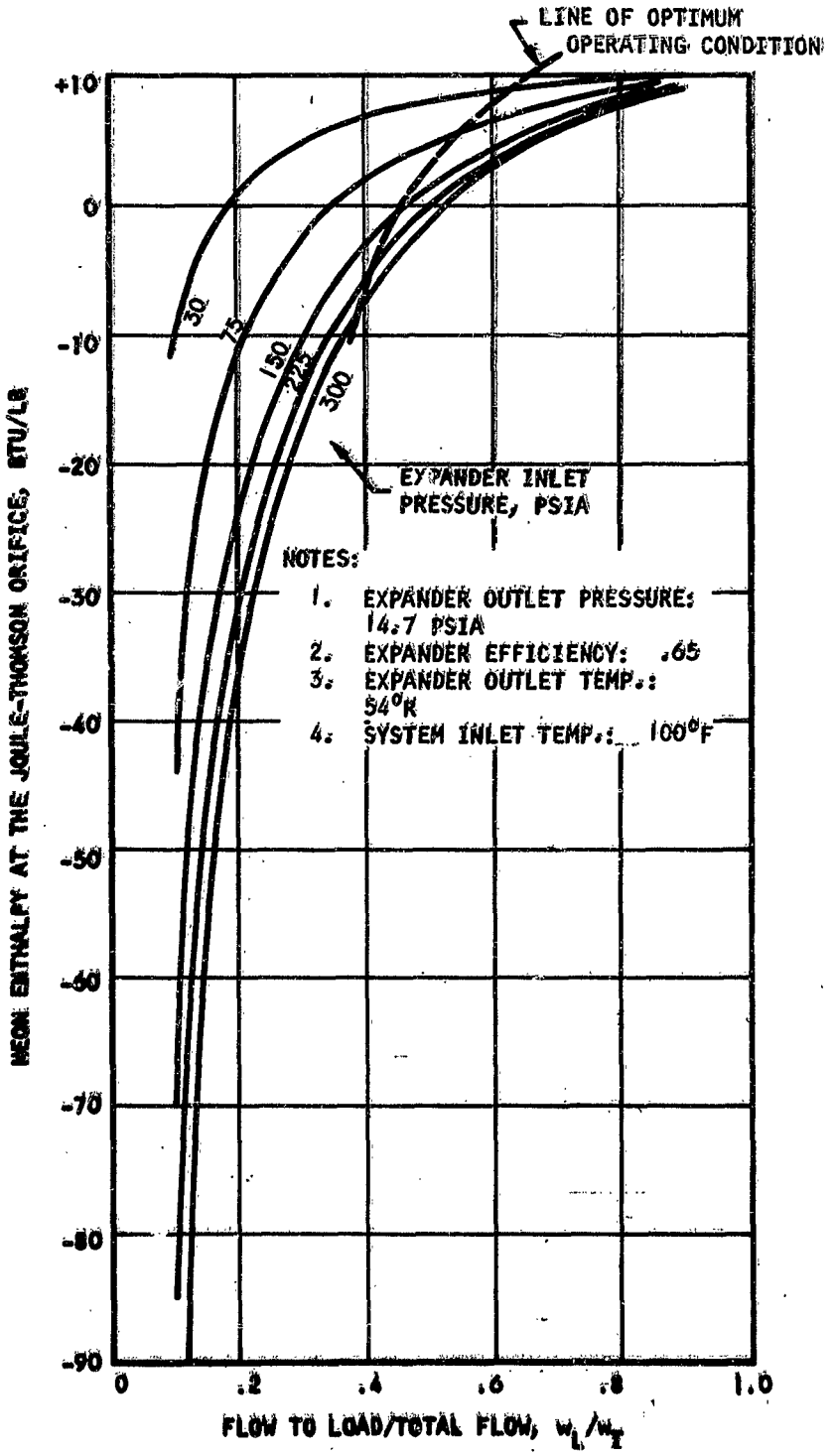

Figure 206. Enthalpy of Neon at the Joule-Thomson Expansion Orifice

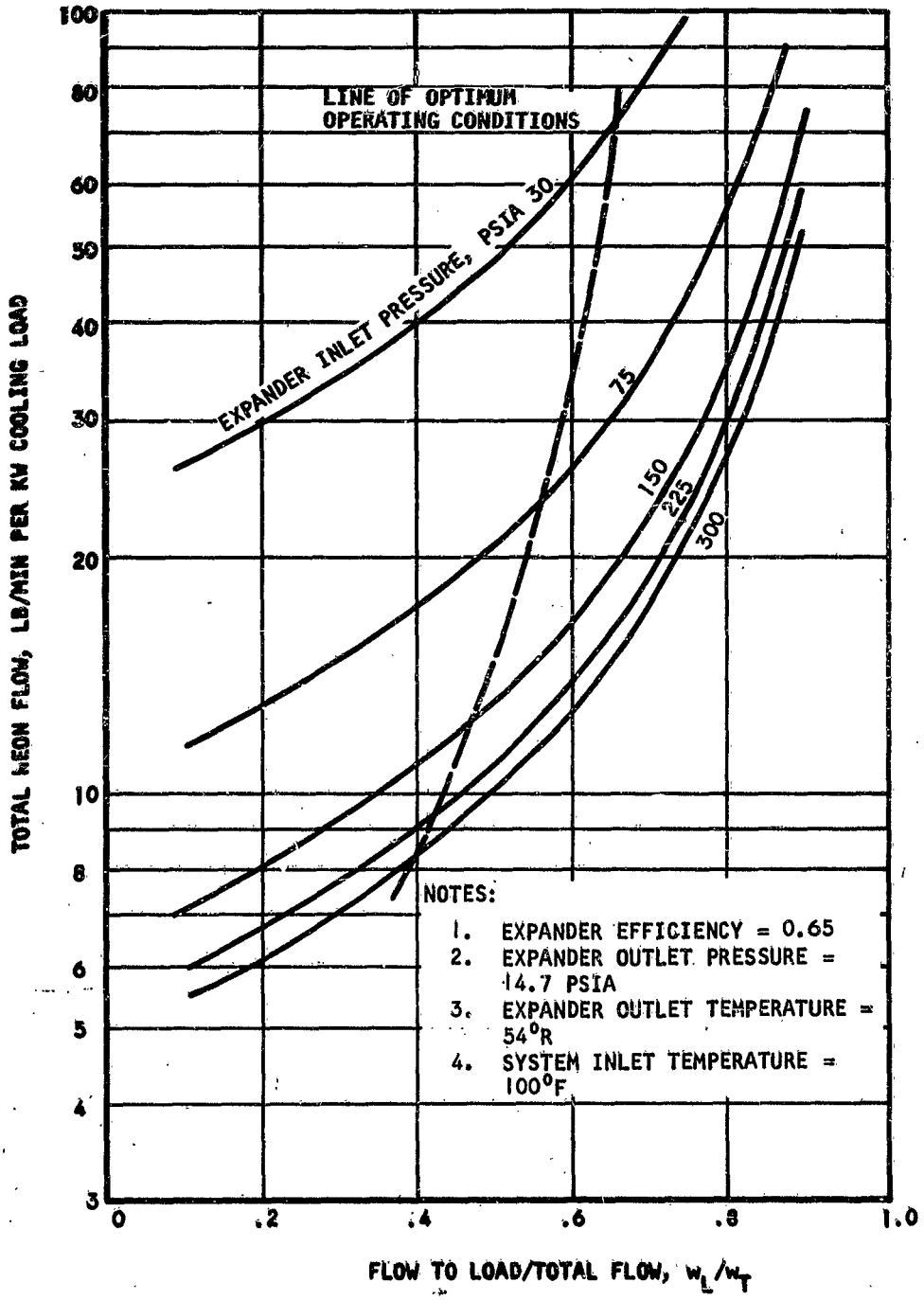

Figure 207. Neon Bypass Expander System Total Flow

For refrigeration at liquid neon temperatures, the cascaded Joule-Thomson system requires 250 lb/min neon flow plus 462 lb/min nitrogen flow (from Figure 41, 42, and 39). The bypass expander system requires 82 lb/min neon flow only (from Figure 50).

Cooling at liquid helium temperatures cannot be compared, since the ideal bypass expander cycle violates the second law of thermodynamics. However, it is evident that the bypass expander cycle has an overwhelming advantage over the simple Joule-Thomson cycle. Consequently, the more detailed analyses involving system weights and power factors, etc., will not be performed for the simple Joule-Thomson cycles.

Stirling Cycle

In 1954, J. W. L. Kohler and C. O. Jonkers of the Phillips Research Laboratories, Eindhoven, Netherlands, announced the development of a gas refrigerating machine which was fundamentally a special case of the Stirling cycle. The Phillips Company had a refrigerator operating at 79°K and producing 5.5 liters per hour of liquid air in 1955 and in 1961 had a smaller machine operating at 30°K.

In the machine developed by the Phillips Company, the cold is produced by the reversible expansion of a gas, either hydrogen or helium. During one cycle, the gas is compressed at ambient temperature and expanded at the desired low temperature, the transition between the two temperature levels being effected by a heat exchanger.

Figure 51 shows the four phases of an ideal Stirling cycle machine operating as follows:

I. The gas is compressed isothermally by piston (2) in space 3. The heat of compression is removed from the working fluid by means of a heat exchanger 4.

II. The gas is transferred from space 3 to space 8 by the movement of the displacer 5. In this constant volume process, the gas passes through a regenerator 6 where it is reversibly cooled down. The heat taken from the gas in this step is stored in the regenerator.

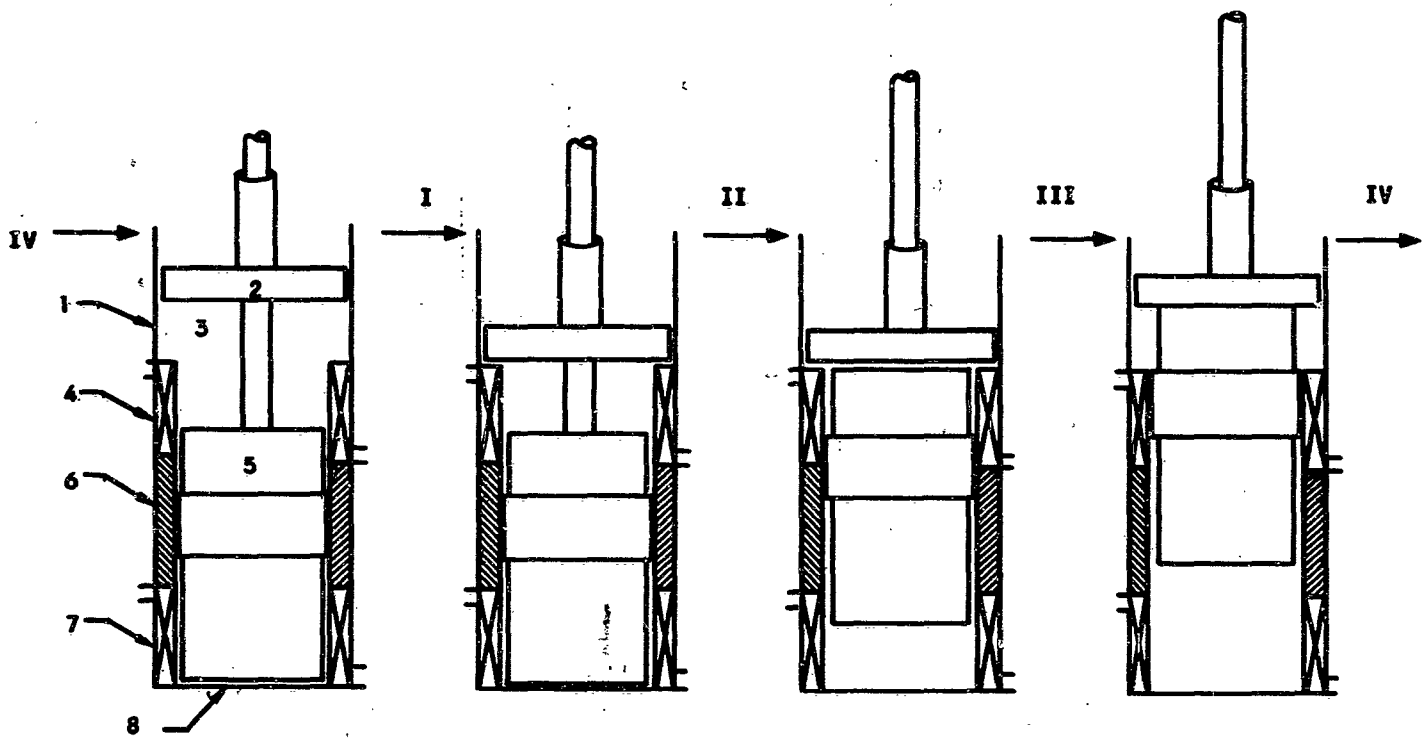

1. CYLINDER
2. PISTON
3. COMPRESSION SPACE
4. HEAT EXCHANGER
5. DISPLACER
6. REGENERATOR
7. HEAT EXCHANGER
8. EXPANSION SPACE

Figure 208. Ideal Stirling Cycle Machine

III. The gas is expanded isothermally in space 8 by the combined movement of the piston 2 and displacer 5 . The refrigeration produced is transferred to the load by means of the cold heat exchanger 7 .

IV. The gas is returned to space 3 by the movement of the displacer 5 In this step, the gas picks up the heat stored in the regenerator 6 during Step II.

Figure 52 is a plot of the ideal cycle on a P-V diagram. Note that this cycle consists of two isotherms and two isochores, however, the isochores may be replaced by isobars or any pair of lines which permit heat exchange by regeneration.

The discontinuous motions of the piston and expander previously described are not feasible in practice; however, the pistons may be driven sinusoidally by some type of drive mechanism. In such a case the cold expansion space must be leading in phase with respect to the hot compression space. This harmonic motion causes the compression and expansion to take place adiabatically which entails some loss in efficiency. This loss will be low for low pressure ratios.

Referring to the P-V diagram, the following expressions can be obtained from elementary thermodynamic relations:

	Work Input to Gas	Heat Input to Gas	Energy Change of Gas
I.	$P_1 V_2 \ln \frac{V_2}{V_1}$	$-P_1 V_2 \ln \frac{V_2}{V_1}$	0
II.	0	$-C_V (T_1 - T_2)$	$-C_V (T_1 - T_2)$
III.	$P_4 V_2 \ln \frac{V_1}{V_2}$	$-P_4 V_2 \ln \frac{V_1}{V_2}$	0
IV.	0	$C_V (T_1 - T_2)$	$C_V (T_1 - T_2)$

From these relations, it can be seen that the ideal cooling capacity per cycle, q_1, can be expressed as

$$q_1 = P_4 V_2 \ln \frac{V_2}{V_1} \qquad (270)$$

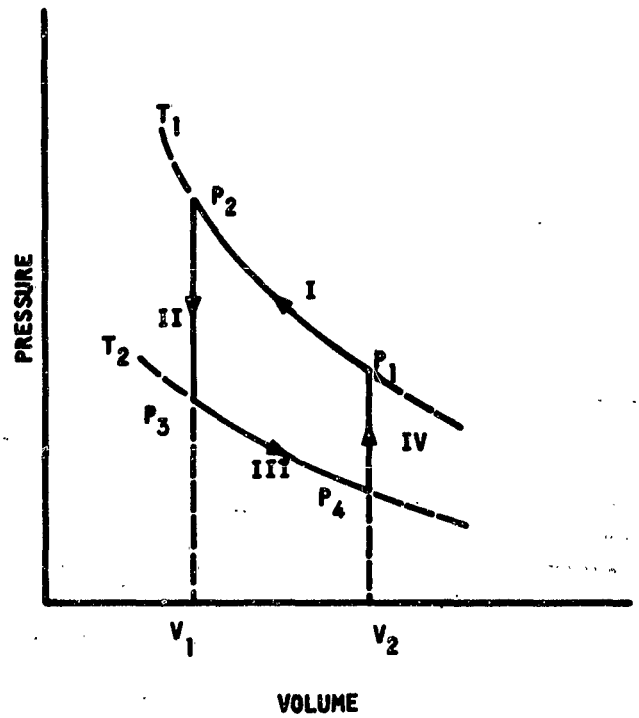

Figure 209. P-V Diagram For Ideal Stirling Cycle (Isothermal Case)

The practical use of a Stirling cycle refrigerator depends very heavily on the efficiency of the regenerator. It has been shown (Reference 18) that, owing to imperfections, an amount of heat, Δq_1, is transmitted through the regenerator from space 3 to space 8 (refer to Figure 51) and that this amount of heat may be expressed as

$$\Delta q_1 \approx 7 (1 - E_r) \left(\frac{T_1 - T_2}{T_2}\right) q_1 \qquad (271)$$

where E_r = regenerator efficiency

T_1 = compression temperature

T_2 = expansion temperature

Reference 18 further states that regenerators consisting of a light, felt-like mass of fine wire can be prepared with efficiencies higher than 99 per cent at frequencies as high as 50 cycles per sec. However, the regenerator acts as a resistance to the gas flow so that the design of a regenerator should compromise between regeneration loss, pressure loss, and loss by dead space.

In the following analysis, the assumptions made are:

1. The working fluid is helium.
2. The warm temperature is 560°R.
3. The cold temperature is 140°R.
4. All heat leaks into the system are considered to be a part of the cooling load.
5. The gas is compressed isothermally.
6. The gas is expanded isothermally.
7. The volume of the gas after expansion is equal to the cross-sectional area of the displacer times its diameter (i.e., "square" displacer stroke).

8. The amount of heat transferred through the regenerator is given exactly by Equation 61.

9. The dead space less due to the heat exchangers is neglected.

Under these assumptions, the diameter of the displacer is given by

$$D = \frac{48W\,T_l\,R}{\pi\,P_l} \qquad (272)$$

where W = total weight of helium being used as a working fluid, lb

R = gas constant for helium, 386.6 ft-lb/lb-$^{\circ}$R

T_l and P_l are as defined in Figure 52

The diameter as a function of the weight of the helium charge is plotted in Figure 53 for various values of P_l.

Combining Equations 60 and 61 yields

$$Q = 1.225\,(21\,E_r - 20)\,C \ln r, \text{ kw/lb} \qquad (273)$$

where Q = Ideal cooling capacity of Stirling engine per pound of helium at 140°R, kw/lb

C = Cycles per minute

r = Compression pressure ratio

Q is plotted in Figures 54, and 55, as a function of C for various compression ratios and regenerator efficiencies.

As was previously mentioned, an actual machine provides the piston and displacer with sinusoidal motions. Using the notation:

V_o = Maximum volume of the expansion space, cm^3

W = Ratio of the swept volumes of the compression and expansion space

ϕ = The phase difference between these spaces

T_C = Temperature in compression space, $^{\circ}$K

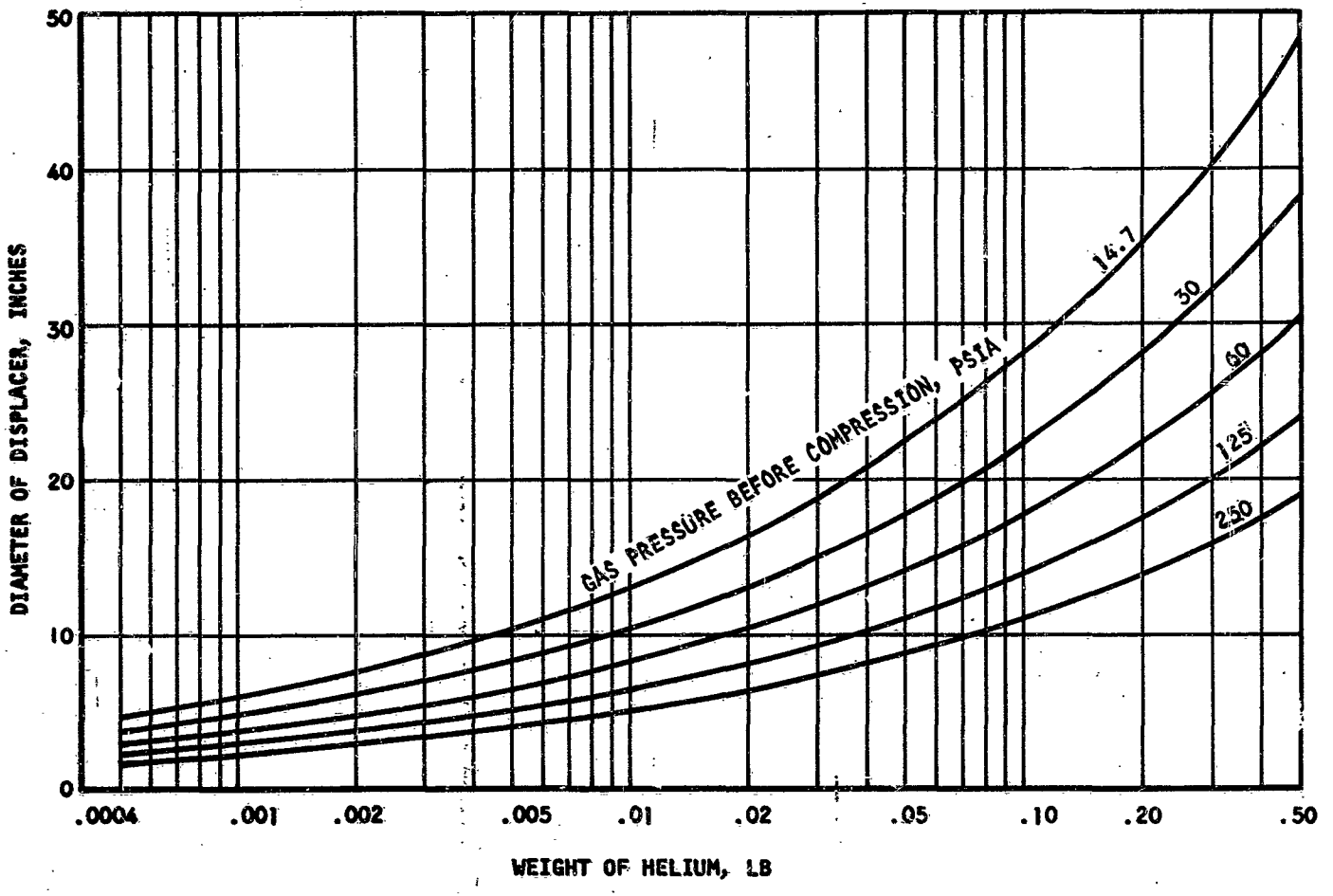

Figure 210. Diameter of Stirling Cycle Refrigerator Displacer

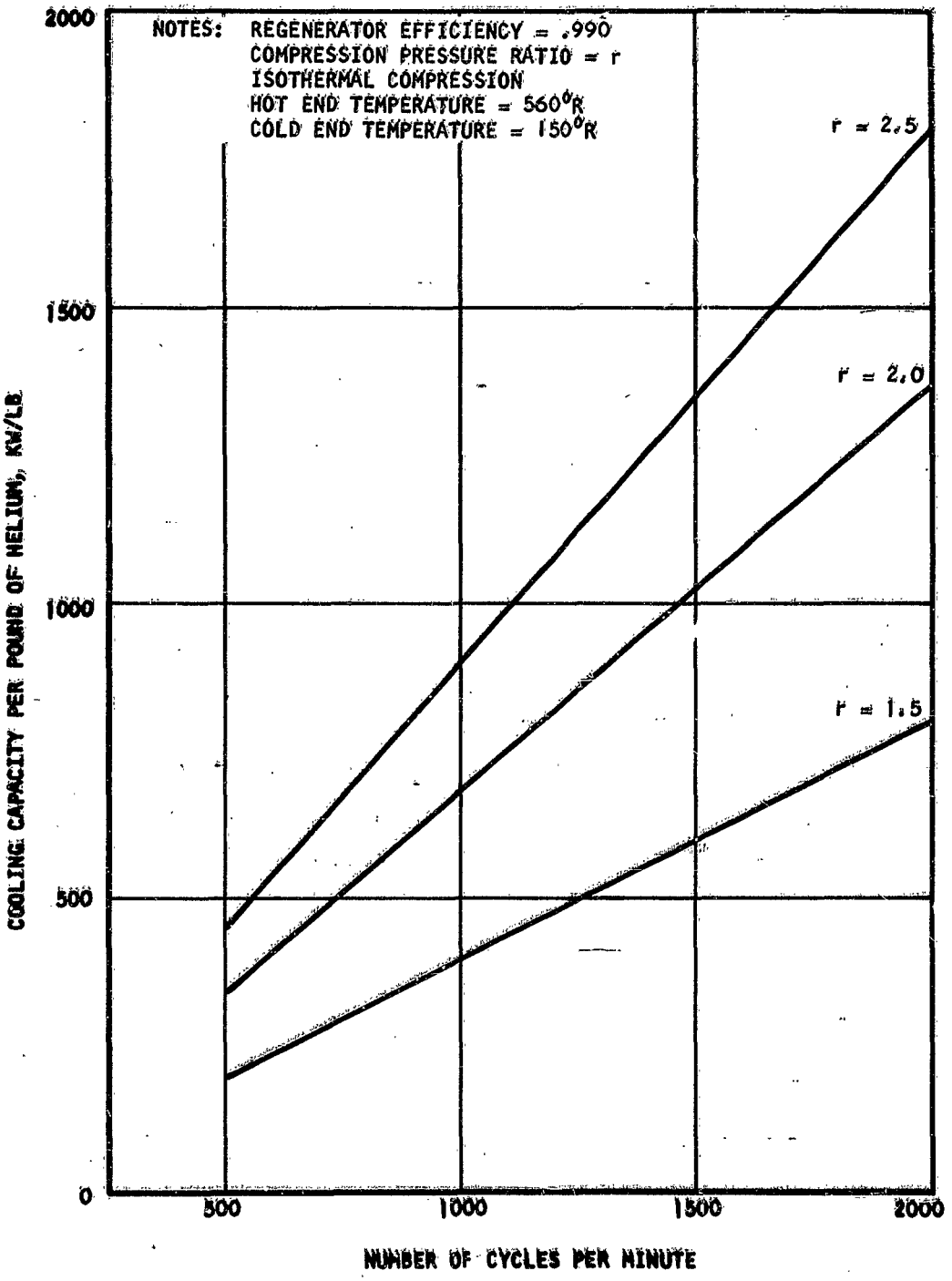

Figure 211. Specific Cooling Capacity of Stirling Cycle Refrigerator (Isothermal Process) (η_R = 0.990)

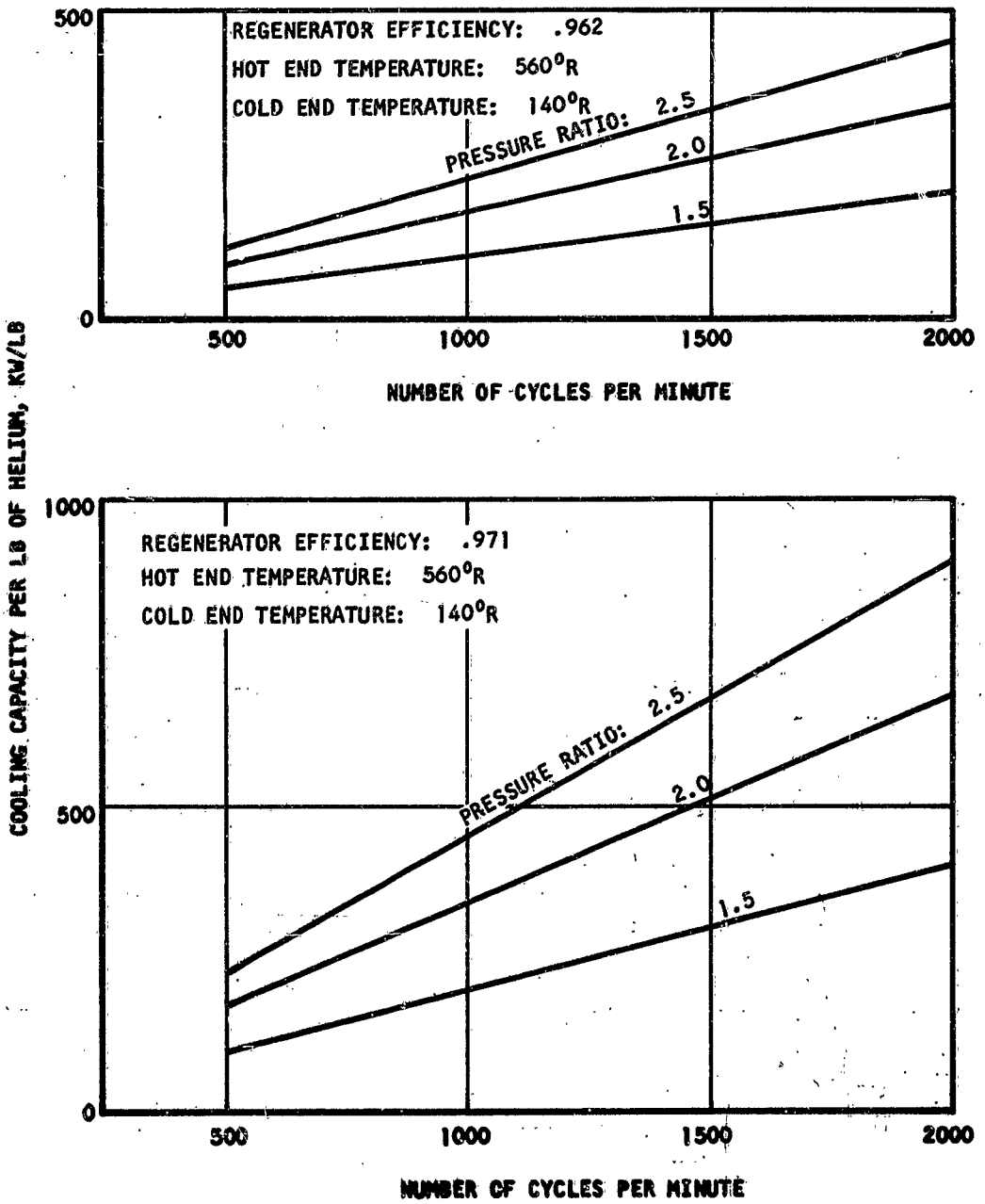

Figure 212. Specific Cooling Capacity of Stirling Cycle Refrigerator (Isothermal Process) (η_R = .971, .962)

T_E = Temperature in expansion space, °K

T_S = Temperature in any dead space, °K

V_S = Volume of any dead space, cm^3

$\tau = T_C/T_E$

$S = \sum \frac{V_S}{V_0} \frac{T_C}{T_S}$

$A = \sqrt{\tau^2 + W^2 + 2\tau W \cos \phi}$

$B = \tau + W + 2S$

$\delta = A/B$

P_{max} = Maximum pressure during the cycle, kgm/cm^2

$P_{mean} = P_{max} \sqrt{\frac{1 - \delta}{1 + \delta}}$

$a = 1 + \sqrt{(1 - \delta^2)}$

n = Cycles per minute

Reference 16 gives the cooling capacity as

$$q_l = \frac{5.136}{a} V_0 P_{mean} \frac{n}{1000} \frac{W \sin \phi}{B}, \text{ watts} \qquad (27k)$$

Again, this expression must be combined with Equation 61 in order to account for losses due to the regenerator. The cycle, as it has been considered to this point, being perfectly reversible, would have the same efficiency as a Carnot cycle. The actual cycle suffers decreases in efficiency due mainly to three causes:

a. Mechanical loss of the drive
b. Pressure loss
c. Adiabatic loss

Losses due to (a) and (b) need no further elaboration. Losses due to (c) arise from the necessity of introducing heat exchangers in order to cool the

gas after compression and in order to exchange heat between the expansion cylinder and the cooling fluid (nitrogen). The walls of the cylinders are extremely poor heat exchangers, consequently, the temperature of the gas varies nearly adiabatically with time. Hence, the mean temperature of the gas in the compression cylinder will be higher than the temperature of the adjoining heat exchanger and similarly, the mean temperature of the gas in the gas in the expansion cylinder will be lower than the temperature of its adjoining heat exchanger. The loss of refrigerative capacity due to this effect is very small, and this effect also has a minor influence on the efficiency (Reference 17).

Some idea of the effect which the actual compression and expansion processes have on the refrigeration capacity may be gained by considering again the ideal cycle. Now the helium will be compressed and expanded polytropically according to the law

$$pv^n = \text{constant} \qquad (275)$$

where p = pressure
v = specific volume
n = a constant depending on the process

For the ideal isothermal case, $n = 1$. For the ideal adiabatic case where no heat is transferred between the helium and its surroundings, $n = \gamma = 1.67$. Hence, $1 \leq n \leq 1.67$. Such a process is indicated schematically in Figure 56 where the dashed lines are isotherms and the solid lines are the actual path followed.

Referring to Figure 56, the following thermodynamic relations can be derived

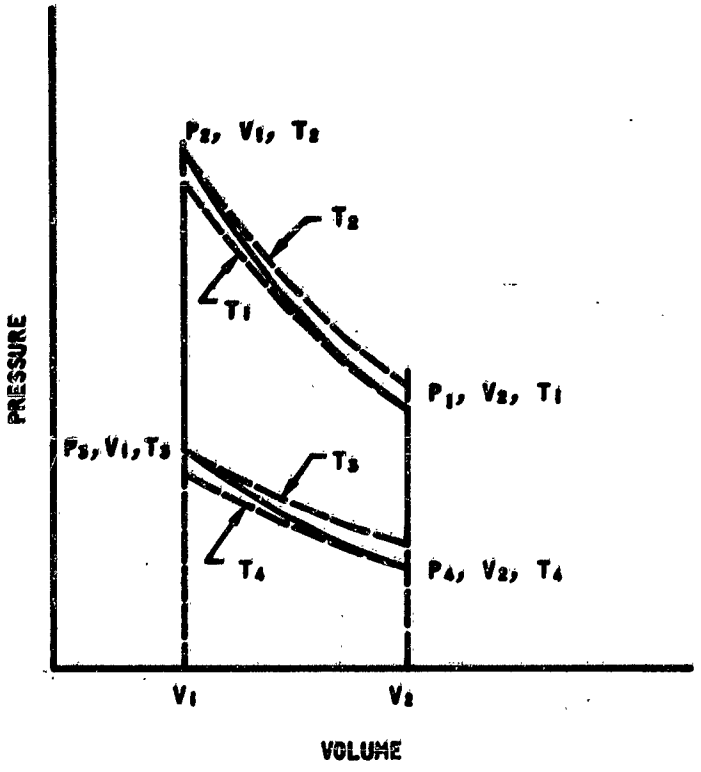

Figure 219. Polytropic Stirling Cycle

	Work Input to Gas	Heat Input to Gas	Energy Change of Gas
I	$\frac{P_2 V_1 - P_1 V_2}{n - 1}$	$C_v \left(\frac{\gamma - n}{1 - n}\right)(T_2 - T_1)$	$C_v (T_2 - T_1)$
II	0	$C_v (T_3 - T_2)$	$C_v (T_3 - T_2)$
III	$\frac{P_4 V_2 - P_3 V_1}{n - 1}$	$C_v \left(\frac{\gamma - n}{n - 1}\right)(T_3 - T_4)$	$C_v (T_4 - T_3)$
IV	0	$C_v (T_1 - T_4)$	$C_v (T_1 - T_4)$

making use of the relation

$$C_v = \frac{R}{\gamma - 1} \tag{276}$$

the ideal cooling capacity of each cycle is given by

$$q_p = \left(\frac{R}{\gamma - 1}\right)\left(\frac{\gamma - n}{n - 1}\right)(T_3 - T_4) \tag{277}$$

Making use of Equation 65, it can be shown that

$$T_3 - T_4 = \left[\left(\frac{P_2}{P_1}\right)^{\frac{n-1}{n}} - 1\right] T_4 \tag{278}$$

hence,

$$q_p = \left(\frac{R}{\gamma - 1}\right)\left(\frac{\gamma - n}{n - 1}\right)\left[r^{\frac{n-1}{n}} - 1\right] T_4 \tag{279}$$

where r is the compression ratio.

Assuming $T_1 = 560^\circ R$

$T_4 = 140^\circ R$

$\gamma = 1.67$

$R = 386.6$ ft-lb/lb $^\circ R$

and also assuming that the regenerative heat loss is given by the same expression as for the isothermal case, the final expression for the cooling capacity is

$$Q = 1.828\,(21E_r - 20)\left(\frac{1.67 - n}{n - 1}\right)\left(r^{\frac{n-1}{n}} - 1\right) C, \text{ kw/lb} \qquad (280)$$

This cooling capacity is plotted in Figures 57, and 58 as a function of C for various values of the compression ratio and n = 1.23.

As an example, suppose that the Stirling cycle refrigerator has a displacer diameter of 6 inches. Figure 53 shows that if the pressure in the cylinder before compression is 14.7 psi, then there is .001 lb of helium being used as a working fluid. Assuming a compression ratio of 2.0 and a regenerator efficiency of .971 and also assuming n = 1.23 at 1000 cycles per minute, the specific cooling capacity from Figure 58 is 193 kw/lb. Hence, the cooling capacity will be .193 kw.

The compression ratio is necessarily low due to the dead space resulting from the volume of the heat exchangers.

From the foregoing discussion it can be seen that a very large number of parameters have to be considered when trying to minimize all losses. A detailed investigation of this problem is outside the scope of this report. Suffice it to say that Stirling cycle refrigerators have been built to operate at an optimum temperature of -190°C from ambient and yielding approximately .085 kw refrigeration for 5.85 kw measured shaft power operating at 1440 rpm and a maximum pressure in the cycle of 35 kg/cm^2.

The machine requires high operating speeds and high operating pressure levels, both of which reduce the reliability over prolonged periods of operation. Furthermore, in order to reach refrigerative capacities of 20 kw several cylinders would be required. In the words of Dr. Kohler, one of the main proponents of Stirling cycle machines, "For very high refrigerating capacities turbine systems are the solution; . . ." (Reference 16).

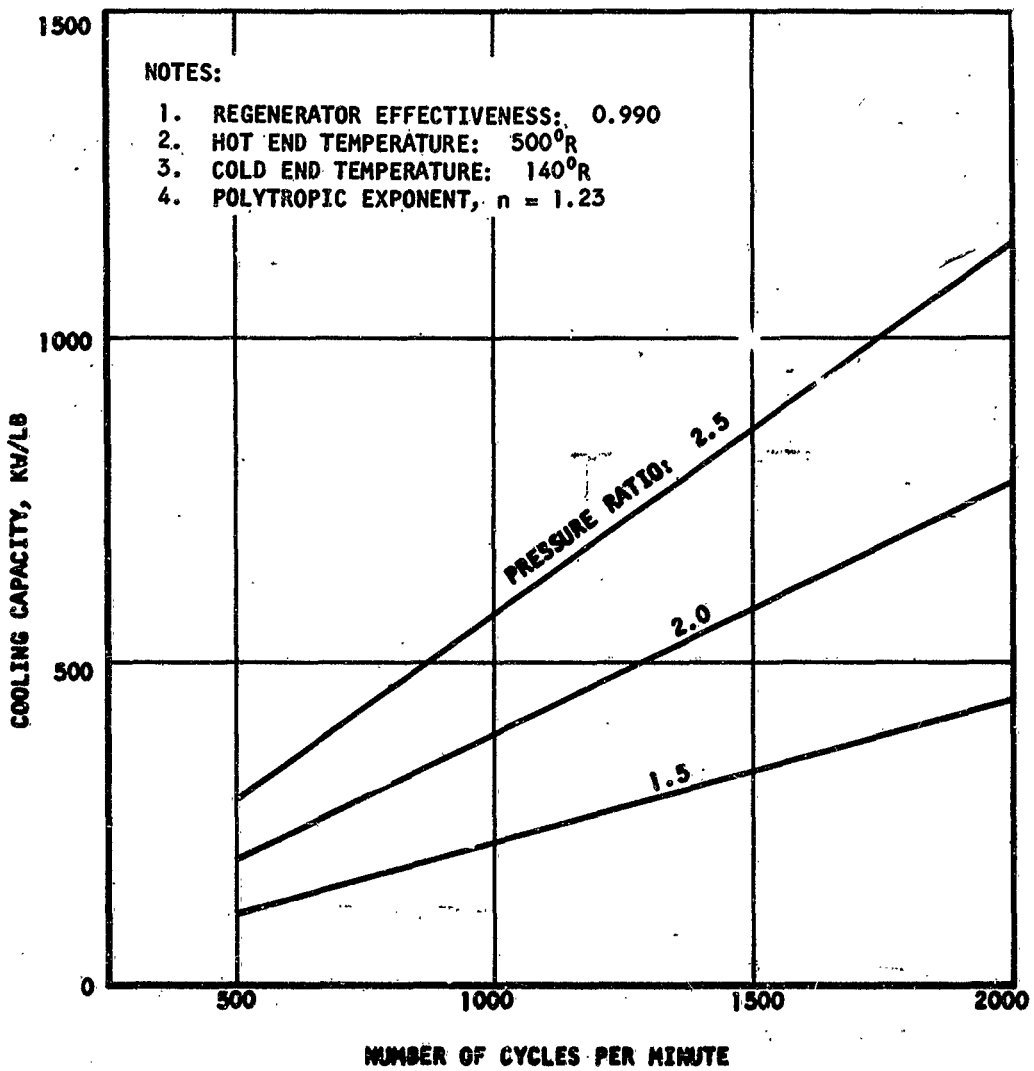

Figure 214. Specific Cooling Capacity of Stirling Cycle Refrigerator (Polytropic Process) (η_R = .990)

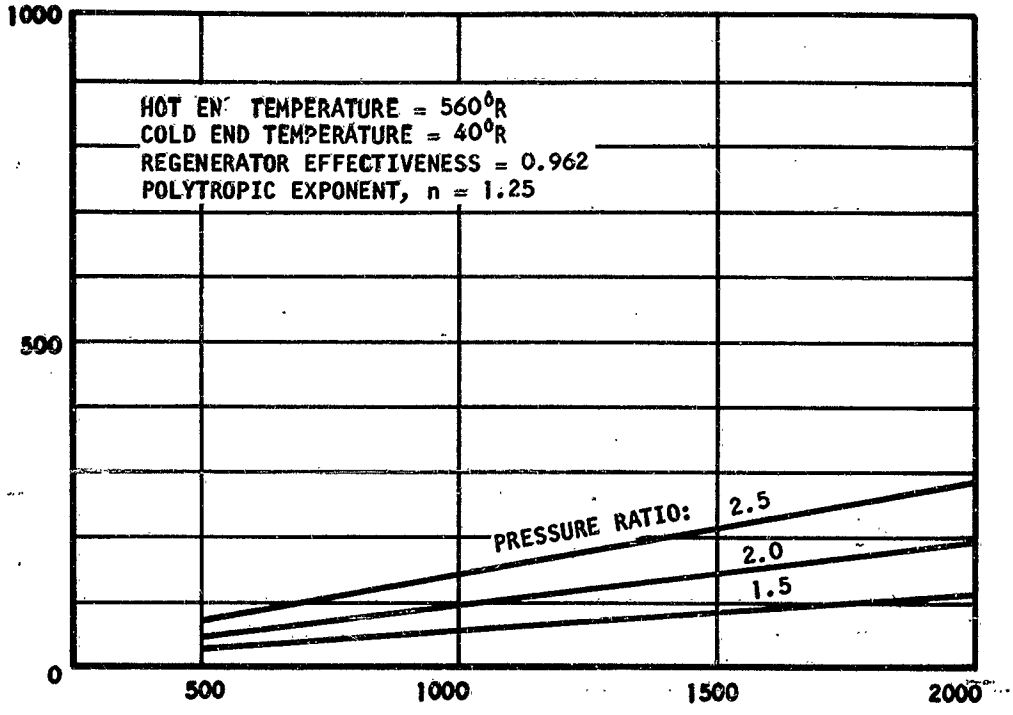

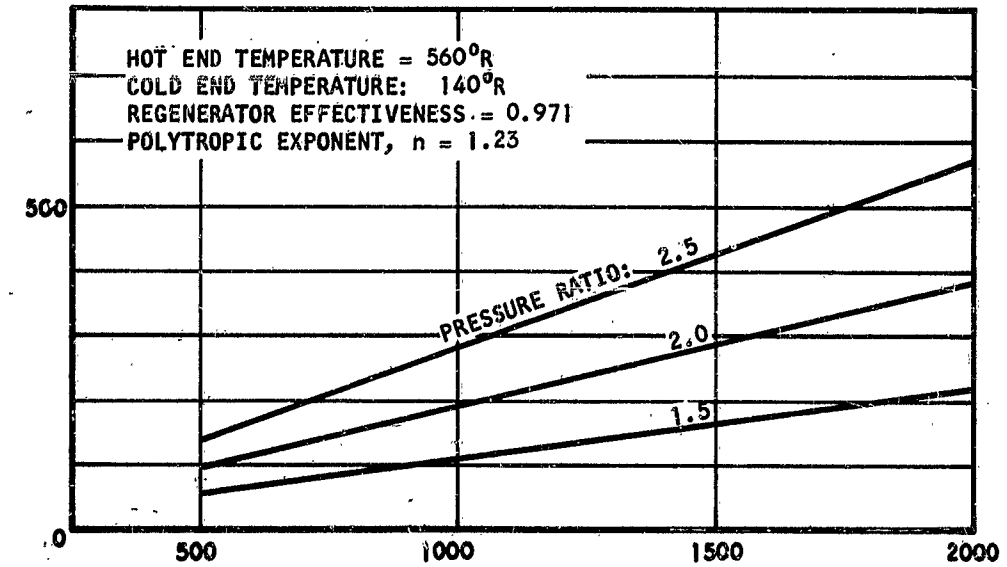

Figure 215. Specific Cooling Capacity of Stirling Cycle Refrigerator (polytropic Process) (η_R = .971, .962)

SECTION VII

NON-IDEAL SYSTEMS

In the previous section, various idealized cycles were considered for cooling large heat loads at liquid nitrogen, neon, and helium temperatures. In the analyses performed, simplifying assumptions were made concerning the components of each system. In this section, system performance is evaluated under more realistic operating conditions.

System components are discussed in Sections II through V of this study. The following design assumptions are taken from these component analyses and form the basis for the system analyses presented here.

a. Heat exchangers: The heat exchangers of the systems considered are designed with a maximum NTU of 9.0. This corresponds to effectiveness of 0.9 on both sides of a regenerator where the capacity rate (wcp) ratio is unity; for capacity rate ratios different from unity the effectiveness on the cold side is allowed to increase above 0.9.

   In all cases where condensation of the working fluid occurs on one side of a heat exchanger, the heat exchanger, for the purpose of analysis, is divided into a condensing portion and into a cooling portion where all the fluid is in the gaseous state. In this manner the "pinch" effect is taken into account in system design.

b. Turbo-expanders: The adiabatic efficiency of the turbo-expanders used in the refrigeration systems considered is taken as 0.85. This value might be optimistic at low flow rates, however, it is felt to be attainable by close control of the manufacturing tolerances. Weight of turbo-expanders are obtained from Figures 27 through 30.

c. Compressors: Centrifugal type compressors are used in all the systems considered. Compressor performance and weight is estimated from the parametric data presented in Section IV.

d. Power Requirement: System power requirement is estimated from the compressor performance assuming that all the power generated by expansion of the working fluid in the system turbo-expanders is used to drive the compressor.

e. Electric Motors: As stated previously (see Section IV) electric motor efficiency is taken as 0.85 (constant), and the motor weight as 0.8 lb per kw.

f. Radiators: The waste heat from the system is rejected to space by means of a radiator. The heat is transferred from the system to the space radiator by means of a heat transport fluid. The radiator area estimates given in this section are based on heat transport fluid temperatures at radiator inlet and outlet of 170°F and 50°F respectively (see Section III).

g. Accessories: Lines, insulation, compressor intercoolers and after-cooler, control system, brackets etc., are assumed to contribute 4 per cent of the total system weight.

In this section, only bypass expander systems are considered. System arrangement and optimum number of expanders are discussed. The system flow rate is determined and estimates of the system weight, power requirement and radiator area requirement are presented as functions of the system cooling loads.

The section is divided in three parts according to the working fluid considered, each working fluid corresponding to a given refrigeration temperature level.

NITROGEN REFRIGERATION SYSTEMS

Single and multiple expander systems are considered for refrigeration at liquid nitrogen temperature (140°F). In the following paragraphs single expander system data are given and its characteristics are plotted. Thermodynamic calculations performed on two-expander systems are also given; these are compared with the single expander systems.

Single Expander System

The system shown schematically in Figure 46 was analyzed with nitrogen as the working fluid and subject to the following conditions (The subscripts are for points defined in Figure 46):

1. $T_7 = 150^\circ F$, $P_7 = 1$ atm. The working fluid state point at expander outlet is chosen to be slightly outside the vapor dome in order to insure that no liquification occurs inside the expander.

2. The temperature of the working fluid at aftercooler outlet, T_1, is taken at $100^\circ F$. The system performance is only mildly dependent on this temperature, therefore this relatively high value was selected to relieve the vehicle thermal management system load.

3. The data available on the working fluids considered in this study is not sufficiently accurate to reflect the effects of pressure drops up to 0.2 per cent in each heat exchanger, therefore no pressure drops were considered.

The equations governing the cycle analysis are the same as those presented in Section VI. It was found that once a heat exchanger effectiveness is assumed, a unique value of the flow ratio, w_L/w_T exists for each set of system inlet parameters; here w_L and w_T are respectively the flow to the load and the total system flow, as defined in Figure 46. Since the total flow rate w_T, is determined from the ratio w_L/w_T, the heat exchanger effectiveness is thus a parameter which lends itself to optimization procedures for the system.

System optimization on the basis of heat exchanger effectiveness is not performed in this study, since it depends essentially on particular vehicle installation parameters. In addition such an optimization study would require extensive use of computers which is outside the scope of this report. For the reasons stated previously (see Section V) the system was analyzed based on a maximum heat exchanger cold side NTU of 9.0.

The results of the thermodynamic analysis performed on the system depicted in Figure 59 are given in Table 3 for compressor delivery pressures of 10, 15, and 20 atm. The pressure in the cold leg of the system was taken as 1 atm in all cases.

From this table it can be seen that the total system flow decreases markedly as the compressor delivery pressure increases.

System Characteristics

Based on the assumptions stated previously the system fixed weight including heat exchangers, compressors, expanders, driving motor and accessories was estimated. The weight is plotted in Figure 60 against the cooling load. Also given in Figure 61 are the system power requirement and radiator area.

The radiator area based on the assumptions listed previously is very large, which suggests that at the higher cooling loads it might be advisable to divorce the cooling loop of the refrigeration system from that of the vehicle. In this manner higher radiator inlet temperatures with correspondingly smaller radiator areas could be obtained. It should be noted here that the radiator area is given for an orbiting vehicle, for which case the radiator equivalent sink temperature is relatively high.

The plot of Figure 60 shows conclusively that operation at the higher pressure ratio is desirable from all points of view. A pressure ratio higher than 20:1 is however unadvisable because of the high number of compression stages and the corresponding loss in compressor efficiency arising from the necessity of matching the speeds of all the stages.

Two-Expander System

A system featuring two expanders was investigated in order to improve on the performance of the single expander system at lower operating pressure. The system considered is shown in Figure 62. For the purpose of analysis and comparison the compressor delivery pressure was taken as 10 atm. Again

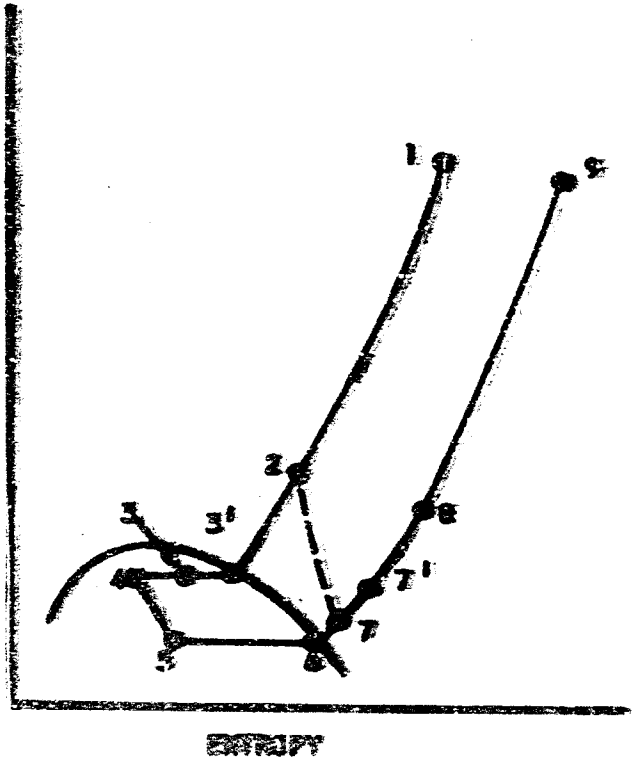

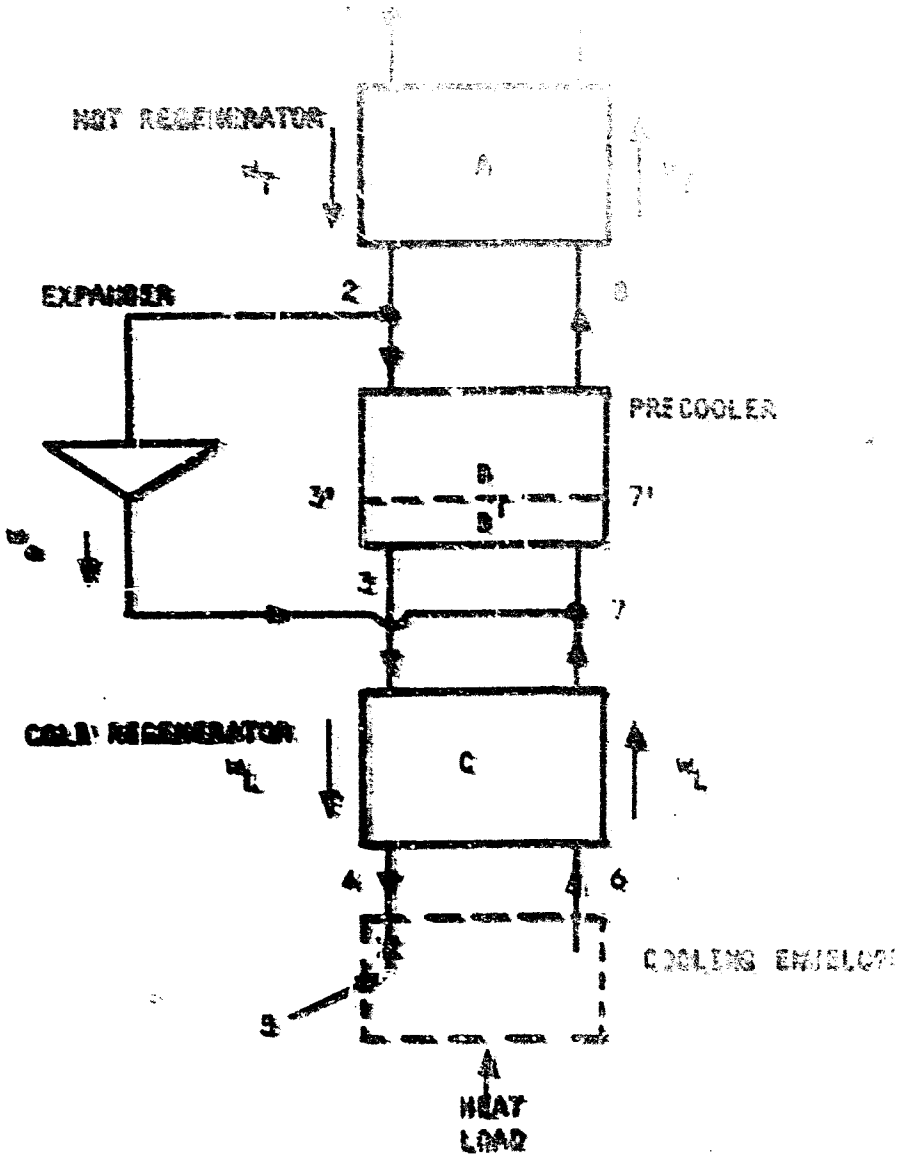

Figure 23b. Bypass Expander System

TABLE 51

NITROGEN SINGLE EXPANDER SYSTEM

Pressure in Hot Leg	10 atm	15 atm	20 atm
T_1	560	560	560
h_1	16.2	15.7	15.3
T_2	280	302.5	326
h_2	-56	-51.5	-46.5
T_3'	187.5	199	209
h_3'	-84.5	-84.5	-86
h_3	-97.7	-102.2	-107.9
T_7	150	150	150
h_7	-86.2	-86.2	-86.2
T_7'	177.1	187.5	196
H_7'	-78.7	-76.2	-74
T_8	240	260	282
h_8	-62.5	-57.6	-52.1
T_9	530.5	530	534
h_9	9.7	9.6	10.5
w_L	4.9	3.6	2.6
w_T	8.7	6.3	4.7
w_e	3.8	2.7	2.1

See Figure 46 for definition of subscripts

Temperatures in °R

Enthalpies in Btu/lb

w_L, w_e, w_T in lb/min per kw cooling

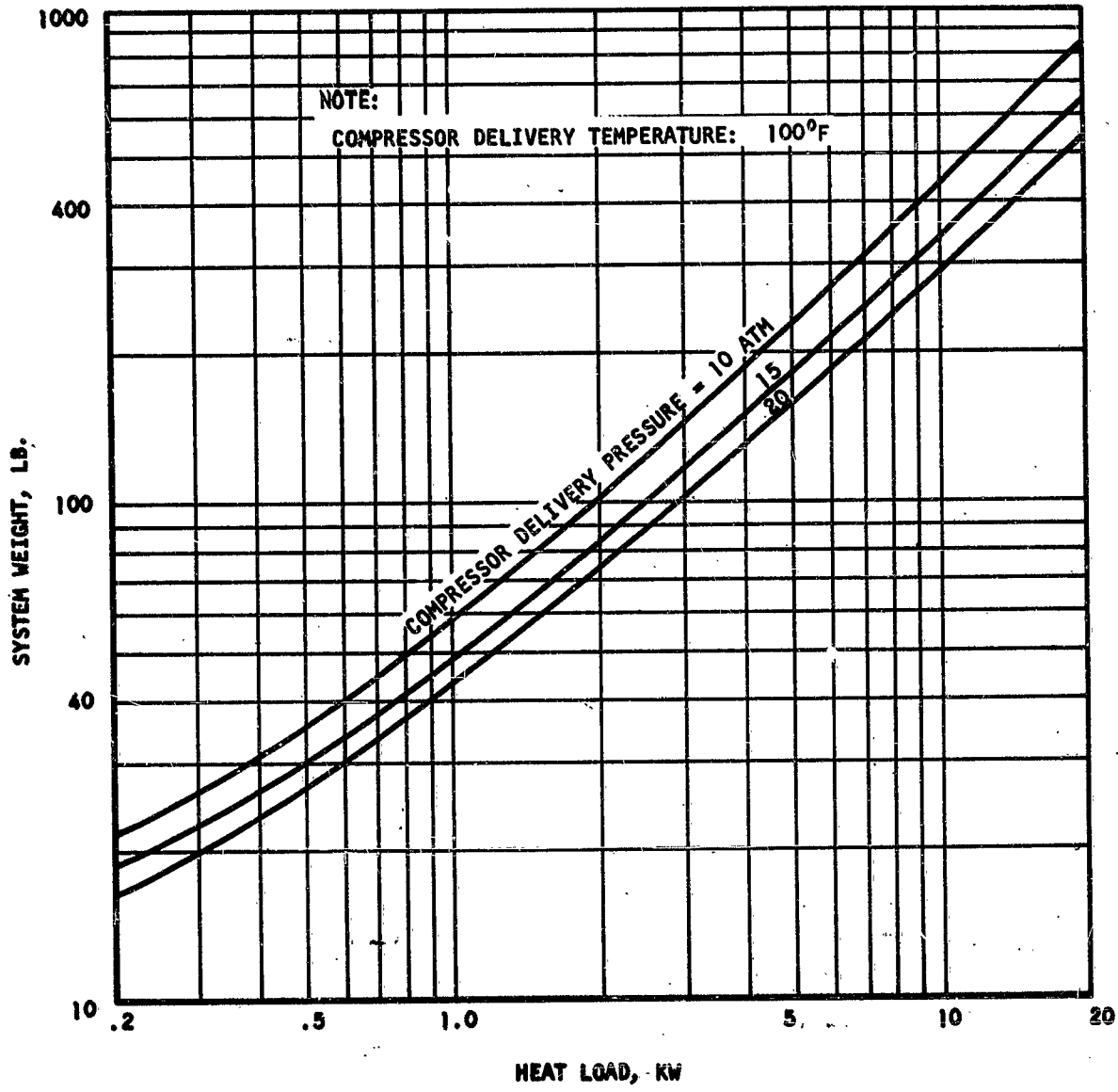

Figure 217. Nitrogen Bypass Expander System Weight

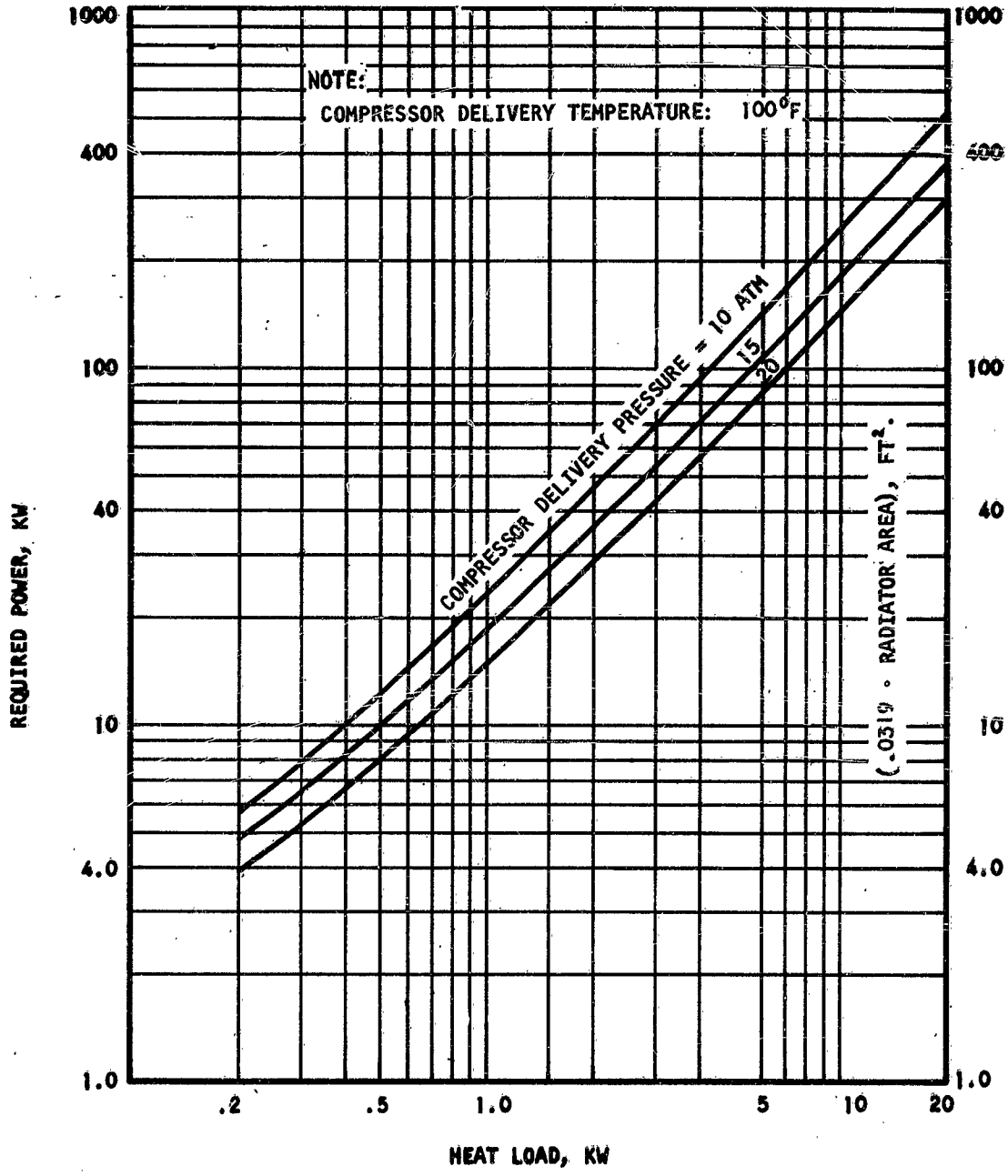

Figure 218. Nitrogen Bypass Expander System Characteristics

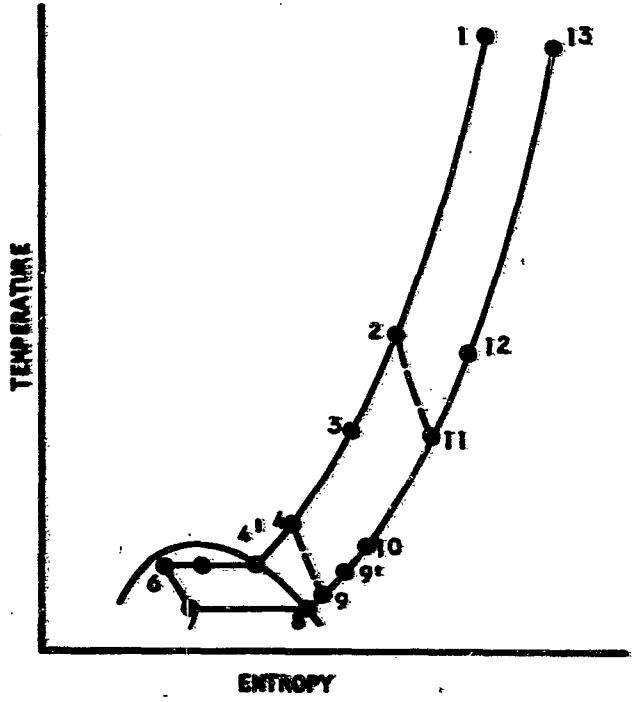

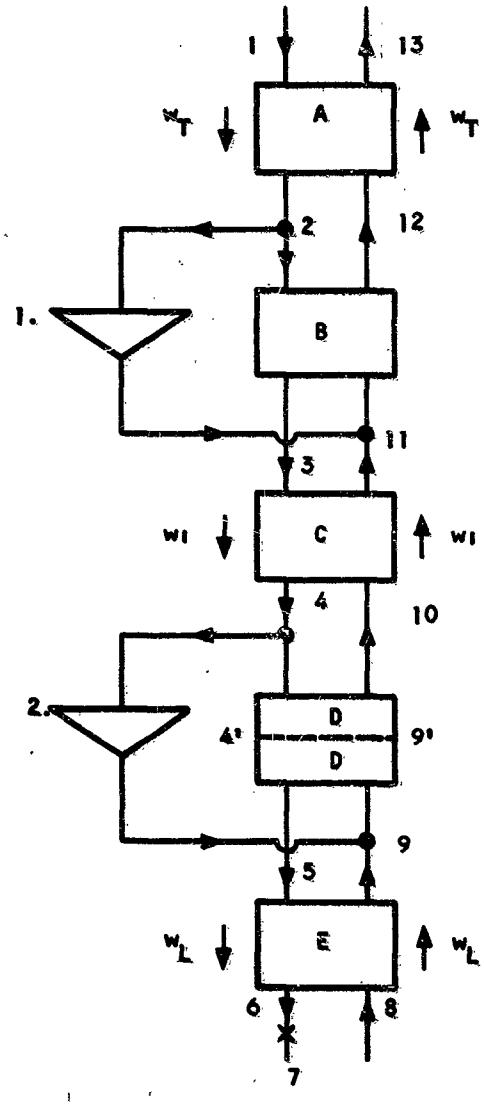

Figure 29. Double Bypass Expander Non-Ideal Cycle I

the cold expander outlet pressure and temperature (Point 9) were taken as 1.0 atm and 150°F; lines and heat exchangers pressure drops were also neglected in the thermodynamic calculations.

The cycle analysis is critically dependent on the effectiveness chosen for the design of the system heat exchangers. This was taken here as 0.90. In these conditions the ratio w_L/w_I (w_L and w_I are defined in Figure 63) is always lower than about 0.8, and the analysis showed that the flow through the upper (warm) expander is very small. This would make it very difficult to manufacture, also its efficiency would be much lower than that assumed (0.85) in the analysis.

In order to reduce the temperature at Point 2 Exchanger "C" of Figure 62 was eliminated since its value seemed very doubtful. The modified system is shown in Figure 63. An analysis of this system based on a maximum heat exchanger NTU on the cold side of 9.0 showed that the upper limit on the ratio w_L/w_I was reduced from 0.85 to 0.66.

The flow through Expander Number 1 is uniquely determined by the flow through Expander 2. The flow rates through the various parts of the system are shown in Figure 64 as a function of the ratio w_L/w_I. Also shown on Figure 64 for comparison purposes are the total flow requirement of the single expander system discussed previously.

The results shown lead to the conclusion that a 10 atm two-expander system does not offer any advantage over a single expander system at a compressor delivery pressure of 20 atm. A similar analysis was performed for the two-expander system at an inlet pressure of 15 atm, and the same conclusion was reached.

In view of these results and of the fact that the added expander would decrease the reliability of the system, it was concluded that a single expander system should be used for cooling at liquid nitrogen temperature.

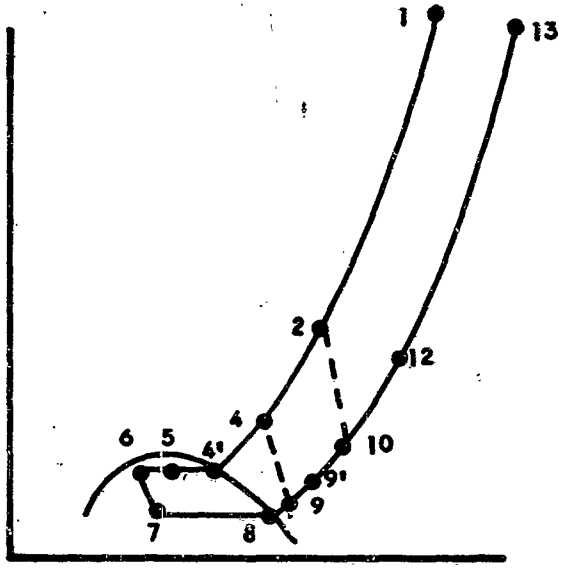

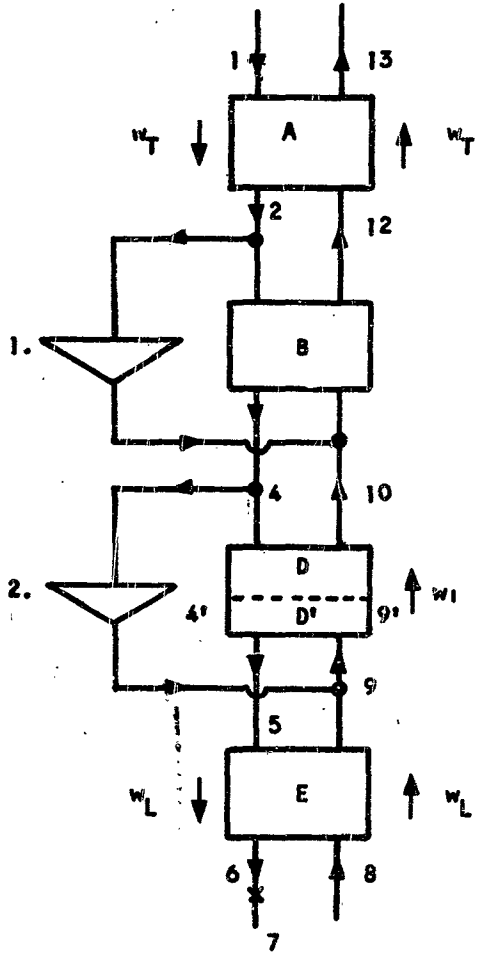

Figure 20. Double Bypass Expander Cycle II

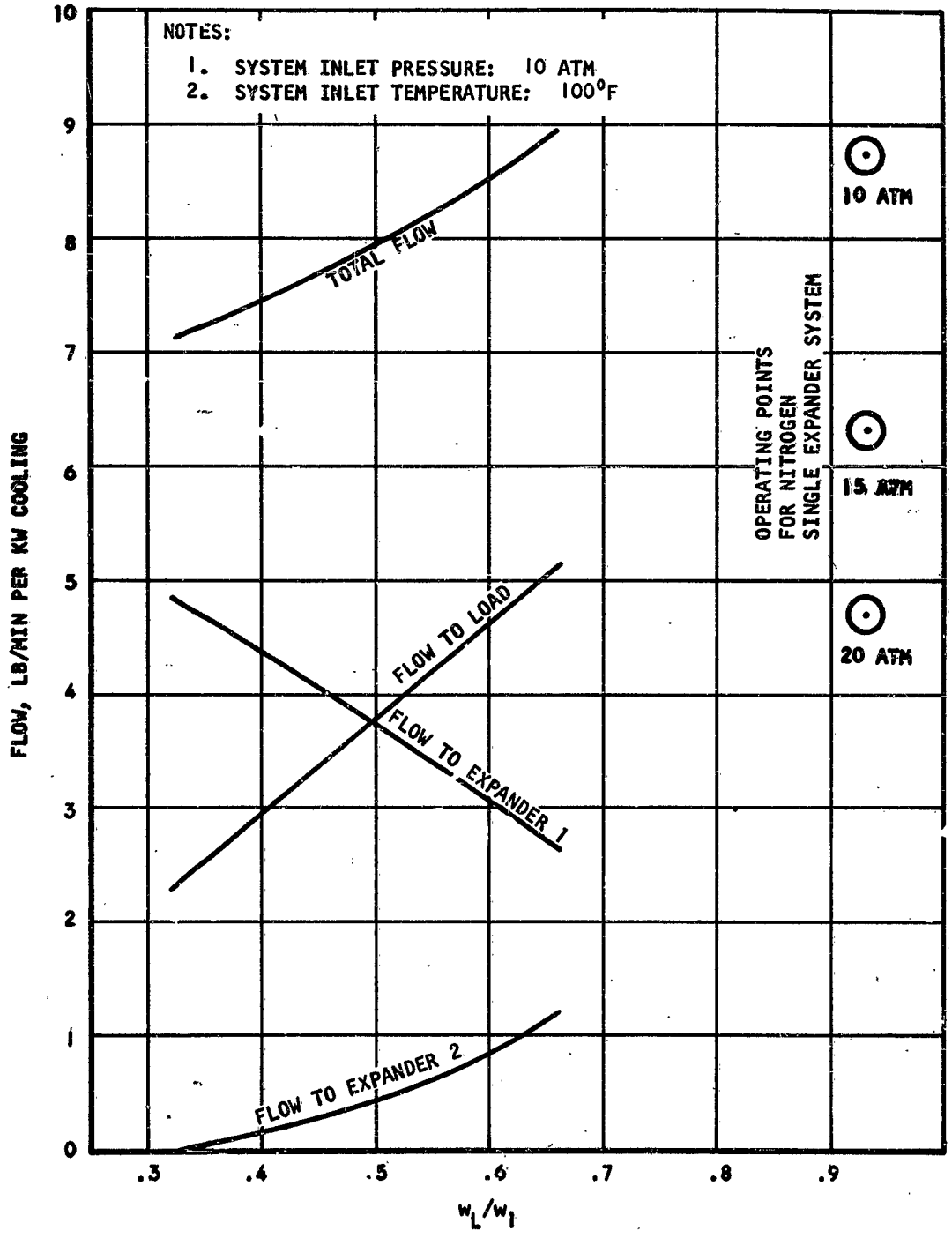

Figure 221. Nitrogen Double Expander System

NEON REFRIGERATION SYSTEMS

The system schematics for the neon systems considered are identical to those of the nitrogen systems already shown. Likewise, the system operation, as shown on temperature-entropy diagram, is the same as for the nitrogen cases.

Thermodynamic Considerations

The neon systems were analyzed subject to the same general conditions as the nitrogen systems, namely:

1. Maximum heat exchanger effectiveness is 0.9.
2. Expander adiabatic efficiencies are 0.85.
3. The pressure drops through the heat exchangers is negligible.
4. The compressor delivery temperature is 100°F.
5. The working fluid state point at outlet of the cold expander is just outside the vapor dome (see Figure 46). For neon, this was taken as 53.7°R at 1 atmosphere pressure.

As for the nitrogen bypass expander cycles, the neon cycles are not overly sensitive to variations in system inlet temperature; hence a relatively high system inlet temperature was used in order to obtain lower radiator area requirements.

Single Expander System

The system shown schematically in Figure 46 was analyzed with neon as the working fluid. The maximum effectiveness of the heat exchangers, together with the efficiency of the expander, determine a unique flow ratio, w_L/w_T, for each set of system inlet parameters. Since the system inlet temperature was held constant at 100°F, the only free variable at the inlet is the pressure.

As was done for the similar nitrogen case, referring to Figure 46, Point 7 is held fixed, and the expander efficiency determines Point 2. Since Point 1 is known from the system inlet parameters, the effectiveness

of the first heat exchanger and the energy balance, determine Points 8 and 9. Point 7' is determined by the effectiveness of the condensing portion of the second heat exchanger plus the fact that Point 3' is on the vapor dome. Therefore, since Points 2, 3', 7', and 8 are known, the flow ratio w_L/w_T is determined by the energy balance in the second heat exchanger. Similarly, Point 3 is determined by w_L/w_T and the energy balance. In any system of this configuration, as the system inlet pressure becomes lower, Point 8 will approach Point 7', and since

$$\frac{h_8 - h_7'}{h_2 - h_3'} = \frac{h_7' - h_7}{h_3' - h_3},$$

an inlet pressure can eventually be reached which will cause Point 3 to lie outside the vapor dome at a temperature lower than that at Point 7. This constitutes an unfeasible system operating condition, since there would be a temperature cross in the second heat exchanger. This effect makes the single expander neon system unfeasible at inlet pressures below approximately 20 atmospheres.

The results of the thermodynamic analysis for this system operating at 20 atmospheres inlet pressure are given in Table 4. The system weight and power requirement are shown plotted in Figures 65 and 66 versus the cooling load in kw. The system radiator area requirement, computed on the basis of a 170°F radiator inlet temperature and 50°F outlet temperature are also given in Figure 66.

Two-Expander System

Two expander systems were also considered for neon in order to determine whether a performance improvement high enough to warrant the increased complexity of the system could be achieved.

The system shown schematically in Figure 62 was analyzed and, as was found for the similar nitrogen system, it was found that the heat exchanger labeled C should be omitted. After making this modification, the system was analyzed for inlet pressures of 10, 15, and 20 atmospheres at an inlet temperature of 100°F.

TABLE 52

NEON SINGLE EXPANDER SYSTEM

$T_1 = 560.0$	$h_1 = 137.5$
$T_2 = 140.0$	$h_2 = 31.8$
$T_3' = 77.1$	$h_3' = 8.4$
$T_7 = 53.7$	$h_7 = 12.0$
$T_7' = 70.0$	$h_7' = 16.3$
$T_8 = 84.0$	$h_8 = 20.0$
$T_9 = 512.6$	$h_9 = 125.7$

w_e = 9.85 lb/min per kw cooling

w_L = 1.848 lb/min per kw cooling

w_T = 11.70 lb/min per kw cooling

Subscripts refer to system points and flows defined by Figure 46.

Pressure in Hot Leg: 20 atm

Pressure in Cold Leg: 1 atm

Temperatures in Degrees R

Enthalpies in Btu/lb

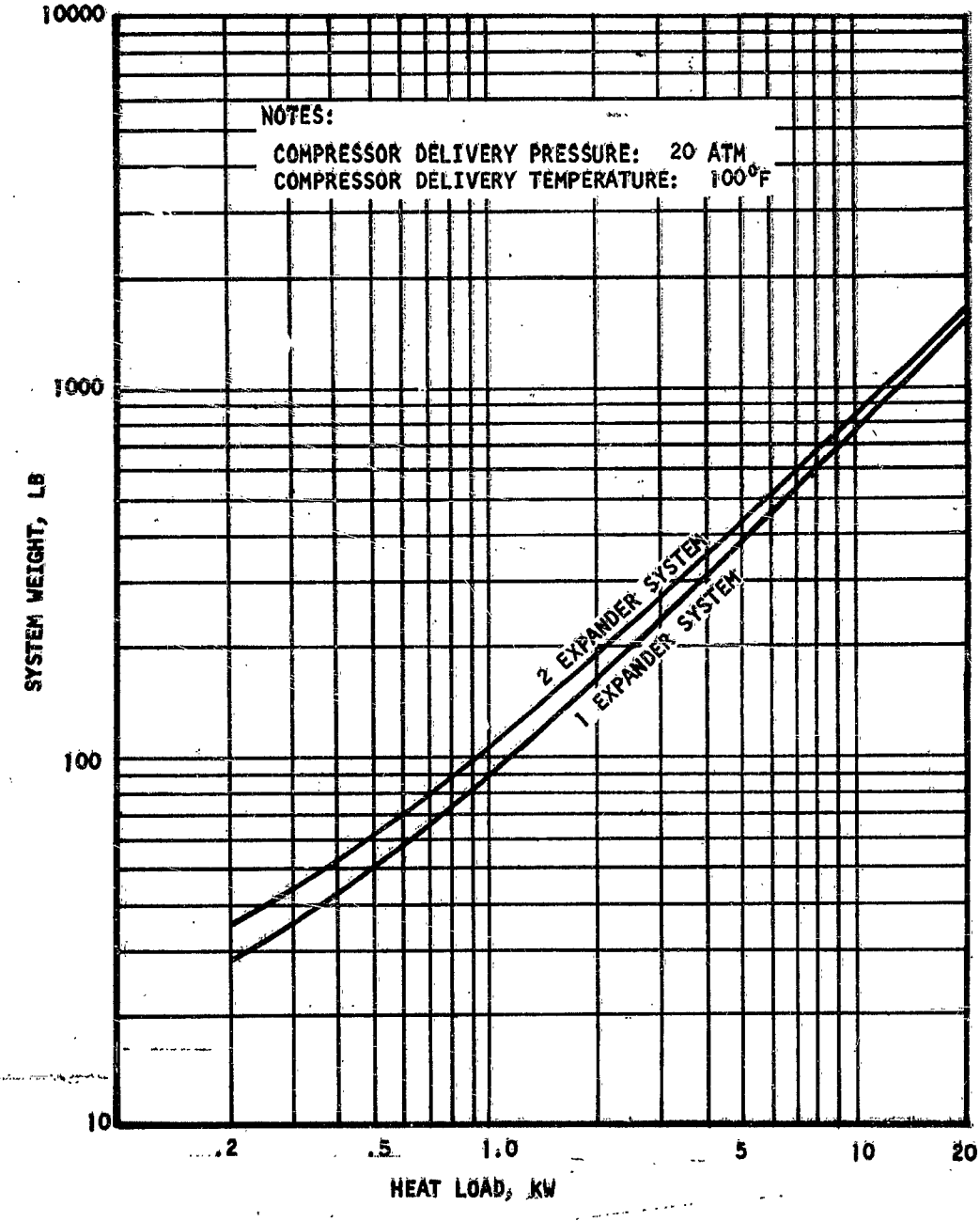

Figure 222. Neon Bypass Expander Systems Weight

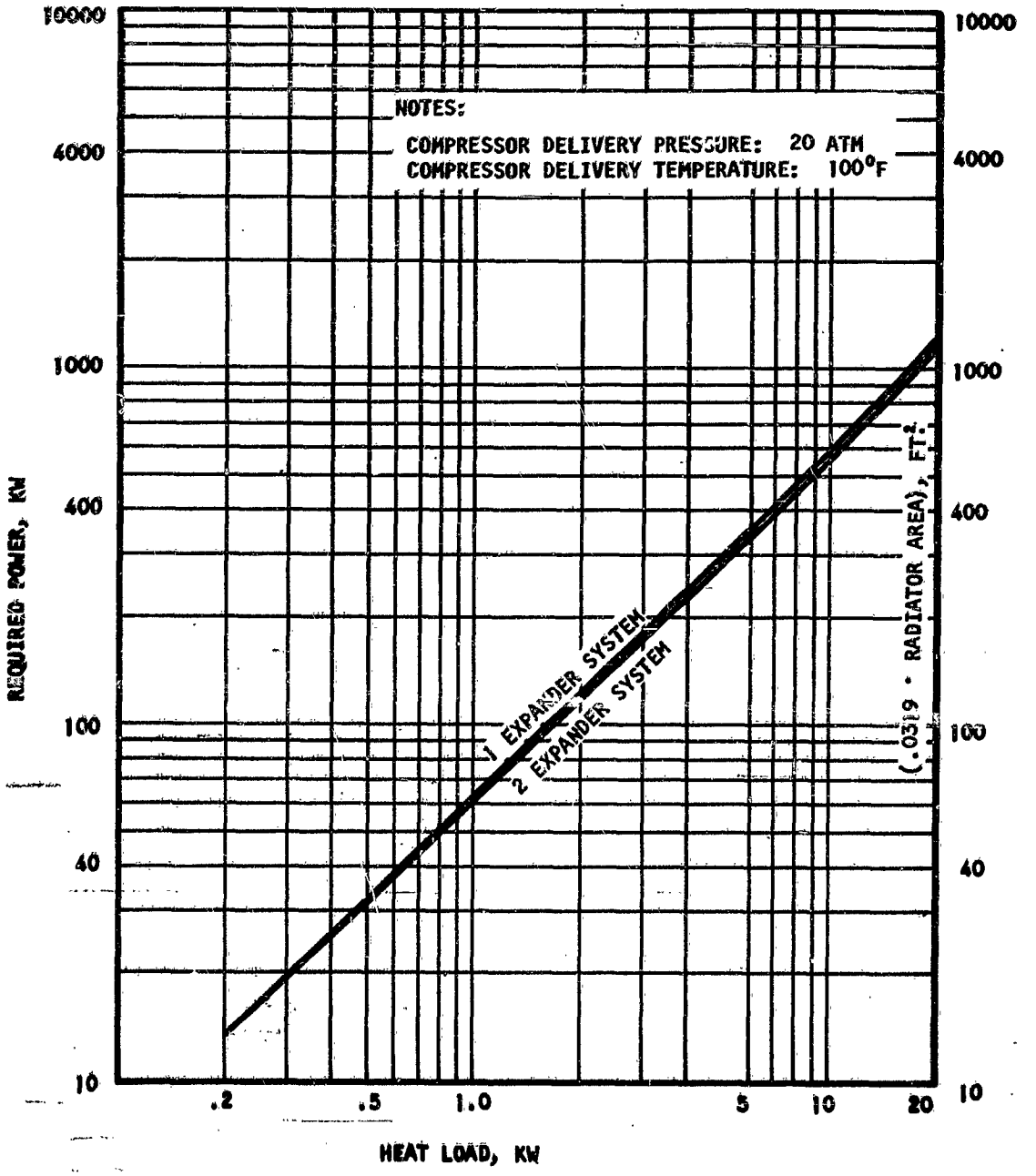

Figure 223. Neon Bypass Expander Systems Characteristics

It was found that the maximum value of the hot side effectiveness of heat exchanger B (refer to Figure 63) determines the maximum value of the flow ratio w_L/w_1. The results of the analyses are presented in Figures 67 through 70. In all cases, the termination of the curve at its maximum value of w_L/w_1 marks the condition where

$$\frac{T_2 - T_4}{T_2 - T_{16}} = 0.9$$

As can be seen in Figure 67, operation at a system inlet pressure of 20 atmospheres offers a wide range of the flow ratio, w_L/w_1, at which to operate with only small changes in total flow rate. Referring to Figure 69, it can be seen that operation at the upper limit of the ratio, w_L/w_1, is to be preferred from the standpoint of achieving maximum expander flow through Expander No. 1 and, therefore, maximum efficiency. The considerable advantage of the 20 atmosphere system over the 10 and 15 atmosphere systems in regard to total flow rates indicates that the 20-atmosphere system should be selected for further examination. The 20-atmosphere system weight, power requirement, and radiator area requirement are plotted in Figures 65 and 66 as functions of the system cooling load.

By examination of the plots of Figures 65 and 66 it can be concluded that the double expander system offers no definite advantages over the single expander system. The latter one is lighter by 10 to 20 per cent depending on the cooling load. The power necessary for operation of the single expander system is however higher by approximately 7 per cent. The selection between these two competing system can only be made as the result of a careful design analysis of the two systems in the light of the installation parameters for a given application.

Here again it should be emphasized that the radiator areas ploted in Figure 66 are critically dependent on the vehicle radiator design which in turn depends on the mission parameters. For large cooling load systems a separate radiator for the refrigeration system would appear preferable.

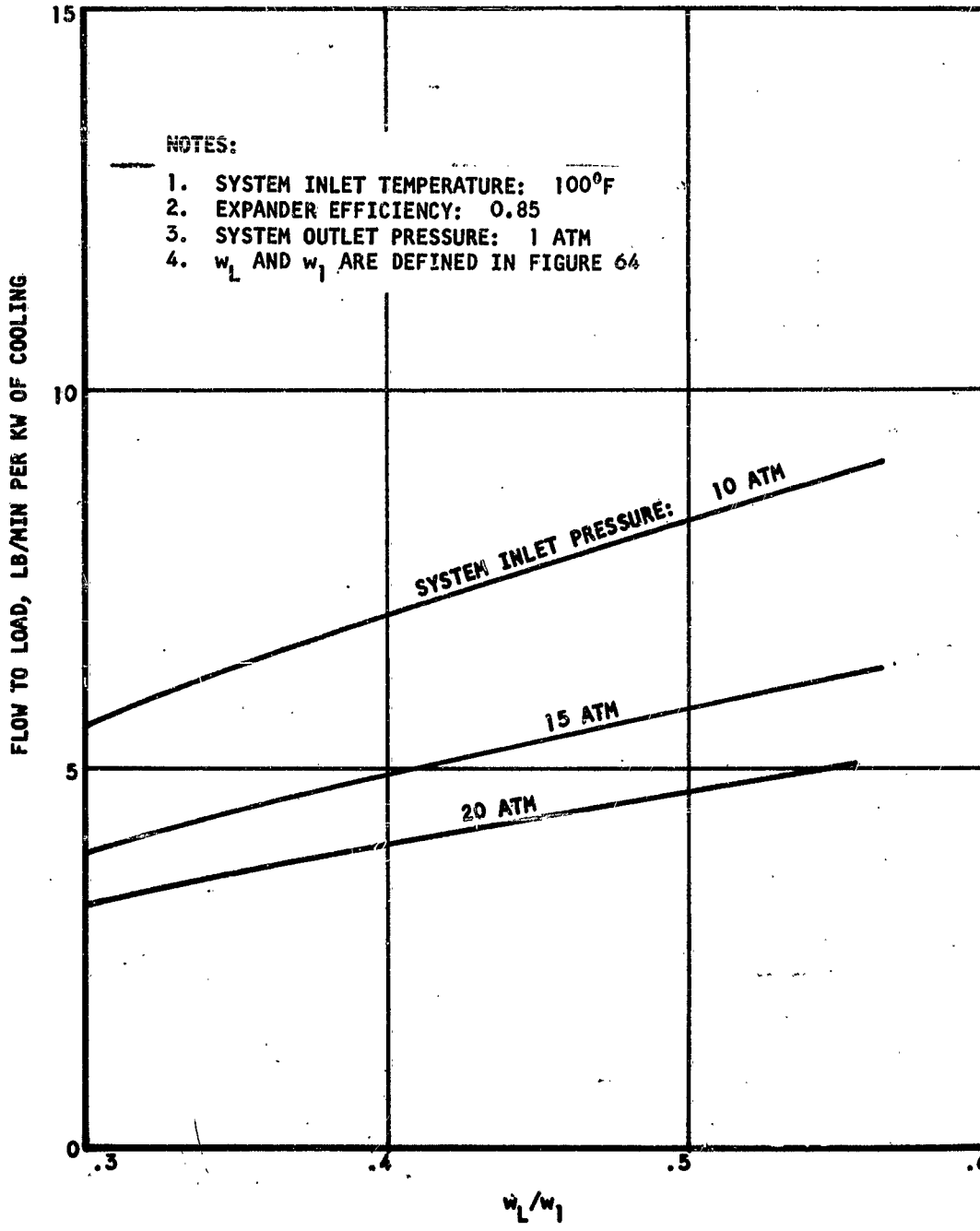

Figure 224. Neon Double Bypass Expander System - Flow to Cooling Load

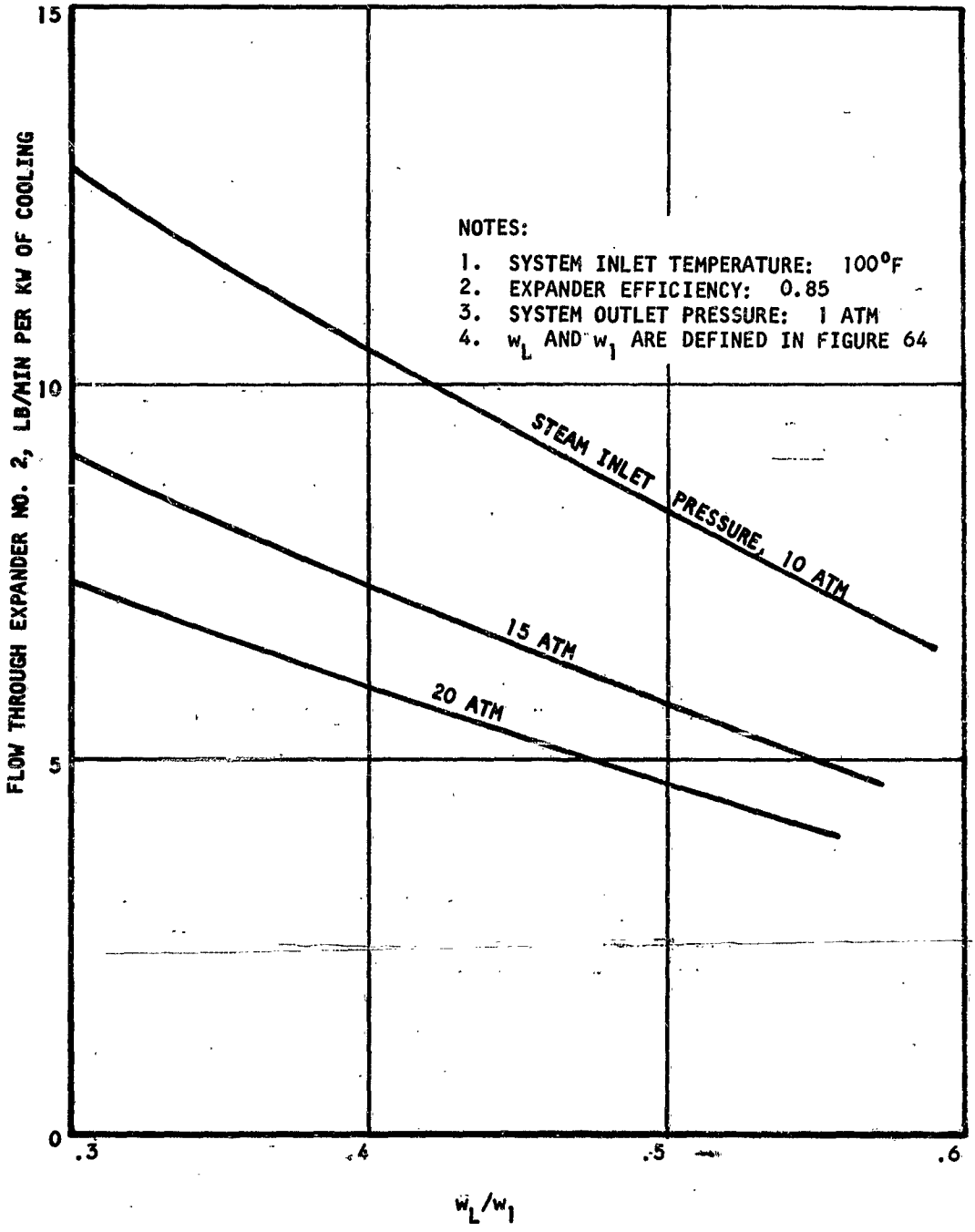

Figure 225. Neon Double Bypass Expander System - Flow through Expander No. 2

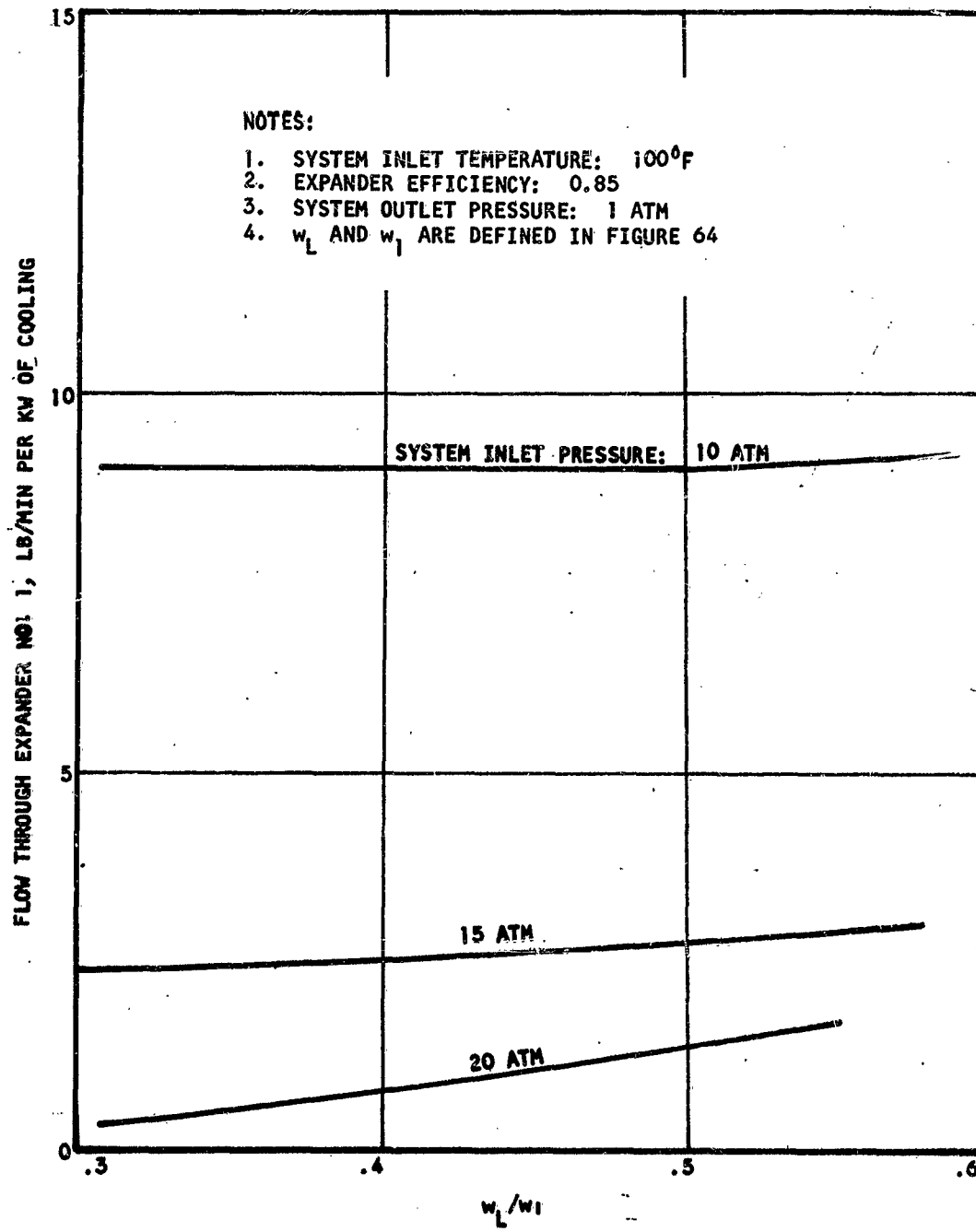

Figure 226. Neon Double Bypass Expander System Flow Through Expander No. 1

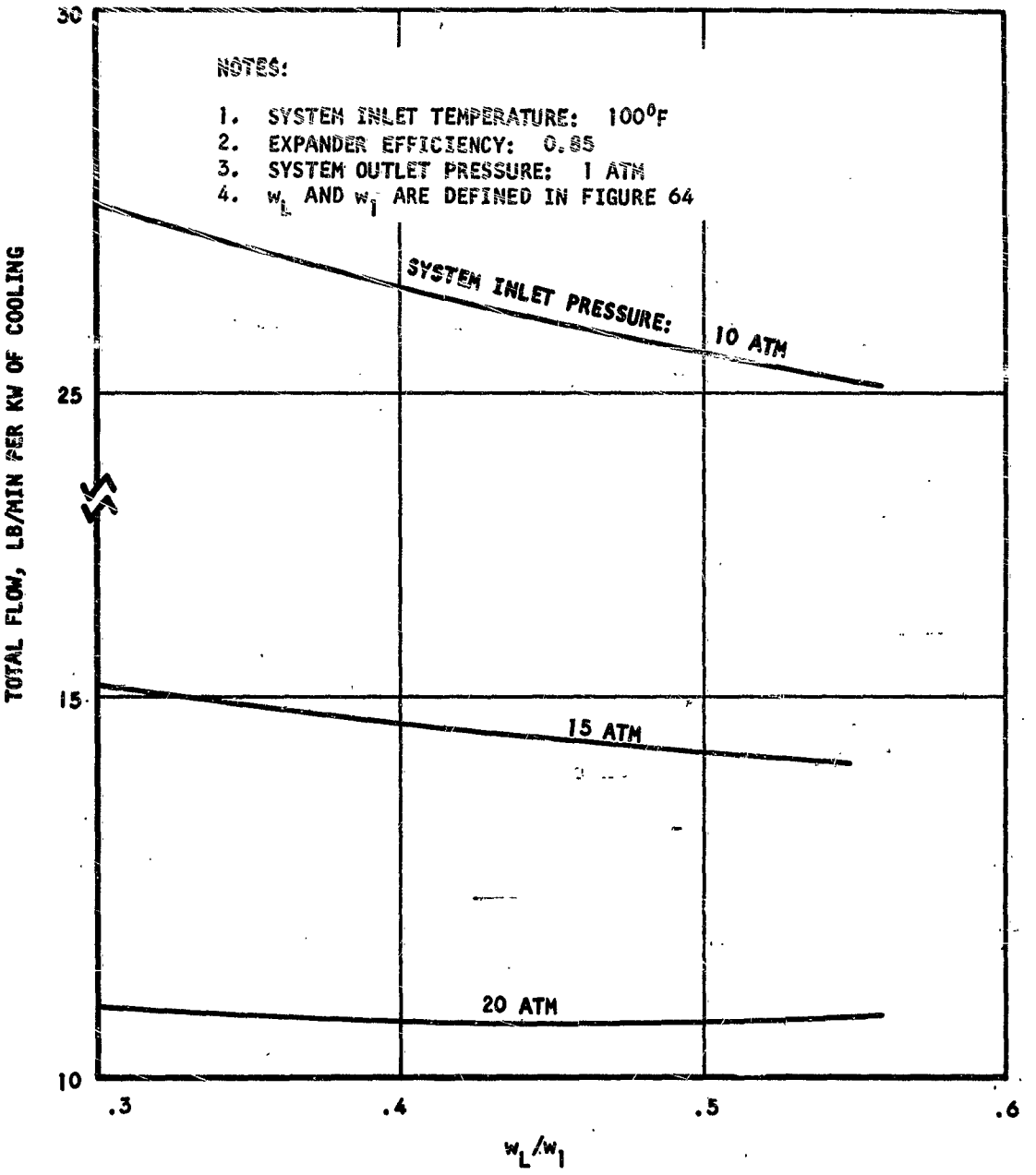

Figure 227. Neon Double Bypass Expander System - Total Flow

HELIUM REFRIGERATION SYSTEMS

Thermodynamic Considerations

As was mentioned in Section VI, a single expander system of the configuration examined for nitrogen and neon becomes unfeasible with helium as a working fluid. Referring to Figure 46, if condensation is attempted in heat exchanger B, the thermodynamic properties of helium confine the system to very low inlet pressures. Also, the extremely large temperature gradient required across heat exchanger A is unfeasible due to the size of the exchanger and heat leaks from the environment.

If condensation is not required in the heat exchangers, low "end-points" effectiveness exchangers are required in order to avoid temperature cross-overs in them. In view of these considerations, multiple expander systems are required for efficient refrigeration at liquid helium temperatures.

In the following analyses, the outlet point of the last expander was chosen to be just outside the vapor dome, as in the nitrogen and neon systems. For helium, this corresponds to a temperature of 4.5°K at a pressure of 1.0 atmosphere.

Two-Expander Systems

The system shown schematically in Figure 71 was analyzed for helium subject to the following conditions:

1. Maximum heat exchanger effectiveness is 0.9.
2. Expander adiabatic efficiencies are 0.85.
3. There are no pressure drops through the heat exchangers.
4. The system inlet temperature is 311°K.

Under these conditions it was found that operation of the system was impossible. It was found that expander number 1 must operate at higher temperatures in order to make this cycle feasible, therefore, a heat exchanger should be introduced between the two expanders.

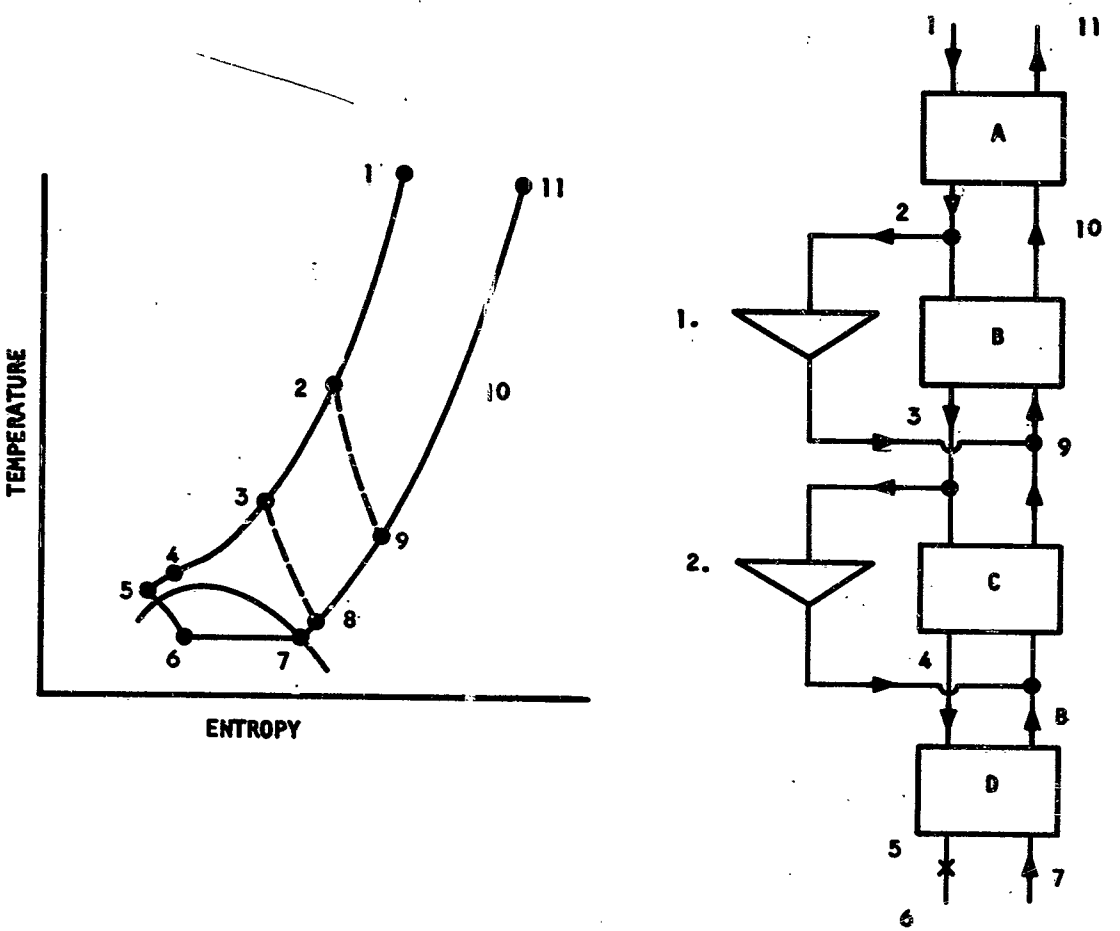

Figure 228. Helium Double Expander System I

The two-expander system thus modified is shown schematically in Figure 72 where the working fluid state points are also shown on a temperature entropy diagram. Subject to the conditions listed above, a thermodynamic analysis of the system was performed. It was found that condition 1 above imposes severe restrictions on the design of the system. The effectiveness on the hot side of the heat exchangers was therefore allowed to increase above the 0.9 limit in cases where the flow ratio in the heat exchangers is different from unity. The maximum NTU was then fixed however at 9.0 which corresponds to a heat exchanger having a flow ratio of unity and effectivenesses of 0.9 on both sides.

The working fluid temperatures throughout the system are shown in Figure 73. The plot shows that T_{i1} and T_{i2} approach each other and become equal at a flow ratio, w_L/w_i of approximately 0.53, therefore the system cannot be operated at higher values of w_L/w_i.

The system was also analyzed for a pressure ratio of 20 to 1. The total flow rates for the two values of the system inlet pressure are shown on Figure 74.

The analysis was also performed for a compressor delivery pressure of 10 atmospheres. In this case the total flow rates lie entirely outside the range of Figure 74 and are too large to merit further consideration.

As can be seen from Figure 74, both systems exhibit minima for the total flow rates. Furthermore, the minimum total flow rate at 15:1 pressure ratio is lower than that at 20:1. The minimum total flow rate for the 15 atmosphere system is 43.5 lb/min per kw cooling and occurs at a flow ratio w_L/w_i value of .33. At this point, the flow through expander number 1 is 14.3 lb/min per kw cooling and the flow through expander number 2 is 19.9 lb/min per kw of cooling.

Three Expander System

The system shown schematically in Figure 75 was analyzed subject to the same general conditions as the two expander system discussed above.

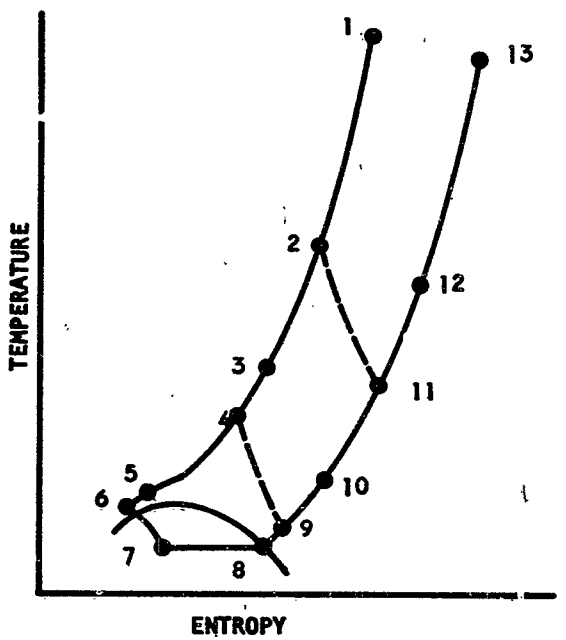

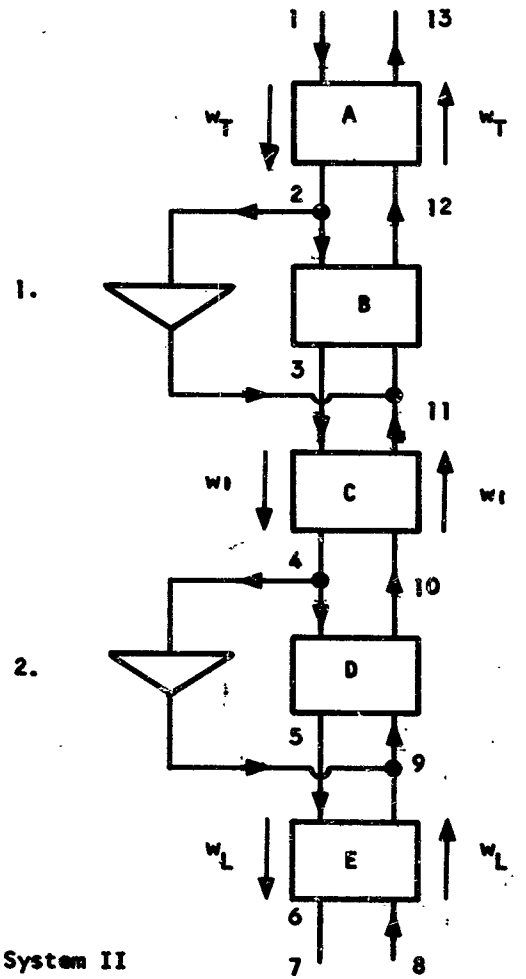

Figure 229. Helium Double Expander, System II

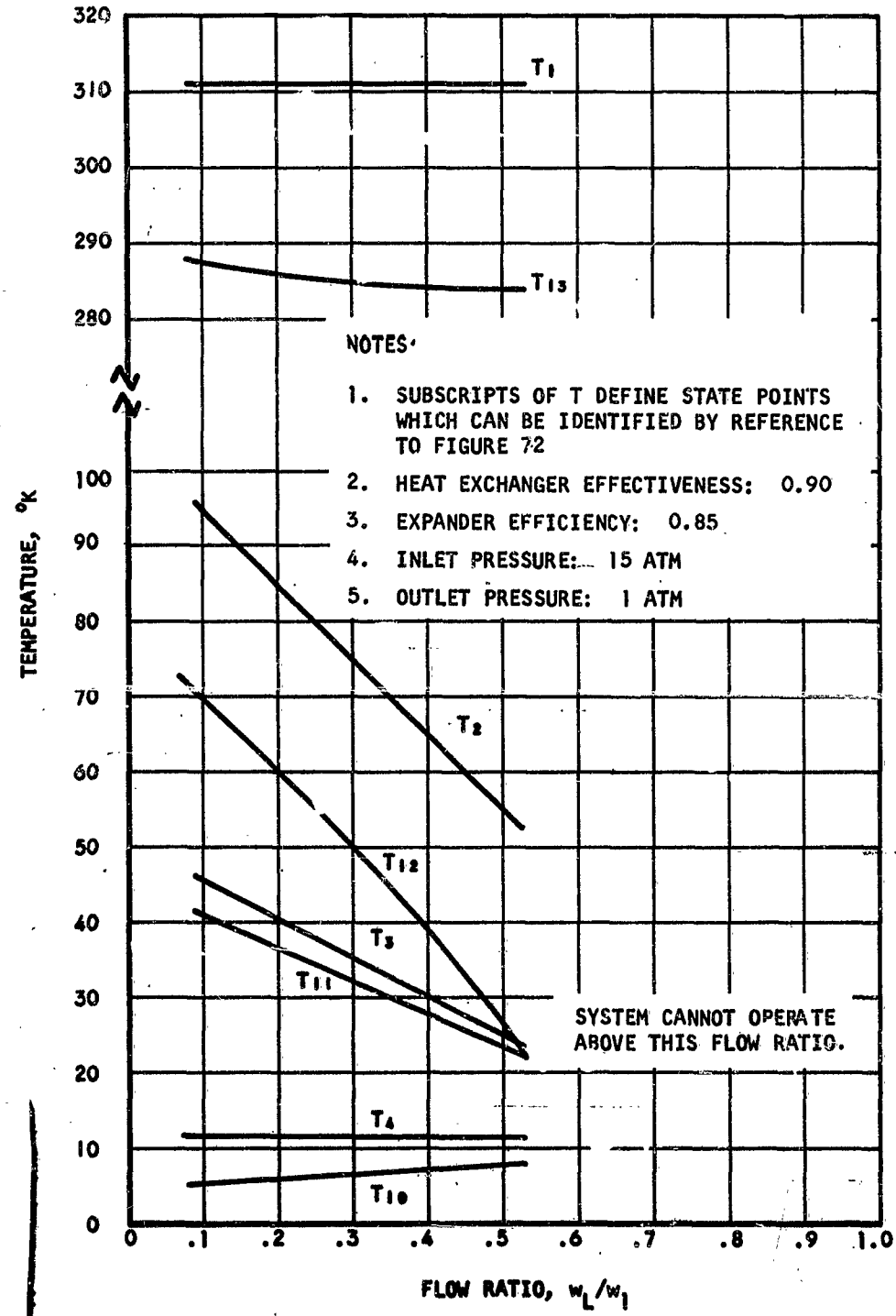

Figure 290. Fluid Temperatures Throughout Helium Two-Expander System

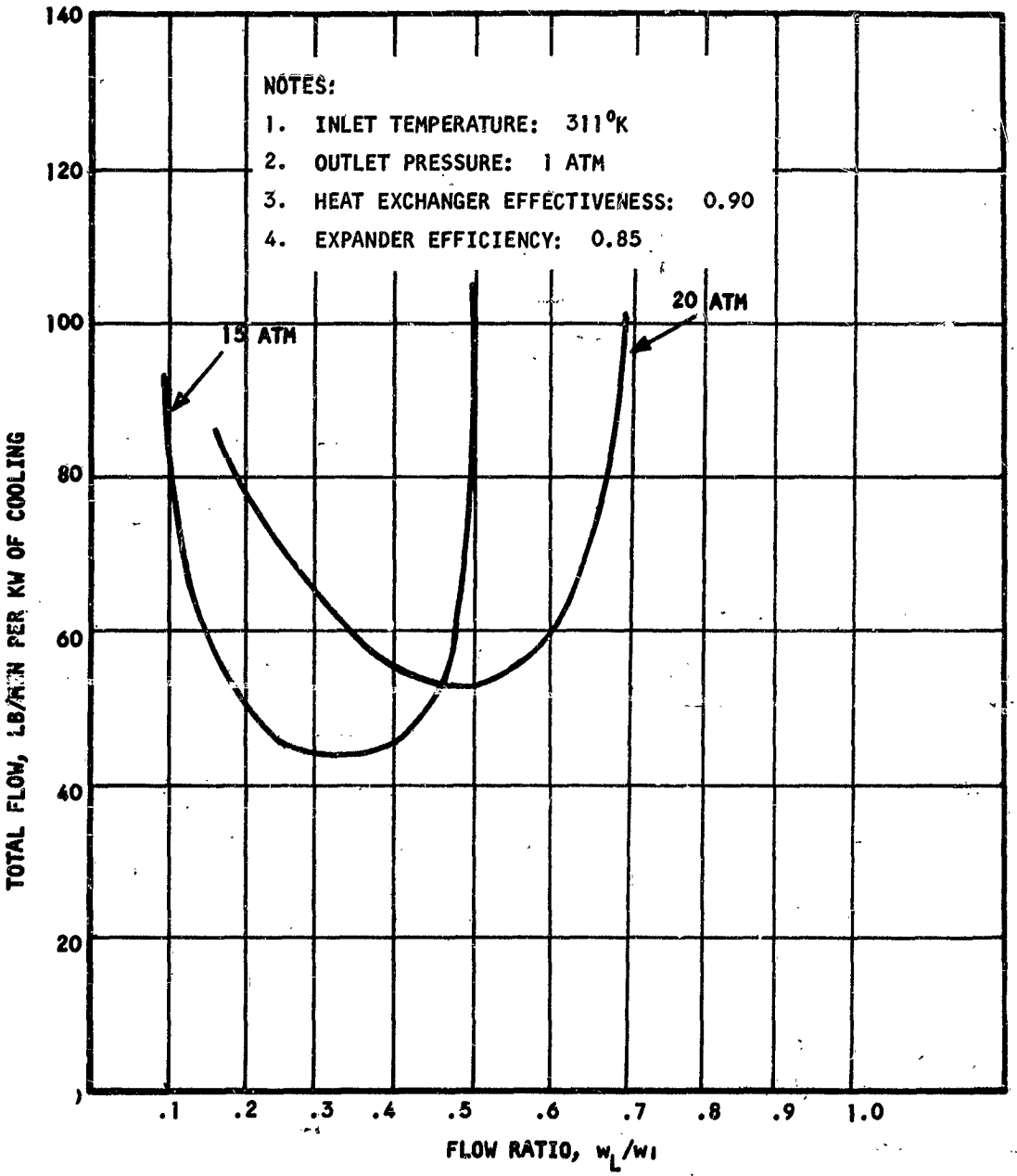

Figure 231. Flow Characteristic of Helium Two-Expander System

The analysis of this cycle becomes rather unwieldy due to the number of independent parameters involved. Referring to Figure 75, the flow ratio w_T/w_1 is uniquely determined for each value of the ratio w_1/w_2. However, w_1/w_2 is independent of w_L/w_2. In the analyses performed, several values of w_L/w_2 were chosen and the range of w_1/w_2 was examined for each one. The values chosen for w_L/w_2 were 0.4, 0.6, and 0.7. It was found that for $w_2/w_L = 0.4$ the values of T_2 ranged around 300°K and consequently the flows through expander number 1 were too low to utilize it efficiently.

The total flow through the system as a function of the ratio w_2/w_1 is shown in Figure 76 for w_L/w_2 of 0.6 and 0.7. The plot shows a minimum total flow of 19.6 lb/min per kw of cooling for $w_L/w_2 = 0.7$ and $w_2/w_1 = 0.8$. The variation of the temperatures throughout the system operating at $w_L/w_2 = 0.7$ are shown in Figure 77.

Operating points of systems of this complexity are better optimized by computer programs. However, examination of the cycle shows that as w_L/w_2 increases T_4 must decrease, thus necessitating increasing flows through expander number 1. At the chosen point, $w_2/w_1 = 0.8$ and $w_L/w_2 = 0.7$, the flows through the expanders are:

Expander no. 1 3.03 lb/min per kw cooling
Expander no. 2 3.30 lb/min per kw cooling
Expander no. 3 4.00 lb/min per kw cooling

It is thus seen that the work done in cooling the helium is being distributed more or less uniformly throughout the system. Hence, it is felt that this operating point is near optimum for the given conditions.

The flow requirement of the three-expander system is about half that of its two-expander counterpart, this in itself is sufficient to justify the use of a third expander. The weight, power, and radiator area requirements of the three-expander system are plotted against the system refrigeration load in Figures 78 and 79, for a pressure ratio of 15:1.

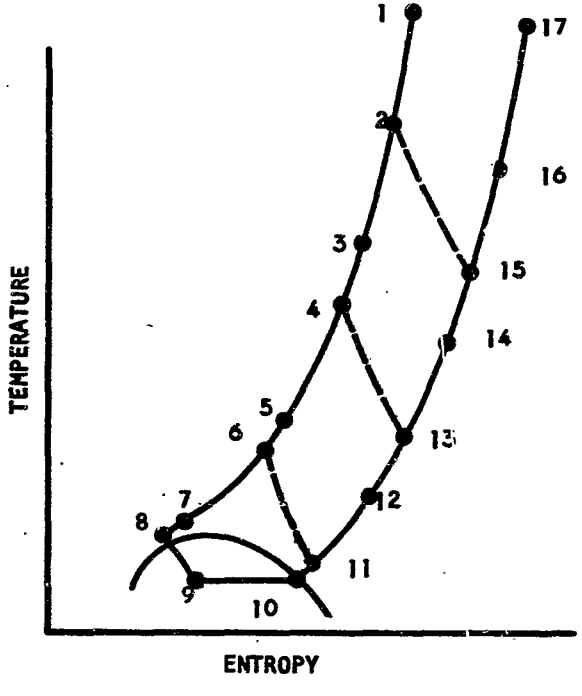

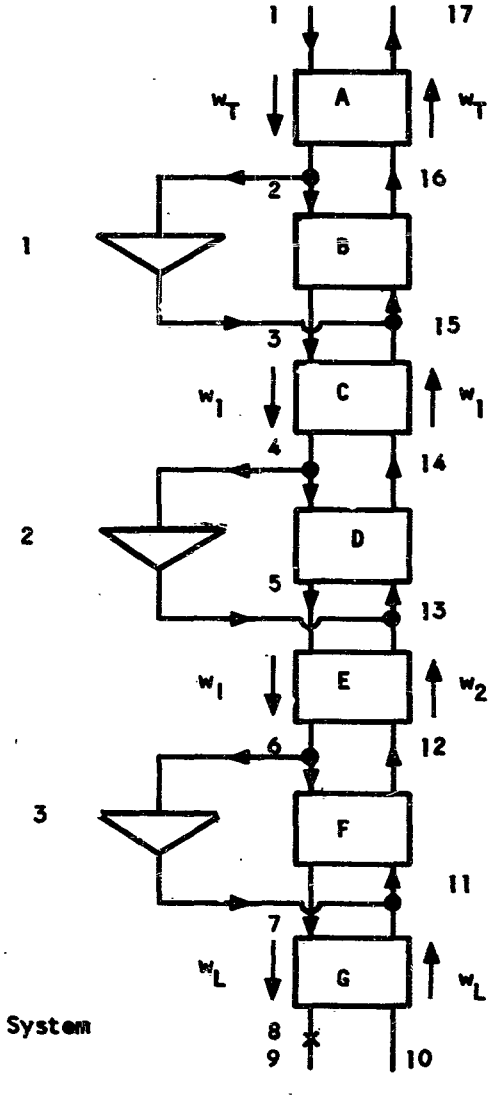

Figure 232. Helium Triple Expander System

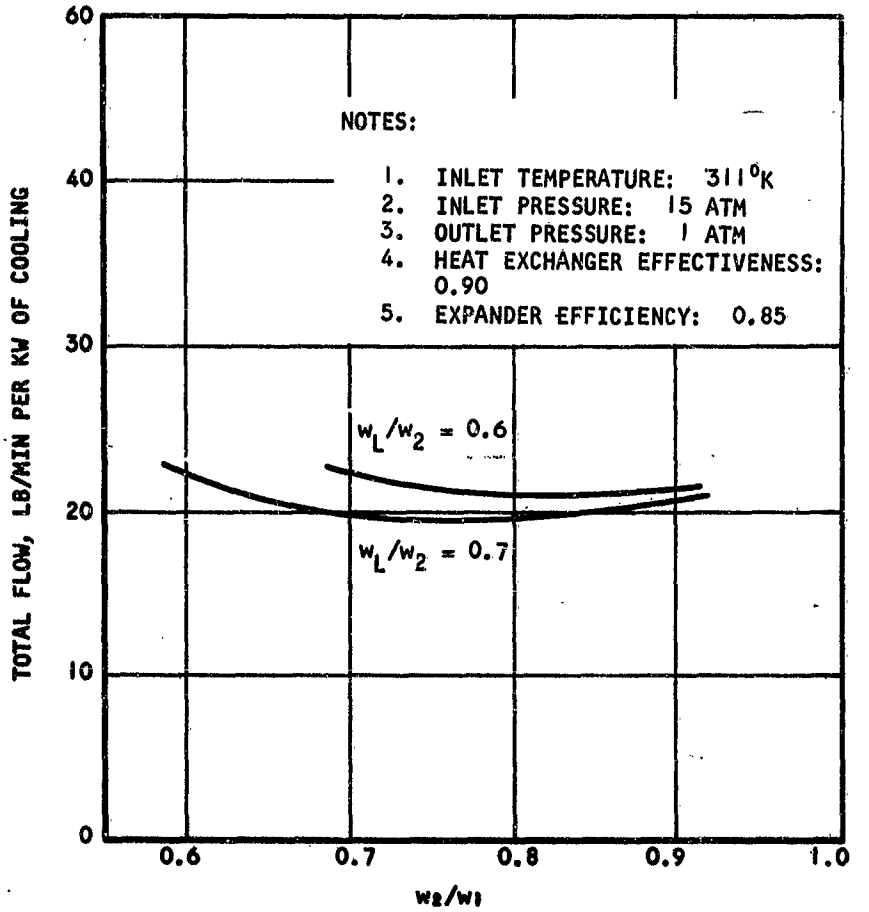

Figure 293. Flow Characteristics of Helium Three-Expander System

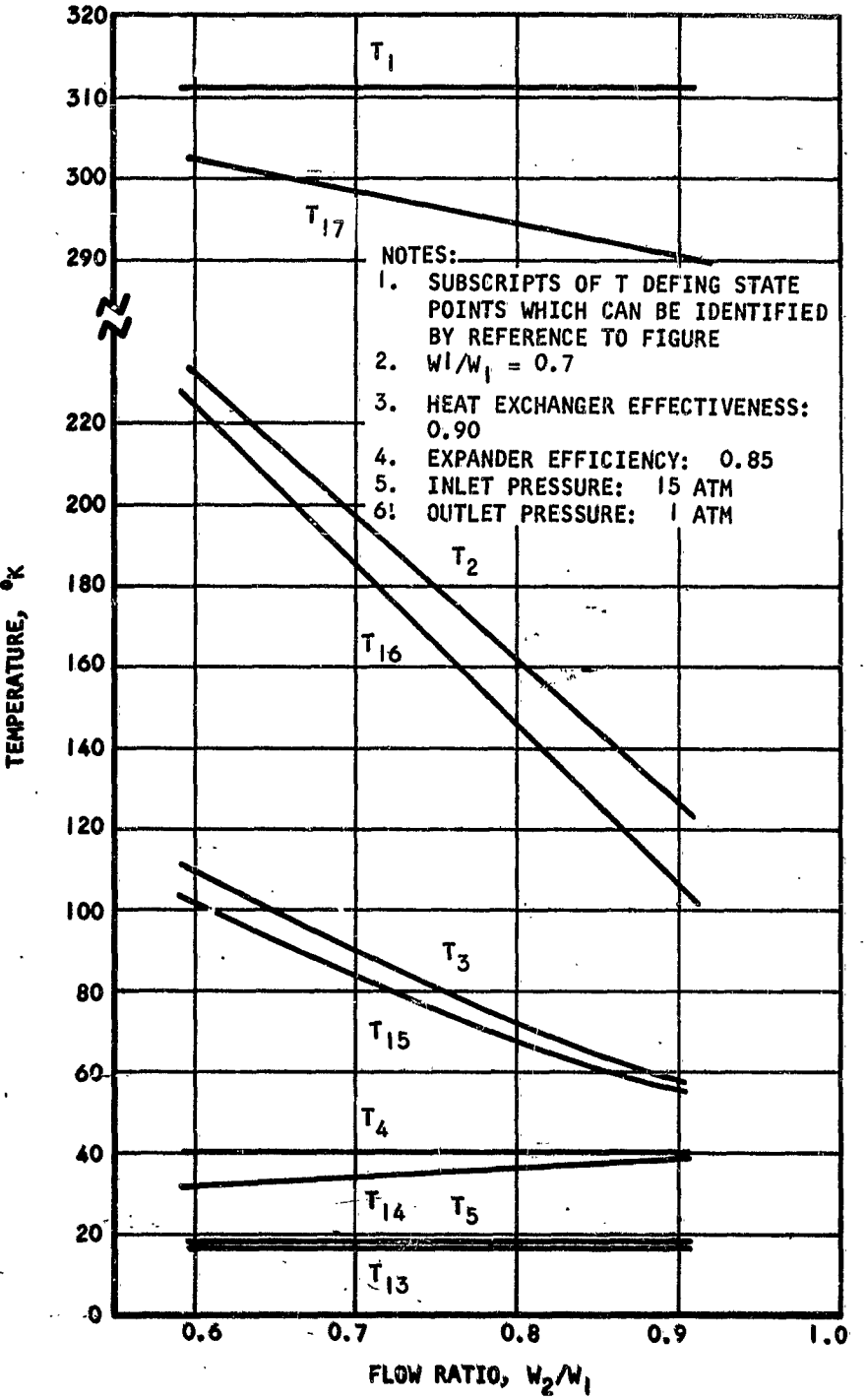

Figure 234. Fluid Temperature Throughout Helium Three-Expander System

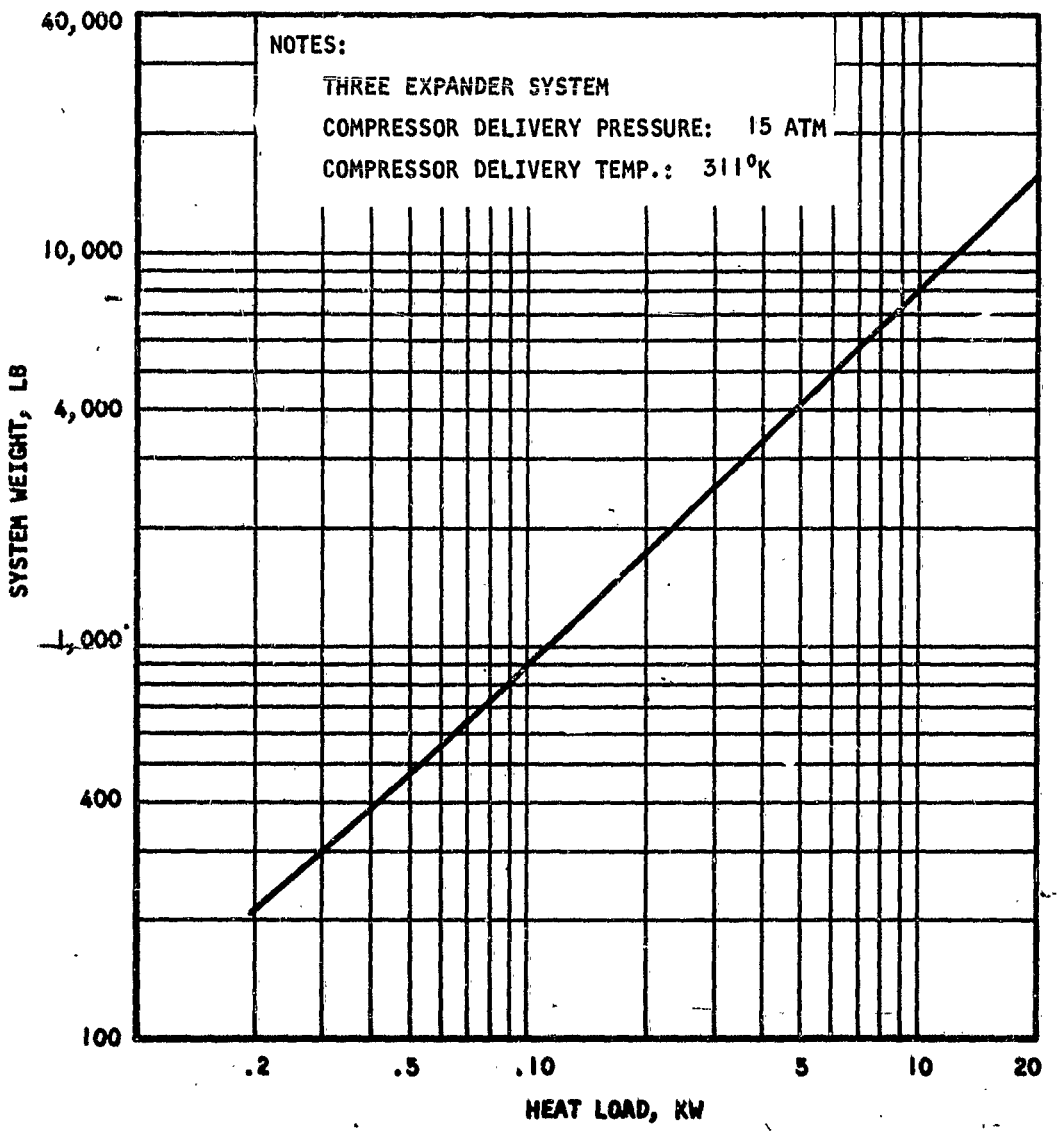

Figure 355. Helium Bypass Expander System Weight

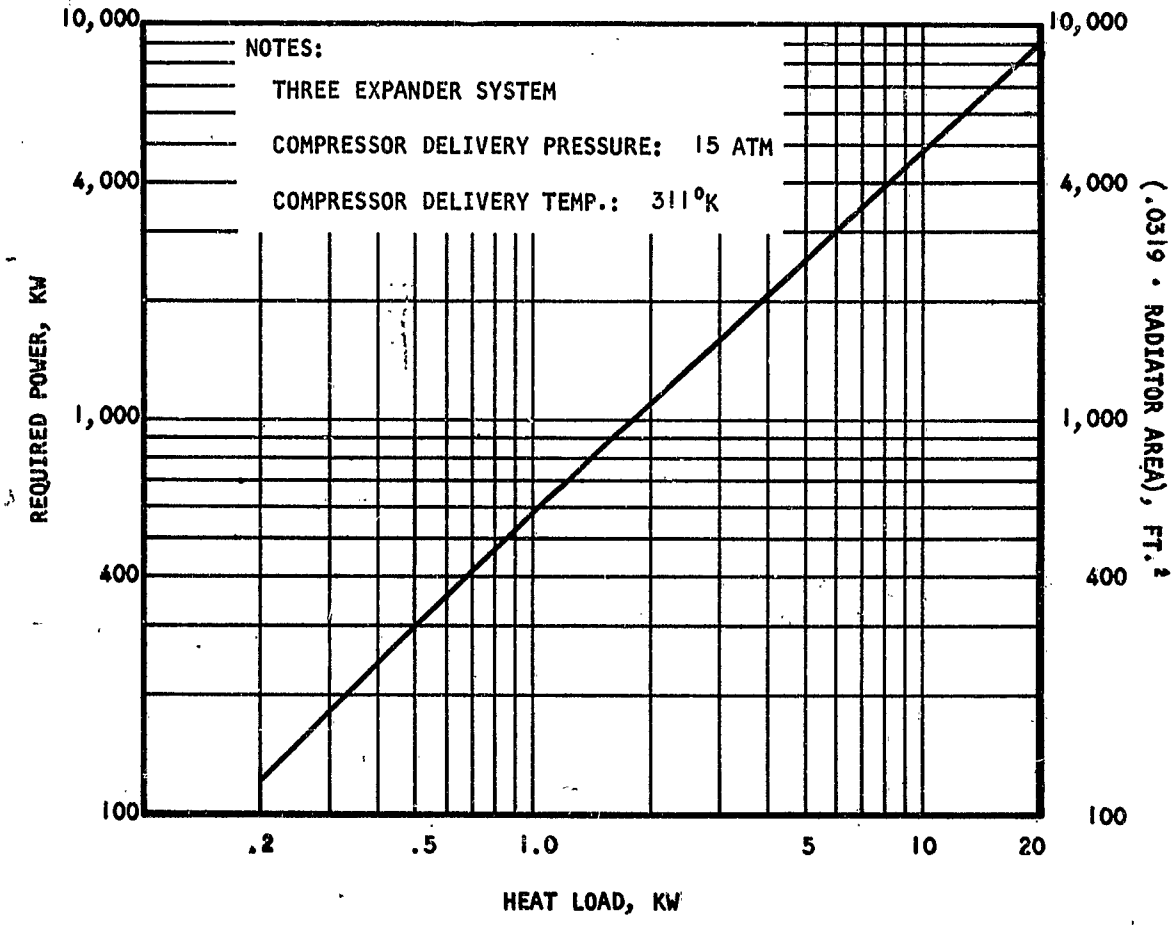

Figure 296. Helium Bypass Expander System Characteristics

SECTION VIII

DISCUSSION AND CONCLUSIONS

The analyses presented in this report are based on numerous assumptions which appear reasonable in a general study of this type. However for any particular space vehicle mission, some of these assumptions can become unrealistic and lead to the selection of systems which are far from optimum. The basic data assumptions and operating conditions used throughout the system analyses are briefly discussed below. Most of these have already been treated in the body of the report.

1. The fluid properties used in the cycle analyses and presented in Section II are only marginally accurate for precise thermodynamic calculations.

2. In this study the waste heat from the refrigeration system is assumed rejected to the vehicle thermal management system. In turn the vehicle heat transport fluid rejects this heat to space through a radiator. An effective radiator sink temperature of 400°R corresponding to an earth orbiting vehicle at relatively low altitude was assumed. These assumptions yield very large radiator areas; it might be preferable, especially for large loads to use a separate radiator operating at a much higher temperature than the 170°F to 50°F assumed.

3. The compressor performance and weight data of Section IV is believed realistic. Motor weight contribute as much as one half to the total system weight. In some installation this weight could be considerably reduced by using a power turbine to drive the refrigeration system compressor, this turbine could be powered by any readily available working fluid.

4. Assumptions regarding the heat exchanger performance had to be made to limit the scope of the study: A maximum heat exchanger NTU of 9.0 was assumed for this purpose because heat exchanger weight increases very rapidly for higher NTU's.

For particular installations a careful trade-off study should be conducted between heat exchanger weights and system power requirements. Also heat exchanger surfaces should be optimized.

5. A thorough investigation of cryogenic refrigeration cycles can only be accomplished by the use digital computers. Such a program would require subroutines for the calculations of fluid properties, as well as subroutines for the estimation of component performance and system integration. This is well outside the scope of this report. General conclusions can be drawn however from the study conducted.

6. The Stirling cycle appears to offer possibilities for cooling loads on the order of 1 kw at the temperature level of liquid nitrogen. Its main disadvantages for long mission duration are its relatively low reliability, as compared with turbo-machine systems, and its inherent leakage which might pose serious problems. For large loads and temperature levels lower than liquid nitrogen, bypass expander cycles of the type described in this report appear more attractive.

7. Refrigeration at liquid nitrogen temperature appears best accomplished by the single bypass expander system. Performance data and weight estimates for this system are given in Sections VI and VII.

8. The choice between a single expander and a two-expander refrigeration system for cooling at liquid neon temperature depends primarily on the vehicle and mission parameters particular to a given application. These systems are treated in Sections VI and VII.

9. For cooling at liquid helium temperature a three-expander system appears to be much better than a two-expander system. Investigation of helium systems utilizing four or more expanders seems to be indicated. Such an investigation would require the use of a computer.

Performance data and weight estimates for the helium three expander system are given in Section VII.

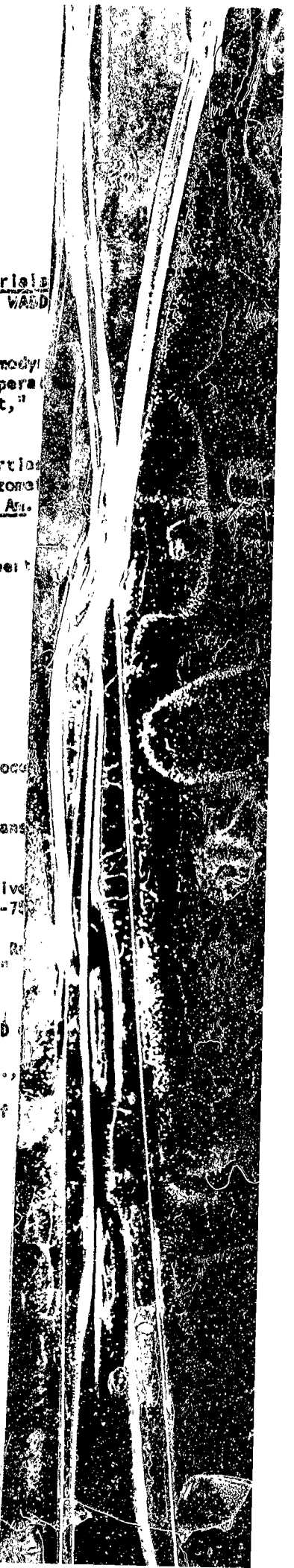

References

1. Johnson, V. J., A Compendium of the Properties of Materials ... Temperatures (Phase 1): Part I - Properties of Fluids, WADD ... Part I, October 1960.

2. Michels, A., Lunbeck, R. J., and Wolkers, G. J., "Thermodyn... Properties of Nitrogen as Functions of Density and Tempera... Between -125° and +150°C and Densities up to 760 Amagat," Physica XVII No. 9, September 1951.

3. Benedict, Hansen, "Pressure, Volume, Temperature Properties ... High Density I. Results obtained with a Weight Piezome... Results obtained by a Piston Displacement Method." J. Am. ... 59, 7224, -2242 (1937).

4. Clatter, ... C., and D. B. Crawford, "Thermodynamic Proper... Nitrogen and Air," Trans. ASME, 71, 885-895 (1949)

5. Chart by E. B. Burnett
U. S. Bureau of Mines
Amarillo, Texas

6. Vandal', E. F., "Thermodynamic Properties of Neon." Proc... the 1958 Cryogenic Engineering Conference, pp. 47-64.

7. Stevenson, J. A. and Grafton, J. C., "Radiation Heat-Trans... for Space Vehicles," ASD-61-119, 1961.

8. Bartas, J. G. and Sellars, W. H., "Radiation Fin Effective... Trans. ASME, Series C, Journal of Heat Transfer, 82, 73-7...

9. Lieblein, S., "Analysis of Temperature Distribution and R... Transfer Along a Rectangular Fin of Constant Thickness," November, 1959.

10. Mackey, D. B., "Space Radiator Analysis and Design," ASD ...

11. Scott, R. B., Cryogenic Engineering, D. Van Nostrand Co., ...

12. Bulje, G. E., A Study on Design Criteria and Matching of ... Journal of Engineering Power, ASME, January 1962.